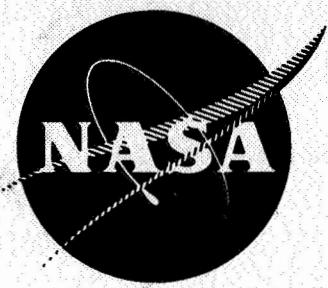


N72-14696

NASA CR-72948



**CASE FILE
COPY**

**CRYOGENIC GLASS-FILAMENT-WOUND
TANK EVALUATION**

by
E. E. Morris and R. E. Landes

**STRUCTURAL COMPOSITES INDUSTRIES, INC.
for
AEROJET-GENERAL CORPORATION**

prepared for
NATIONAL AERONAUTICS AND SPACE ADMINISTRATION

**NASA Lewis Research Center
Contract NAS 3-10289
James R. Barber, Project Manager**

FINAL REPORT

CRYOGENIC GLASS-FILAMENT-WOUND
TANK EVALUATION

by

E. E. Morris and R. E. Landes

STRUCTURAL COMPOSITES INDUSTRIES, INC.
6344 N. Irwindale Avenue
Azusa, California 91702

for

Aerojet-General Corporation
El Monte, California

prepared for

NATIONAL AERONAUTICS AND SPACE ADMINISTRATION

July 1971

CONTRACT NAS 3-10289

NASA Lewis Research Center
Cleveland, Ohio
James R. Barber, Project Manager
Liquid Rocket Technology Branch

FOREWORD

This report is submitted by Structural Composites Industries, Inc., and Aerojet-General Corporation in fulfillment of the contract. It covers all work on the program, which was conducted from July 1967 to February 1971.

The work was done by the Structural Composites Industries, Inc., and Aerojet. E. E. Morris, Manager of the Filament-Wound Tankage and Structures Division, was the Program Manager and principal investigator. R. E. Landes conducted the pressure vessel design analysis and guided filament winding of the test vessels. Metallurgical evaluations were performed by H. E. Bleil with the assistance of J. Garancovsky in mechanical testing.

Pressure-vessel fabrication was accomplished by R. J. Alfring and J. J. Dawson for the metal liners, and E. I. Fullmer and N. R. Dunavant for the glass filament-wound shell.

Vessel testing was conducted under the direction of A. I. Taoyama. Analysis of test data and program results was done by E. E. Morris and R. E. Landes, who prepared this report.

Guidance and many helpful suggestions were provided throughout the program by the NASA Project Manager, J. R. Barber of the Liquid Rocket Technology Branch, Lewis Research Center.

CRYOGENIC GLASS-FILAMENT-WOUND
TANK EVALUATION

by E. E. Morris and R. E. Landes

Structural Composites Industries, Inc.
Aerojet-General Corporation

ABSTRACT

High-pressure glass-filament-wound fluid storage vessels with thin aluminum liners were designed, fabricated, and tested at ambient and cryogenic temperatures which demonstrated the feasibility of producing such vessels as well as high performance and light weight. Significant developments and advancements were made in solving past problems associated with the thin metal liners in the tanks, including liner bonding to the overwrap and high strain magnification at the vessel polar bosses. The vessels had very high burst strengths, and failed in cyclic fatigue tests by local liner fracture and leakage without structural failure of the composite tank wall. The weight of the tanks was only 40 to 55% of comparable 2219-T87 aluminum and Inconel 718 tanks.

CONTENTS

	<u>Page</u>
SUMMARY	xx
I. INTRODUCTION	1
A. Background	1
B. Liners for Glass Filament-Wound Vessels	3
C. Glass Filament-Wound Vessels with Thin Metal Liners	4
D. Materials, Fabrication, and Design Problems and Solutions	6
1. Metal Liner	6
2. Filament-Wound Composite Buildup At Boss	7
3. Mandrel Support for Liner	8
4. Adhesive Bonding of Liner to Glass-Filament Composite Overwrap	8
II. DESIGN, FABRICATION, AND TESTING OF INITIAL VESSEL CONFIGURATIONS	9
A. Criteria	9
B. Aluminum Liner Materials Selection, and Design and Fabrication Concepts	9
1. Aluminum Selection for Liners	10
2. Liner Fabrication Processes	11
3. Other Points of Discussion	15
C. Design	16
1. Liner Material Characterization Analysis	16
2. Vessel Structural and Design Analysis	20

CONTENTS (cont.)

	<u>Page</u>
3. Evaluation of Adhesive Bond Between Aluminum Liner and Glass Filament- Wound Composite _____	22
D. Fabrication _____	24
1. Metal Liners _____	24
2. Aluminum Lined Glass Filament-Wound Vessels _____	31
E. Vessel Testing _____	32
F. Evaluation of Results _____	33
1. Summary of Problems With 1100 Aluminum Liner Fabrication _____	33
2. Summary of Problems With 6061 Aluminum Liner Fabrication _____	33
3. Conclusions and Recommendations _____	34
III. DESIGN, FABRICATION, AND TESTING OF IMPROVED VESSEL CONFIGURATIONS _____	37
A. Design _____	37
1. Dome Characteristics _____	37
2. Polar Boss Design Concepts _____	39
3. Vessel Designs _____	39
B. Fabrication _____	39
1. Electron Beam Weld Schedule Development _____	39
2. Liner Mechanical Testing _____	40
3. Liner and Vessel Fabrication _____	41
C. Testing _____	43
1. Test Plan, Facility, and Instrumentation _____	43

CONTENTS (cont.)

	<u>Page</u>
2. Test Results _____	46
IV. DESIGN, FABRICATION, AND TESTING OF ADDITIONAL VESSELS _____	55
A. Design _____	55
B. Fabrication _____	55
C. Testing _____	58
1. Test Plan, Facility, and Instrumentation _____	58
2. Test Results _____	59
3. Evaluation of Results _____	62
V. CONCLUSIONS AND RECOMMENDATIONS _____	69
References _____	73

Table

Effect of Cryogenic-Temperature Exposure on Welded and Planished 6061-0 Aluminum Alloy _____	1
Peel Adhesion Test Results _____	2
Liner Fabrication Sequence _____	3
Mechanical Properties of 6061 Aluminum Liner Cylindrical Section, Initial Annealing Procedure _____	4
Mechanical Properties of 6061 Aluminum Liner Dome Section, Initial Annealing Procedure _____	5
Mechanical Properties of 6061 Aluminum Liner Dome Section, Modified Annealing Procedure _____	6
Room Temperature Properties of 6061 Aluminum Welded With Various Weld Metals _____	7
Tensile Properties of EB-Weld Specimens of 1100-0 Aluminum _____	8

CONTENTS (cont.)

Table

Tensile Properties of 2219-T62 to 1100-H14 Aluminum EB Welds (Weld Transverse to Specimen Axis) _____	9
Tensile Properties of 2219-T62 to 1100-H14 Aluminum EB Welds (Weld Longitudinal to Specimen Axis) _____	10
Pressure Vessel Fabrication Data (BWB and HB Series) _____	11
Single Cycle Burst Test Data (BWB and HB Series) _____	12
Cyclic Fatigue Loading Test Data (BWB and HB Series) _____	13
Microhardness Traverse in Failure Area, Tank BWB-2 After 25 Pressure Cycles _____	14
Metal Liner Fabrication Data (A Series) _____	15
Pressure Vessel Fabrication Data (A Series) _____	16
Assignment of Vessels to Tests _____	17
Vessel Single Cycle Burst Test Data (A Series) _____	18
Vessel Cyclic Fatigue Loading Test Data (A Series) _____	19
Pressure Vessel Performance Factors _____	20

Figure

Pressure Vessel Performance Factors _____	1
Stress-Strain Characteristics of S-HTS Filaments and Ductile Aluminum Liner Materials _____	2
Fabrication Plan for 6061 Aluminum Liners with Integral Bosses _____	3
6061 Aluminum Liner With Integral Bosses (Engineering Drawing) _____	4
1100 Aluminum Liner With Bonded Bosses (Engineering Drawing) _____	5

CONTENTS (cont.)

Figure

Boss For 1100 Aluminum Liner With Bonded Bosses (Engineering Drawing) _____	6
Aluminum-Lined Glass Filament-Wound Pressure Vessel (Engineering Drawing) _____	7
T-Peel Adhesion vs Cure Schedule _____	8
1100 Aluminum Liner Halfshell, 12-in.-dia. _____	9
6061-T6 Aluminum Boss for 1100 Aluminum Liner _____	10
1100 Aluminum Liner Halfshells, Bonded Boss in Place _____	11
Weld Joint Detail Evolution _____	12
6061 Aluminum Liner Halfshell, Exterior View _____	13
6061 Aluminum Liner Halfshell, Interior View _____	14
Properties of 6061 Aluminum Liner Halfshell, Initial Annealing Procedure _____	15
Section From 6061 Aluminum Liner Halfshell Showing Test Specimens _____	16
Properties of 6061 Aluminum Liner Halfshell, Modified Annealing Procedure _____	17
Properties of 6061 Aluminum Weldments Prepared With Various Filler Wires _____	18
Application of Longitudinal Windings to Liner _____	19
Winding 12-in.-dia. by 18-in.-long Liner _____	20
Application of Circumferential Glass-Filament Winding to Liner _____	21
6061 Aluminum-Lined Glass Filament-Wound Pressure Vessel _____	22
Polar Boss Design Configurations _____	23
Schematic of Plastic Spring Boss (Hinge Boss) _____	24

CONTENTS (cont.)

	<u>Figure</u>
Plastic Spring Boss (Hinge Boss) _____	25
Matched-Rotation Flange Boss (Butt-Welded-Boss) _____	26
1100 Aluminum Liner, Hinged-Boss Configuration (Engineering Drawing)	
Note: 4 Pages - P/N 1269227 - 1 Page P/N 1269226 - 3 Pages _____	27
1100 Aluminum Liner, Butt-Welded-Boss Configuration (Engineering Drawing)	
Note: 3 Pages - P/N 1269231 - 1 Page P/N 1269230 - 1 Page P/N 1269229 - 1 Page _____	28
Aluminum-Lined Glass Filament-Wound Vessel (Engineering Drawing) _____	29
Drawn and Machined 1100 Aluminum Halfshell Forming For Hinged Boss Liner _____	30
Boss, Flange, and Collar For Hinged Boss Liner _____	31
Flange and Drawn and Machined Halfshell Forming For Hinged Boss Liner _____	32
Flange Welded to Drawn and Machined Halfshell Forming For Hinged Boss Liner _____	33
Boss and Collar Welded to Flange of Hinged Boss Liner Halfshell Forming _____	34
Final Machined and Chemically Milled Liner Halfshell for Hinged Boss Liner, Exterior View _____	35
Final Machined and Chemically Milled Hinged Boss Liner, Interior View _____	36
Copper Girth Weld Backup Ring Assembly to Liner Halfshell _____	37
Liner Assembly in Position for EB Girth Welding _____	38
Completed Liner Assembly, Hinged Boss Configuration _____	39

CONTENTS (cont.)

	<u>Figure</u>
Application of Longitudinally Oriented Glass-Filament Overwinding to Aluminum Liner	40
Application of Circumferentially Oriented Glass-Filament Overwinding to Aluminum Liner	41
Completed Aluminum-Lined Glass Filament-Wound Pressure Vessel	42
Liquid Cryogen Test Facility	43
Cryogenic Pressure Test Facility	44
Location of Instruments on Test Vessels	45
Post Test Photograph of Tank BWB-1 After Burst Test	46
Pressure vs Strain for Tank BWB-1 Burst Test	47
Boss Cross-Section from Tank BWB-1	48
Pressure vs Strain for Tank BWB-2 Cyclic Fatigue Test	49
Boss Cross-Section from Tank BWB-2	50
Boss Cross-Section from Tank BWB-2	51
View of Boss to Liner Transition of Tank BWB-2 Showing Local Thinning	52
View of Boss to Liner Transition of Tank BWB-2 Showing Local Thinning	53
View of Tank BWB-2 Section at Boss	54
EB Weld Joint	55
Tank BWB-2 Microhardness Traverse in Failure Area	56
Pressure vs Strain for Tank BWB-3 Burst Test	57
Boss Cross-Section from Tank BWB-3	58
View of Tank BWB-3 Boss Weld Showing 2219 Aluminum Side of Weld With Hot Tear in Weld and Parent Metal	59

CONTENTS (cont.)

	<u>Figure</u>
View of Tank BWB-3 Boss Weld Showing 1100 Aluminum Side of Weld With Hot Tear in Weld Metal _____	60
Boss Cross-Section from Tank BWB-3 _____	61
View of Tank BWB-3 Boss Showing Localized Necking of 1100 Aluminum in Failure Area _____	62
View of Tank BWB-3 Boss Showing 2219 Aluminum Side of Weld _____	63
Post Test Photograph of Tank HB-2 After Burst Test _____	64
Pressure vs Strain for Tank HB-2 Burst Test _____	65
Cross-Section of Tank HB-2 Boss From Vessel Dome That Failed _____	66
Cross-Section of Tank HB-2 Boss from Vessel Dome That Did Not Fail _____	67
Pressure vs Strain for Tank HB-3 Cyclic Fatigue Test _____	68
Photomicrographs of Tank HB-3 Cylinder Wall Sections Showing Lack of EB Weld Penetration at Liner Girth Weld _____	69
Photomicrographs of Tank HB-3 Dome Sections Showing Liner Fracture Site _____	70
Cross-Section of Tank HB-3 Boss From Vessel Subjected to Fatigue Cycling _____	71
Post Test Photograph of Tank HB-1 After Burst Test _____	72
Pressure vs Strain for Tank HB-1 Burst Test _____	73
View of Tank HB-1 Boss Showing Successful Operation of the Hinged Boss _____	74
Group of Completed 1100 Aluminum Liners of Hinged-Boss Configuration, 12-in.-dia. by 18-in.-long _____	75
Glass Filament Overwinding 1100 Aluminum Hinged-Boss Liner _____	76
Buckles in Liner A-1 _____	77

CONTENTS (cont.)

	<u>Figure</u>
Installation of Test Vessel in Holding Frame, With Instrumentation Attached	78
Vessel Holding Frame Positioned in Cryogen Filled Test Container	79
Post Test Photograph of Tank A-3 After Burst Test	80
Pressure vs Strain for Tank A-3 Burst Test	81
Post Test Photograph of Tank A-11 After Cyclic Fatigue Test	82
Pressure vs Strain for Tank A-11 Cyclic Fatigue Test	83
Post Test Photograph of Tank A-12 After Cyclic Fatigue Test	84
Pressure vs Strain for Tank A-12 Cyclic Fatigue Test	85
Post Test Photograph of Tank A-1 After Burst Test	86
Pressure vs Strain for Tank A-1 Burst Test	87
Post Test Photograph of Tank A-4 After Cyclic Fatigue Test	88
Pressure vs Strain for Tank A-4 Cyclic Fatigue Test	89
Post Test Photograph of Tank A-13 After Cyclic Fatigue Test	90
Pressure vs Strain for Tank A-13 Cyclic Fatigue Test	91
Post Test Photograph of Tank A-9 After Burst Test	92
Pressure vs Strain for Tank A-9 Burst Test	93
Post Test Photograph of Tank A-2 After Cyclic Fatigue Test	94
Post Test Photograph of Tank A-6 After Cyclic Fatigue Test	95
Pressure vs Strain for Tank A-2 Cyclic Fatigue Test	96
Pressure vs Strain for Tank A-6 Cyclic Fatigue Test	97

CONTENTS (cont.)

	<u>Figure</u>
Typical Boss and Head-To-Cylinder Junction Specimens Taken from Tanks	98
Cross-Sections of Hinged Boss, Exterior View	99
Cross-Sections of Hinged Boss, Interior View	100
Locations of Liner Failure Sites and Specimens Taken from Tanks for Analysis	101
Photomicrographs of Tank A-3 Cross Section Showing Liner, Glass Filament Overwrap, and Craze Cracking	102
Tank A-1 Boss Cross Section	103
Photomicrographs of Tank A-1 Dome Cross Section Showing Liner Failure Site	104
Photomicrographs of Tank A-11 Dome Cross Section Showing Liner Failure Site	105
Photomicrographs of Tank A-12 Dome Cross Section Showing Liner Fracture Site	106
View of Tank A-11 Liner Failure Site, Looking from Inside Surface	107
View of Tank A-4 Liner Failure Site in Dome, Looking From Inside Surface	108
View of Tank A-4 Liner Failure Site in Cylinder, Looking From Inside Surface	109
Photomicrographs of Tank A-4 Dome Cross Section Showing Liner Fracture Site	110
Photomicrographs of Tank A-4 Cylinder Cross Section Showing Liner Fracture Site	111
Tank A-4 Boss Cross Section	112
View of Tank A-13 Liner Dome Inside Surface Near Head-To- Cylinder Juncture Showing Strain Concentration Lines	113
Outside View of Tank A-13 Head-To-Cylinder Juncture, Showing Filament-Wound Composite Craze Cracking	114

CONTENTS (cont.)

	<u>Figure</u>
View of Tank A-2 Liner Dome Inside Surface Near Head-To-Cylinder Juncture Showing Fracture Site and Work Hardening in Liner	115
Tank A-6 Boss Cross-Section	116
Hoop-Wound Glass-Filament Stress at Vessel Burst vs Temperature	117
Longitudinally Wound Glass-Filament Stress at Vessel Burst vs Temperature	118
Hoop Filament Stress During Cycling vs Cycles to Vessel Failure	119
Longitudinal Filament Stress During Cycling vs Cycles to Vessel Failure	120
Vessel Equivalent Uniaxial Strain Range During Cycling vs Pressure Cycles to Failure (1:1 Load Condition) Compared With 1100 Aluminum Low Cycle Fatigue Data (1:0 Load Condition)	121
	<u>Page</u>
APPENDIX A - LINER MATERIAL CHARACTERIZATION ANALYSIS	A-1
	<u>Table</u>
Effect of Location in Thickness on Tensile Properties of 1.00-in. Thick 6061 Aluminum Plate	A-1
Effect of Thickness on Mechanical Properties of 6061 Aluminum (Not Chemically Milled)	A-2
Effect of Chemical Milling and Degree of Anneal on Mechanical Properties of 6061 Aluminum (Chemically Milled from 0.030 to 0.010-in.)	A-3
Effect of Chemical Milling and Degree of Anneal on Mechanical Properties of 6061 Aluminum (Chemically Milled from 0.020 to 0.010-in.)	A-4
Effect of Final Thickness on Annealed Chemically Milled 6061 Aluminum Mechanical Properties	A-5

CONTENTS (cont.)

Table

Ambient and Cryogenic Temperature Mechanical Properties of Annealed 6061 Aluminum (Chemically Milled from 0.030 to 0.010-in.)	A-6
Ambient Temperature Mechanical Properties of Annealed 6061 Aluminum Weldments (TIG Butt Fusion Welded With 1100 Aluminum Filler Wire)	A-7
Ambient Temperature Mechanical Properties of Annealed 6061 Aluminum Weldments (TIG Butt Fusion Welded With 1100 Aluminum Filler Wire and Beneficiated)	A-8
Effect of Thickness on the Mechanical Properties of Annealed 1100 Aluminum (Not Chemically Milled)	A-9
Effect of Chemical Milling on the Mechanical Properties of Annealed 1100 Aluminum	A-10
Ambient and Cryogenic Temperature Mechanical Properties of Annealed 1100 Aluminum (Chemically Milled from 0.030 - 0.010-in.)	A-11
Ambient Temperature Mechanical Properties of Annealed 1100 Aluminum Weldments (TIG Butt Fusion Welded With 1100 Aluminum Filler Wire)	A-12
Ambient Temperature Mechanical Properties of Annealed 1100 Aluminum Weldments (TIG Butt Fusion Welded With 1100 Aluminum Filler Wire and Beneficiated)	A-13

Figure

Section of 0.010-in. Thick 6061 Aluminum Membrane Showing Edge Attack by Chemical Milling Solution	A-1
Section of 0.010-in. Thick 6061 Aluminum Membrane Showing Slight Intergranular Attack by Chemical Milling Solution	A-2
Effect of Processing on Elongation of 6061 Aluminum	A-3
Tensile and Yield Strength of 6061-0 Aluminum Chemically Milled from 0.030 to 0.010-in. Thickness	A-4
Elongation of 6061-0 Aluminum Chemically Milled from 0.030 to 0.010-in. Thickness	A-5

CONTENTS (cont.)

	<u>Figure</u>
Elongation for Various Gage Lengths of 6061 Aluminum Weld Specimen GW-7	A-6
Tensile and Yield Strength of 6061-O Aluminum, TIG Butt Fusion Welded With 1100 Aluminum Filler Wire and Beneficiated	A-7
Elongation of 6061-O Aluminum, TIG Butt Fusion Welded With 1100 Aluminum Filler Wire and Beneficiated	A-8
Section of 1100 Aluminum 0.010-in. Membrane Showing Uniform Edge Attack by Chemical Milling Solution	A-9
Section of 1100 Aluminum 0.010-in. Membrane Showing Evidence of Some Localized Intergranular Attack by Chemical Milling Solution (Unetched)	A-10
Section of 1100 Aluminum 0.010-in. Membrane Showing Evidence of Slight Intergranular Attack by Chemical Milling Solution (Etchant - 10% NaOH)	A-11
Effect of Processing on Elongation of 1100 Aluminum	A-12
Tensile and Yield Strength of 1100-O Aluminum Chemically Milled From 0.030 to 0.010-in. Thickness	A-13
Elongation of 1100-O Aluminum Chemically Milled from 0.030 to 0.010-in. Thickness	A-14
Tensile and Yield Strengths of 1100-O Aluminum, TIG Butt Fusion Welded With 1100 Aluminum Filler Wire and Beneficiated	A-15
Elongation of 1100-O Aluminum, TIG Butt Fusion Welded With 1100 Aluminum Filler Wire and Beneficiated	A-16
	<u>Page</u>
APPENDIX B - DESIGN ANALYSIS OF PRESSURE VESSEL MEMBRANE, HEAD-TO-CYLINDER JUNCTURE, WINDING PATTERN, AND METAL BOSSES	B-1
Design Criteria	B-1

- All vessels subjected to cyclic fatigue tests failed by local fracture in the aluminum liner. The cyclic fatigue failure mode always consisted of leakage, without any evidence of structural failure of the vessel composite wall.
- The maximum number of pressure cycles achieved by vessels when pressurized between 0 and 60% of burst strength prior to liner fracture was 97 at the liquid hydrogen test temperature.

Failure analysis indicated that elimination of liner strain magnification sites in the vessel domes should increase the cyclic life of the aluminum liners to 400 to 1000 cycles at the 60% load level.

Pressure vessel performance comparisons showed that the vessels had a much higher demonstrated weight efficiency than metal vessels and similar boron and graphite filament-wound vessels. The weight of the glass filament-wound vessels with thin aluminum liners is only 40 to 55% of 2219-T87 aluminum or Inconel 718 spherical and cylindrical vessels having the same burst pressure and volume.

I. INTRODUCTION

A. BACKGROUND

Interest in filament-wound tankage for aerospace applications has increased because of the need for maximum weight-saving and because state-of-the-art advancements have demonstrated that the reliability level needed in specific applications can be attained with filament-wound structures.

Since the early 1950's, when the first serious efforts were made with high-strength, light-weight glass-filament-wound vessels and rocket motor cases, significant successes have been achieved in development of a technology base and reliable application of these composite structures to operational systems.

The potential of filament-wound composite tankage for cryogenic service has been shown in a series of NASA technology development programs. Such vessels with metal liners offer considerable weight savings at ambient and cryogenic temperatures as compared with homogeneous metal construction. Research has been concentrated on evaluation of constituent-material properties, development of effective pressure vessel analytical methods and designs for combining a metal liner with the overwrapped filament composite, and evaluation testing of tanks at ambient and cryogenic temperatures. These programs have produced filament-wound tanks offering significant potential advantages:

- Weight reductions of 20 to 60%.
- Fail-safe characteristics - non-shatterability/increased crack propagation resistance.
- Increased packaging density with no weight penalty (vessel shape not restricted to spheres for minimum weight).

Impermeability, corrosion resistance, and cryogenic temperature capability are achieved for space applications by using a metal liner inside the winding. To minimize tank weight and make maximum use of the filament-wound composites high strength-to-density ratio, a minimum-weight liner is desirable.

Composite tankage designs developed and evaluated under NASA sponsorship have been based on two different liner design approaches. With the first, filament overwindings are used to reinforce a high-strength metal shell which has a thickness about one-half of what a homogeneous vessel would need if not reinforced. Designs are established by using analyses which combine strength and strain characteristics of the filament and metal shells.

Combining the filament-wound composite with a metal shell provides the necessary sealant liner and permits the strength potential of both the filament and metal shells to be exploited. With this approach, glass filaments with epoxy resins have been used exclusively for the high-strength metal shell reinforcement. This concept, with the load bearing metal shell, is referred to as a glass-filament-reinforced (GFR) vessel. In the second approach, filament windings are used to reinforce a very thin metal liner which has the minimum possible thickness required for impermeability and fabrication. The liner carries only a small share of the structural loads. For this approach, glass filaments with epoxy resins have received the most emphasis, and significant work has been conducted on boron and graphite filaments with epoxy resins. Liners used are low-strength ductile metals. This concept, with the non-load bearing liner, is referred to as a metal-lined filament-wound vessel.

Early work involved glass filament reinforcing metal for rocket motor cases (References 1 and 2). Efforts started on cryogenic metal-lined glass filament-wound vessels at Aerojet in 1962 (References 3 to 5). NASA-LeRC sponsored a program to evaluate internally insulated filament-wound LH₂ tanks (References 6 and 7), and then conducted several in-house programs involving studies on problems of liners for filament-wound cryogenic tanks (References 8 to 10). A program was then awarded by NASA-LeRC to investigate design improvements in liners for glass filament-wound tanks to contain cryogenic fluids (Reference 11). Concurrent with this cryogenic tankage effort, two programs were conducted for the U.S. Air Force on thin metal-lined glass filament-wound vessels to contain corrosive storable propellants (References 12 and 13).

Because of the performance potentials demonstrated from the above work, and NASA-LeRC's growing interest in filament-wound cryogenic tankage, three programs were initiated in 1965. One program involved development of resin matrix systems for glass filament-wound cryogenic vessels, including tank testing (Reference 14). The second program involved study of glass-filament-reinforced (GFR) metal vessels with load-bearing, non-buckling metal liners for cryogenic service. Three main efforts were conducted: a parametric study of GFR 2219 aluminum, GFR Inconel X750, GFR 5Al-2.5 Sn titanium, and GFR stainless steel vessels (Reference 15); development of structural analysis techniques and computer programs for GFR metal tanks (Reference 16); and design, fabrication, and testing of GFR Inconel tanks at ambient to liquid hydrogen temperature (Reference 17). The third program (Reference 18) involved development of improved evaluation testing of metal-lined tanks. Concurrent with these activities, two other programs were conducted studying thin metal liners and liner bonding adhesives for cryogenic glass-filament-wound tanks (References 19 and 20).

NASA-LeRC in-house research efforts continued with a series of investigations by Hanson. In Reference 21, boron and graphite filaments were studied along with glass filaments for composites of cryogenic vessels.

Following this, tensile and cyclic-fatigue properties of graphite filament-wound pressure vessels with metal liners were evaluated at ambient and cryogenic temperatures (Reference 22). Later, static and dynamic fatigue behavior of glass-filament-wound pressure vessels was further studied at ambient and cryogenic temperatures (Reference 23). Additional efforts were conducted to evaluate glass filament overwrapped metallic cylindrical pressure vessels (Reference 24); besides demonstrating the performance potentials of glass filament reinforced aluminum cylinders, it was in this work that Johns and Kaufman established constrictive wrap buckling strengths and design criteria of overwrapped metal shell tank liners. Other contracts were awarded by NASA-LeRC to study GFR Cryoformed 301 stainless steel vessels (Reference 25) and GFR 5A1-2.5 Sn titanium pressure vessels (Reference 26).

Lightest weight high pressure vessels for service at ambient to cryogenic temperatures are glass-filament-wound pressure vessels with very thin metal liners, providing a reliable liner design is employed. The magnitude of performance advantage is shown in Figure 1, where the pressure-vessel performance factor, pV/W^* , is presented for metal-lined filament-wound tanks and homogeneous-metal pressure vessels. The weight of the filament-wound vessels is only 50 to 70% of that of the titanium tanks and is considerably less than this when compared with stainless steel, aluminum, and Inconel vessels. Test results for a large number of composite overwrapped metal pressure vessels from the previously referenced programs have demonstrated that glass-filament-wound tanks have the great potential for weight savings in cryogenic tankage indicated by Figure 1.

The program covered by this report was initiated to demonstrate the feasibility of producing closed-end, cylindrical, glass-filament-wound pressure vessels with very thin aluminum liners for operation in the +75 (297°K) to -423 $^{\circ}\text{F}$ (20°K) temperature range. Processes for fabricating thin metal liners, for providing joints in the liner having the necessary properties, and for providing a bond between the liner and filament-wound composite were to be identified, demonstrated, and evaluated by fabricating and testing vessels at +75 (297°K), -320 (77°K), and -423 $^{\circ}\text{F}$ (20°K).

B. LINERS FOR GLASS-FILAMENT-WOUND VESSELS

Although the filament-wound material is light in weight, it is permeable to gases and liquids under pressure. Furthermore, the filament and/or resin components of the composite may be subject to chemical corrosion by contained fluids, such as propellants. This is overcome by using a thin liner

* p = design pressure, psig (N/cm^2); V = internal volume, in.³ (cm^3); W = pressure vessel weight, lbm (g).

inside the filament-wound structure to prevent fluid contact or transmission through the composite wall. Because the performance of a pressure vessel is based on its total weight, operating pressure, and volume, a minimum liner weight is desired. The functional requirements for sealant liners of glass-filament-wound pressure vessels include:

- Impermeability to gases and liquids under pressure.
- Resistance to corrosion by contained fluids.
- Strain compatibility with the composite structure up to its failure stress.
- Resistance to fatigue when subjected to repetitive loading of the composite structure to the operating stress level.
- Toleration of tankage expansion and contraction during temperature cycling.

Materials such as molded elastomer, polymeric films, metal coatings, metal foil, and thin metal sheet have been used for liners. The polymeric materials have been suitable when the pressure-vessel service life has been short, and when some permeation through the structure has been tolerable. To date, the use of elastomeric liners has been restricted to temperatures greater than about -65°F or 220°K because of the loss of extensibility that occurs as the glass transition temperature is reached.

When a polymer liner is functionally adequate for a specific application, the designing of the liner and filament-wound vessel is relatively straight-forward. When stringent limitations are imposed on the leakage of fluids or when operational temperatures are below -65°F (220°K), metal liners must be used because of the present inability of elastomers and polymers to provide the necessary properties. As previously described, these liners may be relatively thick (load-bearing) or very thin (sealant liner). The latter metal liners have been as thin as 0.003-in.-(0.076 mm) and 0.006-in.-(0.152-mm) when made from stainless steel and aluminum foils. When very thin metal liners are used, however, the high operating strains repetitively applied to glass-filament-wound-composite pressure vessels during service have presented extremely difficult problems in keeping the liner bonded to the overwrap in order to sustain fatigue cycling; when liners became unbonded, they locally buckled, and failed by fatigue cracking in the buckles during pressure cycling.

C. GLASS-FILAMENT-WOUND VESSELS WITH THIN METAL LINERS

Problems encountered in using thin high-elongation, foil materials for the liners of glass-filament-wound vessels and strain-cycling the liners into the plastic regions of their stress-strain curves arise

because of (1) thin liner buckling on depressurization of the vessel when the bond between the liner and filament-wound composite fails, and (2) subsequent fatigue failure of the liner in the buckled area: an adhesive bond must be retained between the thin metal liner and filament-wound composite for maximum cyclic-fatigue life capability in the liner. NASA-sponsored research directed specifically at developing cryogenic adhesives for this purpose demonstrated that adhesives can be compounded for the requirements of low-temperature adhesion of thin metal liners to the glass-fiber composite. Using the adhesive developed under the Reference 20 program [consisting of Adiprene L-100/Epi Rez 5101/MOCA (80/20/17)], thin aluminum liners were bonded to filament-wound cylinders in such a manner that the liners did not buckle when subjected to repeated high cyclic strains representative of a pressure-vessel service cycle.

Concurrent with the development of the adhesive bonding system, other work on the Reference 14 program led to the development of a filament-wound composite resin matrix with higher elongation at cryogenic temperature than commonly used resins. This resin [Epon 828/DSA/Empol 1040/BDMA (100/115.9/20/1)] improved composite performance at cryogenic temperatures. The Reference 17 and 18 work developed analytical methods and important design data at ambient to liquid hydrogen temperatures for filament-wound vessels with metal liners.

Each of these developments were brought together in the program covered by this report to develop an optimum design for a cryogenic glass-filament-wound vessel and structural performance data. The vessels developed incorporated

- The cryogenic resin matrix and cryogenic adhesive bond system described above.
- S-HTS glass for the windings.
- Thin aluminum liners of 0.010-in. (0.254 mm) thickness.

Very thin metal liners for filament-wound pressure vessels had been developed and used in earlier efforts. These liners were as thin as 0.002-in.-(0.051-mm-) thick aluminum on a 7 1/2-in.-(19.05-cm-) diameter cylinder with adhesive-bonded overlap seam joints (References 20 and 21). Liners with welded joints were as thin as 0.003 in. (0.076 mm) and 0.006 in. (0.152 mm) when made into 8-in.-(20.3-cm-), 12-in.-(30.5-cm-), and 18-in.-(45.7-cm-) dia. closed-end liner assemblies from aluminum and stainless steel (References 11, 12, 13, 14, and 18). Joints in these liners were not made by butt welding because of the thin gage; instead, an overlap roll-resistance seam weld was employed.

Some test results had indicated that an adhesive bonded overlap joint in the liner might not be reliable when the liner must sustain high operating strains repeatedly applied during pressure-cycling of the vessel (Reference 20). On the other hand, the roll-resistance seam-weld joint in 0.006-in.- (0.152-mm-) thick stainless steel had been shown to be leaktight in oblate spheroids subjected to 100 or more pressure cycles to 2% strain level and in 12-in.- (30.5-cm-) dia. by 37-in.- (94.0-cm-) long cylindrical vessels subjected to 25 cycles to 1% strain level. (References 12 and 13) However, the geometry of the overlapped welded joint could introduce problems in obtaining the high-quality adhesive bond between the metal liner and overwrapped glass filaments needed to keep the liner from buckling. We believed that smooth liner without discontinuities and areas where overwrapped filaments would bridge, such as could be formed by electroforming metal on a removable mandrel or butt-welding liner components together, would provide a better design configuration.

Although progress had been made in the development of processes for the electroforming of thin aluminum liners of good ductility on double-curvature shapes, it appeared that more exploratory development work was needed to demonstrate the potential of electroformed aluminum liners prior to committing a large development program to their use. Accordingly, this program was based on making aluminum liners by welding of liner components.

D. MATERIALS, FABRICATION, AND DESIGN PROBLEMS AND SOLUTIONS

1. Metal Liner

The high strength and low modulus of glass filaments create a requirement for large biaxial strains in the metal liner, and are the most significant factors influencing metal-liner materials selection and design. The aluminum liner membrane used in the vessel must strain under a 1-to-1 biaxial strain field past its yield point to the operating and ultimate stresses of the glass filaments without failure or permeability to fluids under pressure. At ambient temperature, S-HTS glass filaments have an elastic modulus of 12.4×10^6 psi (85.5 GN/m^2) and a representative ultimate filament strength in pressure vessels of 330 000 psi (228 000 N/cm^2), resulting in a failure strain of about 2.7%. At cryogenic temperatures, the strength of the filaments may increase as much as 50% to 495 000 psi (341 000 N/cm^2), while the modulus increases about 10% to 13.6×10^6 psi (93.8 GN/m^2), producing a biaxial failure strain of about 3.6%. Comparative stress-strain diagrams for S-HTS glass filaments and ductile aluminum liner materials at ambient and cryogenic temperatures are shown in Figure 2.

Under the 1-to-1 biaxial-stress-field conditions, metals have a significantly reduced strain capability as compared with their uniaxial ductility. The allowable elongation under 1-to-1 stress-field conditions is less than 50% and closer to 25% of the uniaxial ductility. We use the design rule that the allowable biaxial elongation of a metal under 1-to-1 stress-

field conditions is 25% of the uniaxial value. With a biaxial design allowable equal to 25% of the uniaxial elongation, the aluminum liner materials in the parent metal and weldments must have a uniaxial ductility capability about four times the ultimate glass filament strain, or 10.8% uniaxial elongation at ambient temperature and 14.4% at cryogenic temperatures, to be able to strain as a liner to achieve the full strength potential of the glass-filament-wound shell.

While the metal membrane, which is completely overwrapped and constrained by the filaments, must have high ductility to perform adequately as a liner, the flanges of the axially located bosses of the liner are subjected to bending and shear stresses. If a quite ductile, but low-strength material is used to form both the liner and the bosses of a high-pressure vessel, the flange thickness becomes very thick compared to the membrane and an effective design for a low rigidity and high ductility transition between the boss and membrane may be difficult to develop. It is desirable that bosses have high strength to sustain with minimum flange thickness the imposed bending and shear loads resulting from pressurization of the vessel.

These conflicting requirements for high ductility for the parent metal and welds of the membrane and high strength for the boss flanges lead to the concepts of forming the liner from either (1) two different aluminum materials which are joined by bonding in the boss-to-membrane transitions, or (2) a single material selectively heat-treated to provide high strength to the bosses and ductility to the membrane.

For maximum compatibility with the high glass-filament-wound composite strains in the end domes, the metal boss should have low rigidity and be as small as possible (i.e., the metal liner should have the minimum possible dimensions which do not plastically deform to the same strains as the isotensoid filaments of the vessel end domes). In practice this is accomplished by reducing the body of the boss to the smallest practical dimensions in width and thickness. By keeping the width dimension small, the magnitude of mismatch between deflections of the filament-wound composite on top of the boss and the boss can be reduced, and the strain dumped into the liner membrane at the edge of the boss flange can be minimized. By keeping the thickness small, the boss flange can be blended into the liner membrane over a short distance to reduce the effective width dimension of the boss.

2. Filament-Wound Composite Buildup at Boss

As the boss diameter is reduced, the stacking (buildup) of the longitudinally wrapped composite around the boss is increased with a reduction in efficiency in the filament-wound composite in this region. By increasing the winding-tape width, however, the stackup can be reduced to acceptable levels.

3. Mandrel Support for Liner

It is extremely important to provide firm mandrel support to the thin, soft aluminum liner during fabrication to preclude liner wrinkling or buckling as could be produced by the overwrapped filaments. A pressure mandrel system was selected for use to provide good contact pressure between the liner and the filament-wound composite at all points, resulting in an enhancement of the adhesive bond.

4. Adhesive Bonding of Liner to Glass-Filament Composite Overwrap

Unlike the metal liner, which has both elastic and plastic components in its stress-strain curves, glass filaments are elastic throughout the entire stress-strain range. When a ductile aluminum lined glass-filament-wound vessel is loaded to its operating strain of about 1 to 2%, the metal liner strains elastically to its yield point and then plastically (about 1-1/2 to 1-3/4%) to the operating strain level. On depressurization, the metal liner springs back along its offset stress-strain curve, recovering about 1/4 to 1/2% strain elastically, and then is pushed plastically into high compression as long as the liner does not buckle from the compressive stress. For thin, smooth, metal liners with high diameter-to-thickness ratios, an adhesive bond between the metal liner and filament-wound composite tank wall is required to prevent the liner from buckling under compressive stress. The bond must be capable of straining with the filament-wound composite to operating strain levels, at ambient temperatures and cryogenic temperatures, without losing adhesion to either surface or failing itself. This bond integrity must be maintained during repeated applications of the strain cycle during pressure cycling of the vessel. Should the bond fail, local buckling followed by fatigue failure of the liner and leakage will occur. Thus adhesive bond integrity a most important requirement for thin metal-lined glass-filament-wound tanks which must sustain fatigue cycling.

The adhesive bonding system and procedures investigated, evaluated, and selected under the Reference 20 program for bonding single-curvature cylindrical aluminum liners to filament-wound-composite pressure vessels was chosen for this program on closed-end cylindrical vessels. The procedure consists of cleaning and priming the aluminum liner surface, applying adhesive-resin-saturated nylon scrim cloth to the surface of the liner (without gapping, overlapping, or wrinkling the scrim cloth), and then overwinding the adhesive layer with filament-wound composite and curing the resin systems. The nylon scrim cloth is used in the adhesive bond layer to control glue-line thickness, to impede the propagation of craze cracks from the filament-wound composite to the metal liner, and to improve performance of the bond.

II. DESIGN, FABRICATION, AND TESTING OF INITIAL VESSEL CONFIGURATIONS

A. CRITERIA

At the start of the program, designs were established for two configurations of glass-filament-wound pressure vessels with the following characteristics:

- Liner: Aluminum, 6061-0 and 1100-0 (each vessel design used one material)
- Fiber Reinforcement: S-glass with HTS finish
- Resin Matrix: Epon 828/DSA/Empol 1040/BDMA (100/115.9/20/1 pbw)
- Liner to Composite Adhesive: Adiprene L-100/Epi-Rez 5101/MOCA (80/20/17) with one layer of J P Stevens Nylon Scrim Cloth No. 34168-2
- Burst Pressure: 3000 psi at 75°F (2070 N/cm² at 297°K)
- Shape: Closed-end cylinder
- Size: 12-in.- (30.5-cm-) dia. by 18-in.- (45.7-cm-) long

All components of the vessels were designed for service down to -423°F (20°K). They had aluminum liners approximately 0.010-in.- (0.254-mm-) thick, equivalent in weight to a 0.003-in.- (0.076-mm-) thick stainless steel liner. The thickness selection was made after consideration of fabrication tolerances and costs, handling and mandrel support requirements, and the requirement for absolute sealing.

B. ALUMINUM LINER MATERIALS SELECTION, AND DESIGN AND FABRICATION CONCEPTS

The conflicting requirements for high ductility for the parent metal and welds of the membrane and high strength for the boss flange lead to the concepts of forming the liner from (1) a single aluminum selectively heat-treated to provide high strength in the boss and ductility in the membrane, and (2) two different aluminum materials (high ductility membrane and high strength bosses) which are joined by bonding at the boss-to-membrane transition.

The first approach permits formation of bosses integral with the membrane and eliminates a weld joint at each end of the vessel. (Welded

joints in the metal liner should be kept at a minimum to reduce problems associated with joint mismatch and weld defects, as well as other fabrication processes used in liner fabrication such as chemical milling.) By making the liner from one material, only a single weld located in the girth direction at the center of the cylindrical section is required. The one girth weld in the cylindrical section would be essentially a cast structure as welded, and could not be expected to have the ductility required over the design operating temperature range. However, the weld joint can be beneficiated by cold working followed by annealing to refine the weld structure and give it nearly the same properties as the parent material.

The second approach permits the (1) formation of the liner membrane using the aluminum alloy having maximum ductility, and (2) the incorporation (without welding) of high strength aluminum alloy bosses. These two components would be joined using the adhesive bonding techniques developed under the Reference 20 program.

1. Aluminum Selection For Liners

a. Aluminum Liner With Integral Bosses

Aluminum alloy 6061 was selected for this liner. Data available for this material in the annealed condition shows adequate ductility over the service-temperature range to be usable for the membrane. However, effects on ductility of the fabrication processes and thickness to be employed needed to be evaluated. In the T6 condition, 6061 has satisfactory strength to perform effectively as the boss of the vessel. A liner fabrication technique was selected which would permit incorporation of selectively annealed 6061 aluminum in the liner membrane and 6061-T6 in the bosses. This technique, discussed in Section II-B-2-a, permits the fabrication of one-piece liner half shells requiring only a single circumferential weld.

To improve the ductility of the circumferential weld joint in the membrane, the use of 1100 aluminum-alloy filler wire was contemplated. Further improvement in weld-joint ductility was planned through beneficiation of the weld by means of planishing. The beneficiation treatment of the weld results in cold work in the area to eliminate the cast structure and obtain recrystallization upon annealing.

A metallurgical investigation was conducted prior to 6061 liner fabrication to evaluate and select the proper parameters for use in fabrication of the liners with integral bosses. This program is described in Section II-C-1.

b. Aluminum Liner With Bonded Bosses

Maximum ductility for the membrane at ambient and

cryogenic temperatures is obtainable by use of the Type 1100 aluminum in the annealed condition. For maximum strength in the boss flanges, 2219 aluminum alloy was selected for these components.

A metallurgical investigation was conducted on Type 1100 aluminum prior to liner fabrication to evaluate and select the proper parameters for use in fabrication of these liners. This program is described in Section II-C-2.

2. Liner Fabrication Processes

a. 6061 Aluminum Liner With Integral Bosses

(1) Selection of Fabrication Method

To satisfy requirements needed for a thin metal-liner of glass filament-wound pressure vessels, the liner must incorporate the following characteristics: (a) thin gage in the membrane to give minimum weight while also providing absolute sealing of the filament-wound structure, (b) metallurgical integrity to provide high strain capability in the membrane, and (c) suitable strength in areas not fully supported by filament winding.

The ideal metal structure to best meet the cyclic straining and burst strain requirements of the liner would be of single-piece or unit construction, and would efficiently withstand the end loads adjacent to the boss areas (on the axial center line) and still provide in all other areas the high ductility needed for compatibility with the glass filament-wound structure. To fulfill all these requirements, and make possible the fabrication of a liner within the limits of present-day metal-working technology, required the employment of three metal-manufacturing processes not heretofore used in glass-filament-wound vessel-liner manufacture. These processes are described below.

Chemical Milling - A metal-removal process which made possible the controlled etching of a relatively thin membrane to obtain a minimum thickness not possible with conventional metal-removal methods without inducing harmful metallurgical effects, such as high surface stress induced by cutting tools.

Temper Control - A selective heat-treatment process which provided needed mechanical properties in certain areas of the metal structure so that high strength could be imparted to one or more areas which require high load-carrying ability while other areas concurrently incorporated a relatively low-strength, highly ductile character.

Weld-Joint Beneficiation - This process upgrades the properties of butt-welded joints in wrought material where the character of the weldment permits restoration to a substantial extent the wrought properties of the parent material by planishing under controlled conditions the cast metal of the weldment. Upon welding of the butted edges, the fused metal "wells up" on the side from which the welding is performed. Appropriate backup with copper chill elements, inert-gas shielding, and control of heat sources prevents excessive penetration or droptrough on the weld backside. In the gage to be used for making liner welds the fused metal builds up in thickness to approximately 25% over the original thickness of the joined edges. Since such buildup is practically all on the external side of the weld, it is accessible for cold work by mechanical means to restore as much as possible the original properties of the parent material. This is accomplished by passing the weld seam under a pressure roll with appropriate support from the internal side of the liner to preclude buckling or other damage. The pressure used to level the weld bead is just enough to bring the fused metal back to the original sheet thickness, with the adjacent unwelded metal serving as a thickness control. Because the weld metal is cold-worked, it is necessary to anneal the weld after this operation to insure maximum ductility in the weld. Depending on the purity of the metal fused and the amount of cold work, the beneficiated weld joint will have the same or nearly the same properties as the parent material. Even though the original properties may not be completely restored, the beneficiated weld joint should be significantly better than the "as-welded" joint, which contains essentially a cast structure.

(2) Configuration Selection

In view of the efficiencies afforded by the fabrication processes discussed above and the program objectives of creating the best liner design compatible with available metal materials, "state-of-the-art" metal-fabrication technology, and the overall objectives incident to the liners end use, the 12-in.-(30.5-cm-) dia. by 18-in.-(45.7-cm-) long closed-end cylindrical liner incorporated the following characteristics:

(a) The liner was fabricated of 6061 aluminum alloy plate stock with mechanical properties subject to temper control. By selective heat treatment, bosses and adjacent high load areas incorporated properties of a heat treatment to obtain maximum strength with a transition to areas needing less strength but high ductility.

(b) The liner was essentially of two-piece construction with a single beneficiated circumferential weld joining two similar halves at a midpoint of the cylindrical section. The configuration of the entire liner was a cylinder section with oblate spheroid ends having integral polar bosses in each dome.

(c) The liner membrane was of 0.010-in.- (0.254-mm) nominal thickness in all areas. A transition thickness existed between boss areas and membrane to preclude local stress loading. The manufacturing tolerances for membrane thickness was as follows:

80% of area 0.010 ± 0.002 in.
 $(0.254 \pm 0.051$ mm)

10% of area $0.010 + 0.004/-0.002$ in.
 $(0.254 + 0.102/-0.051$ mm)

10% of area $0.010 + 0.006/-0.002$ in.
 $(0.254 + 0.152/-0.051$ mm)

The variations permitted by these tolerances were to be random in location and were necessary because of inconsistencies of metal conversion and removal processes involved in the overall manufacturing task.

(3) Fabrication Plan

The approach taken for liner manufacture embraced several metal-manufacturing technologies in the following general sequence:

(a) Preform machining to configuration for each liner half from 1.00-in.- (2.54-cm-) thick plate aluminum alloy 6061-T651 as shown in Figure 3A. The choice of 6061-T651 aluminum alloy as the starting material was made because this material condition provides a fully stabilized metal structure for the close-tolerance machining to a 0.036/0.030-in.- (0.091/0.076-cm-) thickness selected for forming. The use of a non-stabilized material condition would have required a rough-machining operation followed by another solution treatment and aging to render the material acceptable for final machining of the membrane area. The stabilized material did not distort or exhibit inherent stress due to the solution treatment, because the stretch stabilization given the material during its fabrication following the solution treatment and prior to aging reduced the internal stress to an insignificant consideration. Further, the use of such stabilized material precluded the possibility of internal stress being relieved due to chemical milling to result in "oil canning" or other effects.

(b) Forming by deep-drawing method to internal contour, utilizing heated dies as required to facilitate forming. This step of the process is depicted in Figure 3B.

(c) Selectively annealing of membrane area, ensuring that boss areas did not exceed the temperature which would remove the original T651 temper, as shown in Figure 3C. Hardness testing of

boss areas was performed to detect any possible loss in hardness in boss areas.

(d) Chemical-milling of the entire area of the membrane, except the area adjacent to the circumferential weld joint, to final design thickness, as indicated in Figure 3D.

(e) Preparing the weld joint by machining to the appropriate length, fusion-butt-welding using the tungsten inert-gas welding process, and beneficiating the weld after welding (see Figure 3E).

(f) Performing weld-joint non-destructive testing utilizing dye-penetrant inspection as an in-process inspection and radiographic inspection as a final inspection.

(g) Induction-annealing of the weld area as required (see Figure 3E).

(h) In-process leak-checking of liner as required.

(i) Machining the area of the weld joint to the final wall thickness of the membrane (this process step is shown in Figure 3B); machining bosses and adjacent areas to final configuration.

(j) Final-inspection, including final helium leak checking.

(k) Final-cleaning in weak chromic acid solution, followed by rinsing in deionized water, and drying in 150 to 180° F (340 to 356 K) atmosphere.

b. 1100-0 Aluminum Liner With Bonded Bosses

Considerations described above for the 6061 aluminum liner with integral bosses were generally applicable for the 1100 aluminum liner. The 1100-0 aluminum liner fabrication process also involved the use of chemical milling and weld-joint beneficiation. The liner was of two-piece construction with a single beneficiated circumferential weld joining two similar halves at the midpoint of the cylindrical section. Thickness tolerances were as for the liner with integral bosses. The liner fabrication plan generally followed that of the 6061 aluminum integral boss configuration, except for starting thickness, selective heat treatment processes, and operations specifically related to formation of the integral bosses.

3. Other Points of Discussion

a. Weld Quality

Procedures were planned for attainment of highest-quality welds and their inspection, followed by weld zone beneficiation by cold work and compacting to ensure integrity. The weld zone was not chemically milled to reduce thickness; in order to guard against any possible degradation of properties from the chemical milling reagents.

b. Protection of Welds During Chemical Milling and Removal of Excess Material

It was planned that chemical milling would be conducted before welding. Excess metal above the desired membrane thickness after beneficiation of the weld was to be removed by machining and hand working.

c. Effect of Chemical Milling on Mechanical Properties

Chemical milling in relatively thin membrane structures does serve to reduce mechanical properties. Before prototype liner fabrication, tests were planned to establish the effect of chemical milling on ductility of the 0.010 or 0.254 mm thick 6061 and 1100 aluminum liner materials.

d. Effect of Weld-Joint Beneficiation on Mechanical Properties

A literature search did not reveal any data on the effect of exposure at cryogenic temperatures on the mechanical properties of weld joints of 6061 aluminum alloy in the annealed condition. Consequently, in support of the program, a preliminary group of butt-welded specimens were prepared by fusion-welding two 0.031-in. (0.787-mm) 6061-0 aluminum-alloy sheets without filler wire. The weld joints were beneficiated by means of planishing using the method to be employed in the proposed liner. Prior to testing, the specimens were annealed to remove cold-work effects on the planished weld by holding at 775°F (686°K) for one hour, cooling in a furnace at 50°F/hr (28°K/hr) to 500°F (533°K), and then removing from the furnace and air-cooling to room temperature.

The results of preliminary tests at $+75$ (297°K), -320 (77°K), and -423°F (20°K) on the annealed planished weld joints are presented in Table 1. These test results showed that high-quality weld joints in 6061-0 aluminum alloy that have been planished and annealed after the planishing operation have elongation values over the temperature range of $+75$

to -423°F (297 to 20°K) considerably in excess of the minimum required. In addition, the comparison with parent metal at ambient temperature indicated that weld-joint efficiency of 100% was obtained.

C. DESIGN

The efforts included liner-material characterization analysis, fabrication process/structural design interaction evaluations, and vessel structural analysis and design.

1. Liner-Material Characterization Analysis

Mechanical data were obtained from 6061 and 1100 aluminum specimens to optimize fabrication procedures and design before liner fabrication. The purpose of this investigation was to determine the effect, if any, that fabrication processing, including chemical milling, would have on the structure and ductility of aluminum alloys 6061 and 1100 chemical-milled from sheet or plate to the $0.010\text{-in.-(}0.254\text{-mm-)}$ thickness of the liner membrane. Tests involved tensile tests at ambient and cryogenic temperatures to establish ductility and strength of liner-membrane parent metal and weldments which had undergone the proposed fabrication sequences, as well as microscopic examination to determine any evidence of intergranular attack. Results of the evaluation are presented in Appendix A and summarized below.

a. 6061-0 Aluminum

(1) Effect of Position in Plate On Properties

Fabrication of liner halfshells with integral bosses required use of $1.00\text{-in.-(}2.54\text{-cm-)}$ thick plate as the starting material. Variation in properties through the plate thickness were investigated. It was found that, on the basis of ductility and grain structure, the liner membrane could be taken from the $1\text{-in.-(}2.54\text{-cm-)}$ thick plate up to a depth of $0.125\text{-in. or }0.318\text{-cm}$ from the surface.

(2) Effect of Thickness on Properties of Non-Chemically Milled Material

Ductility of 6061-0 aluminum $0.012\text{-in.-(}0.305\text{-mm-)}$ thick, when measured over a $2\text{-in.-(}5.08\text{-cm-)}$ gage length, was significantly lower than for specimens $0.030\text{-in.-(}0.762\text{-mm-)}$ thick, but appeared to be adequate to meet liner requirements.

(3) Effect of Chemical Milling and Annealing Procedure on Properties

This evaluation showed that the degree of

chemical milling employed affected ductility. Specimens chemically milled from 0.030-in. to 0.010-in.-(0.762-mm to 0.254-mm-) thickness had slightly less ductility than specimens chemically milled from 0.020-in. to 0.010-in.-(0.508-mm to 0.254-mm-) thickness. The chemical milling solution apparently attacked the aluminum in a non-uniform manner, producing significant thickness variation (waviness) due to intergranular attack. However, to ease fabrication difficulties, it was decided to chemically mill the liner to the 0.010-in.-(0.254-mm-) thickness from material machined to 0.030-in.-(0.762-mm-) thickness.

Modification of the standard annealing procedure to one in which a more rapid cooling rate was incorporated was investigated to guide the choice of selective heat treatment procedures required at the liner integral polar bosses. It was found that cooling from the annealing temperature faster than the standard practice resulted in incomplete annealing and reduction in ductility; accordingly, standard practice was employed in liner fabrication.

(4) Parent Metal Properties at Ambient, Liquid Nitrogen, and Liquid Hydrogen Temperatures

Characterization was made of tensile strength, yield strength, and ductility over the temperature range for 0.010-in. or 0.254-mm specimens, resulting in the following typical properties:

<u>Temperature</u>		<u>Tensile Strength</u>		<u>Yield Strength</u>		<u>Elongation</u>
<u>°F</u>	<u>°K</u>	<u>psi</u>	<u>N/cm²</u>	<u>psi</u>	<u>N/cm²</u>	<u>In 2-In.(5.08-cm)</u>
75	297	15 200	10 500	6800	4700	13.8
-320	77	26 900	18 500	8800	6100	21.7
-423	20	45 600	31 400	-	-	24.7

Ductility as measured over shorter 0.50-in. (1.27-cm) and 0.25-in. (0.635-cm) gage lengths were generally about the same as for the 2-in. (5.08-cm) gage length. Values appeared to be adequate when compared to design property objectives for the material.

(5) Welded Specimen Properties at Ambient, Liquid Nitrogen, and Liquid Hydrogen Temperatures

Available data on aluminum alloy 6061 weld

joints are based mainly on the use of other aluminum-alloy filler wires. To determine the degree of increased weld-joint ductility obtainable by both butt fusion welding (without filler wire) and the use of the softer 1100 alloy as a filler wire, weld joints of both types were made and evaluated which incorporated the proposed liner-fabrication sequence, including chemical milling. These tests were made at 75° F (297° K), -320° F (77° K), and -423° F (20° K) and included tests of 0.010-in.- (0.254-mm-) thick as-welded joints and joints which had been beneficiated by planishing after welding. The beneficiated welds were annealed prior to testing. Control specimens of 0.010-in.- (0.254-mm-) thick parent metal which had undergone the simulated fabrication process were tested simultaneously for comparison.

TIG butt fusion welded and annealed joints (without filler wire) were so brittle, as determined from bend tests, that tensile testing was not performed.

Annealed welds prepared by TIG butt fusion welding with 1100 aluminum filler wire had low elongation values in a 2-in.- (5.08-cm-) gage length. However, the ductility of the specimens was high in the weld joint (approximately 1/4-in gage length) due to the use of soft type 1100 filler wire there, and the readings in 2-in gage length were not representative of ductility of the specimens.

Annealed welds prepared by TIG butt fusion welding with 1100 aluminum filler wire, followed by beneficiation, showed elongation values in 0.25-in.- (0.635-cm-) gage length two to four times the ductility measured over a 2-in.- (5.08-cm-) gage length. The weld joint was quite soft compared with the parent metal, and failure occurred in it. Typical properties were the following:

<u>Temperature</u>		<u>Tensile Strength</u>		<u>Yield Strength</u>		<u>Elongation in 0.25-In.(0.635-cm)</u>
<u>°F</u>	<u>°K</u>	<u>psi</u>	<u>N/cm²</u>	<u>psi</u>	<u>N/cm²</u>	<u>%</u>
75	297	14 200	9800	6800	4700	13.8
-320	77	23 400	16 100	10 000	6900	11.3
-423	20	32 000	22 100	-	-	14.3

Elongation values over the temperature range were marginal compared to the design property objectives. Welded specimen yield strength was comparable to parent metal yield strength. Tensile strengths were lower for welded specimens at all temperatures. Ambient temperature ductility was about the same for both types of specimens, and at cryogenic temperatures, the welded specimen ductility generally tended to remain constant while the parent metal ductility increased.

In view of the findings that weld beneficiation and 1100 aluminum filler wire apparently improved ductility, the use of them was selected for liner manufacture.

b. 1100-0 Aluminum

(1) Effect of Thickness on Properties of Non-Chemically Milled Material

Ductility of 0.010-in.- (0.254-mm-) thick material was lower than for material 0.035-in.- (0.889-mm-) thick, but exceeded the design property objectives for the material.

(2) Effect of Chemical Milling on Properties

Chemical milling from 0.030-in. (0.762-mm) to 0.010-in. (0.254-cm) thickness did not appear to have a detrimental effect on properties. Microscopic examination of specimens revealed a uniform material removal during chemical milling.

(3) Parent Metal Properties at Ambient, Liquid Nitrogen, and Liquid Hydrogen Temperatures

The following typical properties were measured for 0.010-in.- (0.254-mm-) thick specimens:

Temperature °F	°K	Tensile Strength		Yield Strength		Elongation in 2-In. (5.08-cm) %
		psi	N/cm ²	psi	N/cm ²	
75	297	12 300	8500	5400	3700	15.8
-320	77	24 300	16 800	6600	4600	27.5
-423	20	37 900	26 100	-	-	35.2

Elongations over the shorter gage lengths, 0.50-in. (1.27-cm) and 0.25-in. (0.635-cm), were about the same as for the 2.0-in.- (5.08-cm-) gage length, and were adequate to meet liner design requirements.

(4) Welded Specimen Properties at Ambient, Liquid Nitrogen, and Liquid Hydrogen Temperatures

Annealed TIG butt fusion welds with 1100

aluminum filler wire, with and without beneficiation, were evaluated. For annealed as-welded specimens, about one-half the specimens failed in the parent metal; for beneficiated and annealed weld specimens, about three-quarters of the specimens failed in the parent metal, indicating the good weld strength obtained. Typical properties for beneficiated and annealed welded specimens were as follows:

<u>Temperature</u>		<u>Tensile Strength</u>		<u>Yield Strength</u>		<u>Elongation in 2-In. (5.08-cm)*</u>
<u>°F</u>	<u>°K</u>	<u>psi</u>	<u>N/cm²</u>	<u>psi</u>	<u>N/cm²</u>	<u>%</u>
75	297	11 200	7700	4100	2800	17.9
-320	77	24 100	16 600	7100	4900	30.0
-423	20	39 300	27 100	-	-	32.5

Beneficiation of the joint welded with 1100 aluminum filler wire was selected for liner fabrication.

2. Vessel Structural and Design Analysis

Two designs for 0.010-in.-(0.254-mm-) thick aluminum-lined glass-filament-wound closed-end-vessels of 12-in.-(30.5-cm-) dia. by 18-in.--(45.7-cm-) length and having 3000 psig (2070 N/cm²) burst strength at ambient temperature were prepared in accordance with the criteria given in Section II-A. Vessel polar boss diameters were fixed at 10% of the vessel diameter, or 1.2-in. (3.05-cm). One vessel had a 6061 aluminum liner and the other utilized 1100 aluminum. Design-allowable glass-filament strength, vessel membrane analysis (including computer input and output), vessel head-to-cylinder juncture discontinuity analysis, winding pattern analysis, and design analysis of the polar bosses are given in Appendix B. Results are summarized below.

a. Ambient Temperature Design Allowable Glass Filament-Strength

The single-pressure-cycle allowable S-glass filament strengths were 316 000 psi (218 000 N/cm²) for the longitudinal filaments and 354 000 psi (244 000 N/cm²) for the hoop filaments. These values increased to 395 000 psi (272 000 N/cm²) for the longitudinal windings and 443 000 psi (305 000 N/cm²) for the hoop windings at cryogenic temperatures.

* parent metal failures

b. Membrane Analysis Results

Design thicknesses determined for longitudinal and hoop glass filament windings applied over the 0.010-in.- (0.254-mm-) thick aluminum liners to achieve the 3000 psig (2070 N/cm^2) burst strength at ambient temperatures were the following:

Longitudinal filament-wound composite thickness in cylinder and at equator of heads	0.042-in.(0.107-cm)
Equivalent filament thickness in longitudinal and at equator of heads	0.028-in.(0.071-cm)
Hoop filament-wound composite thickness in cylinder	0.075-in.(0.191-cm)
Equivalent filament thickness in hoop direction of cylinder	0.051-in.(0.130-cm)

Cylindrical section length was 10.74 in. (27.28 cm) for the 12-in.- (30.5-cm-) dia. by 18-in.- (45.7-cm-) long closed-end vessel. Vessel design burst pressure increased from 3000 psi (2070 N/cm^2) at ambient temperature to 3750 psig (2590 N/cm^2) at cryogenic temperatures.

c. Head-To-Cylinder Discontinuity Analysis Results

This analysis of the vessel (as designed by the computer) showed the maximum longitudinal filament stress at ambient temperature and 3000 psig (2070 N/cm^2) to be 318 500 psi or $219\ 600 \text{ N/cm}^2$ (0.8% greater than the allowable design stress), in the vessel cylinder section 0.1 in. (0.254 cm) from the tangent plane.

d. Filament-Winding Pattern

The filament-wound vessels had two winding patterns: a longitudinal-in-plane pattern along the cylinder and over the end domes to provide the total filament-wound composite strength in the heads and the longitudinal strength in the cylindrical section; and a circumferential pattern applied along the cylinder for hoop strength in this section. Owens-Corning S/HTS glass 20-end continuous filament roving was selected for vessel winding. The calculated vessel filament-winding pattern consisted of six layers of longitudinal winding (each layer uniformly distributed by winding a 0.268-in.- (0.681-cm-) wide tape, formed from three 20-end rovings, at 140 turns per revolution of the liner), and ten layers of hoop winding (each

layer uniformly distributed by winding a single 20-end roving at 12 turns per inch (4.72 turns/cm) of cylinder section).

e. Complete Vessel Designs

The 6061 aluminum liner design is shown in Figure 4, the 1100 aluminum liner design in Figure 5, the boss for the 1100 aluminum liner in Figure 6, and the aluminum-lined glass-filament-wound pressure vessel in Figure 7.

3. Evaluation of Adhesive Bond Between Aluminum Liner and Glass Filament-Wound Composite

Under the Reference 20 program, an aluminum-to-composite adhesive bonding system for cryogenic service consisting of Adiprene L-100/Epi-Rez 5101/MOCA (80/20/17 pbw) with nylon scrim cloth was evaluated using a curing schedule of 16 hours at room temperature, 1 hour at 150°F (340°K), and 8 hours at 250°F (394°K). On the Reference 24 program, a glass filament-wound composite resin matrix for cryogenic service consisting of Epon 828/Empol 1040/DSA/BDMA (100/20/115.9/1.0 pbw) and designated as cryogenic Resin No. 2 was developed using a curing schedule of 2 hours at 150°F (340°K), followed by 4 hours at 300°F (422 K). Both polymeric material systems were planned for use in vessel fabrication. In order to identify (1) the compatibility of the two systems, and (2) the single vessel curing schedule that had to be used for both the adhesive and resin, the evaluation described below was conducted.

a. Experimental Procedure

T-peel adhesion tests were made at ambient and liquid nitrogen temperatures on specimens consisting of 0.010-in.-(0.254-mm-) thick 6061 aluminum as the adherent, the adhesive described above with a single layer of nylon scrim cloth imbedded in the adhesive along the bonding surface, and 181 glass cloth impregnated with Resin No. 2 as the supporting member. Both J P Stevens nylon scrim cloth styles S-1852-2-400 and 34168-2 were evaluated; the Type 34168-2 had been previously used before under the Reference 20 program, and the Type S-1852-2-400 had a slightly more open weave. The fabrication procedure used for specimen preparation simulated that of the metal-lined filament-wound tankage fabricated and tested later in the program. Strips of 2024 aluminum 1-in. by 4-in. by 1/8 in. (2.5-cm by 10.2-cm by 0.32-cm) were used on the backside of the 181 glass cloth impregnated laminate to provide rigidity for the adhesion testing. The detailed fabrication procedure is given in Appendix C.

b. Results

The T-peel adhesion was determined using Federal Test Methods Specification No. 601, Method 8031. Testing of specimens fabricated with the

Type S-1852-2-400 nylon scrim cloth was accomplished first. Six specimens each were given the following elevated temperature cures:

<u>Time, Hours</u>	<u>Temperature</u>	
	$^{\circ}$ <u>F</u>	$^{\circ}$ <u>K</u>
4	300	422
6	300	422
8	250	394
16	250	394
24	250	394

Three specimens each were tested for each condition of cure and test temperature (ambient or liquid nitrogen temperature). The T-peel adhesion results are shown graphically in Figure 8 and listed in Table 2. The average, high, and low values of each group of three specimens are indicated. The results indicate that the 4 hours at 300°F (422°K) cure produced the highest values at both room and cryogenic temperatures. However, reasonably good results were obtained on the specimens cured 24 hours at 250°F (394°K) which may indicate reasonably equivalent cures for the specified resin system. The lower values and wide spread in adhesion results of the shorter cures at 250°F (394°K), particularly at ambient temperature, indicate that the resin system is not completely cured even though the adhesive system may have reached optimum cure.

Next, specimens were fabricated from the Type 34168-2 nylon scrim cloth (scoured and heat set) and cured at 300°F (422°K) for 4 hours and 250°F (394°K) for 8 hours; test specimens cured 12 hours at 300°F (422°K) were also included to determine the effect of an overcure on bond strength. Peel tests were conducted at ambient, LN₂, and LH₂ temperatures, with the results given in Table 2.

The test results show a slightly lower value for the 4 hours at 300°F (422°K) cure in room temperature tests (17.0 lbf/in or 29.8 N/cm) than was obtained when S-1852-2-400 nylon scrim cloth was used (23.5 lbf/in or 41.1 N/cm). The value of 20 lbf/in or 29.1 N/cm for the 8 hours at 250°F (394°K) cure was somewhat higher than the average value of 16.6 lbf/in or 29.1 N/cm obtained previously with the other nylon scrim cloth. The cryogenic test results at -320°F (77°K) for the 4 hours at 300°F (422°K) cure (17.0 lbf/in or 29.8 N/cm) was higher than obtained with the laminate containing S-1852-2-400 nylon scrim cloth (12.5 lbf/in or 21.9 N/cm).

The adhesion of 20 lbf/in (35.0 N/cm) obtained on

the 12 hours at 300°F (422°K) cure indicates that no loss of bond strength for this adhesive system is produced by a long cure at the 300°F (422°K) temperature. This indicates that a satisfactory margin of safety exists in the use of a 300°F (422°K) curing temperature. Based on these results, the Type 34168-2 nylon scrim cloth and a cure of 4 hours at 300°F or 422°K (the standard Resin No. 2 cure) was selected for vessel fabrication.

Approximately equivalent adhesion values were obtained on test specimens assembled either before or after a 16 hour room temperature gel cure of the adhesive, indicating that gel curing does not reduce the bonding properties of the adhesive. This result was considered important considering that in fabrication of the filament-wound tanks, several hours elapse between application of the adhesive and the winding of the vessel.

D. FABRICATION

1. Metal Liners

As previously described, 12-in.-(30.5-cm-) dia. by 18-in.-
-(45.7-cm-) long aluminum liner fabrication involved two tasks:

- Develop and produce 0.010-in.-
(0.254-mm-) thick
1100-0 aluminum liners with bonded 6061-T6 aluminum
bosses, using a single girth weld to join mating
1100 aluminum half liners.
- Develop and produce 0.010-in.-
(0.254-mm-) thick
6061 aluminum liners with integral 6061-T6 bosses
and 6061-0 membrane, using a single girth weld to
join mating halves.

Detailed procedures were prepared to guide fabrication of the 6061 and 1100 aluminum liners; they are presented in Appendices D and E. The manufacture of both types of liners follows the general sequence indicated in Table 3, with in-process inspections described in Appendices D and E. Tasks common to both liners were:

- Precision deep drawing to provide liner halfshells
to exact internal configuration to eliminate machining
on internal surfaces (successfully accomplished
for both liner types).
- Precision sizing to provide liners capable of being
machined to 0.030-in.-
(0.762-mm-) thickness in
membrane without buckling, "oil-canning," wrinkling,
and other conditions associated with the thin wall

(successfully accomplished for both liner types).

- Precision machining of membrane to wall thickness of 0.030-in. or 0.762-mm (successfully accomplished for both liner types).
- Precision chemical milling to provide membrane wall thickness of 0.012-in. (0.305-mm) prior to closure welding (successfully accomplished for both liner types).
- Precision TIG welding to provide welds of high integrity in both liner types using 1100 aluminum filler wire (problems were encountered in accomplishment of this task).

All liners were required to pass a helium-leak check with a mass spectrometer at a pressure differential of 5-7 psia ($3.4\text{-}4.8 \text{ N/cm}^2$).

a. 1100 Aluminum Liners

Figure 9 shows a drawn and machined liner half-shell before girth weld joint preparation. A 6061-T6 boss, for bonding in the halfshell, is shown in Figure 10. A halfshell with boss bonded in place is depicted in Figure 11.

Adhesive bonding of 6061 aluminum bosses to the 1100 aluminum halfshells before welding at the girth was done with the adhesive used for bonding the metal liner to the filament-wound composite. A bonding technique was developed, as described in Appendix D, which involved cleaning of the adhering surfaces, priming, coating of both surfaces with adhesive, and curing under vacuum bag pressure.

Girth closure welding was undertaken on the 1100 aluminum liner before the 6061 aluminum liner. The primary problem encountered was obtaining liners without cracks in the girth weld joint. Cracking has occurred both during and after halfshell closure welding. Eight 1100 aluminum liners had to be closure welded to get two units with leak-tight girth welds; one of the two required no repair welds while the other needed extensive repair welds in order to pass helium leak test. Delayed cracking of girth weld joints was noted in some of the liners. The cause of the cracking is not known, but is probably related to the following factors associated with procedures and tooling:

- TIG welding of the relatively thin and narrow weld joint detail, with adjacent 0.012-in.-(0.305-mm)- thick liner membrane material.
- Excessive chill of the weld by the backup ring.

- Differential thermal expansion of assembly components.
- Restraint of liner axial movement during welding.

The evolution of weld joint details is shown in Figure 12. Initially, the joint was as shown in Figure 12A, with relieved copper backup ring (later removed by etching with nitric acid), to minimize weld drop through, minimize shell distortion, and permit planishing. No pre-heat of the weld joint was attempted initially.

Since as small as possible of a weld was wanted, the welding of both units was accomplished with the minimum heat input and minimum 1100 aluminum weld filler wire needed to achieve fusion. However, because of the mass of aluminum adjacent to the joint line and its heat dissipation characteristics, heat input to achieve fusion was high, leading to a thicker and wider weld than desired. Weld cracking resulted from use of the joint configuration.

The weld joint configuration shown in Figure 12B was next tried, and also resulted in weld cracking. Following this, the joint shown in Figure 12C was used, after review and evaluation of previous efforts and additional trial welding of full diameter rings simulating the liner joint conducted. This joint had two edges with sufficient material to ensure butt-up and joint alignment, and a proper geometry for welding - material was provided only as required to permit development of enough heat for welding in a small localized area. Welding of a liner was accomplished without evidence of cracking, the weld area was annealed, and then dressed off for planishing. Upon weld planishing, some small cracks developed. Repairs were made and the repairs dressed, until no cracks were evident from dye penetrant inspection. The liner was reannealed and then planished. As final weld dressing was accomplished by hand with emery paper before the final planishing operation, cracks at the parent metal-to-weld liner were observed.

Possible causes for the cracking were reviewed, including: flexing of the weld fixture during welding and in subsequent handling, excessive chill of the weld by the backup ring, differential thermal expansion of assembly components (liner halfshells, backup ring, external rings), and restraint of liner halfshell axial movement during welding. Corrective action was taken in each of these areas for the welding of another liner including: steel support rod addition to weld fixture for increased rigidity, transportation of the liner assembly in a vertical rather than horizontal position, preheat of the weld fixture and liner halfshell assembly in an oven to 350°F (450°K) before welding, and loosening of the external stainless steel restraining clamps. Additionally, it was decided to minimize dressing of the weld because of possible inadvertent parent metal thinning.

With these changes made, two liners were successfully welded, the weld dressed, planished, and annealed without weld cracking or the necessity for any repairs. These liners were leak tested and used for vessel fabrication.

Another important factor related to the membrane and filler wire material. The general procedure in TIG welding aluminum and its alloys is to weld with a filler metal of higher alloy than the parent metal so that the weld when molten or on cooling will have strength as equivalent as possible to the material being joined and the thermal stresses are then balanced or compensated. In the case of the 1100 aluminum liner, the metal being joined is welded with the same filler metal which when molten or hot is weaker than the cooler parent metal. Consequently, stresses can produce cracking as the metal structure is heated and cooled in the welding process.

The use of 1100 material for both weld parent metal and filler material induces high stresses in the weld. This is because of 1100 aluminum's higher melting point to flow as weld metal, its higher thermal conductivity, and its higher thermal expansion coefficient as compared with other weld fillers. To minimize stresses, the weld backup ring should permit circumferential shrinkage of the weld on cooling as well as axial shrinkage. However, the need to have mating edges fit closely for TIG welding led to the use of an interference fit between halfshells and the back-up ring for welding all of the 1100 aluminum liners. This in turn prevented axial contraction of liner halfshells and it is believed on cooling weld tensile stresses were set up leading to cracking parallel to the weld seam. Additionally the interference fit between the halfshells and backup ring, which required that the weaker member be under slight stress to hug the other member, only made for greater stresses when the weld bead was developed in the molten state and then contracted when cooled. The stresses which were induced tended to be taken out at the thinner heat affected zone of the liner weld.

In retrospect, the backup ring should have probably been looser fitting to permit liner shrinkage during welding; we estimate that the backup ring should be 0.010 - 0.014-in. (0.254 - 0.356-mm) smaller in diameter than the halfshells. With this looser fit between the tooling and halfshells, full diameter tacking should be employed to insure proper alignment and fitup of mating halves. In addition, we think the backup ring should have had more relief to permit slightly more weld bead to naturally form on the weld backside; where only a very small relief was provided (about 0.010-in or 0.254-mm), there was a tendency for excess drop-through to form which in turn distorted the weld joint and membrane by pushing against the backup ring and displacing the weld joint area outwardly. The backup ring relief configuration recommended is shown in Figure 12D.

We think that the use of a thicker wall thickness during the TIG welding would only have magnified the problems encountered in girth welding because the heat input to fuse the thicker material would then

be much greater to bring the metal affected to the welding temperature. With increased heat there would be more expansion of the curved mating parts, and greater thermal stress effect which could result in more severe buckling, shrinkage, and possible cracking.

A secondary problem associated with the 1100 aluminum liner, noted only on the two liners that were produced with leak tight weld joints (and which passed helium leak testing), was leakage of the bonded 6061 aluminum boss during vessel fabrication. One pressure vessel liner structure was completely filament overwrapped and put in an oven for cure; a leak at the bonded boss developed during cure at 300°F (422°K), causing loss of the pressure mandrel. A second vessel was completely wrapped; at the completion of winding, a leak developed at the bonded boss, resulting in loss of this unit. Leakage during cure of the first vessel was attributed to weakening of the boss bonding adhesive at 300°F (422°K). Cause of leakage of the second vessel is unknown; however, the possibility of boss bond weakening from excessive heat during welding of fittings to the boss extensions exists.

Based on the difficulties encountered, it was decided not to proceed further with work on the 1100 aluminum liner, and to concentrate efforts on the 6061 aluminum liner.

b. 6061 Aluminum Liners

Type 6061 aluminum halfshells, of 0.010-in. or 0.254-mm membrane thickness and with 6061-O condition in the membrane and 6061-T6 condition in the integral boss, are shown in Figures 13 and 14. These shells are in the final configuration used for closure welding.

(1) Characterization of Halfshells

Hardness and tensile tests were conducted on specimens cut from 6061 aluminum liner halfshell dome and cylindrical sections to provide characterization of the units. The hardness tests showed that "T6" properties existed in the boss and that "O" properties existed in the membrane, as required by the liner design and as expected from the fabrication process.

Data from the characterization are presented in Tables 4 and 5, and shown graphically in Figure 15 for the first halfshell evaluated.* These data show the transition from "T6" to "O" condition at the boss-to-liner membrane juncture;** however, the distance over which the transition occurred was greater than desired.

* The thin membrane in the cylinder section is due to excessive chemical milling of the unit.

** For reference, the following Rockwell hardness (15T scale) is associated with various tempers: 48 for 6061-O; 65 for 6061-T4; and 78 for 6061-T6.

Another selective annealing procedure was used on a halfshell to reduce the transition distance for "T6" to "O". Specimens were cut from the halfshell, as shown in Figure 16, and tested. Data are presented in Table 6, and are shown graphically in Figure 17. The revised annealing procedure improved the membrane properties, and produced the most rapid transition of properties of any other procedure evaluated. The revised procedure was therefore employed in annealing halfshells for use in the liner assemblies.

(2) Additional Characterization of
6061 Aluminum Weld Joints

A limited evaluation of simulated 6061-0 liner weldments made by (1) butt fusion welding, (2) welding with 4043 filler wire, and (3) welding with 5356 filler wire was conducted for comparison with the extensive data (Appendix A) already developed for 6061-0 aluminum welded with 1100 filler wire. The 1100 filler wire had been selected earlier for liner welding to impart maximum ductility to the weld joint. Its use, however, was found during fabrication of the type 1100 aluminum liners to complicate welding because of its higher melting point and low strength. Melting points for the alloys are given below:

<u>Designation</u>	<u>Melting Range</u>		<u>Mean</u>	
	<u>°F</u>	<u>°K</u>	<u>°F</u>	<u>°K</u>
1100	1190 - 1215	917 - 931	1203	924
6061	1080 - 1200	856 - 922	1140	889
4043	1065 - 1170	847 - 906	1118	877
5356	1055 - 1180	842 - 911	1118	877

Specimens of each type were welded, and tested at room temperature. Results are presented in Table 7 and shown graphically in Figure 18. All specimens failed in the heat affected zone or the weld. In welded specimens, tensile and yield strength was about the same for all methods evaluated. Elongation of 2-in. (5.08-cm), 1-in. (2.54-cm), 1/2-in. (1.27-cm), and 1/4-in. (0.635-cm) gage length, respectively, was about the same for 6061 butt fusion welded or welded with 1100, 4043, or 5356 weld rods. Maximum ductility was obtained with 6061 welded with 1100 filler with subsequent planishing; however, the increase in ductility was not great compared with the other methods investigated.

Welding evaluations of 12-in.-(30.5-cm-) dia. rings showed that 4043 weld wire improved girth weld quality and ease of welding over the 100 filler wire. Based on these data and the difficulties previously encountered in welding the 1100 aluminum liners, it was decided to evaluate both 4043 and 1100 weld wire in closure welding 6061 aluminum liner halfshells.

(3) Liner Fabrication

Welding of this liner presented some of the same problems as the 1100 aluminum liner. In the 6061 liner, the 1100 aluminum filler wire used for welding of some liners was weaker than the parent metal. A "burn-down" flange of 6061 as well as 1100 filler metal (join configurations as depicted in Figure 12C and D) were used. The first 6061 liner was successfully welded, using the Figure 12C weld joint configuration, but was made unacceptable when chemical reagents used for copper weld joint backup ring removal produced a few holes through the liner membrane. Another problem noted was that the backup ring groove geometry was not optimum, and it was modified.

After incorporation of processing changes that were indicated (including the Figure 12D weld joint configuration) another liner (A-4) was welded with 1100 filler wire. Dye penetrant inspection showed the weld to be crack-free. Stress relief of the weld was completed, and the weld was dressed off to minimize weld bead height. After this operation, two cracks were noted at and along the heat affected zone. These were successfully repaired; however, the repairing produced a thicker weld joint than desired. The copper backup ring was removed without attack of the liner membrane by control of reagent concentration and reaction temperature. This unit was subjected to and passed helium mass spectrometer leak testing before filament overwinding.

Another liner (A-3) was welded with 1100 filler wire and processed up to helium leak testing. During the leak testing, small leaks (10^{-6} to 10^{-5} scc/sec of helium) were detected at three specific sites in the girth weld and at one site in the membrane. These leaks were repair welded, the unit leak tested, and accepted for filament overwinding.

The next 6061 liner (A-6) was welded using 4043 weld wire. Welding was accomplished without any need of repair. This was the best appearing liner procured up to this time, and of much higher quality than liners welded with 1100 filler wire. After completion of processing, the liner was given helium leak testing. A single small leak was detected in the liner membrane which was repaired. The liner was re-leaked tested, accepted, and filament overwound.

Another 6061 liner (A-5) closure welded

with 4043 weld wire appeared to be of as good integrity as liner A-6, passed helium leak tested successfully, and was overwound.

2. Aluminum-Lined Glass Filament-Wound Vessels

Two wooden mandrels simulating the 1100 and 6061 liner assemblies were fabricated and used to develop procedures for application of nylon scrim cloth to the liner as part of the adhesive system between the liner and overwrapped glass filament composite. It was determined that a single piece of Type 34168-2 nylon scrim cloth could be made to conform to each liner head contour without wrinkling or without the necessity for cutting or tailoring it in the head section. The scrim cloth was thus applied to the liner in only three sections - two heads and a cylinder - thereby minimizing the number of joints; the scrim cloth layer on the liner had two girth joints on the cylindrical section and a single longitudinal joint on the cylinder. Careful application of the scrim cloth resulted in joints free of gaps or wrinkles, with very few overlapped areas.

The wooden mandrels were used for programming of the filament winding machine, and final checkout of tooling and the glass roving in-process resin impregnation system. Several trial windings were made on the wooden mandrels; to gain experience in application of the design winding pattern and to improve the planned sequence of operations to be followed in vessel fabrication.

The filament-wound composite of two simulated vessels were completely wound and cured on wooden mandrels. The winding was accomplished smoothly without incident in both cases. The first vessel was vacuum bag cured, using two layers of Dacron bleeder cloth. Inspection of this vessel after cure revealed a sound appearing structure, with the exception of some excessive stackup of winding at the bosses, and roving bridging and resin starvation in one local area at each boss against the liner. Resin content in the composite was a low 13 to 14 weight percent everywhere except near the boss where it was about 20 percent. In winding the second unit, resin filled with CAB-O-SIL to increase viscosity was locally applied by brush at the bosses to increase resin content there and to eliminate the resin starved area noted in the first simulated vessels composite.

Aluminum-lined glass-filament-wound vessels were fabricated in accordance with the fabrication procedure given in Appendix F. Figures 19 to 21 show the winding patterns used in vessel fabrication, and Figure 22 shows a completed vessel.

Type 6061 aluminum liner A-4 was filament-overwound and cured successfully, and subjected to testing.

Two attempts were made at overwinding 6061 aluminum

liner A-3. On the first attempt, after it was completely overwrapped, a leak developed at a repair weld area near the boss and the pressure stabilized mandrel was lost. The area that leaked was repair welded again, the liner re-leak tested, and winding attempted, with leakage occurring at the start of winding in the same area. Both leakage failures were attributed to creation of a "hardpoint" at the repaired area, which probably caused fatigue of the liner repair from flexing as it rotated in a horizontal position during application of longitudinal and hoop windings.

Liner A-6 was filament-overwrapped and cured with no problem.

Liner A-5 was completely overwrapped without incident. However, as it was being prepared for cure, oil from the pressure mandrel was detected in the wound composite. The windings were carefully removed as the pressure level inside the mandrel was reduced, and the leakage site was found to be in the liner membrane at the transition between the chemically milled area and the area machined for the girth weld flange. Because this area was leaktight under the helium-mass-spectrometer-leak-test, it is believed that the leak must have resulted from (1) local overstress of the liner (possible thin spot) by the pressure mandrel, and/or (2) fatigue of the area during liner rotation and flexing as windings were applied to the liner.

E. VESSEL TESTING

Tank A-4 was subjected to a room temperature burst test using water as the pressurizing medium. A preliminary 200 psig (138 N/cm^2) leak test was conducted without any evidence of leakage prior to the destructive test. The vessel was then pressurized at 1200 psi/min or $827 \text{ N/cm}^2/\text{min}$ ($\approx 1\% \text{ strain/min}$) until failure. Vessel failure, consisting of a liner leak, occurred at 1400 psig (965 N/cm^2), compared with the design structural burst pressure of 3000 psig (2070 N/cm^2).

Tank A-6 was tested in the same manner as A-4, with vessel failure occurring at 2200 psig (1520 N/cm^2) and consisting of liner leaks in the polar boss section.

Post test examination of both vessels showed that liner failure was located in the polar boss-to-liner membrane transition area. This condition was believed to be associated with the liner strain magnification occurring in this area due to boss rigidity and glass filament-wound composite extensibility, as well as the transition in the aluminum liner properties from 6061-T6 to 6061-0.

F. EVALUATION OF RESULTS

1. Summary of Problems with 1100 Aluminum Liner Fabrication

Considerable effort was expended in attempting to obtain acceptable liners. Although steady improvements were made through fabrication process changes, review of the efforts made and results obtained indicated that the fabrication procedure would not produce the quality of 1100 aluminum liners needed without a high rejection rate.

The primary problem was obtaining liners without cracks in the girth weld joint; cracking occurred both during and after halfshell closure welding. Eight 1100 aluminum liners had to be closure welded to get two units with leak-tight girth welds; one of the two had no repair welds while the other required extensive repair welds in order to pass helium-leak testing. Delayed cracking of the girth weld joint was noted in some of the liners. The cause of the cracking was not definitely determined, but is believed to have been associated with (1) TIG welding of the relatively thin gage material, (2) excessive chill of the weld by the backup ring, (3) differential thermal expansion of assembly components, (4) restraint of liner axial movement during welding and/or (5) possible contamination of the aluminum membrane material during polishing the liner inside surface.

A secondary problem, uncovered with the two liners that were produced with leak-tight weld joints, was leakage of the bonded boss during vessel fabrication. One vessel was completely wrapped over the liner and put in the oven for cure; a leak at the bonded boss developed during cure at 300°F (422°K), causing loss of the pressure mandrel, and of the wound vessel. A second vessel was completely wrapped; at the completion of winding, a leak developed at the bonded boss, resulting in loss of this unit.

2. Summary of Problems With 6061 Aluminum Liner Fabrication

Welding of this liner presented some of the same characteristics as the 1100 aluminum liner, as well as some new problems.

Some liners which were successfully welded were made unacceptable when chemical reagents used for copper backup ring removal produced small holes through the liner membrane. This problem was solved by investigation, and then control, of reagent concentration and reaction temperature.

Type 1100 aluminum filler wire was used in initial 6061 aluminum liner girth welded joints, to maximize weld joint ductility. However, girth weld joint cracking, requiring extensive repairing, was encoun-

tered with 6061 aluminum liners welded with 1100 filler wire. The cause of the cracking is believed to be associated with the higher melting point of 1100 aluminum, its lower strength, and the five factors enumerated in the preceding section for 1100 aluminum liners.

In the liner halfshell, 6061-0 properties were provided in the membrane and 6061-T6 in the integral bosses. The transition from "T6" to "0" was at the boss-to-liner membrane juncture; however, the distance over which the transition occurred was greater than desired.

One of the liners welded with 1100 filler wire was filament overwrapped, cured, and tested. Failure, consisting of liner leaks at about one-half of design burst pressure, occurred around each of the polar bosses. Failures were liner fractures around the boss at the boss-to-membrane transition where properties changed from "T6" to "0".

After a mechanical property evaluation showed that 4043 aluminum weld wire produced a weld of only slightly lower ductility than 1100 weld wire, and offered the possibility of improved quality and ease of welding compared with the 1100 filler wire, it was used for liner welding. Liners welded with the 4043 weld wire were of improved quality with the weld generally free of cracks and leak-tight; weld bead size was more uniform and smaller than with 1100 filler wire because the need for repair welding was essentially eliminated.

One of the liners welded with 4043 filler wire was filament overwrapped, cured, and tested. Failure, consisting of leaks at about three-quarters of design burst pressure, occurred around each of the polar bosses. Examination of the vessel after test showed that fractures occurred at the boss-to-membrane transition (as for the 6061 liner welded with 1100 filler wire); no failure at the girth weld was evident.

3. Conclusions and Recommendations

a. Liner Material

Parent metal test data at ambient to LH₂ temperature showed that 1100 aluminum has 50 to 100% greater uniaxial ductility capability than 6061-0 aluminum; Type 1100 aluminum weldments have higher ductilities than 6061-0 aluminum weldments (welded with 1100 aluminum filler wire). The increased ductility for 1100 aluminum indicated that this material has the properties necessary for metal liners of glass filament-wound vessels to operate at ambient to LH₂ temperatures. The need for maximum biaxial ductility in the metal sealant liners and the excellent properties demonstrated by 1100 aluminum in comparison with 6061-0 aluminum, lead to selection of 1100 aluminum for the remainder of liner work under the program.

b. Revisions to 1100 Aluminum Liner
Fabrication Processes and Boss Design

The use of the electron-beam (EB) welding method would provide considerably less heat input during welding, would be completely automatic, and would be conducted in a vacuum, all of which were anticipated to eliminate or greatly reduce the problems encountered in TIG welding. Feasibility was demonstrated by successfully preparing flat butt welded specimens of 1100 aluminum ranging from 0.010 to 0.063-in.-(0.254-mm to 1.600-mm-) thickness, as were specimens of 0.010-in.-(0.254-mm-) thickness with 0.050 x 0.050-in. (1.27 x 1.27-mm) and 0.035 x 0.040-in. (0.889 x 1.016-mm) flanges at the weld joint. Based on these successful results, 12-in.-(30.5-cm-) dia. circular rings of 0.010-in.-(0.254-mm-) thickness with 0.032 x 0.032-in. (0.813 x 0.813-mm) flanges were prepared; EB welding of this configuration was completely successful, with no weld cracking, and a relatively small resultant weld bead on inner and outer joint surfaces. From this work EB welding was recommended for the additional efforts in liner fabrication.

Elimination of the adhesive bonded joint at the boss-to-membrane transition was also recommended; instead, a mechanical joint, welded to insure impermeability, should be employed. Welds should be provided in a noncritical region of the boss-to-membrane transition (if possible) to eliminate possible leak paths. Because of the critical nature of the boss-to-liner transition in metal-lined glass-filament-wound vessels, the mismatch of deflections, and the strain magnifications known to exist in this region due to the rigidity of the boss designs employed thus far and the extensibility of the filament-wound composite on top of the boss, detailed structural analysis of this region of the pressure vessel should be conducted.

c. Plan for Design, Fabrication, and
Testing of Improved Vessel Configurations

It was concluded and recommended that the program effort should be concentrated to accomplish the following:

- Development of a structural analysis of the boss region of glass-filament-wound pressure vessel domes, and redesign of liner bosses of the aluminum-lined glass-filament-wound tanks being evaluated in the program.
- Development of electron-beam welding procedures for 12-in.-(30.5-cm-) dia. by 18-in.-(45.7-cm-) long 1100 aluminum liners of 0.010-in.-(0.254-mm-) thickness.

- Evaluation of two designs (different bosses) for the 1100 aluminum-lined glass-filament-wound vessels by fabrication of three vessels of each type, and ambient temperature testing of them in burst and fatigue tests.
- Fabrication and testing of additional vessels of the best design in cyclic fatigue and burst tests at ambient, LN₂, and LH₂ temperatures.

III. DESIGN, FABRICATION, AND TESTING OF IMPROVED VESSEL CONFIGURATIONS

A. DESIGN

Structural analysis of the boss sections of metal-lined glass-filament-wound pressure vessel domes was conducted to establish redesigns of the liner bosses and the boss-to-liner transition. The purpose of this work was to minimize strain magnifications known to exist in this vessel region due to the previously used rigid boss designs and the extensibility of the glass-filament-wound composite on top of the bosses. Design criteria for the vessel, and filament-wound composite details were as described in Section II, except that 1100 aluminum was the single liner membrane material considered.

The work involved dome characterization in the vicinity of the polar bosses; development and evaluation of improved boss design concepts; and review and selection of two configurations for detailed design and analysis. These two new detailed boss designs were then incorporated into the previously developed vessel configurations to result in two complete vessel designs for fabrication and evaluation.

The detailed results of the study were published as an interim report issued under the contract entitled Analysis of Filament-Wound Dome and Polar Boss of Metal-Lined Glass-Filament-Wound Vessels (Reference 27). The results are summarized briefly below.

1. Dome Characteristics

A method was developed for analysis and detailed investigation of the dome ends of metal-lined glass-filament-wound vessels in the vicinity of an axially located polar boss, representing an extension and supplement to the methods generally used for membrane analysis of filament-wound composite pressure-vessel shells (domes and cylinder), and for discontinuity analysis of the dome-to-cylinder juncture.

The analytical method was developed for and applied to the specific pressure-vessel design configuration of interest: a 12-in.- (30.5-cm-) dia. by 18-in.- (45.7-cm-) long closed-end, cylindrical, glass-filament-wound vessel lined with 0.010-in.- (0.254-mm-) thick aluminum, with aluminum polar bosses with diameters equal to 10% of the vessel diameter located axially on each dome end, designed for a burst pressure of 3000 psi (2070 N/cm²) at 75°F (297°K).

The metal-lined glass-filament-wound vessel domes were characterized when subjected to internal pressure and boss reaction loads with emphasis on the axial polar boss regions. The meridional wrap angle as a function of radial distances was determined; most of the vessel head had longitudinal wrap angles less than 20 degrees (0.35 rad). Hoop radius of curvature and filament-wound composite thickness were determined as a

function of wrap angle. Elastic properties, deflections, rotations, and strains were found by orthotropic analysis and netting analysis.

It was from orthotropic analysis that the glass-filament-wound dome had an increasing strain up the dome; at the point where the metal liner-to-boss transition would be located, the strain was 11% greater than at the equator. The maximum meridional strain occurred on top of where the boss would be located and was 50% greater than at the equator.

Netting analysis resulted in essentially constant meridional strain up the dome.

Although radial deflection could be computed easily, the deflection in an orthogonal direction was needed to locate the deflected point in space; the equations governing this orthogonal deflection required extensive numerical solution. Instead, empirical data on dome deflections were reviewed. It was determined that, for glass-filament-wound vessels, two zones of approximately linear load vs deflection exist due to the departure from orthotropic properties with increasing strain. Above the transition load (approximately 25% of ultimate) where crazing initiates, the deformation behaves as predicted by netting analysis. Above the crazing threshold, deflections of points on the domes were essentially normal to the unpressurized surface. Based on this, it was determined that the netting analysis should be used for glass-filament-wound vessels for establishing strains, stresses, and deflections.

In the area of the dome immediately adjacent to the boss, the composite thickness increases rapidly, and discontinuity forces and moments exist here due to changes in section properties and curvature, necessitating a discontinuity analysis of the section. The discontinuity analysis analyzed the filament-wound composite buildup at the boss as a ring-plate and accounted for the flange bearing loads (distributed or concentrated) of a free-floating boss. Ring loads, deflections, and rotations were determined. The results were almost independent of the theory used to establish elastic properties. Radial deflection at the composite ring-plate-to-membrane junction was independent of the type of flange bearing load (distributed or concentrated) and its position, but rotation was strongly influenced by the magnitude and point of load application. For example, at the vessel design burst pressure, the radial deflection was 0.040 in. or 0.102 cm (i.e., the "slip" between the free-floating boss flange and composite ring-plate is 0.040 in. or 0.102 cm); the rotation of the composite section at the junction ranged from 1.5 to 3° (0.026 to 0.052 rad) depending on location of the bearing load. Since results of the discontinuity analysis were independent of theory used to establish elastic properties, it was concluded that netting theory properties are sufficient for establishing vessel designs.

2. Polar Boss Design Concepts

The various polar boss configurations for glass filament-wound metal-lined vessels considered during the study are shown schematically in Figure 22. The schematics indicate regions of the liner estimated to be in the elastic or plastic ranges. Areas of possible debonding caused by deflection and rotation of the composite on top of the boss are indicated. Configurations 4 and 12 of Figure 22 were selected for detailed design. Configuration 4, the matched rotation flange boss, incorporates a high strength aluminum alloy boss with flange taper to the 1100 aluminum membrane to permit equal rotation of the filament-wound composite and boss flange, and to uniformly distribute the boss reaction load. Mismatch of radial deflections could cause debonding as shown in Figure 22; plastic-to-elastic condition occurs in the transition area. This design is subsequently referred to as the "butt-welded-boss" liner.

In Configuration 12, the plastic spring boss, pressure in the vessel is used to expand the 1100 aluminum liner past yield plastically against the opening in the filament-wound composite dome. The liner is flexible up to the opening and in the opening, and thickens as it exits from the opening in the filament-wound composite. A slip surface is provided on the other high strength aluminum alloy boss member which takes out the boss reaction load. Another schematic of this configuration is shown in Figure 24, depicting its operation. Enough flexibility is provided to accommodate filament-wound composite deflection. Pressure acts to form the liner and reduce bond stresses. This configuration is subsequently called the "hinged boss" liner.

3. Vessel Designs

Detailed structural analyses and designs for the two selected metal polar bosses are given in Reference 27. Basic features of the hinged boss are shown in Figure 25 and of the butt welded boss in Figure 26. In both designs, 2219 aluminum alloy is utilized for portions of the boss requiring high strength, and 1100 aluminum is utilized for the liner itself. These two boss designs were incorporated into the membrane analysis pressure vessel designs previously established during the work described in Section II. The aluminum liner with hinged boss is shown in Figure 27, the aluminum liner with butt welded boss in Figure 28, and the complete aluminum-lined glass-filament-wound vessel in Figure 29.

B. FABRICATION

1. Electron-Beam Weld Schedule Development

Evaluation of EB weldments of 1100-0 aluminum was made. Flat panels were prepared by welding together two sheets of 0.010-in.-

(0.254-mm-) thick aluminum with 0.025 x 0.025-in. (0.635 x 0.635-mm) flanges at the mating edges. Test specimens were prepared by shearing and machining standard tensile coupons from the flat panels. The welds of some test specimens were worked down after welding while others were left as welded. Test data are summarized in Table 8, where tensile strength, yield strength, and elongation in 2, 1, 1/2, and 1/4 inch (5.08, 2.54, 1.27, and 0.635 cm) are shown. Most specimens failed in the parent metal with high ductilities, and the data compare favorably with information developed previously under the program.

Full diameter aluminum rings of 12-in.-(30.5-cm-) dia. and 0.010-in.- (0.254-mm-) thickness with 0.032 x 0.032-in. (0.813 x 0.813-mm) flanges were girth EB-welded with no weld cracking and a relatively small resultant weld bead on inner and outer joint surfaces.

Additional sets of 12-in.-(30.5-cm-) dia. weld specimens were made based on a butt girth weld joint configuration 0.025-in.- (0.145-mm-) thick. This joint configuration was selected based on previous EB-weld evaluation of flat specimens which showed that quality butt welds could be produced in the 0.025-in.- (0.145-mm-) thick material. The girth weld joint used was 0.025-in.- (0.145-mm-) thick over a total length of 0.40-in. (1.016-cm), which then tapered down on each side over a length of 0.75-in. (1.905-cm), to the liner membrane thickness of 0.010-in. (0.254-mm). Each set of girth weld simulators was assembled over an inner copper backup ring support. The specimens had very uniform thicknesses and diameters and we obtained a butt joint with only slight gapping, (less than 0.002-in. or 0.051-mm) within the tolerances permissible for EB-welding of 0.025-in.- (0.145-mm-) thick material.

The specimens were successfully welded, and had narrow heat affected zones, little weld bead on inner and outer surfaces, and absence of cracking (as determined from dye penetrant and x-ray film). As a result of the work, an acceptable weld joint configuration and weld schedule (voltage, amperage, focus current, and speed) for welding of the 12-in.- (30.5-cm-) dia. by 18-in.- (45.7-cm-) long aluminum liners was developed.

Trial EB-welds were also successfully prepared to simulate welding the 2219 aluminum of the bosses to the 1100 aluminum of the liner membrane.

2. Liner Mechanical Testing

Tests were conducted at ambient temperature on EB-welded specimens of 2219-T62 to 1100 aluminum with welds running both longitudinally and transversely along the specimens. The results are given in Tables 9 and 10.

For specimens with welds running longitudinally, failure

always initiated in the 2219 aluminum, and then propagated across the weld into the 1100 aluminum. For the transverse welded samples, failure always initiated in the 1100 aluminum in the heat affected zone.

3. Liner and Vessel Fabrication

Fabrication process procedures developed and used in draw formed, machined, chemically milled, and EB-welded liner manufacture are presented in Appendix G. The filament-winding procedure used in overwinding the aluminum liners to produce vessels is given in Appendix F. Figures 30 to 42 show the typical fabrication sequence for the hinged-boss configuration liners and filament-wound vessels; procedures used for the butt-welded-boss configuration liners and vessels were similar. Three vessels of each of the two configurations were fabricated, and the fabrication data are summarized in Table 11.

a. Vessels With Butt Welded Boss (BWB) Liners

(1) Fabrication of Initial Liner

Assembly of the liners required EB-welding of a boss to each of the liner halfshells, and girth EB-welding the halfshells together, using a copper backup ring at the girth weld to assure proper fitup and alignment. Welding of an initial liner was initiated. Both boss welds required re-welding several times in order to fuse small cracks generated during the first penetration pass. The cracks were successfully fused but some buckling of the thin liner occurred during the multiple passing. As a result one weld suffered one burn-through hole and the other had two. The holes were repaired with a manual TIG weld using 1100 aluminum filler wire and re-welded in the electron-beam machine with the head well-clamped in a heat-sink fixture. No further hole burning in the boss welds was encountered. The girth EB-weld of this liner assembly resulted in two burn-through holes about 90° (1.57 rad) apart on the cleaning pass and a third one near the second hole, during the penetrating pass, possibly a result of slight mismatch or gap at the girth weld. The holes were manually TIG-repaired with 1100 aluminum filler wire and an Argon backup, and then re-welded with EB locally, taking several passes to smooth out the repaired area, before the weld was judged to be acceptable. After completion of liner assembly welding, the copper backup ring inside the liner was removed by nitric acid etching. The liner was then x-rayed and the liner leak tested. In the soap bubble leak test that preceded the planned helium leak test, several liner leaks were found in the membrane area. The situation was reviewed with the liner component and copper ring removal vendor, who accepted blame for the deficiency, and replaced the liner components at no additional cost to the program.

(2) Vessel BWB-1

One of the boss welds showed a small crack after the first penetration pass. A second pass fused the crack and both boss welds were accepted to the dye penetrant and x-ray inspection requirements.

The girth weld did not seal over a 3/4-in.- (1.9-cm-) long slight mismatch area on the first EB sealing pass. This area was filled with 1100 aluminum and locally sealed with the EB. On the subsequent EB full penetration pass, two burn-through holes about 1/2-in.- (1.3-cm-) long occurred. Filler metal was added here, and the burned-through areas were successfully sealed with full penetration EB passes.

Because of the leaks noted on the initial liner fabricated, liner BWB-1 was soap-bubble tested with no indication of leaks prior to nitric acid etch removal of the copper girth weld backup ring. The backup ring was then removed by etching, and the liner weld x-rayed. Two spherical porosities in a repair area of 0.010-in.- (0.254-mm-) dia. and 0.020-in.- (0.508-mm-) dia. located 0.200-in.- (0.508-cm-) apart were noted and accepted. The liner was accepted for further processing and helium leak tested.

The liner was assembled in a vacuum chamber and subjected to a helium mass spectrometer leak test, which the liner successfully passed. However, due to operator error, the liner was accidentally overpressurized beyond its yield point. Although some plastic deformation occurred, inspection of the leak-tight liner resulted in a decision to use it for filament-winding a pressure vessel for burst testing. Corrective action was taken to preclude overpressurization of future liners.

Vessel overwinding and curing was accomplished in accordance with the procedures of Appendix F without difficulty; operations consisted of cleaning and priming the liner, applying adhesive coated nylon scrim cloth to the liner, followed by overwinding with longitudinal and circumferential patterns of resin impregnated glass roving and resin curing.

(3) Vessel BWB-2

The first boss weld was completed with one cleaning and one penetration pass without incident. The second weld showed a large crack in the middle of the weld which required about six additional passes to obtain complete fusion. The cracking of this weld is believed to be inherent in the nature of the restrained joint and since multiple electron-beam fusing can be used to close the crack, no attempts at corrective action were taken.

During seal welding of the girth joint,

one area did not seal. It was filled with 1100 aluminum, and successfully sealed. In the penetration pass, two holes occurred, which were sealed by manual TIG welding with 1100 aluminum filler wire and argon backup. This liner then passed a soap bubble leak test and the copper backup ring was removed.

X-ray of the girth weld joint revealed several small porosities in the TIG repaired areas. The liner was accepted for further processing, and successfully passed a helium mass spectrometer leak test. The vessel was overwrapped without problems.

(4) Vessel BWB-3

The liner assembly and aluminum-lined glass filament-wound vessel were fabricated without problems.

b. Vessels With Hinged Boss (HB) Liners

Liner welding and filament overwinding to produce vessels HB-1, HB-2, and HB-3 was accomplished without particular problems, except the one described below, because the processing was similar to that previously developed and optimized for the vessels with butt welded boss liners.

In fabrication of the first two units of the hinged boss configuration, the first attempts to remove the copper backup ring by nitric acid etching did not completely remove the copper. The liners were further processed to remove all the copper. In leak testing, it was found that the two liners had pin-hole leaks in the membrane. Failure analysis revealed that the cause of the pin holes was that both of the tanks were submerged in tap water overnight in an attempt to completely rinse the etching fluid from the entrapped area of the boss joints (this procedure had not been used for previous liner assemblies in which the copper backup rings had been removed without incident). This extended exposure to tap water caused corrosion and pitting of the liners. Corrective action, consisting of rinsing the liner with deionized water rather than prolonged submergence in tap water, was instituted for subsequent liner assemblies. Components for the defective liners were replaced, and liner assemblies were fabricated free of pin holes which passed the helium leak testing.

C. TESTING

1. Test Plan, Facility, and Instrumentation

a. Test Plan

Three vessels each of the two designs were sub-

jected to design verification tests at ambient temperature. For each design, one vessel was burst tested at ambient temperature and one at liquid nitrogen temperature, and one additional vessel fatigue cycled at ambient temperature between 0 and 60% of original burst strength.

For burst tests and cyclic fatigue tests, a rate of pressurization that produced a strain of approximately 1%/minute in the longitudinal and circumferential directions was used.

Each vessel was equipped with extensometers for strain measurement and thermocouples for measurement of cryogenic temperatures. Data were recorded continuously during testing on internal pressure, exterior-surface temperature (cryogenic tests only), and deflection vs pressure relationships at three points distributed to provide hoop and longitudinal strains. One set of hoop-strain measurements was made at the vessel cylindrical-section center, and two sets of axial-strain measurements were made along the cylinder section.

b. Test Facility

Liquid nitrogen (LN_2) was used to pressurize the vessels for the (-320°F or 77°K) tests, with the pressurization rate regulated by gas-controlled valves. Inhibited water was used for pressurization in the room-temperature tests. The cryogenic-test facility is shown schematically on Figure 43. The test fixture (Figure 44) consisted of a vacuum chamber with provisions for instrument leads and vacuum-jacketed pressurization lines. The chamber interior and exterior were coated with aluminum paint, and a layer of aluminum foil was installed inside to provide additional insulation.

To aid in maintaining minimum test temperatures, the vessels installed in the vacuum chamber were equipped with external cooling coils through which liquid nitrogen was flowed at essentially atmospheric pressure. A cylinder of reflective-type insulation was used around the exterior cooling coils. The vacuum chamber was pumped down to 4×10^{-4} mm Hg (5.3 cN/m²) to assure the required temperatures. The tank temperatures were maintained as low as possible, and thermal equilibrium was obtained before testing was initiated. Thermal equilibrium for the liquid nitrogen testing was defined as a vessel flange or skin temperature of -300°F (89°K), or less, with -310°F (83°K), or less, at the vessel outlet vent line.

c. Instrumentation

Temperatures, longitudinal and circumferential strains, and internal pressures were monitored throughout testing; Figure 45 shows the instrument locations.

The electronic and digital equipment used for

these measurements was calibrated periodically, against standards traceable to the National Bureau of Standards.

Platinum resistance thermometers and copper-constantan thermocouples were used in the LN₂ tests. The measurements were made on the exterior surface near the tangency at one end of the tank. In addition, the temperatures of the cryogenic fluids inside and outside the tank were recorded.

The Aerojet-developed "bow-tie" extensometers were used to make strain measurements. They consist of a piece of beryllium-copper sheet in a configuration that provides two cantilever beams fitted with bonded strain gages. Metal-foil strip, approximately 0.25 in. (0.63 cm) wide, was used to link the beam ends to the gage-length end points. Both the extensometers and the foil strips were positioned against the test-vessel surface.

For girth (hoop) measurements, the thin metal strip was placed around the cylinder and secured to opposite ends of the extensometer; circumferential deflection resulted in a proportional output of the gages on the cantilever beams. For longitudinal-deflection measurements, metal strips were affixed to instrumentation-pin terminals wound into the tank near the ends of the cylindrical section. The strips were run along the cylinder longitudinally toward its center; the cantilever-beam ends were connected to the ends of the strips at the midsection of the tank. A longitudinal deflection produced a proportional strain-gage output.

The accuracy of the strain gages depends on the gage factor, which is extremely sensitive to cryogenic-temperature variations. To provide the required accuracy, the concept of controlled-temperature strain transduction was employed: Heaters were provided to maintain the gage temperatures within their compensation range, and a sensor was added to record the vessel-surface temperature in the vicinity of the extensometer. This sensor was used to verify that the heat input to the extensometer did not warm the tank surface in the region of the transducer. Thermal insulation was used under the heated extensometers to minimize heat transfer to the vessel. The test data showed that no significant vessel warming was produced.

Before testing, each extensometer was installed on the vessel and shunt calibrated under ambient conditions throughout its anticipated range of deflection. The gage factors did not vary under cryogenic conditions, because the heaters kept the gages essentially at the ambient temperature; monitoring during the cryogenic tests revealed that the gages were usually maintained at $75 \pm 20^{\circ}\text{F}$ ($297 \pm 11^{\circ}\text{K}$). Because the gage factor varies only 1% per 100°F (56°K) change in the 75°F (297°K) range, there was negligible loss in accuracy.

To calibrate for longitudinal displacements, the

distance between the bow-tie attachment points or terminals (L_2) was carefully measured. The instrument and its metal-strip extensions were then stretched to the maximum expected deflection, using accurately determined positions (ΔL_2). The strain was calculated as $\Delta L_2/L_2$ to indicate the total between the two attachment points. To calibrate the girth extensometer, the tank circumference (L_1) was measured and the bow-tie attachment band was moved to produce the maximum expected deflection (ΔL_1). The girth strain was calculated as $\Delta L_1/L_1$. Calibration was performed under ambient conditions, and a shift in the zero point occurred due to thermal contraction when the tank was cooled to cryogenic levels. To correct for this shift it was only necessary to reset the recorder to zero, because the repeatability under ambient conditions was essentially linear and the heaters maintained ambient temperatures.

2. Test Results

Test results at ambient and liquid nitrogen temperatures are summarized in Tables 12 and 13. The tables indicate the type of test each vessel was given, the test temperature, the load level used for fatigue loading, the pressure cycles achieved, the burst pressures, the modes of failure, filament ultimate stresses and strains, and pertinent remarks. Comments on the individual vessel tests, amplifying data given in the tables and figures are given below.

a. Butt-Welded Boss Liner Configuration Vessels

(1) Room Temperature Burst Test

Vessel BWB-1 was installed in a test stand, instrumented with longitudinal and circumferential extensometers, and pressurized to its burst point using a 1%/minute strain rate. Failure occurred at 2983 psig (2057 N/cm²), or 98.7% of the nominal design burst pressure of 3000 psi (2070 N/cm²). The vessel, after testing, is shown in Figure 46. The failure consisted of an energetic failure of the glass hoop windings at the midpoint of the cylinder section. The hoop windings failed from the cylinder midpoint to within two inches of the head-to-cylinder junction at each end of the vessel. The longitudinal windings and liner also ruptured. Breaks in the liner were oriented longitudinally across the weld. Visual inspection of the vessel interior revealed good bonding of the liner to the filament-wound composite and no apparent cracks at the boss welds.

The pressure vs strain data obtained from the test are shown in Figure 47, as well as the design ultimate pressure vs strain points. Longitudinal strain measurements were determined by measuring deflection along the length of the vessel cylinder section. Hoop strain measurements were calculated from circumferential deflections of the vessel. In addition to one set of measurements at the cylinder midsection, additional sets of data were taken at each cylinder end. The pressure-strain data were

uniform and close to the design values. Hoop filament stress at failure was 383 000 psi (264 000 N/cm²).

Sections were cut from the vessel, and examinations made of all weld areas. X-ray and dye penetrant inspection showed that no cracks or other metal flaws had been produced in the girth or boss welds by the burst test. Macrographic inspection of sections cut from the vessel at the polar boss did reveal that local plastic deformation and necking occurred in the 1100 aluminum about 0.050-0.070-in. (0.127-0.178-cm) from the 2219 aluminum to 1100-aluminum liner-membrane welds (see Figure 48). This necking appeared to circumscribe the vessel bosses. The boss welds were sound and had a uniform cross-section without undercut or other stress concentrating configurational features. The bond between the filament-wound composite and liner appeared to be intact without any voids between the opening in the filament-wound composite and the boss body protruding from the filament-wound composite.

Examination of the section cut from the vessel showed that the metal bosses had a tendency to be pushed inward during fabrication (filament-overwrapping of the pressure-stabilized thin aluminum liner) due to design features of the winding shaft which let the boss-to-boss length "float" rather than be fixed.

(2) Room Temperature Cyclic Fatigue Test

Vessel BWB-2 was pressure cycled at between 0 and 60% of design burst (1800 psig or 1240 N/cm²) until failure occurred after 25 pressure cycles. The vessel failure consisted of a leak, and appeared to be located at one of the vessel bosses.

Pressure vs strain data for the test are shown in Figure 49 for cycles number 1, 2, 10, 20, and 23. There was a small amount of permanent set after the first cycle which did not increase with additional cycling. Strains were uniform and close to design values.

Sections were cut from the vessel, and the vessel was inspected in the same manner as vessel BWB-1. X-ray inspection indicated one crack approximately 1/2-in.-(1.27-cm-) long at one of the bosses on the outer edge of the weld, and two cracks approximately 1-in.-(2.54-cm-) long 180° (3.14 rad) apart at the edge of the boss weld on the end of the tank which leaked during test. Exact location of the crack relative to the weld was not possible (i.e., in weld, heat affected zone, parent metal). Dye penetrant inspection revealed only one 1/2-in. (1.27-cm) crack (on the end that had two crack indications by x-ray examination).

Visual examination showed small, smooth liner buckles at some local points around the bosses in the 1100 aluminum

Examination of microphotographs revealed:

- Cold work flow lines into the failure area.
- Wide cracks relative to their depth in the failure area which would make the detection of the failure initiation by dye penetrant methods quite insensitive.
- Through-wall liner failure in the 1100 aluminum approximately 0.055-in. (0.140-cm) from the weld joining the liner to the boss.
- That apparently both tensile and compressive yielding had occurred in the 1100 aluminum.
- The weld was sound and had a uniform cross section without undercut or other stress-concentrating features.
- No cracking in the weld of the 2219 aluminum boss material.
- That liner thickness were:

Weld	0.041-0.035-in. (0.104-0.089-cm)
------	-------------------------------------

2219 Aluminum at Weld	0.0375-in. (0.095-cm)
-----------------------	--------------------------

1100 Aluminum at Necking	0.0219-in. (0.056-cm)
--------------------------	--------------------------

1100 Aluminum at Parent Metal Bulge	0.0422-in. (0.107-cm)
--	--------------------------

(3) Liquid Nitrogen Burst Test

This test was conducted by positioning vessel BWB-3 in the cryogenic test vacuum chamber, cooling the vessel down to -320°F (77°K) by filling it with LN₂ while maintaining a high vacuum externally, and pressurizing the vessel to its burst point with LN₂.

The vessel failed at a pressure of 2570

liner away from and around the 2219 aluminum boss. Macrographic inspection of sections cut from the boss area of the tank revealed the following:

- The failure sites (breaks through liner) were located where buckling of the 1100 aluminum liner had not occurred (see Figure 50). In an area approximately 3/4-in.- (1.9-cm-) long, where buckling of the liner had occurred, the localized thinning was much less pronounced than as noted at the failures, as can be seen from Figure 51. Local thinning is shown in Figures 52 and 53. "Oilcanning" had apparently reduced the tendency to highly localized strain.
- Difficulty in interpreting the radiographic inspection where the cracks occurred was due to compressive yielding of the 1100 aluminum liner which produced thicker material on the outside of the cracks (shown in Figure 54). The greater thickness occurring in a uniform circular configuration made it appear on the x-ray film to be weld edge, although it was actually deformed parent material.
- As was the case for vessel BWB-1, the bosses had a tendency to be pushed inward during filament overwinding of the liner.
- Voids existed between the 2219 boss and the filament-winding around it. The bond between the filament-wound composite and the boss appeared to be broken between the boss body and the area of high plastic deformation and necking.

Microhardness traverse of the boss region sections cut from the vessel (1) confirmed the localized work hardening which occurred in the failure area; (2) indicated that alloying between 1100 aluminum and 2219 aluminum occurred during the EB-welding producing greater hardness and strength in the weld than the 1100 aluminum parent metal; and (3) indicated that the heat affected zone extended approximately 0.080-in. (0.203-cm) into the 2219 aluminum (from the weld edge). The EB-weld joint is shown in Figure 55. Data from the microhardness traverse are presented in Table 14 and plotted in Figure 56.

psig (1770 N/cm^2) when pressure could no longer be increased due to leakage through the liner in the head region. Test vessel skin temperature at the start of the burst test was -314°F (81°K) and -300°F (89°K) at the vessel burst point.

Pressure vs strain data from the test are given in Figure 57. The hoop-strain data became inconsistent with design predictions when pressure increased over 1500 psig (1030 N/cm^2). Test records indicated that some vacuum loss occurred in the test chamber at 1200 psig (830 N/cm^2) and above (perhaps due to some minor leakage through the liner at its eventual failure site).

Post-test metallurgical examination showed that one boss weld had cracked almost all of the way around. Figure 58 shows the failure. The crack was located partially in the 2219 aluminum alloy boss and partially in the fusion zone itself. Figure 59 shows a hot tearing of the weld on the 2219 aluminum side during weld-metal solidification and Figure 60 shows hot tears in the weld on the 1100 aluminum side. The tears are probably due to excessive restraint of the boss-weld configuration and the cumulative shrinkage resulting from multiple weld passes required to complete this particular weldment.

The other boss failed in the 1100 metal adjacent to the weld. Figure 61 shows a section of the joint, exhibiting a neck-down resulting from a strain magnification which occurs between the soft ductile 1100 aluminum liner and the high-strength non-yielding 2219 boss*. Figure 62 shows the same view at higher magnification*. Figure 63 shows the 2219 side of the same section and exhibits a slight tearing of the 2219 near the weld. The tearing is believed to be the result of localized stress concentrations occurring during welding. Both the thinning of the 1100 alloy and the hot-tearing of the 2219 alloy and the weld metal are believed to be inherent in the combination of materials, processes, and weld joint.

The aluminum liner had an area of damage in one halfshell, due to mishandling (dropping) of it during an x-ray operation. Also, one of the heads had significant buckling in it as a result of several boss reweld operations required to obtain an acceptable weld; both of these areas were hand-straightened prior to girth welding.

The liner membrane areas of each head which were buckled due to mishandling on one end and multiple welding on the other showed no evidence of failure at the ultimate pressure. It is possible, however, that the hand-straightening of the dent in the dropped unit was contrib-

* In Figures 61 and 62, the broken pieces were placed together for the photograph, causing overlap of the necked-down sections of the liner in the fracture area.

utory to the highly localized stress in the boss weld, which finally failed in thinning.

b. Hinged-Boss Liner Configuration Vessels

(1) Room Temperature Burst Test

Vessel HB-2 was pressurized to its burst point of 3003 psig (2071 N/cm^2) using a 1%/minute strain rate. The massive failure occurred in the longitudinal filaments in the head of the vessel, appearing to originate at the axial polar boss; the head of the vessel opened up like a "flower" as it failed at the burst pressure (see Figure 64).

The nominal design burst pressure for the vessel is 3000 psig (2069 N/cm^2) and the result is almost identical to the burst pressure of 2983 psig (2057 N/cm^2) obtained from the ambient temperature test of the butt-welded boss liner configuration vessel. Pressure vs strain data from the test are presented in Figure 65. The data are uniform and quite close to the values predicted from the design analysis. Hoop filament stress at vessel burst was 375 000 psi ($259 000 \text{ N/cm}^2$).

Figures 66 and 67 exhibit cross sections of the hinged-joint bosses. Figure 66, showing the boss from the vessel dome where the failure was located, indicates no thinning of the liner section as a result of the working of the hinged-joint. The bending of the 2219 aluminum collar further exhibits that the hinged-joint functioned as designed. Figure 67, from the vessel dome that did not fail at 3003 psig (2071 N/cm^2), shows more of the spring action and a slight thinning of the 1100 membrane in the head section adjacent to the boss flange. Another area of thinning (not shown in Figure 67) occurred just outboard of the flange and spread over an annular distance about 1/4-inch-(0.64-cm-) wide around the flange. It appears that the hinged-joint distributed the strain over a much wider area than experienced with the butt-welded bosses.

In all regions of the vessel interior not damaged as a result of the test, the liner appeared to be well bonded to the filament-wound composite tank wall. Liner HB-2 met the design requirements of an ambient single-cycle burst pressure of 3000 psig (2069 N/cm^2) without any evidence of liner failure prior to failure of the glass-filament-wound composite.

(2) Room Temperature Cyclic Fatigue Test

Test vessel HB-3, instrumented with longitudinal and hoop strain measurement extensometers, was pressure cycled between 0 and 60% of single-cycle burst pressure (i.e., 1800 psig or 1240 N/cm^2) until failure occurred. After 18 pressure cycles, a small leak occurred,

consisting of slight weeping through the windings over a 90° (1.58 rad) sector of the girth-weld area at the cylinder section midpoint. Pressure cycling was continued and at 65 cycles another leak occurred in the vessel in one head just away from the head-to-cylinder juncture. The pressure cycling was continued to 70 cycles, and then stopped. Figure 68 shows pressure vs strain data for cycles number 1, 2, 29, 49 and 68. After the first cycle, virtually no additional permanent set in the vessel was noted. Strains were close to design values and uniform.

The vessel was sectioned revealing complete bonding of the liner to the filament-wound composite (i.e. lack of buckles in the liner). From inspection of the vessel liner interior and from pretest x-rays, it is clear that the cylinder section leakage was attributable to localized lack of complete penetration in the EB girth weld. A section was cut from the tank in this region and was examined by a metallurgist as part of the failure analysis. Figure 69 shows two different cross sections of the liner girth joint, the overwrapped filaments, and the liner-to-composite bond. The lack of EB-weld penetration is clearly evident.

Densitometer readings of the x-ray film of the girth weld prior to filament-winding showed about 80% penetration of the joint in a local area. Since no technique had been developed for repair weld (without a back-up ring) of the thin girth section, the liner was filament-wound and tested. Analysis of the photo-micrographs of the two separate sections made after vessel test showed the following weld penetration measurements:

	<u>Section A</u>	<u>Section B</u>
Penetration of Total Thickness at Weld	62%	83%
Weld and Parent Metal Thickness	0.0423 in. (0.107 cm)	0.0364 in. (0.092 cm)
Parent Metal Thickness 1/8-Inch (0.32-cm) From Weld	0.0331 in. (0.084 cm)	0.0318 in. (0.081 cm)
Actual Weld Thickness	0.0261 in. (0.066 cm)	0.0302 in. (0.077 cm)
Unwelded Parent Metal Thickness	0.0161 in. (0.041 cm)	0.0063 in. (0.016 cm)
Weld Thickness (% of PM Thickness)	79%	95%

The lack of penetration of the girth weld

provided a natural site for localized strain due to thinner weld metal and the notch-effect at the root of the weld.

A localized crack on the liner inside surface was clearly evident where the leakage in the vessel head was noted in the vessel dome near the head-to-cylinder juncture after 65 pressure cycles. Figure 70 shows cross sections of the vessel wall at the liner fracture site. The failure in the head section noted after 65 cycles appeared to originate possibly as a result of slight voids and resin-rich areas in the composite which allowed the liner membrane to crease into the weakened area. The localized nature of the crease in the liner caused localized wall thinning and localized failure (note significant composite crazing over liner fracture in Figure 70).

A band of surface roughness about 1.5-in.- (3.8-cm-) wide extended completely around the inside surface of the head just past the tangency point. Micro-examination of the area indicated this was a mechanically-induced effect (probably during forming) rather than "orange-peeling" which would have shown disturbance of the grain boundaries of the material and a larger grain-size.

Figure 71 shows the excellent performance of the hinged-joint boss of the liner. The photo shows slight buckling and thinning of the liner head, as well as slight deformation of the liner where it contacted the lower portion of the 2219 aluminum collar. The slight nature of these deformations demonstrate that the liner boss was able to sustain the operating conditions through the 70 fatigue cycles and probably could function satisfactorily for a considerably larger number of cycles.

(3) Liquid Nitrogen Burst Test

The test on Tank HB-1 was conducted as described in Section III-C-2-a. The vessel burst at a pressure of 4240 psig (2920 N/cm^2), a 40% increase over the room temperature burst strength of this vessel configuration. The failure was massive, and the test vessel was essentially totally blown apart into many pieces except for one head (see Figure 72). Pressure-vs-strain curves for the test are given in Figure 73. The two longitudinal extensometers were lost about halfway to the burst point. The hoop-strain data look good, and the value at the vessel burst point is very close to design predictions of strain for the burst pressure obtained. Hoop filament stress at vessel burst was 532 000 psi ($367 000 \text{ N/cm}^2$). Figure 74 shows one of the hinged-joint bosses after failure of the vessel. This figure also shows the successful operation of the hinged-joint. The membrane and outer supporting collar both dished outward but functioned satisfactorily all the way to the high 3.5% strain associated with the 4240 psig (2920 N/cm^2) burst pressure. The figure also shows voids in the weld crown which, however, had no effect on the operation of the liner assembly.

Figure 74 (like Figure 71 from the cyclic-fatigue test unit) shows deformation of the 1100 aluminum liner into the lower edge of the 2219 aluminum collar as a result of the internal pressure in the area. The minor nature of this deformation indicates the adequacy of the composite supporting material and the capability of the liner boss to accomodate the operating characteristics of the aluminum-lined glass-filament-wound pressure vessel.

c. Evaluation

Evaluation of the test results obtained lead to the selection of the hinged-boss liner as the configuration offering the highest performance potential in cyclic fatigue capability and burst strength for thin aluminum-lined glass-filament-wound vessels for operation at room and cryogenic temperatures. Additional vessels of this type were fabricated and tested, as described in the following section.

IV. DESIGN, FABRICATION, AND TESTING OF ADDITIONAL VESSELS WITH HINGED-BOSS LINERS

Nine additional 12-in.-(30.5-cm-) dia. by 18-in.--(45.7-cm-) long thin aluminum-lined glass-filament-wound vessels, incorporating the 0.010-in.--(0.254-mm-) thick 1100 aluminum liner of the hinged boss configuration, were fabricated and tested.

A. DESIGN

Vessel design was identical to the hinged boss configuration already described in Section III-A.

B. FABRICATION

Liner and filament-wound vessel fabrication were performed using the process specifications described in Section III-B. Metal liner fabrication data are given in Table 15, and pressure vessel fabrication data are presented in Table 16. Figure 75 shows a group of completed liners, and Figure 76 shows liner overwindings.

Practice EB girth welds were made with reduced heat input on a set of full-scale liner halfshells in order to purposely develop areas of incomplete penetration in the weld. These areas were then re-welded at different machine settings to determine an appropriate control setting for any welds which might show incomplete penetration in the x-ray operation following removal of the backup ring. We found that a machine setting approximately that of the original weld would penetrate the joint completely without burning holes in the weld joint. This increased heat "receptiveness" in a reduced heat-sink situation is probably attributable to the partial weldment already in existence.

An evaluation to determine optimum annealing procedures for the 1100 aluminum liner assembly with high strength 2219-T62 boss components was conducted. It was determined that liner annealing could safely be performed after all welding, back-up ring removal, girth weld x-ray, and helium leak testing were completed. The annealing procedure selected and used for all liners was to subject the liner to 600°F (590°K) for one hour, to give a "dead-soft" 1100 aluminum membrane condition, prior to filament-overwinding. Evaluation of the 2219 alloy components showed that they had adequate strength to meet design requirements after exposure to the annealing temperature for one hour.

Liner A-1 was fabricated and passed helium leak test, but was buckled when an external pressure differential inadvertently occurred during venting of the vacuum chamber (see Figure 77). The buckling shown was largely removed by straightening by internal pressurization after being filament overwrapped with dry glass roving, and the vessel made with this liner later achieved a very high performance level.

Liners for Tanks A-2, A-4, A-6, and A-7 were fabricated and passed helium leak testing without problems.

Helium leak testing of Liners A-3, A-5, A-8, and A-9 indicated leakage at the non-structural weld between the boss, hat section, and external collar. Rewelding was successful on Liner A-5, but Liners A-3, A-8, and A-9 still showed slight leakage at this joint. Repair of these three liners to pass the helium leak test was unsuccessful after repeated EB rewelds at the boss/liner/collar joint. Liner A-8 was collapsed in the EB weld chamber during one of the attempted repairs and had to be scrapped. It was decided to manually TIG weld a fillet of 1100 aluminum around the external 2219 aluminum collar-to-1100 aluminum dome intersection of Liners A-3 and A-9. Although this repair sealed the helium leakage, the relative massive fillet weld completely eliminated any possible hinge action of the bosses repaired. It is believed that problems encountered with this weld joint were probably due to initial contamination in the joint when it was EB-welded the first time, and that subsequent EB-weld repair attempts were fruitless because of contamination at the inside surface of the joint from products of reaction produced by nitric acid removal of the copper backup ring (conducted prior to the helium leak testing which revealed the leakage).

In filament-overwinding of these eight completed liners, no problems were encountered with Tanks A-2, A-3, A-4, A-6, and A-9. The three other liners A-1, A-5, and A-7 experienced local fracture of the thin 1100 aluminum membrane in the dome area away from the boss during filament-winding operations while pressure stabilized. Investigation revealed that the heads which failed had membrane thicknesses equal to or slightly less than the minimum design wall thickness of 0.010-inch (0.254-mm) upon receipt from the liner halfshell forming vendor. In addition, it was found that the membrane fractures each were located on a 5-in.- (12.7-cm-) dia. circle; this circle coincided with one of the diameters at which a protective chemical milling maskant had been cut off with a sharp knife during the tapering of the head which is achieved by a chem-milling process. As a result of the thinness of the area, and possible scratching with the knife, and subsequent chemical milling and pressurization of the liner during winding which possibly further thinned the area, the fractures occurred. Micro-sections of one of the areas showed thinning down to 0.0015 inches (0.038 mm) but evidence of local work hardening was not discerned, indicating either an extremely localized work hardening or a complete absence of it. Other locations which also were the sites of possible knife scratching of the maskant during step tapering did not

cause fracture problems. Liner A-1 was repaired by manual TIG welding in the fractured membrane area (and around the entire 5-in.- (12.7-cm-) dia. suspect area of the membrane) and reprocessed into a successfully filament-wound and cured vessel.

The liners had been designed to permit halfshell salvage from a complete liner assembly by cutting the liners on one side or the other of the girth weld located at the cylinder midsection. The non-failed halfshells of Liners A-5 and A-7 were salvaged in this way and joined by a new EB girth weld joint to form Liner A-13. During helium leak testing Liner A-13 was found to have small pinhole leaks (two in the hat section weld and two in the girth weld) which were successfully TIG repaired. This liner was then successfully processed into a filament-wound vessel.

Whenever liner rework was necessary, the rework was always followed by helium leak testing and annealing in order to restore the 1100 aluminum portion of the liner assembly to the "dead-soft" condition prior to filament overwinding.

Liner A-10 was fabricated without problems, but after filament-overwinding during resin curing a small fracture occurred in the knuckle area of one liner head. The cured composite structure was stripped by soaking in an acid solution in an attempt to reclaim the liner. It was impossible to salvage this liner without significant damage (due to collapsing as a result of unsupported winding tension in the filaments during the stripping procedure).

Liners A-11 and 12 were fabricated and required TIG repair of pinhole leaks to pass helium leak testing (see Table 15); they were subsequently overwrapped without problems to make test vessels.

Work proceeded on Liners A-14, A-15, and A-16 which were fabricated from previously unacceptable liner halfshells (thin membranes, with pin-hole leak sites) in an attempt to obtain additional liners for overwinding. All units required considerable repair welding to pass helium leak test. Each of the liners locally fractured at thin spots in the aluminum membrane during filament overwinding, and further attempts at weld repairing were abandoned.

The nine test vessels successfully fabricated were given final inspection and subjected to structural testing, as described in the next section.

C. TESTING

1. Test Plan, Facility, and Instrumentation

a. Test Plan

Vessel testing consisted of burst and cyclic fatigue tests at room, liquid nitrogen, and liquid hydrogen temperatures. One vessel was subjected to burst testing at each temperature, and two vessels were given cyclic fatigue testing at each temperature by pressurization between 0 and 60% of single cycle burst strength.

All records for the nine vessels were reviewed to establish a qualitative ranking for use in assigning vessels to specific tests. Results of this evaluation are summarized in Table 17.

Testing was conducted using a pressurization rate producing approximately 1% strain/minute in the vessel. Vessels were equipped with extensometers for measurement of strain in the longitudinal and hoop directions of the vessel cylindrical section. One set of hoop strain measurements and two sets of longitudinal strain measurements were made in the cylinder section, and the data were recorded continuously.

b. Facility

Room temperature testing was conducted as previously described in Section III-C, using deionized distilled water as the pressurizing medium. Cryogenic temperature testing was performed by mounting the vessel in a frame and attaching and calibrating the deflection measurement instrumentation (Figure 78), positioning the frame holding the vessel in an insulated container, and filling the container with the cryogenic test fluid (Figure 79). Liquid nitrogen was used as the pressurizing medium for -320°F (77°K) tests, and liquid hydrogen for the -423°F (20°K) tests.

c. Instrumentation

Longitudinal and circumferential strains, and pressure, were monitored throughout the testing. This instrumentation was essentially the same as already described in Section III-C-1-c, except that (1) temperature measurements were not taken, as the vessels were at normal ambient temperatures or submerged in the cryogenic fluid throughout the tests and at steady-state 60-70°F (289 - 294°K), -320°F (77°K), or -423°F (20°K) conditions, and (2) the "bow-tie" extensometers were mounted on the vessel holding fixture out of the cryogenic test fluid, with steel wires running from the cantilever beam ends to the vessel gage length end points. Deflection measurement extensometers were calibrated as installed in the test rig immediately prior to testing, using the procedure already described.

2. Test Results

Test results at ambient, liquid nitrogen, and liquid hydrogen temperatures are summarized in Tables 18 and 19. The tables indicate the type of test given, the test temperature, the load level used for fatigue loading, the pressure cycles achieved, the failure pressure, modes of failure, filament stresses and strains, and pertinent remarks. Comments on the individual vessel tests, amplifying data recorded in the tables, are given below:

a. Ambient Temperature Tests

(1) Single Cycle Burst

Tank A-3 was installed in a test stand, filled with deionized distilled water, and deflection measurement instrumentation attached for measuring cylinder section circumferential and longitudinal strains. The vessel was then pressurized at a rate producing 1% strain/minute (approximately 1000 psi/min. or 690 N/cm²/min.) until burst occurred at 2250 psig (1550 N/cm²). Failure originated in the vessel end dome in the region of the polar boss; the continuous longitudinal windings opened up like a flower and the entire hinge boss was ejected from the vessel. The structural failure was at lower than design burst, due to the massive TIG weld repairs made at the liner boss, as described in Sections IV-B and IV-C-3. The failed tank is shown in Figure 80. At the burst pressure the calculated stresses were 280 000 psi (193 000 N/cm²) in the hoop filaments and 234 000 psi (161 000 N/cm²) in the longitudinal filaments. Pressure vs strain data are shown in Figure 81 and the maximum strains recorded in Table 18.

(2) Cyclic Fatigue Life

The above burst data were compared to data obtained from previous ambient temperature burst tests for this vessel design (discussed in Section III-C-2-b) in order to reaffirm values for the 60% pressure level required for pressure cycling tests. Because of the massive repair weld in the region where failure occurred, it was decided that the low burst pressure of Tank A-3 was not a good representation of the strength of this series of vessels. Thus, the 60% load levels was retained at 1800 psi (1240 N/cm²) for ambient temperature tests.

Tank A-11 was set up for and subjected to pressure cycling between 0 and the 60% load level. Vessel failure, consisting of a leak in the aluminum liner, occurred on the 17th cycle in the knuckle region of the head approximately one inch (2.54 cm) from the head-to-cylinder junction (see Figure 82). The peak stresses during cycling were 223 000 psi (154 000 N/cm²) in the hoop filaments and 186 000 psi (128 000 N/cm²) in the longitudinal filaments. Pressure vs strain plots are shown for the 1st, 11th,

and 15th pressure cycles in Figure 83. As noted in the figure, permanent set after the first pressure cycle was limited to the hoop direction of the cylinder; strain levels remained constant during subsequent cycling.

Tank A-12 was fatigue cycled to the same load level (60%) as Tank A-11. During the 25th pressure cycle a leak occurred in the same area of the vessel head (see Figure 84) as was noted for Tank A-11. The peak stresses during cycling were 222 000 psi ($153\ 000\ N/cm^2$) in the hoop filaments and 185 000 psi ($128\ 000\ N/cm^2$) in the longitudinal filaments. Figure 85 presents pressure vs strain plots for the 2nd, 10th, and 20th pressure cycles. Only minor increases in hoop and longitudinal strain occurred as the number of cycles increased.

b. Liquid Nitrogen Tests

(1) Single Cycle Burst

Tank A-1 was installed in a test stand, deflection measurement instrumentation attached, and the assembly surrounded with a liquid nitrogen bath. When steady-state conditions were achieved, the vessel was pressurized with liquid nitrogen to a maximum pressure of 3870 psig ($2670\ N/cm^2$), whereupon pressure could not be increased further due to system limitations. Pressure was maintained at this pressure level, producing a hoop strain of 3.12%, for about three minutes prior to decreasing to 1800 psig ($1240\ N/cm^2$), where the pressure was maintained while attempts were made to increase the test system pressure level capability. During these efforts vessel pressure was inadvertently decreased to zero. When the vessel was again pressurized in an attempt to burst it, a leak developed in the liner at a pressure of 2250 psig ($1550\ N/cm^2$). The leak was located in the knuckle area of the head just forward of the head-to-cylinder junction. The tank after testing is shown in Figure 86. Stresses at the maximum pressure of 3870 psig ($2670\ N/cm^2$) were 497 000 psi ($343\ 000\ N/cm^2$) in the hoop filaments and 415 000 psi ($286\ 000\ N/cm^2$) in the longitudinal filaments. First cycle pressure vs strain data are shown in Figure 87.

(2) Cyclic Fatigue Life

Tank A-4 was prepared for liquid nitrogen test as described for Tank A-1 and pressure cycled between 0 and 2400 psig ($1650\ N/cm^2$) for 93 cycles because the 2400 psig was approximately 60% of the average LN₂ burst strength of this vessel design (i.e. HB-1 achieved 4240 psig burst and A-1 attained 3870 psig). During the first fatigue cycle the pressure was inadvertently increased to 2500 psig ($1720\ N/cm^2$). Leakage was noted on the 94th cycle when the maximum pressure which could be obtained was 2200 psig ($1520\ N/cm^2$). The calculated stresses at the cycle pressure of 2400 psig ($1650\ N/cm^2$) were 297 000 psi ($205\ 000\ N/cm^2$) in the hoop filaments and 248 000 psi ($171\ 000\ N/cm^2$) in the longitudinal filaments. The leakage areas are shown in Figure 88 and the pressure vs strain data are given in Figure 89. Permanent set occurred in the longitudinal direction of the tank after the 1st

pressure cycle, but this did not occur in the hoop direction.

Tank A-13 was pressure cycled at liquid nitrogen temperature, duplicating the Tank A-4 test, but failure of this tank occurred on the 16th cycle at a pressure of 2250 psig (1550 N/cm^2). The tank after testing is shown in Figure 90. The peak stresses during cycling were 299 000 psi ($206 000 \text{ N/cm}^2$) in the hoop filaments and 250 000 psi ($172 000 \text{ N/cm}^2$) in the longitudinal filaments. Figure 91 presents pressure vs strain plots for the 2nd, 10th, and 15th pressure cycles.

c. Liquid Hydrogen Tests

(1) Single Cycle Burst

Tank A-9 was installed in the test fixture, deflection measurement instrumentation attached, and the assembly submerged in a liquid hydrogen bath. The tank was pressurized with gaseous hydrogen to 30 psig (21 N/cm^2) for a period of time which allowed the gaseous hydrogen to become liquefied. The tank was then pressurized at a rate of 1000 psi/min ($690 \text{ N/cm}^2/\text{min}$) with liquid hydrogen until a pressure of 2380 psig (1640 N/cm^2) was obtained. Excessive boil-off occurred at this point, and the pressure was decreased to zero in order to leak check the test system. When the vessel was again pressurized in an attempt to burst it, excessive leakage occurred at a vessel boss at a pressure of 1760 psig (1210 N/cm^2). The boss which failed had been repair welded during liner fabrication using a rather massive TIG weld (same as described for Tank A-3) and the premature failure was attributed to this repairing; the leakage area is shown in Figure 92. Stresses at the maximum pressure of 2380 psig (1640 N/cm^2) were 295 000 psi ($203 000 \text{ N/cm}^2$) in the hoop filaments and 245 000 psi ($169 000 \text{ N/cm}^2$) in the longitudinal filaments. Longitudinal strain vs pressure are shown in Figure 93, but no signal was obtained from the hoop extensometer.

(2) Cyclic Fatigue Life

Tanks A-2 and A-6 were installed in the liquid hydrogen test facility and subjected to cyclic fatigue at the 60% load level (2400 psi or 1650 N/cm^2) determined from the previous liquid nitrogen burst tests. Tank A-2 sustained 97 pressure cycles before a leak occurred in the knuckle area of the head (see Figure 94), while Tank A-6 experienced a leak failure after 75 pressure cycles, the location of which could not be found in post test analysis; Tank A-6 after testing is shown in Figure 95. The peak stresses for both vessels, were 298 000 psi ($206 000 \text{ N/cm}^2$) in the hoop filaments and 248 000 psi ($171 000 \text{ N/cm}^2$) in the longitudinal filaments. Pressure vs strain plots for Tanks A-2 and A-6 are shown in Figures 96 and 97, respectively. Permanent set occurred in both vessels in both directions as a result of the first pressure cycle; only minor changes in strain levels occurred during subsequent pressure cycles.

3. Evaluation of Test Results

a. Failure Modes and Analysis

After testing, tanks were analyzed in more detail for failure modes, hinge boss operation, and glass-filament-wound composite/aluminum liner characteristics after burst and cyclic fatigue testing. Polar bosses and tank membrane areas were cut from the tanks and sectioned; Figure 98 shows typical boss and head-to-cylinder junction specimens. Figures 99 and 100 shows exterior and interior views of sectioned polar bosses. Figure 101 schematically depicts location of head-to-cylinder section specimens and cylinder section specimens taken from the tanks as well as liner leakage failure sites.

(1) Tanks Pressurized to Burst

Tanks A-3 and A-9 (tested to burst at room and liquid hydrogen temperatures) both failed prematurely due to massive TIG weld repairs made at the polar bosses to solve liner leakage problems during liner fabrication. The TIG welds impeded function of the boss hinge, and caused early failures.

Figure 102 is a photomicrograph taken from a dome of Tank A-3 (see Figure 101) showing the metal liner, glass filament overwrap, and composite craze cracking.

Tank A-1 (tested to 3870 psig or 2670 N/cm^2 and to over 3% biaxial strain at liquid nitrogen temperature) demonstrated one of the highest strength performances of the tanks tested, and had induced in it a high single cycle strain condition in the polar boss. Since the tank did not fail structurally during the test, sections taken from the tank after testing to very high stress and strain conditions were very revealing at showing action of the hinge boss and tank wall membrane. Figure 103 shows the action and excellent condition of the hinge boss after the test.

The tank did not fail at 3870 psig (2670 N/cm^2); it was depressurized and subsequently repressurized until liner failure occurred at 2250 psig (1550 N/cm^2) in the knuckle area of the head just above the head-to-cylinder juncture (Figure 101). Photomicrographs of the wall cross-section at the failure location showing the longitudinally oriented liner break site are shown in Figure 104.

(2) Tanks Pressure Cycled to Failure

Tanks A-11 and A-12 pressure cycled to failure at room temperature failed by leakage after 17 and 25 cycles to about 1.6% strain level and 60% of ultimate strength, with failures located in the

liner at the head area just above the head-to-cylinder juncture (see Figure 101). Photomicrographs of wall cross-sections showing the longitudinally oriented liner break sites are presented in Figures 105 and 106. Figure 107 shows an inside view of the liner of Tank A-11 with the liner fracture clearly evident and parallel liner strain concentration lines running longitudinally, which are spaced about 0.25 to 0.30-in. (0.64 to 0.76-cm) apart, compared with the longitudinal winding tape width of 0.26-in. or 0.66-cm (nominal) used in liner overwinding. The strain concentration sites seem to be located at the edges of the longitudinal winding tape. A similar condition was observed on the liner of Tank A-12.

Tanks A-4 and A-13 were pressure cycled at liquid nitrogen temperature at about 2% strain level and 60% of ultimate strength until liner leakage occurred at 93 and 15 cycles respectively. Liner fractures were longitudinally oriented and located on the head just away from the tank head-to-cylinder juncture for Tank A-4. Figures 108 and 109 show the metal liner fracture in the head near the head-to-cylinder juncture and in the liner cylinder-section adjacent to the girth weld, looking from the inside surface. Figure 110 is a photomicrograph of the dome cross-section at the liner fracture site, and Figure 111 shows the liner failure in the cylinder section. A cross-section of a hinge boss of Tank A-4 is presented in Figure 112, showing satisfactory operation and condition after 93 cycles to 2400 psi (1650 N/cm^2) at -320°F (77°K) and approximately 2% strain level. The failure site for Tank A-13 could not be located in the post failure analysis. Figure 113 does show the inside of the tank end dome at the knuckle with local longitudinal strain concentration sites in the liner clearly evident, spaced about 0.25 to 0.30-in. (0.64 to 0.76-cm) apart (compared with winding tape width of 0.26-in. or 0.66-cm). Figure 114 shows the tank filament-wound composite outside surface with craze cracking similarly spaced.

Tanks A-2 and A-6 were pressure cycled at liquid hydrogen temperature to about 2% strain and 2400 psig (1650 N/cm^2) until liner leakage failure occurred at 97 and 75 cycles respectively. Figure 115 indicates the end dome metal liner failure for Tank A-2 looking from the inside surface after the cycling test (note work hardening in liner). Wall section photomicrographs were of similar appearance to those already presented. Figure 116 presents the hinge boss cross-section from Tank A-6 after 75 cycles to 2400 psig (1650 N/cm^2) at -423°F (20°K) and 2.10% strain level, indicating its satisfactory operation.

b. Test Temperature Effect On Ultimate Filament Strength of Pressure Vessels

Single cycle burst test data obtained from both series of pressure vessels (HB/BWB and A) were grouped together for evaluation of the temperature effect on pressure vessel filament strength. Appendix H presents the methods used to calculate filament stresses and includes sample

calculations to show their application. It should be noted that the analysis considers the loads carried by the metal liner and oriented filaments in both directions. Results of calculations based on the analysis of Appendix H are recorded in Tables 12, 13, 18, and 19 for the HB/BWB and A series vessels, respectively.

Hoop and longitudinal filament stresses for all vessels burst are shown in Figures 117 and 118, respectively, as a function of the test temperature. At ambient temperature, vessels exhibited an average ultimate strength of 380 000 psi ($262\ 000\ N/cm^2$) in the hoop filaments and 317 000 psi ($219\ 000\ N/cm^2$) in the longitudinal filaments.

At the liquid nitrogen (LN_2) test temperature, Figures 117 and 118 indicate a 40% increase in the strength of both hoop and longitudinal filaments. The average ultimate strength was 532 000 psi ($367\ 000\ N/cm^2$) in the hoop filaments and 444 000 psi ($306\ 000\ N/cm^2$) in the longitudinal filaments. Although only one burst data point was available to establish the LN_2 strength, Tank A-1, which did not fail, due to test system limitations, exhibited stress levels of 497 000 psi ($343\ 000\ N/cm^2$) in the hoop filaments and 415 000 psi ($286\ 000\ N/cm^2$) in the longitudinal filaments.

c. Pressure vs Strain Characteristics

Pressure vs strain data recorded for the cylindrical section of all vessels tested during the program generally showed uniform hoop and longitudinal strains very close to those predicted by the design analysis.

Raw data obtained for the end-to-end deflection of Vessel A-12 during application of the second fatigue cycle indicated a 2.17% overall maximum strain (corresponds to 1800 psi or $1240\ N/cm^2$) in comparison to a 1.32% longitudinal strain for the cylinder section. During peak pressure on the 10th and 25th cycle, the total strain of the vessel was 2.28% and the longitudinal strain of the cylinder was 1.38%. Thus, at ambient temperature and the 60% load level the 21.7-in.-(55.1-cm) long vessel deflected approximately 1/2 inch or 1.27 cm while the cylinder elongated 1/10 inch or 0.25 cm.

Although vessel deflection data were uniform for load cycles greater than one (Tank A-12), first cycle deflection data obtained from the ambient single cycle burst test of Tank A-3 indicated the heads of the vessel were actually contracting during the initial states of pressurization. The overall effect was a zero net deflection of the vessel up to approximately 1500 psi ($1030\ N/cm^2$) and then uniform deflection up to the burst pressure of 2250 psi ($1550\ N/cm^2$). The non-uniformity of vessel deflection during initial stages of the first pressure cycle and the uniformity of data for subsequent pressure cycles is probably due to orthotropic

behavior of the glass/resin composite prior to resin fracture (crazing).

d. Cyclic Fatigue Life

Hoop and longitudinal filament failure stresses for all vessels (BWB/HB and A series) subjected to single cycle and cyclic fatigue loading tests at ambient and cryogenic temperatures are shown in Figures 119 and 120, respectively, as a function of the number of cycles to cause failure. As previously discussed, three of the single cycle vessels exhibited failure of the composite and four were liner failures (Vessel A-1 failed on second burst attempt cycle); all cyclically loaded vessels failed by liner leakage.

Since all vessels subjected to fatigue loading failed in the metal liner, the works of Manson (Reference 28) and Coffin (Reference 29) on metal fatigue in the low-cycle range (1/4 to 1000 cycles) were reviewed for application to these vessels. According to numerous investigators low-cycle fatigue of metals is governed by the cyclic plastic strain range, and the power law relation between cyclic life (N_f) and uniaxial plastic strain range ($\Delta\epsilon_p$) proposed by both Manson and Coffin in the form

$$\Delta\epsilon_p = MN_f^Z$$

has been amply verified. Before this relation could be applied to the metal liners tested on this program, the material constants, M and Z, for annealed 1100 aluminum had to be determined as well as a correction factor for the 1:1 biaxial strain conditions existing in the tank liner.

Manson, in Reference 28, experimentally evaluated the material constants for 1100 aluminum, but later found the material to be in the H12 condition rather than the annealed condition. Coffin, in the discussion section of Reference 28, provided his own experimental data and showed an excellent curve fit using room temperature values of 0.85 for the material coefficient M and -0.5 for the exponent Z. Coffin's resulting equation for uniaxial strain range as a function of cycles to failure was

$$\Delta\epsilon_p = 0.85 N_f^{-0.5}$$

Ives, et.al. (Reference 30) compared equibiaxial strain (equibiaxial stress) fatigue data with uniaxial strain (imparted by 2:1 biaxial stress) fatigue data in terms of an equivalent strain. The equivalent strain may be defined as the axial strain of a specimen subjected to a uniaxial load (1:0 biaxial stress). Their theoretically derived value for equivalent strain was found to be twice the measured biaxial strain for equibiaxially stressed specimens and 1.155 times the measured axial strain for 2:1 biaxially stressed specimens. The resulting correlation of experimentally obtained room temperature strain data for various steels in the 10^2

to 10^5 cycle range was very good.

Based on the above discussion, the maximum 1:1 cyclic strain levels, which were average tank cylinder surface strains measured over a long gage length, (see Tables 13 and 19) for all vessels subjected to fatigue loading were converted to equivalent strain by multiplying the values by a factor of two; the resulting equivalent strains for the tanks are shown in Figure 121 as a function of cyclic life. The previously described Coffin relation for 1100 aluminum at room temperature has also been included in the figure for comparison. All test data fall below the Coffin curve which indicates a greater cyclic potential for the metal liners than was realized.

However, it should be noted that the vessels did not fail in the cylinder section where strain was recorded, but generally in the vessel domes just away from the head-to-cylinder juncture. As such, the data in Figure 121 are not failure strains for the section being measured. These low test values are probably caused by very local high magnitude strain concentrations at the failure sights of the domes (as discussed in Section IV-C-3-a); as described there, the location and orientation of metal liner dome fractures appeared to coincide with resin craze planes in the filament-wound composite. Based on the Coffin curve, elimination of strain magnification sights in the domes should increase the cycle life of metal liners in the tanks to 400 - 1000 cycles for the 60% load level.

e. Pressure Vessel Performance

The pressure vessel performance factors ($p_b V_o / W$) shown in Table 20 were computed from measured values of burst pressure (p_b), internal volume (V_o) and total tank weight (W) except as noted in the table. The data from all single cycle burst strength determinations (HB, BWB, and A series) are included in the table; leak type failures are not representative and have been excluded from the table. It should be noted, the units of performance factor were not reduced to the usual standard in. notation, but instead were retained in the form in.-lbf/lbm* to depict vessel efficiency by relating the capability of the pressure vessel to store energy (in-lbf or joules) to the container weight penalty (lbm or grams).

The average room temperature burst performance factor was 0.73×10^{-6} in-lbf/lbm (182 J/g) and at -320°F (77°K) was 1.01×10^{-6} in-lbf/lbm (251 J/g). The maximum deviation from the average performance factors at the two temperatures was only 2.7%.

* 1×10^6 in-lbf/lbm = 249 joules/gram (J/g)

The thin aluminum-lined glass-filament-wound vessels demonstrated considerable weight savings as compared with homogeneous metal construction. For example, 2219-T87 aluminum and Inconel 718 (STA) homogeneous metal pressure vessels have the following maximum theoretical performance factors at room temperature:

Material	<u>Vessel Performance Factor, $p_b V_o / W$</u>			
	<u>Sphere</u>		<u>Cylinder</u>	
	<u>in.-lbf/lbm</u>	<u>J/g</u>	<u>in.-lbf/lbm</u>	<u>J/g</u>
2219-T87 Aluminum	0.41×10^6	102	0.30×10^6	75
Inconel 718 (STA)	0.42	105	0.31	77

In comparison with these metal vessel weights for a given $p_b V_o$ capability, the composite tanks weigh only 40 to 55% of the 2219-T87 or Inconel 718 (STA) tanks, depending on shape of the metal tanks. In addition to weight savings, the aluminum-lined glass-filament-wound tanks offer the following advantages:

- Increased packaging density with no weight penalty; vessel shape not restricted to spheres for minimum weight, as composite vessels of spherical, spheroidal, and cylindrical shape all have about the same $p_b V_o / W$ performance factor.
- Leakage failure mode, without fragmentation or shatterability.
- Improved reliability through safety factor increase.

The table below compares the efficiency of the 12-in.-(30.5-cm-) dia. by 18-in.-(45.7-cm-) long S-glass/epoxy filament-wound composite tanks fabricated during this program with tanks constructed from other fiber reinforced composites; performance factors based on composite weight without metal liners or bosses have been used in the table to show a direct comparison of filament-wound composite material efficiency.

Test Environment	<u>Maximum Demonstrated Filament-Wound Composite Vessel Performance Factors</u>					
	<u>S-Glass/Epoxy</u>		<u>Boron/Epoxy (Reference 31)</u>		<u>Graphite/Epoxy (Reference 32)</u>	
	<u>in-lbf/lbm</u>	<u>J/g</u>	<u>in-lbf/lbm</u>	<u>J/g</u>	<u>in-lbf/lbm</u>	<u>J/g</u>
Ambient	0.95×10^6	237	0.72×10^6	179	$0.37 -$	0.47×10^6 92-117
Liquid Nitrogen	1.37	341	0.47	117	0.32 - 0.41	80-102
Liquid Hydrogen	--	--	0.63	157	0.34 - 0.46	85-115

All of the graphite/epoxy and boron/epoxy pressure vessels were 8-in.-(20.3-cm-) dia. by 13-in.- (33.0-cm-) long and incorporated thin stainless steel foil liners. The performance and weight saving advantage of glass filaments over boron and the various currently available forms of graphite filaments is evident from the table. The primary disadvantage of S-glass filaments is the high strain levels associated with their high efficiency; these strains greatly tax the capability limits of the thin metal liners especially during fatigue cycling.

A comparison of the three composite materials, in terms of vessel weight, was obtained by applying the corresponding maximum performance factors to a 500 in³ (8200 cm³) vessel approximately 8-in.- (20.3-cm-) dia. by 12-in.- (30.5-cm-) long designed for a burst pressure of 3000 psi (2070 N/cm²) at ambient temperature. The resulting weight of the S-glass/epoxy composite was 1.6 lbm (720 g) as compared to a boron/epoxy composite weight of 2.1 lbm (950 g) and a graphite/epoxy composite weight of 3.2 lbm (1450 g). The required additional metal hardware weight would be the same for all three types of vessels.

V. CONCLUSIONS AND RECOMMENDATIONS

A. The principal objective of the program --to demonstrate the feasibility of producing closed-end, cylindrical, glass-filament-wound pressure vessels with thin (0.010-in.--or 0.254-mm-thick) aluminum liners for operation in the 75° F (297° K) to -423° F (20° K) temperature range--was accomplished.

B. Significant developments and advancements were made in solving past problems with thin-metal-lined glass filament-wound vessels. The work provided further demonstration of the ability of the bond between the liner and the overwrapped composite to keep the liner from buckling during high strain range vessel pressure cycling, and of the ability of the bond to maintain its strength and integrity until failure of the metal liner by high strain range fatigue. The problem of strain magnification in the metal liner near the vessel polar bosses was solved by development of a novel "hinge boss" design configuration.

C. Initial material, process, fabrication, and vessel test evaluations lead to the following conclusions associated with aluminum liners:

1. The best ductility capability for the aluminum sealant liners to operate at ambient to LH₂ temperatures was provided by type 1100 aluminum.

2. TIG welding the thin aluminum liner joints to meet the design objectives of weld properties, quality, and geometry was not successful. Electron-beam welding of the joints, however, eliminated or greatly reduced the problems encountered in TIG welding, and resulted in weld joints which did meet design objectives.

D. Better understanding of the critical nature of the polar boss-to-liner membrane transition, the mismatch of deflections there, and the strain magnifications known to exist in this region due to the rigidity of boss designs usually employed and the extensibility of the glass-filament-wound composite on top of the boss flange was obtained from extensive structural analysis of the vessel polar port area. Detailed investigation of the end domes of the metal-lined glass-filament-wound vessel configuration studies under this program in the vicinity of the axially located polar bosses resulted in the following theoretical observations:

1. Analysis of the membrane portion of the vessel indicated that below the resin crazing threshold (25% ultimate load), where orthotropic behavior dominates, meridional strains increased in value as the port was approached reaching a maximum value 50% greater than the strain at the equator; above the resin crazing threshold, where deformations can be predicted by netting theory, meridional strain was essentially constant over the entire dome.

2. Discontinuity analysis of the filament-wound composite shell at the boss-flange to membrane juncture indicated that radial deflection was independent of the flange bearing load (distributed or concentrated) and its position for the range of parameters investigated; rotational effects were strongly influenced by the magnitude and point of application of the bearing load. Any mismatch in rotation of mating aluminum and filament-wound composite structural components indicated potentially large shear-distortion effects which could induce peal action and eventual destruction of the aluminum-to-composite adhesive bond.

E. Several polar boss design concepts were developed and evaluated using results of the efforts described in C. and D. above, resulting in selection of improved vessel configurations for further study. One of these incorporated a "hinge boss" in which pressure in the vessel is used to expand the 1100 aluminum liner past yield plastically against the opening in the filament-wound composite dome. The liner is flexible up to the opening and in the opening, and thickens as it exits from the opening in the filament-wound composite; a high strength aluminum alloy boss member is provided which takes out boss reaction loads but which does not impede the hinge action of the liner at the boss.

F. The fifteen 12-in.-(30.5-cm-) dia. by 18-in.-(45.7-cm-) long 1100 aluminum-lined improved configuration pressure vessels that were fabricated and tested demonstrated burst strengths and strain-vs-pressure characteristics predicted by the design analysis. The following conclusions were drawn from these tests:

1. The adhesive/scrim cloth bonding system maintained a bond between the aluminum liner and the filament-wound composite shells during all burst and cyclic fatigue tests at ambient to liquid hydrogen temperatures.

2. The hinge boss design exhibited impermeability to fluids and strain compatibility between aluminum parts and the filament-wound composite during burst and cyclic fatigue tests at ambient to liquid hydrogen temperatures.

3. At ambient temperature, vessels achieved their design burst strength of 3000 psi (2070 N/cm^2), and exhibited an average ultimate strength of 380 000 psi ($262 000 \text{ N/cm}^2$) in the hoop filaments and 317 000 psi ($219 000 \text{ N/cm}^2$) in the longitudinal filaments.

4. At the liquid nitrogen test temperature both hoop and longitudinal filaments had a 40% increase in strength to 532 000 psi ($367 000 \text{ N/cm}^2$) for the hoop filaments and 444 000 psi ($306 000 \text{ N/cm}^2$) for the longitudinal filaments which is consistent with values obtained in previous evaluations and by other investigators with smaller and simpler test vessels.

5. Generally, all vessels subjected to cyclic fatigue tests failed by local fracture in the aluminum liner portion of the vessel dome just above the head-to-cylinder juncture; fractures in the liner were due to high strain range fatigue of the metal, and appeared to coincide with resin craze planes in the filament-wound composite. Failure analysis showed strain concentration lines in the liner domes in the head-to-cylinder junction region running parallel to the direction of the longitudinal wrap, and spaced the same as the longitudinal filament-winding tape width. The strain concentration sites seemed to be located at the edges of the longitudinal winding tape.

6. Vessel failure mode under cyclic fatigue conditions always consisted of leakage, without any structural failure of the vessel whatsoever. The maximum number of pressure cycles achieved by vessels when pressurized between 0 and 60% of burst strength prior to liner fracture was 97 at the liquid hydrogen test temperature.

7. Comparison of vessel liner fatigue life to published data for low-cycle, high-strain-range fatigue of simple 1100 aluminum specimens, on an equivalent (uniaxial) strain basis, indicated that elimination of strain magnification sights in the domes should increase the cyclic life of the aluminum liners to 400 to 1000 cycles at the 60% load level.

8. Pressure vessel performance comparisons, based on single cycle burst strength, showed that glass filament-wound vessels had a much higher demonstrated weight efficiency than metal vessels and similar boron and the various forms of graphite filament-wound vessels. More specifically, the weight of the glass filament-wound vessels is only 40 to 55% that of homogeneous 2219-T87 aluminum or Inconel 718 spherical and cylindrical vessels having the same burst pressure and volume.

E. Additional studies of metal-lined glass-filament-wound pressure vessels are recommended to further improve designs and processes, for fabricating thin metal liners and vessels to attain increased cyclic fatigue life and greater vessel reliability. The areas of investigation should include:

1. Definition of design approaches improving liner and end-fitting fabrication approaches and reliability, as well as reducing scrap rates, reworks, and costs of the thin walled fragile liner assemblies.

2. Improvement of the cyclic fatigue performance of the thin metal-lined portion of the glass-filament-wound pressure vessels.

3. The definition of new and novel end-fitting designs that provide for maximum biaxial extensibility and compatibility with liner materials and fabrication processes.

4. Demonstration of reliability of the tanks via a complete qualification test program.

REFERENCES

1. Glass Filament Reinforced Homogeneous Chambers. Aerojet Report MF-546, 25 March 1964.
2. Odell, C. N.; and Albert, W. E.: The Filament-Reinforced Motor Case. Aerospace Engineering Magazine, April 1962.
3. Preliminary Development Studies of Glass Filament-Wound Cryogenic Tankage. Aerojet-General Report No. 2445 (Special), December 1962.
4. Thermal Shock Tests of Glass-Filament-Wound All-Fiberglass Reinforced-Plastic Cryogenic Sandwich Specimens. Aerojet-General Report No. 2471 (Special), February 1963.
5. Fatigue Test of Patterned Low-Stress Metallic Liner for Glass Filament-Wound Liquid-Propellant Tankage. Aerojet-General Report No. 2490 (Special), February 1963.
6. Design and Fabrication of an Internally Insulated Filament-Wound LH₂ Tank. NASA CR-127, November 1964.
7. Heidelberg, L. J.: Evaluation of a Subscale Internally Insulated Fiberglass Propellant Tank for LH₂. NASA TN-D-3068, October 1965.
8. Hanson, M. P.; et al: Preliminary Investigation of Filament-Wound Glass-Reinforced Plastics and Liners for Cryogenic Pressure Vessels. NASA TN-D-2741, 1965.
9. Frischmuth, R. W., Jr.: Investigation of Thin Films as Floating Liners for Fiberglass Cryogenic Propellant Tanks. NASA TN-D-3205, January 1966.
10. Frischmuth, R. W., Jr.: Experimental Investigation of Glass Flakes as a Liner for Fiberglass Cryogenic Propellant Tanks. NASA TM-X-1193, January 1966.
11. Design Improvements in Liners for Glass-Fiber Filament-Wound Tanks to Contain Cryogenic Fluids. NASA CR 54-854, Aerojet-General Corporation, January 1966.
12. Sanger, M. J.; and Molho, R.: Exploratory Evaluation of Filament-Wound Composites for Tankage of Rocket Oxidizers and Fuels. AFML-TR-65-381, Aerojet-General Corporation, October 1965.
13. Sanger, M. J.; Molho, R.; and Morris, E. E.: Stainless Steel Lined Glass Filament-Wound Tanks for Propellant Storage. AFML-TR-66-264, Aerojet-General Corporation, December 1966.

14. Molho, R.; and Soffer, L. M.: Cryogenic Resins for Glass Filament-Wound Composites. NASA CR-72114, Aerojet-General Corporation, January 1967.
15. Morris, E. E.; Darms, F. J.; Landes, R. E.; and Campbell, J. W.: Parametric Study of Glass-Filament-Reinforced Metal Pressure Vessels. NASA CR 54-855, Aerojet-General Corporation, April 1966.
16. Darms, F. J.; and Landes, R. E.: Computer Program for the Analysis of Filament-Reinforced Metal-Shell Pressure Vessels. NASA CR-72124, Aerojet-General Corporation, May 1966.
17. Morris, E. E.: Glass-Fiber-Reinforced Metallic Tanks for Cryogenic Service. NASA CR-72224, Aerojet-General Corporation, June 1967.
18. Lewis, A.; and Bush, G.: Improved Cryogenic Resin/Glass-Filament-Wound Composites. NASA CR 72163, Aerojet-General Corporation, April 1967.
19. Toth, J. M.; et al: Investigation of Structural Properties of Fiber-glass Filament-Wound Pressure Vessels at Cryogenic Temperatures. NASA CR 54393, Douglas Aircraft Company, September 1965.
20. Toth, J. M.; et al: Investigation of Smooth-Bonded Metal Liners for Glass Fiber Filament-Wound Pressure Vessels. NASA CR 72165, Douglas Aircraft Company, May 1967.
21. Hanson, M. P.: Glass, Boron, and Graphite Filament-Wound Composites and Liners for Cryogenic Pressure Vessels. NASA TM-X-52350, April 1967.
22. Hanson, M.P.: Tensile and Cyclic Fatigue Properties of Graphite Filament-Wound Pressure Vessels at Ambient and Cryogenic Temperatures. NASA TM-X-52539, April 1969.
23. Hanson, M.P.: Static and Dynamic Fatigue Behavior of Glass Filament-Wound Pressure Vessels at Ambient and Cryogenic Temperatures. NASA TN-D-5807, May 1970.
24. Johns, R. H.; and Kaufman, A.: Filament-Overwrapped Metallic Cylindrical Pressure Vessels. NASA-LeRC, in Journal of Spacecraft, July 1967.
25. Development of a Filament-Overwrapped Cryoformed Metal Pressure Vessel. NASA CR-72753, Arde, Inc, January 1971.
26. Composite Overwrapped Metallic Tanks. Contract NAS 3-12023 with Martin Marietta Corporation (work in progress).

27. Landes, R.E.; and Morris, E. E.: Analysis of Filament-Wound Dome and Polar Boss of Metal-Lined Glass Filament-Wound Pressure Vessels. NASA CR-72599, Aerojet-General Corporation, January 1970.
28. Manson, S.S.; and Hirschberg, M. H.: Fatigue Behavior in Strain Cycling in the Low and Intermediate-Cycle Range. Fatigue- An Interdisciplinary Approach; Proceedings of the Sagamore Army Materials Research Conference, Raquette Lake, N.Y., August 1963, Syracuse University Press, 1964.
29. Tavernelli, J. F.; and Coffin, L. F.: Experimental Support for Generalized Equations Predicting Low-Cycle Fatigue. Journal of Basic Engineering, Trans. ASME, Series D, December 1962.
30. Ives, K.D.; Kooistra, L. F.; and Tucker, J. T.: Equibiaxial Low-Cycle Fatigue Properties of Typical Pressure-Vessel Steels. Journal of Basic Engineering, Trans. ASME, December 1966.
31. Cycle Test of Boron Filament-Wound Vessels. Contract NAS 3-12006, with Aerojet-General Corporation (work in progress).
32. Morris, E. E.; and Alfring, R. J.: Closed-End Cylindrical Graphite Filament-Wound Vessels. Aerojet Report 3779 to NOL under Contract N60921-16-C0021, August 1969.

TABLE 1
 EFFECT OF CRYOGENIC-TEMPERATURE EXPOSURE ON WELDED 6061-0 ALUMINUM ALLOY

Type Of Specimen (a)	Test Temperature °F	Test Temperature °K	Tensile Strength psi	Tensile Strength N/cm ²	Yield Strength psi	Yield Strength N/cm ²	Elongation % in 2 in (5.08 cm)	Fracture Location
Parent Metal	75	297	19 700	13 600	7800	5400	24.5	Within gage length
Parent Metal	75	297	19 000	13 100	8400	5800	21.5	Center of gage length
Welded	75	297	19 500	13 400	8100	5600	17.5	Parent metal - within gage length
Welded	75	297	19 500	13 400	8300	5700	17.5	Parent metal - within gage length
Welded	75	297	19 500	13 400	7900	5400	17.5	Parent metal - within gage length
Welded	-320	77	34 600	23 900	11 100	7700	31.5	Parent metal - within gage length
Welded	-320	77	34 600	23 900	11 600	8000	31.5	Center of weld
Welded	-320	77	35 300	24 300	12 300	8500	34.5	Parent metal - within gage length
Welded	-423	20	53 700	37 000	12 000	8300	24.0	Parent metal at extensometer mark
Welded	-423	20	57 500	39 600	-	-	40.5	Parent metal - no extensometer
Welded	-423	20	45 700 ^b	31 500	14 300 ^b	9900	13.0 ^b	Failed in weld

a Specimens were 0.031-in.-(0.079-cm)-thick, fusion-butt-welded without filler wire;
 Welds were planished and then specimens annealed at 775°F (686°K), cooled at 50°F/hr (28°K/hr)
 to 500°F (533°K), and then air-cooled to room temperature from 500°F (533°K).

b Weld joint apparently had defect not visually detectable.

TABLE 2

PEEL ADHESION TEST RESULTS
0.010-IN-THICK 6061 ALUMINUM BONDED^a TO GLASS FILAMENT COMPOSITE^b

Nylon Scrim Cloth	Elevated Temperature Cure (c)	Specimen Number	Test Temperature °K	T-Peel		180° Peel N/cm
				°F	1bf/in	
JP Stevens S-1852-2-400	4 hours at 300°F (420°K)	PA-1-1	75	297	22	38.5
		PA-1-2			25	43.8
		Average		23.5	41.1	22.5
	6 hours at 300°F (420°K)	PA-2-1	75	297	20	35.0
		PA-2-2			20	35.0
		PA-2-3			26	45.5
		Average		22	38.5	21.7
	8 hours at 250°F (390°K)	PA-3-1	75	297	12	21.0
		PA-3-2			15	26.3
		PA-3-3			23	40.3
		Average			16.6	29.1
						14.8
						26.0

^a Adhesive Bond System: Adiprene L-100/Epirez 5101/MOCA (80/20/17 pbw) with indicated nylon scrim cloth

^b Composite: 181 glass cloth impregnated with Epon 828/Empol 1040/DSA/BDMA (100/20/115.9/1.0 pbw); 1.00-in.-(2.54-cm-) wide

^c Cure: 16 hours at ambient temperature, 1 hour at 150°F (340°K), plus indicated elevated temperature cure

TABLE 2 (cont.)

Nylon Scrim Cloth	Elevated Temperature Cure	Specimen Number	Test Temperature °F °K	T-Peel		Peel Strength 180° Peel N/cm	
				1bf/in	N/cm	1bf/in	N/cm
JP Stevens S-1852-2-400	16 hours at 250°F (390°K)	PA-4-1	75 297	14	24.5	14	24.5
		PA-4-2		10	17.5	10.5	18.4
		PA-4-3		11	19.3	10	17.5
		Average		11.6	20.4	11.5	20.1
34168-2	24 hours at 250°F (390°K)	PA-5-1	75 297	22	38.5	14	24.5
		PA-5-2		22	38.5	18	31.5
		PA-5-3		20	35.0	20	35.0
		Average		21.3	37.3	17.3	30.3
	8 hours at 250°F (390°K)	1	75 297	15	26.3		
		2		26	45.5	—	—
		3		20	35.0		
		Average		20.3	35.6		
		4	-320	77	8	14.0	
		5		10	17.5	—	—
		6		11	19.3		
		Average		9.7	16.9		
		7	-423	20	17.5	30.6	
		8		18	31.5	—	—
		9		17	29.8		
		Average		17.5	30.6		

Table 2, Sheet 2 of 3

TABLE 2 (cont.)

Nylon Scrim Cloth	Elevated Temperature Cure	Specimen Number	Test Temperature °F °K	Peel Strength				
				1bf/in	N/cm	1bf/in	N/cm	
34168-2	4 hours at 300°F (420°K)	10	75	297	18	31.5		
		11			18.5	32.4	-	
		12			15	26.3	-	
		<u>Average</u>			<u>17.2</u>	<u>30.1</u>		
		13	-320	77	23.5	41.1		
		14			11	19.3	-	
	12 hours at 300°F (420°K)	15			16	28.0	-	
		<u>Average</u>			<u>16.8</u>	<u>29.5</u>		
		16	-423	20	18	31.5		
		17			6.5	11.4	-	
		18			35	61.3	-	
		<u>Average</u>			<u>19.8</u>	<u>34.7</u>		
		1	75	297	16.5	28.9		
		2			26	45.5	-	
		3			18	31.5	-	
		<u>Average</u>			<u>20.2</u>	<u>35.3</u>		

TABLE 3
LINER FABRICATION SEQUENCE

<u>1100 Aluminum Liner</u>	<u>6061 Aluminum Liner</u>
Cut blank from 1/8-inch (0.32-cm) sheet.	Cut blank from 1-inch (2.54-cm) plate
Form contour and anneal half shells.	Upset plate for boss projection and machine membrane to 1/8-inch (0.32-cm) (except at boss).
Cut hole for boss installation.	Anneal preform.
Machine to preweld configuration (membrane thickness of 0.030-inch (0.076-cm) approx. except at weld joint).	Form contour and anneal half shells.
Reduce membrane to 0.012-inch (0.305-mm) by chemical milling, except at weld joint area.	Solution treat and age to T6 condition.
Adhesively bond boss into dome of each liner half shell.	Machine to preweld configuration (membrane thickness of 0.030-inch or 0.076-cm approx., except at boss and weld joint).
Machine half shell girth weld joints.	Reduce membrane to 0.010-inch (0.254-mm) by chemical milling, except at boss and weld joint area.
Girth closure weld half shells.	Machine half shell girth weld joints.
Remove excess metal at weld joint.	Girth closure weld half shells.
Planish girth weld seam.	Remove excess metal at weld joint.
Final machine weld seam.	Planish girth weld seam.
Locally anneal weld joint, chemically mill to 0.010-in.-(0.254-mm-) thickness.	Final machine weld seam.
Weld extensions on both bosses.	Anneal membrane area (except bosses).
Clean and inspect liner assembly.	Clean and inspect liner.

Table 3

TABLE 4
**MECHANICAL PROPERTIES OF 6061 ALUMINUM LINER
 CYLINDER SECTION, INITIAL ANNEALING PROCEDURE**

Specimen No.	Type Specimen	Specimen Thickness (a) in mm	Tensile Strength psi N/cm ²	Yield Strength psi N/cm ²	Elongation, %				Remarks	
					2-in. (5.08-cm)	1-in. (2.54-cm)	1/2-in. (1.27-cm)	1/4-in. (0.635-cm)		
1	Longitudinal Cylinder Membrane	0.0075 0.0080 0.0070	0.191 0.203 0.178	10,400 12,700 12,000	7200 8750 8300	8200 8200 8000	5700 5700 5500	1.5 3.0 3.5	2.0 4.0 6.0	3.0 5.0 8.0
2										
3										
4										
<u>Average</u>		<u>0.0075</u>	<u>0.191</u>	<u>11,550</u>	<u>8000</u>	<u>8200</u>	<u>5700</u>	—	—	<u>10.0</u>
5	Circumferential Cylinder Membrane	0.0070 0.0060 0.0088	0.178 0.152 0.224	12,400 11,700 12,700	8500 8100 8750	8600 8500 7600	5900 5850 5200	2.5 4.5 5.5	3.5 6.0 6.0	7.0 7.0 7.0
6										
7										
8										
<u>Average</u>		<u>0.0076</u>	<u>0.193</u>	<u>12,400</u>	<u>8550</u>	<u>8370</u>	<u>5770</u>	—	—	<u>8.8</u>

^a Specimen thickness varied 10% along specimen gage length, and value given is minimum; failure generally occurred at thinnest section.

^b Not included in average.

TABLE 5

MECHANICAL PROPERTIES OF 6061 ALUMINUM LINER
DOME SECTION, INITIAL ANNEALING PROCEDURE

Specimen No.	Specimen Thickness In. cm	Tensile Strength		Yield Strength N/cm ²	Elongation, %		
		psi	N/cm ²		2-in (5.08-cm) (2.54-cm)	1-in (2.54-cm) (1.27-cm)	1/2-in (1.27-cm) (0.635-cm)
9	0.0180	0.0457	35 400	24 400	32 800	22 600	2.0
14	0.0172	0.0437	37 500	25 900	35 200	24 300	1.7
Average	<u>0.0176</u>	<u>0.0447</u>	<u>36 500</u>	<u>25 200</u>	<u>34 000</u>	<u>23 500</u>	<u>—</u>
10	0.0170	0.0432	24 400	16 800	18 300	12 600	5.0
15	0.0182	0.0462	26 100	18 000	21 100	14 500	5.0
Average	<u>0.0176</u>	<u>0.0447</u>	<u>25 300</u>	<u>17 400</u>	<u>19 700</u>	<u>13 600</u>	<u>—</u>
11	0.0175	0.0445	21 400	14 800	13 700	9400	6.5
16	0.0165	0.0419	21 400	14 800	12 600	8700	7.5
Average	<u>0.0170</u>	<u>0.0432</u>	<u>21 400</u>	<u>14 800</u>	<u>13 150</u>	<u>9100</u>	<u>—</u>
12	0.0155	0.0394	19 000	13 100	10 900	7500	10.0
17	0.0165	0.0419	17 800	12 300	10 500	7200	9.0
Average	<u>0.0160</u>	<u>0.0406</u>	<u>18 400</u>	<u>12 700</u>	<u>10 700</u>	<u>7350</u>	<u>—</u>
13	0.0160	0.0406	16 900	11 700	10 400	7200	9.0
18	0.0165	0.0419	16 100	11 100	9700	6700	10.0
Average	<u>0.0163</u>	<u>0.0413</u>	<u>16 500</u>	<u>11 400</u>	<u>10 050</u>	<u>6950</u>	<u>—</u>

Table 5

TABLE 6

MECHANICAL PROPERTIES OF 6061 ALUMINUM LINER
DOME SECTION, MODIFIED ANNEALING PROCEDURE

Specimen No.	Specimen Thickness In cm	Tensile Strength		Yield Strength psi N/cm ²	Elongation, %					
		psi	N/cm ²		2-in. (5.08-cm)	1-in. (2.54-cm)	1/2-in. (1.27-cm)	1/4-in. (0.635-cm)		
1	0.0118	0.0300	30 500	21 000	28 100	19 400	3.2	6.0	10.0	14.0
2	0.0115	0.0292	27 500	19 000	25 600	17 700	3.0	5.0	9.0	14.0
Average	<u>0.0117</u>	<u>0.0296</u>	<u>29 000</u>	<u>20 000</u>	<u>26 800</u>	<u>18 600</u>	<u>3.1</u>	<u>5.5</u>	<u>9.5</u>	<u>14.0</u>
3	0.0122	0.0310	21 200	14 600	13 200	9100	6.0	8.0	9.0	15.0
4	0.0122	0.0310	21 800	15 000	13 300	9200	6.5	8.5	10.0	16.0
Average	<u>0.0122</u>	<u>0.0310</u>	<u>21 500</u>	<u>14 800</u>	<u>13 200</u>	<u>9100</u>	<u>6.3</u>	<u>8.3</u>	<u>9.5</u>	<u>15.5</u>
5	0.0112	0.0284	16 200	11 200	9600	6600	5.0	6.5	8.0	14.0
6	0.0118	0.0300	19 400	13 400	10 700	7400	7.5	9.0	11.0	16.0
Average	<u>0.0115</u>	<u>0.0292</u>	<u>17 800</u>	<u>12 300</u>	<u>10 200</u>	<u>7000</u>	<u>6.3</u>	<u>7.7</u>	<u>9.5</u>	<u>15.0</u>

Table 6

TABLE 7
ROOM TEMPERATURE MECHANICAL PROPERTIES OF 6061 ALUMINUM
WELDED WITH VARIOUS WELD METALS
(SPECIMENS STRESS RELIEVED AFTER WELDING: WELD BEAD LEFT AS-WELDED TO SIMULATE LINER WELD)

Type Weld	Specimen No.	Specimen Thickness		Tensile Strength N/cm ²	Yield Strength N/cm ²	Elongation, %	Failure Location
		Membrane in cm	Weld in cm			1-in. (2.54-cm)	1/2-in. (1.27-cm)
Fusion (no weld wire)	1	0.0138	0.0351	0.0435	0.1105	13 900	8000
	2	0.0138	0.0351	0.0435	0.1105	15 600	10 800
	3	0.0110	0.0279	0.0393	0.0998	12 300	8500
	Average	0.0129	0.0357	0.0421	0.1069	13 900	9600
1100 weld metal	4	0.0145	0.0368	0.0575	0.1461	15 300	10 500
	5	0.0140	0.0356	0.0585	0.1486	14 900	10 300
	6	0.0140	0.0356	0.0565	0.1435	15 500	10 700
	Average	0.0142	0.0360	0.0575	0.1461	15 200	10 500
4043 weld metal	7	0.0135	0.0343	0.0595	0.1511	15 800	10 900
	8	0.0138	0.0351	0.0515	0.1308	15 500	10 700
	9	0.0138	0.0351	0.0515	0.1308	14 400	9900
	Average	0.0137	0.0348	0.0542	0.1376	15 200	10 500
5356 weld metal	10	0.0125	0.0318	0.0675	0.1715	13 000	9000
	11	0.0125	0.0318	0.0595	0.1511	14 300	9900
	12	0.0135	0.0343	0.0570	0.1448	14 800	10 200
	Average	0.0128	0.0326	0.0613	0.1558	14 000	9700
None-parent metal specimen	1	0.0100	0.0254	-	-	14 600	10 100
	2	0.0105	0.0288	-	-	14 300	9900
	3	0.0103	0.0262	-	-	12 800	8800
	Average	0.0103	0.0262	-	-	13 900	9600

Table 7

TABLE 8
TENSILE PROPERTIES OF EB WELD SPECIMENS
OF 1100-O ALUMINUM
(WELD TRANSVERSE TO SPECIMEN AXIS)

Type Specimen	Specimen No.	Thickness		Tensile Strength		0.2% Yield Strength		Elongation, %		Failure Location		
		At Weld in	In Membrane cm	psi	N/cm ²	psi	N/cm ²	2-in. (2.54-cm) 1/2-in. (5.08-cm) 1-in. (2.54-cm) 1/4-in. (0.635-cm)				
Transverse Welded/As-welded	2-1	-	0.0118	0.0300	10 500	7250	5000	3450	11.5	21.0	32.0 Parent Metal	
	2-1A	-	0.0125	0.0318	10 600	7300	4900	3400	12.0	15.0	32.0 Parent Metal	
	2-2	0.0240	0.0610	0.0292	10 400	7200	3400	2350	9.0	15.0	28.0 Parent Metal	
	2-3	0.0245	0.0622	0.0268	9300	6400	3600	2500	6.5	12.5	28.0 Parent Metal	
	2-4	0.0250	0.0635	0.0305	10 700	7400	3400	2350	16.5	20.5	30.0 Parent Metal	
Transverse Welded/Weld Dress After Welding	1-5	0.0125	0.0318	0.0112	0.0284	10 800	7450	5200	3600	15.0	13.0	20.0 HAZ
	1-6	0.0120	0.0305	0.0111	0.0282	10 500	7250	4900	3400	14.0	16.0	17.0 HAZ
	1-7	0.0125	0.0318	0.0110	0.0279	10 400	7200	4800	3300	10.5	13.0	20.0 Parent Metal
	1-7A	-	0.0113	0.0287	-	-	-	-	13.0	15.0	20.0 Parent Metal	

Table 8

TABLE 9

TENSILE PROPERTIES OF 2219-T62 TO 1100-H14 ALUMINUM EB WELDS
(WELD TRANSVERSE TO SPECIMEN AXIS)

Specimen No. (a)	0.2% Yield Strength		Ultimate Strength (b)		Elongation, %			
	psi	N/cm ²	psi	N/cm ²	2-in. (5.08-cm)		1-in. (2.54-cm)	1/2-in. (1.27-cm)
					2-in. (5.08-cm)	1-in. (2.54-cm)	1/2-in. (1.27-cm)	1/4-in. (0.635-cm)
H-1	14 700	10 100	15 700	10 800	2.2	4.5	9.0	16.0
H-2	15 900	11 000	17 000	11 700	2.5	5.0	9.0	16.0
H-4	17 300	11 900	18 600	12 800	2.5	5.0	9.0	16.0
5-1	15 300	10 500	17 700	12 200	2.5	5.5	10.0	18.0
5-2	16 400	11 300	23 800	16 400	2.5	5.0	10.0	18.0
5-3	16 200	11 200	18 100	12 500	2.5	5.0	10.0	18.0
5-4	15 300	10 500	17 000	11 700	2.5	5.0	10.0	18.0
D-1	14 900	10 300	16 200	11 200	2.5	5.0	10.0	18.0
D-2	15 000	10 350	16 200	11 200	2.5	5.0	10.0	18.0
D-3	14 900	10 300	16 200	11 200	2.5	5.0	10.0	16.0
D-4	15 700	10 800	16 700	11 500	2.5	5.0	10.0	18.0
4-1	15 500	10 700	17 100	11 800	2.5	5.0	10.0	18.0
4-4	15 500	10 700	17 200	11 850	2.5	5.0	10.0	18.0
4-3	15 800	10 900	17 300	11 900	2.5	5.0	10.0	18.0
4-4	15 700	10 800	17 300	11 900	2.5	5.0	10.0	18.0

a

Specimen thickness 0.0405 in (0.1029 cm)

b

Failure location was in the heat affected zone (HAZ) for all specimens

TABLE 10

TENSILE PROPERTIES OF 2219-T62 TO 1100-H14 ALUMINUM EB WELDS
(WELDS LONGITUDINAL TO SPECIMEN AXIS)

Thickness in cm	Specimen No.	0.2% Yield Strength psi N/cm ²	Ultimate Strength (a) psi N/cm ²	Elongation, %		
				2-in. (5.08-cm)	1-in. (2.54-cm)	1/2-in. (1.27-cm) 1/4-in. (0.635-cm)
0.0401	0.1019	A	20 900	14 400	31 500	21 700
				10.7	13.5	17.0
						20.0
0.0405	0.1029	C	22 400	15 450	32 300	22 300
		E	20 600	14 200	32 300	22 300
		F	22 000	15 200	33 100	22 800
		G	22 200	15 300	33 500	23 100
		1	22 400	15 450	37 000	25 500
		2	20 300	14 000	29 200	20 100
		3	20 600	14 200	32 700	22 550
		6	24 000	16 550	39 400	27 200
		7	20 400	14 100	32 200	22 200
		8	20 900	14 400	30 200	20 800
				8.0	8.5	11.5
					10.5	15.0
						20.0

^a All failures occurred in the 2219-T62 aluminum

TABLE 11
PRESSURE VESSEL FABRICATION DATA

Vessel Serial Number (a)	Filament Winding Sequence	Metal Liner	Scrim System (b)	Weights, grams			Cured Vessel (c)	Cylinder Outside Diameter			Vessel Overall Length					
				Roving Deposited	Longitudinal	Hoop		Prior to Overwrap	Completed Vessel	in	cm	in	cm			
BWB-1	1	691	(d)	1441	770	2211	3221	2530	12.200	30.988	12.558	31.897	21.75	55.25	21.32	54.15
BWB-2	2	744	(d)	1208	775	1983	3249	2505	(d)	---	12.421	31.549	21.60	54.86	21.40	54.36
BWB-3	4	719	75	1220	860	2080	3336	2542	12.027	30.549	12.298	31.237	(d)	---	21.78	55.32
HB-1	6	746	75	1192	863	2055	3388	2567	12.028	30.551	12.291	31.219	21.59	54.84	21.89	55.60
HB-2	3	752	76	1275	854	2129	3412	2584	12.033	30.564	12.320	31.293	21.56	54.76	21.70	55.12
HB-3	5	761	89	1198	844	2042	3361	2511	12.032	30.561	12.291	31.219	21.66	55.02	21.72	55.17

a BWB denotes "Butt Welded Boss" design, HB denotes "Hinge Boss" design

b Scrim system includes Nylon Cloth and Adhesive

c Composite weight = cured vessel weight minus liner and scrim system weights

d Data not recorded

TABLE 12
SINGLE CYCLE BURST TEST DATA

Vessel Serial Number (a)	Test Temperature °F	Burst Pressure psig	Maximum Strain, % (c)	Fiber Stress at Failure Pressure (d)				Location of Failure	Remarks
				Hoop	Longitudinal LG-1	Hoop	Longitudinal MN/m²		
BWB-1	75	297	2983	2057	3.26 ^e	2.51	2.32	383	2640
								320	2210
								Hoop filaments in cylindrical section	Three circumferential extensometers used; one at cylinder mid-plane, and one at each end of cylinder
HB-2	75	297	3003	2071	2.86	2.21	2.17	375	2590
								314	2170
								Massive failure in longitudinal filaments of head; "flower" burst	
BWB-3	-320	77	2570 ^f	1772	1.48	2.00	1.83	316	2180
								264	1820
								Liner leak in boss area of head	Slight vacuum loss at 1200 psig (830 N/cm²) and above. Abnormal pressure strain curves.
HB-1	-320	77	4240	2923	3.50	(g)	(g)	3670	4444
								3060	3060
								Massive failure of entire vessel	Slight drop in test chamber vacuum noted as pressure increased above 3000 psig (2070 N/cm²)

a BWB denotes "Butt Welded Boss" design, HB denotes "Hinge Boss" design

b Pressurization rate was 1000 psi/min (690 N/cm²/min)

c See Figure 45 for extensometer location

d See Appendix I for sample calculation.

e Average of three strain readings: 3.00, 3.30, and 3.50%.

f Leak type failure, value corresponds to maximum pressure.

g Extensometers failed during test: LG-1 at 2236 psi (1542 N/cm²), LG-2 at 2708 psi (1867 N/cm²).

TABLE 13
CYCLIC FATIGUE LOADING TEST DATA

Vessel Serial Number (a)	Test Temperature °F °K	Load Level (b)		Fiber Stress @ Cyclic Load Level (c)		Strain @ Cyclic Load Level, % (d)		Cycles to Failure	Location of Failure	Remarks
		% Ultimate	Ambient	Pressure Level psig N/cm ²	Hoop ksi MN/m ²	Longitudinal ksi MN/m ²	Hoop LG-1 LG-3			
BWB-2	75 297	60	1800 1240	224 1540	187 187	1290 1280	1.82 1.70	1.37 1.39	25 18/65	Leak in area of vessel boss
HB-3	75 297	60	1800 1240	221 1520	185 185	1280 1280	1.70 1.70	1.39 1.39	18/65	Leak in girth weld area at cylinder section midpoint and later at vessel dome near head-to-cylinder juncture

a BWB denotes "Butt Welded Boss" design, HB denotes "Hinge Boss" design

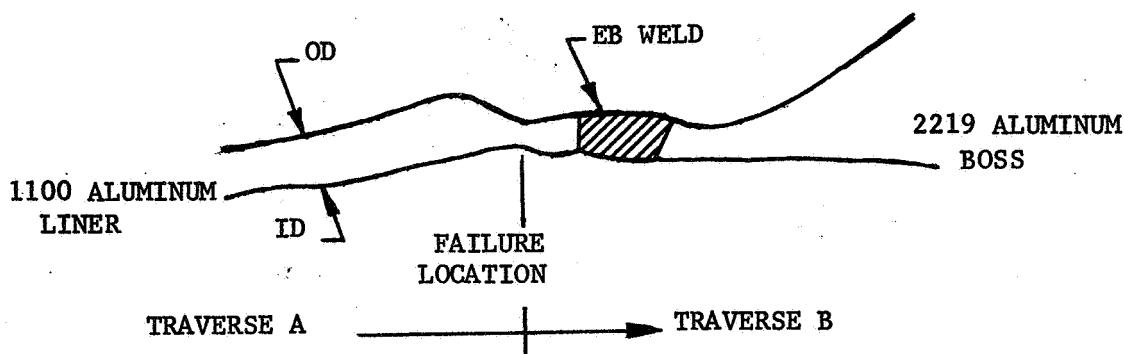
b Pressurization rate was 1000 psi/min (690 N/cm²/min)

c See Appendix I for sample calculation

d 1st cycle strain readings; see Figure 45 for extensometer locations

TABLE 14

MICROHARDNESS TRAVERSE IN FAILURE AREA, TANK BWB-2
(BOSS B) AFTER 25 PRESSURIZATION CYCLES



<u>Distance From Failure Location</u> <u>Mils</u>	<u>mm</u>	<u>Knoop Hardness Number (50.gm load)</u>	
		<u>Traverse A</u>	<u>Traverse B</u>
0	0	43	43
4	0.1	46	44
8	0.2	43	46
12	0.3	42	43
16	0.4	40	46
20	0.5	40	46
25	0.6	38	43
30	0.8	38	41
35	0.9	37	43
40	1.0	37	43
45	1.1	36	42
50	1.3	35	41
55	1.4	35	39
60	1.5	36	55
65	1.7	35	57
70	1.8	36	58
80	2.0	35	58
90	2.3	35	63
100	2.5	33	63
110	2.8	35	65
120	3.0	33	58
130	3.3	33	53
140	3.6	33	59
150	3.8	33	58
160	4.1	34	108
180	4.6	33	114
200	5.1	35	108
210	5.3		137

1100 Al

Weld

Weld

2219 Al

TABLE 14 (cont)

<u>Distance From Failure Location</u>		<u>Knoop Hardness Number (50.gm load)</u>	
<u>Mils</u>	<u>mm</u>	<u>Traverse A</u>	<u>Traverse B</u>
220	5.6		117
230	5.8		117
240	6.1		137
		1100 A1	2219 A1
		<u>5/8 in. (1.59 cm) from failure</u>	<u>Remote from Weld</u>
		31	145
		30	141
		31	149

TABLE 15

METAL LINER FABRICATION DATA

Liner Serial Number (a)	Half-Shell Serial Number (b)	Half-Shell Weight, Grams (b)	Average Liner Thickness (c)												Remarks					
			C			D			E			F			G			H		
in	mm	in	mm	in	mm	in	mm	in	mm	in	mm	in	mm	in	mm	in	mm	in	mm	
A-1 1	409	0.012	0.30	0.013	0.33	0.014	0.36	0.016	0.41	0.021	0.53	0.017	0.43	0.018	0.43	0.014	0.41	0.016	0.46	
	3	433	0.015	0.38	0.016	0.41	0.018	0.46	0.022	0.56	0.022	0.56	0.016	0.41	0.014	0.41	0.016	0.41	0.016	0.36
A-2 6	435	0.014	0.36	0.015	0.38	0.016	0.41	0.016	0.41	0.022	0.56	0.019	0.48	0.020	0.51	0.011	0.28	0.011	0.51	
	16	387	0.012	0.30	0.015	0.38	0.015	0.38	0.013	0.33	0.016	0.41	0.013	0.33	0.011	0.28	0.011	0.28	0.011	0.51
A-3 5	425	(d)	---	(d)	---	(d)	---	(d)	---	(d)	---	(d)	---	(d)	---	(d)	---	(d)	---	
	12	410	0.011	0.28	0.015	0.38	0.014	0.36	0.012	0.30	0.019	0.48	0.018	0.46	0.016	0.41	0.016	0.41	0.016	0.41
A-4 8	402	0.013	0.33	0.014	0.36	0.014	0.36	0.019	0.48	0.018	0.46	0.015	0.38	0.016	0.41	0.016	0.41	0.016	0.41	
	15	381	0.012	0.30	0.014	0.36	0.013	0.33	0.016	0.41	0.017	0.43	0.015	0.38	0.014	0.36	0.015	0.38	0.014	0.36
A-5e 7	391	0.012	0.30	0.013	0.33	0.013	0.33	0.015	0.38	0.019	0.48	0.015	0.38	0.013	0.33	0.013	0.33	0.013	0.33	
	10	403	0.012	0.30	0.014	0.36	0.015	0.38	0.018	0.46	0.021	0.53	0.020	0.51	0.019	0.48	0.019	0.48	0.019	0.48
A-6 4	405	0.012	0.30	0.014	0.36	0.015	0.38	0.018	0.46	0.020	0.51	0.017	0.43	0.015	0.38	0.015	0.38	0.015	0.38	
	11	403	0.011	0.28	0.013	0.33	0.013	0.33	0.020	0.51	0.020	0.51	0.018	0.46	0.018	0.46	0.018	0.46	0.018	0.46
A-7e 2	429	0.014	0.36	0.014	0.36	0.015	0.38	0.019	0.48	0.022	0.56	0.019	0.48	0.018	0.46	0.015	0.46	0.018	0.46	
	9	374	0.011	0.28	0.012	0.30	0.013	0.33	0.018	0.46	0.018	0.46	0.015	0.38	0.011	0.28	0.011	0.28	0.011	0.28

Table 15, Sheet 1

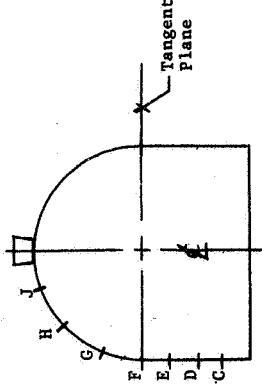
a Corresponds to vessel serial number

b Includes all boss components prior to girth-weld and copper ring etchout

c See schematic for location of thickness measurement; thicknesses were measured prior to final chemical milling operation

d Data inadvertently misplaced

e Liner assembly scrapped as a unit



Location of Thickness Measurements

TABLE 15 (cont)

METAL LINER FABRICATION DATA

Liner Serial Number (a)	Half-Shell Weight, Grams (b)	Average Liner Thickness (c)												Remarks
		C in mm	D in mm	E in mm	F in mm	G in mm	H in mm	J in mm						
A-8 ^d	13 408	0.013 0.33	0.015 0.38	0.015 0.38	0.015 0.38	0.016 0.41	0.018 0.46	0.016 0.41	0.015 0.38	0.015 0.38	0.017 0.43	0.015 0.38	0.017 0.43	Liner collapsed in electron beam vacuum chamber during attempted repair of boss weld. Entire liner scrapped.
A-8 ^d	14 389	0.011 0.28	0.013 0.33	0.013 0.33	0.014 0.36	0.017 0.43	0.026 0.66	0.025 0.64	0.025 0.64	0.023 0.58	0.023 0.58	0.023 0.58	0.023 0.58	Leak detected at boss weld of half-shell #19; no satisfactory repair. Membrane sealed to collar with massive TIG fillet weld completely eliminating hinge action.
A-9	19 460	0.013 0.33	0.017 0.43	0.017 0.43	0.016 0.41	0.026 0.66	0.025 0.64	0.023 0.58	0.023 0.58	0.023 0.58	0.023 0.58	0.023 0.58	0.023 0.58	Satisfactory repair. Membrane sealed to collar with massive TIG fillet weld completely eliminating hinge action.
A-9	20 449	0.011 0.28	0.016 0.41	0.016 0.41	0.015 0.38	0.023 0.58	0.023 0.58	0.023 0.58	0.020 0.51	0.020 0.51	0.018 0.46	0.018 0.46	0.018 0.46	Fracture occurred in knuckle area of one half-shell during cure of filament overwrap. Salvage attempted, but liner collapsed due to unsupported tensioned filaments during stripping procedure. Liner scrapped.
A-10 ^d	23 423	0.011 0.28	0.014 0.36	0.016 0.41	0.015 0.38	0.023 0.58	0.020 0.51	0.018 0.46	0.018 0.46	0.018 0.46	0.018 0.46	0.018 0.46	0.018 0.46	Fracture occurred in knuckle area of one half-shell during cure of filament overwrap. Salvage attempted, but liner collapsed due to unsupported tensioned filaments during stripping procedure. Liner scrapped.
A-10 ^d	24 417	0.011 0.28	0.013 0.33	0.015 0.38	0.015 0.38	0.023 0.58	0.020 0.51	0.018 0.46	0.018 0.46	0.018 0.46	0.018 0.46	0.018 0.46	0.018 0.46	Fracture occurred in knuckle area of one half-shell during cure of filament overwrap. Salvage attempted, but liner collapsed due to unsupported tensioned filaments during stripping procedure. Liner scrapped.
A-11	21 433	0.012 0.30	0.014 0.36	0.016 0.41	0.015 0.38	0.023 0.58	0.022 0.56	0.018 0.46	0.018 0.46	0.018 0.46	0.017 0.43	0.017 0.43	0.017 0.43	Six pin-holes in cylindrical section of half-shell #22 repair welded. No weld problems.
A-11	22 420	0.012 0.30	0.014 0.36	0.015 0.38	0.014 0.36	0.022 0.56	0.021 0.53	0.017 0.43	0.017 0.43	0.017 0.43	0.017 0.43	0.017 0.43	0.017 0.43	Six pin-holes in cylindrical section of half-shell #22 repair welded. No weld problems.
A-12	17 437	0.010 0.25	0.013 0.33	0.014 0.36	0.014 0.36	0.024 0.61	0.023 0.58	0.018 0.46	0.018 0.46	0.018 0.46	0.018 0.46	0.018 0.46	0.018 0.46	Three small TIG repairs required near tangency plane of half-shell #17. Leak-check showed leakage of 5.16×10^{-6} cc/sec at undetected sight.
A-12	25 441	0.013 0.33	0.014 0.36	0.016 0.41	0.013 0.33	0.024 0.61	0.022 0.56	0.019 0.46	0.019 0.46	0.019 0.46	0.019 0.46	0.019 0.46	0.019 0.46	Unit comprised of salvaged half-shells from S/N A-5 and A-7. Two small TIG repairs in "hat" weld of both half-shells. Two small TIG repairs in girth weld.
A-13	2 429	0.014 0.36	0.014 0.36	0.015 0.38	0.019 0.48	0.022 0.56	0.019 0.48	0.018 0.46	0.018 0.46	0.018 0.46	0.018 0.46	0.018 0.46	0.018 0.46	Unit comprised of salvaged half-shells from S/N A-5 and A-7. Two small TIG repairs in "hat" weld of both half-shells. Two small TIG repairs in girth weld.
A-13	10 403	0.012 0.30	0.014 0.36	0.015 0.38	0.018 0.46	0.021 0.53	0.020 0.51	0.019 0.48	0.019 0.48	0.019 0.48	0.019 0.48	0.019 0.48	0.019 0.48	Unit comprised of salvaged half-shells from S/N A-5 and A-7. Two small TIG repairs in "hat" weld of both half-shells. Two small TIG repairs in girth weld.
A-14 ^d	18 (e)	0.012 0.30	0.016 0.41	0.016 0.41	0.014 0.36	0.026 0.66	0.024 0.61	0.021 0.48	0.021 0.48	0.021 0.48	0.021 0.48	0.021 0.48	0.021 0.48	Sixteen TIG repairs in half-shell #28; eight TIG repairs in half-shell #18. Slight buckle in girth section. Leaking occurred during filament winding and liner was scrapped.
A-14 ^d	28 (e)	0.011 0.28	0.013 0.33	0.014 0.36	0.013 0.36	0.018 0.46	0.019 0.48	0.019 0.48	0.019 0.48	0.019 0.48	0.019 0.48	0.019 0.48	0.019 0.48	Liner assembly scrapped
														Data not recorded

^a Corresponds to vessel serial number^b Includes all boss components prior to girth weld and curing etchout^c See schematic for location of thickness measurement (Sheet 1)^d Liner assembly scrapped^e Data not recorded

TABLE 16
PRESSURE VESSEL FABRICATION DATA

Vessel Serial Number	Filament Winding Sequence	Metal Liner	Scrim System (a)	Weights, Grams				Composite Material (b)	Internal Volume in ³	Cylinder Outside Diameter Prior to Overwrap in cm	Vessel Overall Length Completed in cm	Vessel Overwrap in cm	Remarks					
				Longo	Hoop	Deposited Total	Cured Vessel											
A-4	1	765	78	1186	852	2038	3250	2407	1825	29.910	12.029	30.554	12.310	31.267	21.51	54.64	21.62	54.91
A-6	2	787	(c)	1194	871	2065	3206	2347 ^d	1818	29.790	12.024	30.541	12.285	31.204	21.53	54.69	21.67	55.04
A-2	3	806	(c)	1202	875	2077	3263	2385 ^d	1968	32.250	12.026	30.546	12.369	31.417	22.00	55.88	21.66	55.02
A-11	4	838	(c)	1231	783	2014	3247	2337 ^d	1848	30.280	12.041	30.584	12.359	31.392	21.53	54.69	21.67	55.04
A-1	5	817	74	1169	799	1968	3304	2413	1882	30.840	12.257	31.133	12.621	32.057	21.65	54.99	21.69	55.09
A-3	6	820	66	1189	801	1990	3230	2344	(c)	---	12.034	30.566	12.339	31.341	21.64	54.97	21.62	54.91
A-9	7	897	65	1211	880	2091	3377	2415	1829	29.970	12.031	30.559	12.310	31.267	21.65	54.99	21.53	54.69
A-13	8	780	81	1214	877	2091	3300	2439	1936	31.730	12.063	30.640	12.375	31.433	21.73	55.19	21.51	54.64
A-12	9	856	65	1272	864	2136	3282	2361	1820	29.820	12.028	30.551	12.321	31.295	21.76	55.27	21.70	55.12

a Scrim system includes Nylon Cloth and adhesive

b Composite material weight = cured vessel weight minus liner and scrim system weights

c Data not recorded

d Values based on an assumed scrim system (average) weight of 72 grams

TABLE 17

ASSIGNMENT OF VESSELS TO TESTS

VESSEL SERIAL NUMBER	TEST ASSIGNMENT		
	TEMPERATURE	BURST	CYCLIC FATIGUE
A-1	Liquid nitrogen	X	
A-2	Liquid hydrogen		X
A-3	Ambient	X	
A-4	Liquid nitrogen		X
A-6	Liquid hydrogen		X
A-9	Liquid hydrogen	X	
A-11	Ambient		X
A-12	Ambient		X
A-13	Liquid nitrogen		X

Table 17

TABLE 18
SINGLE CYCLE BURST TEST DATA, A SERIES

Vessel Serial Number	Test Temperature °F °K	Maximum Pressure (a) psig	Maximum Strain, % (b)	Fiber Stress @ Maximum Pressure (c)			Location of Failure	Remarks
				Hoop	Longitudinal	Hoop		
				LG-1	LG-2-4	ksi MN/m²		
A-3	61 289	2250 ^d	1550	2.12	1.75	1.46	280 1930	234 1610 Longitudinal filaments @ repair welded boss (flower burst)
A-1	-320 77	3870	2670	3.12	3.18	3.05	497 3430	415 2860 Leak in knuckle area of head just above head-to-cylinder junction
A-9	-423 20	2380	1640	(e)	1.48	1.81	295 2030	245 1690 Leak at repair welded boss

a Pressurization rate was 1000 psi/min (690 N/cm²/min)

b See Figure 45 for extensometer location

c See Appendix I for sample calculation

d Vessel burst pressure

e Extensometer failure, no signal

TABLE 19
CYCLIC FATIGUE LOADING TEST DATA, A SERIES

Vessel Serial Number	Test Temperature °F	Ultimate Burst Pressure psi	Load Level (a)	Fiber Stress @ Cyclic Load Level (b)				Strain @ Cyclic Load Level, % (c)				Cycles To Failure	Location of Failure	Remarks			
				Hoop		Longitudinal		Hoop		Long							
				ksi	MN/m²	ksi	MN/m²	ksi	MN/m²	ksi	MN/m²						
A-11	65	292	60	1800	1240	223	1540	186	1280	1.68	1.25	1.24	17	Leak in knuckle area of head one inch above head-to-cylinder junction.			
A-12	64	291	60	1800	1240	222	1530	185	1280	1.48	1.34	1.29	25	Leak in knuckle area of head just above head-to-cylinder junction.			
A-4	-320	77	60	2400	1650	297	2050	248	1710	2.01	1.96	1.82	93	Leak in knuckle area of head.			
A-13	-320	77	60	2400	1650	299	2060	250	1720	2.13	1.67	1.68	15	--			
A-2	-423	20	60	2400	1650	299	2060	249	1720	2.22	2.02	1.98	97	Leak in knuckle area of head.			
A-6	-423	20	60	2400	1650	297	2050	247	1700	2.10	1.87	1.74	75	--			

a pressurization rate was 1000 psi/min (690 N/cm²/min)

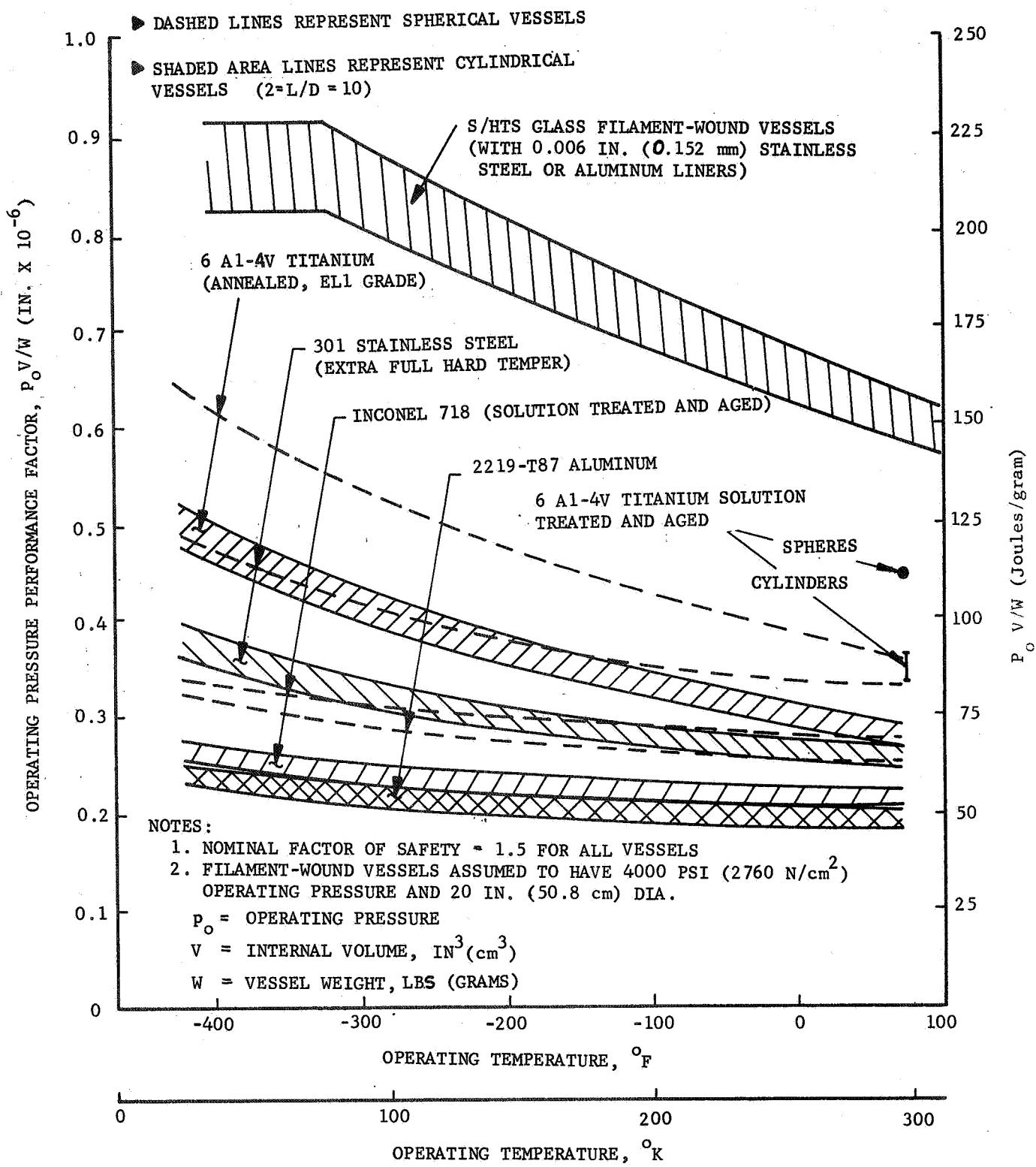
b See Appendix I for sample calculation

c 1st cycle strain readings, see Figure 45 for extensometer locations

TABLE 20
PRESSURE VESSEL PERFORMANCE FACTORS

Test Temperature °F °K	Vessel Serial Number	Burst Pressure, P_b psi	Internal Volume, V_o in ³	Vessel Weight, W lbm	grams	Performance Factor ($P_b V_o^{\alpha} / W$)				
						Specific Vessel Temperature	Average For Temperature in-lbf/lbm			
75	297	BWB-1	2983	2057	1784 ^a	29 200	7.10	3221	0.75 x 10 ⁶	187
		HB-2	3003	2071	1784 ^a	29 200	7.52	3412	0.71	177
-320	77	HB-1	4240	2923	1784 ^a	29 200	7.47	3388	1.01	252
		A-1	3870	2670	1882	30 800	7.28	3304	1.00	249
									1.01	251

^a Calculated volumes, data not recorded



Pressure Vessel Performance Factors

Figure 1

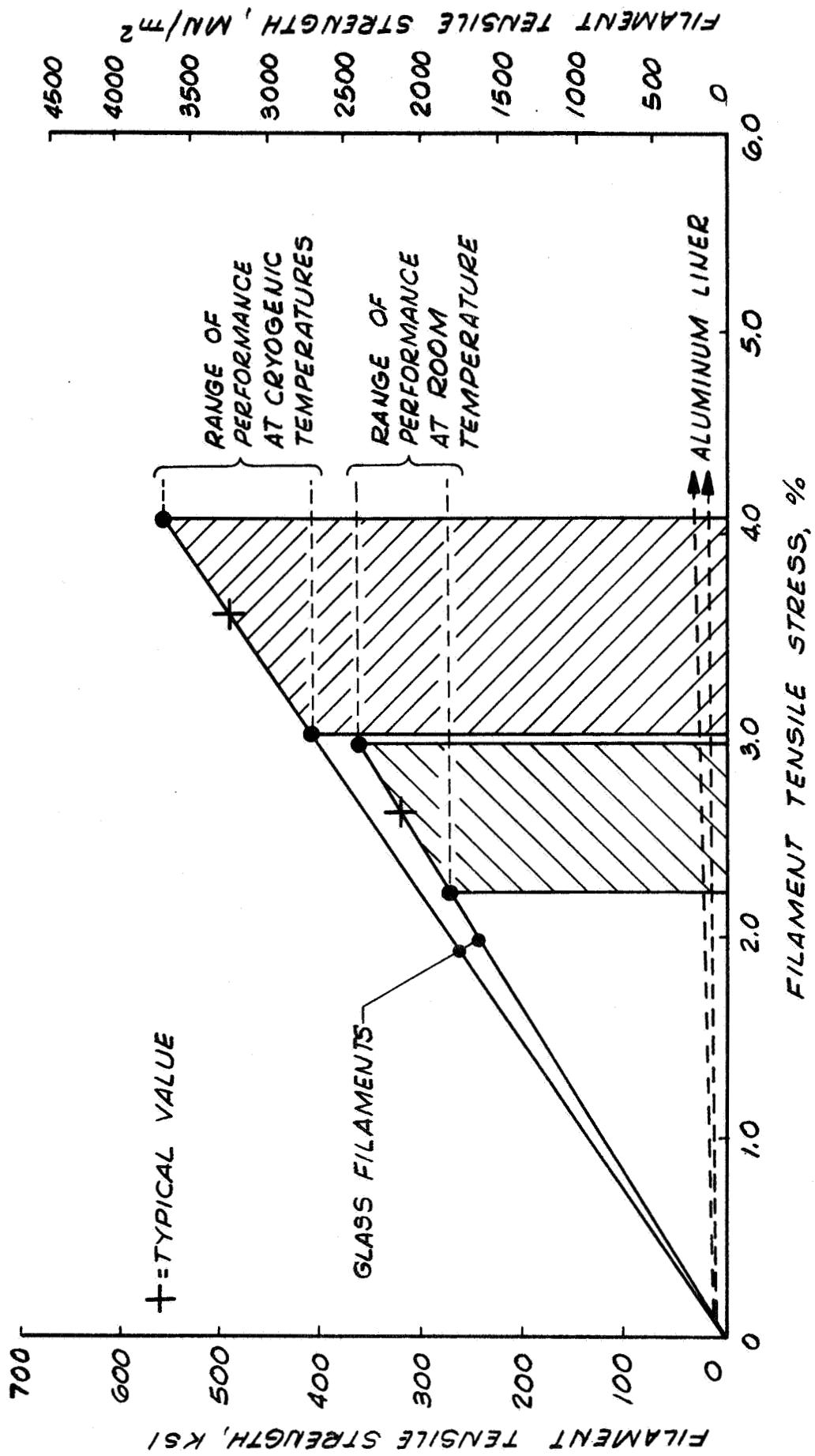


Figure 2

Stress-Strain Characteristics of S-HTS Filaments and Ductile Aluminum Liner Materials

Fabrication Plan For 6061 Aluminum Liners With Integral Bosses

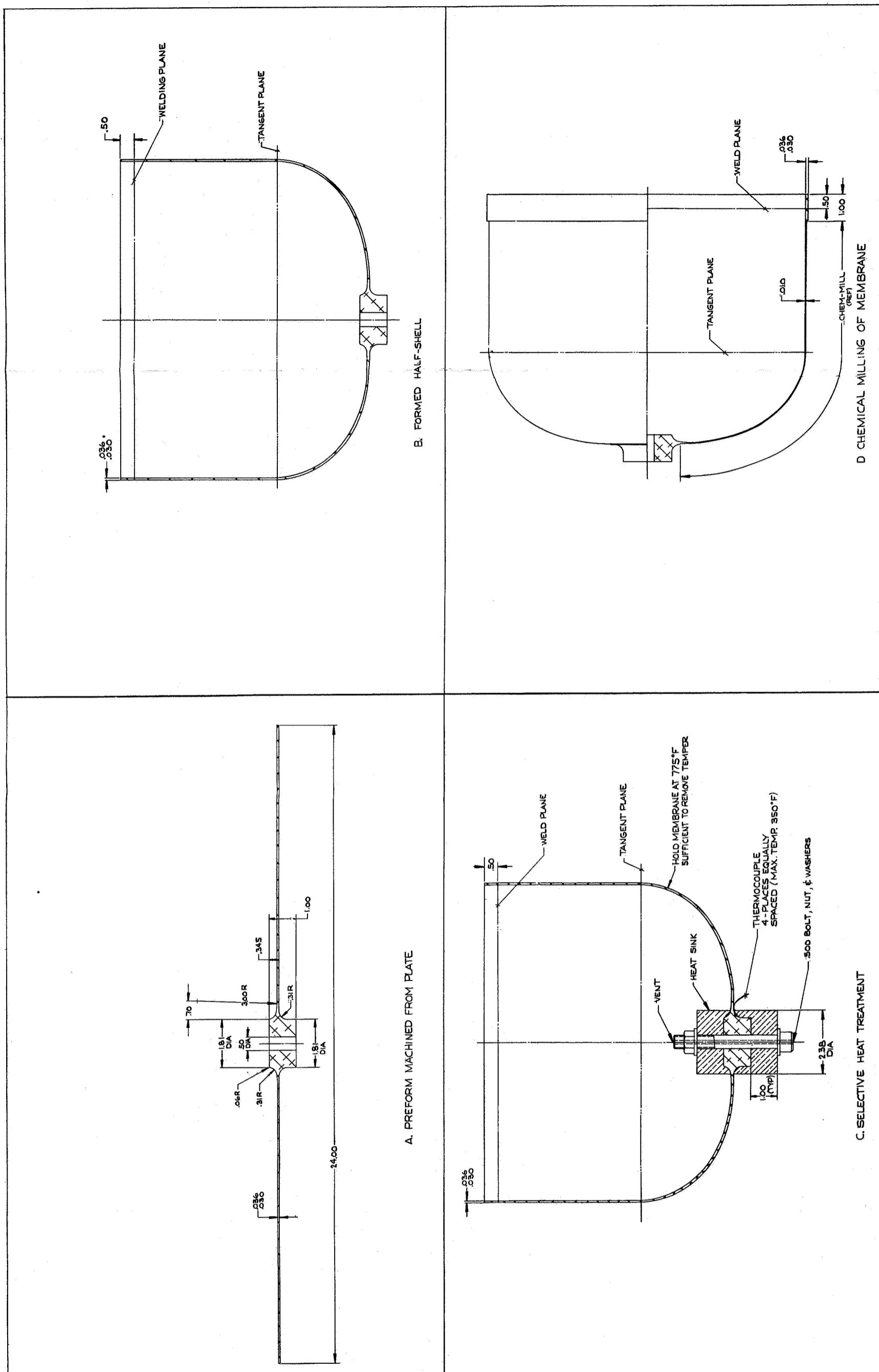
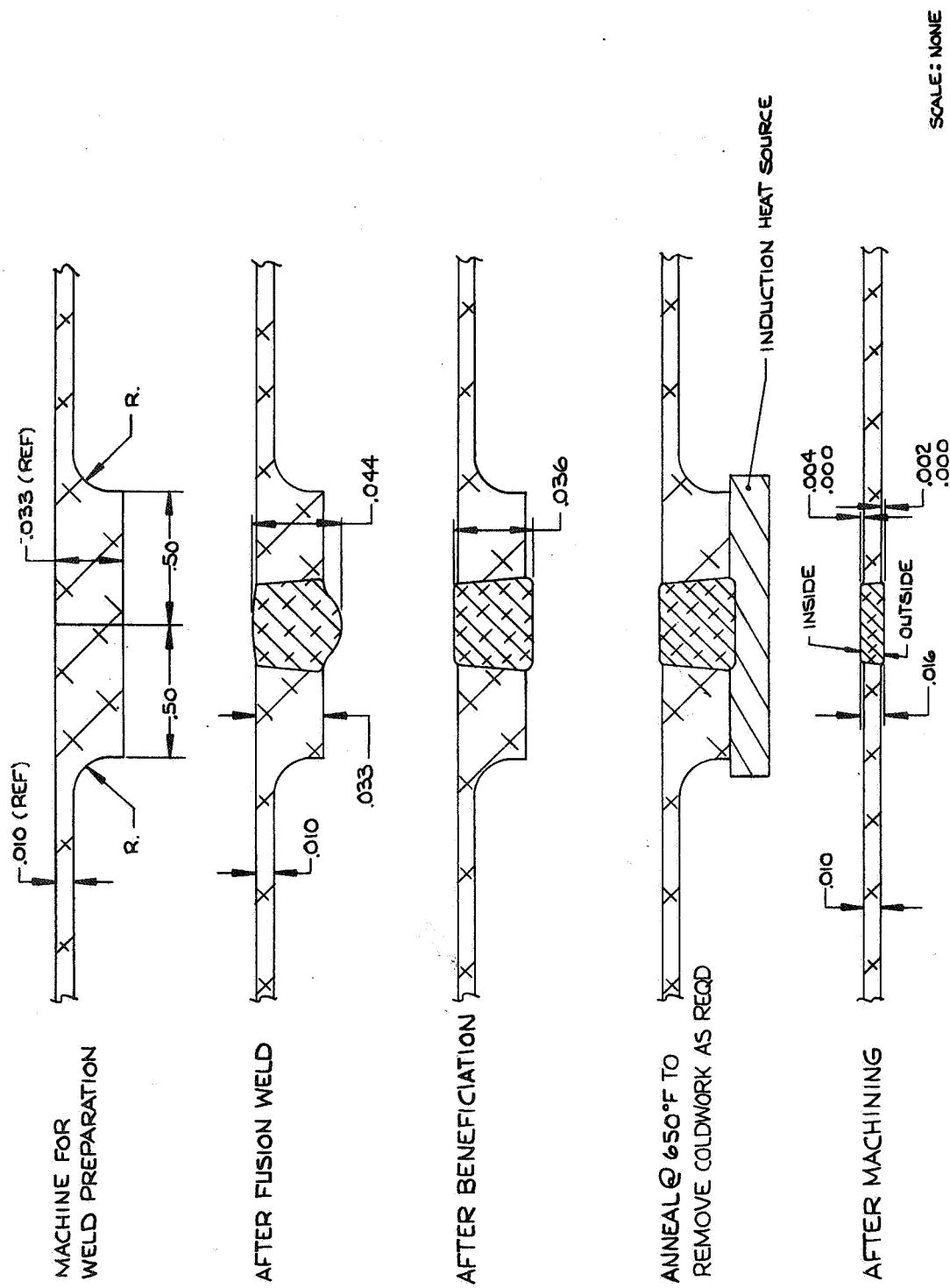


Figure 3
Sheet 1 of 2



E. FUSION WELDING AND WELD BENEFICIATION

Fabrication Plan For 6061 Aluminum Liners With Integral Bosses

Figure 3
Sheet 2 of 2

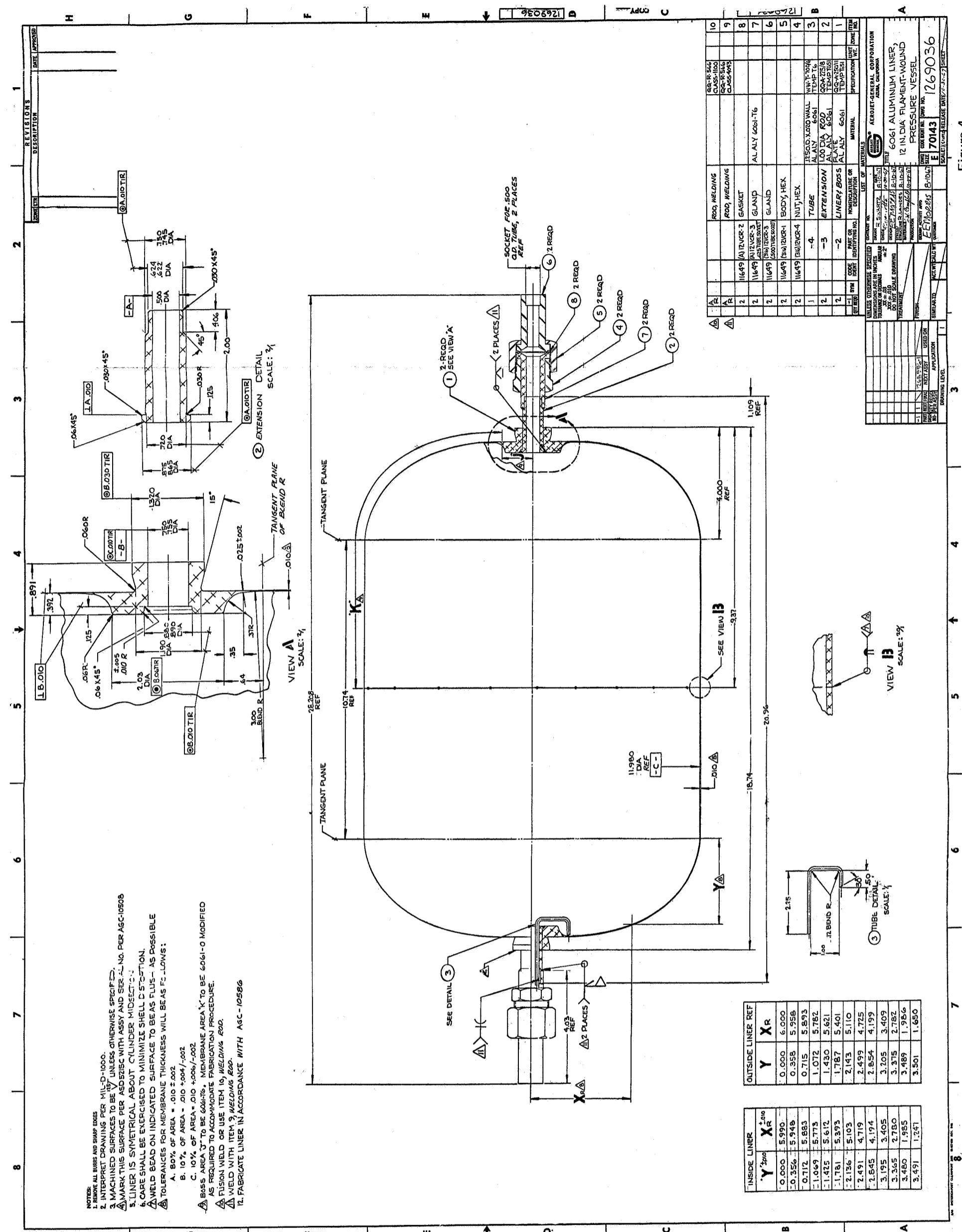
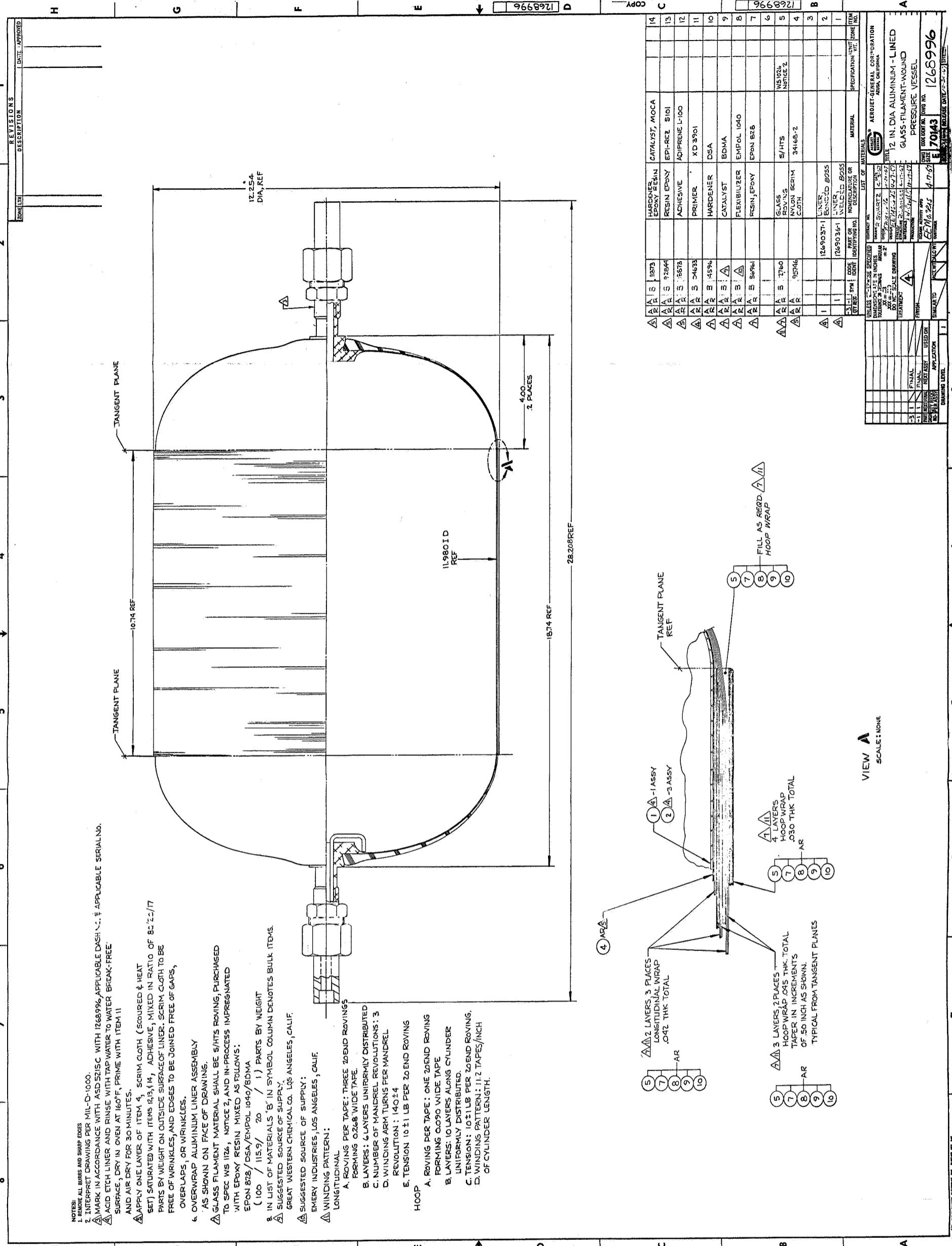


Figure 4
6061 Aluminum Liner With Integral Bosses
(Engineering Drawing)



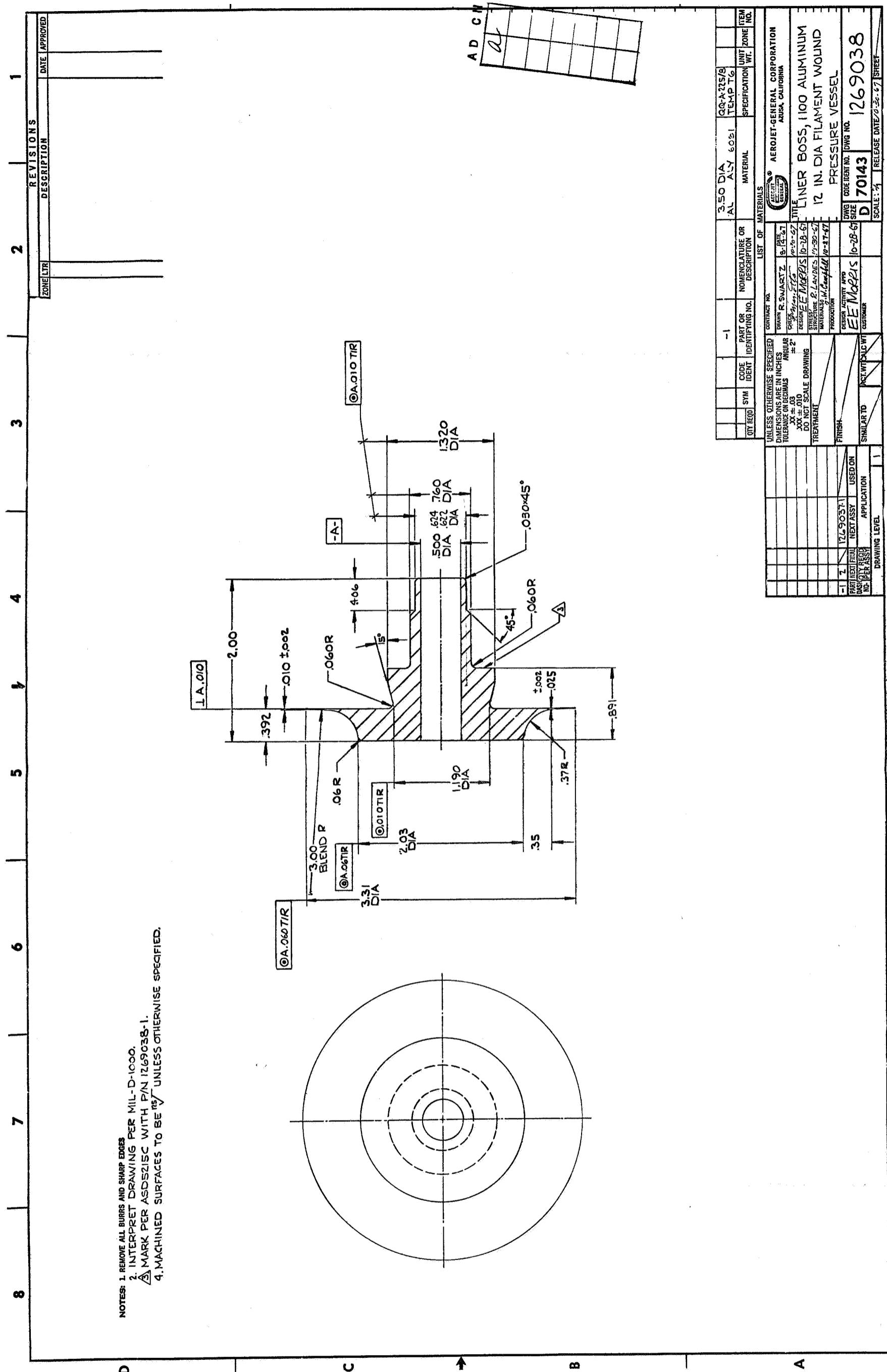


Figure 6 Boss for 1100 Aluminum Liner with Bonded Bosses (Engineering Drawing)

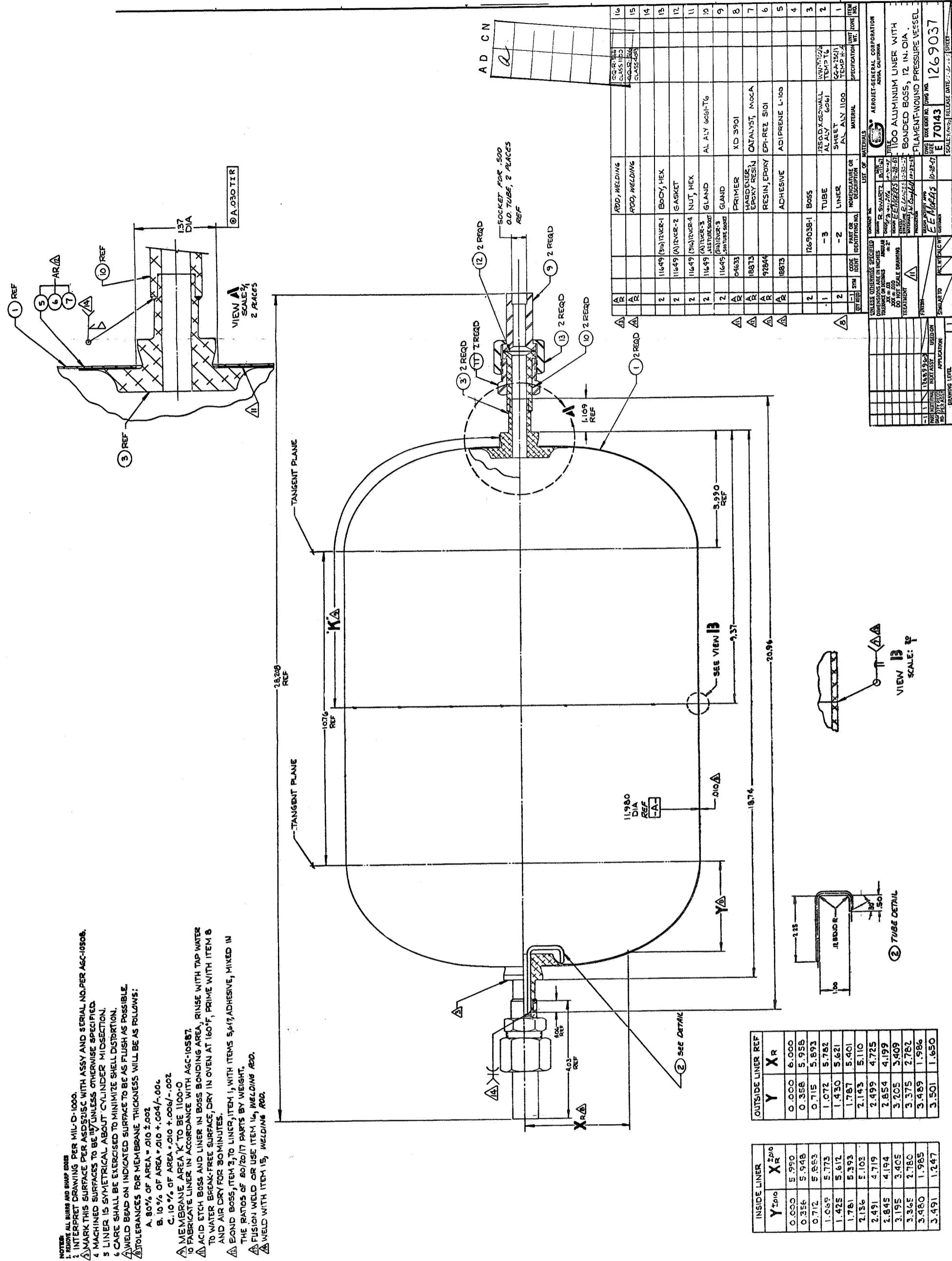
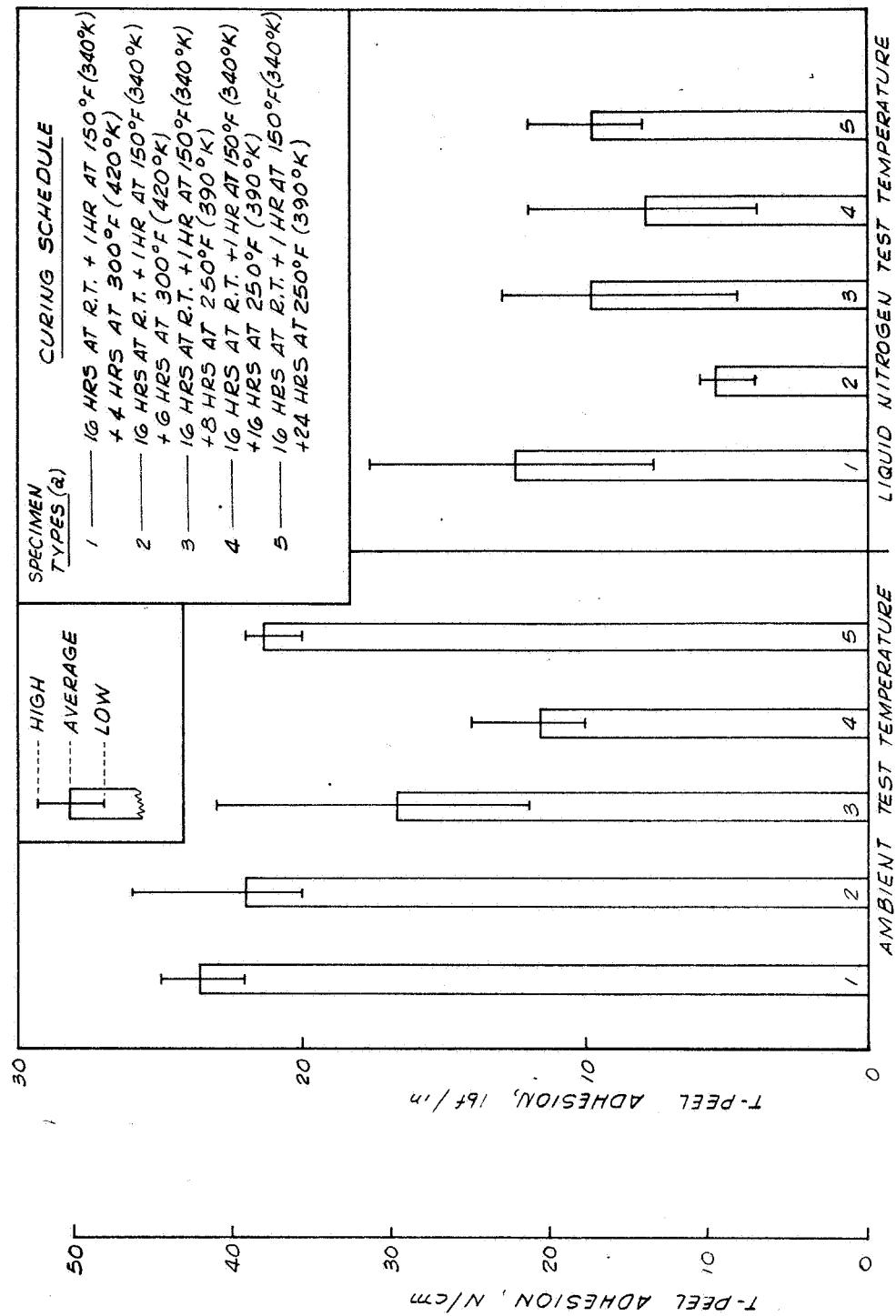


Fig. 7 1100 Aluminum Liner with Bonded Bosses (Engineering Drawing)



a 0.010-in-thick 6061 Aluminum bonded to Glass Filament Composite;
 Adhesive Bond System: Adiprene L-100/Epirez 5101/MOCA(80/20/17 pbw) with
 S-1852-2-400 Nylon scrim cloth; Glass Filament Composite: Epon 828/Empol 1040/
 DSA/BDMA(100/20/115.9/1.a pbw) impregnated in 181 glass cloth.

T-Peel Adhesion vs Cure Schedule

Figure 8

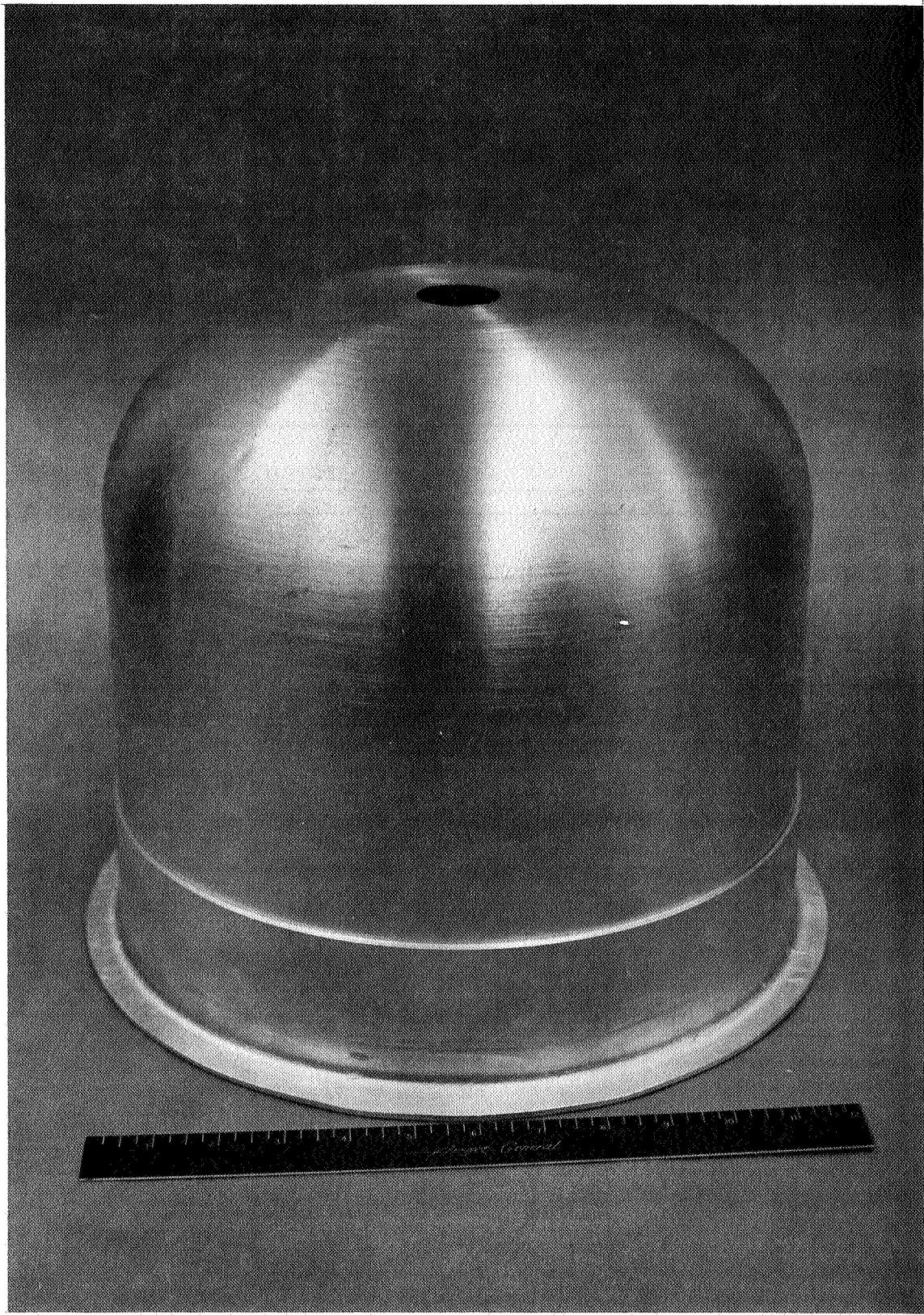
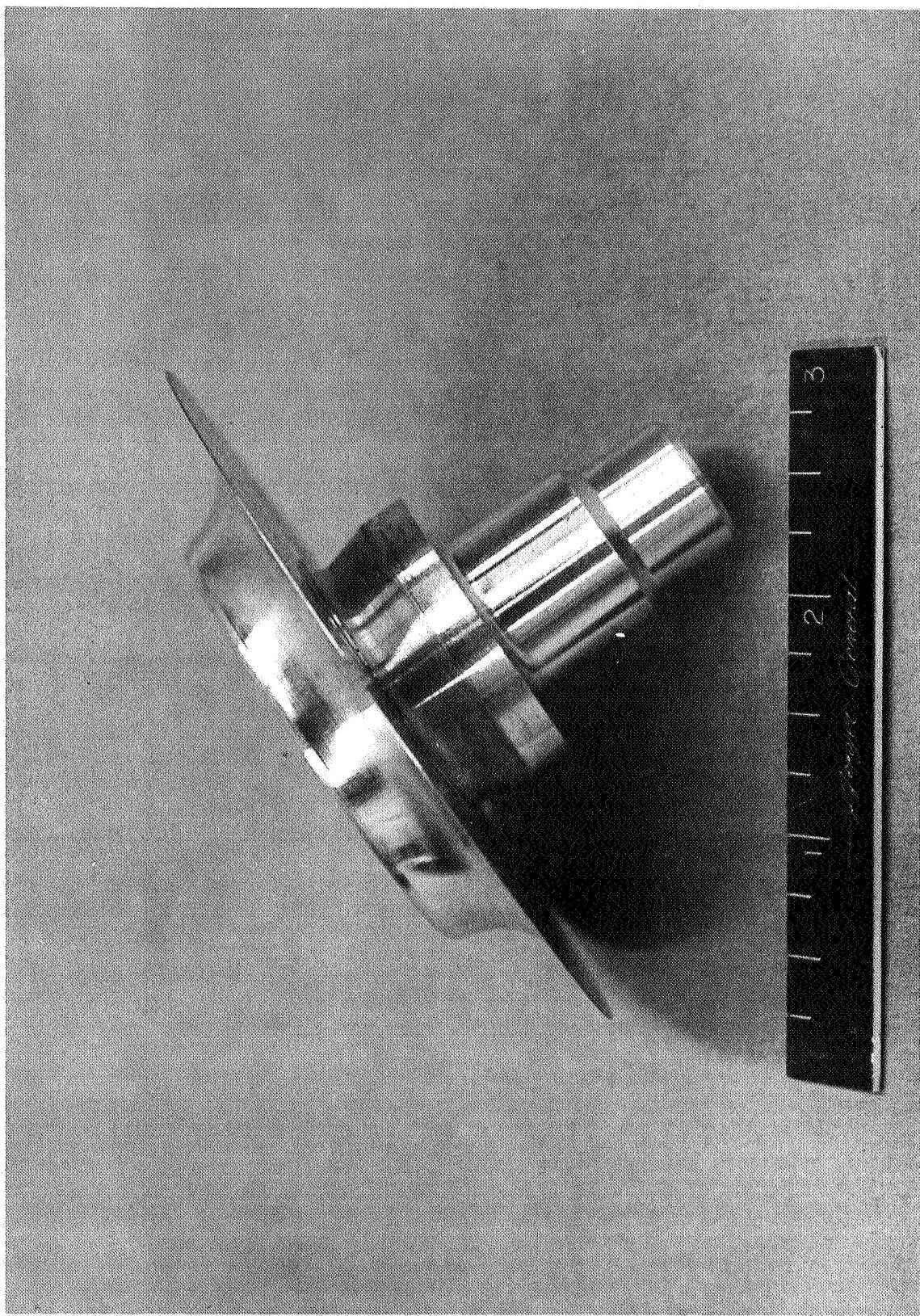


Figure 9
1100 Aluminum Liner Half Shell, 12-in.-dia.

Figure 10
6061-T6 Aluminum Boss for 1100 Aluminum Liner



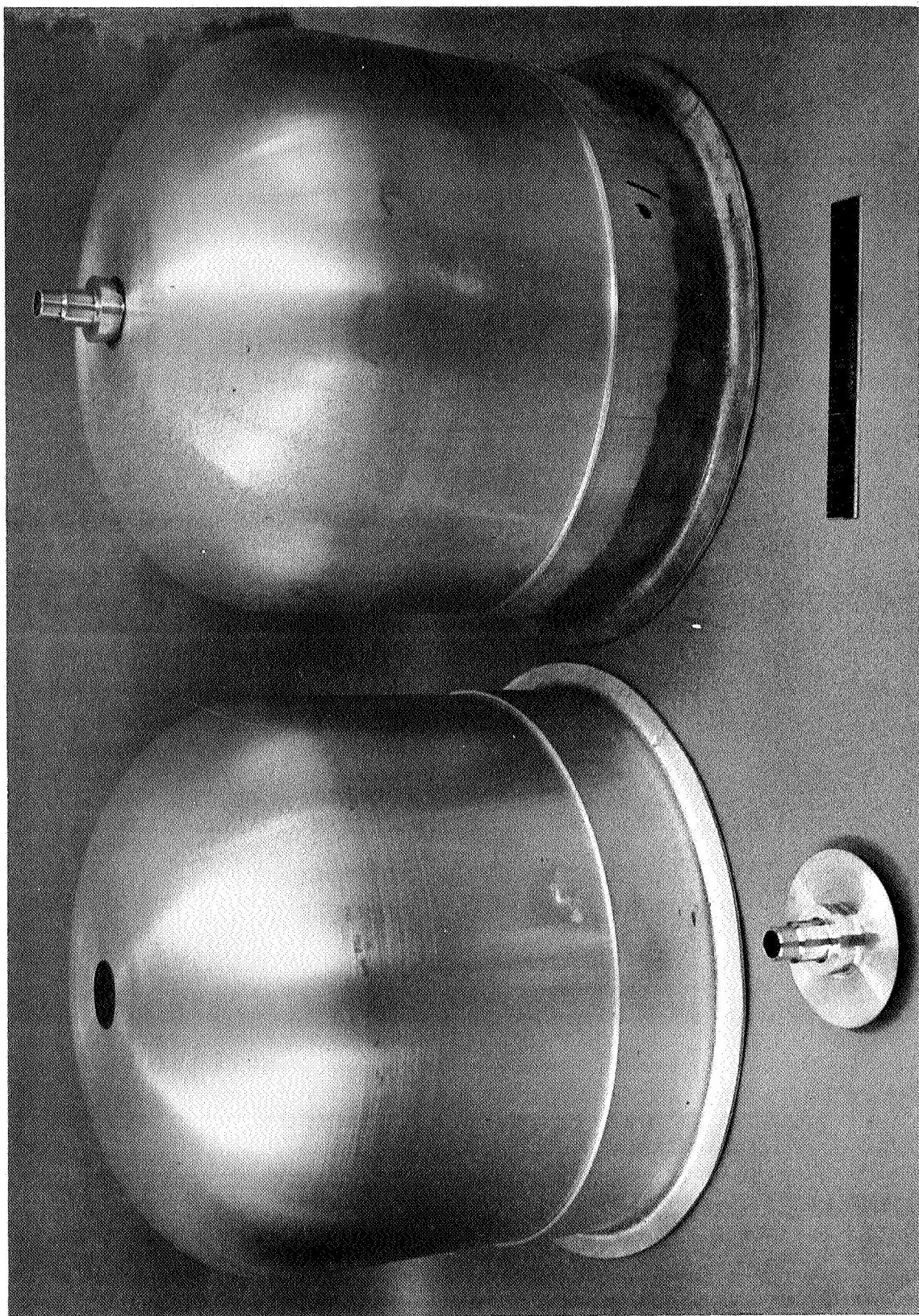
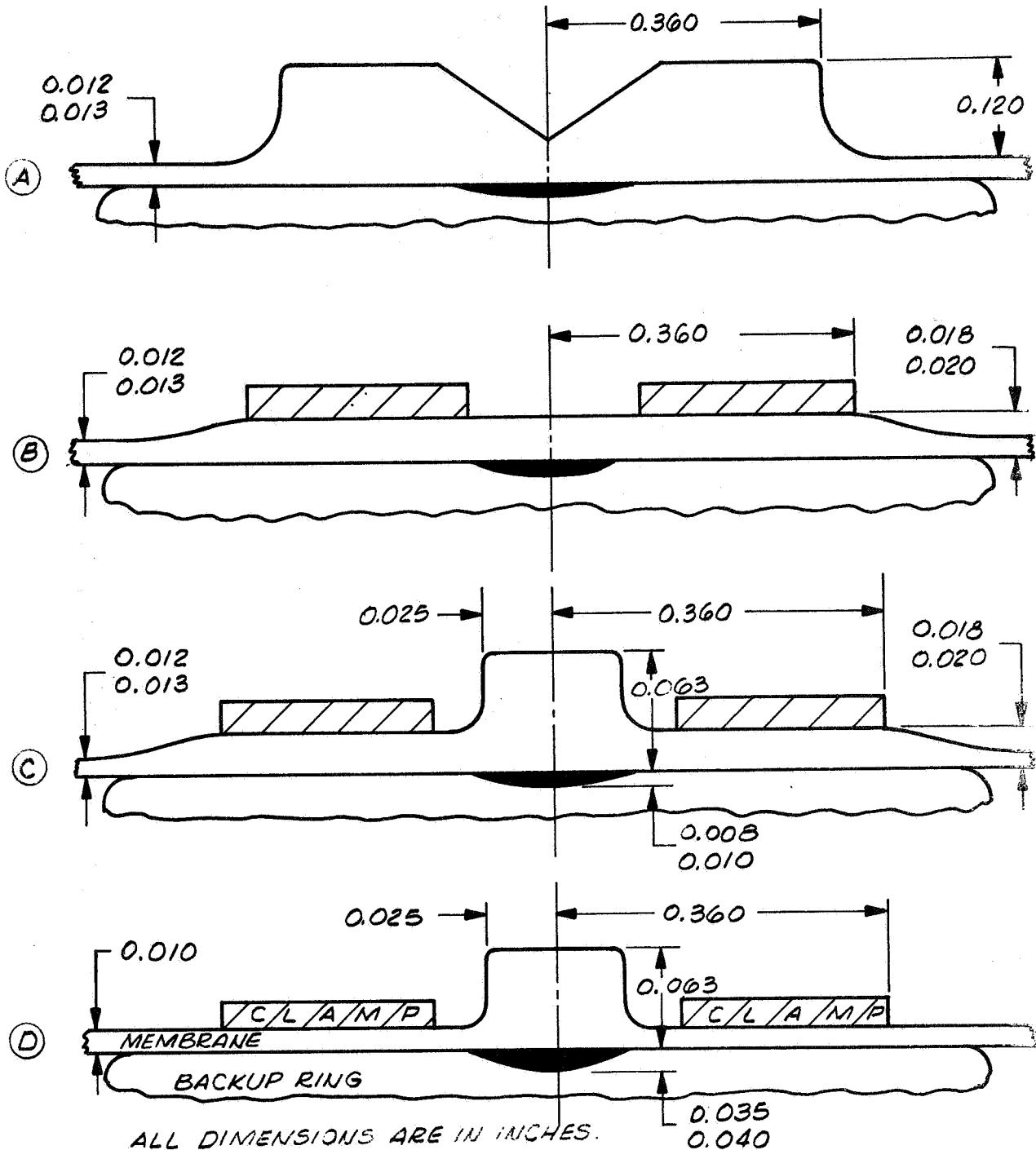


Figure 11
1100 Aluminum Liner Half Shells, Boss Bonded in Place



Weld Joint Detail Evolution

Figure 12

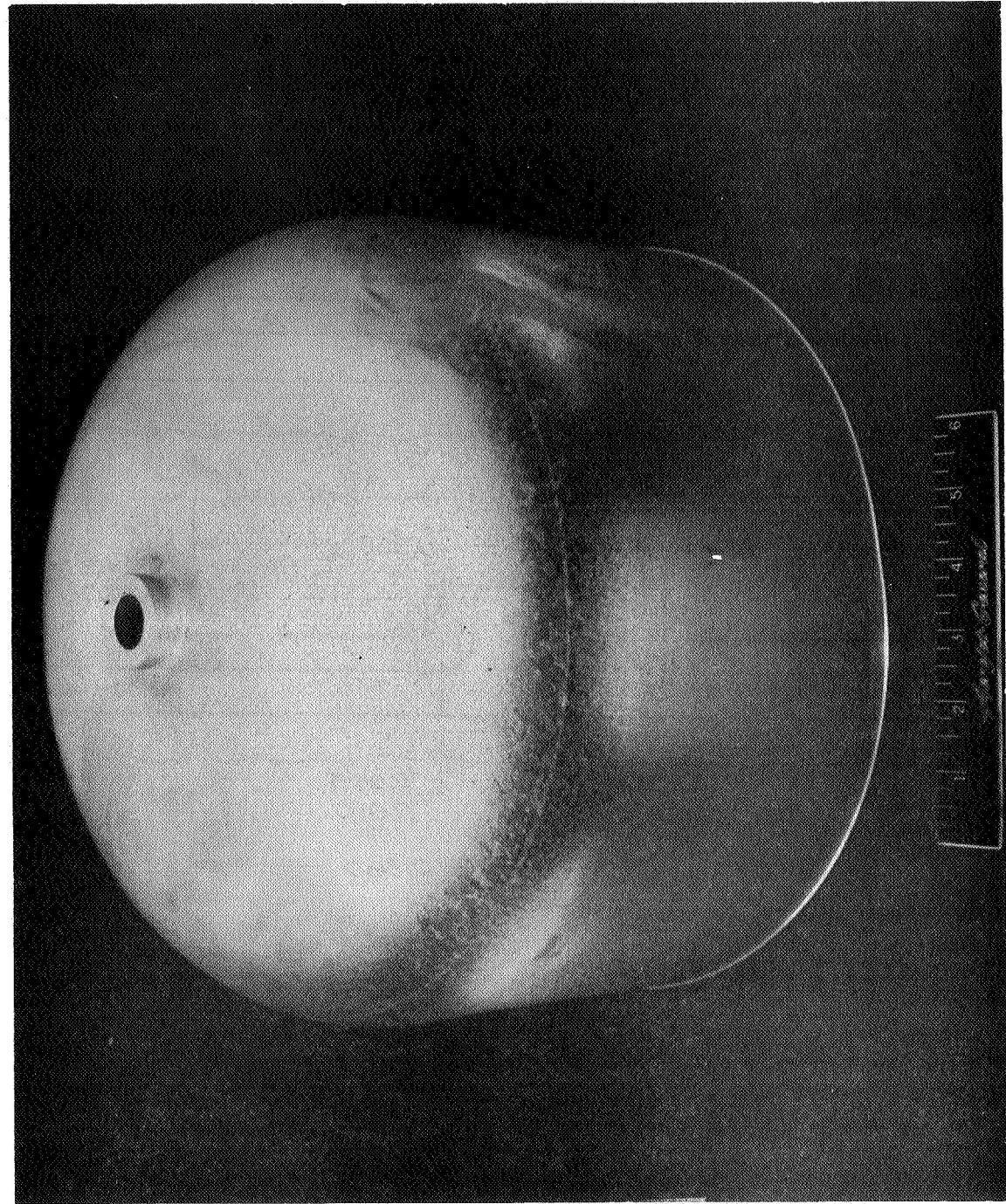


Figure 13
6061 Aluminum Liner Half Shell, Exterior View

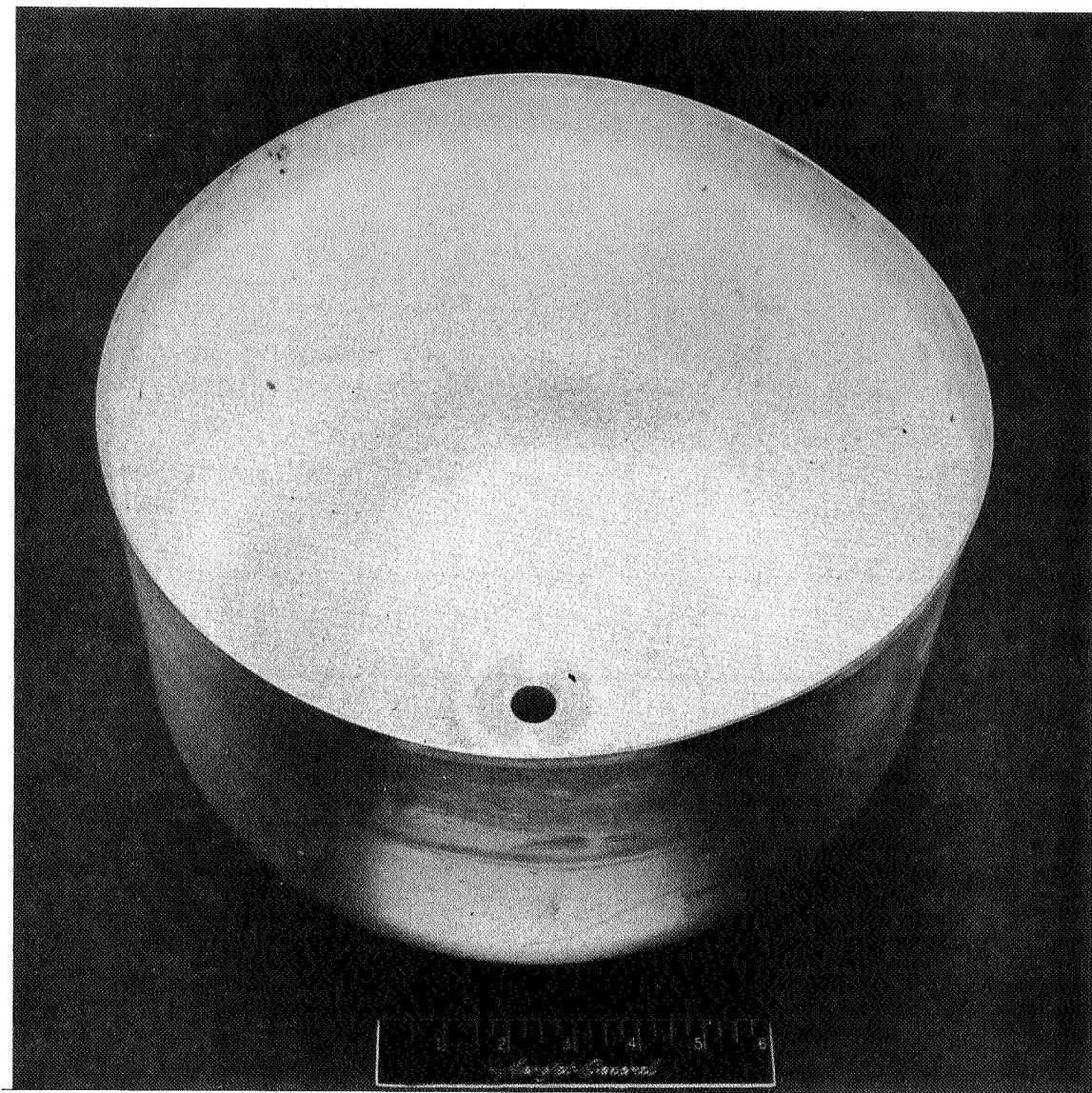
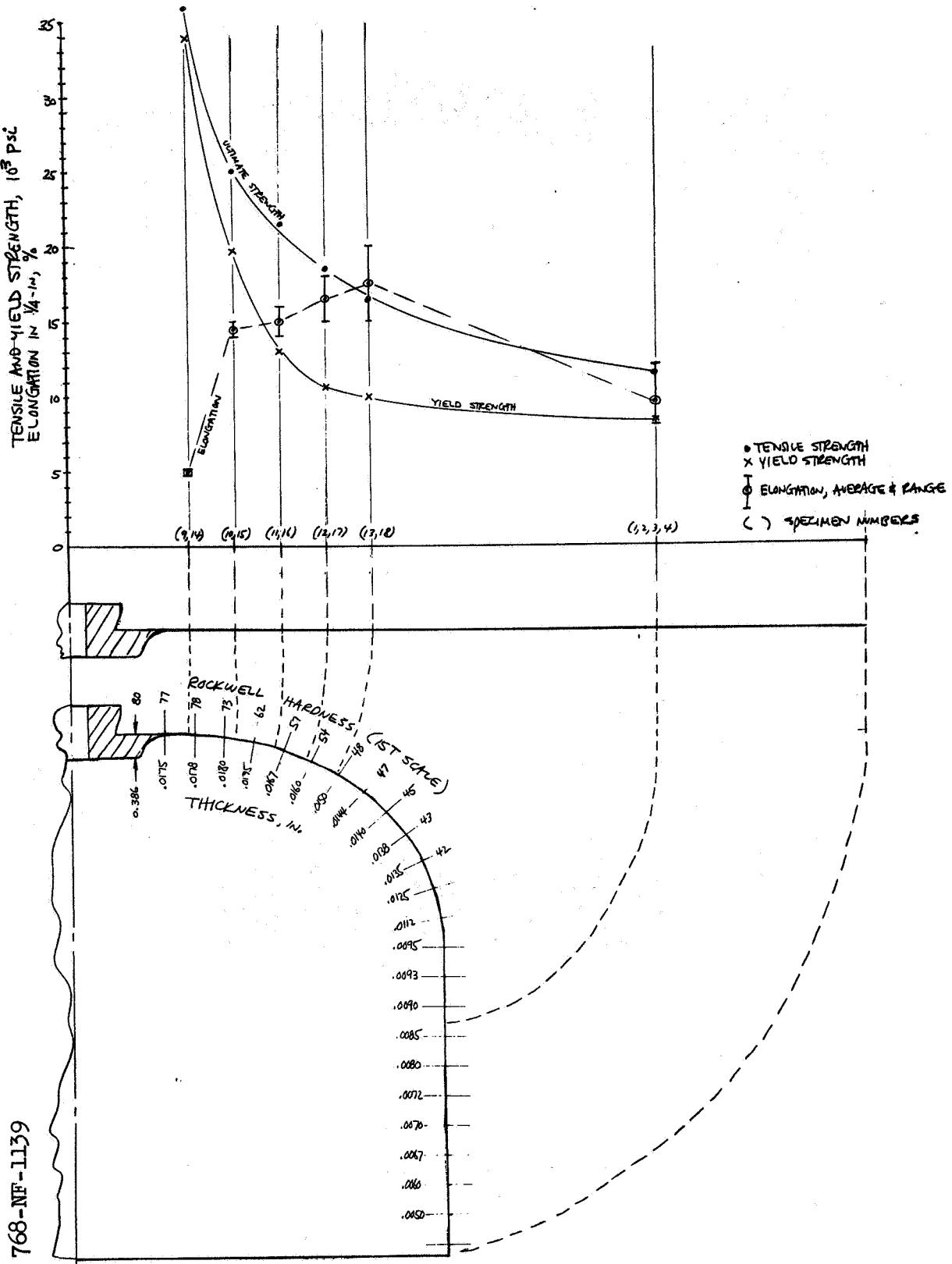


Figure 14
6061 Aluminum Liner Half Shell, Interior View



Properties of 6061 Aluminum Liner Half Shell, Initial Annealing Procedure

Figure 15

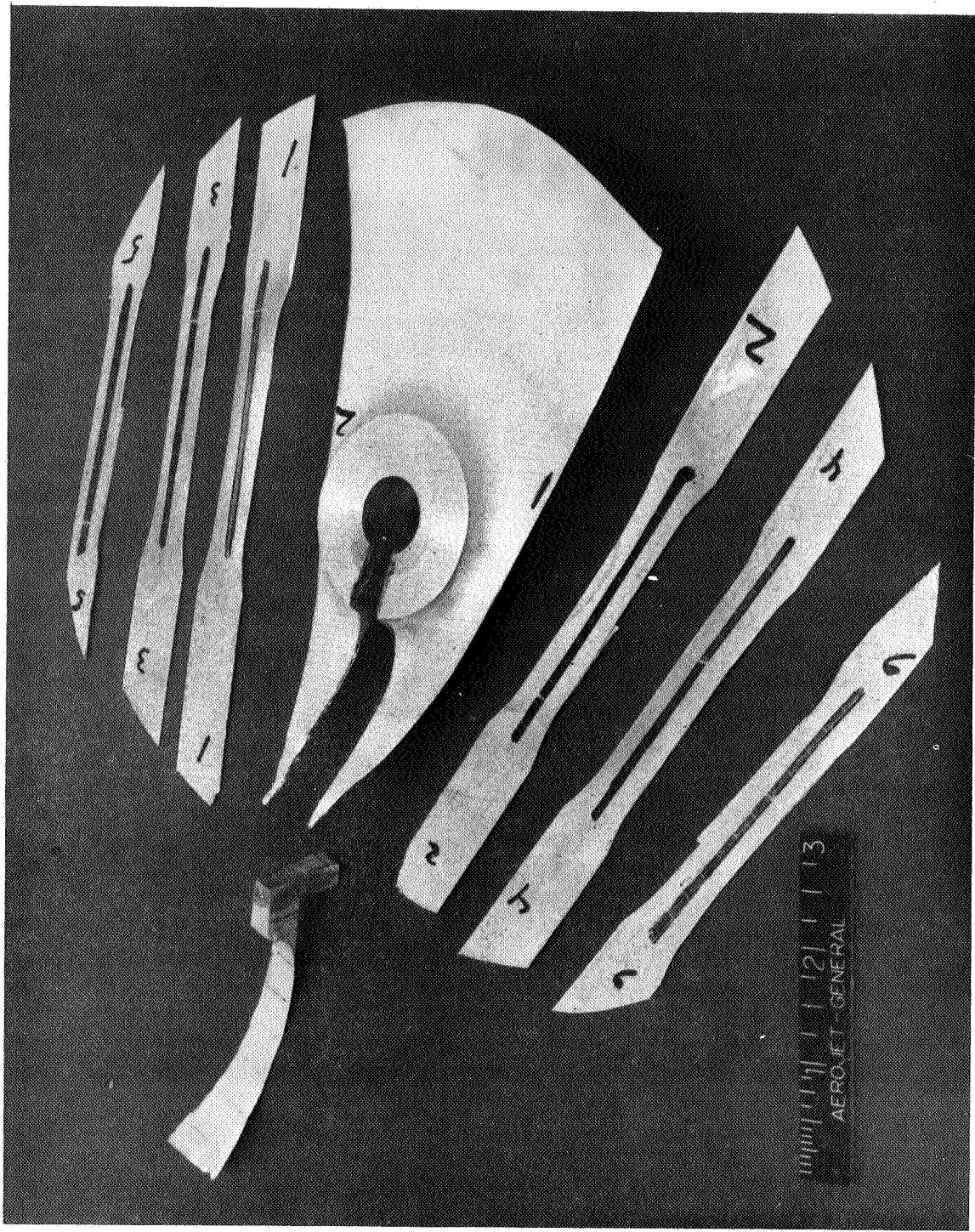
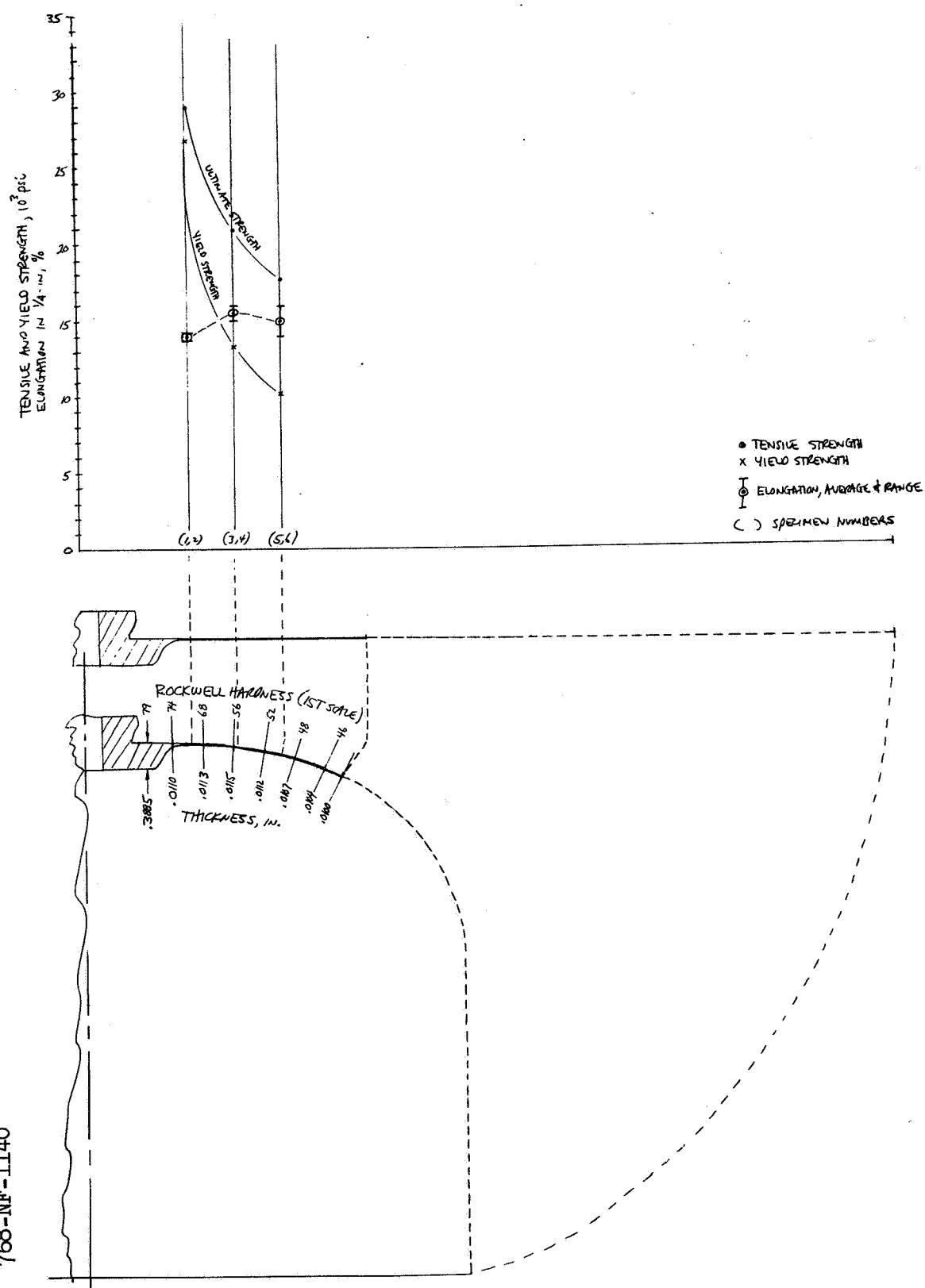


Figure 16
Section from 6061 Aluminum Liner Half Shell Showing Test Specimens



Properties of 6061 Aluminum Liner Half Shell, Modified Annealing Procedure

Figure 17

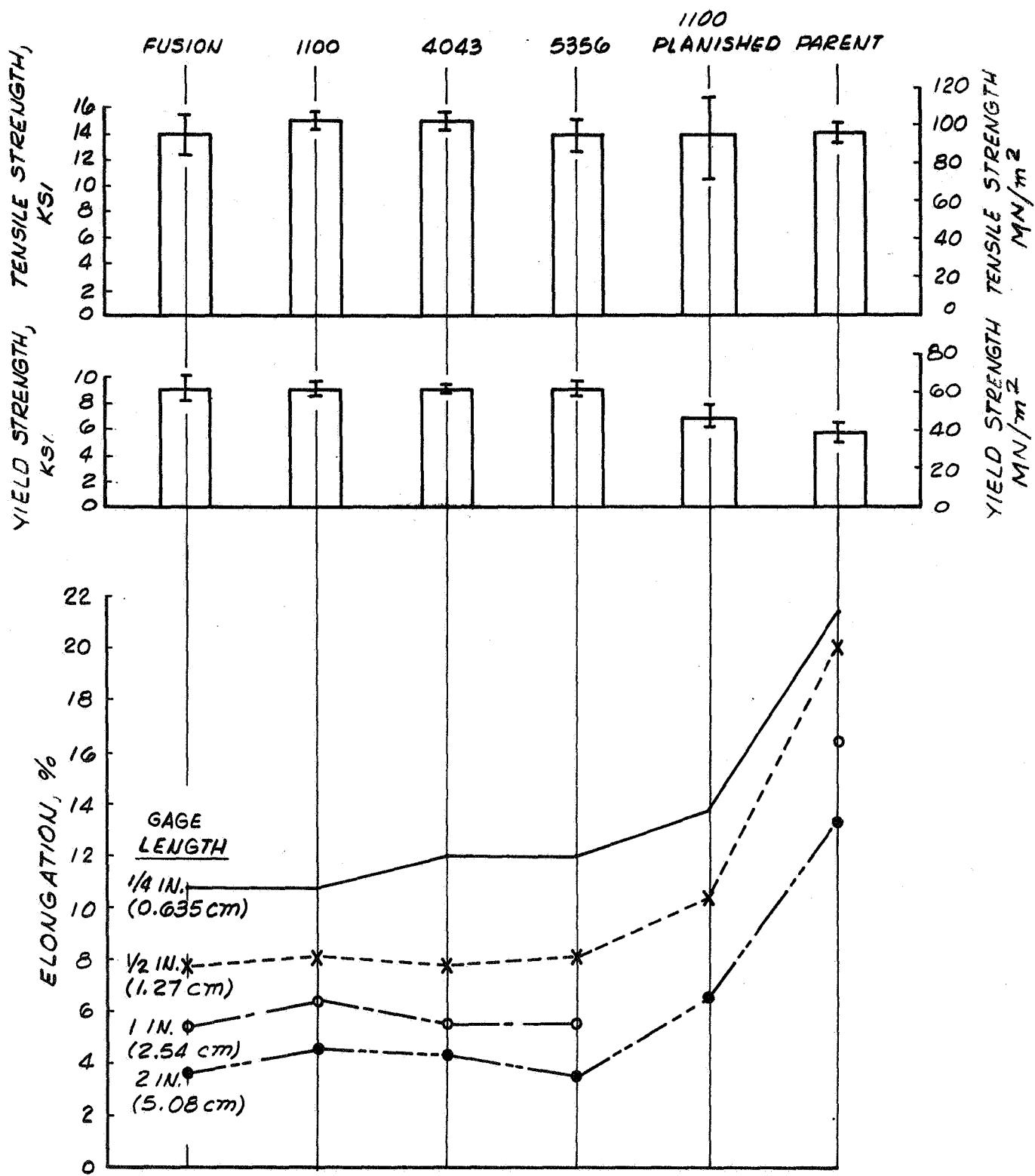


Figure 18

Figure 19
Application of Longitudinal Windings to Liner

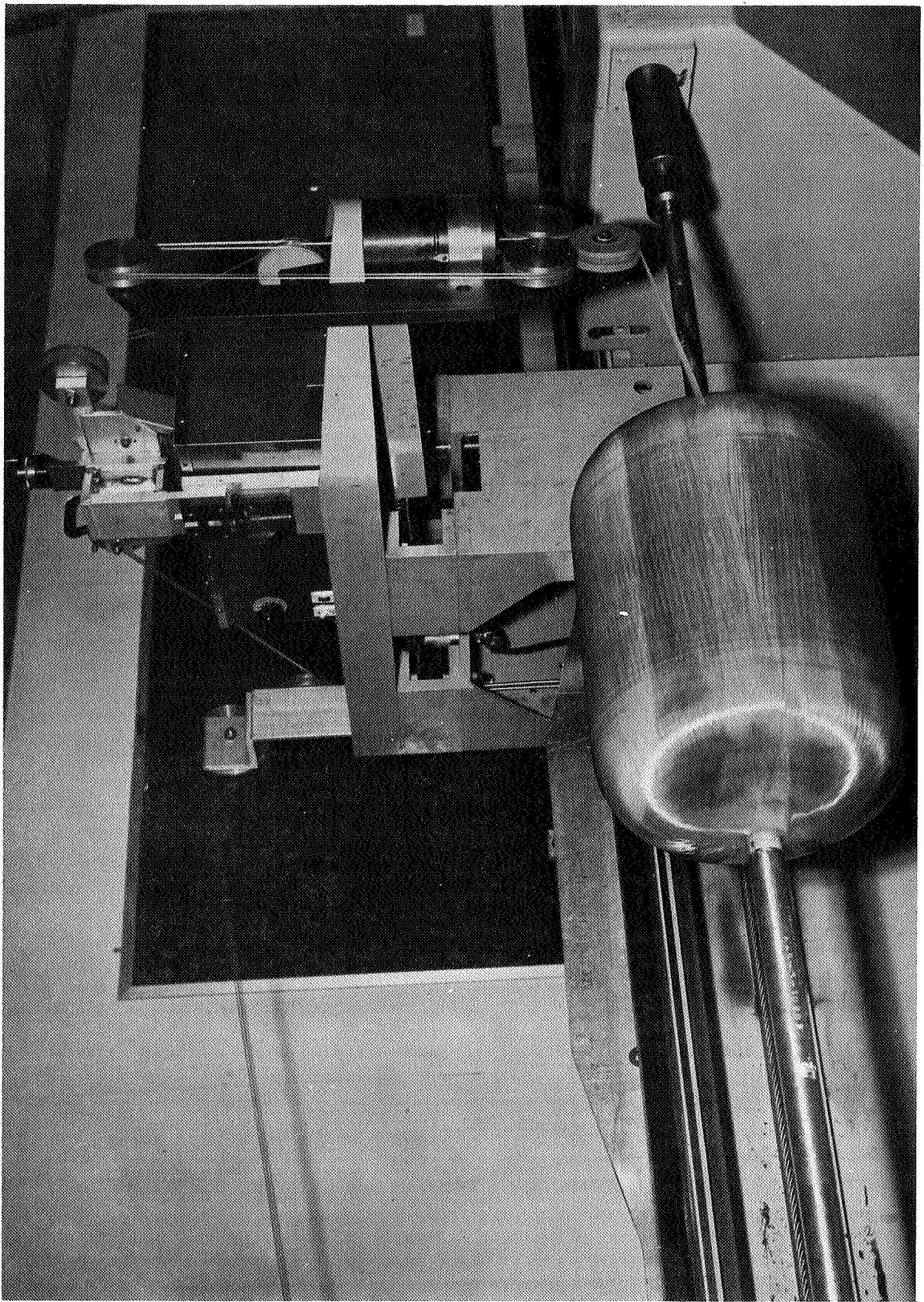
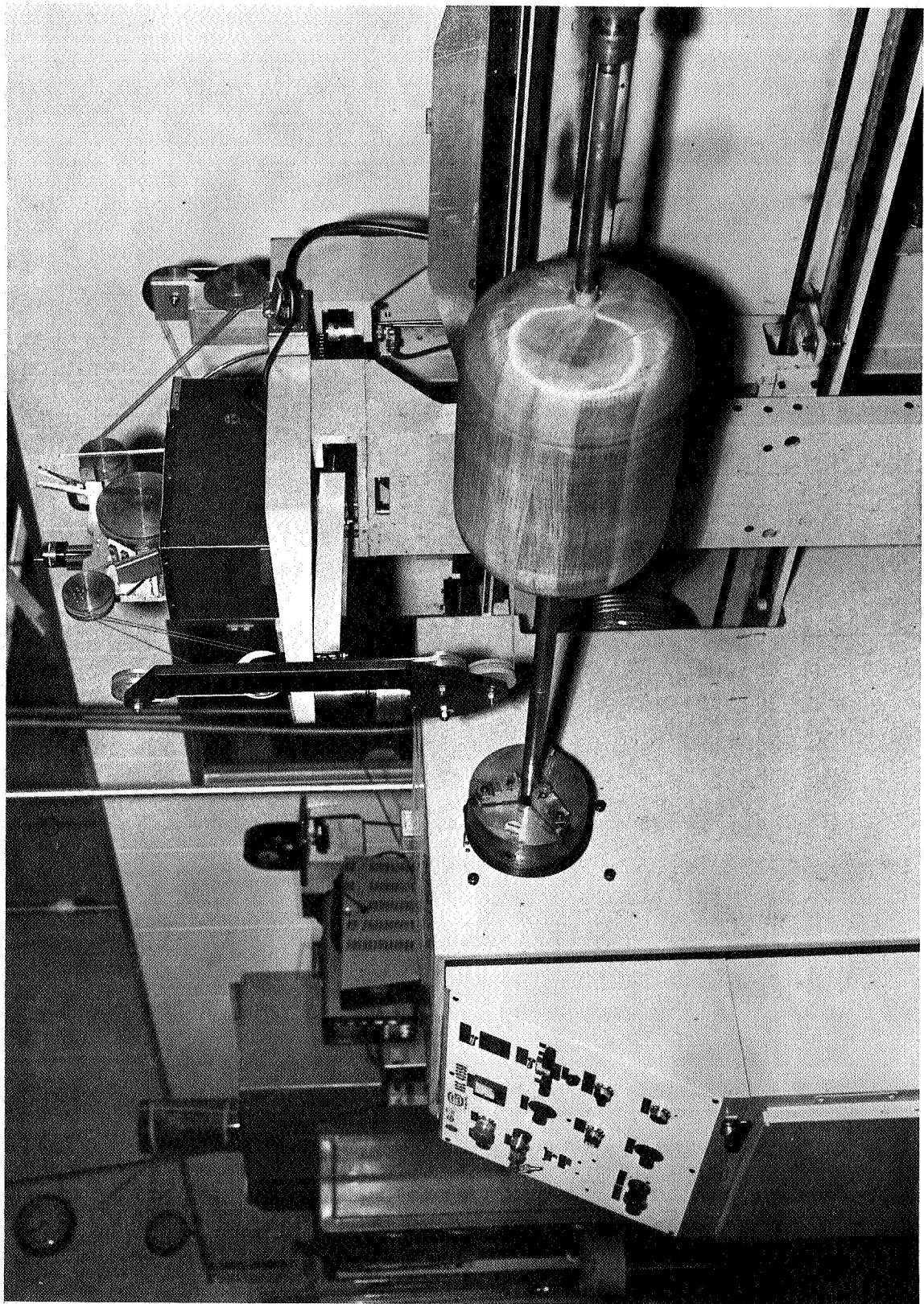


Figure 20
Winding 12-in.-dia. by 18-in.-long Mandrel



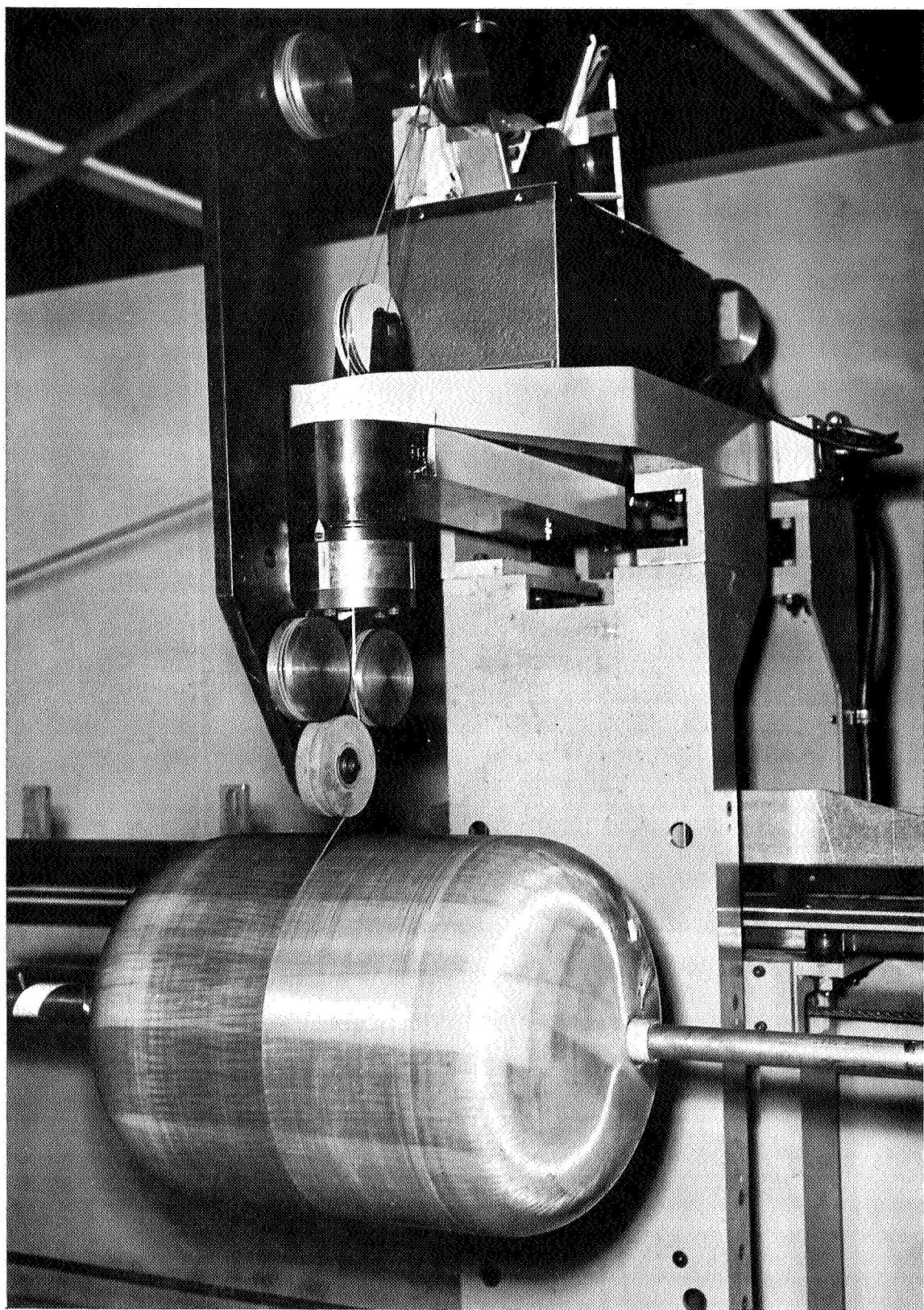
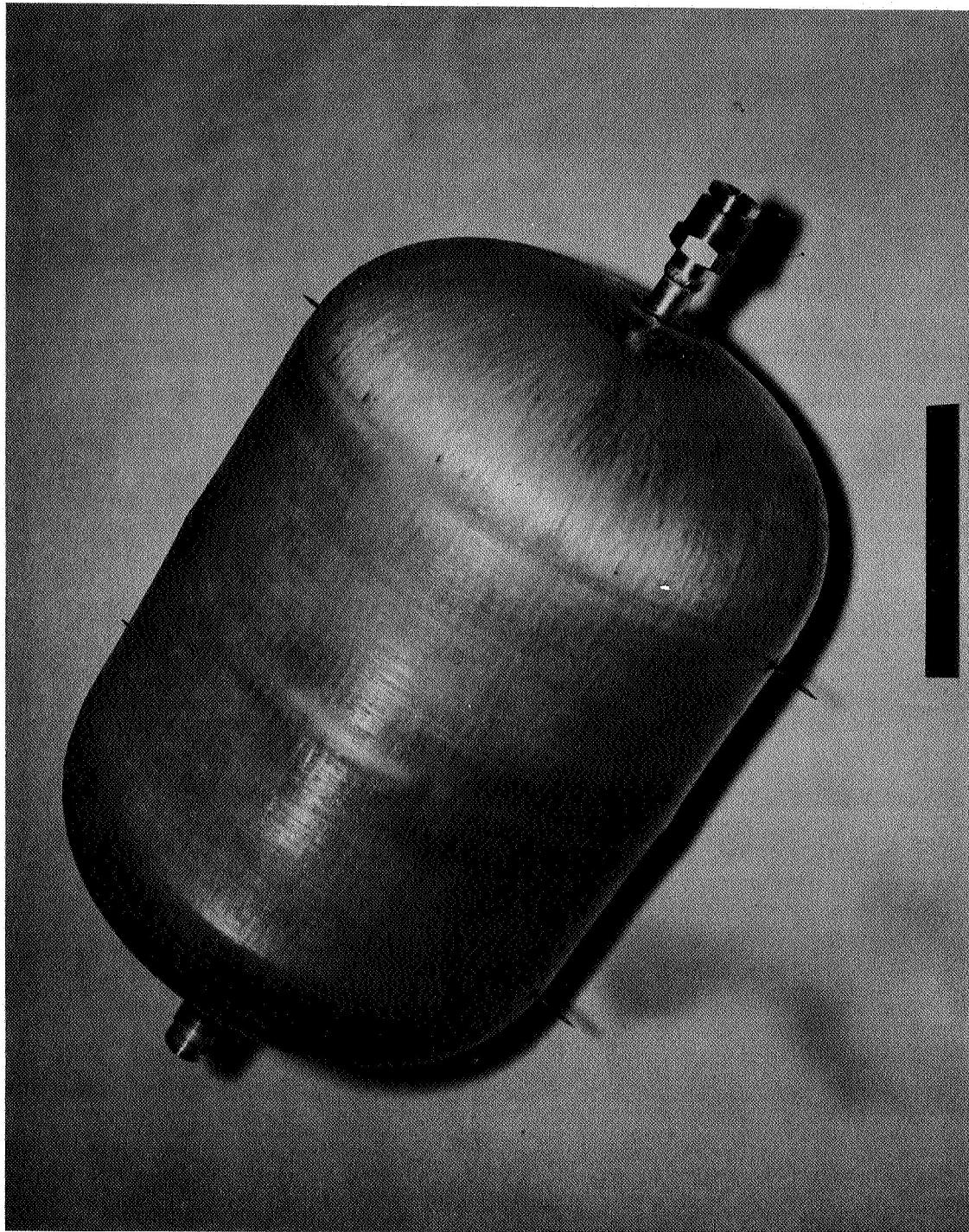


Figure 21
Application of Circumferential Glass Filament Winding to Liner

Figure 22
6061 Aluminum Lined Glass Filament-Wound Pressure Vessel



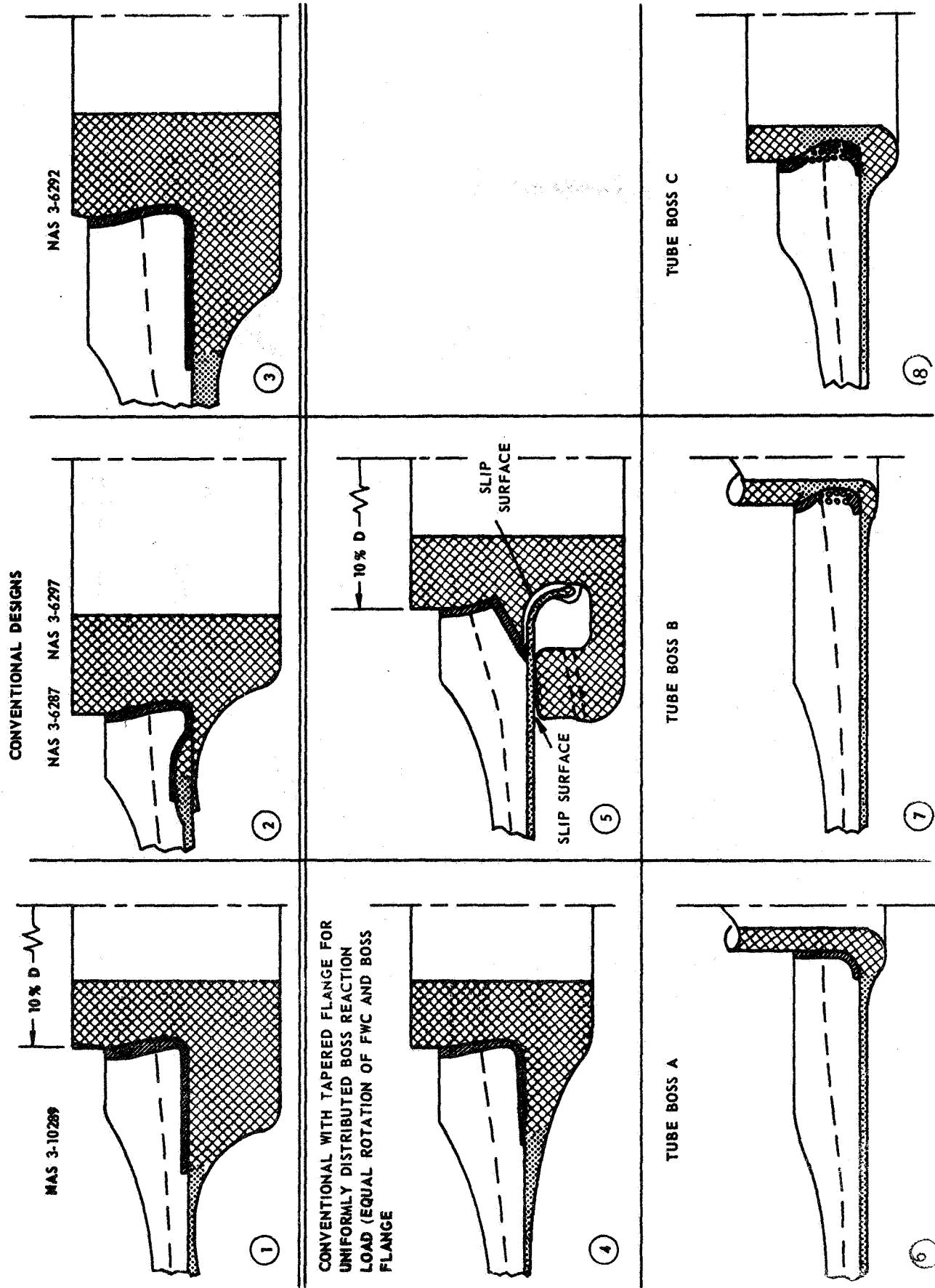


Figure 23, Sheet 1 of 2

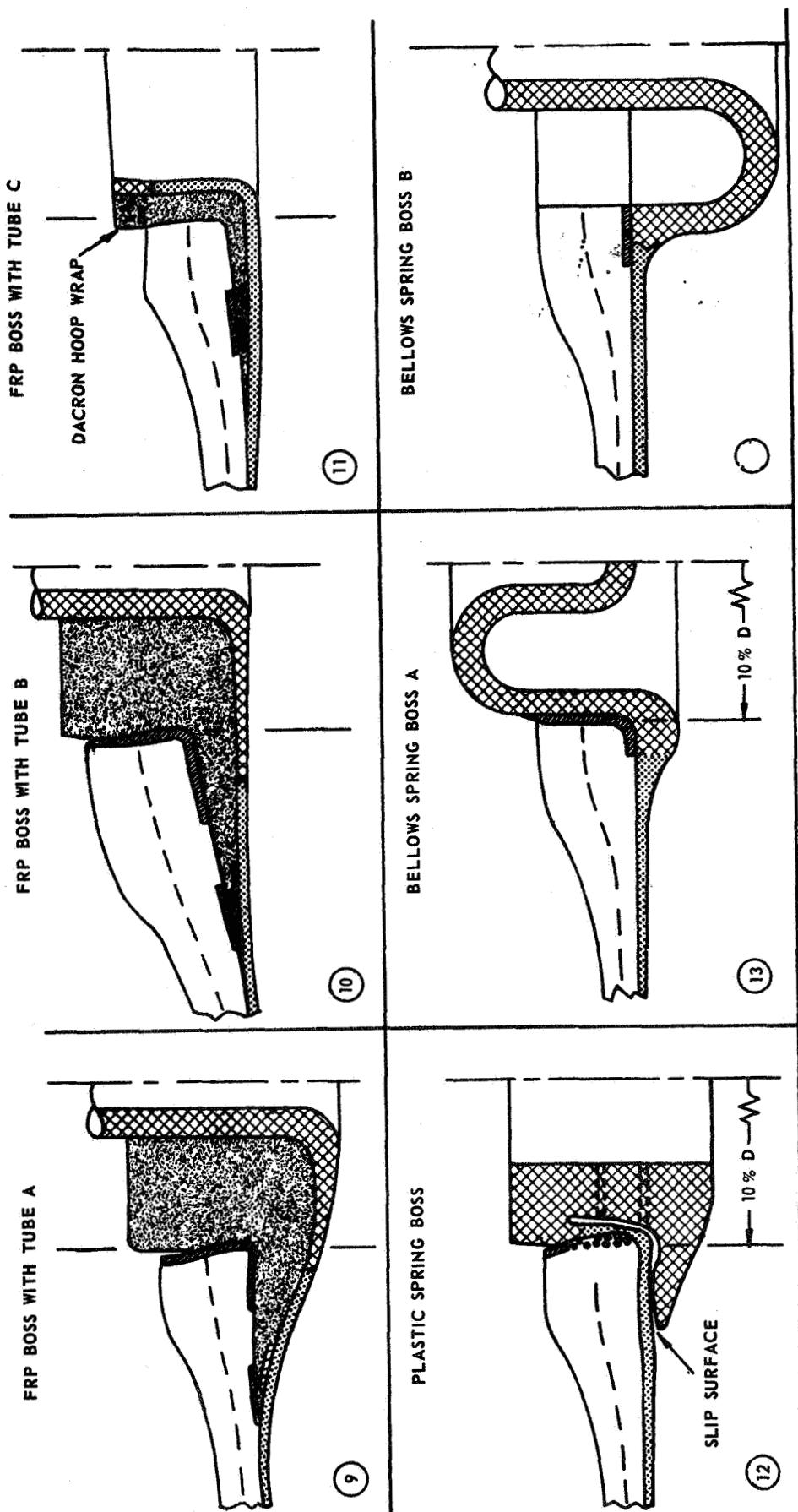
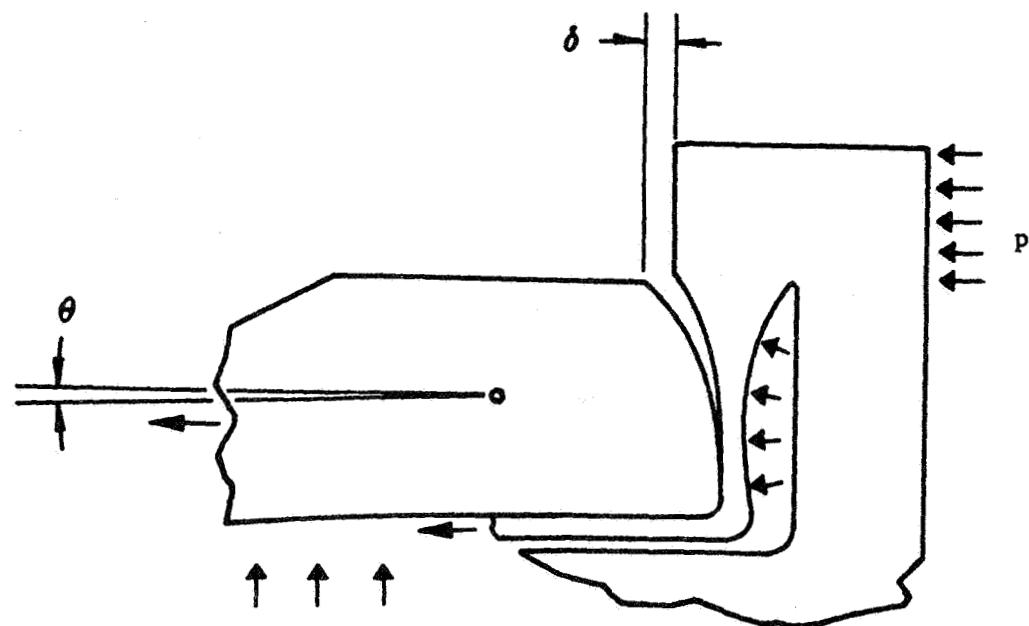
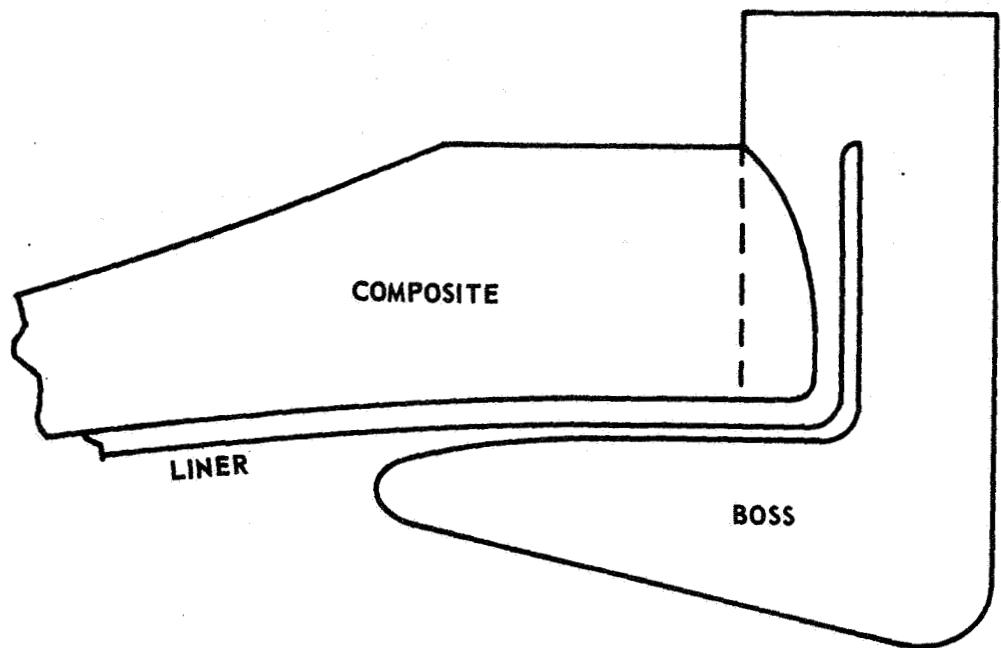


Figure 23, Sheet 2 of 2

METAL ABOVE YIELD STRESS
 XXXXXXXX
 METAL BELOW YIELD STRESS
 Wavy Line Pattern
 POSSIBLE UNBONDING

Polar Boss Design Configurations



Schematic of Plastic Spring Boss
(Hinge Boss)

Figure 24

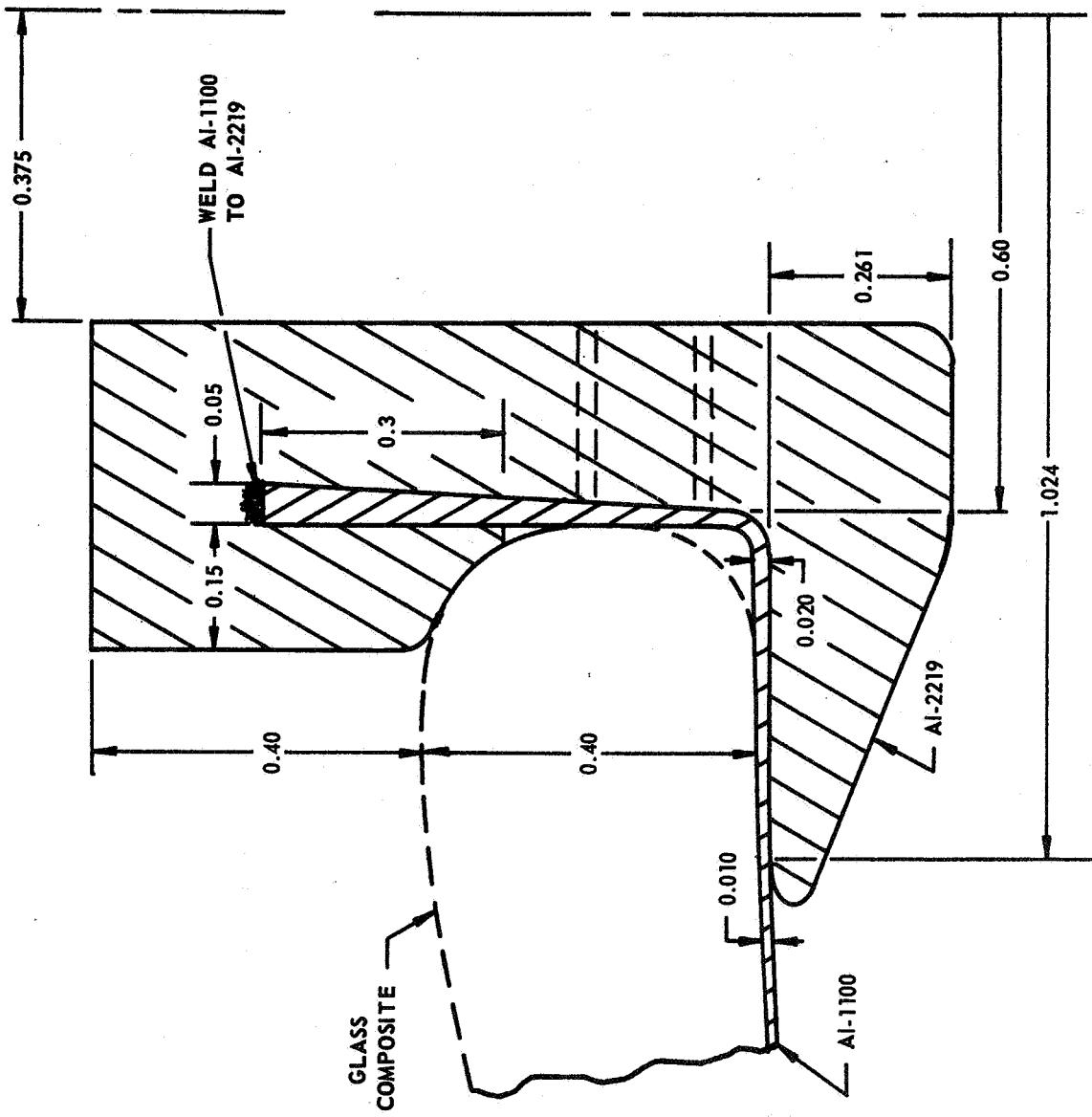


Figure 25

Plastic Spring Boss (Hinge Boss)

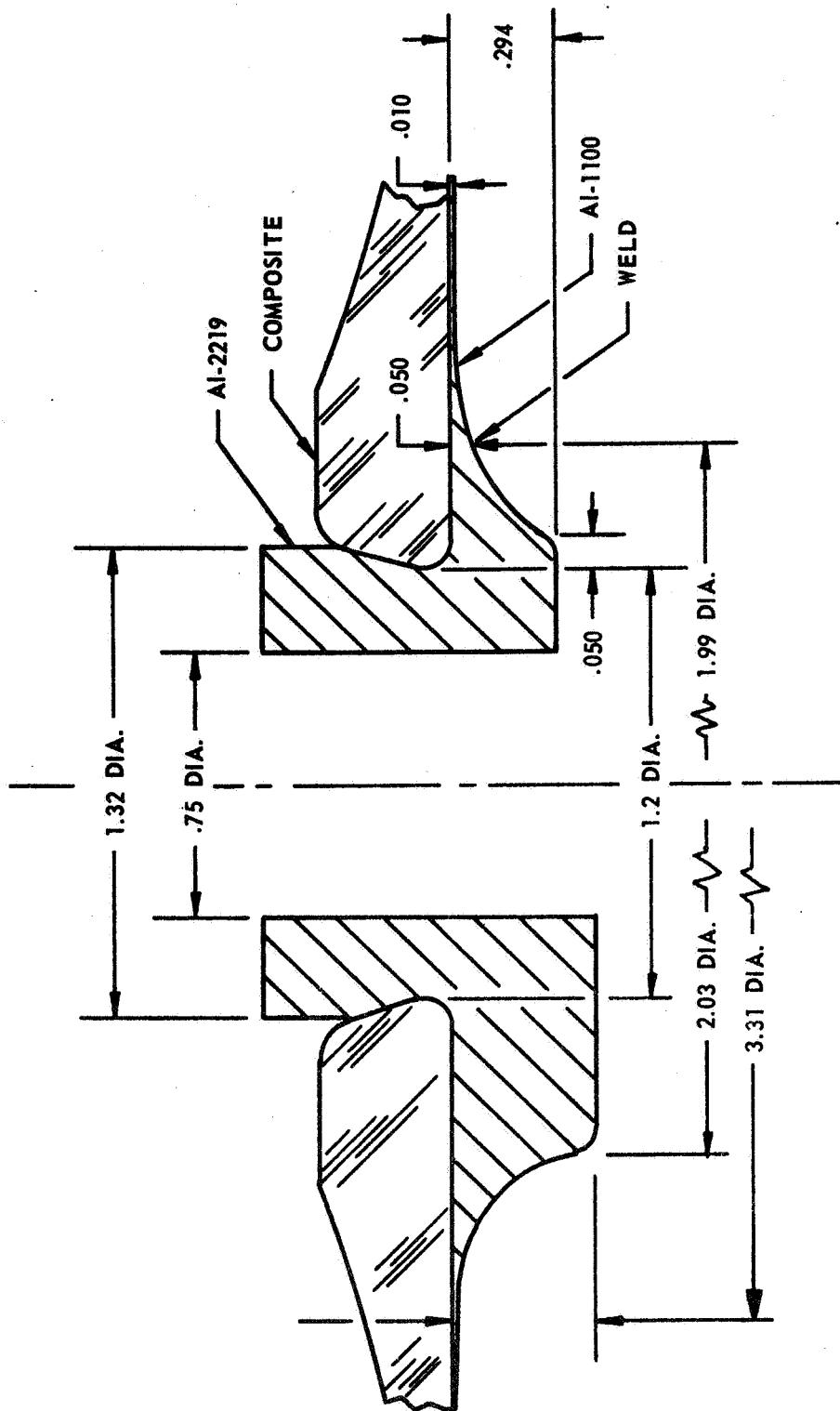
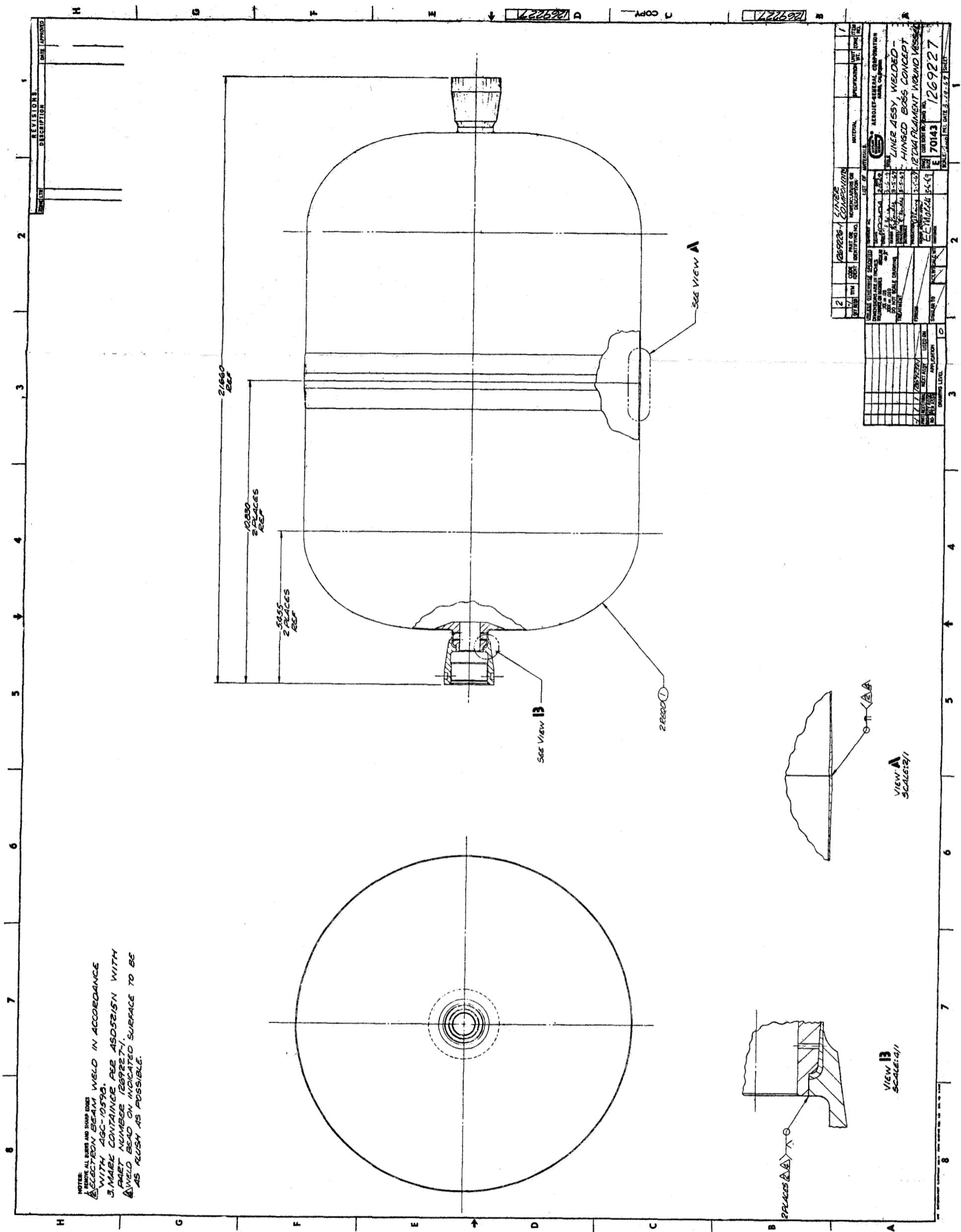


Figure 26

MATCHED ROTATION FLANGE BOSS

Matched-Rotation Flange Boss
(Butt-Welded-Boss)



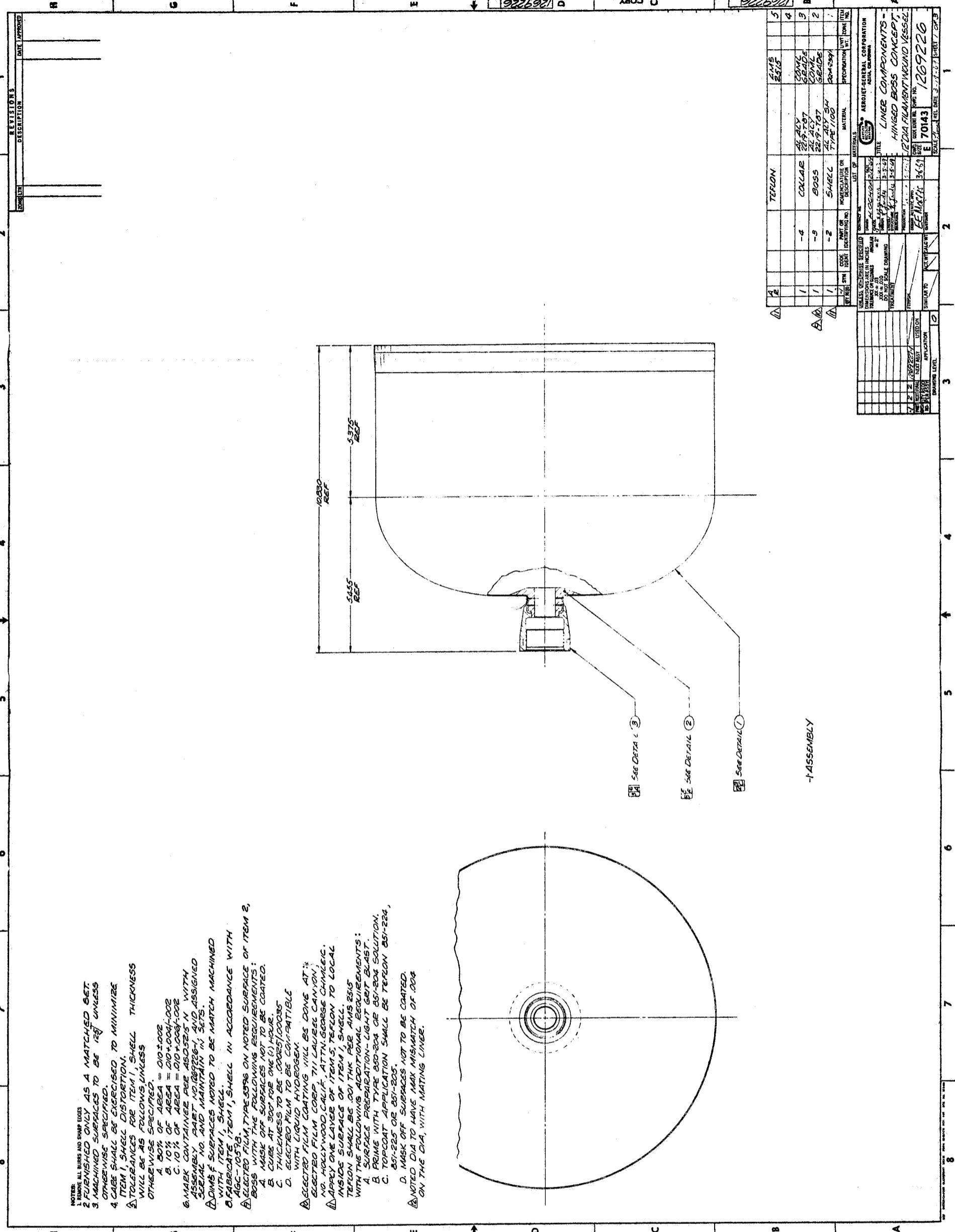


Fig. 27 1100 Aluminum Liner, Hinged-Boss Configuration (Engineering Drawing) – Sheet 2

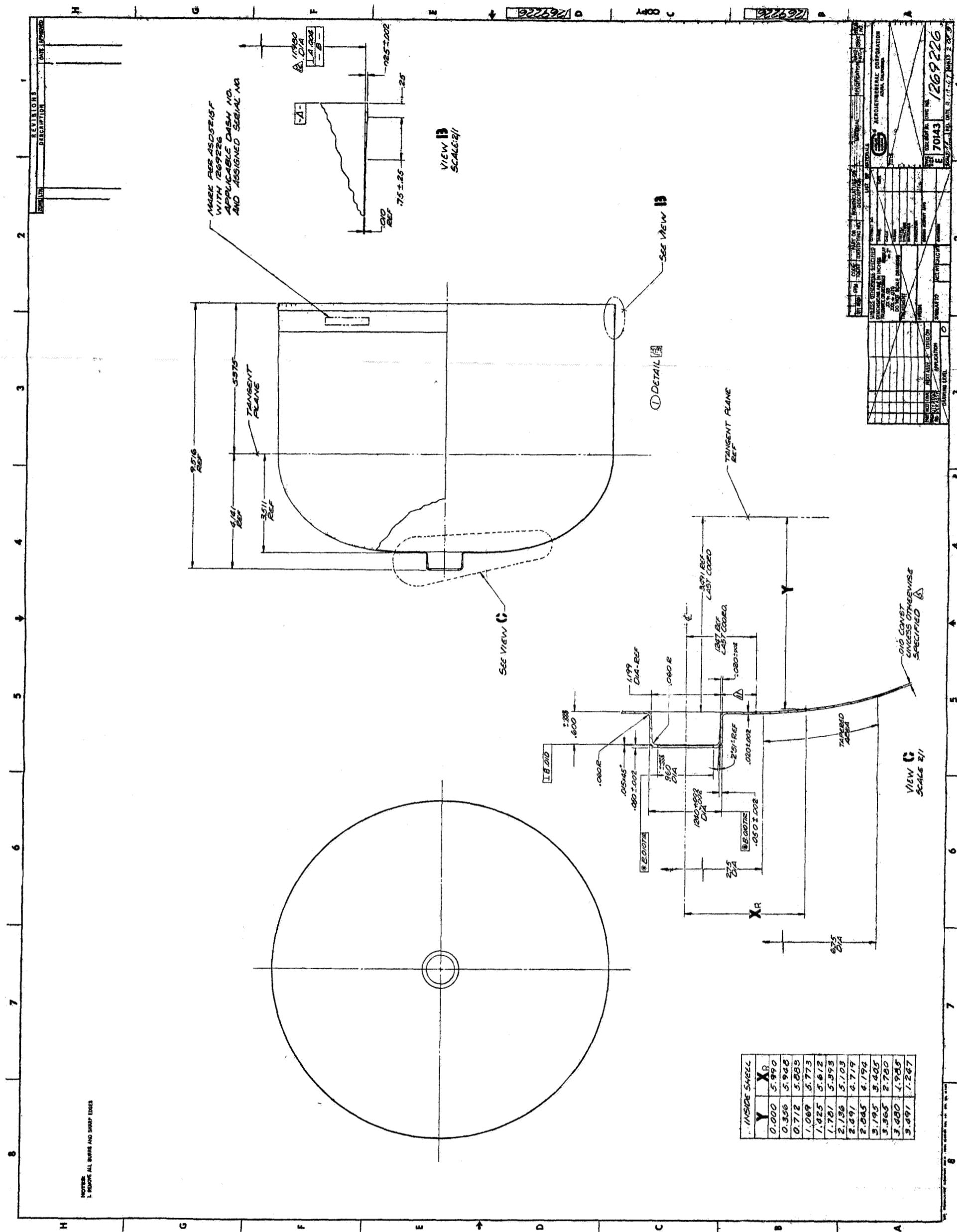


Fig. 27 1100 Aluminum Liner, Hinged-Boss Configuration (Engineering Drawing) – Sheet 3

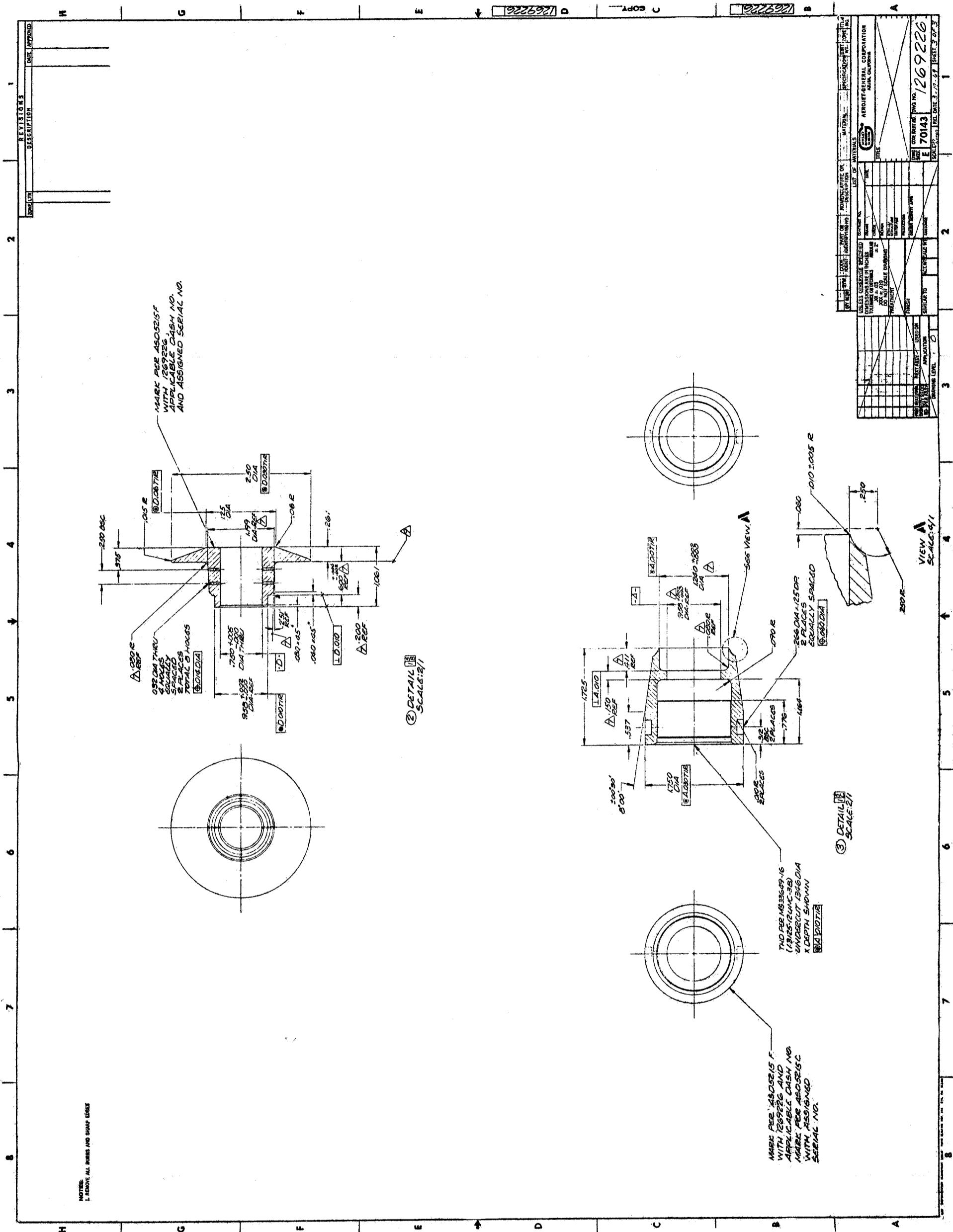


Fig. 27 1100 Aluminum Liner, Hinged-Boss Configuration (Engineering Drawing) – Sheet 4

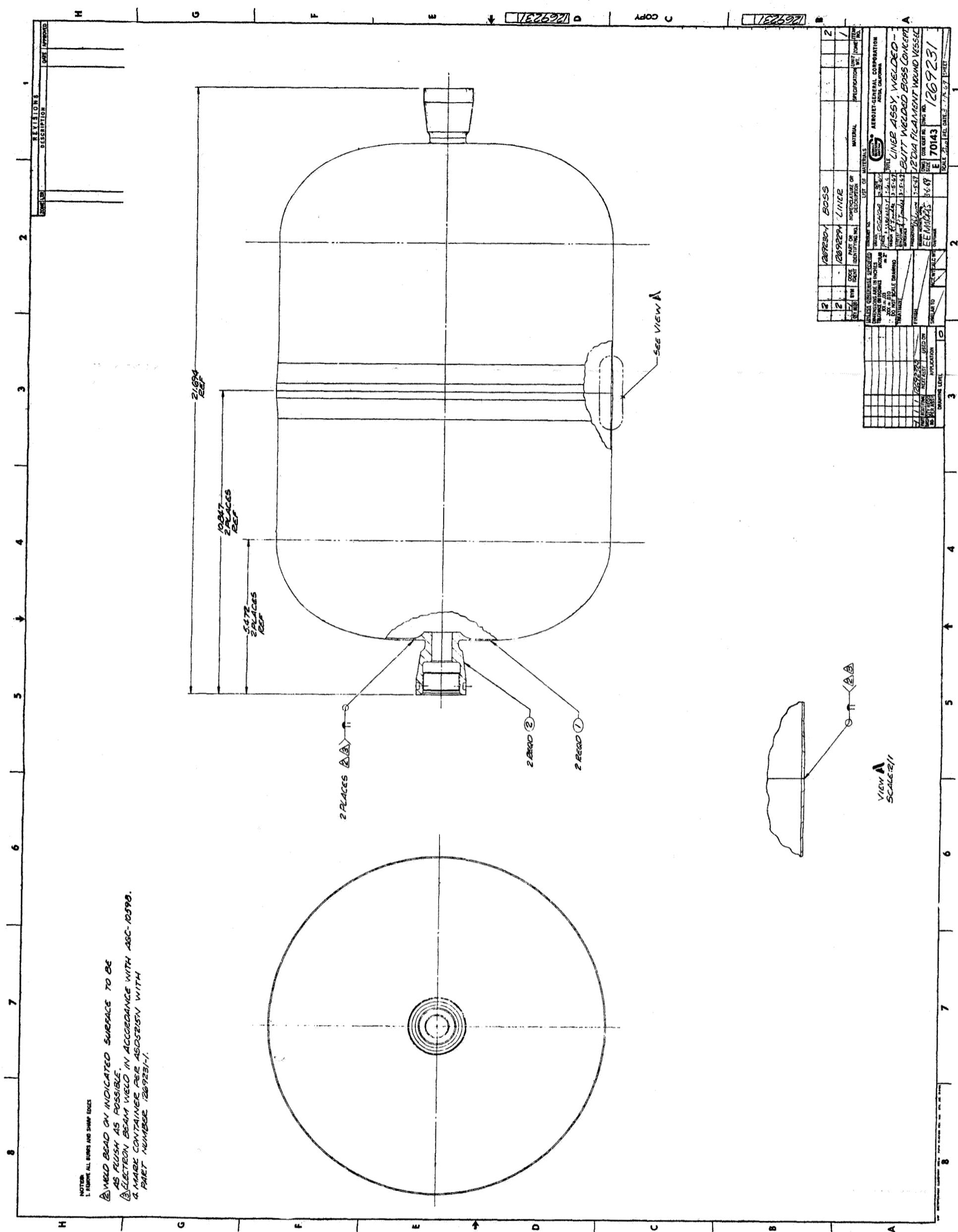


Fig. 28 1100 Aluminum Liner, Butt-Welded Boss Configuration (Engineering Drawing) – Sheet 1

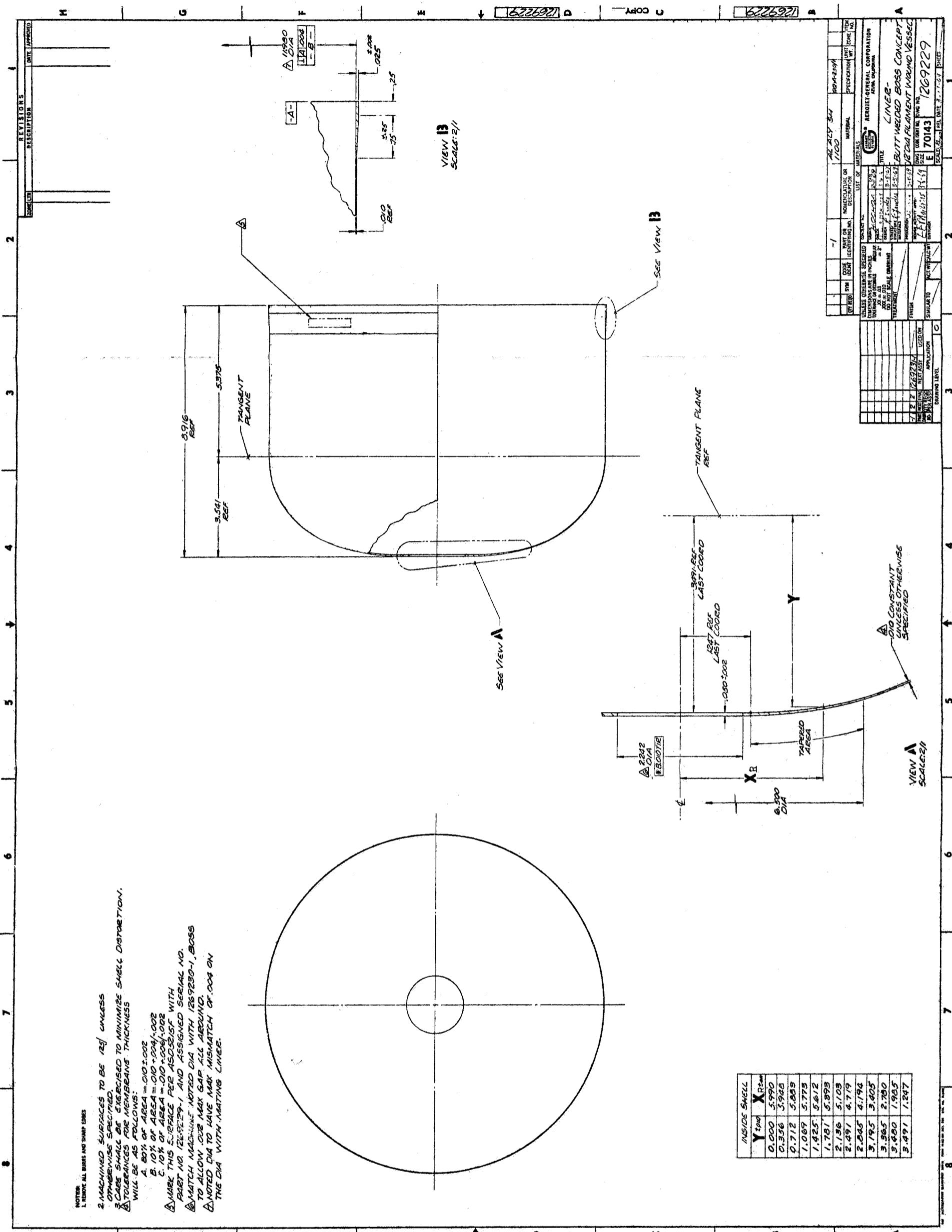
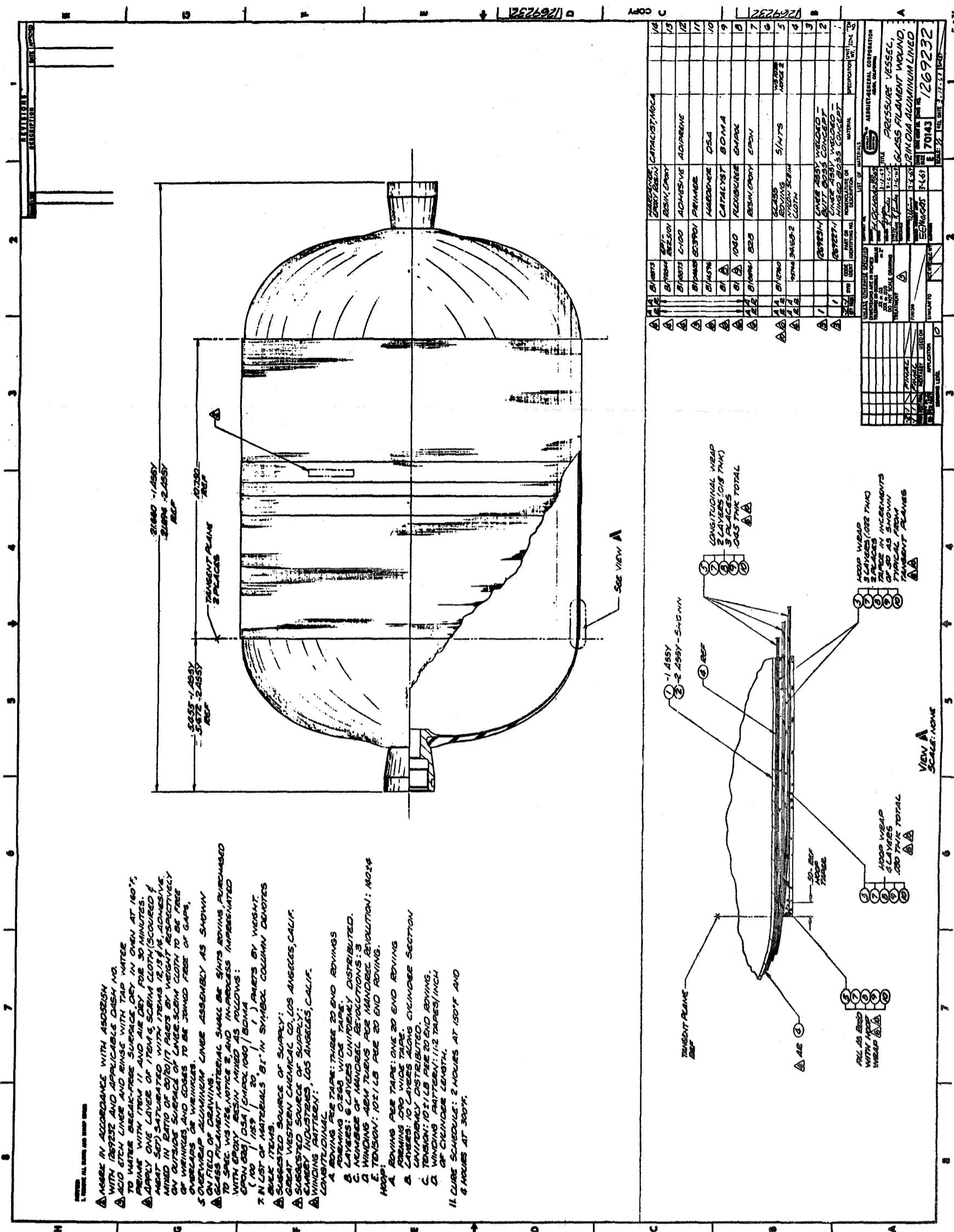


Fig. 28 1100 Aluminum Liner, Butt Welded Boss Configuration (Engineering Drawing) – Sheet 2



Aluminum-Lined Glass-Filament-Wound Vessel

Figure 29



Figure 30
Drawn and Machined 1100 Aluminum Halfshell Forming for Hinged Boss Liner

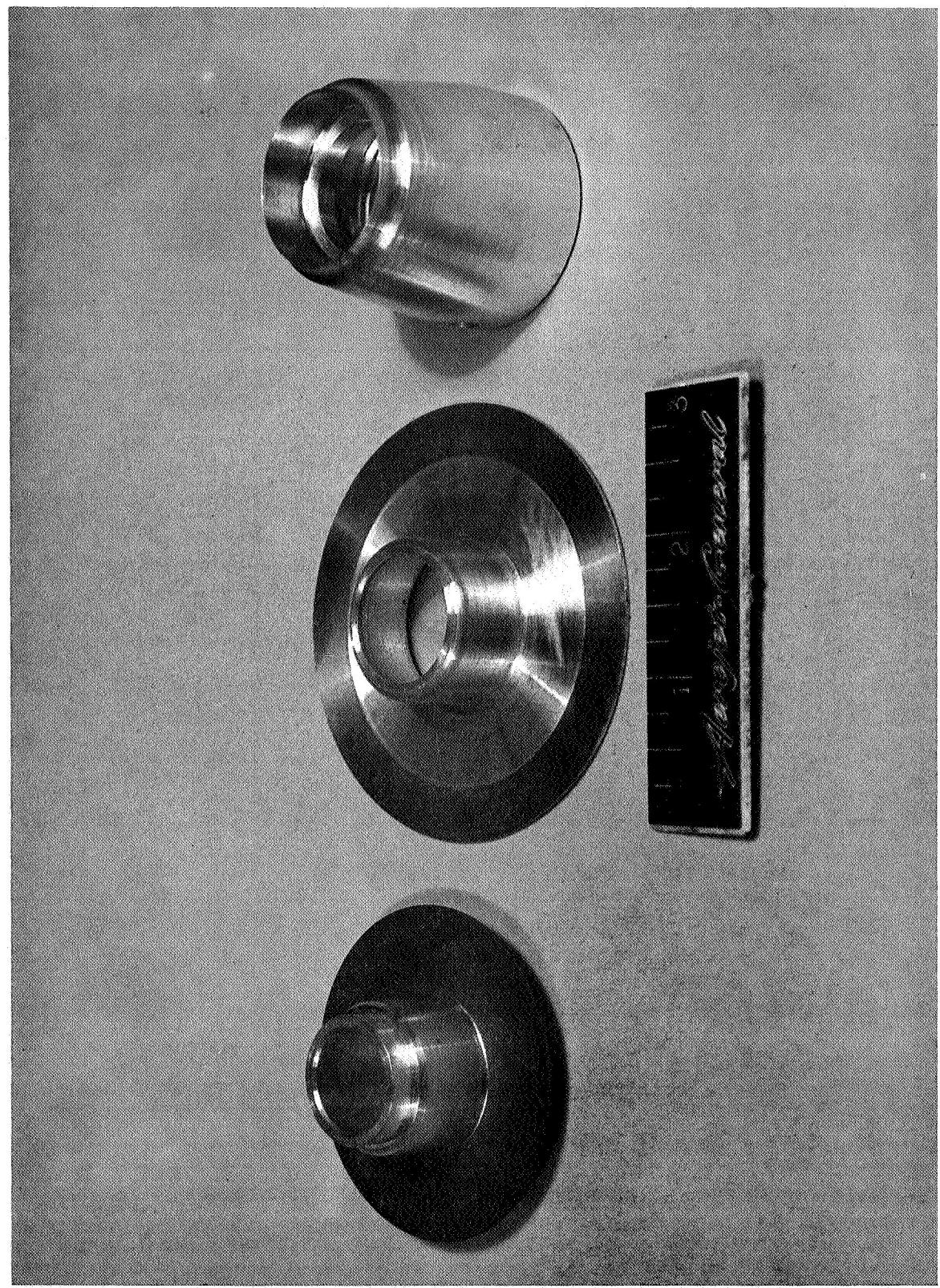


Figure 31
Boss, Flange, and Collar for Hinged Boss Liner

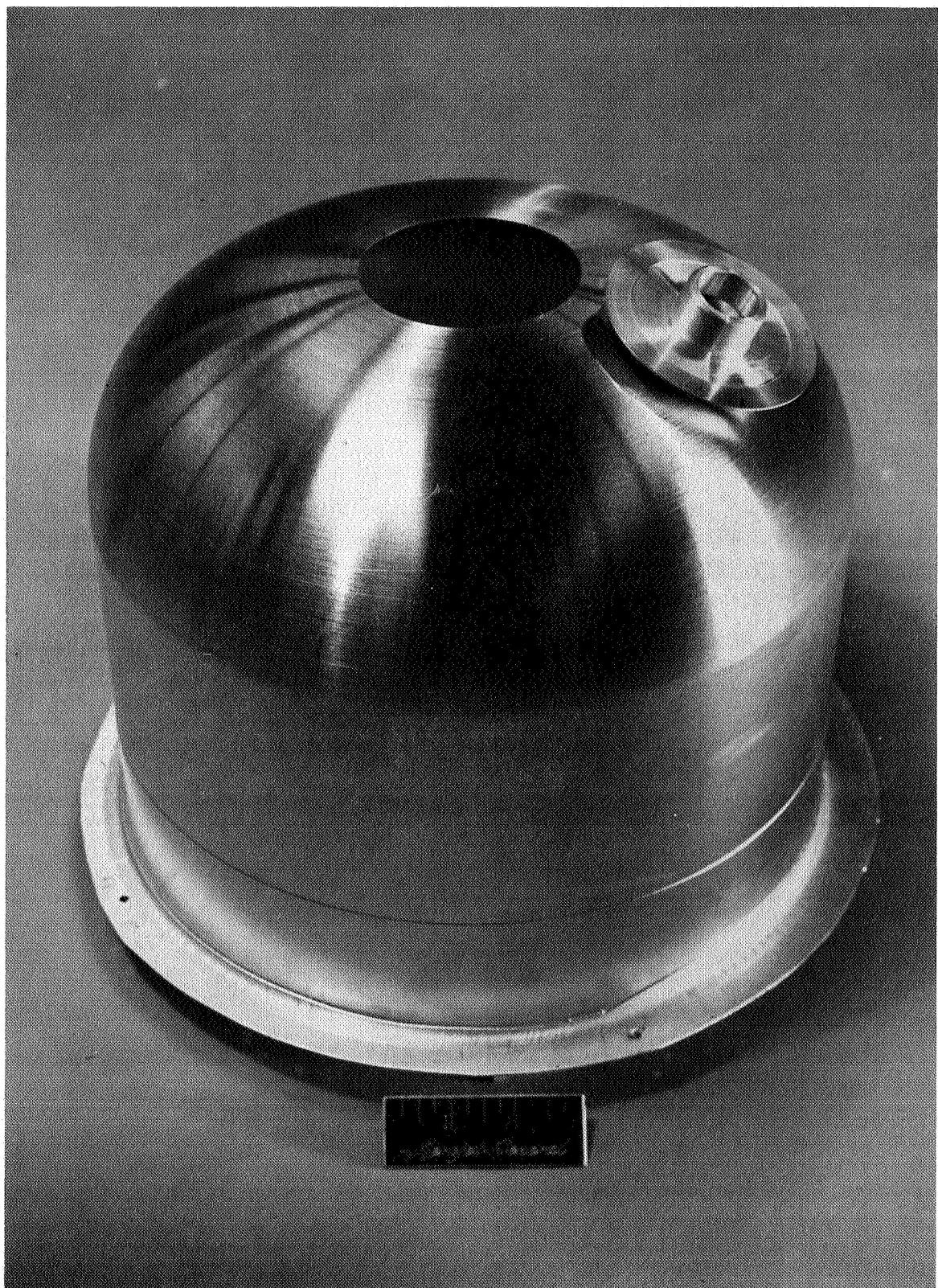


Figure 32
Flange and Drawn and Machined Halfshell Forming for Hinged Boss Liner



Figure 33
Flange Welded to Drawn and Machined Halfshell Forming for Hinged Boss Liner

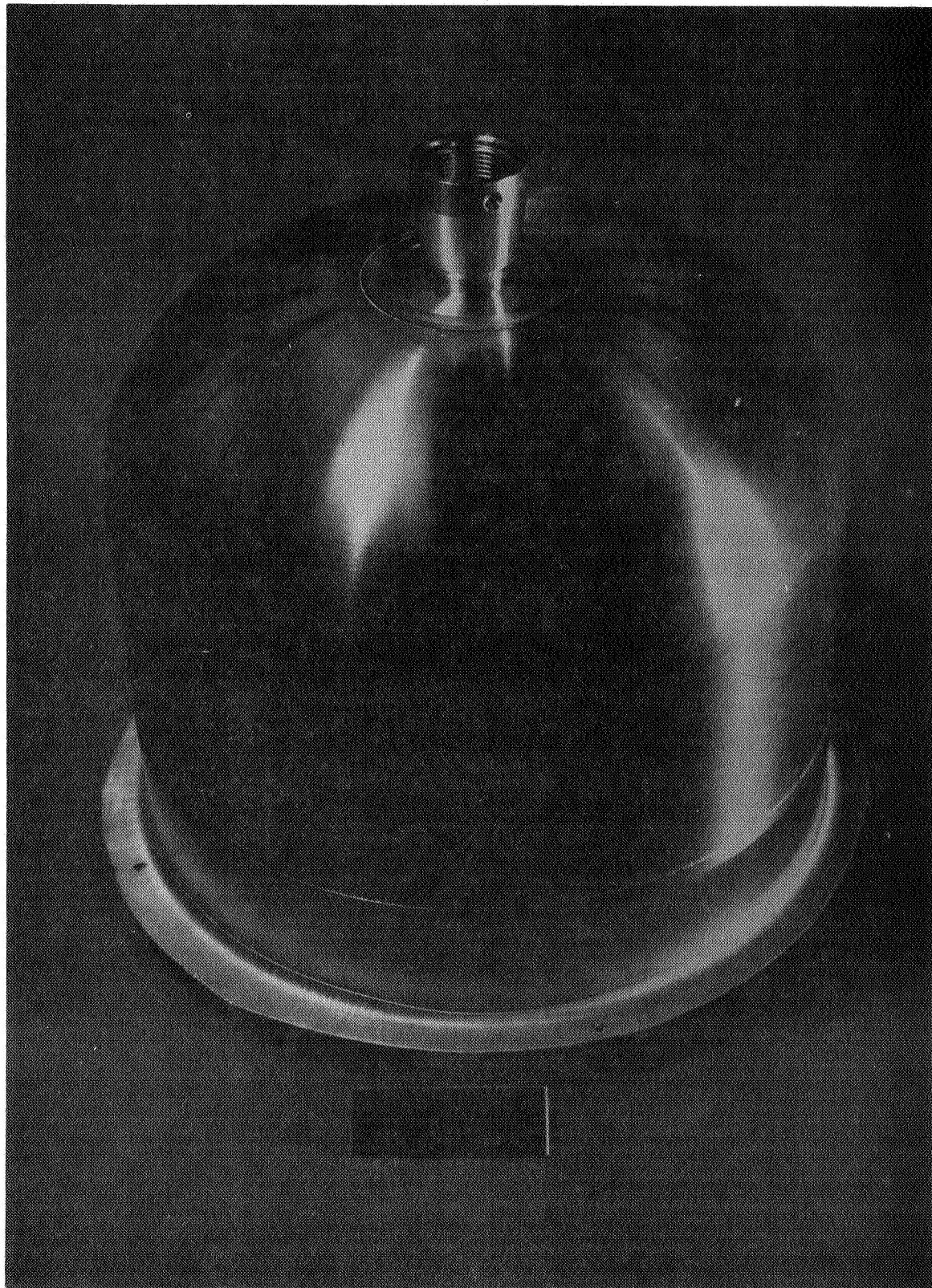


Figure 34
Boss and Collar Welded to Flange of Hinged Boss Liner Halfshell Forming

Figure 35
Final Machined and Chemically Milled Liner Halfshell for Hinged Boss Liner, Exterior View

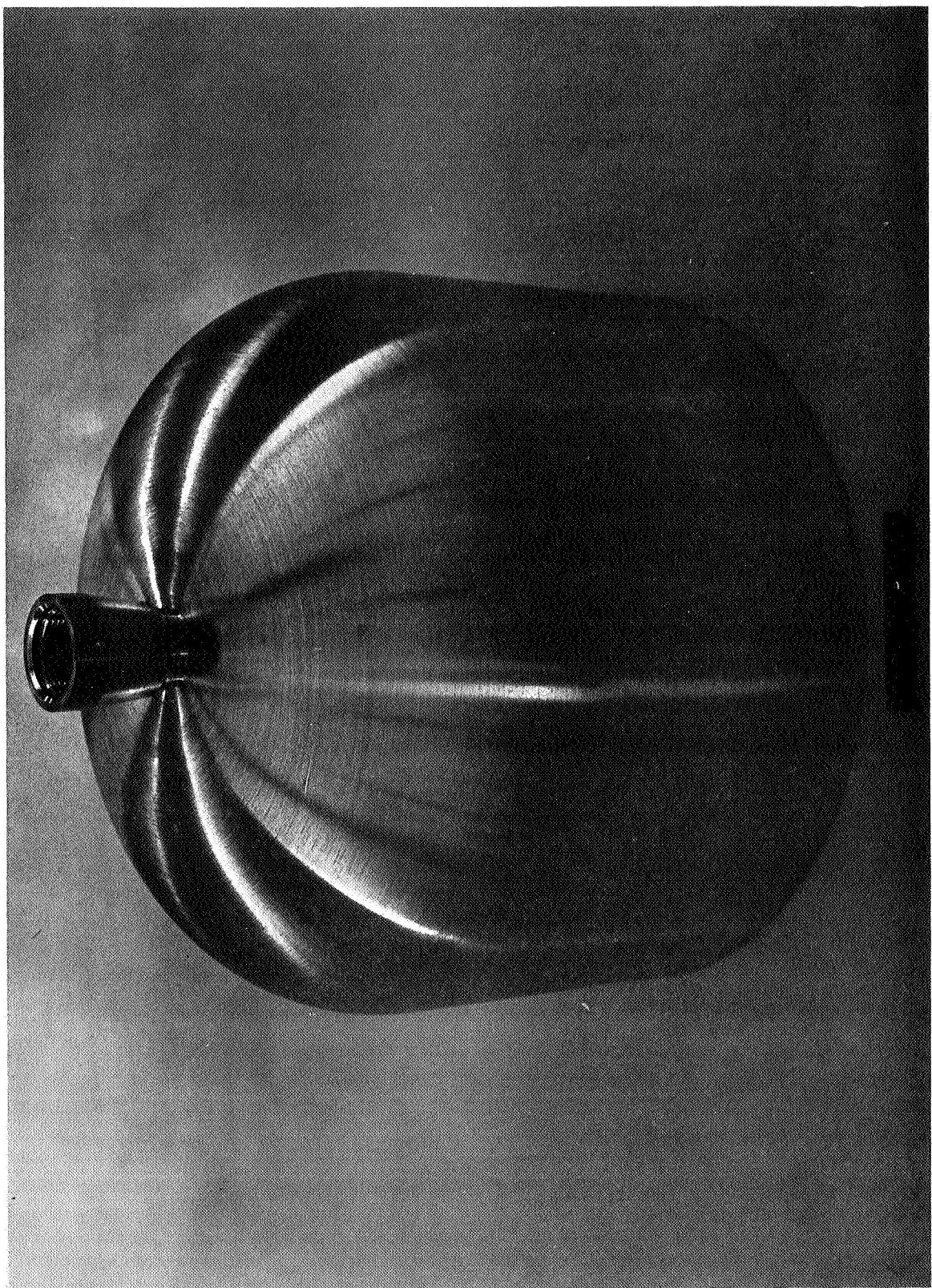
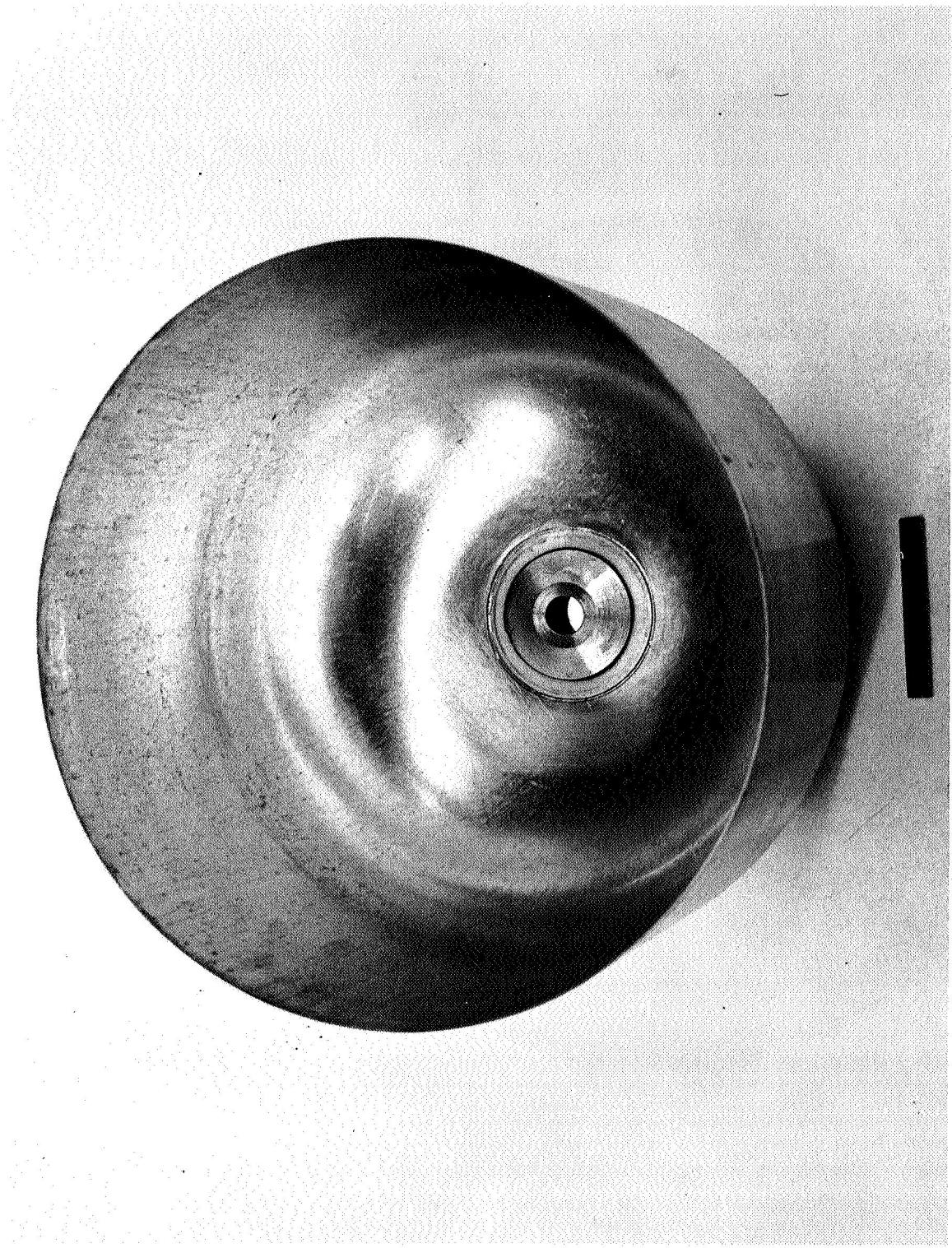


Figure 36
Final Machined and Chemically Milled Hinged Boss Liner, Interior View



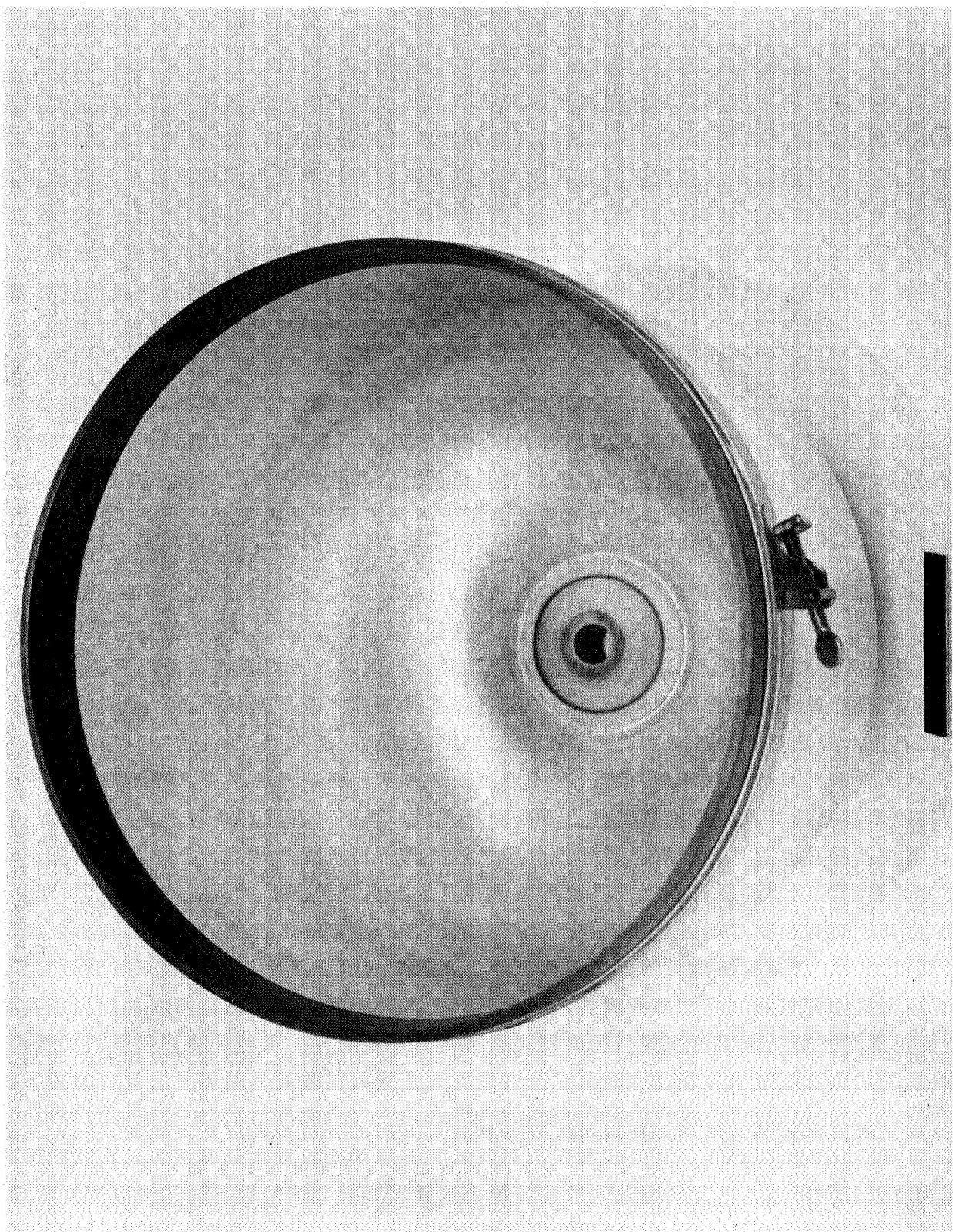


Figure 37
Copper Girth Weld Backup Ring Assembly to Liner Halfshell

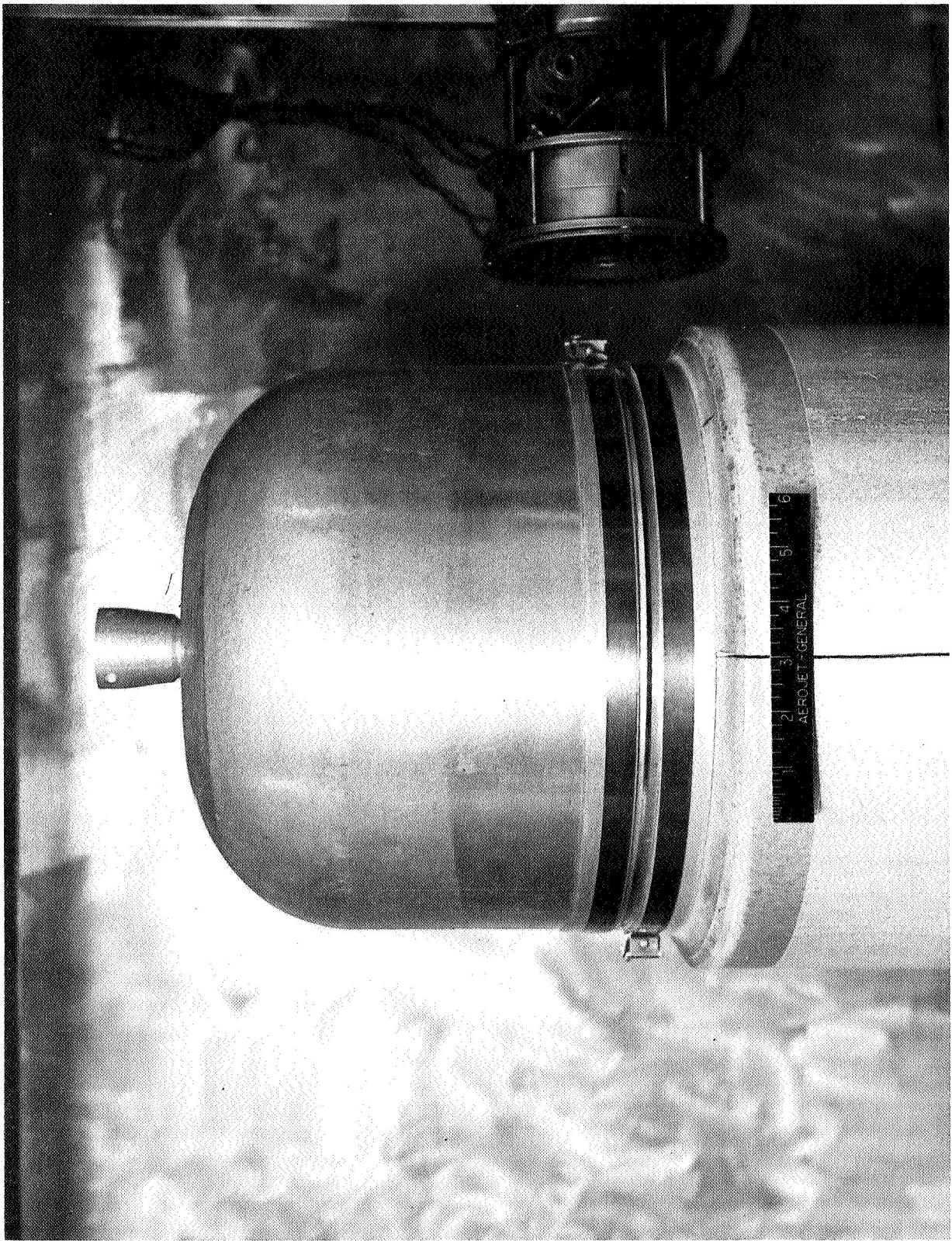


Figure 38
Liner Assembly in Position for EB Girth Welding

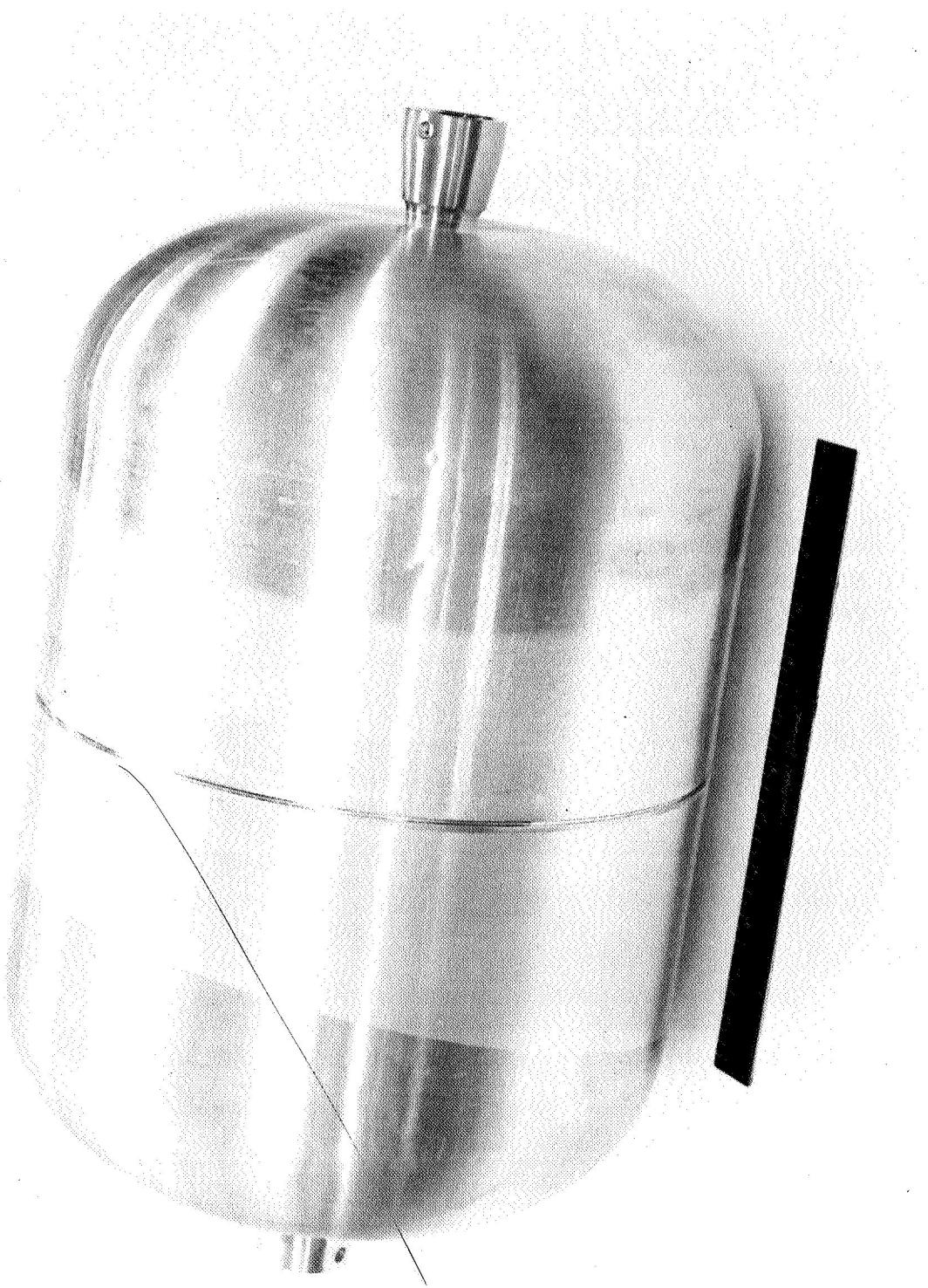


Figure 39
Completed Liner Assembly, Hinged Boss Configuration

Figure 40
Application of Longitudinally Oriented Glass-Filament Overwinding to Aluminum Liner

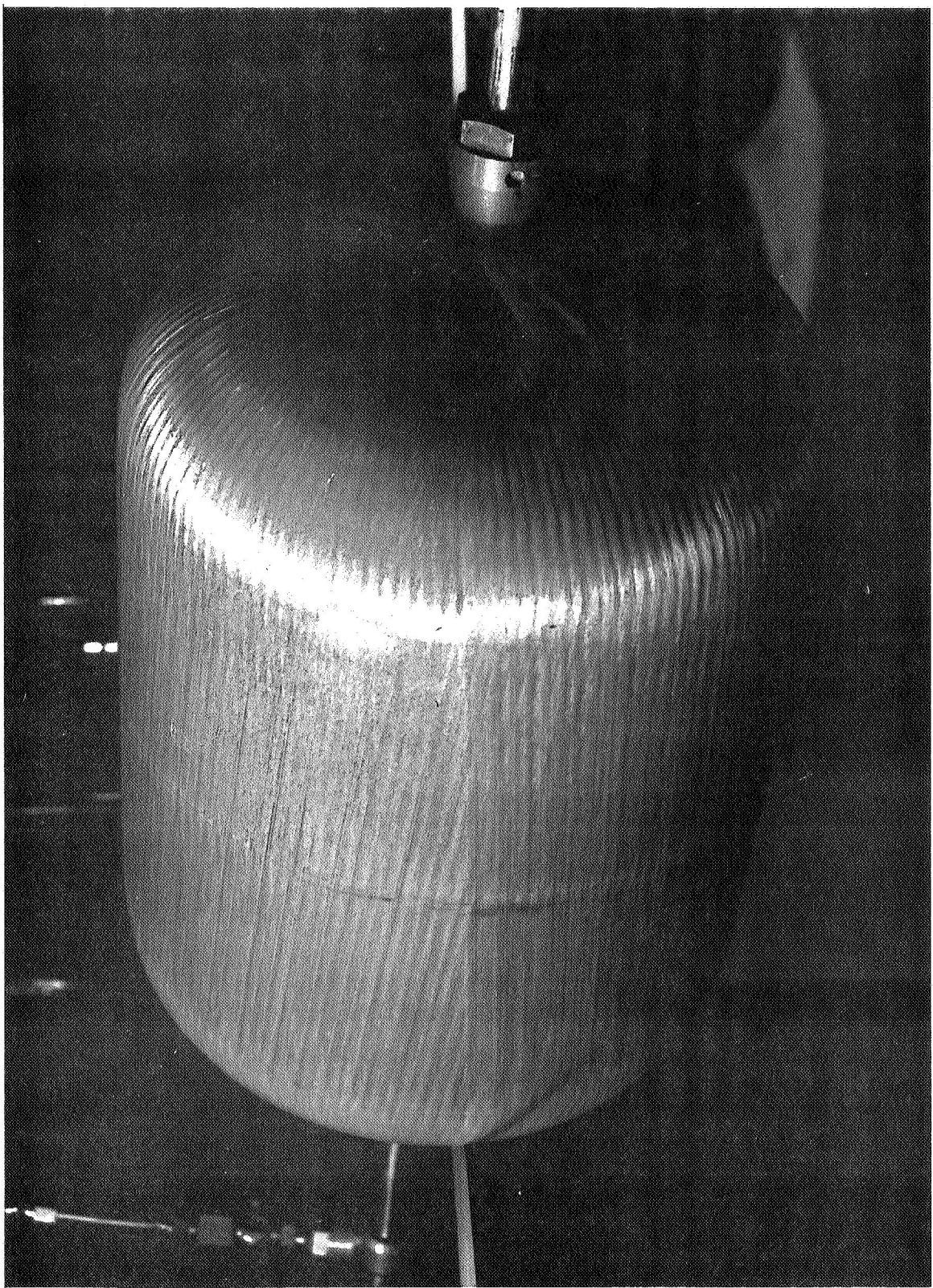
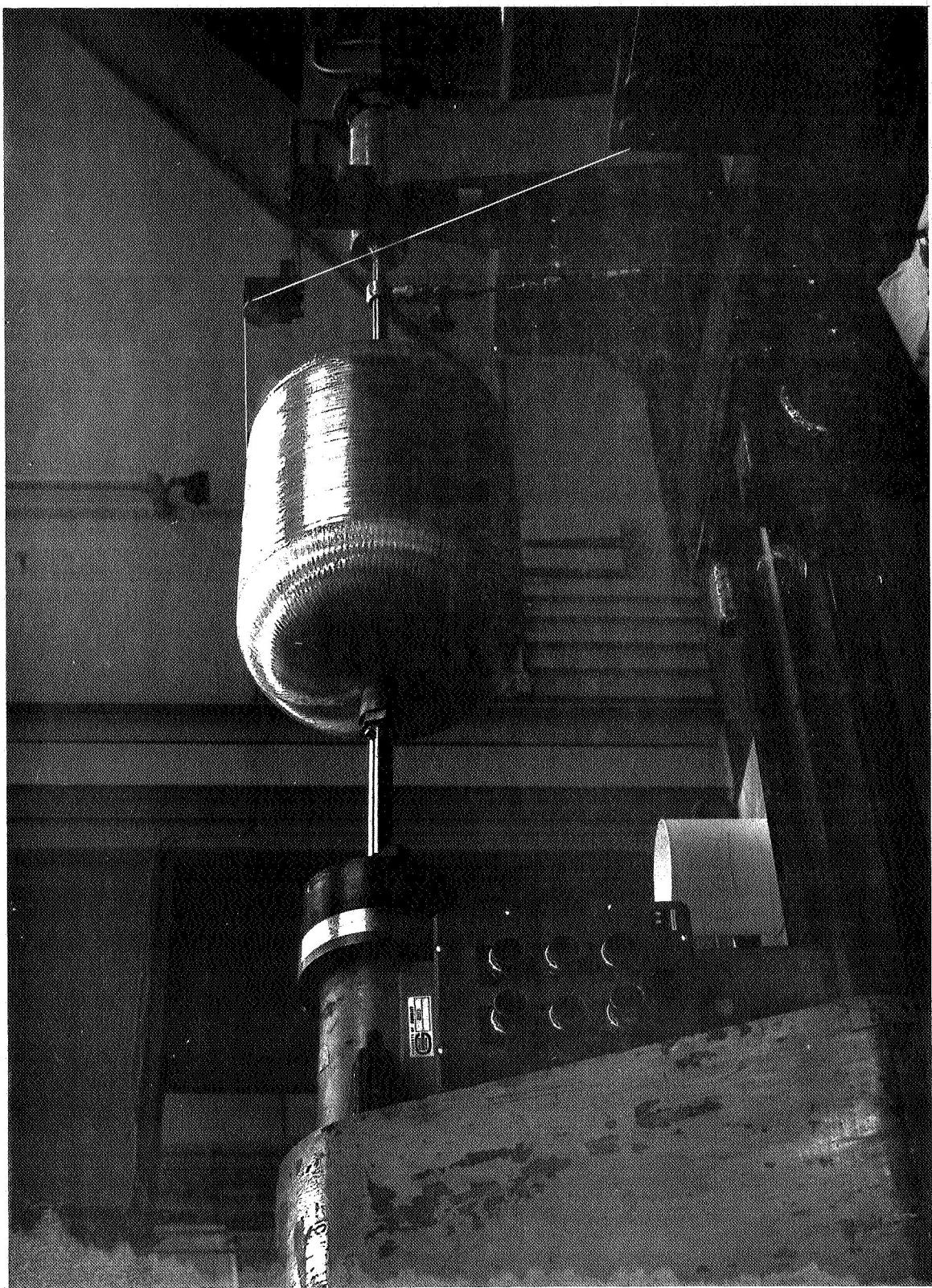


Figure 41
Application of Circumferentially Oriented Glass-Filament Overwinding to Aluminum Liner



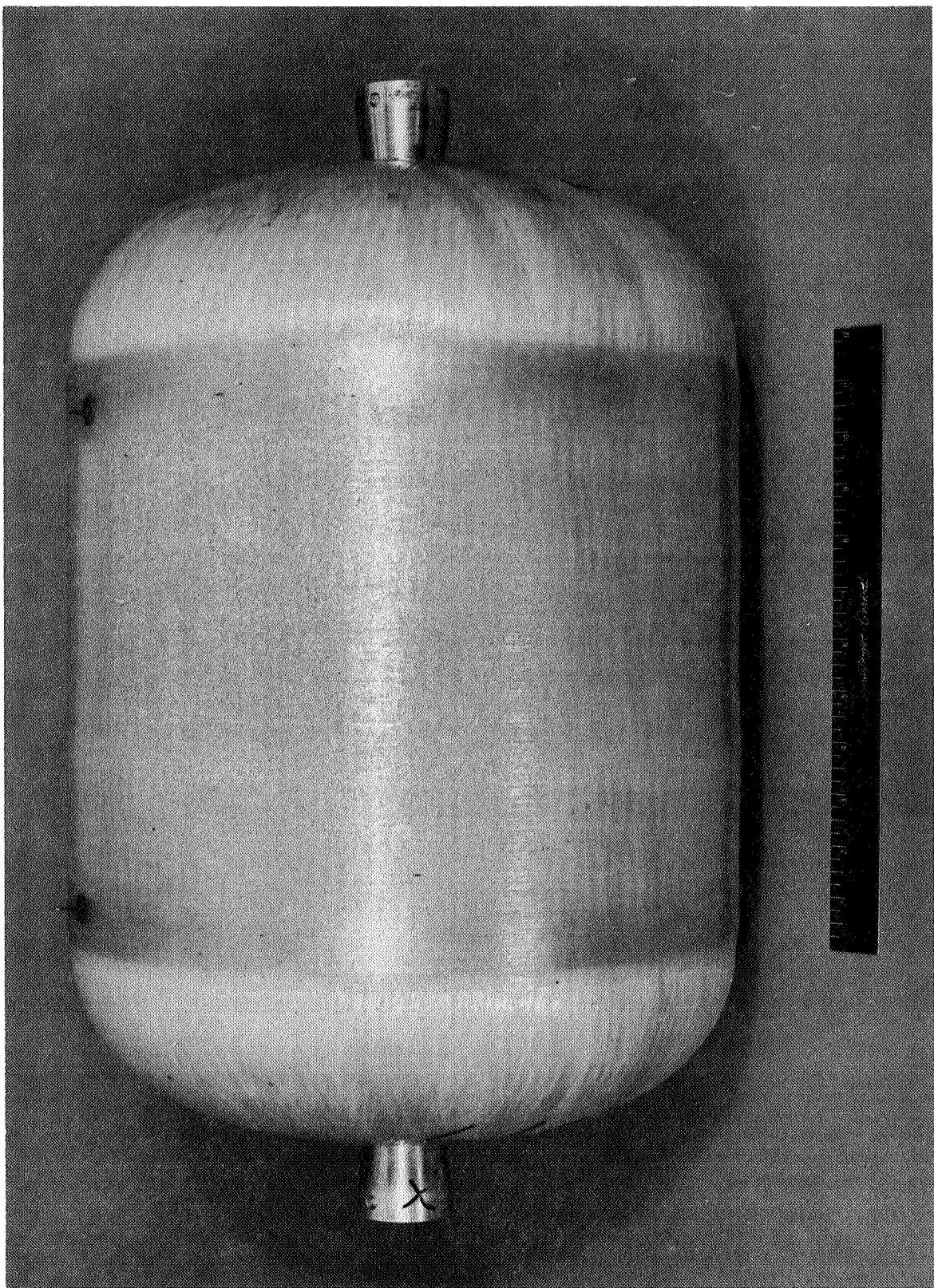


Figure 42
Completed Aluminum-Lined Glass Filament-Wound Pressure Vessel

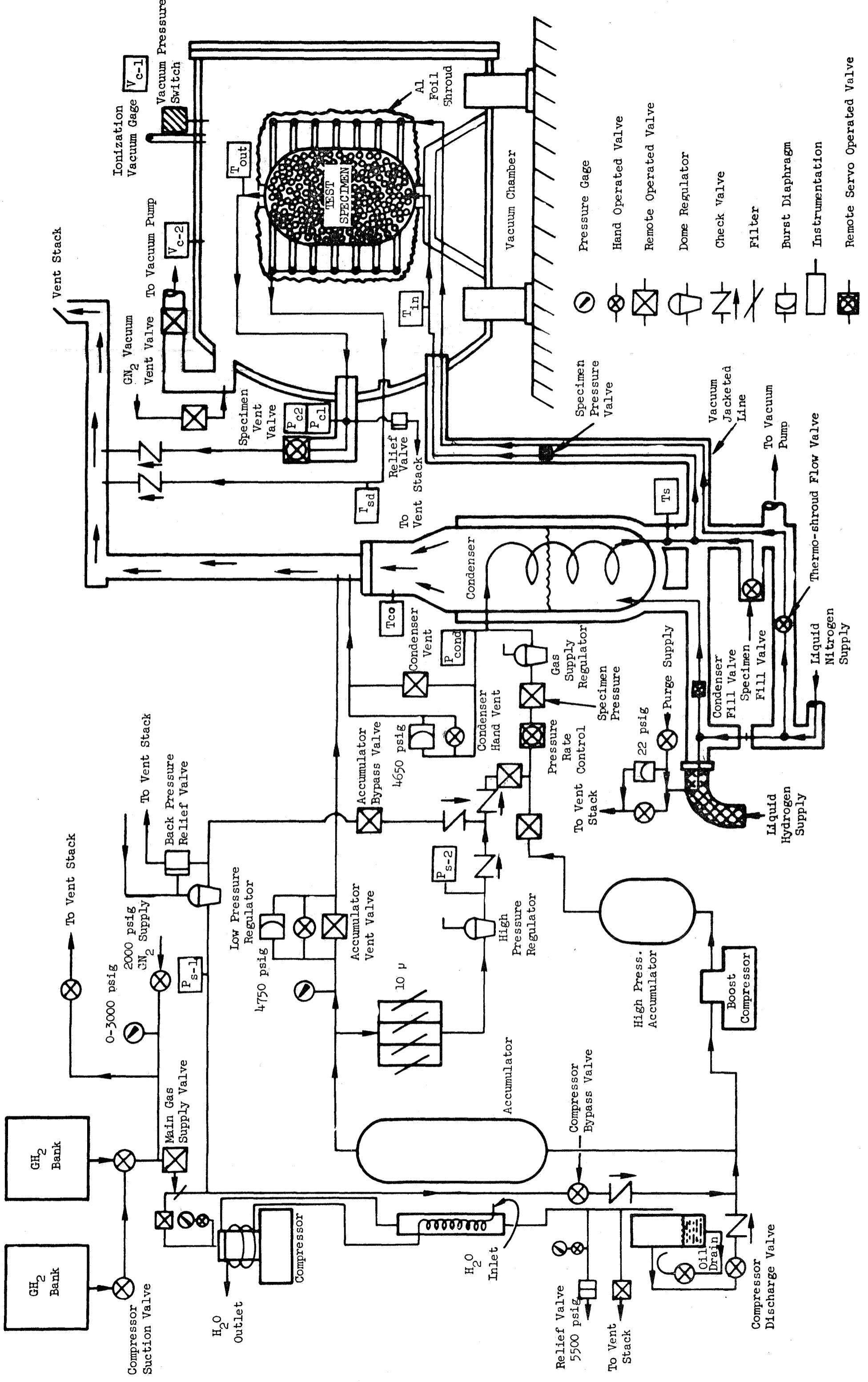


Fig. 43 Liquid Cryogen Test Facility

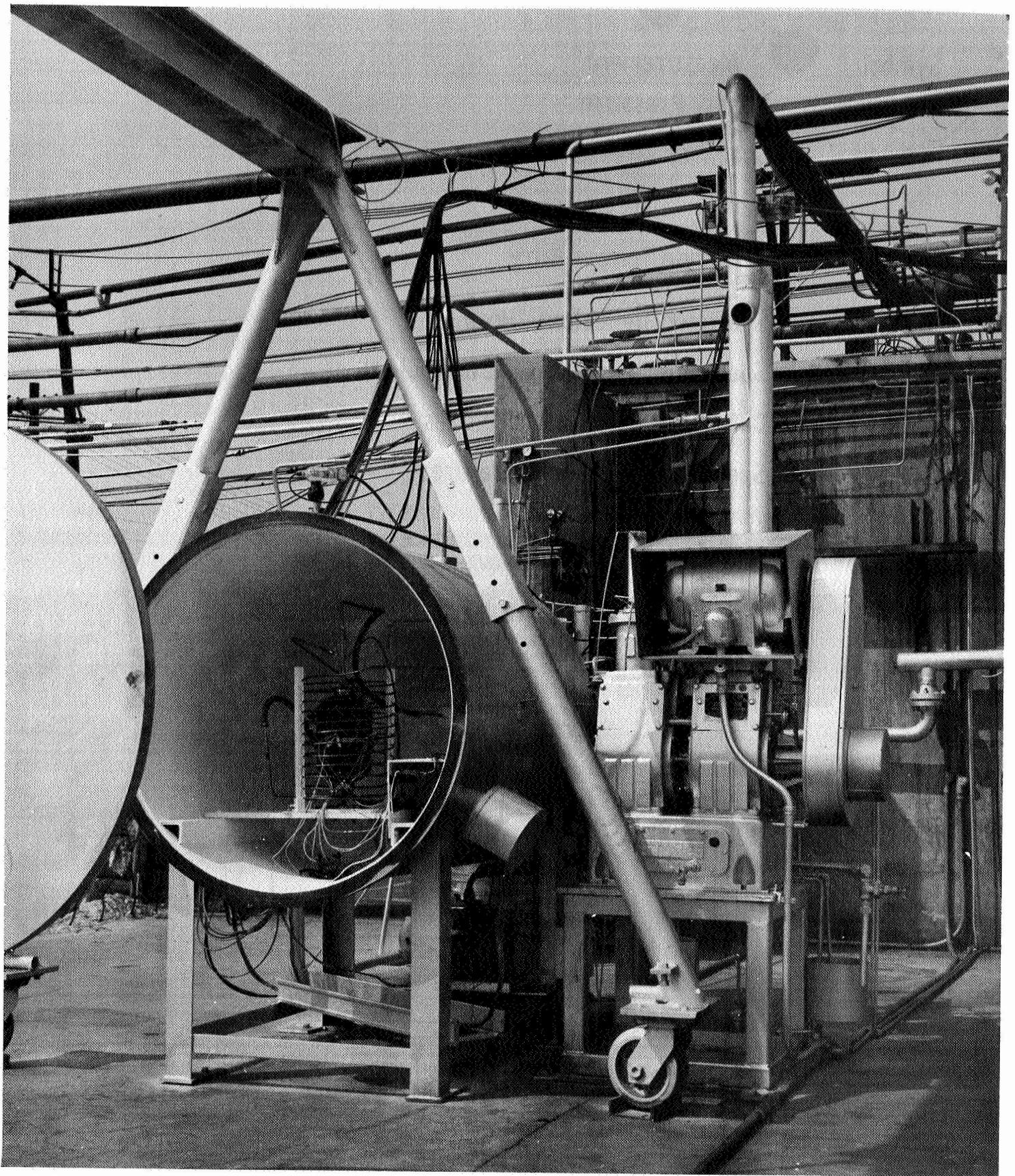


Fig. 44 Cryogenic Pressure-Test Facility

Symbol	Measurement
P_s	Supply Pressure
P_c	Specimen Pressure
T_s	Supply Temperature
T_0	Specimen Temperature
SG_1	Specimen Deflection, Hoop
$SG_{2,3}$	Specimen Deflections, Longitudinal
$TSG_{1,2,3}$	Deflection Beam Temperatures
$TC_{1,2}$	Specimen (Skin) Temperatures

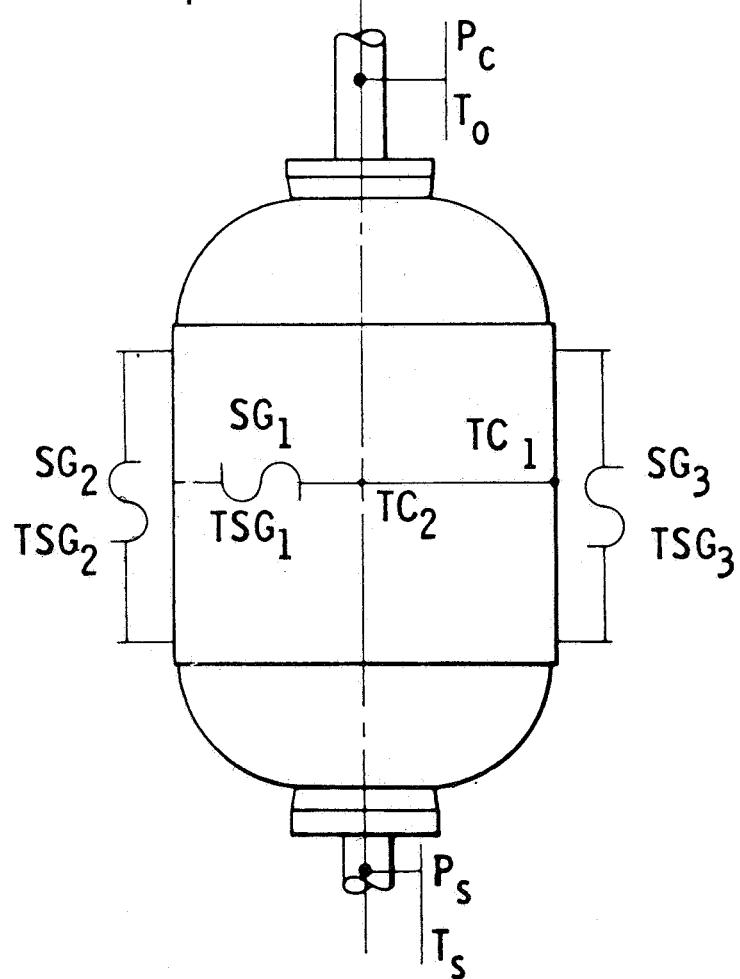


Fig. 45 Location of Instruments on Test Vessels

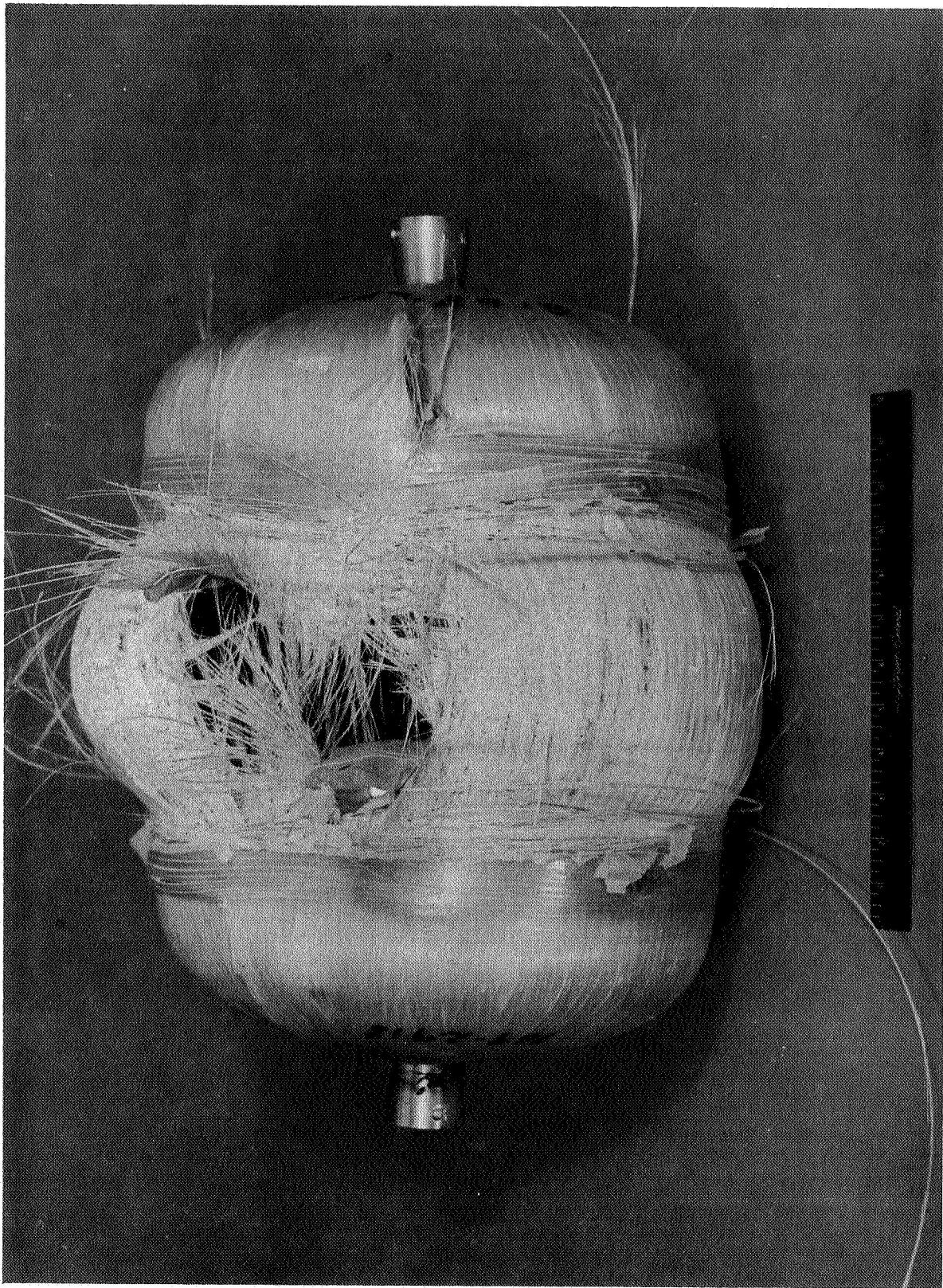
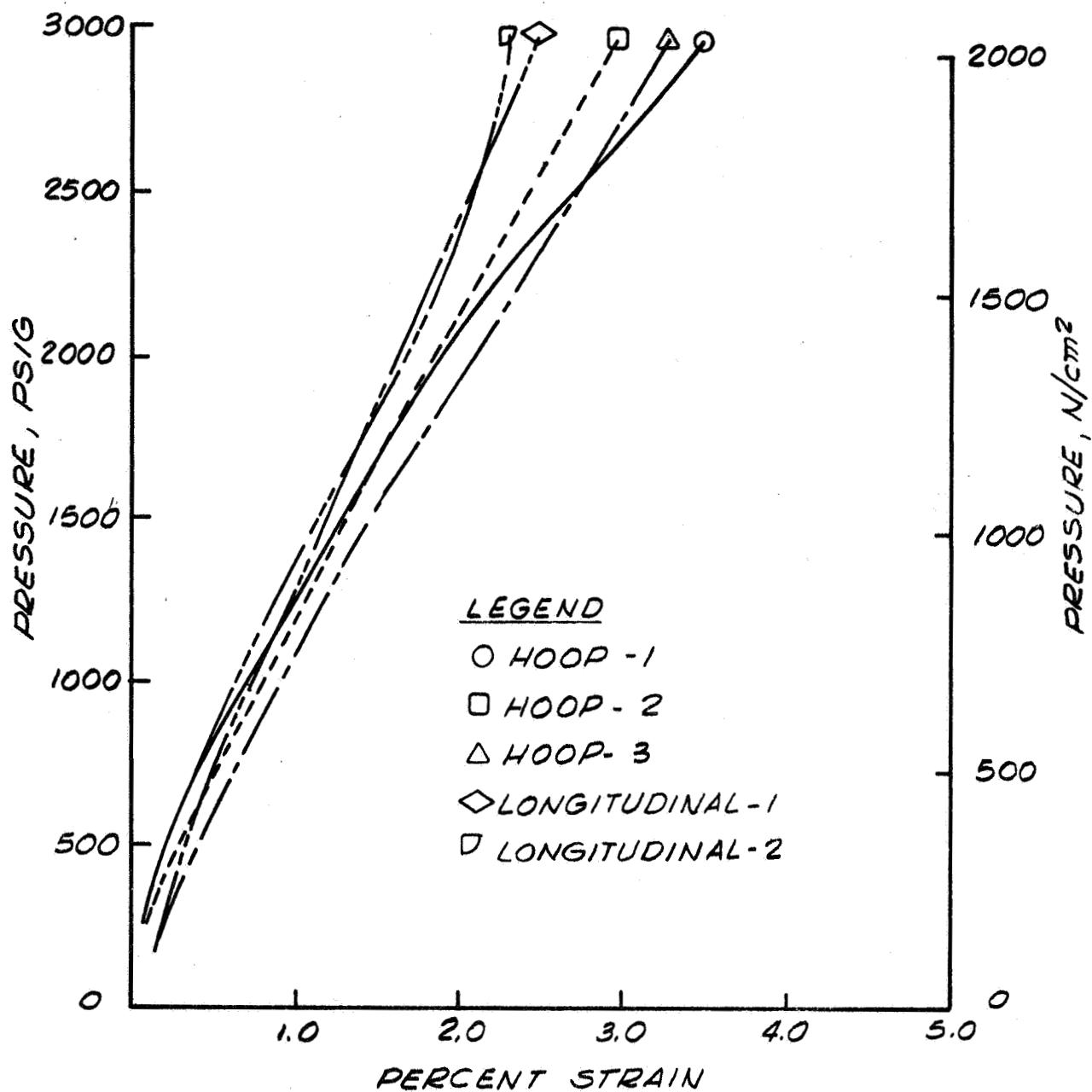
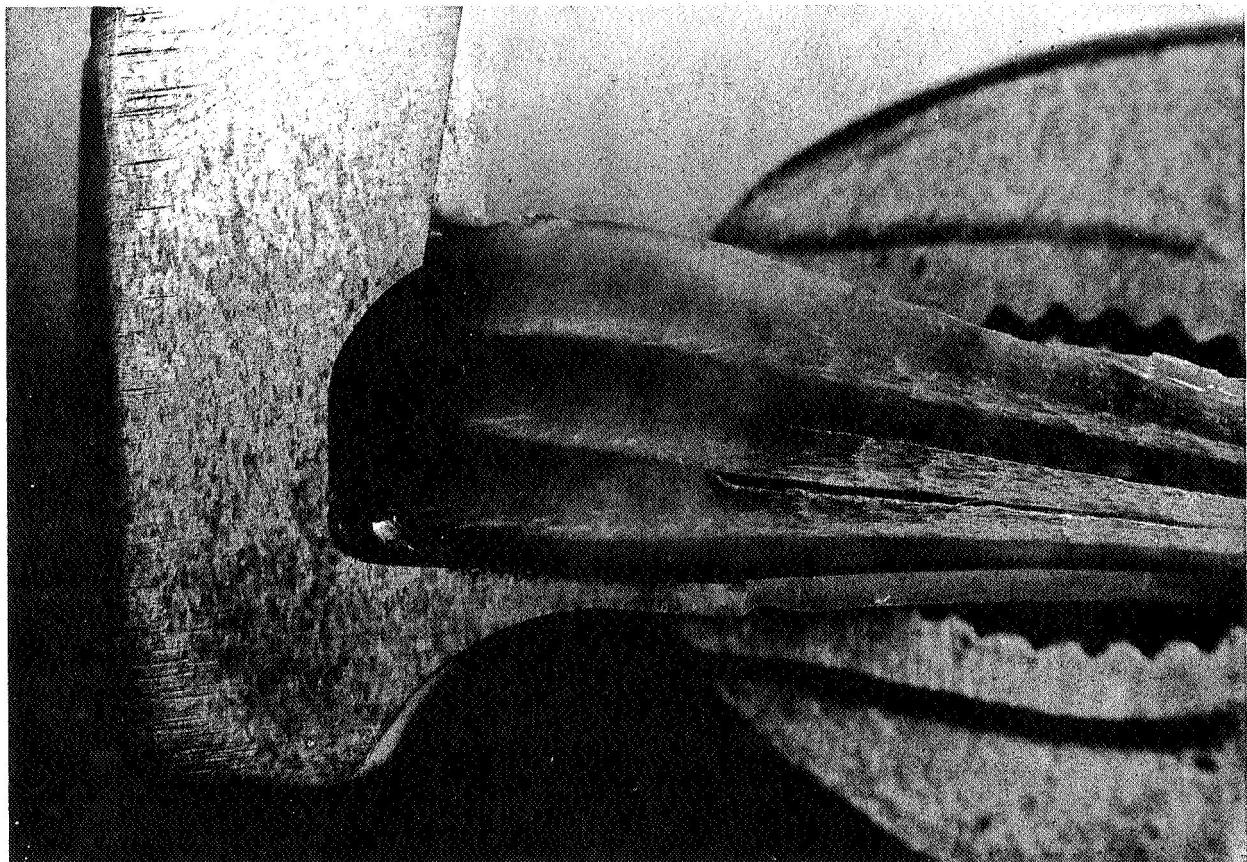


Figure 46
Post Test Photograph of Tank BWB-1 After Burst Test



Pressure vs Strain for Tank BWR-1 Burst Test

Figure 47

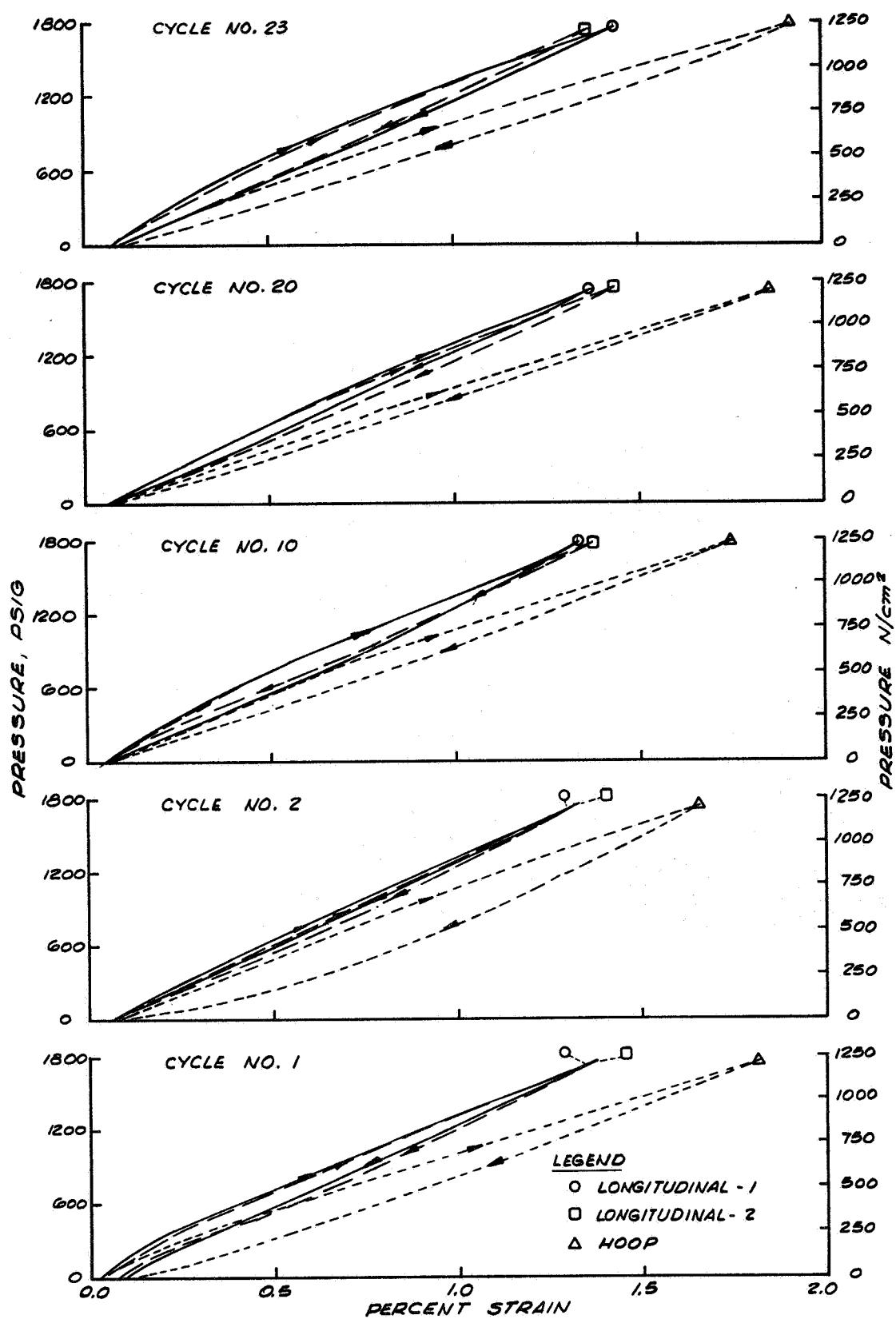


A3475

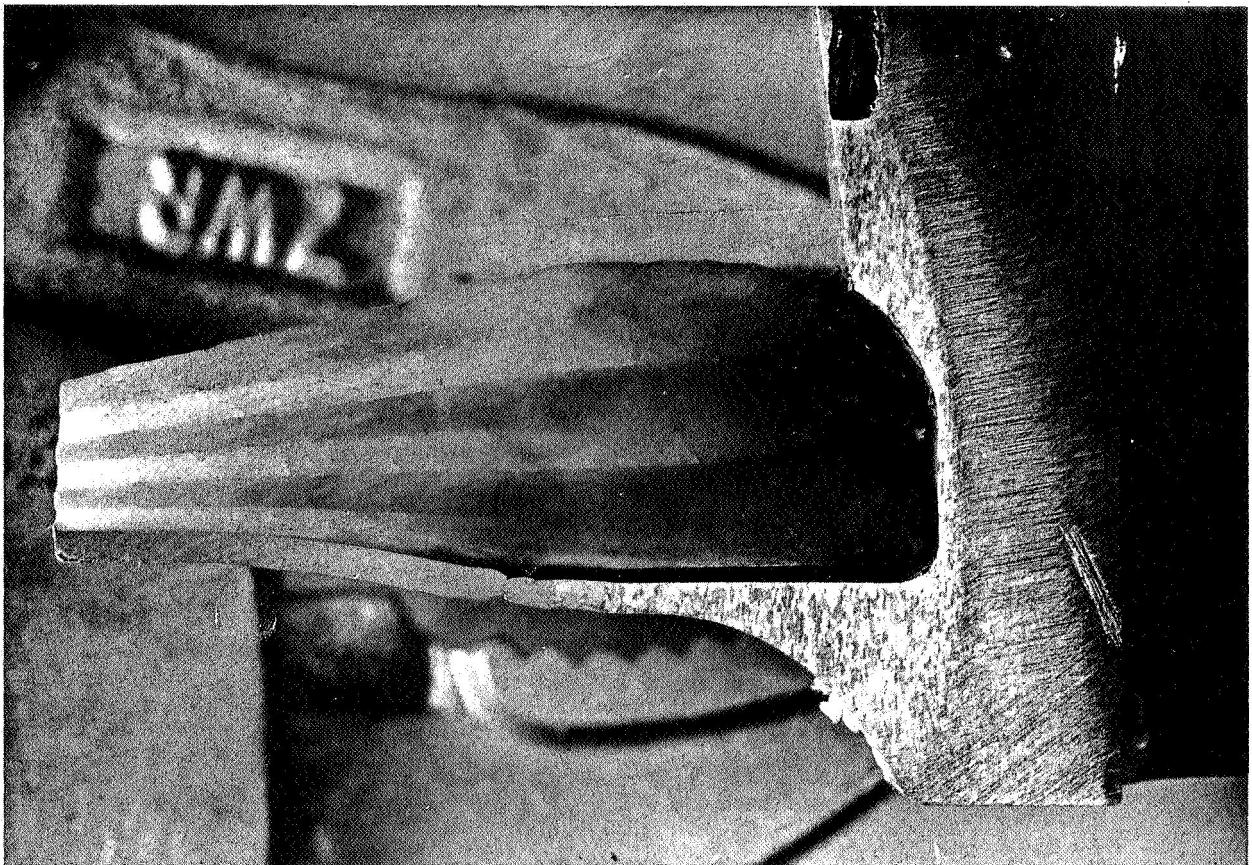
Keller's Etch

4X

Figure 48
Boss Cross-Section from Tank BWB-1



Pressure vs Strain for Tank BWB-2 Cyclic Fatigue Test

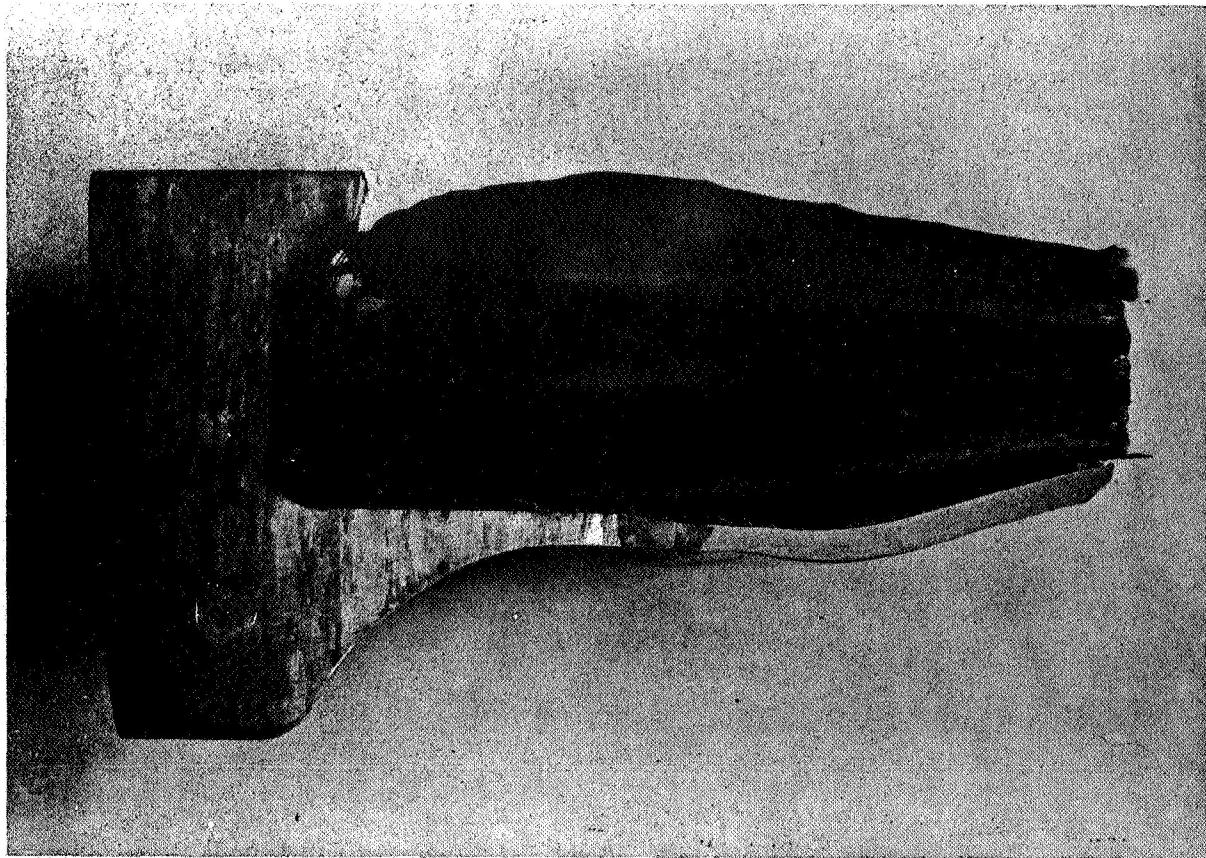


A3476

Keller's Etch

4X

Figure 50
Boss Cross-Section from Tank BWB-2

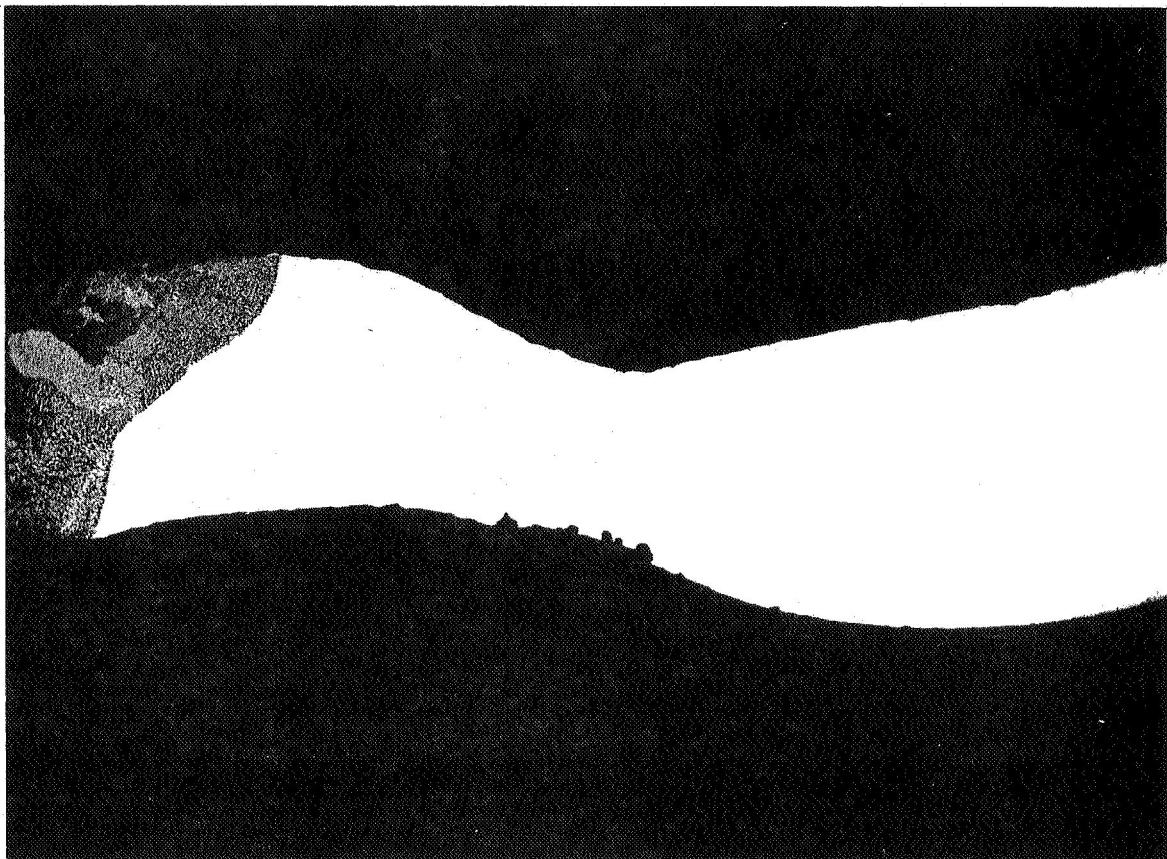


A3473

Keller's Etch

4X

Figure 51
Boss Cross-Section from Tank BWB-2



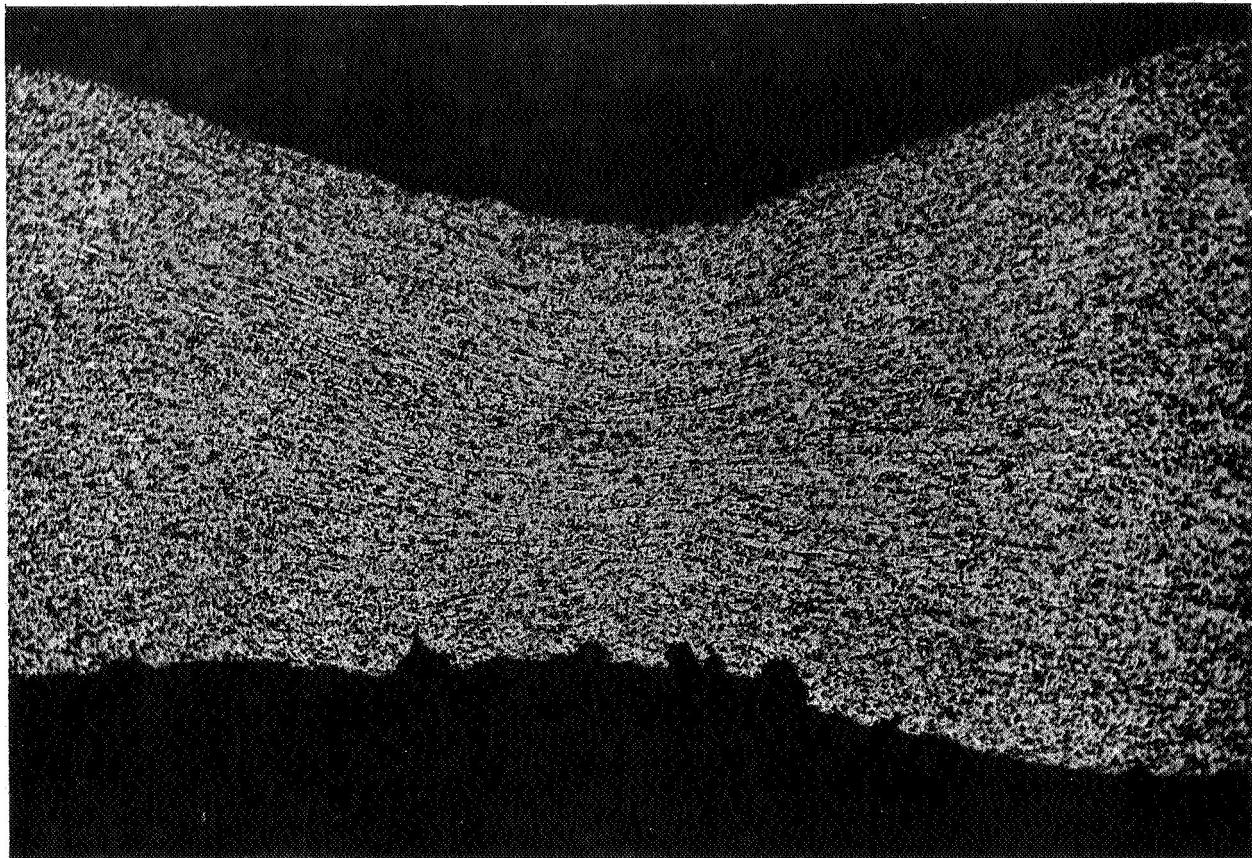
A3470

Keller's Etch

40X

Figure 52

View of Boss to Liner Transition of Tank BWB-2 Showing Local Thinning



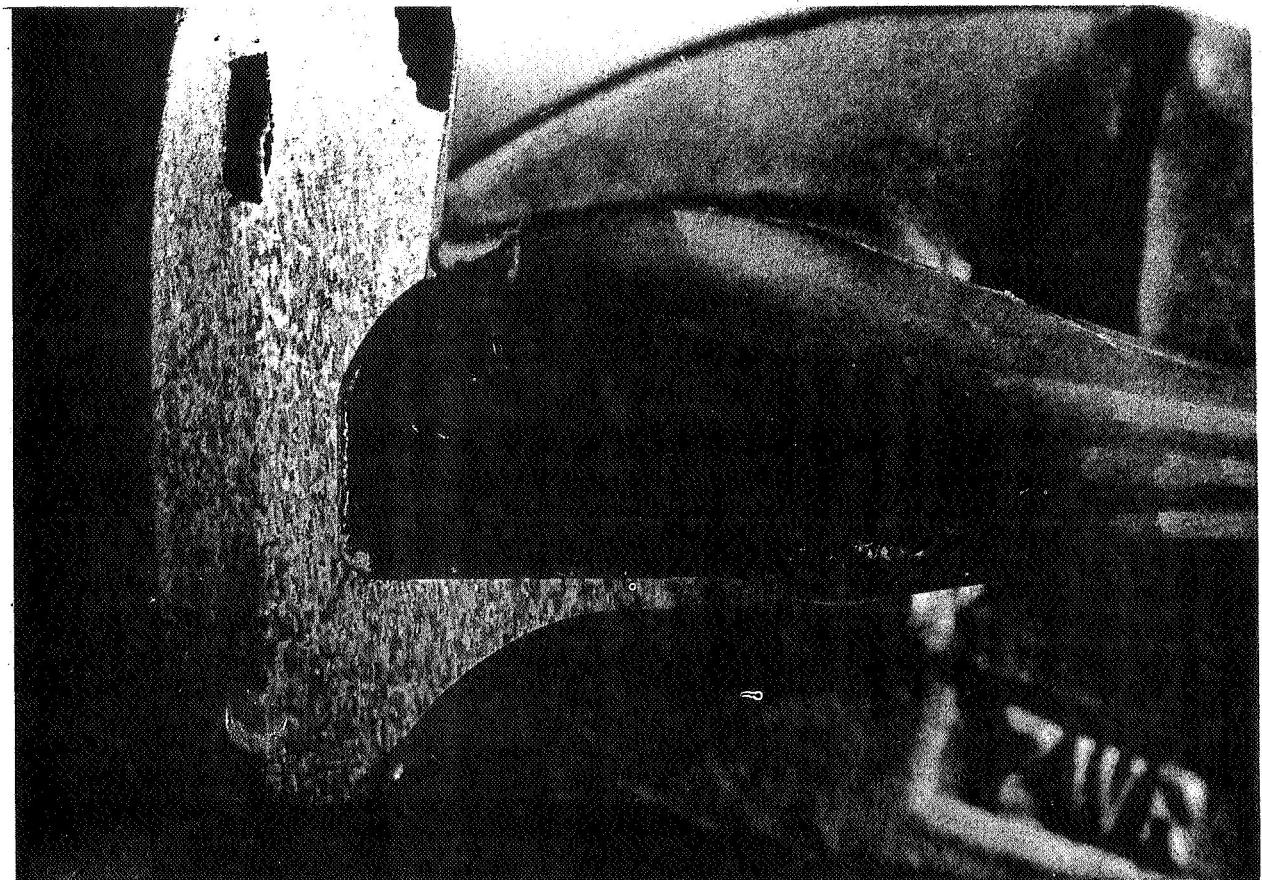
A3⁴72

Keller's Etch

100X

Figure 53

View of Boss to Liner Transition of Tank BWB-2 Showing Local Thinning

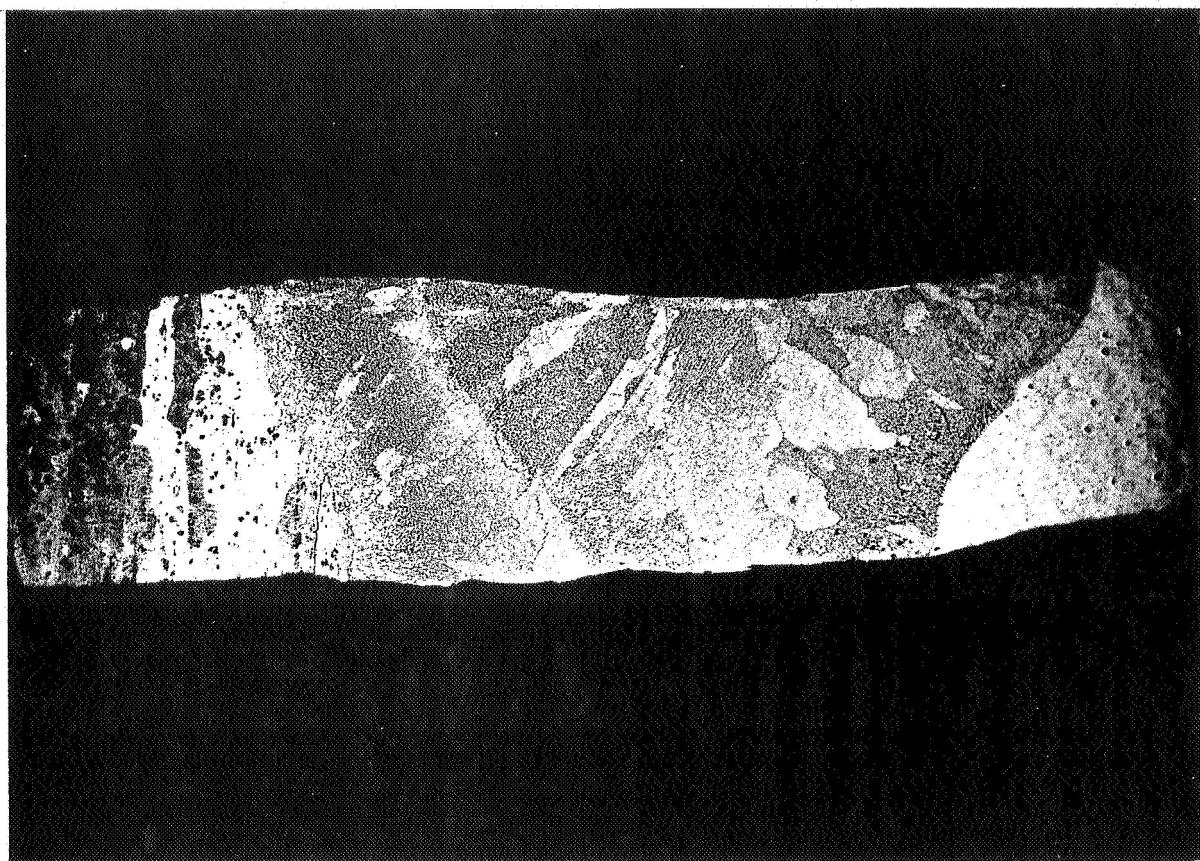


A3475

Keller's Etch

4X

Figure 54
View of Tank BWB-2 Section at Boss



A3471

Keller's Etch

40X

Figure 55
EB Weld Joint

1169-NF-1374

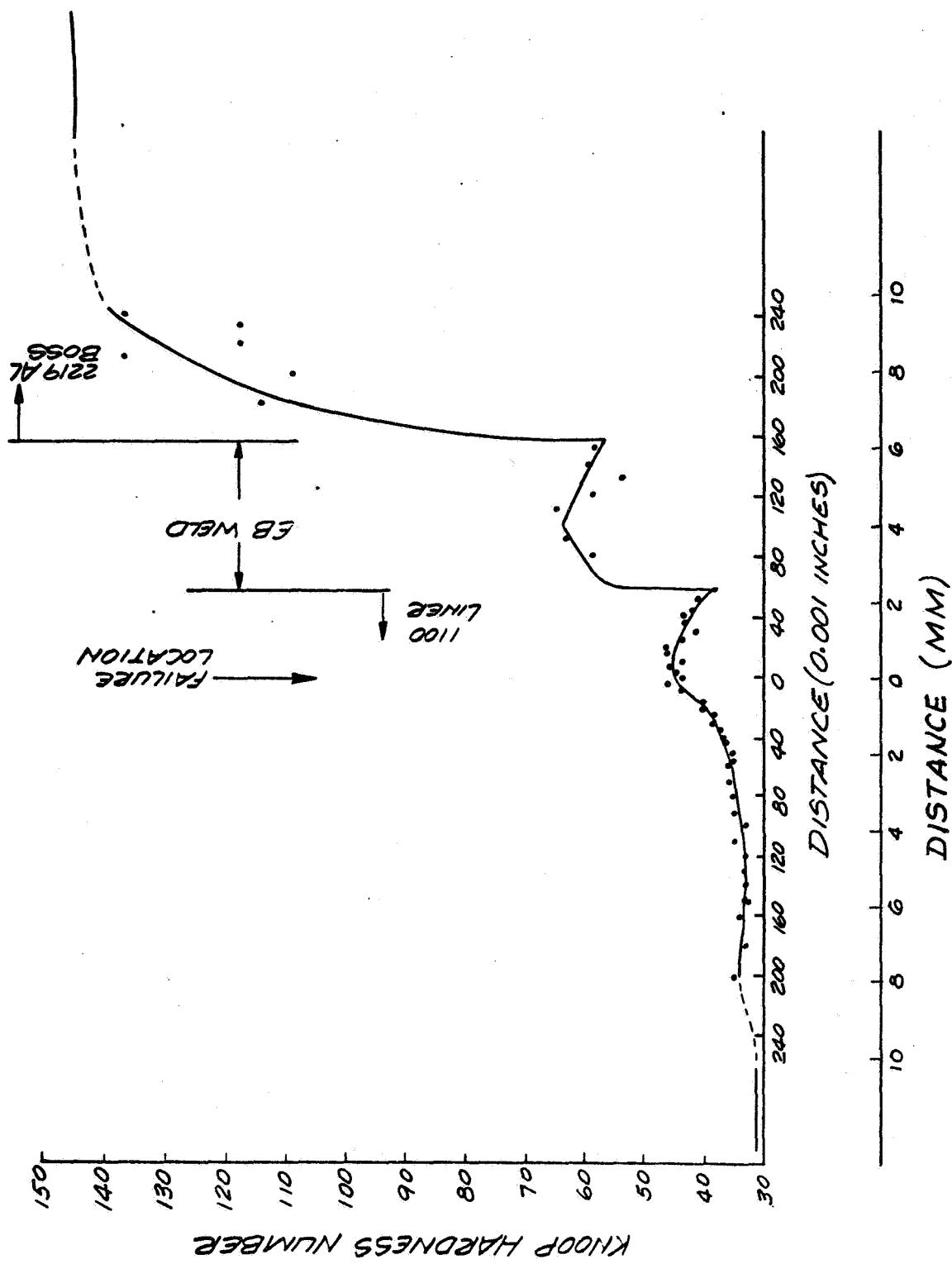
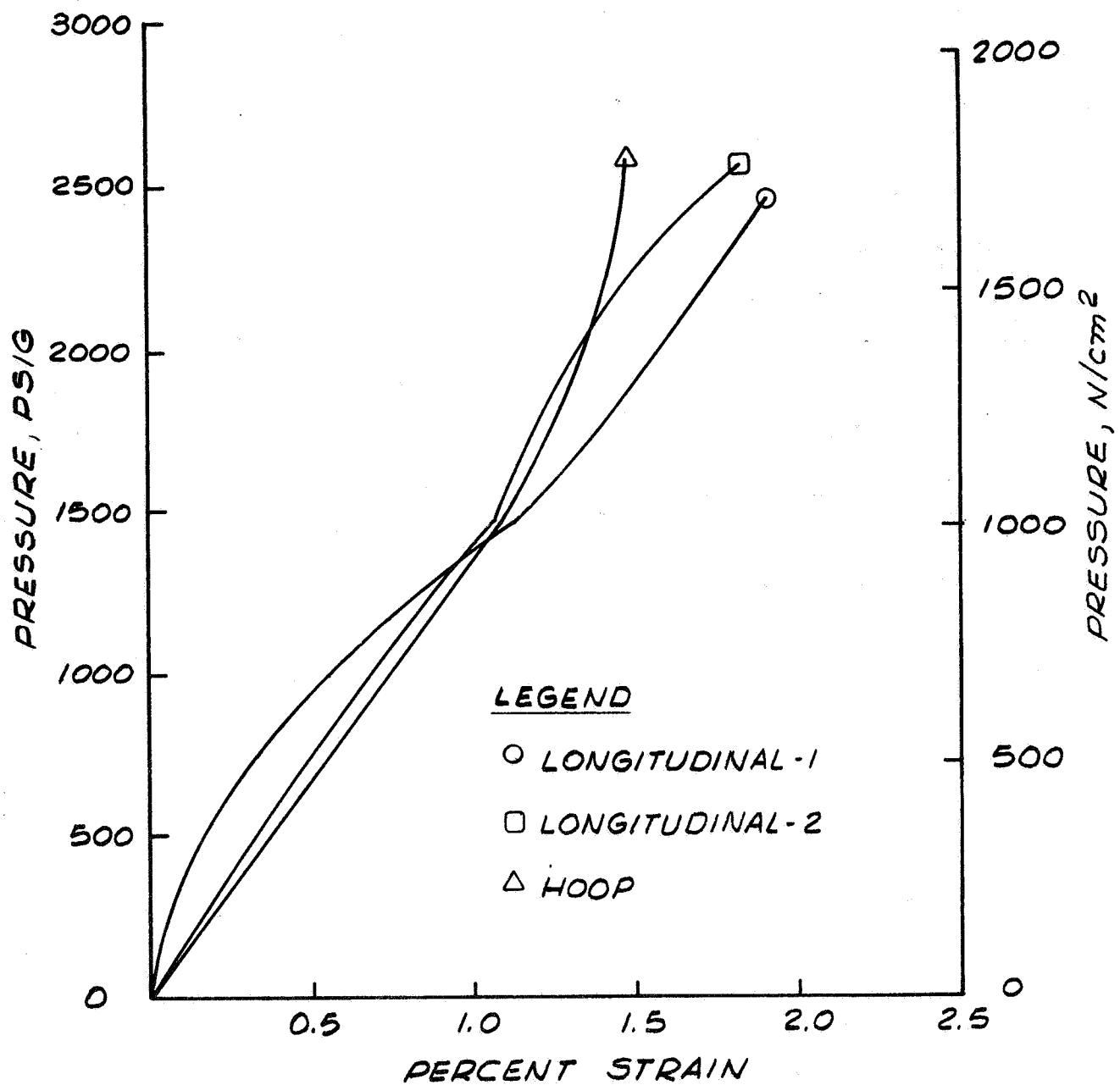


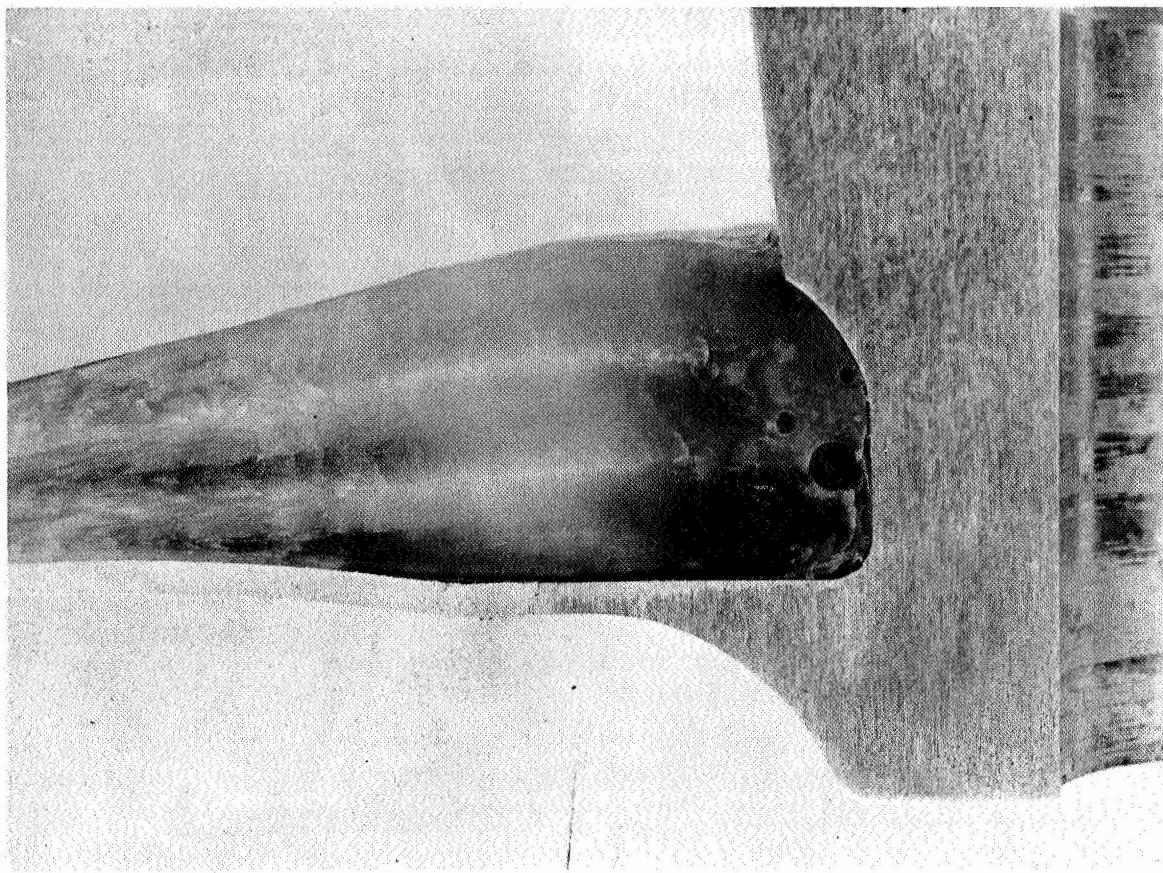
Figure 56

Tank BWB-2 Microhardness Traverse in Failure Area



Pressure vs Strain for Tank BWB-3 Burst Test

Figure 57

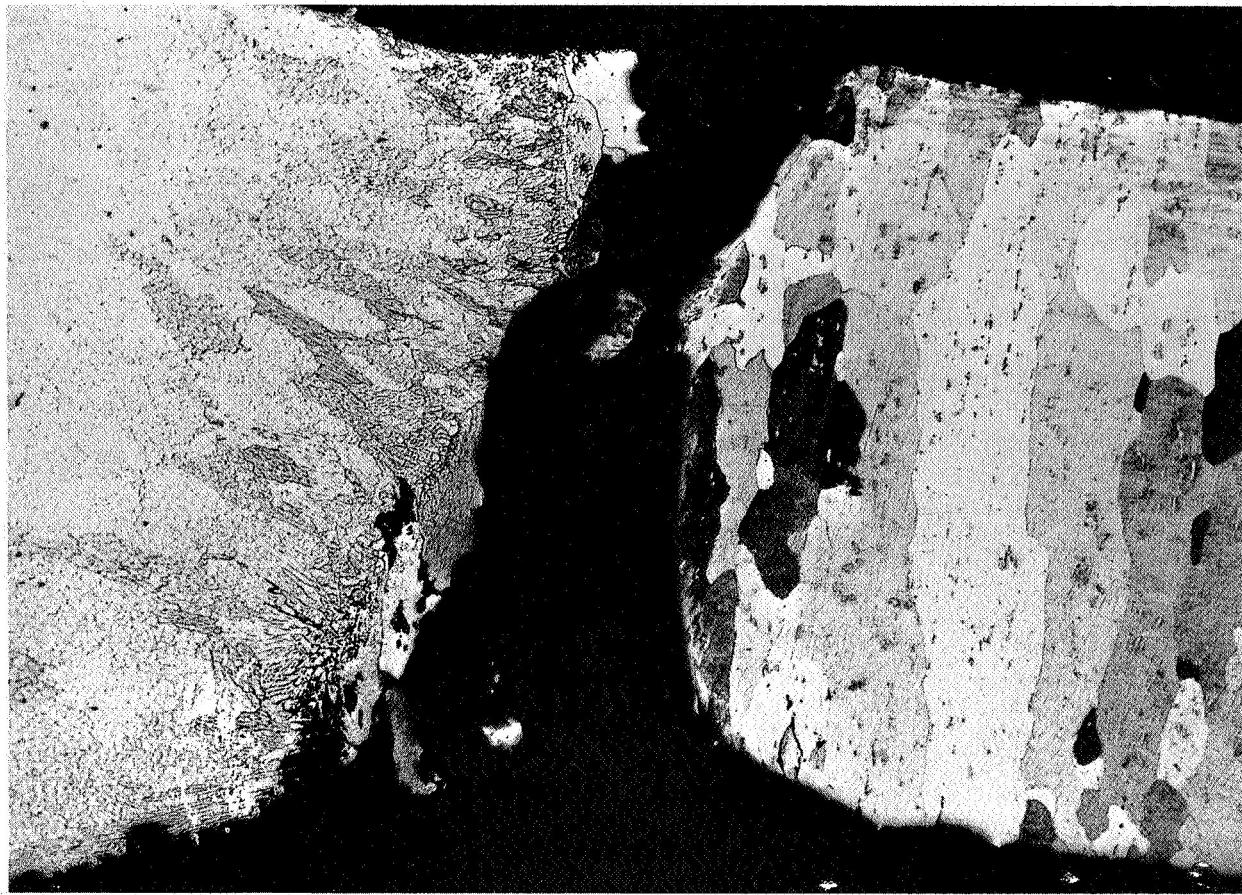


0036

Keller's Etch

4X

Figure 58
Boss Cross-Section from Tank BWB-3



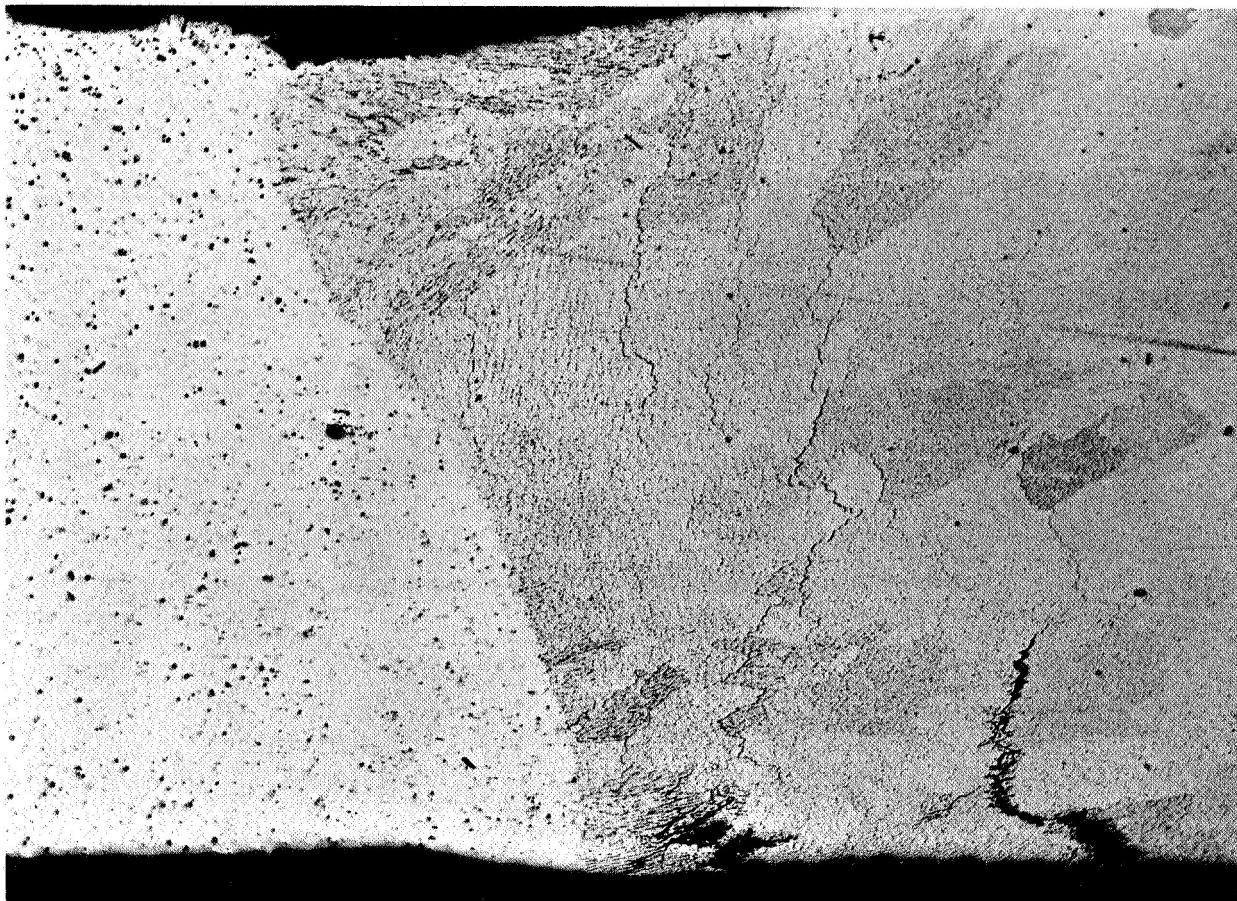
0039

Keller's Etch

100X

Figure 59

**View of Tank BWB-3 Boss Weld Showing 2219 Aluminum Side of Weld with Hot Tear
in Weld and Parent Metal**



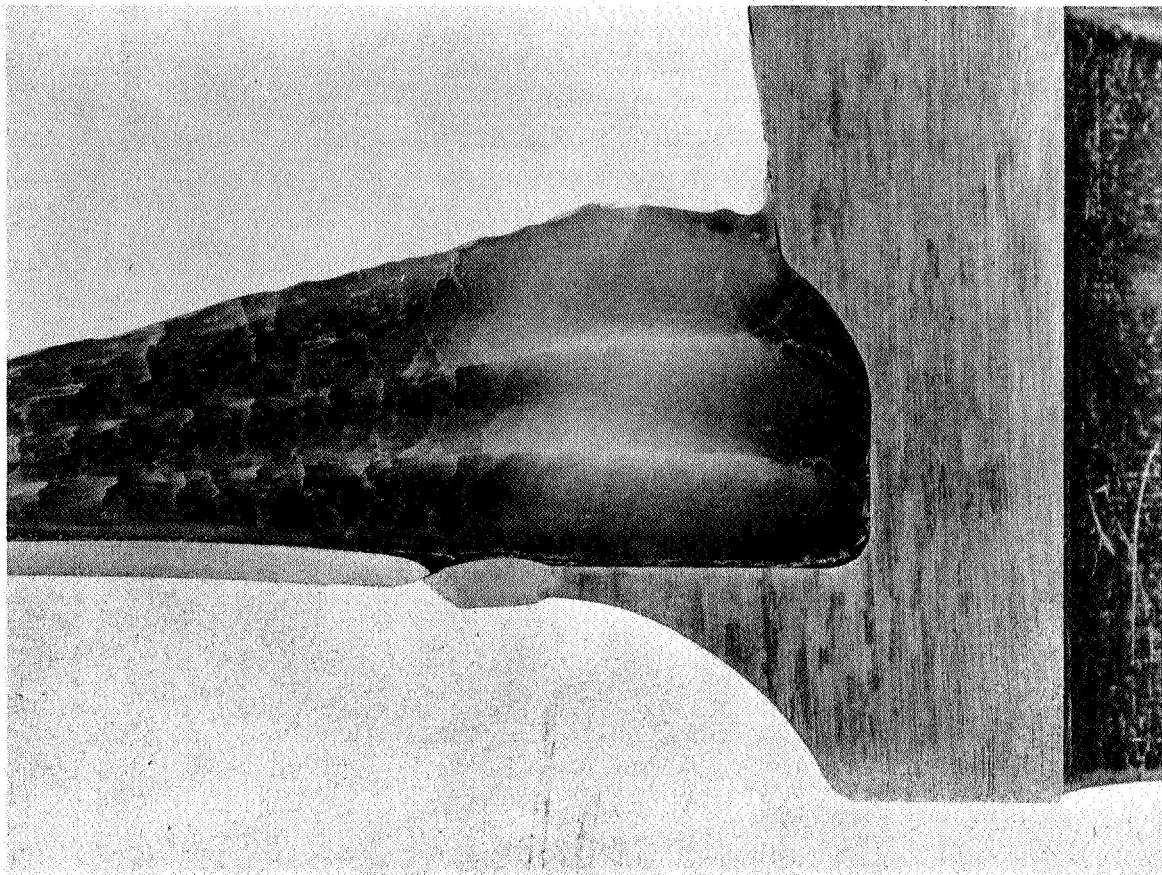
0040

Keller's Etch

100X

Figure 60

**View of Tank BWB-3 Boss Weld Showing 1100 Aluminum Side of Weld with Hot Tear
in Weld Metal**

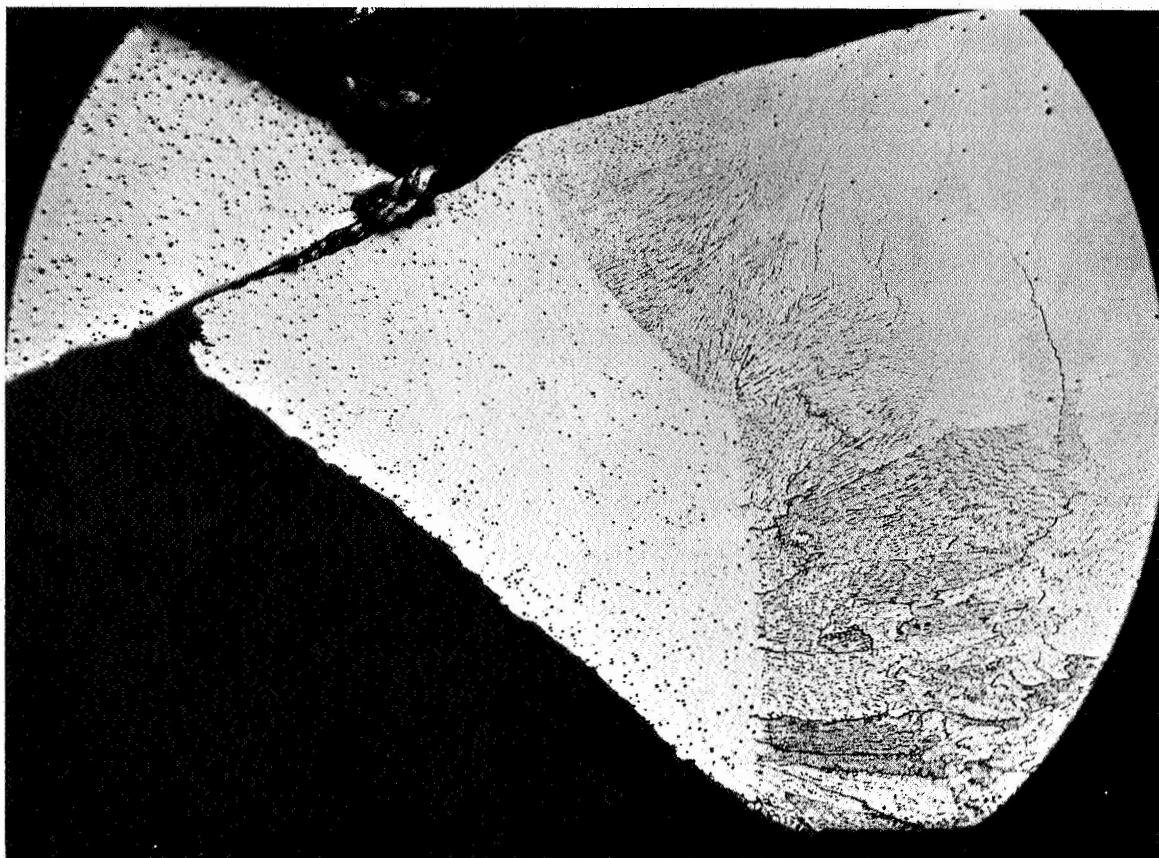


0037

Keller's Etch

4X

Figure 61
Boss Cross-Section from Tank BWB-3



0041

Keller's Etch

75X

Figure 62

**View of Tank BWB-3 Boss Showing Localized Necking of 1100 Aluminum
in Failure Area**



0042

Keller's Etch

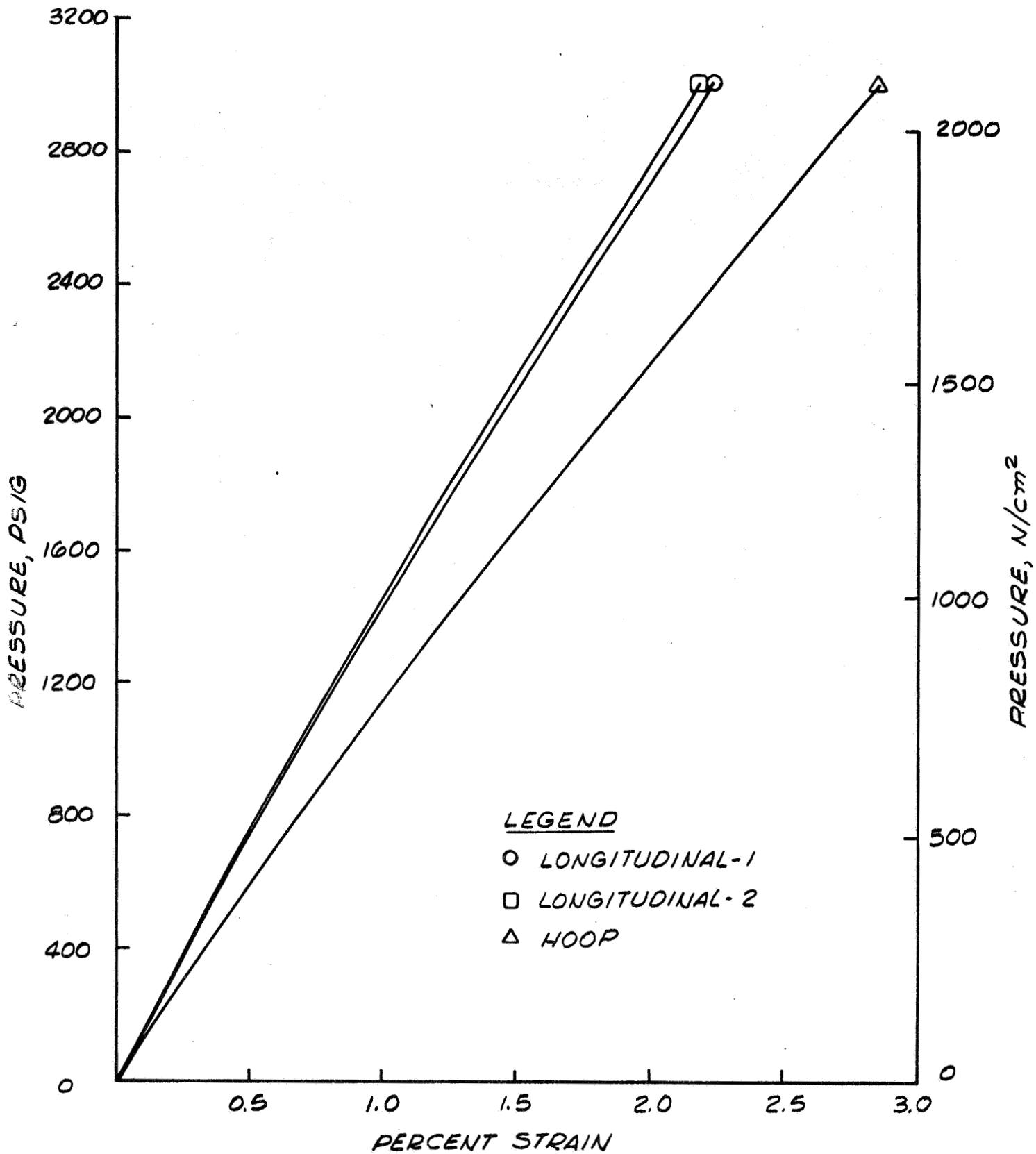
75X

Figure 63

View of Tank BWB-3 Boss Showing 2219 Aluminum Side of Weld

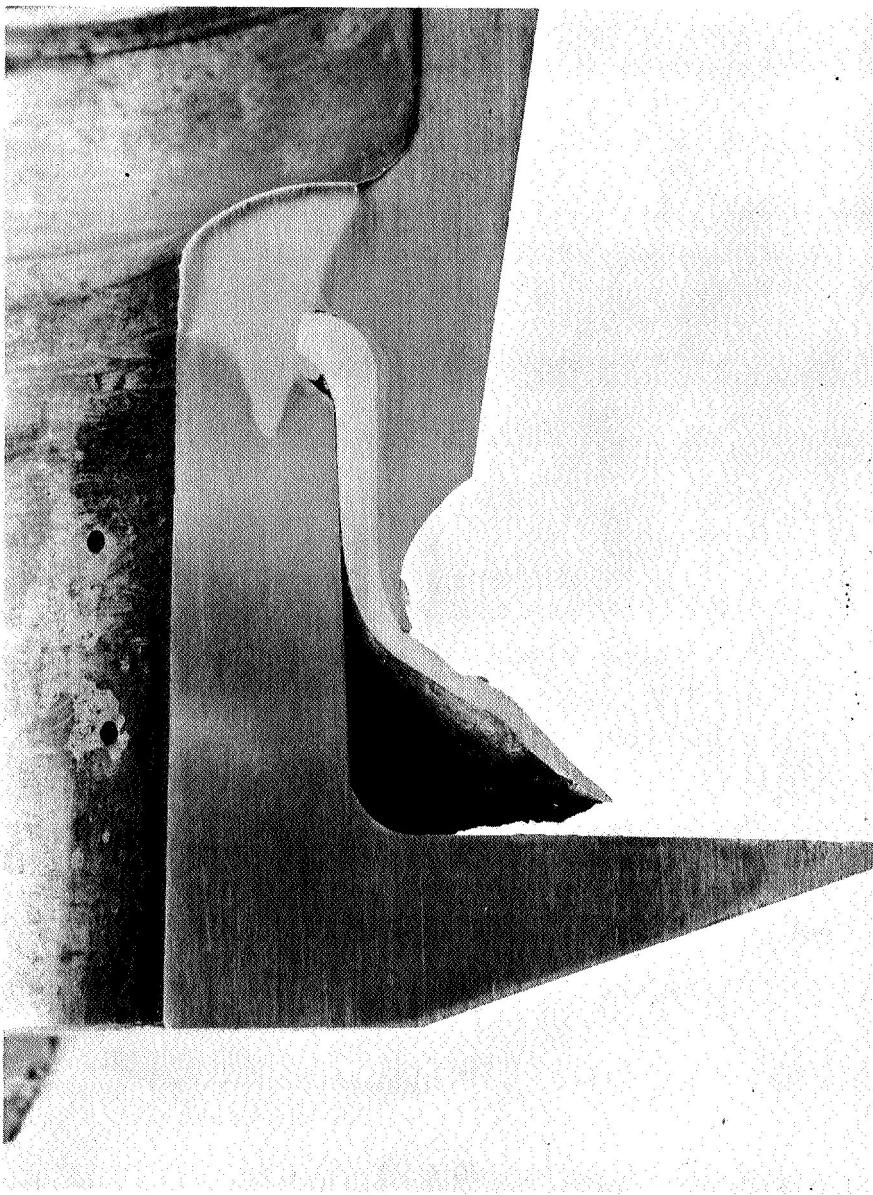


Figure 64
Post Test Photograph of Tank HB-2 After Burst Test



Pressure vs Strain for Tank HB-2 Burst Test

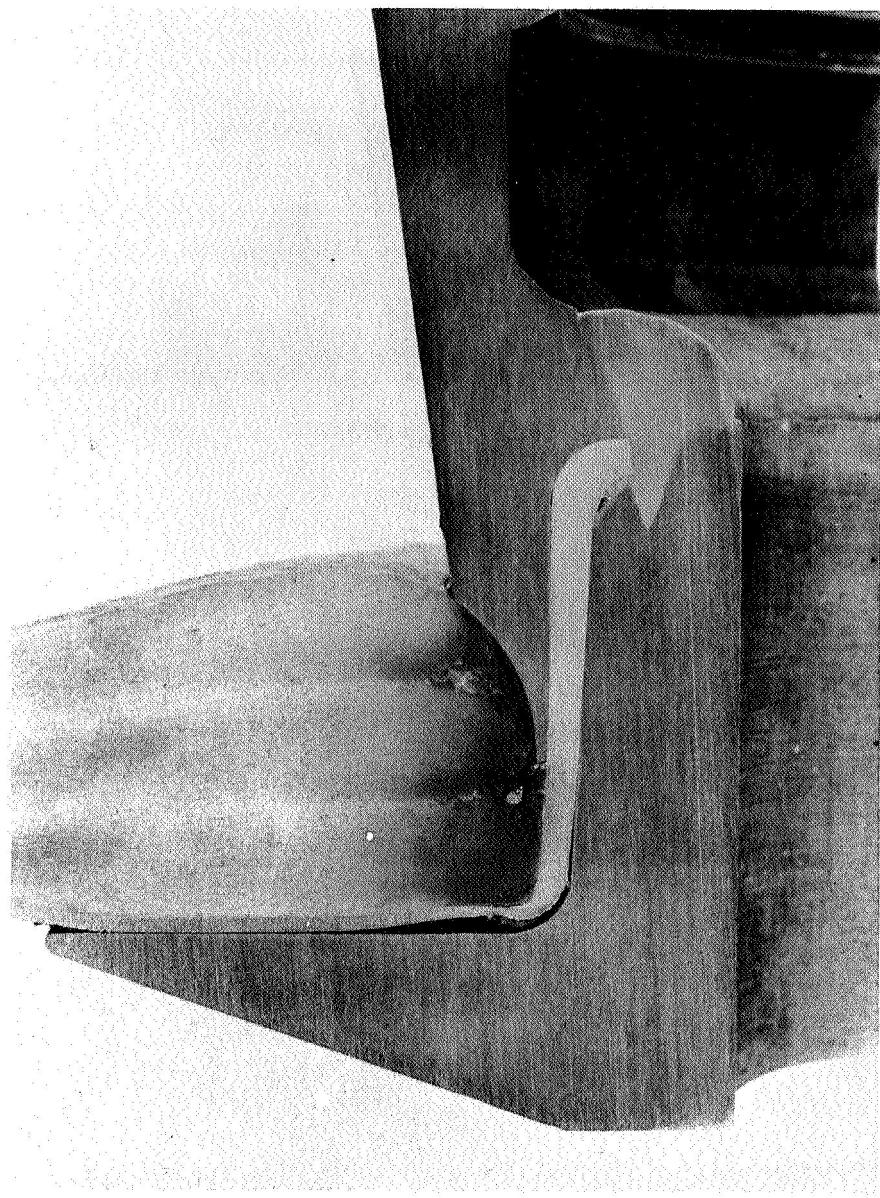
Figure 65



0029

4X

Figure 66
Cross-Section of Tank HB-2 Boss from Vessel Dome That Failed

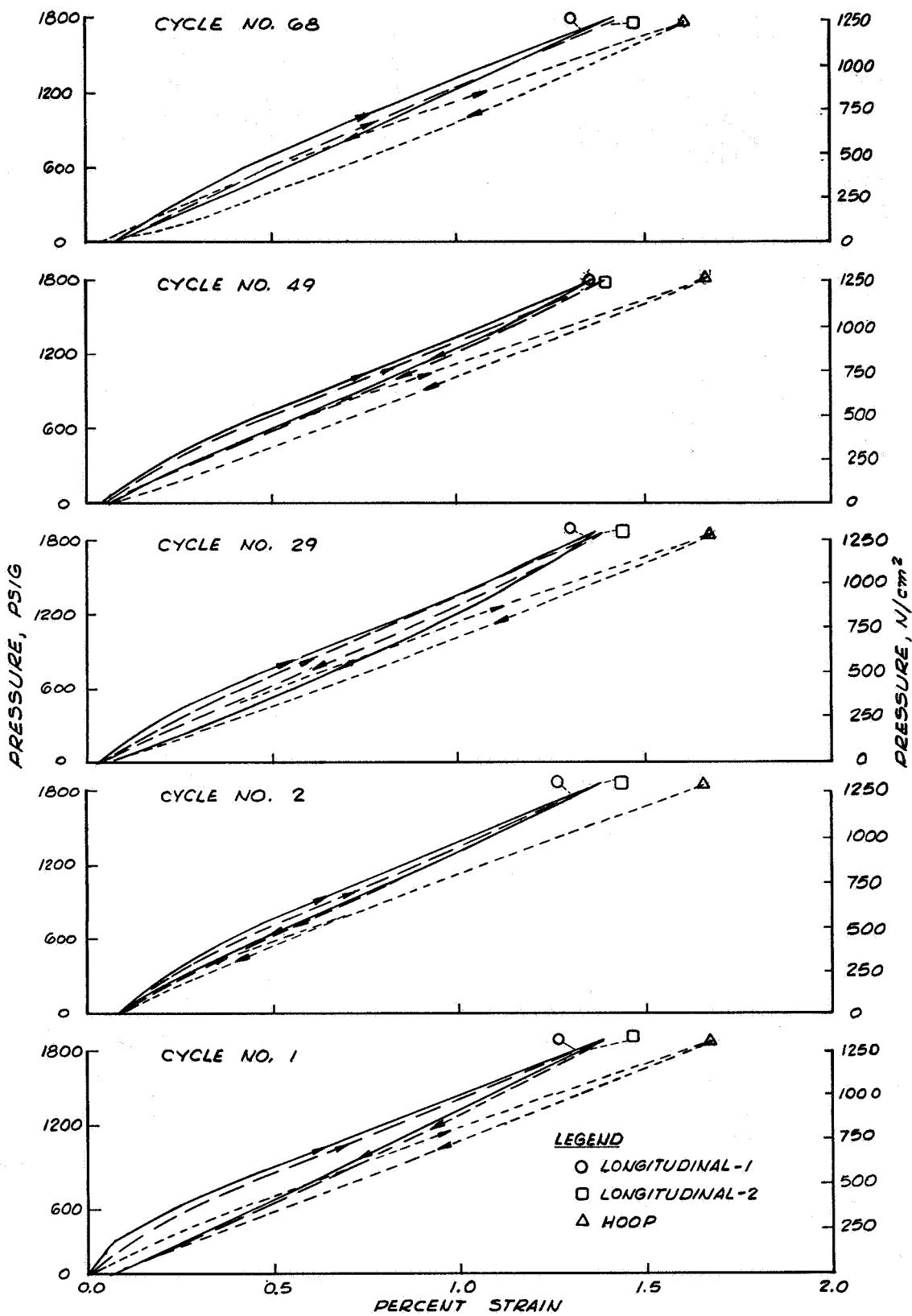


0030

4X

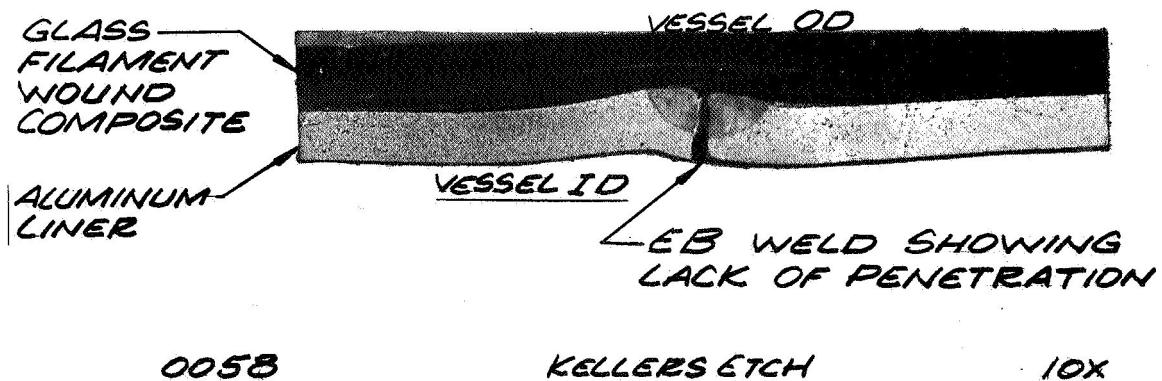
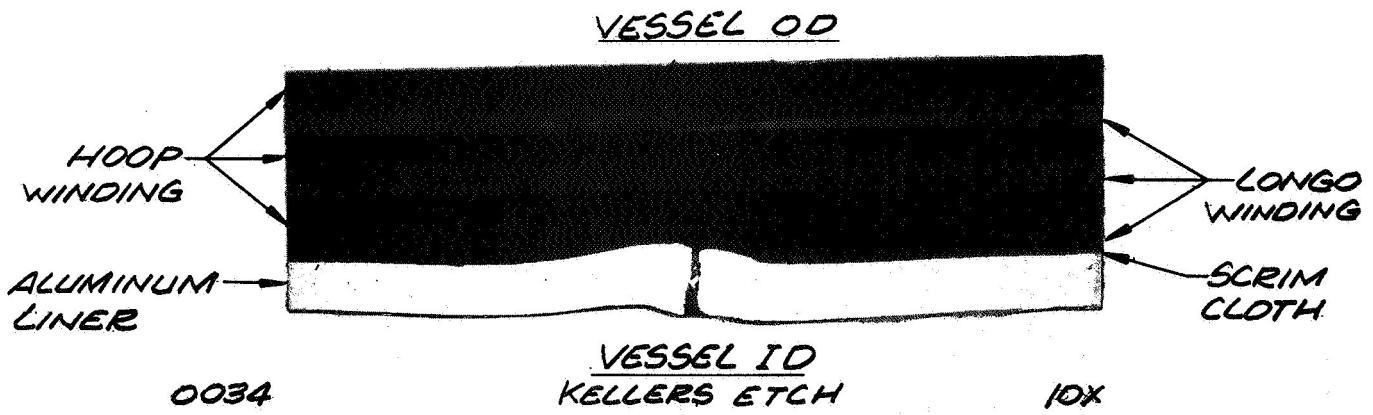
Figure 67

Cross-Section of Tank HB-2 Boss from Vessel Dome That Did Not Fail

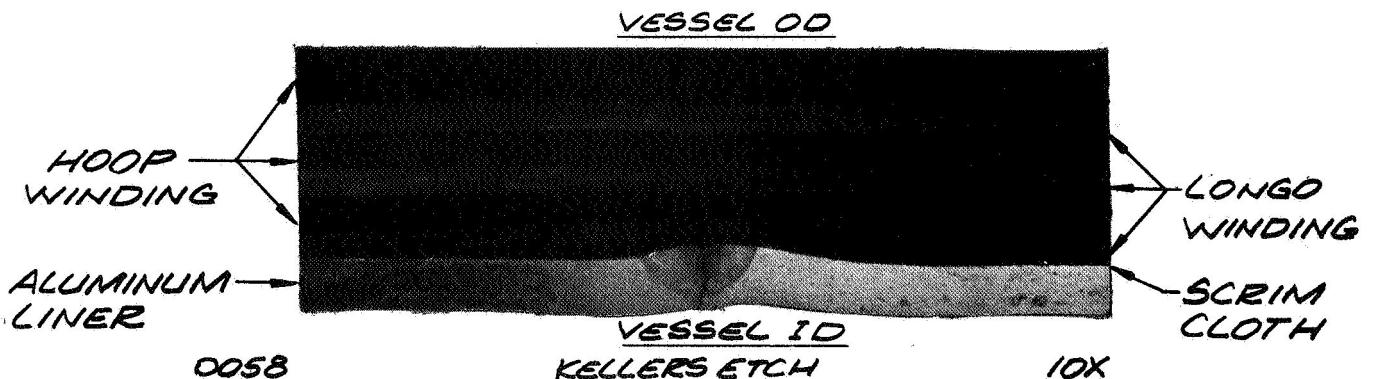


Pressure vs Strain for Tank HB-3 Cyclic Fatigue Test

Figure 68



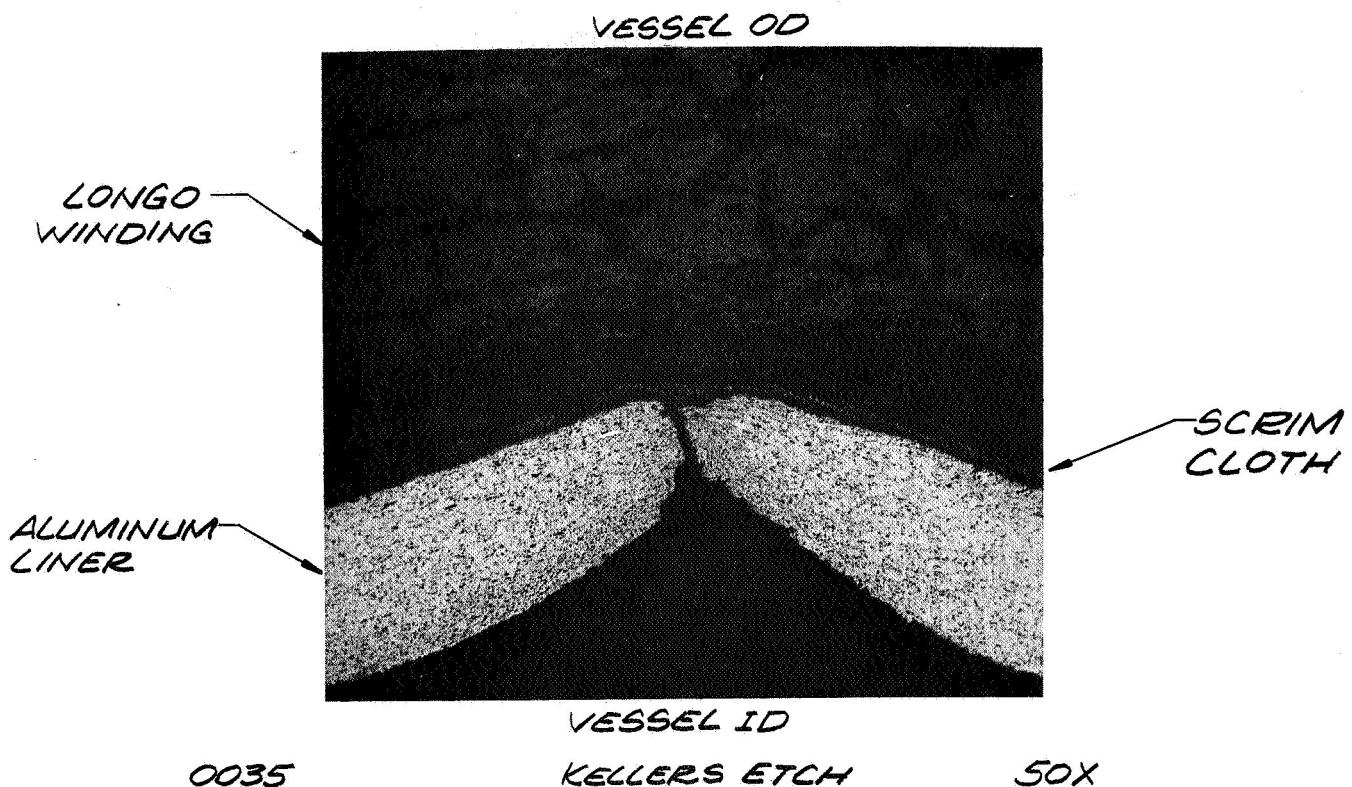
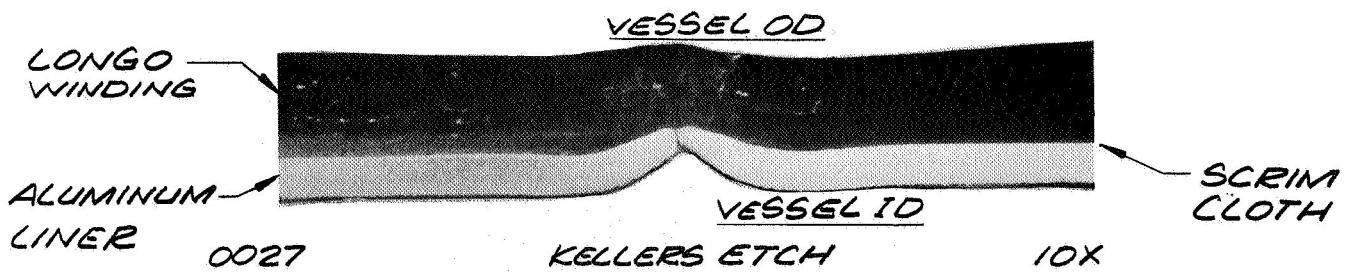
SECTION A



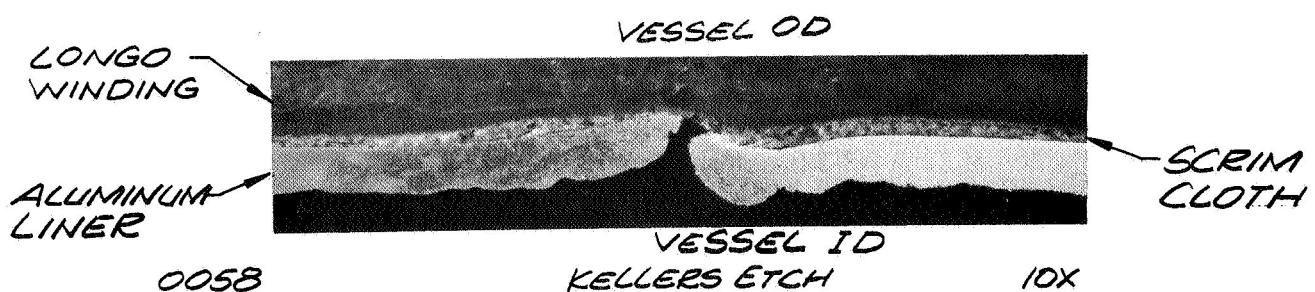
SECTION B

Photomicrographs of Tank HB-3 Cylinder Wall Sections Showing Lack of EB Weld Penetration at Liner Girth Weld

Figure 69

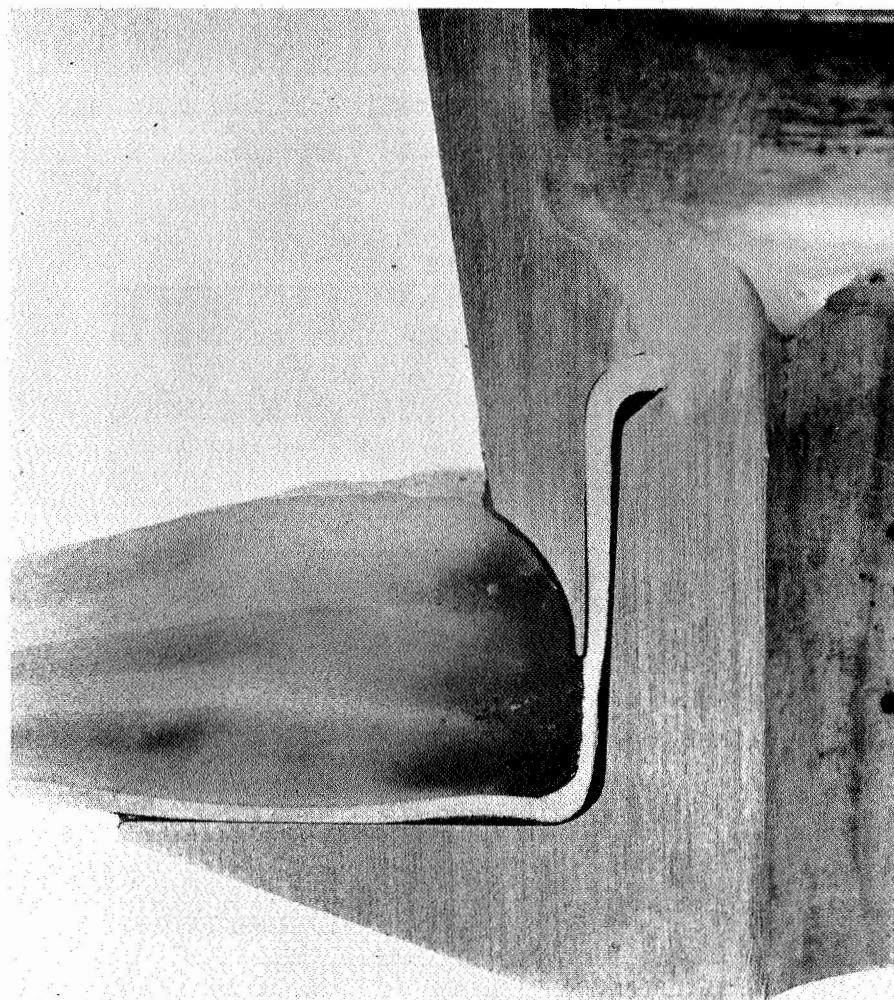


SECTION A



SECTION B

Photomicrographs of Tank HB-3 Dome Sections Showing Liner Fracture Site



0032

4X

Figure 71
Cross-Section of Tank HB-3 Boss from Vessel Subjected to Fatigue Cycling

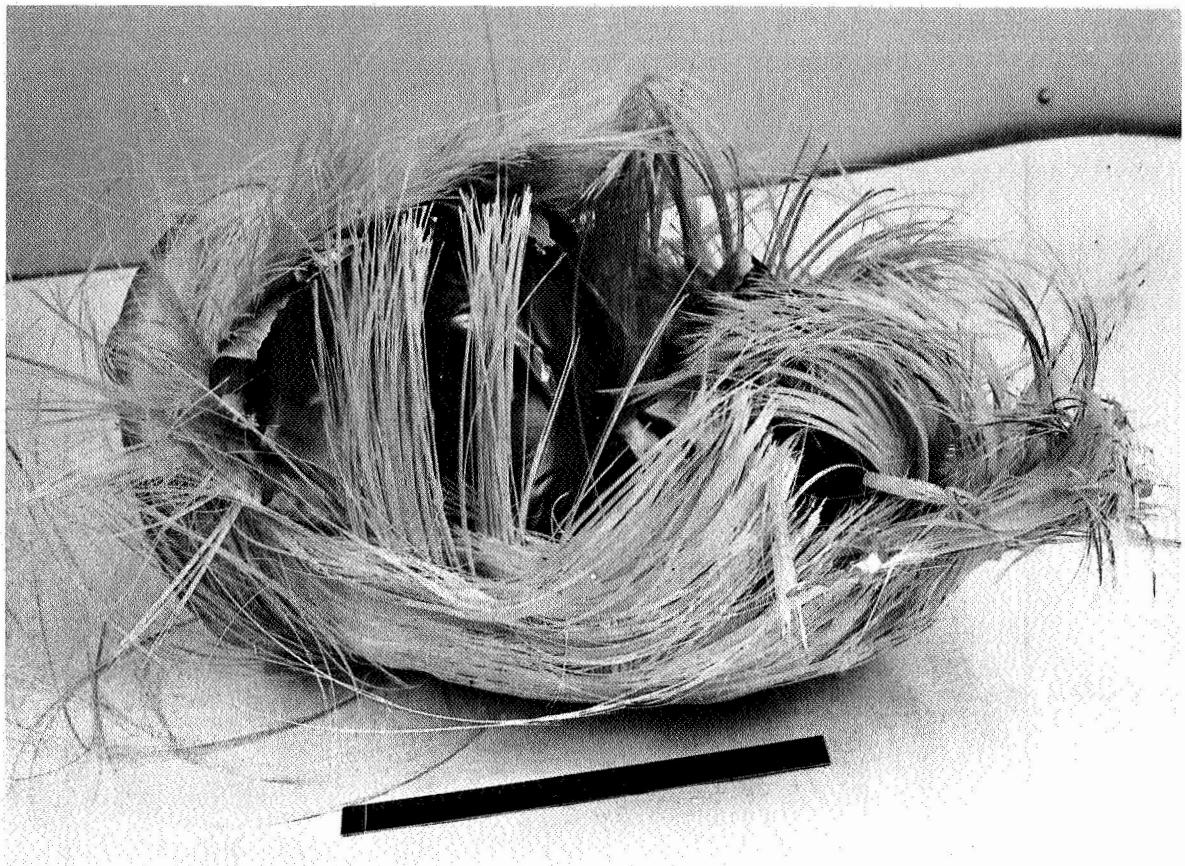
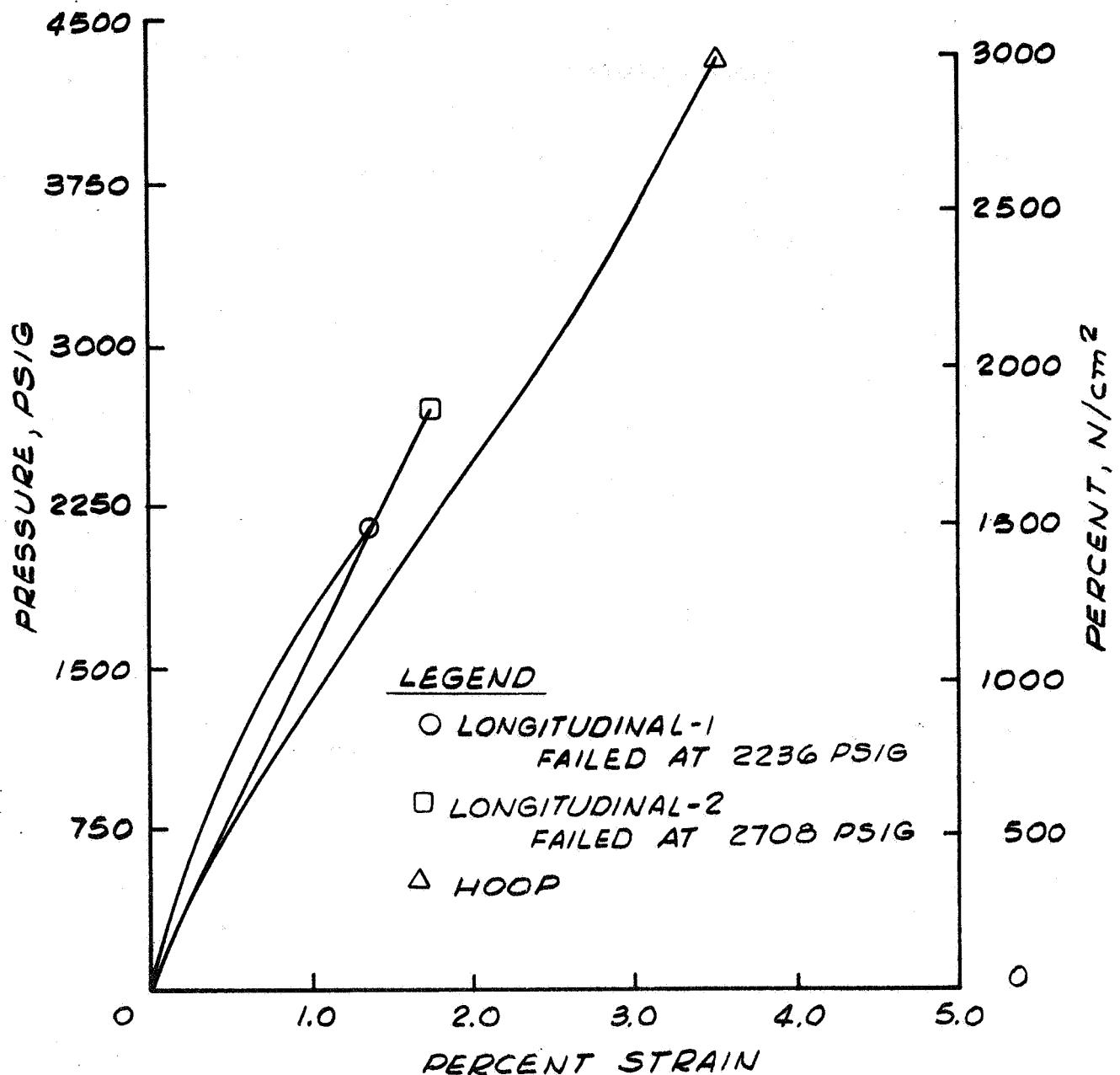
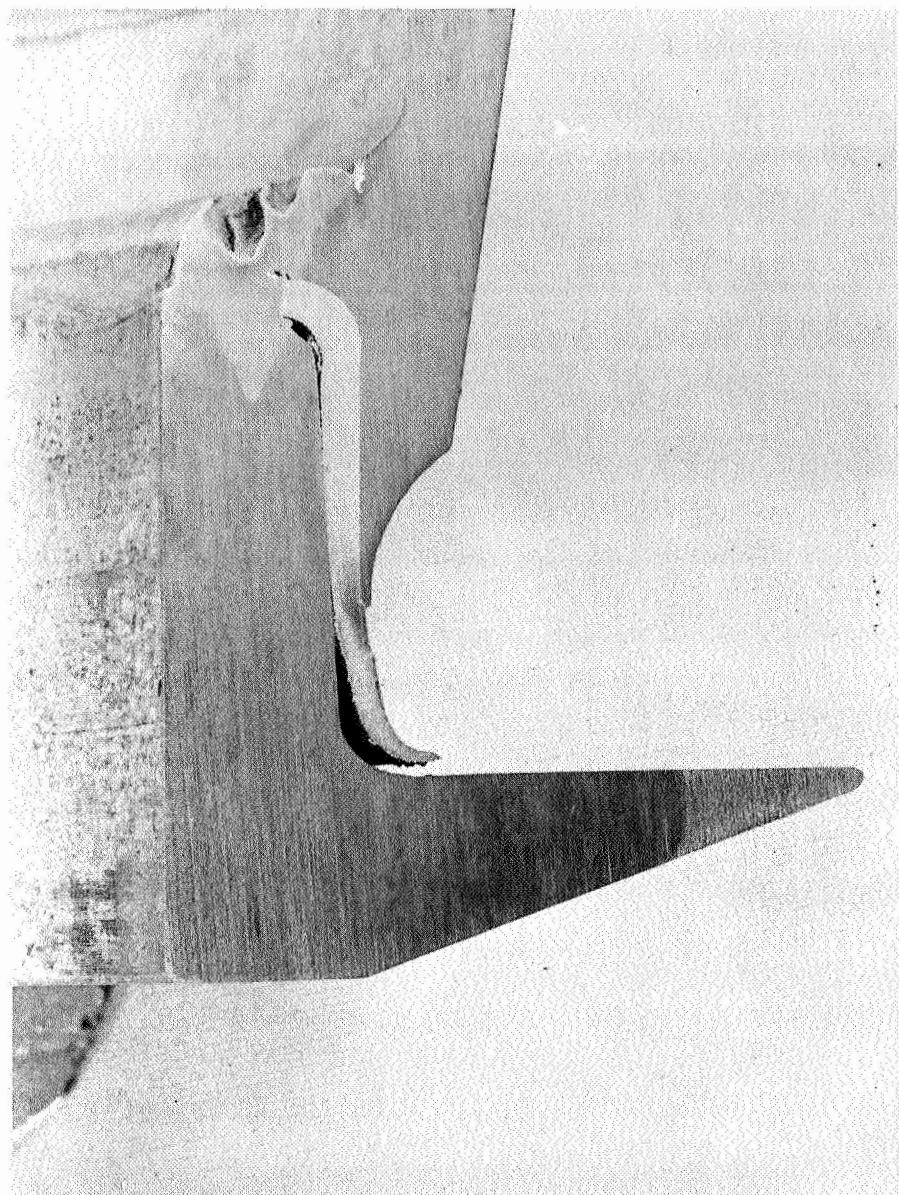


Figure 72
Post Test Photograph of Tank HB-1 After Burst Test



Pressure vs Strain for Tank HB-1 Burst Test

Figure 73



0031

4X

Figure 74
View of Tank HB-1 Boss Showing Successful Operation of the Hinged Boss

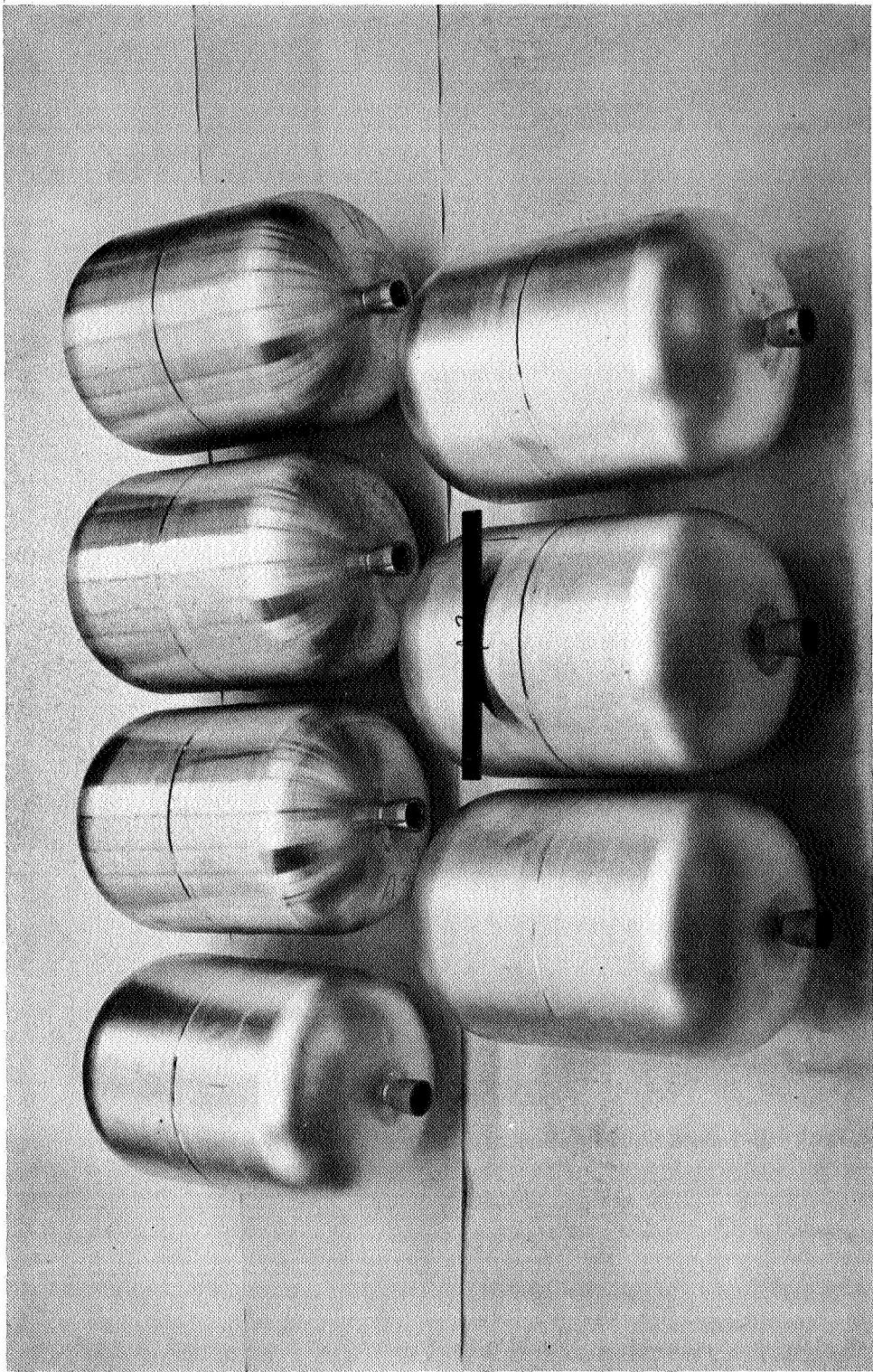


Figure 75
Group of Completed 1100 Aluminum Liners of Hinged-Boss Configuration,
12-in.-dia. by 18-in.-long

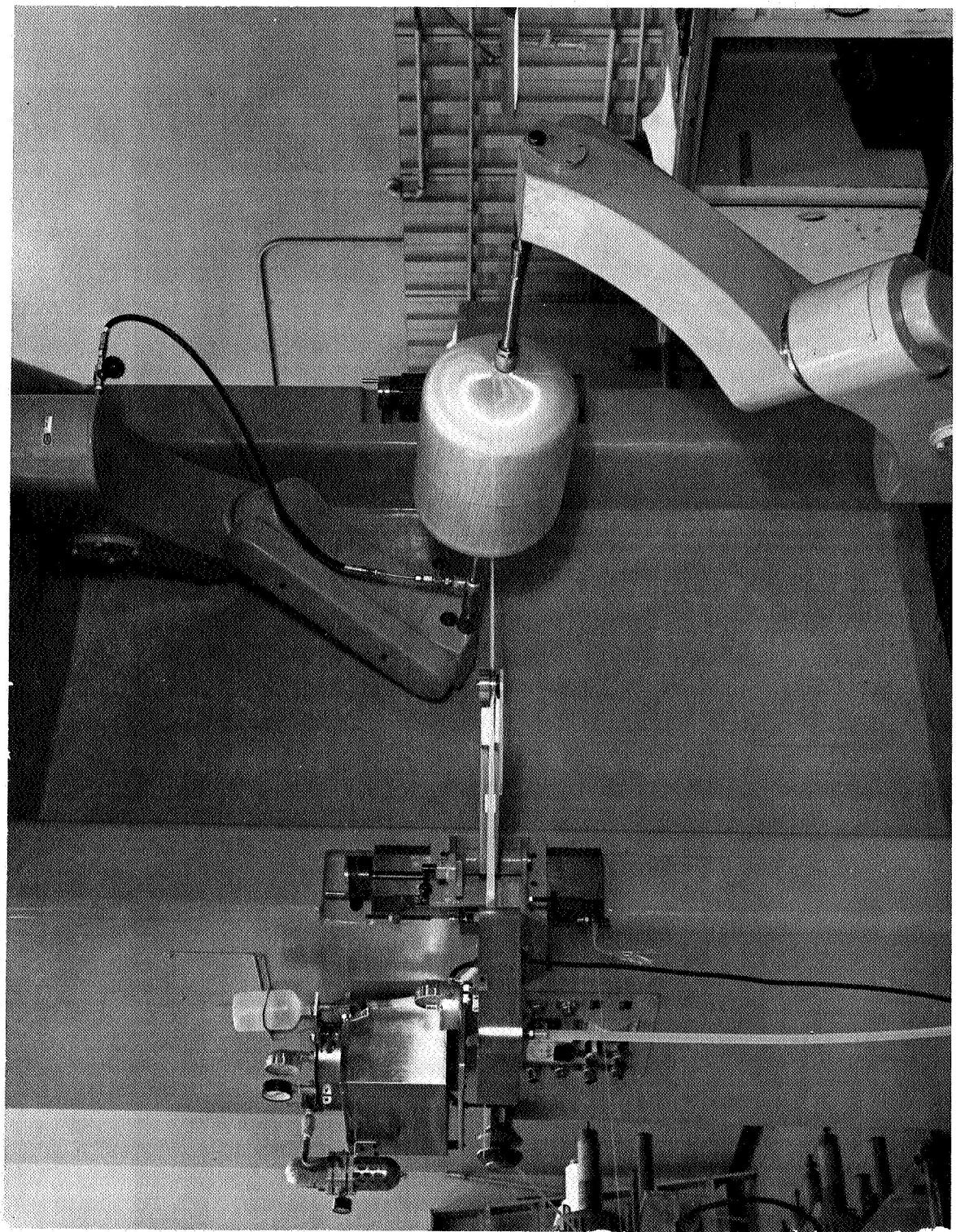


Figure 76
Glass Filament Overwinding 1100 Aluminum Hinged-Boss Liner

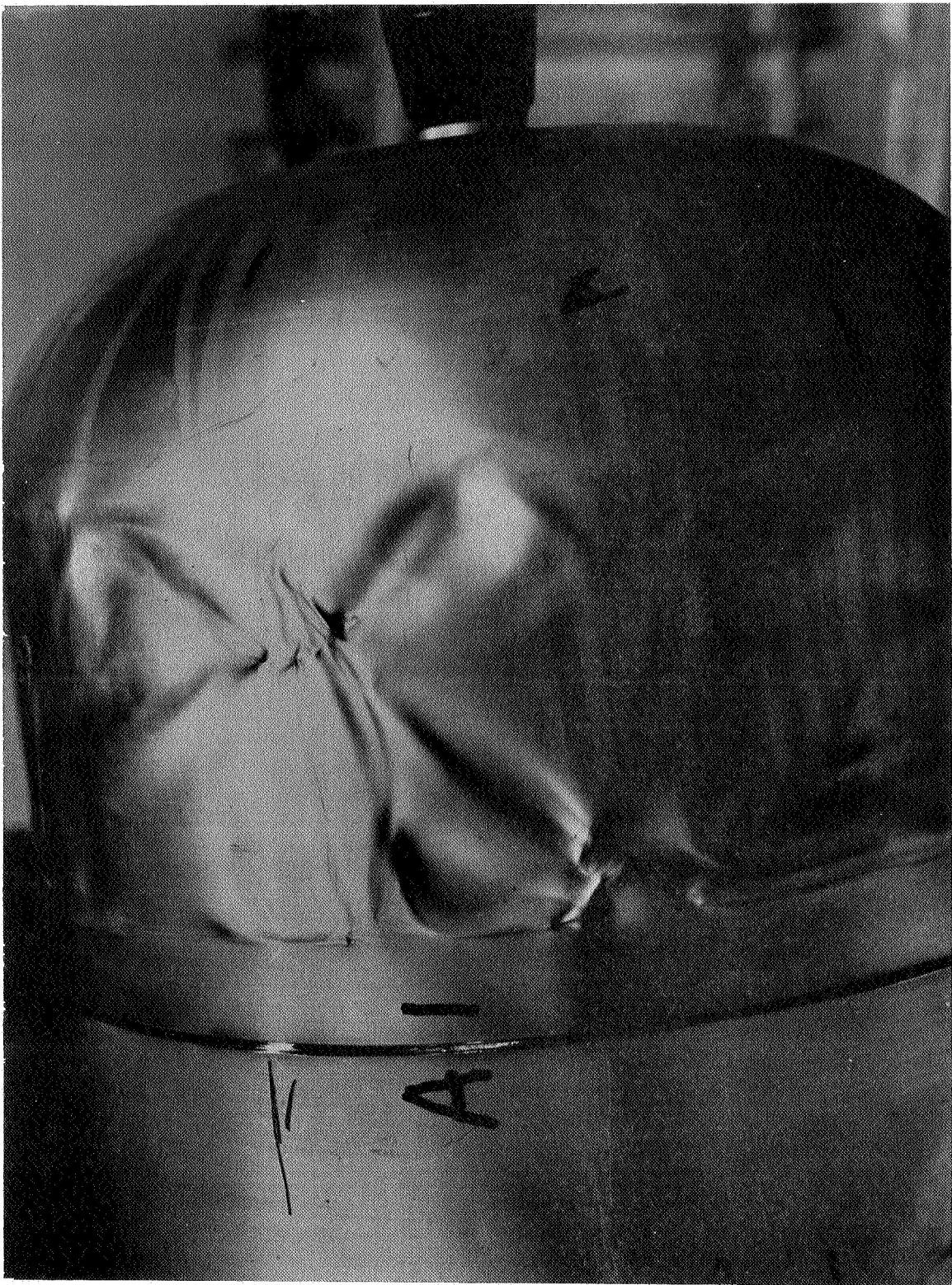


Figure 77
Buckles in Liner A-1

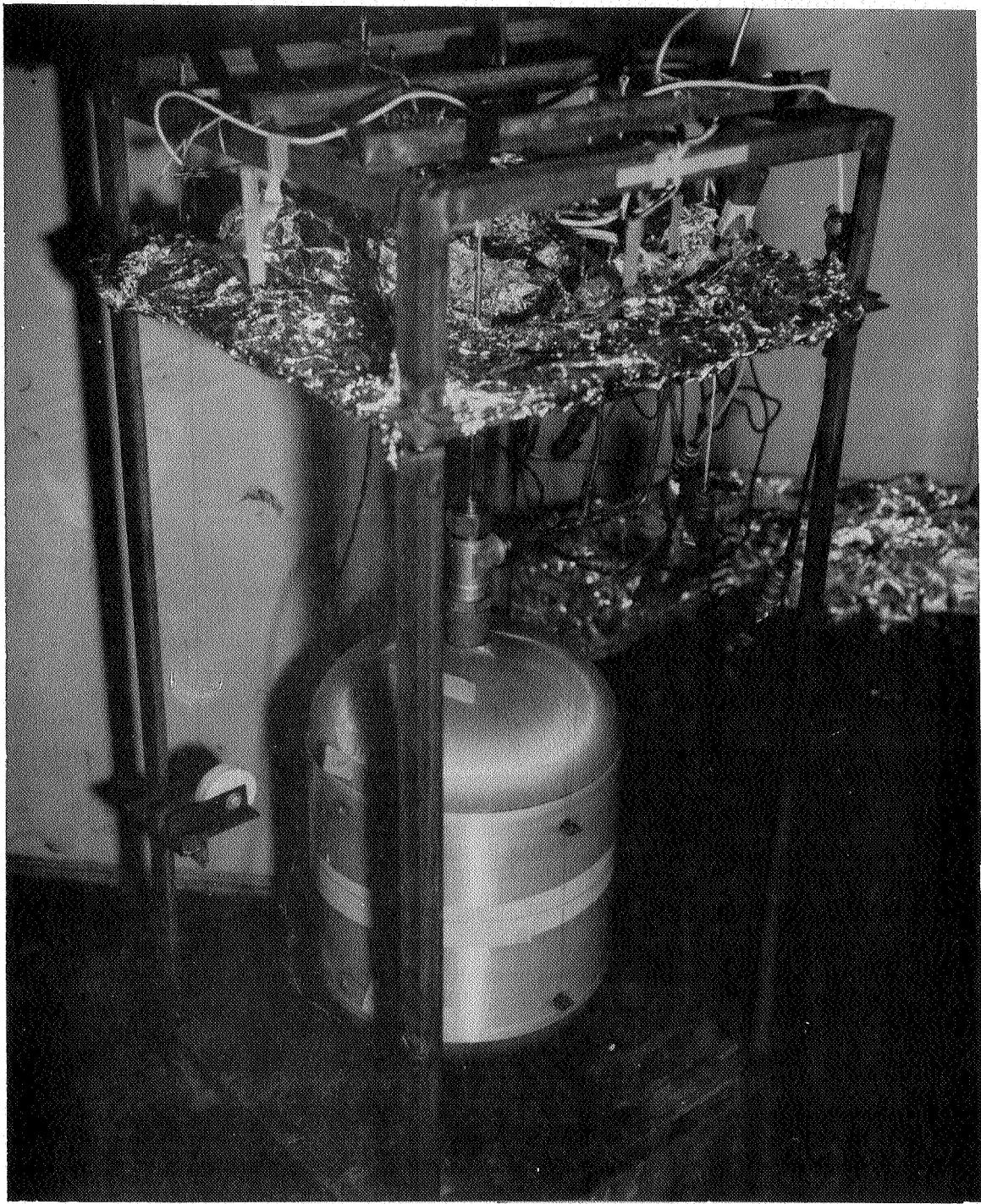


Figure 78
Installation of Test Vessel in Holding Frame, With Instrumentation Attached

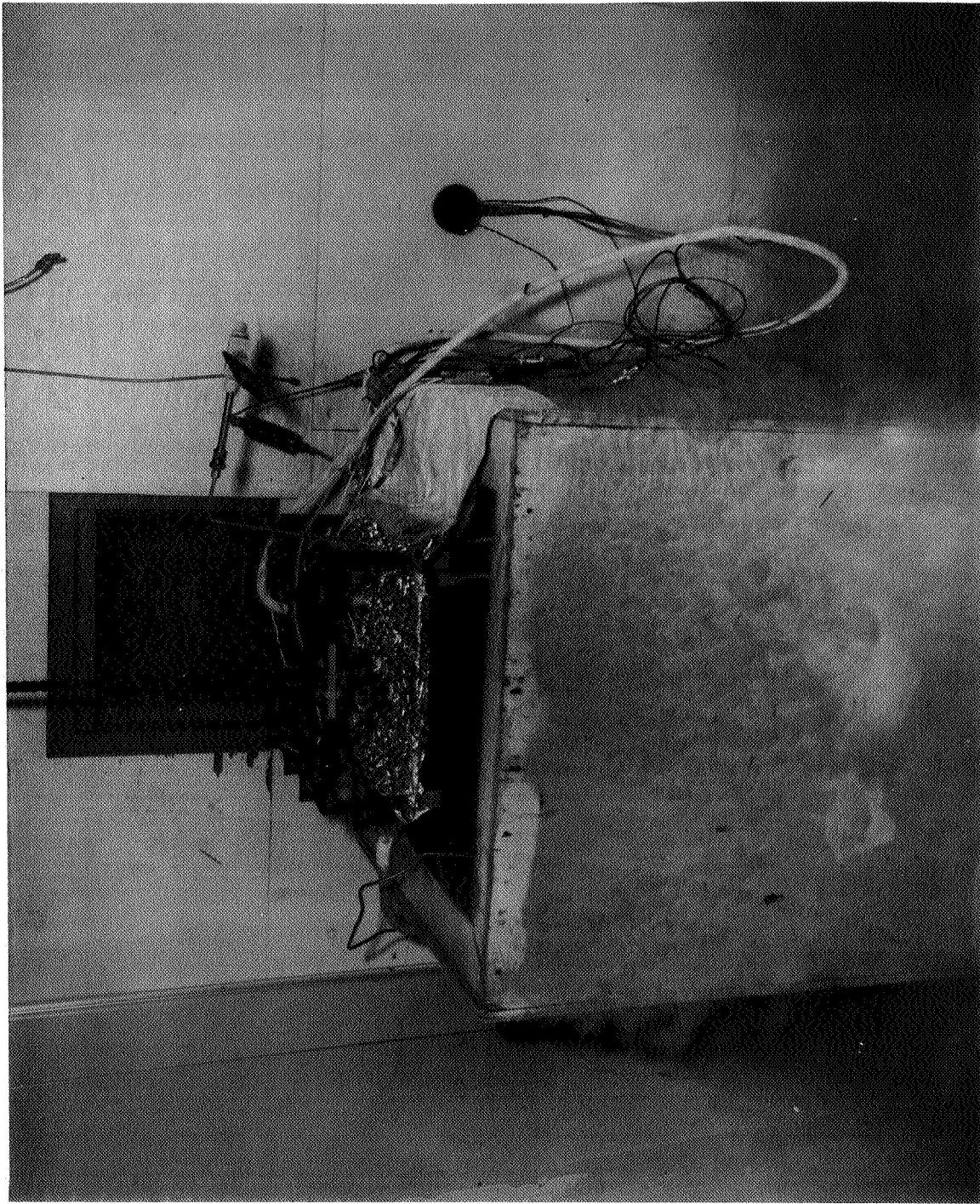
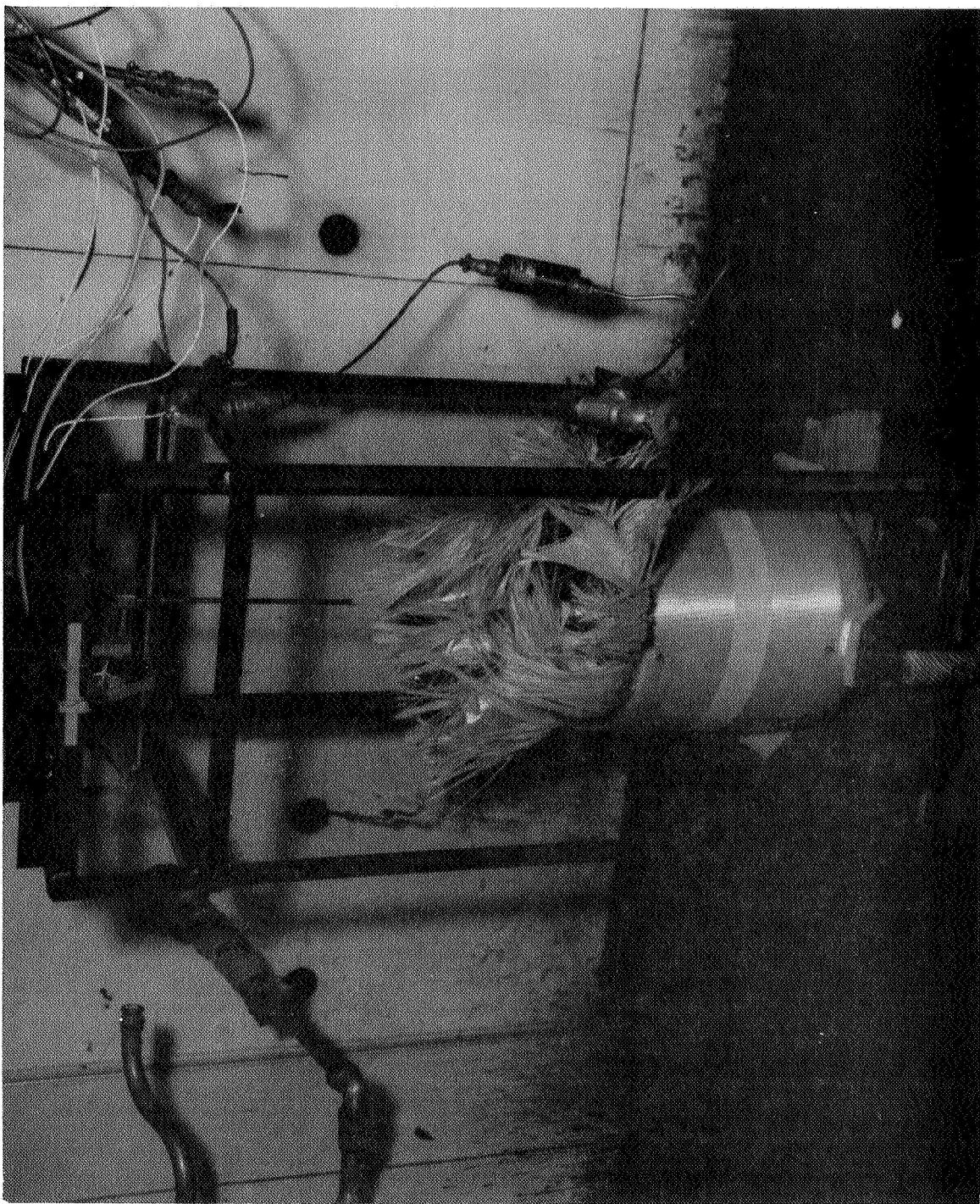
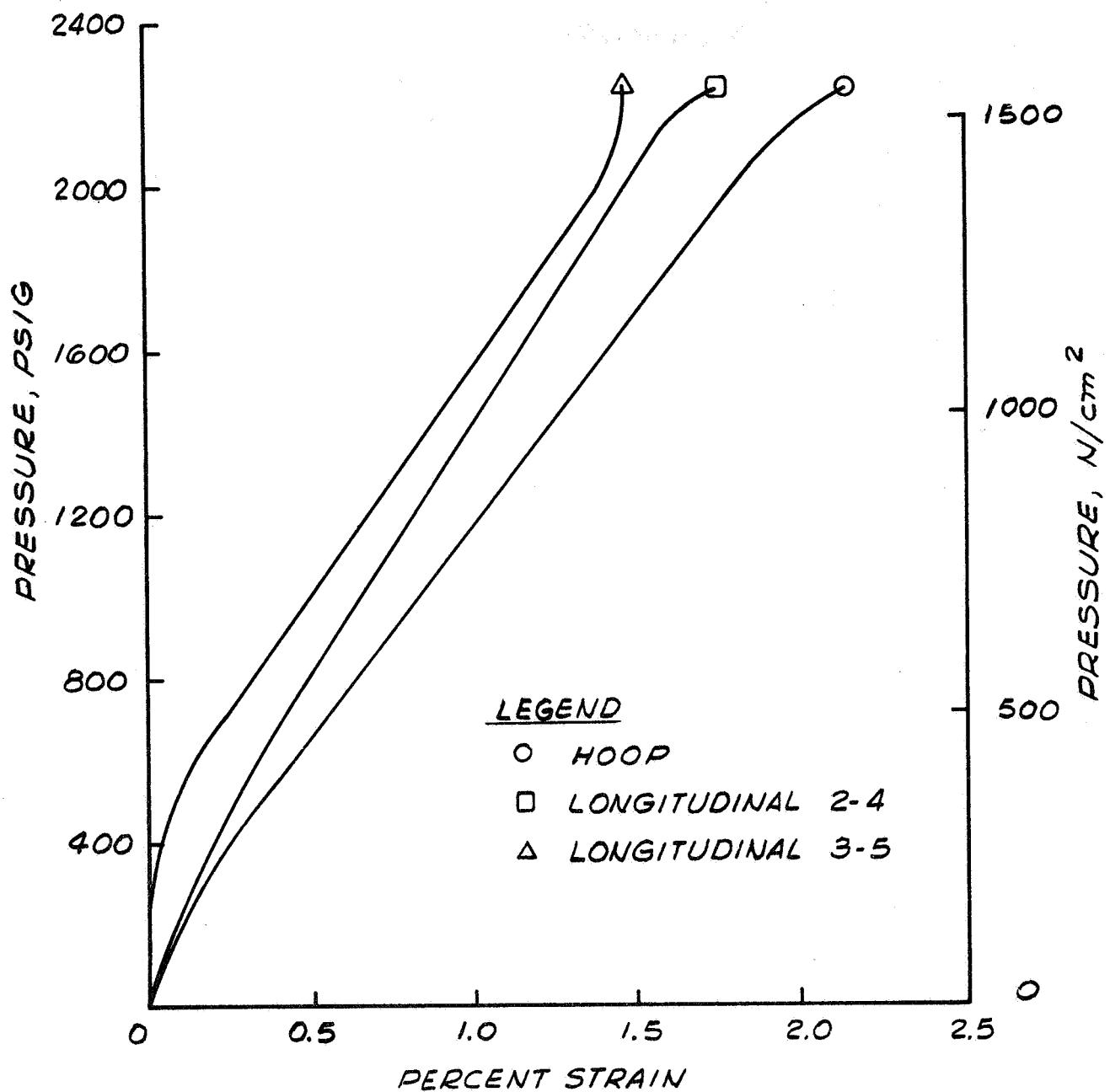


Figure 79
Vessel Holding Frame Positioned in Cryogen Filled Test Container

Figure 80
Post Test Photograph of Tank A-3 After Burst Test

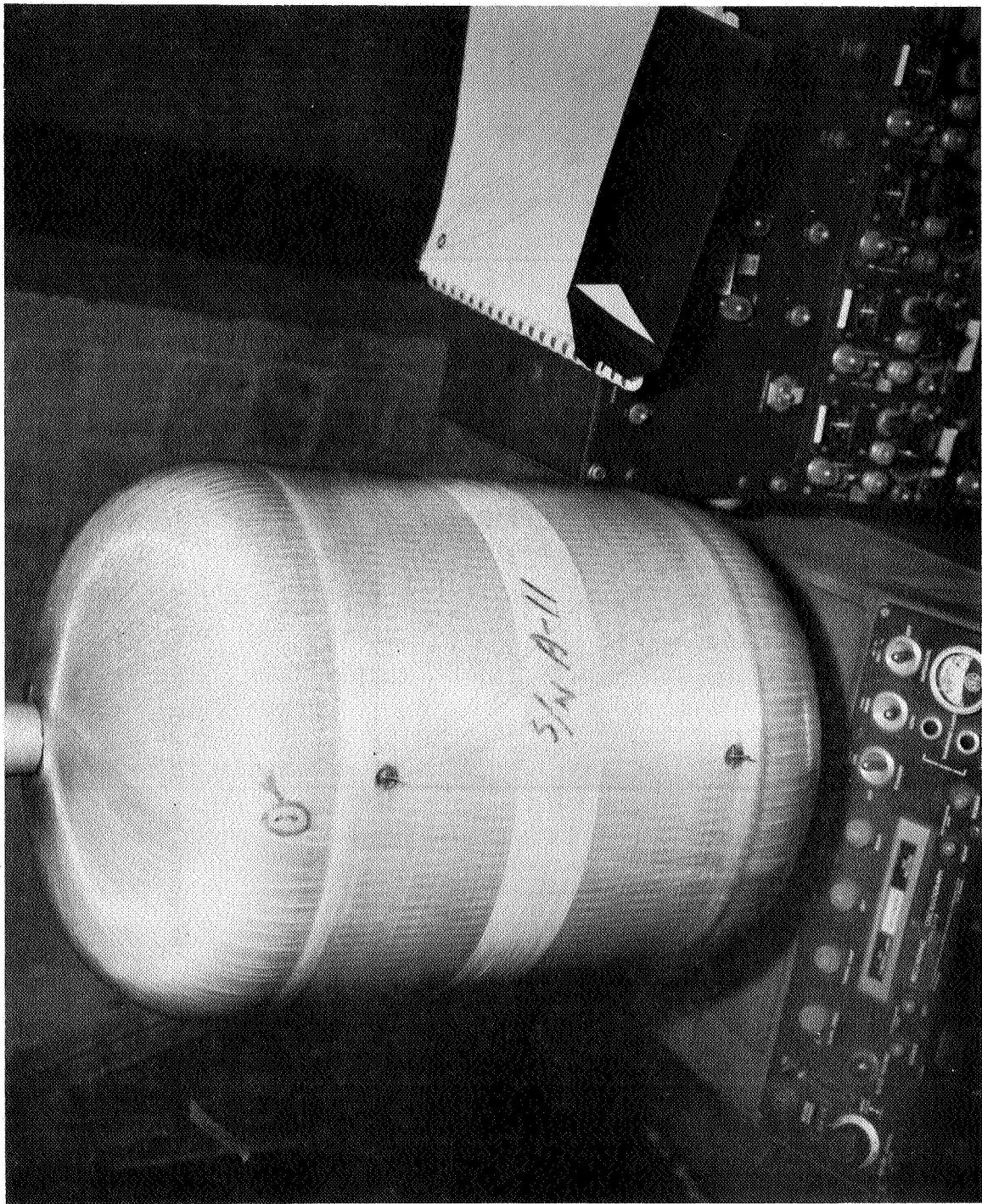




Pressure vs Strain for Tank A-3 Burst Test

Figure 81

Figure 82
Post Test Photograph of Tank A-11 After Cyclic Fatigue Test



Pressure vs Strain For Tank A-11 Cyclic Fatigue Test

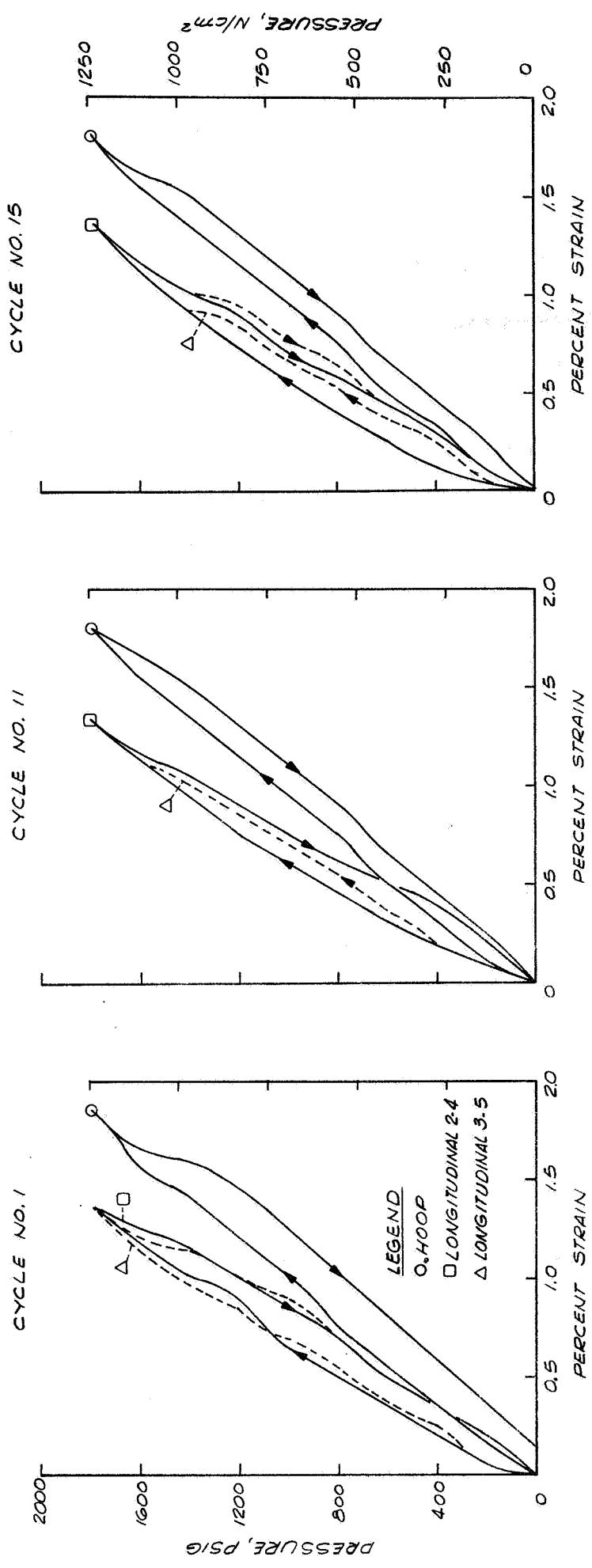
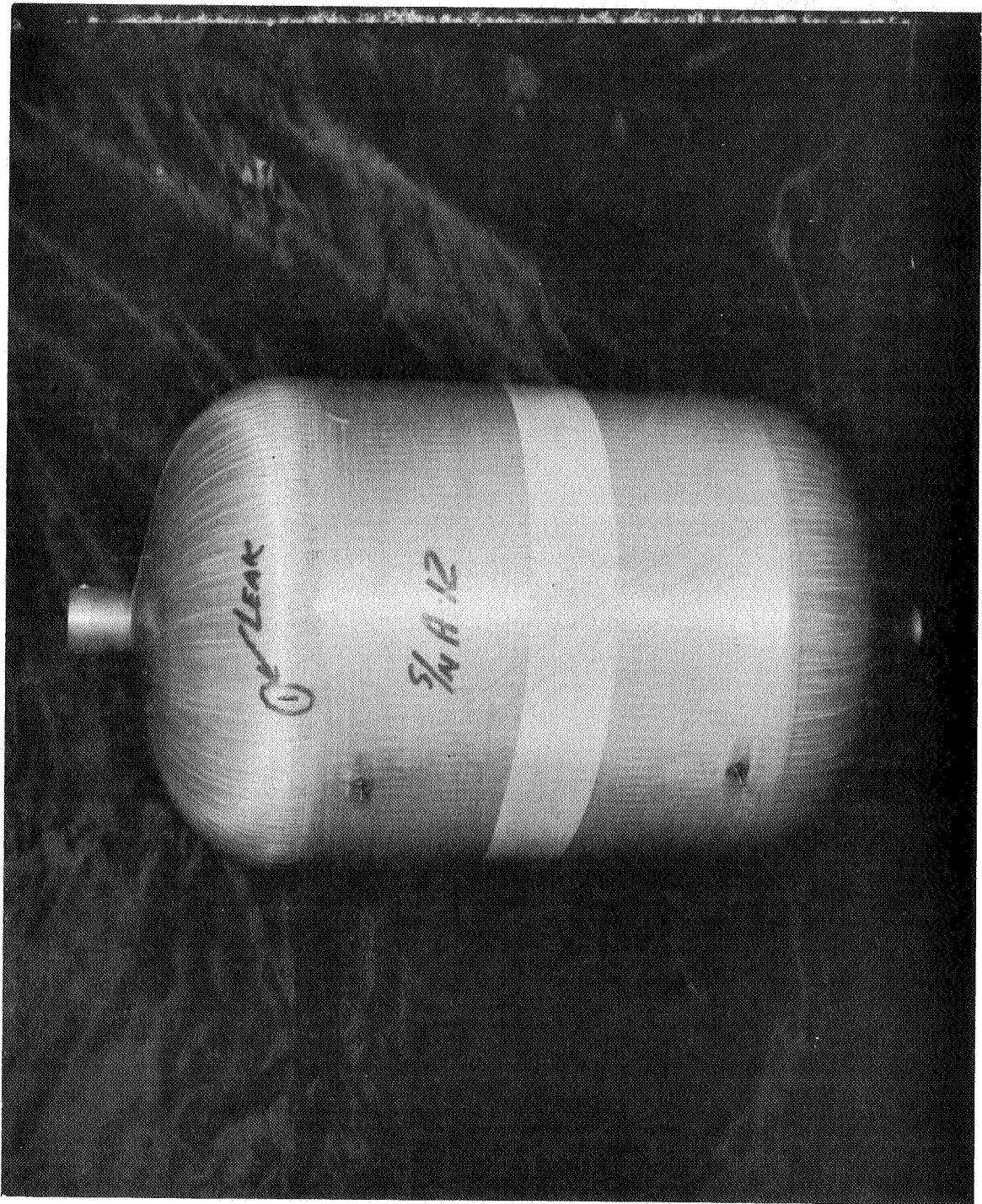
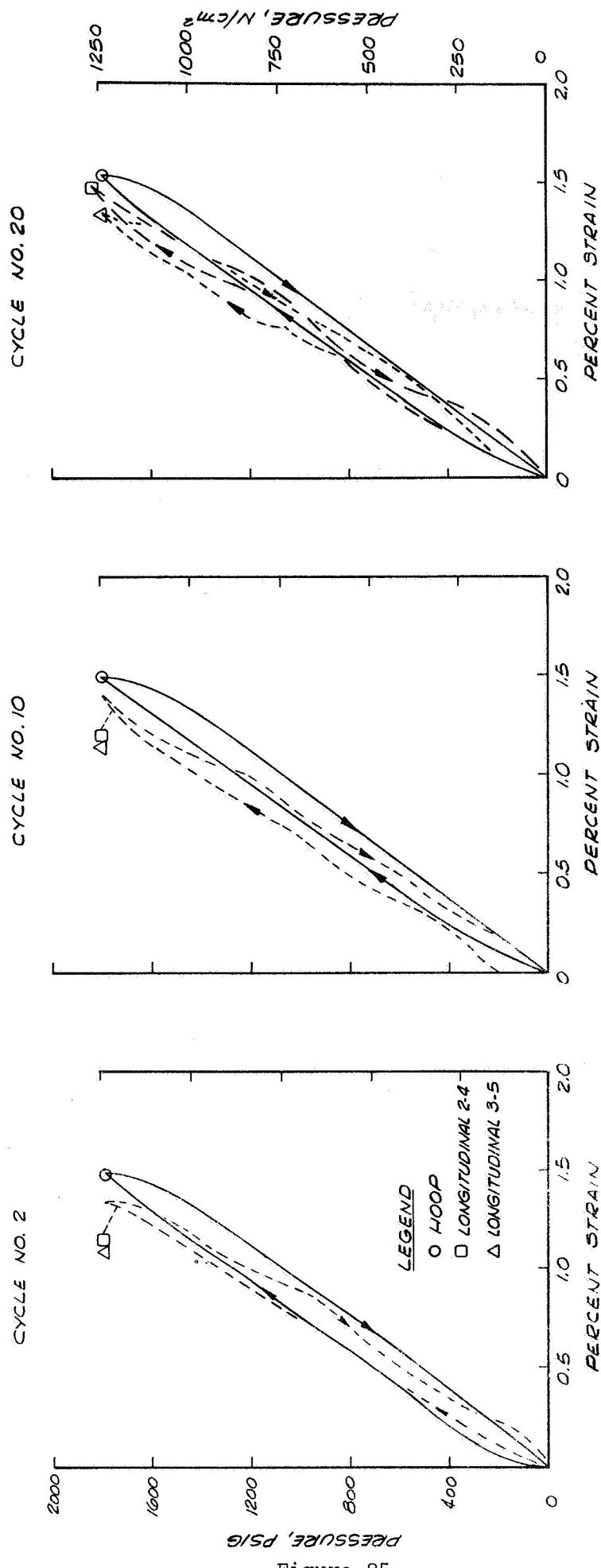


Figure 83

Figure 84
Post Test Photograph of Tank A-12 After Cyclic Fatigue Test

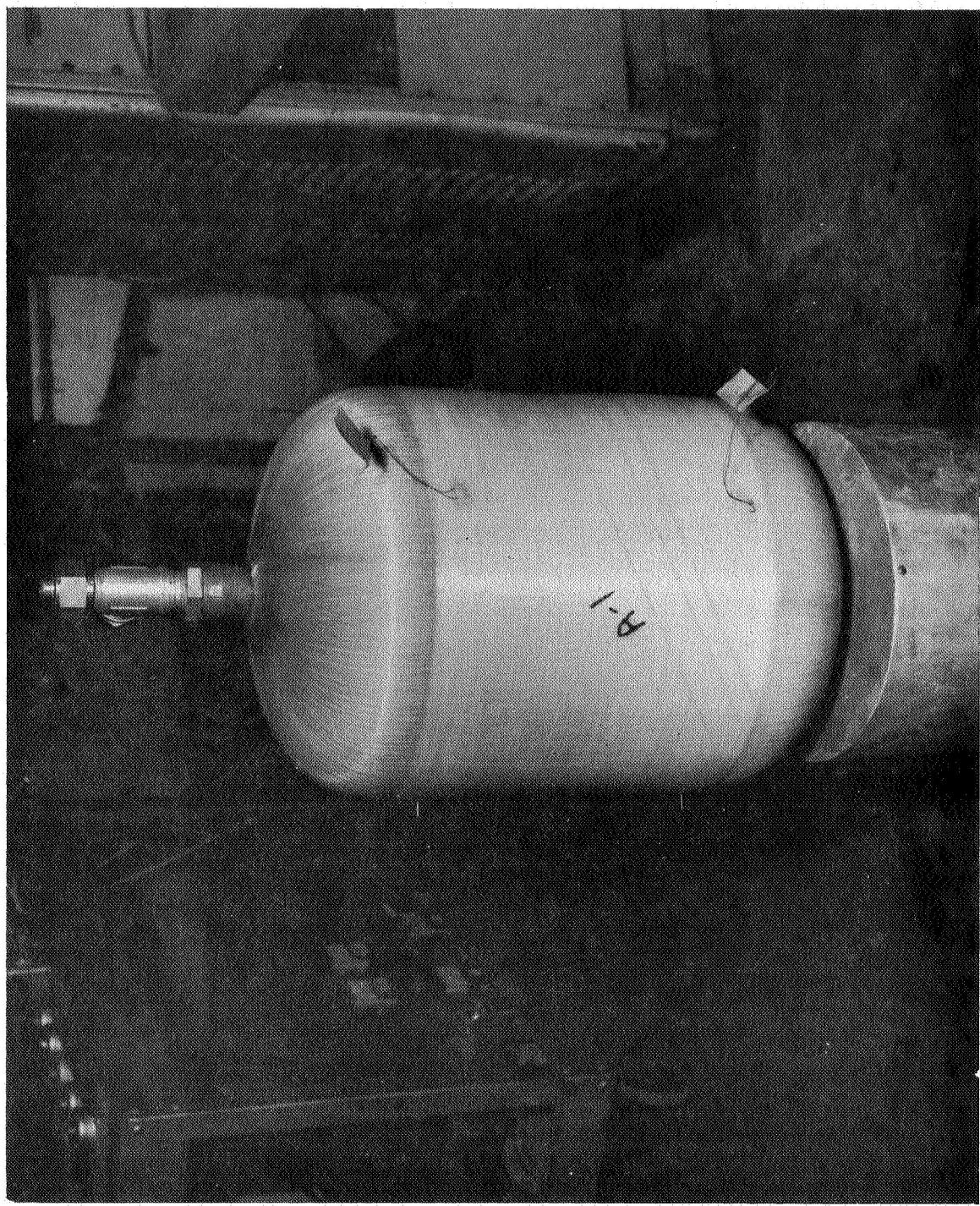


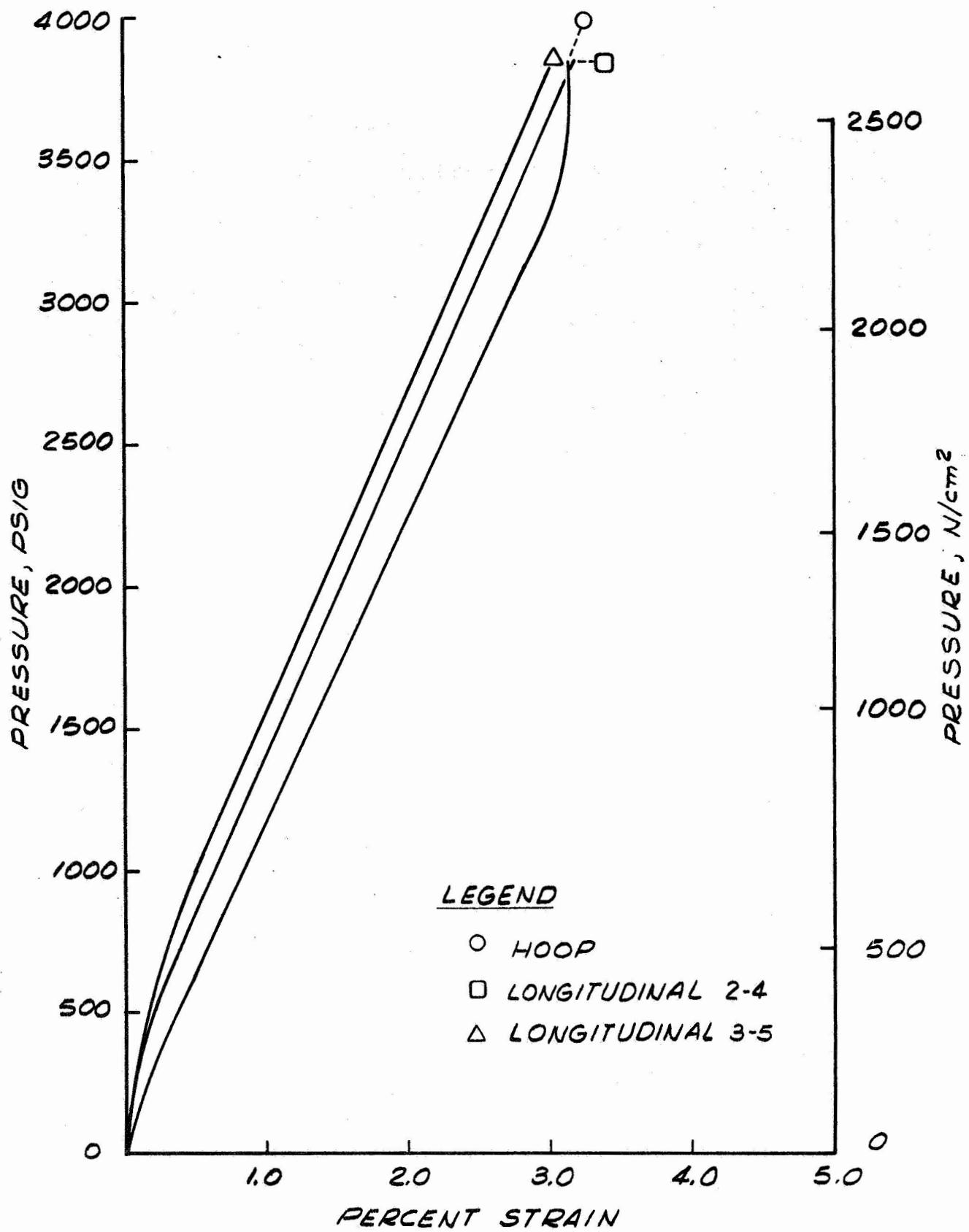


Pressure vs Strain for Tank A-12 Cyclic Fatigue Test

Figure 85

Figure 86
Post Test Photograph of Tank A-1 After Burst Test

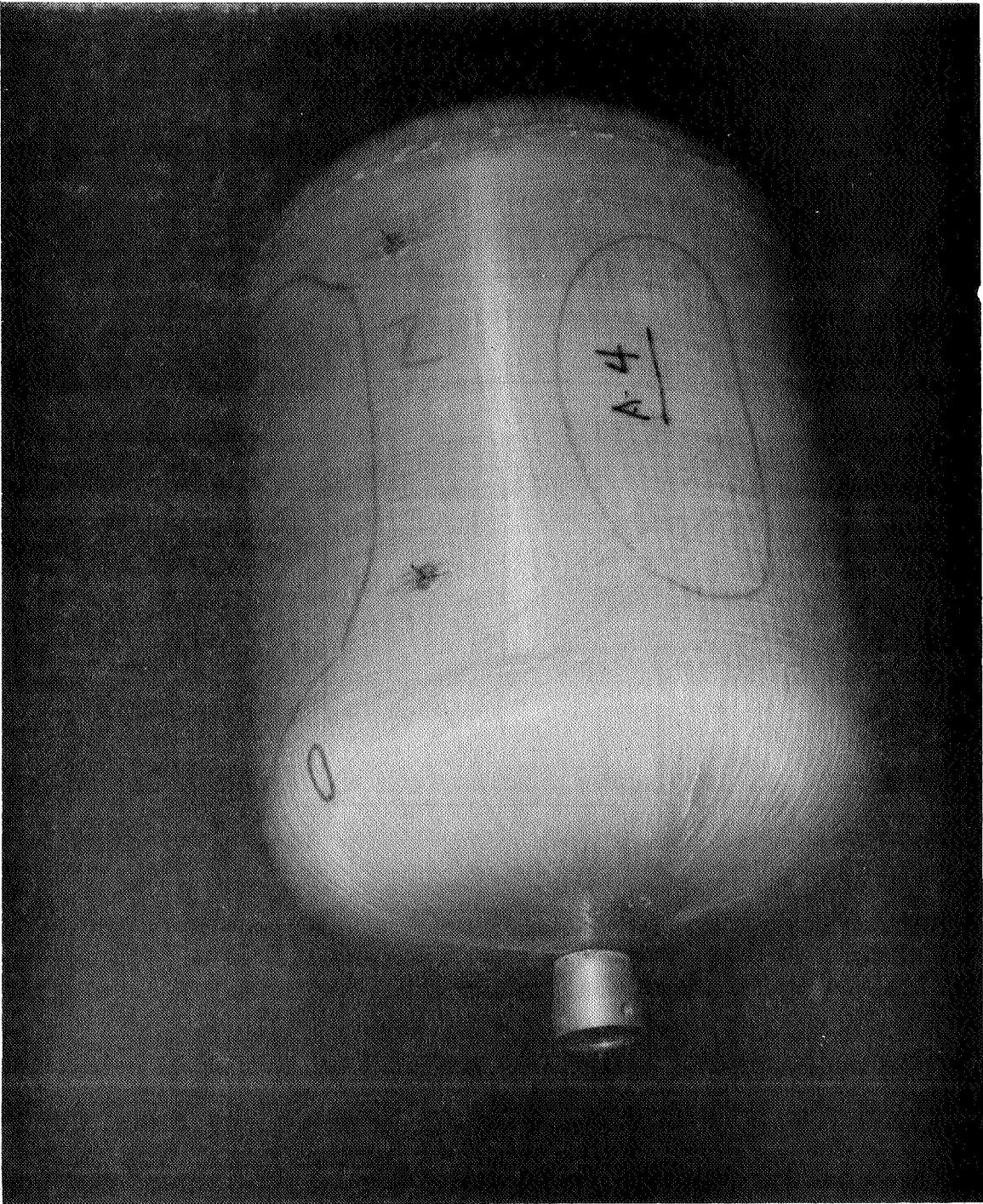


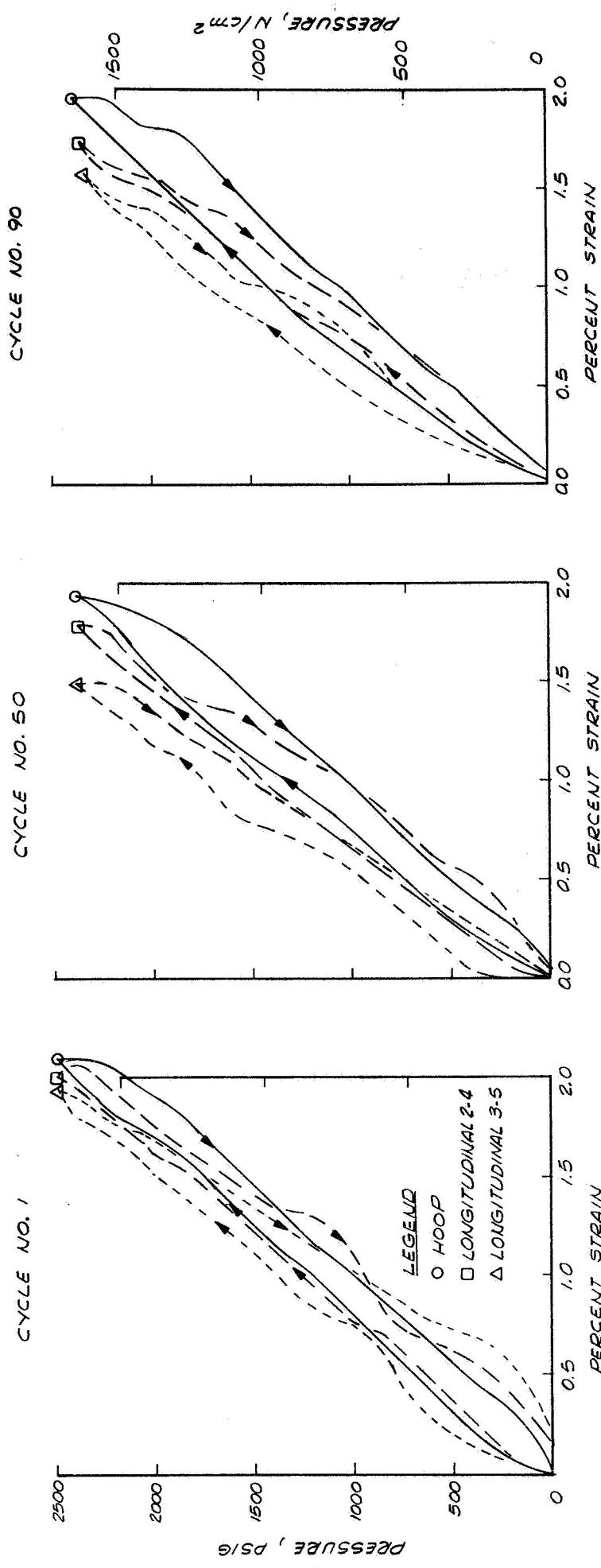


Pressure vs Strain for Tank A-1 Burst Test

Figure 87

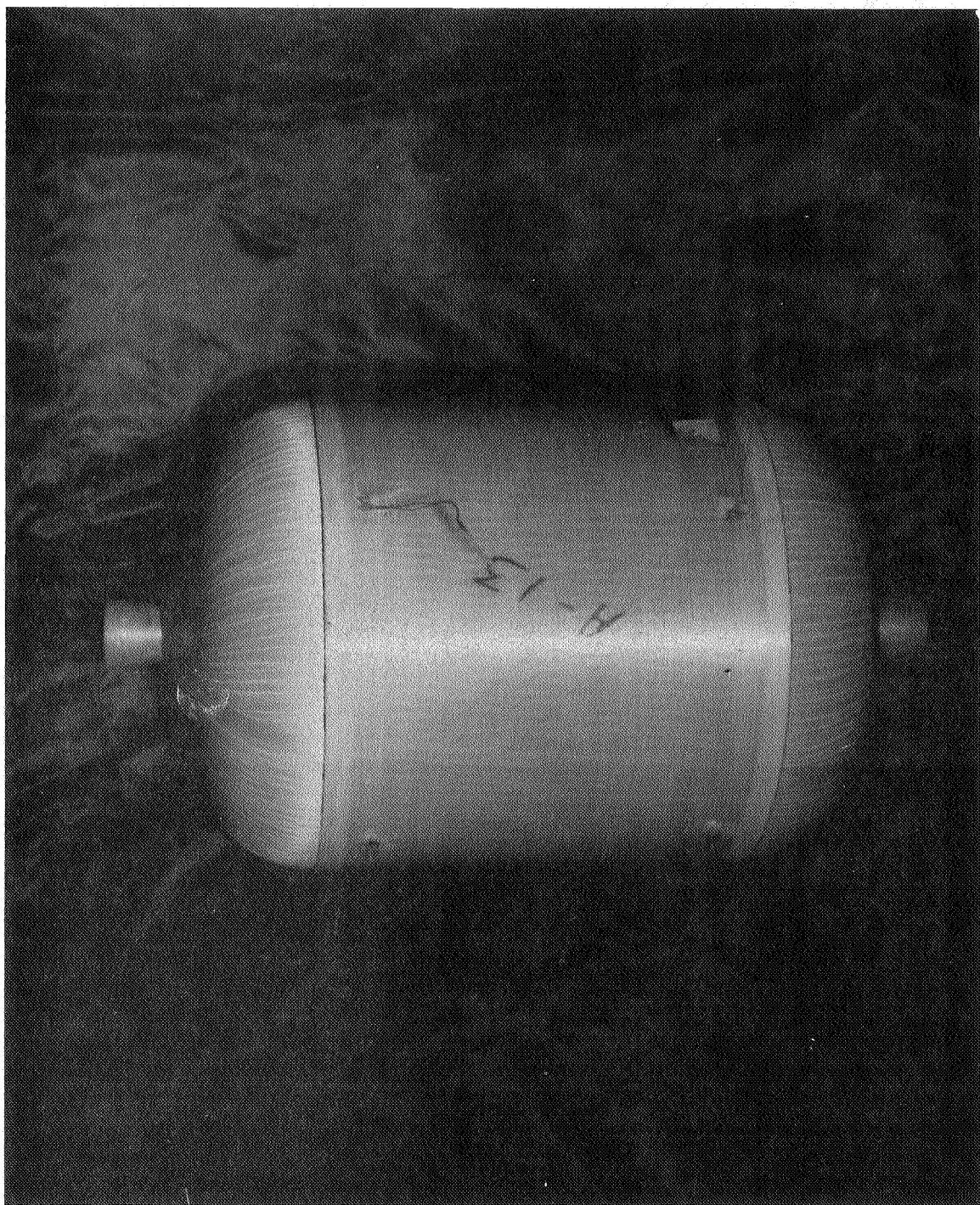
Figure 88
Post Test Photograph of Tank A-4 After Cyclic Fatigue Test





Pressure vs Strain for Tank A-4 Cyclic Fatigue Test

Figure 90
Post Test Photograph of Tank A-13 After Cyclic Fatigue Test



Pressure vs Strain for Tank A-13 Cyclic Fatigue Test

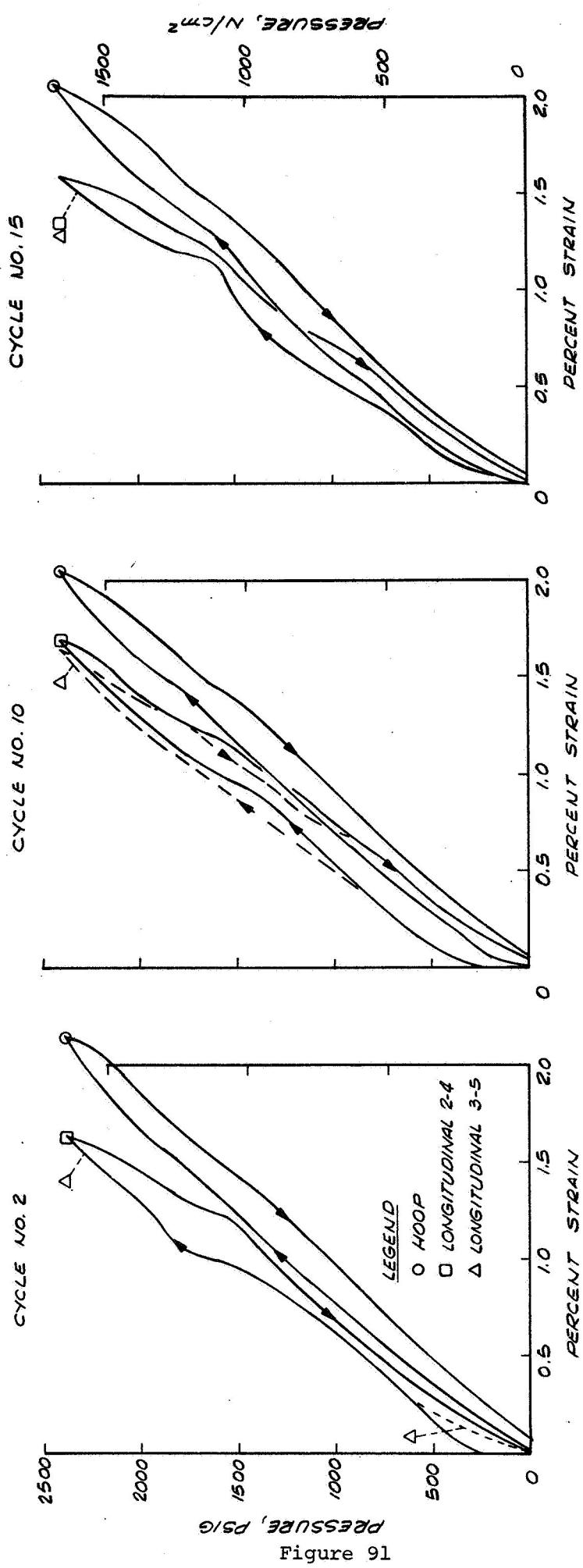
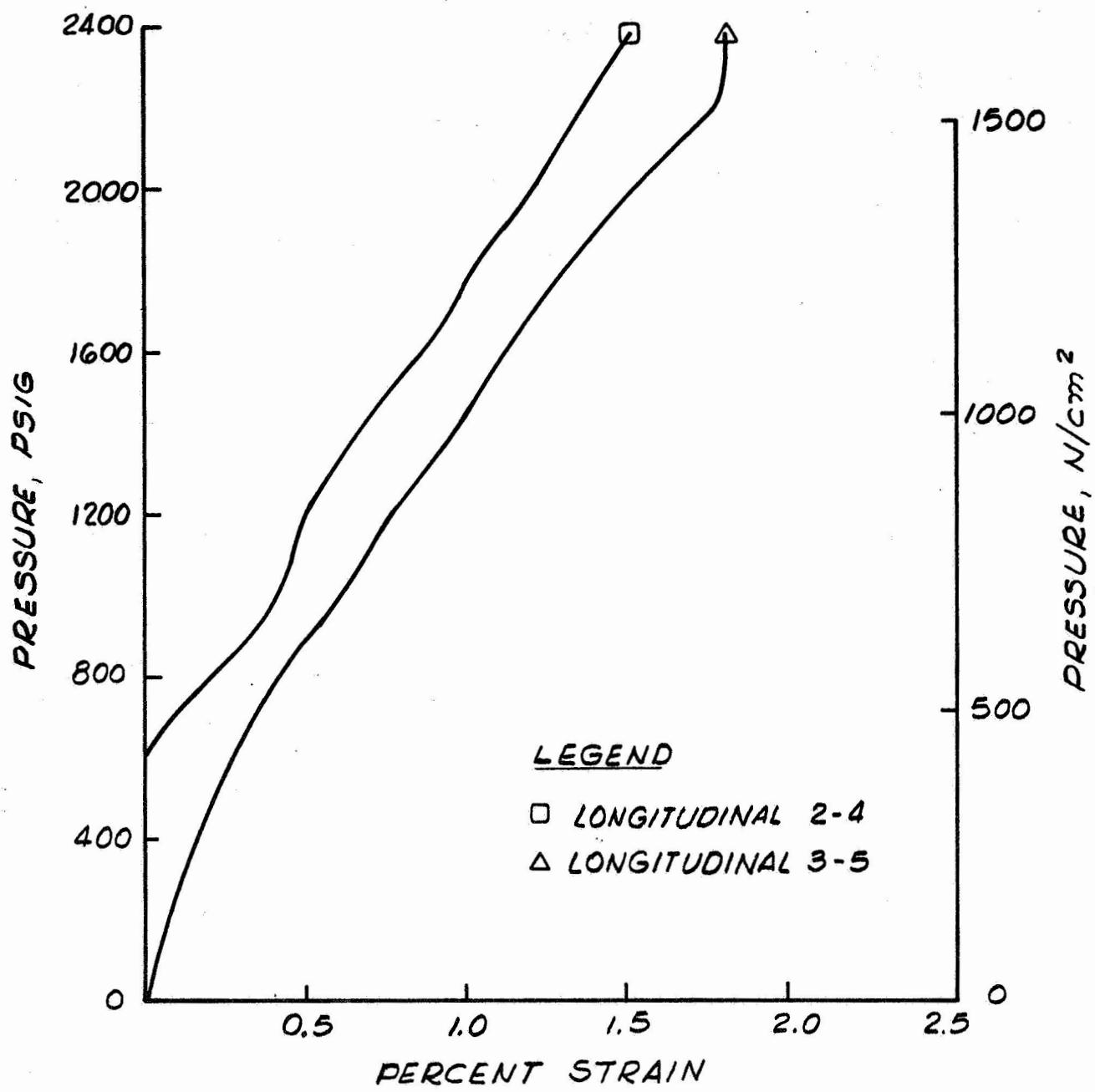


Figure 91

Figure 92
Post Test Photograph of Tank A-9 After Burst Test

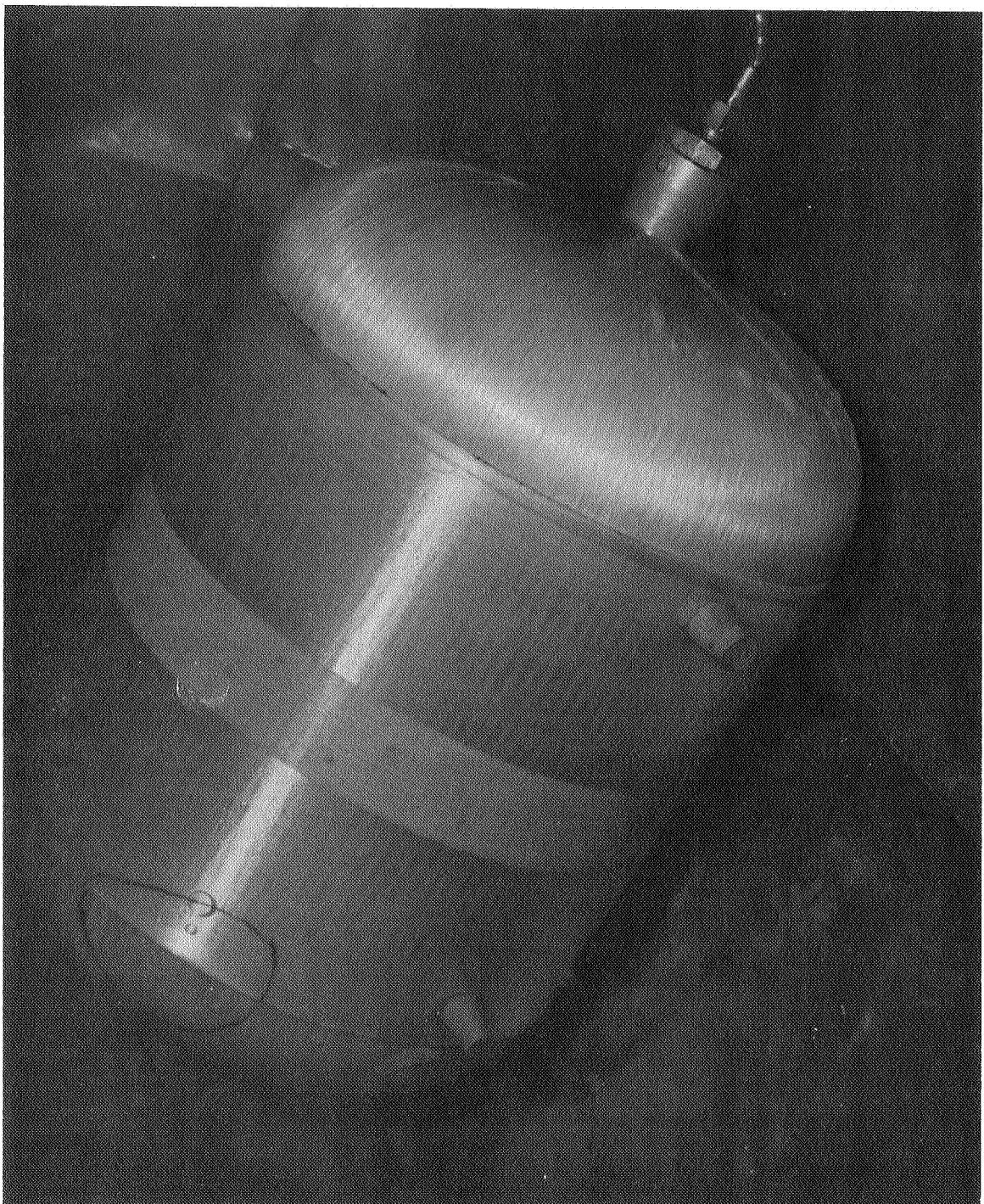




Pressure vs Strain for Tank A-9 Burst Test

Figure 93

Figure 94
Post Test Photograph of Tank A-2 After Cyclic Fatigue Test



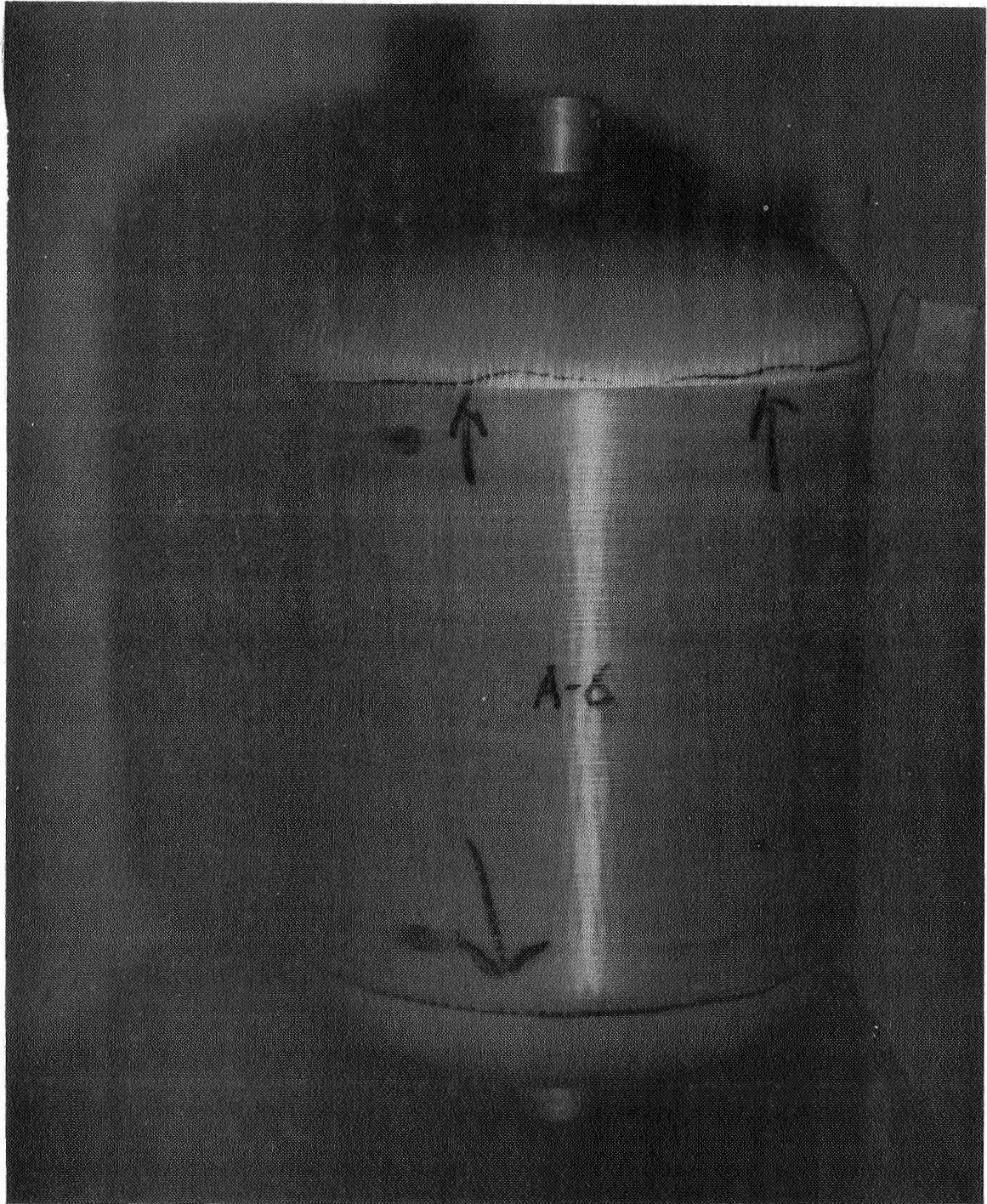
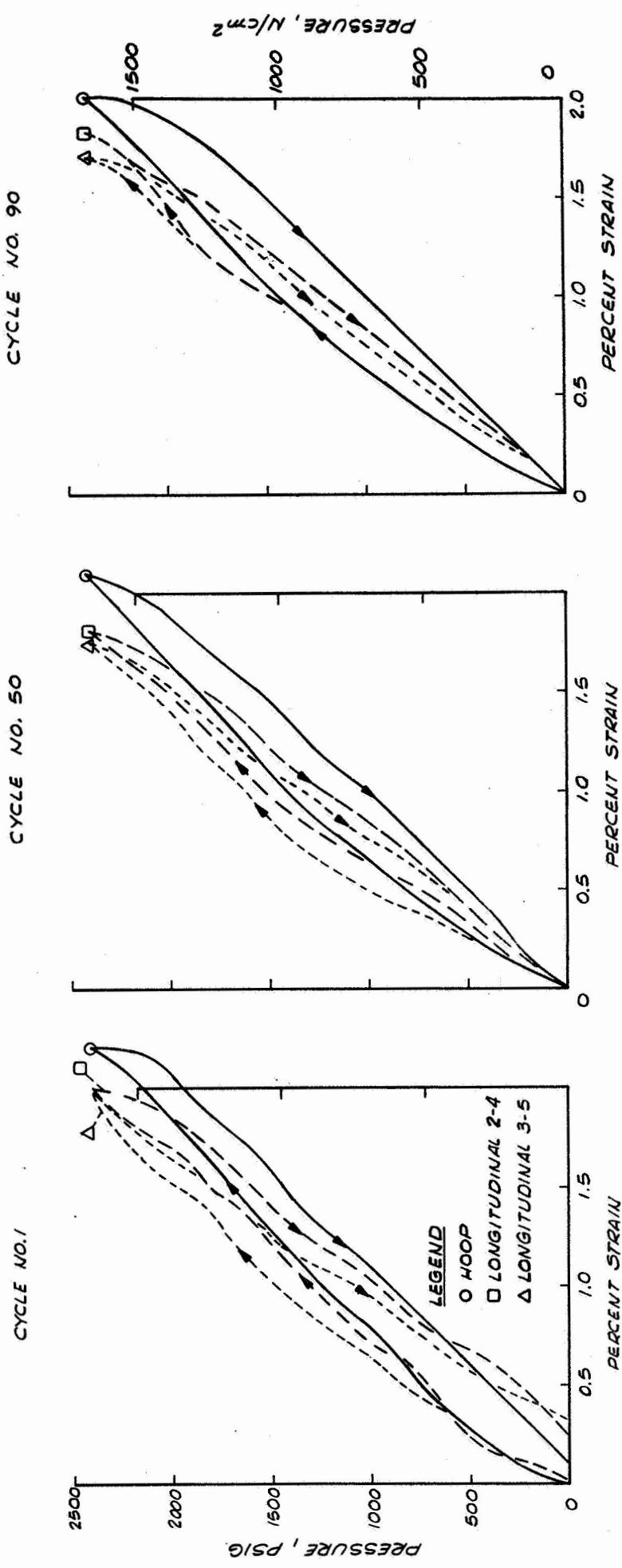
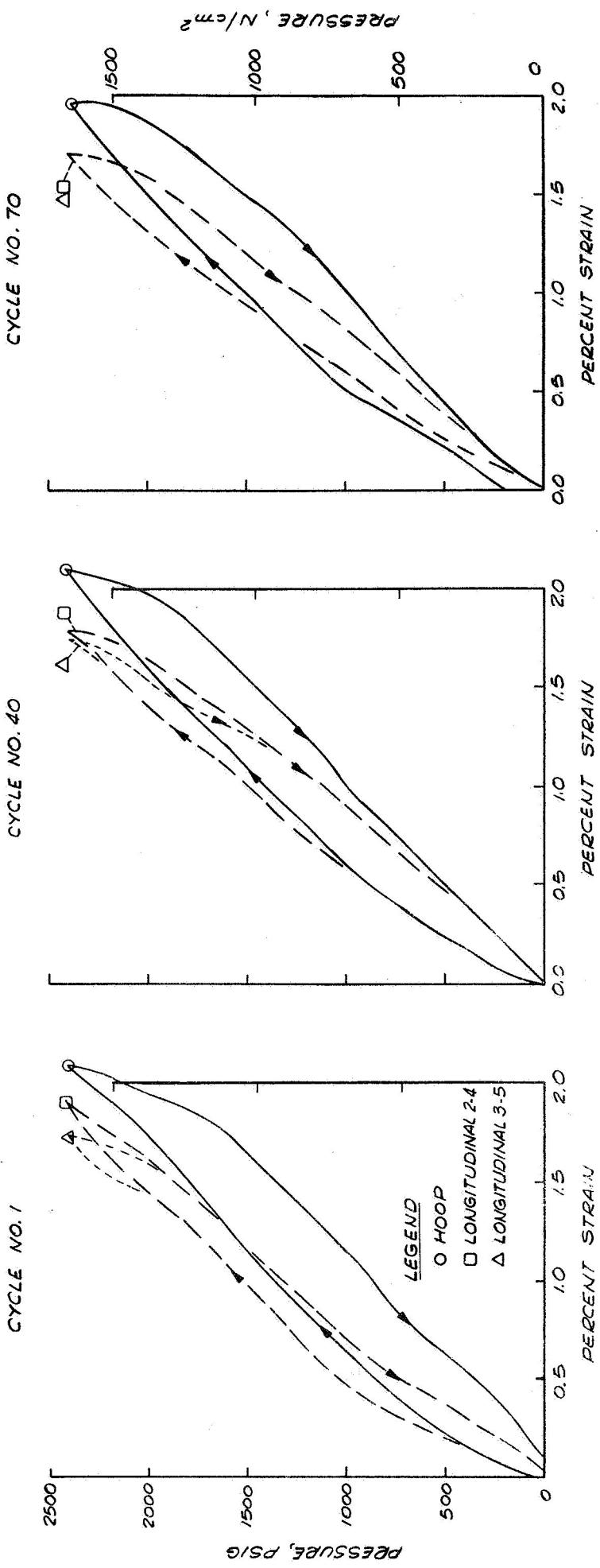


Figure 95
Post Test Photograph of Tank A-6 After Cyclic Fatigue Test



Pressure vs Strain for Tank A-2 Cyclic Fatigue Test

Figure 96



Pressure vs Strain for Tank A-6 Cyclic Fatigue Test

Figure 97

Figure 98
Typical Boss and Head-To-Cylinder Junction Specimens Taken from Tanks

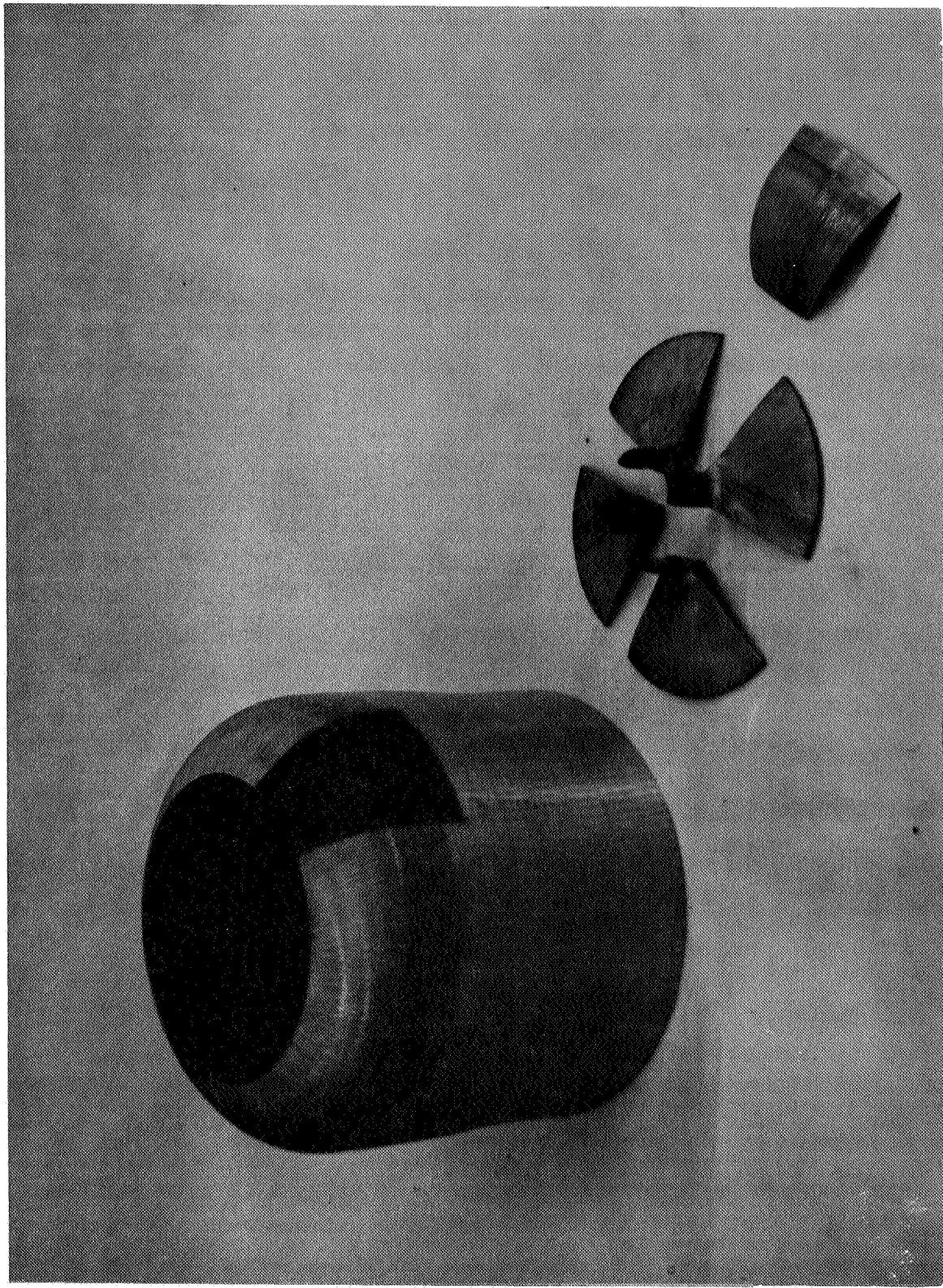


Figure 99
Cross-Section of Hinged Boss, Exterior View

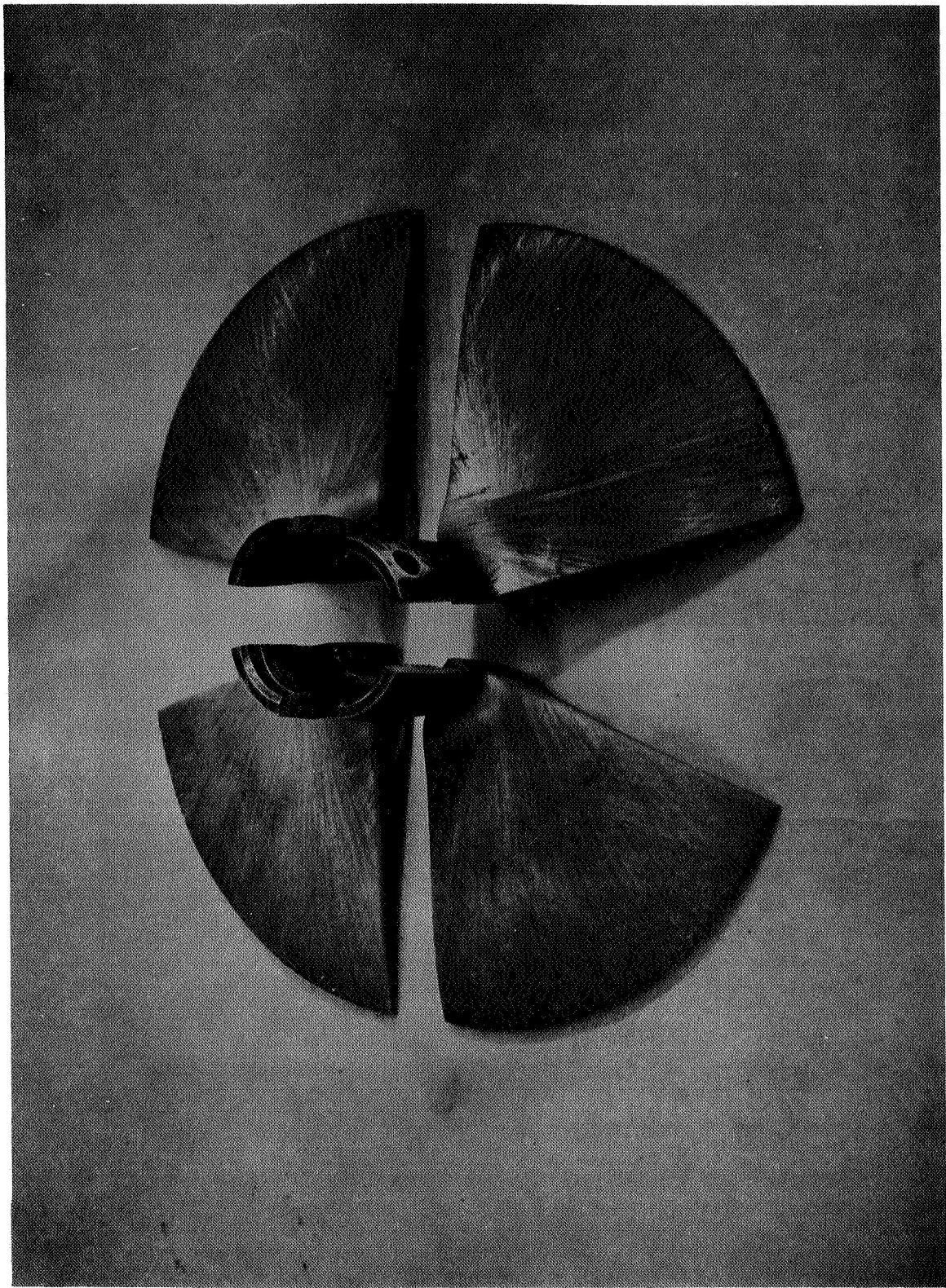
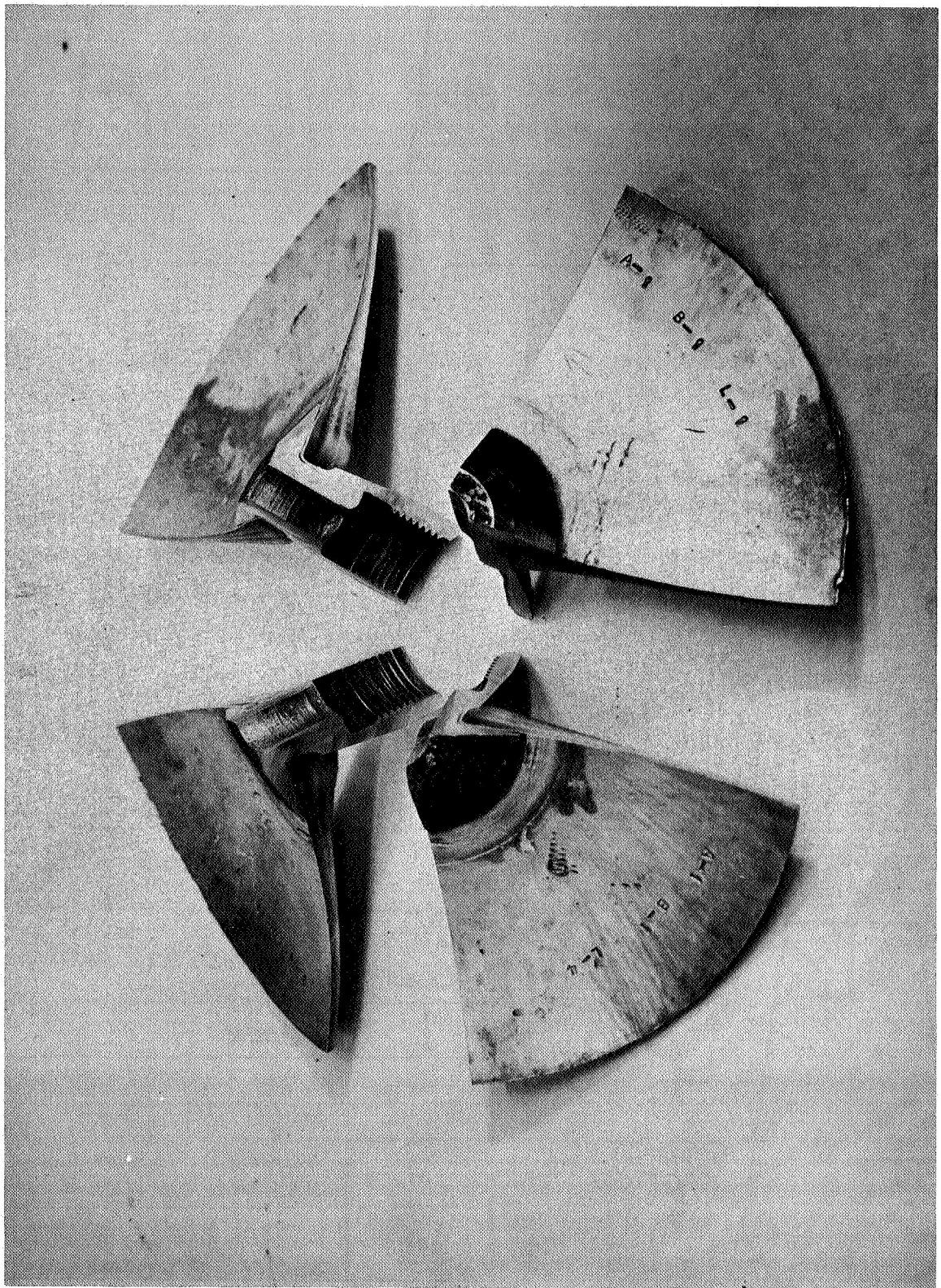
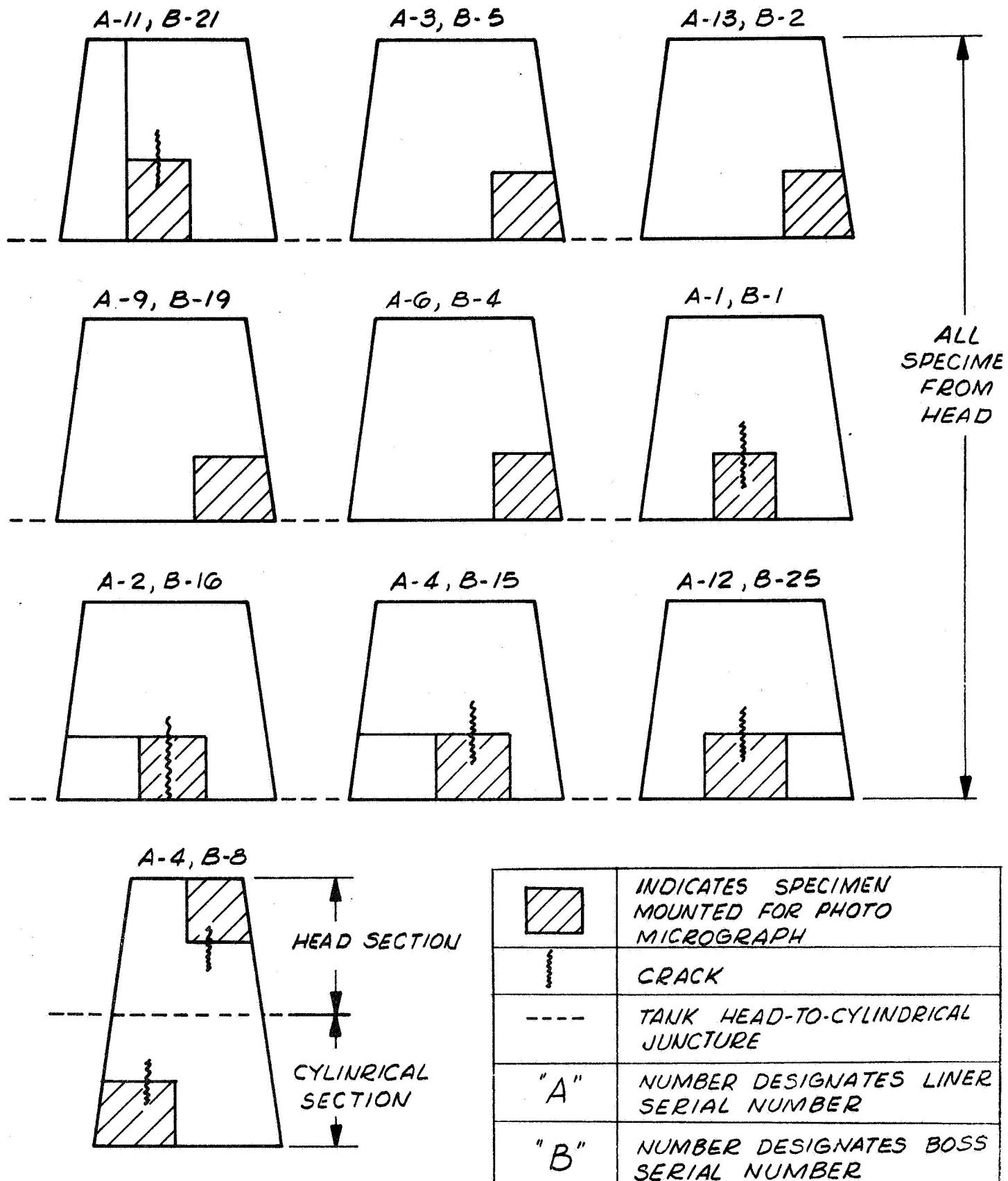


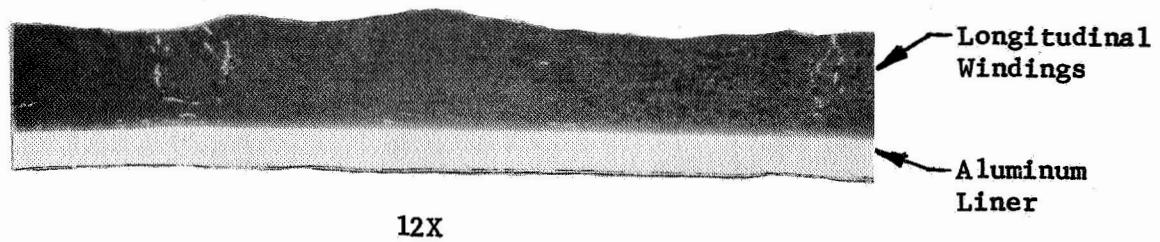
Figure 100
Cross-Sections of Hinged Boss, Interior View



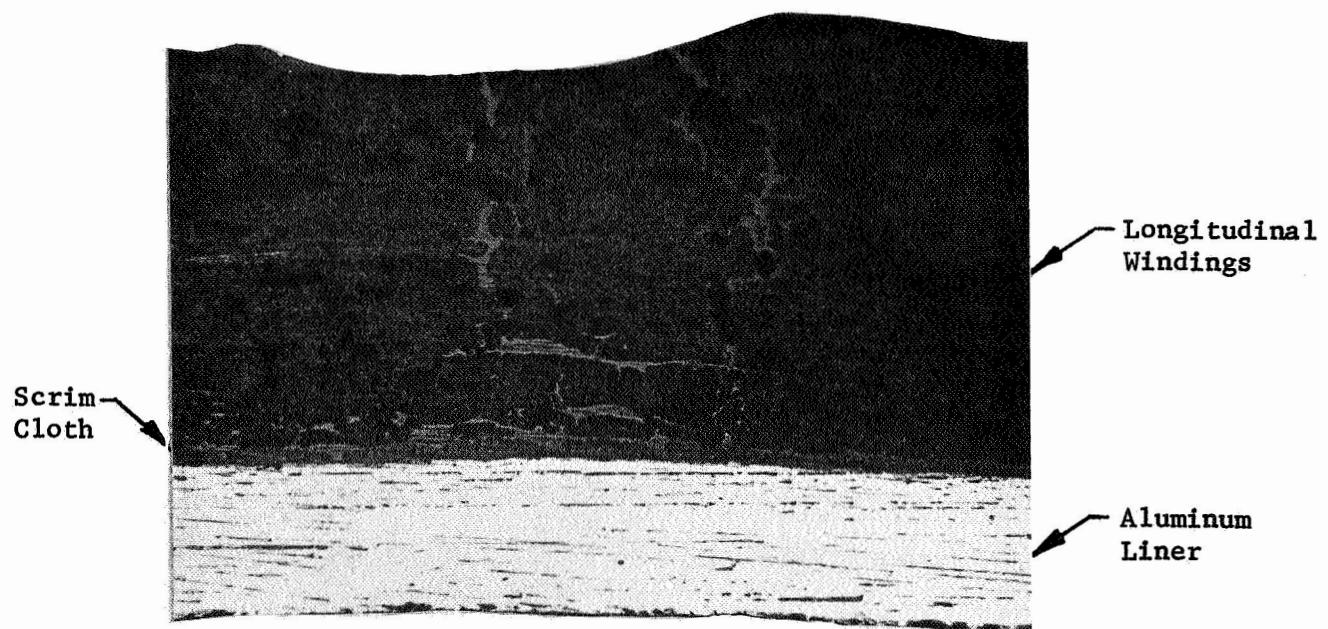


Locations of Liner Failure Sites and Specimens Taken from Tanks for Analysis

Figure 101



12X



74X

Photomicrographs of Tank A-3
Cross Section Showing Liner, Glass
Filament Overwrap, and Craze Cracking

Figure 102

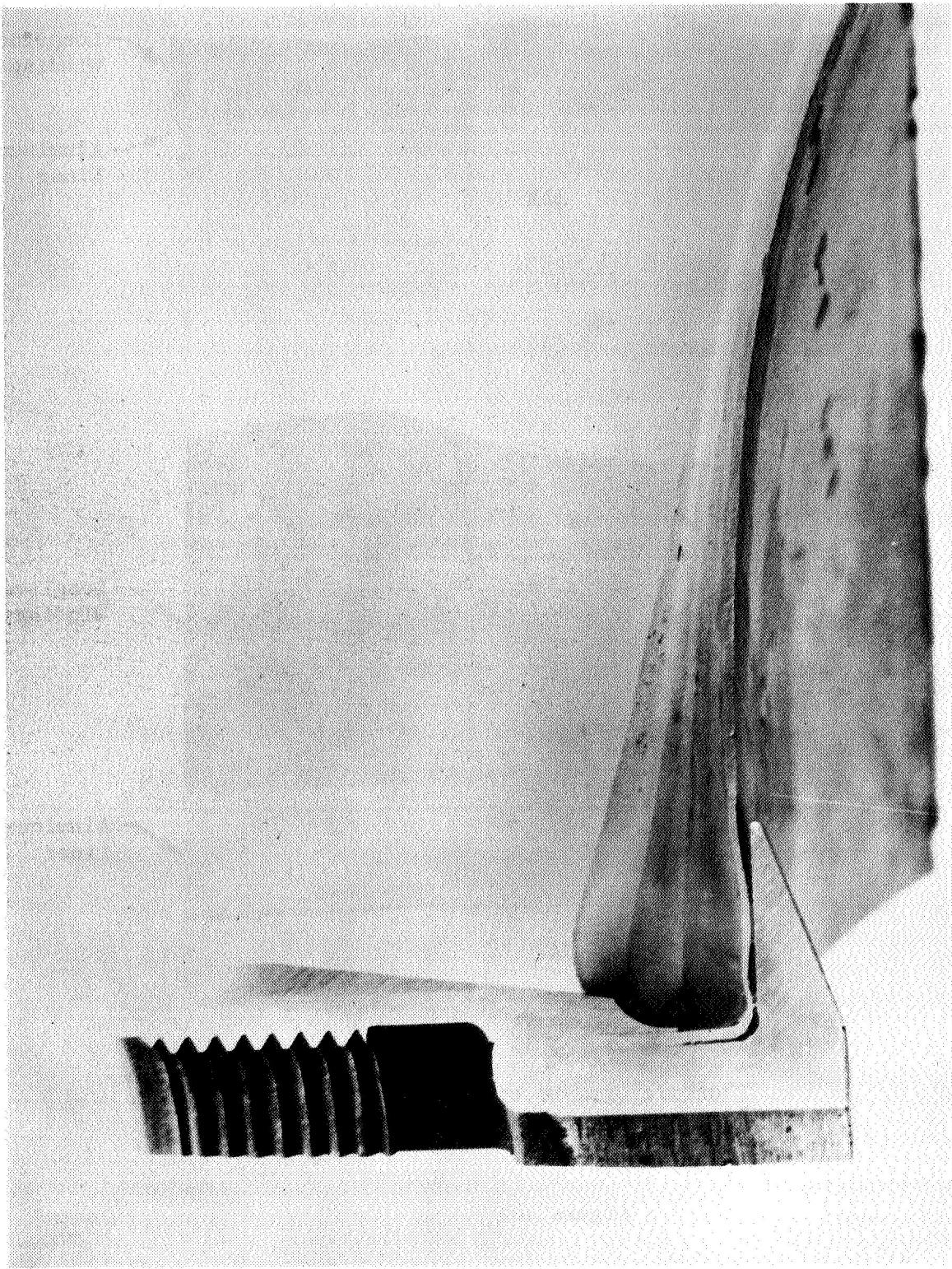


Figure 103 Tank A-1 Boss Cross Section



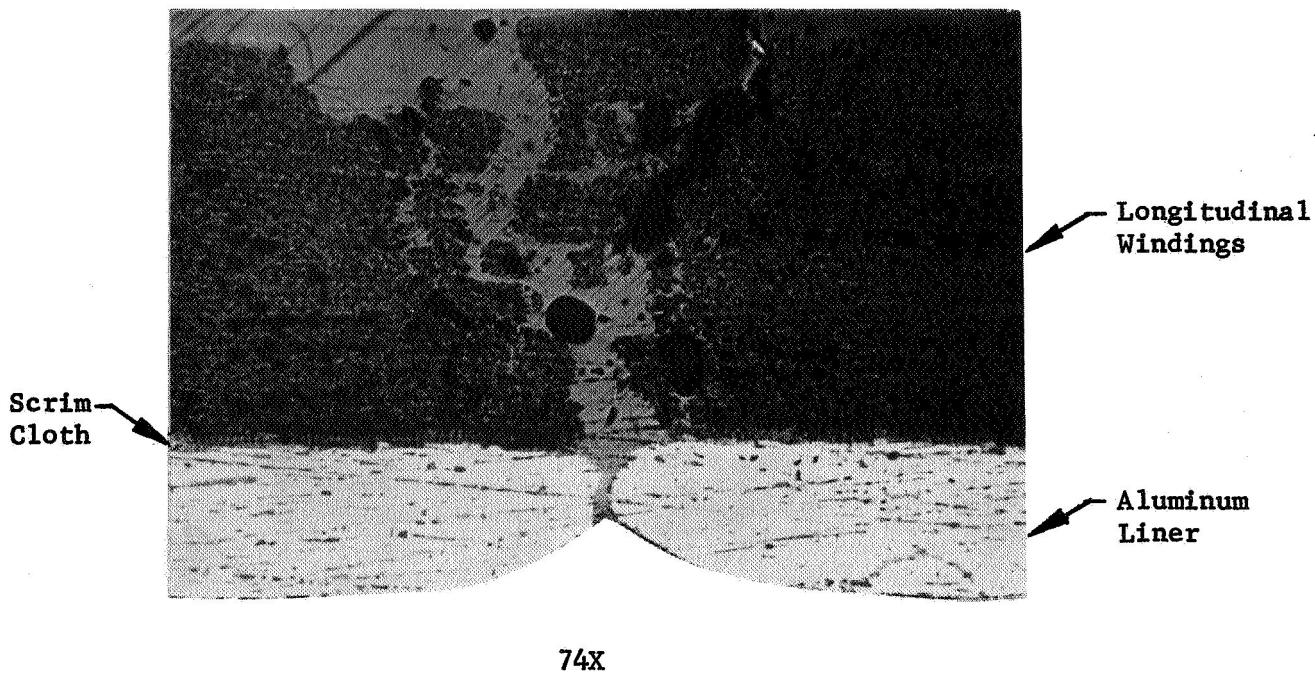
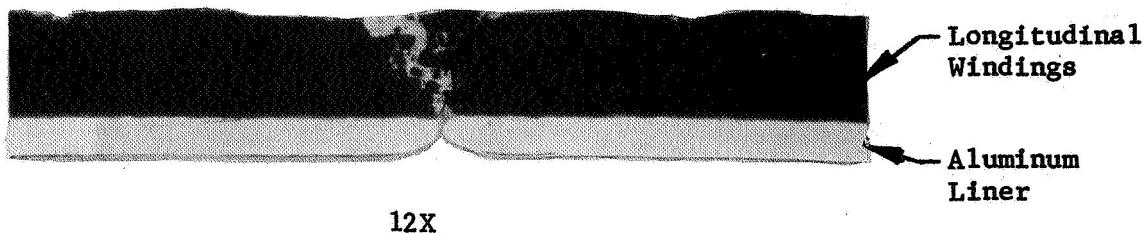
12X



74X

Photomicrographs of Tank A-1
Dome Cross Section Showing Liner Failure Site

Figure 104

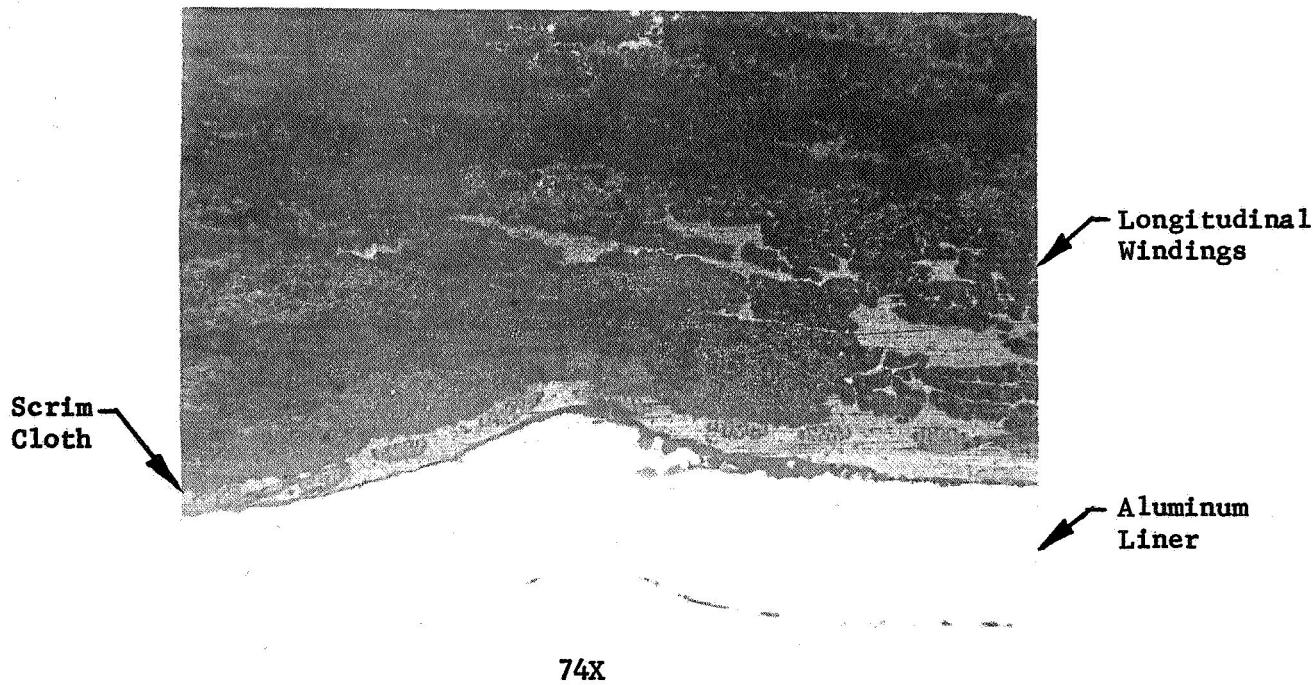


Photomicrographs of Tank A-11
Dome Cross Section Showing Liner Failure Site

Figure 105



12X



74X

Photomicrographs of Tank A-12
Dome Cross Section Showing Liner Fracture Site

Figure 106

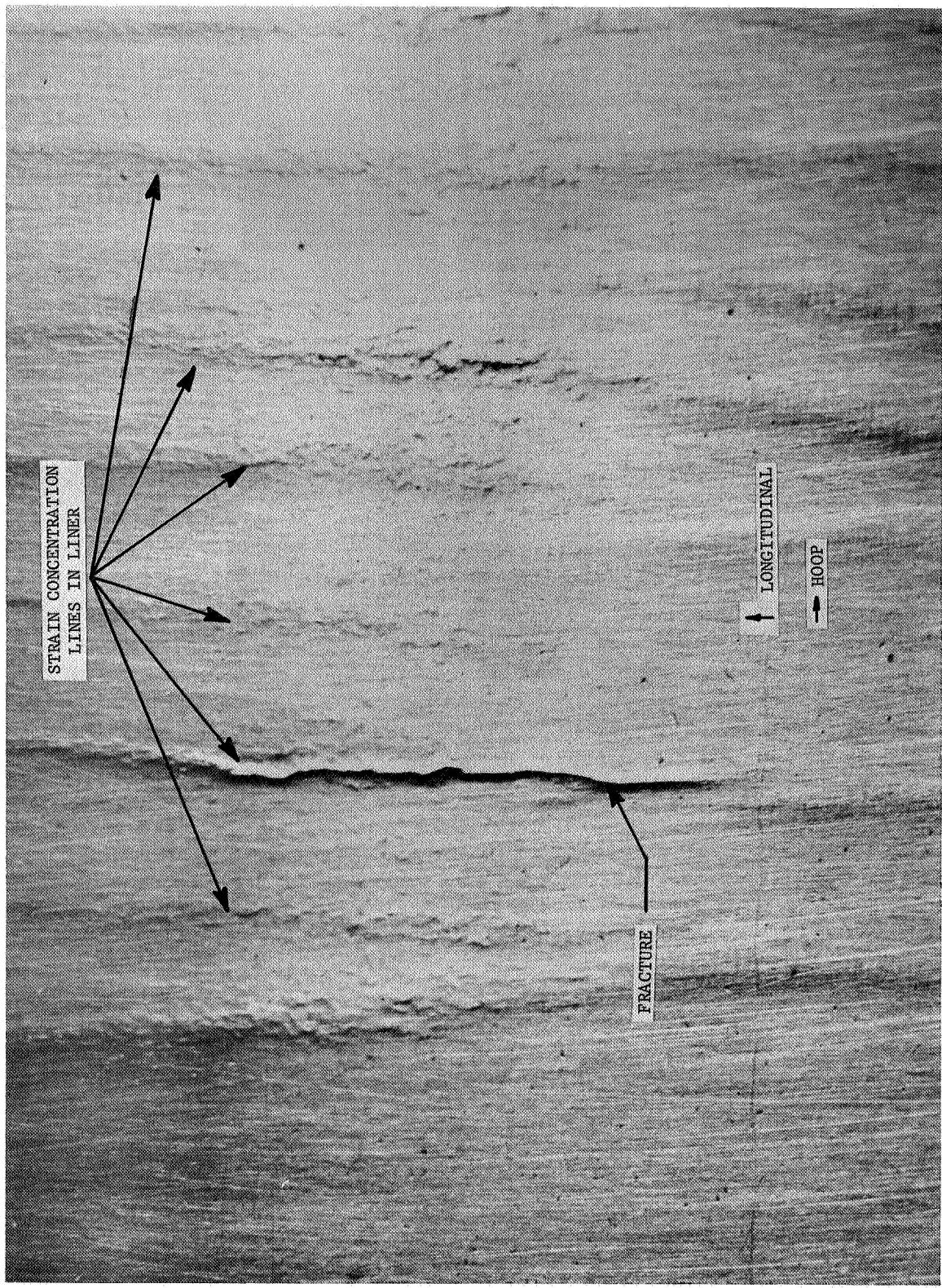


Figure 107
View of Tank A-11 Liner Failure Site, Looking from Inside Surface

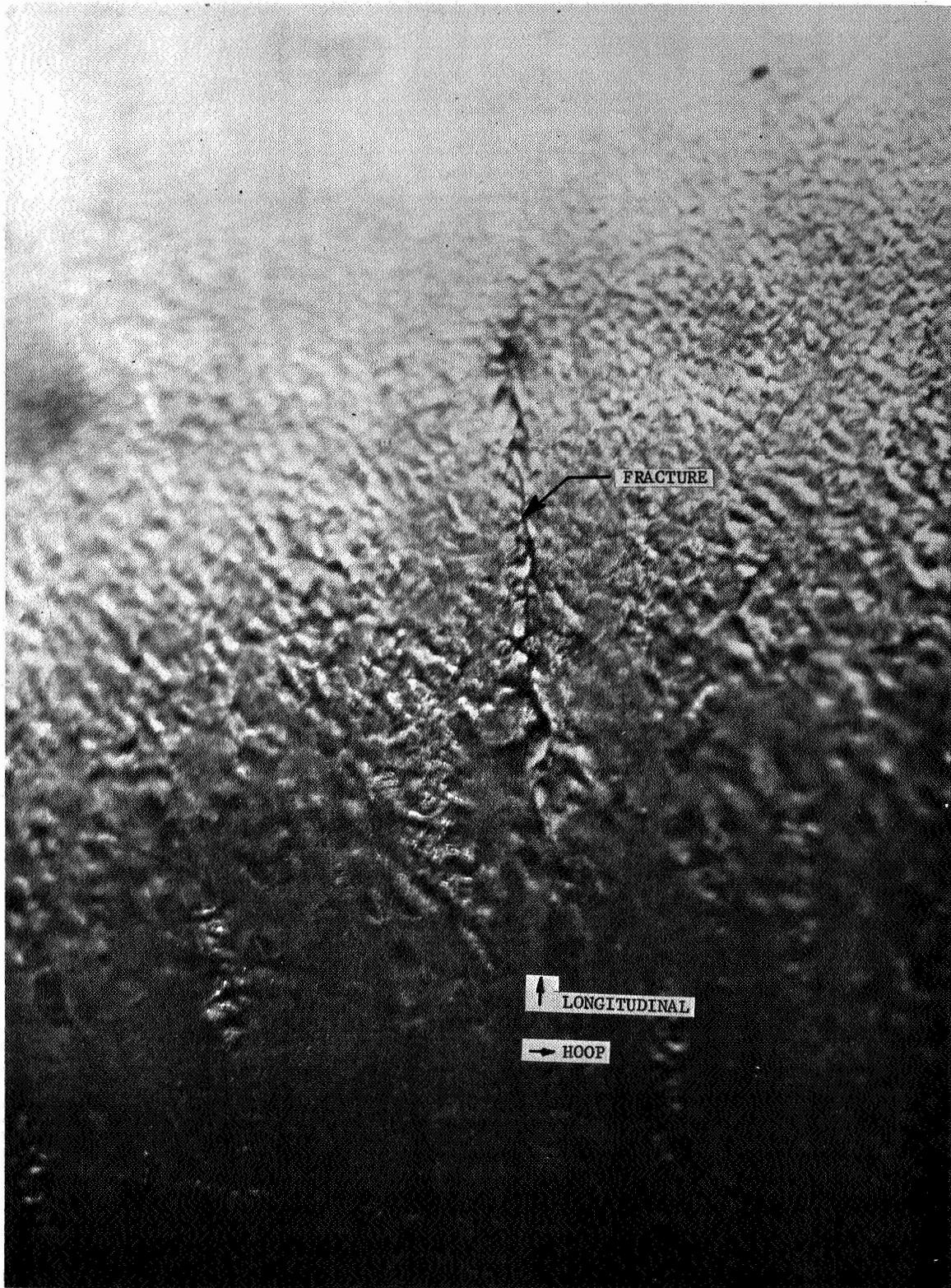


Figure 108
View of Tank A-4 Liner Failure Site in Dome, Looking from Inside Surface

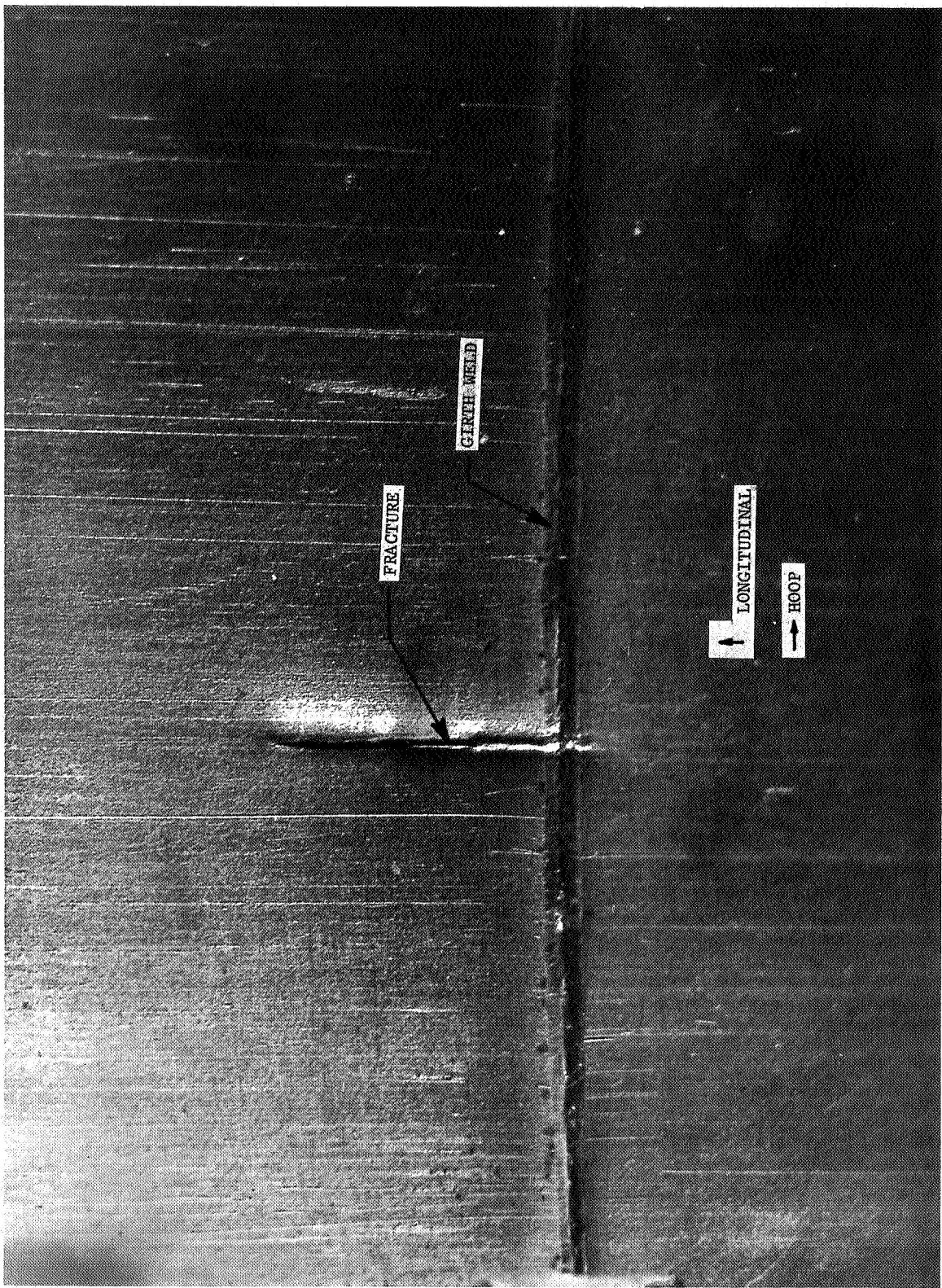
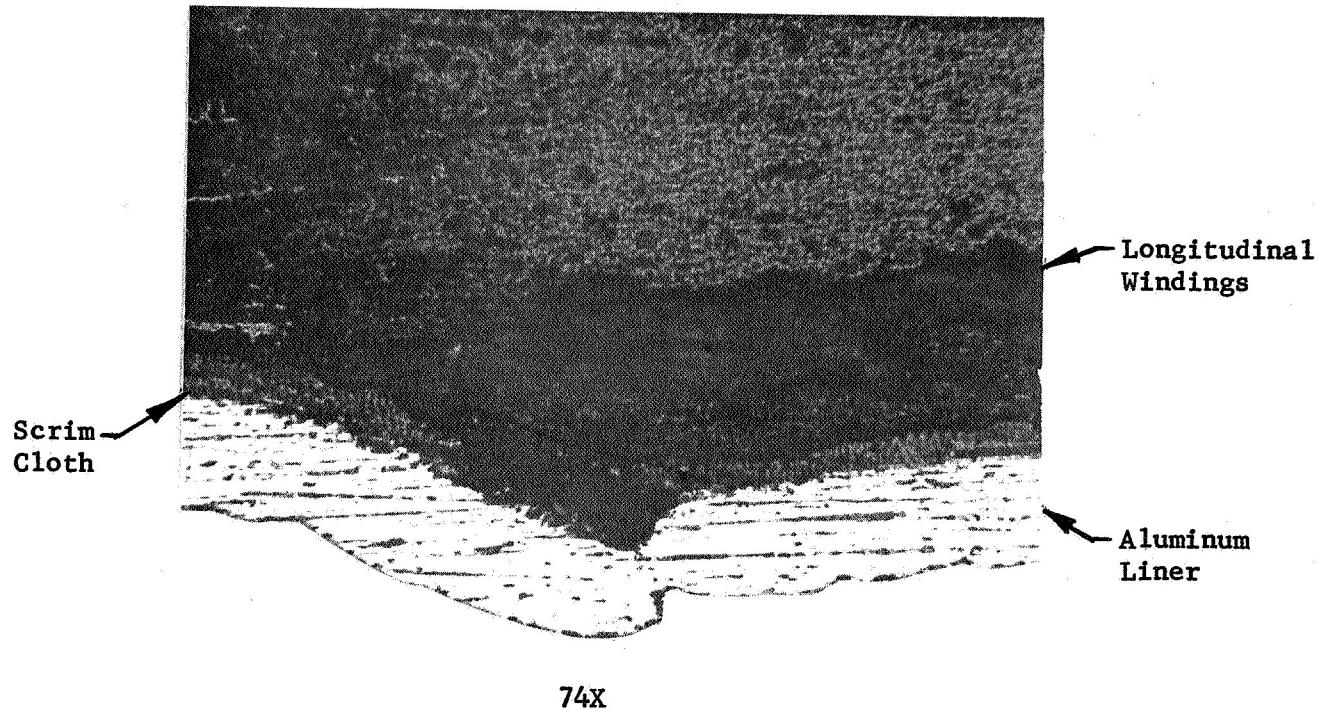
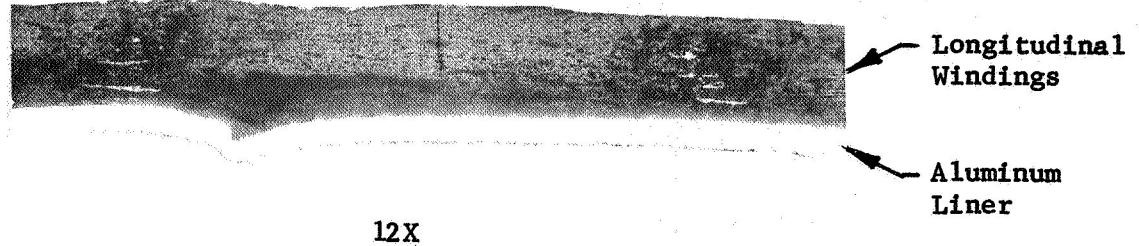
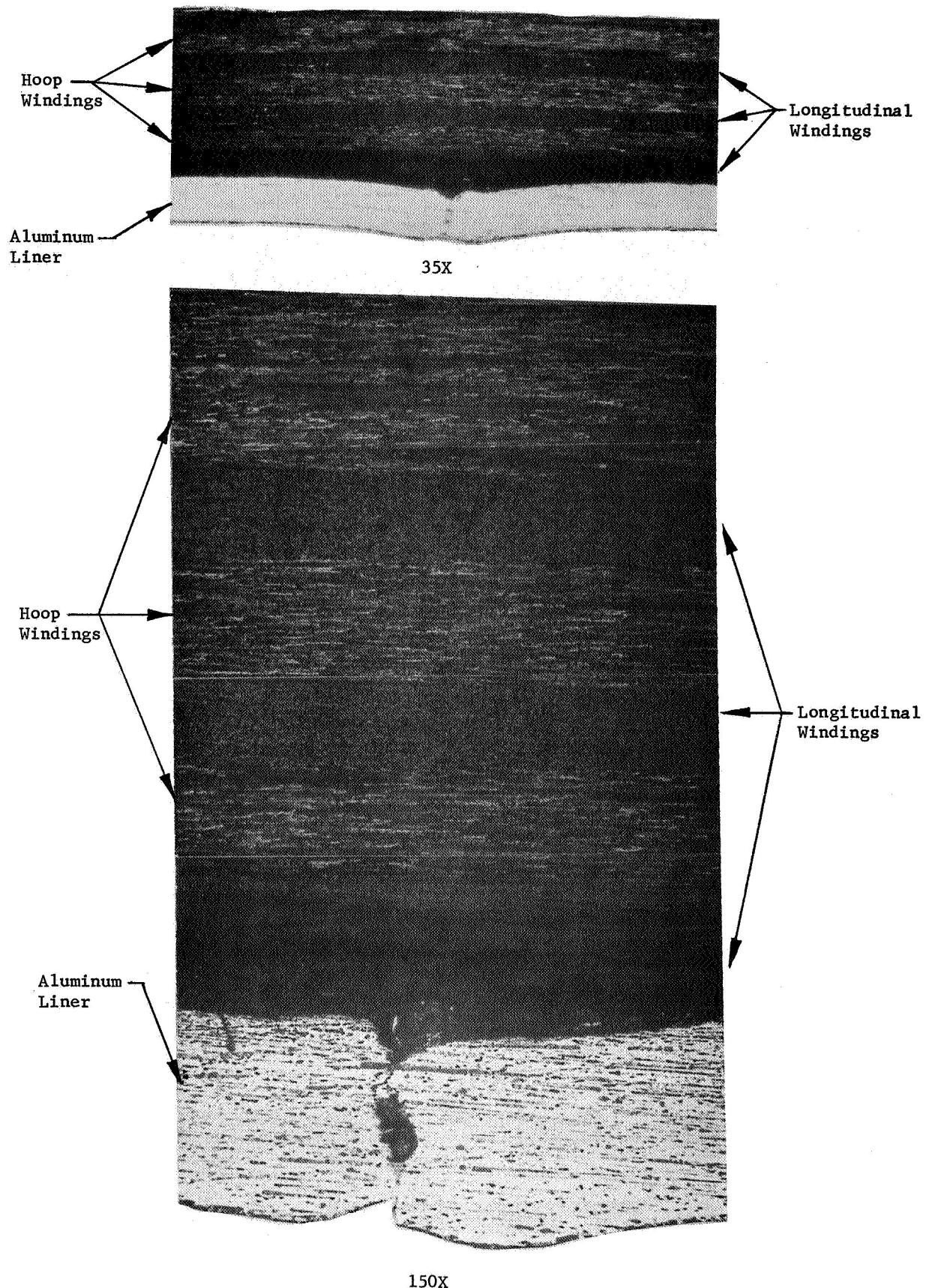


Figure 109
View of Tank A-4 Liner Failure Site in Cylinder, Looking from Inside Surface



Photomicrographs of Tank A-4
Dome Cross Section Showing Liner Fracture Site

Figure 110

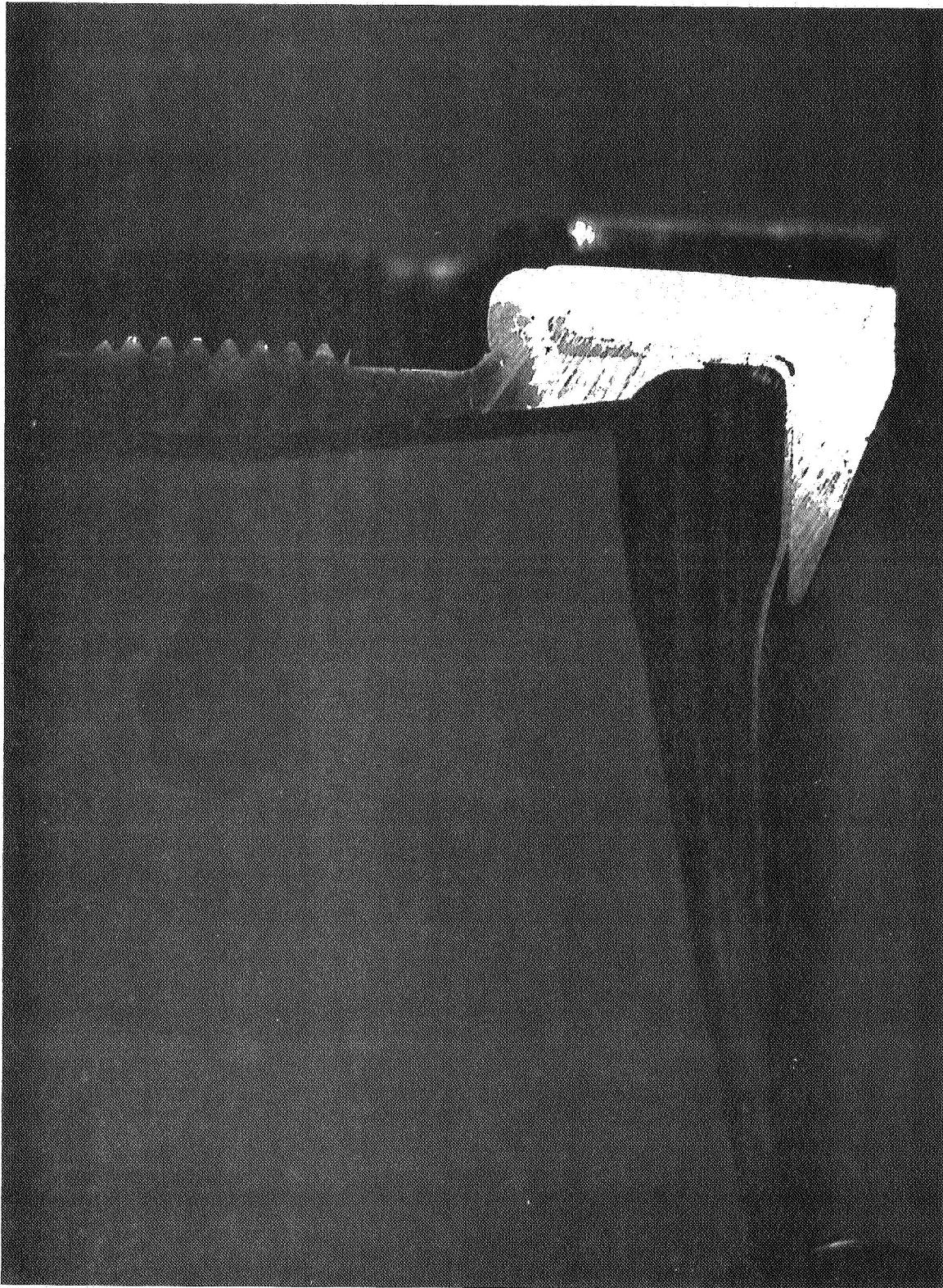


Photomicrographs of Tank A-4 Cylinder
Cross Section Showing Liner Fracture Site

Figure 111

Figure 112

Tank A-4 Boss Cross Section



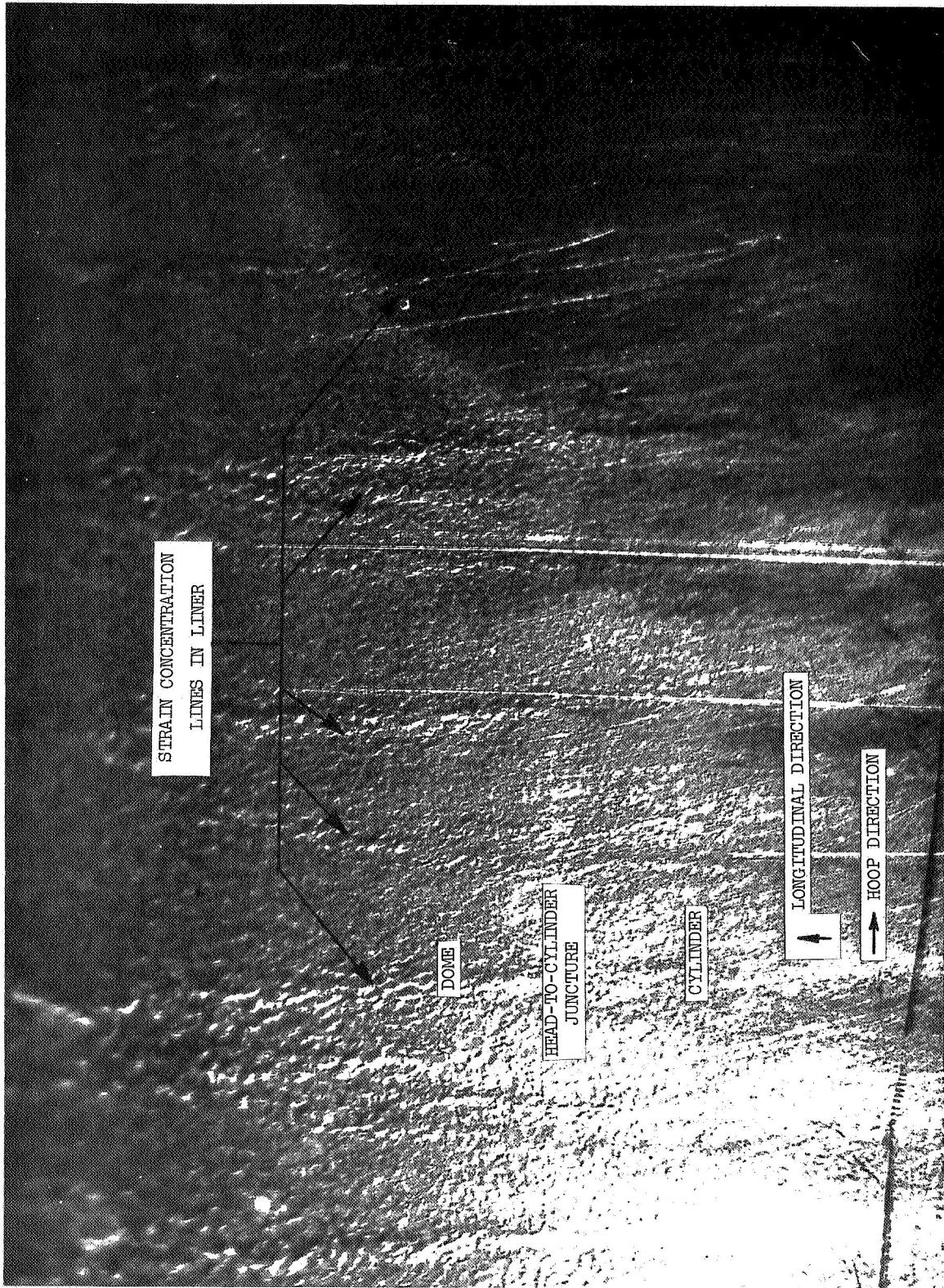


Figure 113
View of Tank A-13 Liner Dome Inside Surface Near Head-To-Cylinder
Juncture Showing Strain Concentration Lines

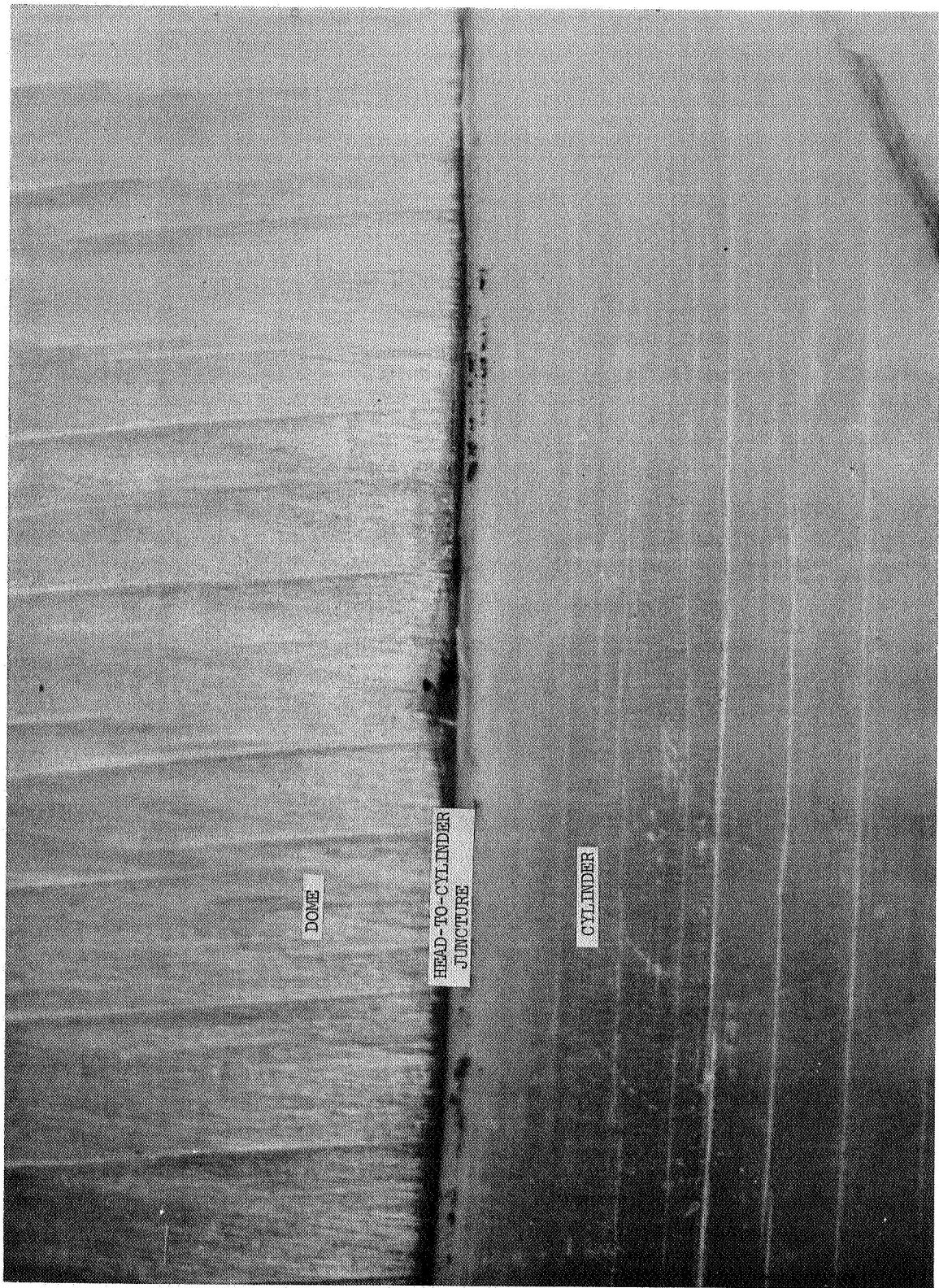


Figure 114
Outside View of Tank A-13 Head-To-Cylinder Juncture,
Showing Filament-Wound Composite Craze Cracking

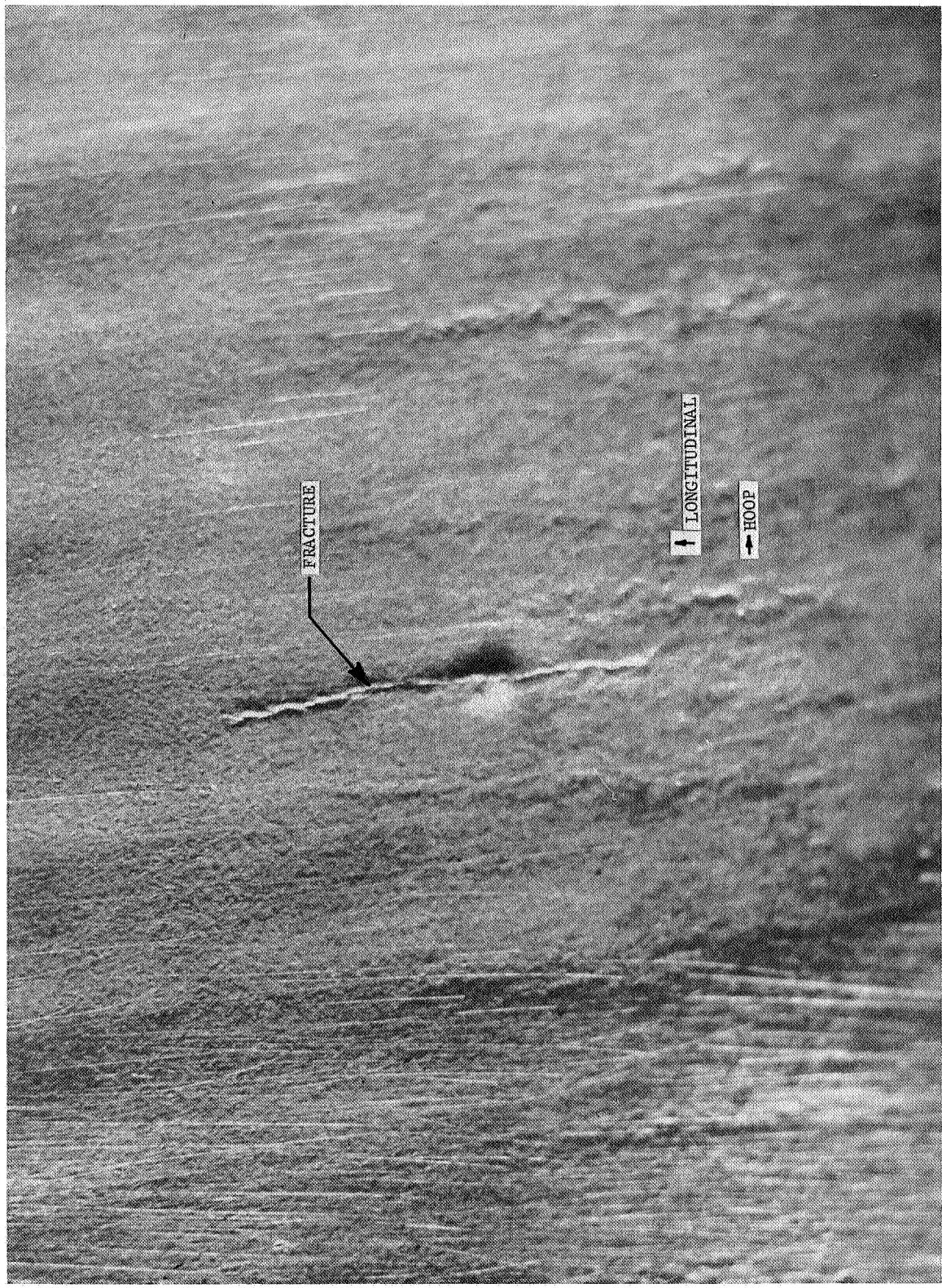


Figure 115
View of Tank A-2 Liner Dome Inside Surface Near Head-To-Cylinder Juncture
Showing Fracture Site and Work Hardening in Liner

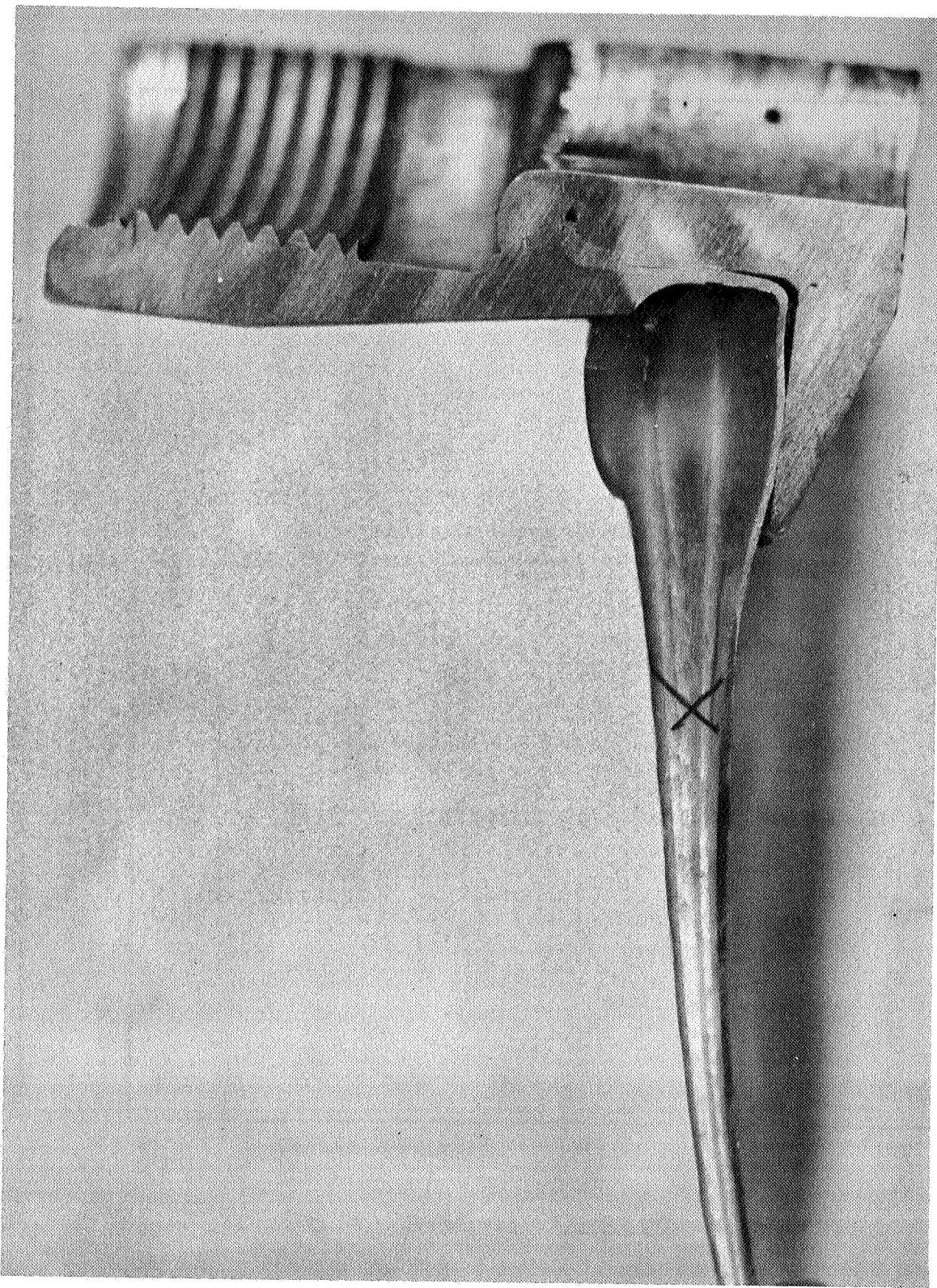


Figure 116
Tank A-6 Boss Cross-Section

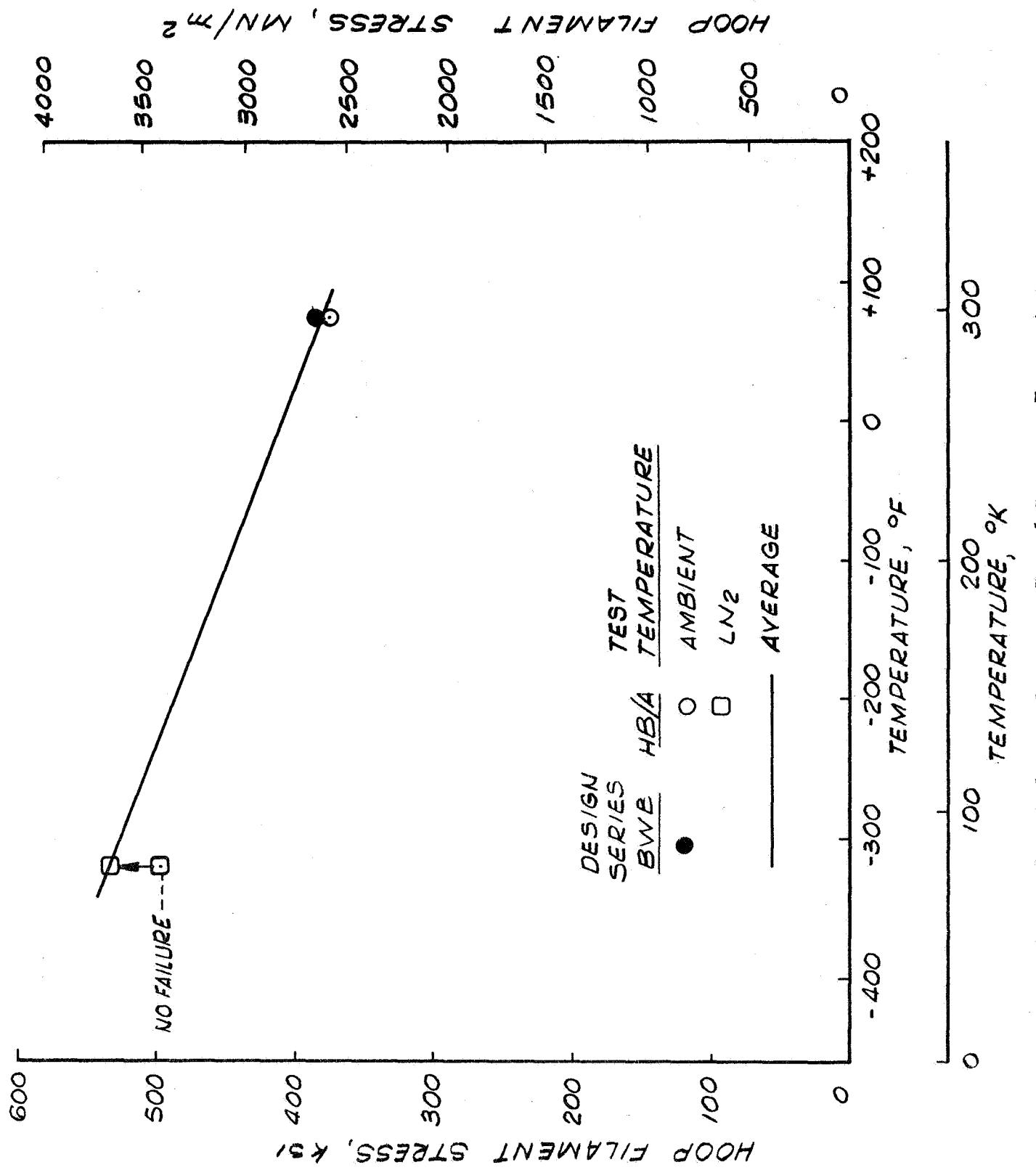


Figure 117

Hoop-Wound Glass-Filament Stress at Vessel Burst vs Temperature

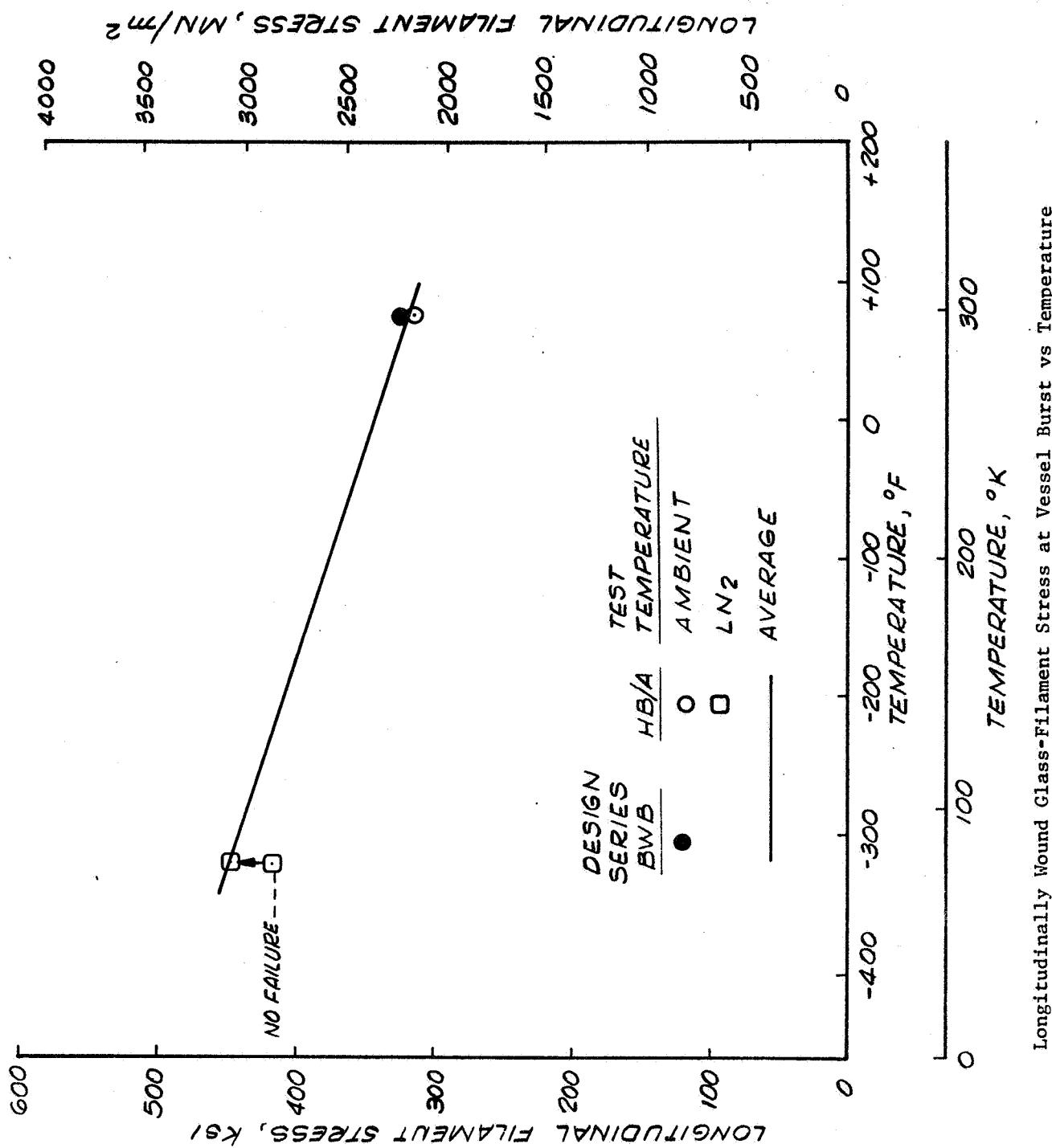
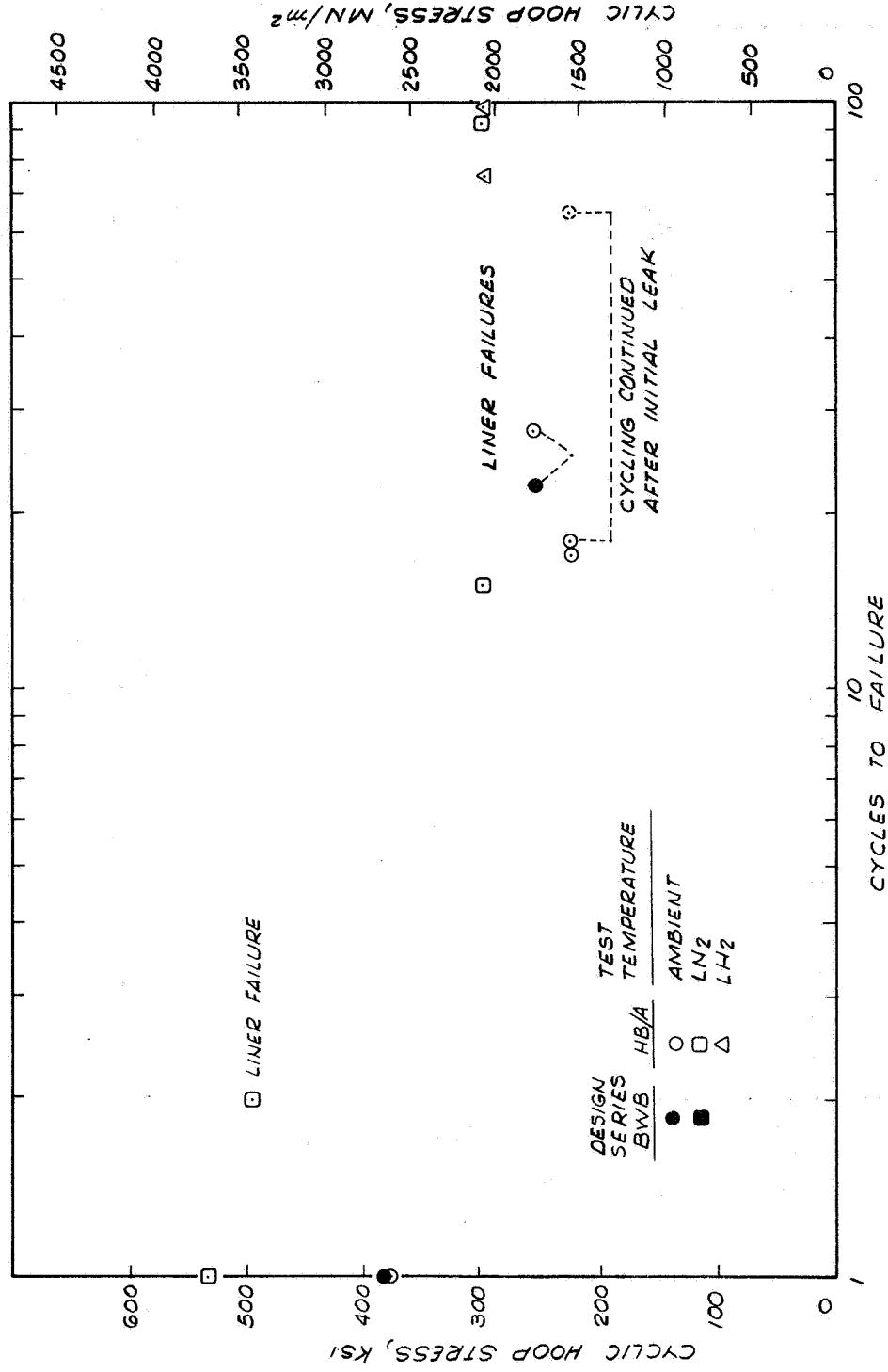


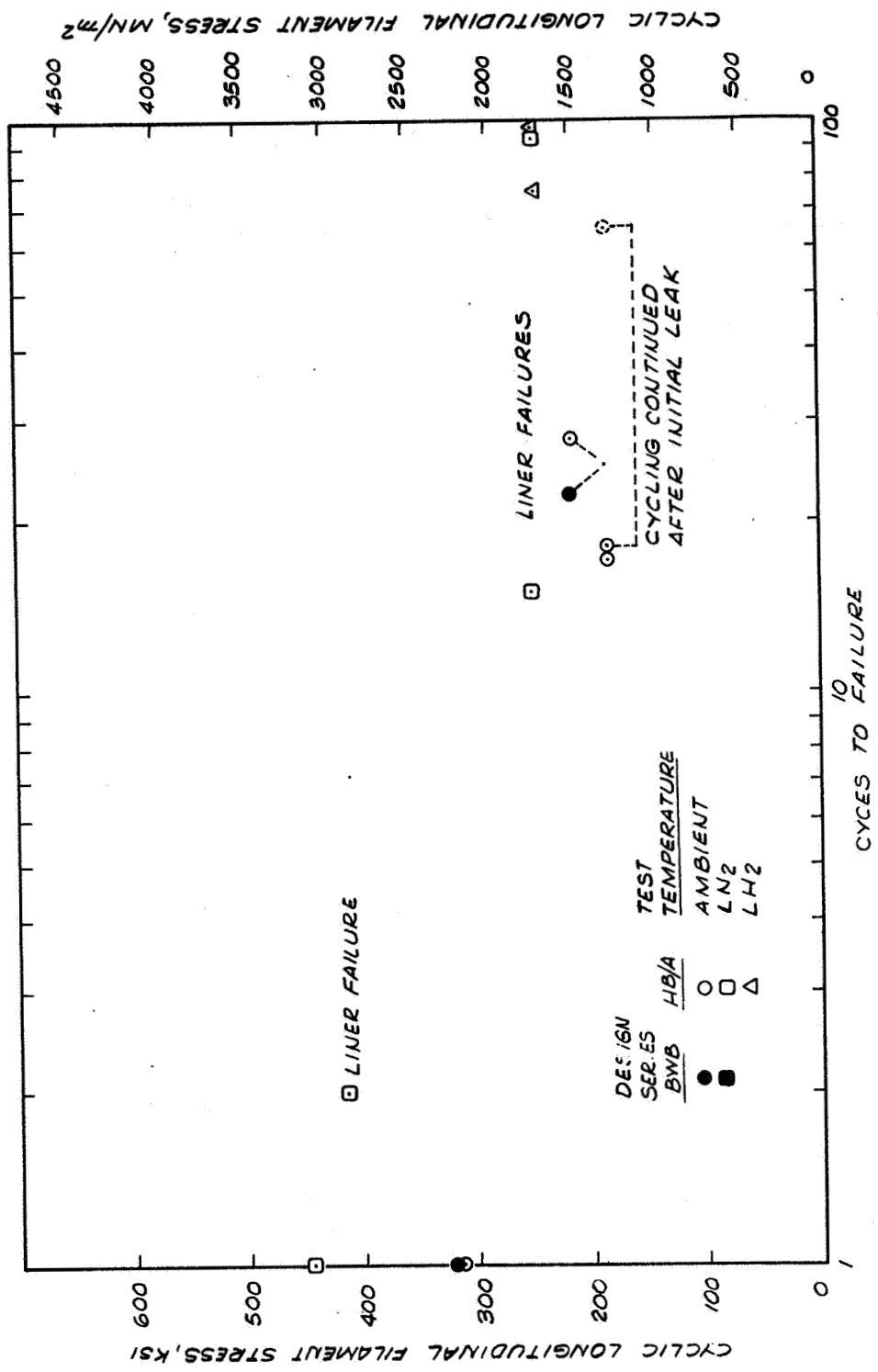
Figure 118

Longitudinally Wound Glass-Filament Stress at Vessel Burst vs Temperature



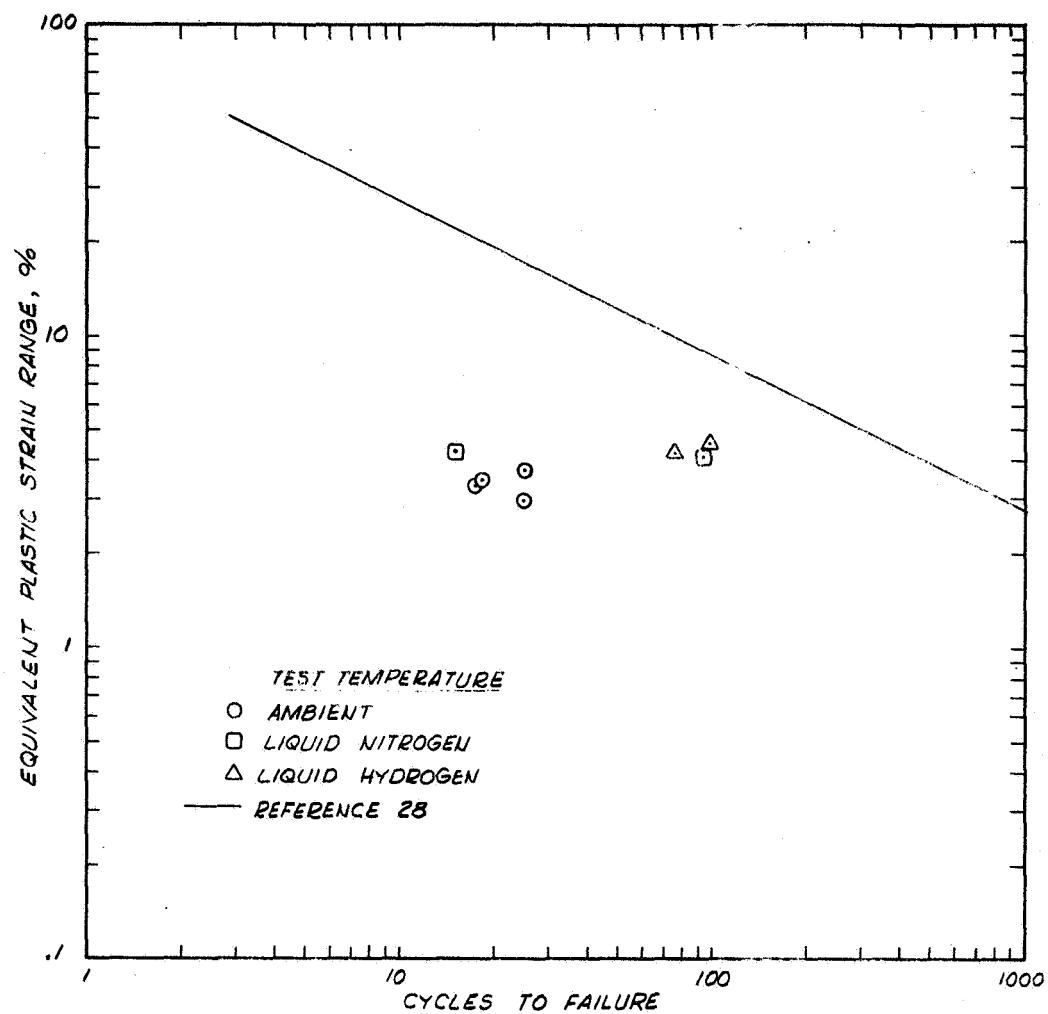
Hoop Filament Stress During Cycling vs Cycles to Vessel Failure

Figure 119



Longitudinal Filament Stress During Cycling vs Cycles to Vessel Failure

Figure 120



Vessel Equivalent Uniaxial Strain Range During Cycling vs Pressure Cycles to Failure
(1:1 Load Condition) Compared With 1100 Aluminum Low Cycle Fatigue Data
(1:0 Load Condition)

Figure 121

APPENDIX A

LINER MATERIAL CHARACTERIZATION ANALYSIS*

I. 6061 ALUMINUM

A. EFFECT OF POSITION IN PLATE ON PROPERTIES OF 6061-0 ALUMINUM

To fabricate the halfshells of the 6061 aluminum alloy liner with integral bosses, 1.00-in. thick 6061-T651 aluminum alloy plate was utilized as the starting material. In the fabrication of plate of this thickness, the effect of mechanical work is more pronounced at and near the outer surfaces. As a result, a variation in mechanical properties can exist in the plate between the outer surfaces and its center. Consequently, specimens of 0.020 in. thickness were taken from locations in a 1-inch thick plate ranging from 0.030 to 0.270-in. from the plate surface to determine the effect of location on strength and ductility. Since the liner membrane was in the annealed condition, these specimens were annealed prior to testing. The anneal treatment utilized consisted of heating the specimens at 775°F for one hour, cooling in the furnace to 500°F at a rate not faster than 50°F per hour, and then air cooling to room temperature.

The results of the tensile tests on the annealed specimens from various locations in the thickness of the 6061 aluminum alloy plate are shown in Table A-1. Maximum ductility of 21.0 to 25.0% accompanied with a slight decrease in strength was indicated for the area at 0.210 to 0.270-in. below the surface. However, the material after annealing also provides adequate ductility from a depth of 0.030-in. to a depth of 0.150 in. (16.5 to 19.0% at 75°F as compared to a minimum requirement of 10.8%). On the basis of ductility of 0.020 in. thick specimens, all positions in the plate which were evaluated possess adequate ductility.

Micro examination of the annealed tensile specimens did not reveal any significant variation in grain structure due to the location in the plate. Likewise, macro and micro examinations of sections of both 6061-0 and 6061-T651 aluminum alloy plates failed to reveal any detectable variations in the grain structure through the thickness of the plate examined. Consequently, it was not possible to select an optimum location in the plate thickness for the liner membrane on the basis of grain structure variation.

In the technique proposed to fabricate the liner halfshells with an integral boss, the desired location for the membrane portion was in the area not exceeding 0.125-in. below the surface of the plate. Since the tensile results in this area showed adequate ductility at 75°F, it was decided that the membrane section could be taken from an area not deeper than 0.125 in. below the plate surface.

* Presentation of this investigation in both S.I. and English systems would reduce the clarity of this Appendix. The English system only is used.

B. SPECIMEN PREPARATION FOR SUBSEQUENT TESTS

Specimens for evaluation of the parent metal were prepared in the following manner from aluminum alloy 6061 plate of 1.0-in. thickness in the T651 heat treated stress relieved temper.

1. Material to a depth of 0.030 in. was removed from one surface of the 1.0-in. thick plate mechanically by means of a machining operation.

2. Using a series of machining cuts, sufficient material was removed starting at the other surface of the plate to obtain a membrane of 0.030-in. thickness.

3. Tensile specimen coupons 1-in. wide by 8-in. long were sheared from the 0.030 in. membrane material both longitudinal and transverse to the direction of rolling.

4. A portion of the 0.030-in. membrane material was further reduced to approximately 0.010 in. thickness by means of mechanical machining operations. Tensile specimen coupons were then sheared from the 0.010 in. material in both the longitudinal and transverse directions.

5. A second portion of the 0.030 in. membrane material was reduced to 0.020-in. thickness by the removal of 0.005-in. from each surface mechanically through machining techniques. An additional 0.005-in. was then removed from each surface by means of chemical milling operations to provide a membrane of 0.010-in. thickness. Both longitudinal and transverse tensile coupons were sheared from the 0.010-in. thick membrane material.

6. The remaining portion of the 0.030-in. material was reduced to 0.010-in. thickness by the removal of 0.010-in. from each surface by means of chemical milling operations. Both longitudinal and transverse tensile coupons were sheared from the 0.010-in. membrane material.

7. All tensile specimen coupons were then annealed at 775° F as specified in Specification MIL-H-6088 for heat treatable alloys.

C. EFFECT OF THICKNESS ON PROPERTIES OF NON-CHEMICALLY MILLED 6061-0 ALUMINUM ALLOY

Two Portions of a 1-inch thick 6061-T651 aluminum alloy plate were machined to provide a membrane of 0.030/0.035-in. thickness and a membrane of 0.012-in. thickness. The center of both membranes was located 0.045-in. below one of the surfaces of the original plate. Both membranes were annealed at 775° F for one hour, cooled in the furance to 500° F at a rate not faster than 50° F per hour, and then air cooled to room temperature.

Tensile specimens longitudinal and transverse to the direction of rolling of the original plate were prepared and tested for each membrane.

The results of the tensile tests at 75° F on the annealed membranes are shown in Table A. The reported values for tensile and yield strengths for both membranes were substantially equivalent in both rolling directions. All values were well below the 22 000 psi and 12 000 psi specified as maximum for tensile strength and yield strength, respectively, in Specification QQ-A-250/11 for all thicknesses of 6061-0 aluminum alloy. However, the ductility of the thinner membrane, as measured by percent elongation in a 2-in. gage length, is significantly lower than that reported for the 0.036-in. membrane. The range of 14.0 to 17.5% for the longitudinal specimens and 10.5 to 13.0% for the transverse specimens indicates the membrane of 0.012-in. thickness may provide adequate ductility. Since a minimum of 10.8% at 75° F is indicated to provide enough liner ductility to achieve the full strength potential of the glass-filament-wound shell, the low values of 10.5 and 11.0% in the transverse direction could possibly make a membrane of 0.010 to 0.012-in. thickness marginal.

D. EFFECT OF CHEMICAL MILLING AND ANNEALING PROCEDURE ON 6061 ALUMINUM ALLOY

Two membranes 0.030-in. in thickness obtained in the manner described previously were further reduced to a nominal thickness of 0.010-in. using one or the other of the following processes:

1. Removal of 0.010-in. from each side by means of chemical milling.

2. Removal of 0.005-in. from each side mechanically by machining followed by removal of an additional 0.005-in. from each side by means of chemical milling.

Tensile specimens cut from the 0.010-in. membranes were then subjected to two annealing procedures and tested at 75° F. One group of specimens was cooled from 775° F at the required rate of not faster than 50° F per hour to 500° F. The other group of specimens was cooled to 500° F at a considerably faster rate. The results of these tests are shown in Tables A-3 and A-4.

The specimens cooled from 775° F at the accelerated rate to 500° F were not completely annealed. Although the tensile and yield strength values were quite well below specification maximum allowables for annealed in accordance with the procedure specified in Specification MIL-H-6088 for the heat treatable alloys, a slight decrease in strength with an accompanying increase in ductility was obtained. The membrane chemical milled from 0.030-in. to 0.010-in. thickness shows adequate elongation in the longitudinal direction

(12.0 to 15.0%). However, in the transverse direction, although a range of 9.5 to 12.0% is indicated, the 9.5 and 10.0% values obtained on three specimens indicates that the membrane processed in this manner may possibly be marginal. The membrane obtained by chemical milling from 0.020 to 0.010-in. thickness appears to be slightly better than the one obtained by chemical milling from 0.030 to 0.010-in. as indicated by more uniformly higher elongation values (15.0 to 16.5% in longitudinal specimens and 10.5 to 12.5% in transverse specimens).

The chemical milling solution apparently attaches the 6061 aluminum alloy in a non-uniform manner as indicated by the notched-like edges shown in the micro-sections of Figures A-1 and A-2. In a thin membrane of 0.010-in. nominal thickness, a significant thickness waviness or variation can occur due to intergranular attack which can result in a significant apparent reduction in the percent elongation in that area. This is indicated by the extremely low values shown for specimen H-9 of Table A-3 (7.0%) and for specimen B-4 of Table A-4 (5.5%).

When the material is chemical milled to a final membrane nominal thickness of 0.014 to 0.015-in., the increased thickness does not appear to be susceptible to the detrimental notch effect described above. Test results on specimens cut from 0.014-in. thickness membrane material reported in Table A-5 provided adequate ductility in both directions (15.0 to 19.0% elongation for longitudinal specimens and 11.5 to 14.5% for transverse specimens).

A summary of the effect of processing operations on the percent elongation of the 6061 aluminum alloy membrane is shown in Figure A-3. The extremely low values shown for the incompletely annealed transverse specimens establishes the necessity for close control of the cooling rate from 775°F in the annealing operation. The thickness effect at 0.010-in. can be critical as indicated by the marginal elongation values shown for the fully annealed transverse specimens resulting from the non-uniform attack by the chemical milling solution. A slight increase in the membrane thickness to 0.014/0.015-in. appears to provide adequate ductility in both the longitudinal and transverse specimens.

E. PARENT METAL PROPERTIES AT 75, -320, AND -423°F

Specimens were prepared by machining a 1-inch thick 6061-T651 aluminum alloy plate to provide a membrane of 0.030/0.035-inch thickness; the center of this membrane was located 0.045-inch below one of the surfaces of the original plate. The 0.030-inch membrane was further reduced to a nominal thickness of 0.010-inch by removal of 0.010-inch from each side by means of chemical milling. Tensile specimens were cut from the 0.010-inch membranes and annealed by cooling from 775°F at the required rate of not faster than 50°F per hour to 500°F.

The results of the tensile tests on the annealed membranes are presented in Table A-6. Average results and the range of values for tensile strength, yield strength, and ductility are plotted as a function of test temperature in Figures A-4 and A-5.

At 75°F the tensile and yield strength values were quite well below specification maximum allowables for annealed material. Tensile strength increased from about 15 200 psi at 75°F to about 26 900 psi at -320°F and 45 600 psi at -423°F. Yield strengths were about 6 800 psi at 75°F, and 8 800 psi at -320°F. They were not determined at -423°F.

A minimum uniaxial ductility of 10.8% at ambient temperature and 14.4% cryogenic temperatures was desired. Elongation (in 2-inch gage length) for membrane chemically milled from 0.030-inch to 0.010-inch thickness shows adequate ductility in the longitudinal direction at 75°F (an average of 13.8%), at -320°F (an average of 21.7%) and at -423°F (an average of 24.7%). In the transverse direction, elongation (in 2-inch gage length) is possibly marginal at 75°F (an average of 10.0%); it is adequate at -320°F (an average of 14.7%), and at -423°F (an average of 21.5%).

Elongations over shorter 0.50 and 0.25-inch gage lengths are reported in Table A-6 for comparison with the elongation values over a 2.0-inch gage length. As shown there, for parent metal specimens elongations were generally about the same regardless of gage length.

F. WELDED SPECIMEN PROPERTIES AT 75, -320, AND -423°F

Test specimen membranes were prepared as described above for parent metal specimens. The membranes were sheared and joined using one of the weld procedures given below:

TIG butt fusion welded (without filler wire)

TIG butt fusion welded with 1100 aluminum filler wire.

TIG butt fusion welded with 1100 aluminum filler wire, beneficiated after welding.

The 1100 aluminum filler wire was used in some of the 6061 aluminum weld specimens to improve weld joint ductility. Specimens were completely annealed after welding and beneficiations.

1. TIG Butt Fusion Welded (Without Filler Wire)

After these specimens were prepared, it was determined from bend tests that the weld joint was so brittle that tensile test evaluation was not warranted.

2. TIG Butt Fusion Welded With 1100 Aluminum Filler Wire

Results from 75°F tensile tests of these weld specimens are summarized in Table A-7. The average ultimate tensile strength was about 12 400 psi and the yield strength was about 6900 psi. Although very low values for elongation over the 2-inch gage length were obtained, it was observed that the weld joint (with the softer 1100 aluminum filler wire) - about 0.125-inch wide - was undergoing considerable deformation. Testing conducted later measured ductility in this area, and therefore elongation values in 2-inch length are for qualitative use only.

No correlation could be established between weld x-rays and test results (e.g., low tensile strength of specimen FW-6 suggests presence of defect, yet x-ray showed this test specimen to be acceptable to the high standard imposed of no porosity greater in size than T/4 and no cracks or other propagating defects allowed).

3. TIG Butt Fusion Welded With 1100 Aluminum Filler Wire, Beneficiated After Welding

Test results from this series of specimens are summarized in Table A-8. After low ductility values over a 2-inch gage length were noted for specimens GW-1 through GW-5 and HW-1 through HW-5 in conjunction with observed local elongation of the weld joint (with the softer 1100 aluminum filler wire), it was decided to mark all remaining test specimens so that elongation over 0.50-inch and 0.25-inch (centered on weld joint) could be determined. Where this was done, it was established that the 0.125-inch wide weld joint was in fact undergoing considerable elongation; see data for specimens GW-6 through GW-11 and HW-6 through HW-9. Elongation over 0.25-inch (centered on the 0.125-inch wide weld) was two to four times as high as that indicated over a 2-inch gage length. This effect is shown graphically in Figure A-6 where average elongation values for 2.0, 0.50, and 0.25-inch gage lengths are plotted. These data show that the weld joint is quite soft compared with the parent metal, and that elongation values over a 2-inch gage length should not be used to evaluate the weld joint of the 6061-O aluminum specimens welded with 1100 aluminum filler wire. The elongation data over a 0.25-inch gage length was used instead for evaluation of the weldments.

Average results and the range of values for tensile strength, yield strength, and ductility are plotted as a function of test temperature in Figures A-7 and A-8. Longitudinal grain direction tensile strength increased from about 14 200 psi at 75°F to 23 400 psi at -320°F, and 32 000 psi at -423°F; in the transverse direction tensile strength increased from 10 300 psi at 75°F to 23 300 at -320°F. Yield strength values increased from about 6800 psi at 75°F to 10 000 psi at -320°F; they were not determined at -423°F.

Elongation values (in a 0.25-inch gage length over the weld) were marginal at 75°F to -423°F. In the longitudinal direction, average values were 13.8% at 75°F, 11.3% at -320°F, and 14.3% at -423°F. In the transverse direction the values were 9.8% at 75°F, and 9.5% at -320°F.

Comparisons of the data for welded and unwelded specimens showed that yield strengths were about the same. Tensile strengths were lower for the welded specimens at all temperatures, and range in strength values was much greater for the weldments. Room temperature ductility was about the same for both types of specimens, but at -320° and -423°F, the welded ductility decreased while the parent metal ductility increased.

II. 1100 ALUMINUM

A. SPECIMEN PREPARATION

Specimens of 1100 aluminum were prepared to evaluate the effect of chemical milling and the liner thickness of 0.010 in. on the material properties and to evaluate parent metal and weldments over the temperature range of 75 to -423°F. The specimens were fabricated using simulated liner fabrication operations and sequence starting with materials in the same form and condition as will be used in liner fabrication. The starting material was aluminum alloy 1100 sheet of 0.125-in. thickness in the H14 cold worked temperature.

Specimens for evaluation of the parent metal were prepared in the following manner:

1. Material to a depth of 0.035-in. was removed from one surface of the 0.125-in. thick sheet mechanically by means of a machining operation.

2. Using a series of cuts by means of machining operations, an additional 0.060-in. of material was removed from the other surface of the 0.125-in. thick sheet. A membrane 0.030-in. in thickness remained from the original 0.125 in. thick sheet.

3. Tensile specimen coupons 1-in. wide by 8-in. long were sheared from the 0.030 in. membrane material with the grain longitudinal and transverse to the direction of rolling.

4. A portion of the 0.030-in. membrane material was further reduced to 0.010-in. thickness by means of mechanical machining operations. Tensile specimen coupons 1-in. wide by 8-in. long were sheared from this material in the longitudinal and transverse grain directions.

5. The balance of the 0.030-in. membrane material was reduced to 0.010-in. thickness by removal of 0.010 in. of material from each surface by means of chemical milling operations. Tensile specimen coupons were then sheared from the chemically milled reduced material in both the longitudinal and transverse directions.

6. All tensile specimen coupons were then annealed at 650°F as specified in Specification MIL-H-6088 for cold worked alloys to put the material in the -0 condition.

A preliminary microscopic examination at 200X magnification of the edge of the chemical milled material in the unetched condition did not reveal any evidence of detrimental attack by the chemical milling solution.

Further microscopic evaluation after etching and at higher magnification was subsequently conducted to definitely establish freedom from intergranular attack.

B. EFFECT OF THICKNESS ON PROPERTIES OF NON-CHEMICALLY MILLED 1100 ALUMINUM

Two portions of a 0.125-in. thick 1100-H14 aluminum sheet were machined to provide a membrane of 0.030/0.035-in. thickness and a membrane of 0.010-in. thickness. The center of both membranes was located 0.045 in. below one surface of the original sheet. Both membranes were annealed in accordance with the procedure specified in Specification MIL-H-6088 for non-heat treatable aluminum alloys. Tensile specimens longitudinal and transverse to the direction of rolling of the original sheet were prepared and tested for each membrane.

The results of the tensile tests at 75°F on the two annealed 1100 aluminum membranes are shown in Table A-9. The ultimate tensile strength for both membrane thicknesses is substantially equivalent. However, the 0.010-in. membrane showed a marked increase in yield strength as compared to that for the 0.035-in. nominal thickness membrane (approximately 5000 psi for the 0.010-in. thickness as compared to 2000 psi for the 0.035-in. thickness). The elongation in the transverse specimens was not significantly lowered by the reduction in thickness, with respect to the intended application. However, in the longitudinal specimens, the elongation range for the 0.010-in. membrane was 12.2 to 16.0% as compared to 27.5 to 34.0% for the 0.035-in. membrane. These reduced values are adequate since they are considerably above the desired 10.8% minimum.

C. EFFECT OF CHEMICAL MILLING ON 1100 ALUMINUM ALLOY

A membrane 0.035-in. in thickness obtained in the manner described above was further reduced to 0.010-in. nominal thickness by removal of 0.010-in. from each side by means of chemical milling. Tensile specimens were cut from the 0.010-in. membrane, annealed, and tested at 75°F. The results of these tests are shown in Table A-10.

The chemical milling operation did not appear to have a detrimental effect on the 1100 aluminum. The elongation of all specimens was greater than the 10.8% minimum desired (11.0 to 18.5% for the longitudinal specimens and 14.5 to 26.0% for the transverse specimens).

A microscopic examination of the chemical milled 1100 aluminum membrane revealed the answer to the apparently better performance. The attack of the chemical milling solution is, in general, more uniform than was the case with the 6061 aluminum alloy (see Figure A-9). However, a slight localized intergranular attack may occur as shown in Figures A-10 and

A-11. Because of the higher inherent ductility of the 1100 aluminum this does not appear to be as detrimental as in the case of the 6061 aluminum alloy.

A summary of the effect of processing operations on the percent elongation of the 1100 aluminum alloy membrane is shown in Figure A-12. Although the reduction to 0.010-in. thickness results in a significant lowering of the percent elongation longitudinal to the direction of rolling, sufficient ductility remains to meet the desired minimum value of 10.8%. Because of its inherent ductility, chemical milling does not appear to have a detrimental effect on the 1100 aluminum material.

D. PARENT METAL TESTS AT 75, -320, AND -423° F

Specimens were prepared by machining a 0.125-inch thick 1100-H14 aluminum sheet to provide a membrane of 0.030/0.035-inch thickness; the center of this membrane was located 0.045-inch below one of the surfaces of the original sheet. The 0.030-inch membrane was further reduced to a 0.010-inch nominal thickness by removal of 0.010-inch from each side by means of chemical milling. Tensile specimens were cut from the 0.010-inch membranes and annealed in accordance with the procedure of specification MIL-H-6088 for non-heat-treatable aluminum alloys.

The results of tensile tests at ambient and cryogenic temperatures on the annealed membrane are presented in Table A-11. Average results and the range of values for tensile strength, yield strength, and ductility are plotted as a function of test temperature in Figures A-13 and A-14.

Tensile strength increased from about 12 300 psi at 75° F to about 24 300 psi at -320° F and 37 900 psi at -423° F. Yield strengths were about 5400 psi at 75° F and 6600 psi at -320° F.

Elongation (in 2-inch gage length) for membrane chemically milled from 0.030-inch to 0.010-inch thickness showed adequate ductility over the temperature range. Average values in the longitudinal direction were 15.8% at 75° F, 27.5% at -320° F, and 35.2% at -423° F. In the transverse direction, elongations were 20.3% at 75° F, 35.5% at -320° F, and 44.0% at -423° F.

Elongations over the shorter 0.50 and 0.25-inch gage lengths are presented in Table A-11. Gage length did not greatly affect measured elongation for the parent metal specimens.

E. WELDED SPECIMEN TESTS AT 75, -320, AND -423° F

The weld test specimen membranes were prepared as described above for the parent metal specimens. The membranes were sheared and joined using one of the procedures given below:

TIG butt fusion welded with 1100 aluminum filler wire.

TIG butt fusion welded with 1100 aluminum filler wire, beneficiated after welding.

The beneficiation process consisted of cold working the weld joint by seam rolling to restore as much as possible the original properties of the parent metal. After welding (and beneficiation where applicable) specimens were completely annealed prior to testing using the same procedure as employed for the parent metal specimens.

1. TIG Butt Fusion Welded With 1100 Aluminum Filler Wire

Results from 75°F tensile tests are summarized in Table A-12. Average tensile strengths were 11 700 psi in the longitudinal direction and 12 800 psi in the transverse direction; yield strengths were 4100 psi in the longitudinal direction and 3900 psi in the transverse direction. About one-half of these welded specimens failed in the parent metal indicating good weld strength.

For the specimens failing in the parent metal, average elongation over a 2-inch gage length was 16.7% for the longitudinal direction, and 19.9% for the transverse direction; these values are about the same as attained at 75°F for unwelded specimens. As discussed for 6061 aluminum, elongation measured over a 2-inch gage length for welded specimens is not considered representation, because of local high ductility in the weld joint. Although weld elongation data were not obtained for this set of specimens over a 0.25-inch gage length, it was determined over a 0.50-inch gage length (centered on the 0.125-inch wide weld). For specimens failing in the weld area, average elongation over a 0.50-inch gage length was 12.7% for the longitudinal direction and 10.3% for the transverse direction.

2. TIG Butt Fusion Welded With 1100 Aluminum Filler Wire, Beneficiated After Welding

Test results are summarized in Table A-13, and presented graphically in Figures A-15 and A-16. About three-quarters of these welded specimens failed in the parent metal, indicating good weld strength and the weldment improvement brought about through beneficiation. At -423°F, only one out of eight specimens failed at the weld joint.

Average tensile strengths in the longitudinal direction increased from 11 200 psi at 75°F to 24 100 psi at -320°F and 39 300 psi at -423°F. In the transverse direction, the tensile strengths were 11 500 psi at 75°F; 22 800 psi at -320°F; and 38 700 psi at -423°F. Longitudinal yield

strengths were 4100 psi at 75°F and 7100 psi at -320°F. Transverse values were 4100 psi at 75°F, and 6300 psi at -320°F.

For specimens failing in the parent metal average longitudinal grain direction elongations in 2-inch were 17.9% at 75°F, 30.0% at -320°F, and 32.5% at -423°F; transverse elongations were 16.1% at 75°F; 28.1% at -320°F; and 33.9% at -423°F. These values are close to those obtained for unwelded specimens. Weld elongation over a 0.50-inch gage length were obtained at 75°F; for specimens failing in the weld the elongation was about 10.5% for the longitudinal specimens at 12.0% for a transverse specimen. At -320°F and -423°F, weld elongation data were obtained for a 0.25-inch gage length. Values at -320°F were 14.5% for longitudinal specimens failing in the weld and 14.0% for a single transverse specimen. At -423°F, only one weld failure was obtained. Elongation over a 0.25-inch gage length was 16.0%.

A limited evaluation was conducted at ambient temperature of specimens with welds along their length parallel to the direction of load application; data are in Table A-13. Average ductility for these specimens was 16.5%.

TABLE A-1

EFFECT OF LOCATION IN THICKNESS ON TENSILE PROPERTIES OF 1.00-IN. THICK
6061 ALUMINUM ALLOY PLATE ^a

Location in Plate	Specimen No.	0.2% Yield Strength psi	Ultimate Tensile Strength psi	Elongation % in 2 in.
0.030 in. below surface	1	7222	18 981	19.0
	2	6923	18 942	19.0
0.090 in. below surface	1	7156	18 992	18.0
	2	6944	18 611	18.0
0.150 in. below surface	1	6545	18 182	17.0
	2	6471	18 039	16.5
0.210 in. below surface	1	6226	17 736	21.5
	2	5981	17 570	21.0
0.270 in. below surface	1	6000	17 714	25.0
	2	6075	17 664	23.0

^a All specimens fully annealed prior to testing

Table A-1

TABLE A-2
 EFFECT OF THICKNESS ON MECHANICAL PROPERTIES OF 6061 ALUMINUM ALLOY
 PARENT METAL - NOT CHEMICAL MILLED

Fabrication Process	Type Specimen (a)	Specimen No.	Specimen Thickness inches	Tensile Strength psi	0.2% Yield Strength psi	Elongation % in 2 in.
Machined to 0.030/0.035	Longitudinal	U-1	0.0365	17 400	6700	25.0
		U-2	0.0350	17 500	6600	25.0
		U-3	0.0360	17 500	6700	23.5
		U-4	0.0361	17 600	6700	22.0
		U-5	0.0365	17 300	6700	23.5
		U-6	0.0360	17 600	6700	23.5
	Transverse	V-1	0.0362	17 600	7100	17.0
		V-2	0.0364	17 700	7100	20.5
		V-3	0.0365	17 600	7100	19.0
		V-4	0.0365	17 600	7000	20.0
		V-5	0.0365	17 400	7000	18.0
		V-6	0.0365	17 600	7100	18.5
Machined to 0.012	Longitudinal	X-1	0.0113	16 100	6500	14.5
		X-2	0.0113	16 200	6400	16.5
		X-3	0.0113	16 400	6400	17.5
		X-4	0.0113	15 800	6400	15.0
		X-5	0.0113	16 000	6400	16.0
		X-6	0.0113	15 800	6400	14.0
	Transverse	W-1	0.0115	15 600	6500	11.0
		W-2	0.0115	15 900	6600	13.0
		W-3	0.0115	15 800	6700	13.0
		W-4	0.0115	15 200	6600	10.5
		W-5	0.0115	15 400	6500	11.5
		W-6	0.0115	15 300	6500	11.5

^a All specimens were completely annealed

TABLE A-3

EFFECT OF CHEMICAL MILLING AND DEGREE OF ANNEAL ON MECHANICAL PROPERTIES OF 6061
ALUMINUM ALLOY - PARENT METAL (CHEMICAL MILLED FROM 0.030 TO 0.010)

Fabrication Process	Type Specimen	Degree of Anneal	Specimen No.	Specimen Thickness inches	Tensile Strength psi	0.2% Yield Strength psi	Elongation % in 2 in.
Chemical Milled from 0.030 to 0.010	Longitudinal	Incomplete	G-1	0.0105	16 800	9000	8.0
			G-2	0.0110	17 200	9000	10.0
			G-3	0.0105	17 500	8500	11.0
			G-4	0.0113	17 000	8700	9.0
			G-5	0.0109	16 900	8700	9.0
			G-6	0.0105	16 500	8900	9.5
	Complete		G-7	0.0107	14 700	5800	14.0
			G-8	0.0105	15 200	6400	13.0
			G-9	0.0107	15 000	5800	15.0
			G-10	0.0105	15 700	6900	15.0
			G-11	0.0104	15 200	6800	12.0
			G-12	0.0108	15 500	6600	13.5
Transverse	Incomplete		H-1	0.0100	16 700	9200	7.5
			H-2	0.0098	16 700	9000	7.2
			H-3	0.0112	18 000	9100	8.5
			H-4	0.0108	16 200	8200	8.0
			H-5	0.0105	17 100	8800	7.5
			H-6	0.0102	17 600	9200	8.0
	Complete		H-7	0.0103	15 100	6600	10.0
			H-8	0.0103	15 300	6500	10.0
			H-9	0.0090	14 900	7100	7.0
			H-10	0.0100	15 700	7500	9.5
			H-11	0.0105	15 200	6600	12.0
			H-12	0.0105	15 200	6700	11.5

Table A-3

TABLE A-4

EFFECT OF CHEMICAL MILLING AND DEGREE OF ANNEAL ON MECHANICAL PROPERTIES OF
 6061 ALUMINUM ALLOY - PARENT METAL (CHEMICAL MILLED FROM 0.020 TO 0.010)

Fabrication Process	Type Specimen	Degree of Anneal	Specimen No.	Specimen Thickness inches	Tensile Strength psi	0.2% Yield Strength psi	Elongation % in 2 in.
Chemical Milled from 0.020 to 0.010	Longitudinal	Incomplete	A-1	0.0108	17 000	8000	13.0
			A-2	0.0109	16 400	8400	9.0
			A-3	0.0109	16 700	8000	11.0
	Complete	A-4	0.0105	15 800	6100	6100	15.0
		A-5	0.0108	15 800	6200	6200	16.5
		A-6	0.0105	15 800	6400	6400	15.0
		A-7	0.0108	15 700	6500	6500	15.0
	Transverse	Incomplete	B-1	0.0103	17 000	8400	6.5
			B-2	0.0103	16 400	8400	6.0
			B-3	0.0108	17 000	8400	7.0
	Complete	B-4	0.0095	13 600	7100	7100	5.5
		B-5	0.0100	15 200	6700	6700	10.5
		B-6	0.0103	15 200	6800	6800	11.5
		B-7	0.0102	15 500	7200	7200	12.5
		B-8	0.0102	15 200	7200	7200	11.0
		B-9	0.0102	15 500	7300	7300	11.0

Table A-4

TABLE A-5

EFFECT OF FINAL THICKNESS ON ANNEALED CHEMICAL MILLED 6061 ALUMINUM ALLOY
 MECHANICAL PROPERTIES - PARENT METAL

Fabrication Process	Type Specimen (a)	Specimen No.	Specimen Thickness inches	Tensile Strength Psi	0.2% Yield Strength psi	Elongation % in 2 in.
Chemical Milled from 0.030 to 0.014	Longitudinal	L-1	0.0142	16 800	7500	15.5
		L-2	0.0150	17 900	7000	16.0
		L-3	0.0148	17 300	7500	19.0
		L-4	0.0148	17 400	7400	15.5
		L-5	0.0150	17 300	7500	15.0
		L-6	0.0145	17 700	7000	15.0
	Transverse	T-1	0.0145	17 800	7300	14.5
		T-2	0.0146	17 800	7700	14.5
		T-3	0.0140	17 000	8200	14.5
		T-4	0.0141	17 200	7200	13.0
		T-5	0.0141	17 300	7300	11.5
		T-6	0.0142	17 300	7200	13.0

a

All specimens were completely annealed

Table A-5

TABLE A-6

MECHANICAL PROPERTIES OF 6061 ALUMINUM ALLOY AT 75, -320, AND -423° F
COMPLETELY ANNEALED PARENT METAL (CHEMICALLY MILLED FROM 0.030- TO 0.010-in. THICKNESS)

Test Temperature °F	Type Specimen (Grain Direction)	Specimen No.	Specimen Thickness in.	Tensile Strength psi	0.2% Yield Strength psi	% in 2 in.	% in 0.50 in.	% in 0.25 in.
75	Longitudinal	G-7	0.0107	14 700	5800	14.0	-	-
		G-8	0.0105	15 200	6400	13.0	-	-
		G-9	0.0107	15 000	5800	15.0	-	-
		G-10	0.0105	15 700	6900	15.0	-	-
		G-11	0.0104	15 200	6800	12.0	-	-
		G-12	0.0108	15 500	6600	13.5	-	-
		AVERAGE	0.0106	15 200	6400	13.8	-	-
		H-7	0.0103	15 100	6600	10.0	-	-
		H-8	0.0103	15 300	6500	10.0	-	-
		H-9	0.0090	14 900	7100	7.0	-	-
		H-10	0.0100	15 700	7500	9.5	-	-
		H-11	0.0105	15 200	6600	12.0	-	-
		H-12	0.0105	15 200	6700	11.5	-	-
		AVERAGE	0.0101	15 200	6800	10.0	-	-
-320	Longitudinal	G-13	0.0107	27 100	7500	25.0	23.0	22.0
		G-14	0.0112	27 600	9200	22.5	22.0	22.0
		G-15	0.0100	26 000	-	17.5	16.0	16.0
		AVERAGE	0.0106	26 900	8400	21.7	20.3	20.0
-423	Transverse	H-13	0.0102	27 200	9400	13.2	18.0	14.0
		H-14	0.0107	25 000	8700	12.0	10.0	12.0
		H-15	0.0102	27 000	8300	19.0	21.0	20.0
		AVERAGE	0.0104	26 400	8800	14.7	16.3	15.3
-423	Longitudinal	G-16	0.0102	46 600	-	23.0	22.0	22.0
		G-17	0.0100	46 100	-	27.5	30.0	30.0
		G-18	0.0103	42 700	-	23.5	24.0	25.0
		AVERAGE	0.0102	45 100	-	24.7	25.3	26.0
-423	Transverse	H-16	0.0110	43 600	-	22.5	24.0	24.0
		H-17	0.0105	46 500	-	19.5	20.0	20.0
		H-18	0.0105	46 800	-	22.5	21.0	22.0
		AVERAGE	0.0107	45 600	-	21.5	21.7	22.0

Table A-6

TABLE A-7

MECHANICAL PROPERTIES OF 6061-0 ALUMINUM WELDMENTS AT 75° F., COMPLETELY
 ANNEALED, TIG BUTT FUSION WELDED WITH 1100 ALUMINUM FILLER WIRE (MEMBRANE CHEMICALLY
 MILLED FROM 0.030- TO 0.010-IN. THICKNESS BEFORE WELDING)

Test Temperature °F	Type Specimen	Specimen No.	Specimen Thickness in.	Tensile Strength psi	0.2% Yield Strength psi	Elongation (a)			Failure Location (b)
						% in. 2 in.	% in. 0.50 in.	% in. 0.25 in.	
75	Longitudinal Grain/Transverse Weld	LW-1	0.0117	15 200	6800	8.5	-	-	Weld
		LW-2	0.0110	10 200	6700	3.5	-	-	Weld
		LW-3	0.0115	16 200	6500	12.5	-	-	At Weld
		LW-4	0.0113	16 400	6800	13.0	-	-	Parent Metal
		EW-1	0.0120	9100	6400	1.8	-	-	Weld
		EW-2	0.0120	14 200	7300	6.5	-	-	Weld
		EW-3	0.0115	10 000	6600	3.0	-	-	Weld & H.A.Z.
		EW-4	0.0120	10 500	6500	3.0	-	-	Weld
		EW-5	0.0122	14 300	6500	7.5	-	-	Weld
		Transverse Grain/ Transverse Weld	0.0118	12 900	6400	4.0	-	-	At Weld
Transverse Grain/ Transverse Weld	Transverse Grain/ Transverse Weld	FW-2	0.0118	12 900	6400	4.0	-	-	Weld
		FW-3	0.0140	10 600	6800	2.5	-	-	Weld
		FW-4	0.0140	15 200	6900	7.5	-	-	H.A.Z.
		FW-6	0.0140	6700	6000	2.5	-	-	Weld
		FW-7	0.0118	11 400	8100	2.5	-	-	At Weld

a Elongation values for qualitative use only

b H.A.Z. = Heat Affected Zone; At Weld = Weld or Heat Affected Zone

Table A-7

TABLE A-8

MECHANICAL PROPERTIES OF 6061-0 ALUMINUM WELDMENTS AT 75° F., COMPLETELY ANNEALED,
 TIG BUTT FUSION WELDED WITH 1100 ALUMINUM FILLER WIRE, BENEFICIATED AFTER
 WELDING (MEMBRANE CHEMICALLY MILLED FROM 0.030-IN. TO 0.010-IN.
 THICKNESS BEFORE WELDING)

Test Temperature °F	Type Specimen	Specimen No.	Specimen Thickness in.	Tensile Strength psi	0.2% Yield Strength psi	Elongation (a)			Failure Location (b)
						% in 2 in.	% in 0.50 in.	% in 0.25 in.	
75	Longitudinal Grain/ Transverse Weld	GW-1	0.0132	16 500	6600	11.2	-	-	H.A.Z.
		GW-2	0.0145	12 300	6200	3.5	-	-	Weld
		GW-3	0.0135	15 800	6500	10.5	-	-	H.A.Z.
		GW-4	0.0118	12 400	6200	4.0	-	-	Weld
		GW-5	0.0114	14 600	7900	3.7	-	-	Weld
		GW-6	0.0144	11 100	6500	2.0	6.0	-	Weld
		GW-7	0.0133	14 500	6500	6.7	8.0	14.0	H.A.Z.
		GW-8	0.0140	16 400	6500	13.0	10.0	6.0 ^c	parent Metal
		GW-9	0.0138	16 500	6800	11.5	13.0	14.0	At Weld
		GW-10	0.0145	16 500	6500	13.0	18.0	15.0	H.A.Z.
		GW-11	0.0145	10 400	6300	3.2	6.0	12.0	Weld
		AVERAGE	0.0135	14 200	6600	N/A	N/A	13.8	
Transverse Grain/ Transverse Weld	Transverse Weld	HW-1	0.0140	10 200	6700	2.5	-	-	H.A.Z.
		HW-2	0.0140	10 700	6700	2.5	-	-	Weld
		HW-3	0.0145	9300	6800	2.5	-	-	At Weld
		HW-4	0.0140	11 000	6800	2.5	-	-	Weld
		HW-5	0.0142	14 500	6900	6.0	-	-	H.A.Z.
		HW-6	0.0142	9900	6600	2.5	4.0	10.0	Weld
		HW-7	0.0138	11 400	7100	2.5	4.0	10.0	Weld
		HW-8	0.0136	8600	6700	2.5	6.0	10.0	Weld
		HW-9	0.0145	6800	6500	2.5	4.0	9.0	Weld
		AVERAGE	0.0141	10 300	6800	N/A	N/A	9.8	

See Sheet 2 for footnotes

TABLE A-8 (con't.)

Test Temperature °F	Type Specimen	Specimen No.	Specimen Thickness in.	Tensile Strength psi	0.2% Yield Strength psi	% in 2 in. 0.50 in.	Elongation (a) % in 0.25 in.	Failure Location (b)
-320	Longitudinal Grain/ Transverse Weld	GW-12	0.0145	25 800	-	10.0 20.0	10.0 13.0	Weld
		GW-13	0.0140	29 300	9400	4.0	10.0 ^c	Parent Metal
		GW-14	0.0140	15 100	8800	8.0	14.0	Weld
		AVERAGE	0.0142	23 400	9100	N/A	11.3	
		HW-10	0.0135	26 600	10 400	9.0	10.0	
	Transverse Grain/ Transverse Weld	HW-11	0.0135	16 200	10 000	3.0	7.0	H.A.Z. Weld
		HW-12	0.0140	24 100	9600	7.5	6.0	Weld
		HW-13	0.0140	26 300	-	10.0	12.0	Weld
		AVERAGE	0.0138	23 300	10 000	N/A	9.5	
		GW-15	0.0113	34 300	-	20.5	14.0	
-423	Longitudinal Grain/ Transverse Weld	GW-16	0.0145	27 800	-	10.0	14.0	
		GW-17	0.0120	28 700	-	9.0	10.0	
		GW-18	0.0135	37 200	-	18.5	17.0	
		AVERAGE	0.0128	32 000	-	N/A	20.0 14.3	
								Parent Metal

a

Elongation values for 2-in.-gage length for qualitative use only, except Specimens GW-8, GW-13 and GW-15, as noted. Elongation in 0.25-in.-gage length considered representative of ductility of 0.125-in.-wide weld joint for specimens failing in Weld or H.A.Z. Representative ductility of Specimen GW-8 considered to be 13%; of GW-13, 20%; and of GW-15, 20.5%; because of parent metal failures.

b H.A.Z. = Heat Affected Zone; At Weld = Weld or Heat Affected Zone

c Not included in Average

TABLE A-9
 EFFECT OF THICKNESS ON THE MECHANICAL PROPERTIES OF 1100 ALUMINUM -
 NON-CHEMICAL MILLED PARENT METAL - ANNEALED

Fabrication Process	Type Specimen	Specimen No.	Specimen Thickness inches	Tensile Strength psi	0.2% Yield Strength psi	Elongation % in 2 in.
Machined to 0.030/0.035	Longitudinal	Z-1	0.0345	12 400	1900	30.5
		Z-2	0.0342	12 200	2000	30.5
		Z-3	0.0345	12 400	1800	27.5
		Z-4	0.0342	12 400	1800	34.0
		Z-5	0.0345	12 400	1800	28.5
		Z-6	0.0345	12 400	2400	30.0
	Transverse	Y-1	0.0340	12 400	1800	23.5
		Y-2	0.0345	12 400	2300	22.5
		Y-3	0.0340	12 400	1900	24.0
		Y-4	0.0345	12 400	1800	26.5
		Y-5	0.0345	12 300	1800	24.0
		Y-6	0.0345	12 500	1800	26.5
Machined to 0.010	Longitudinal	L-1	0.0108	11 700	5100	16.0
		L-2	0.0110	12 000	5600	15.0
		L-3	0.0112	10 900	5000	12.0
		L-4	0.0110	11 200	-	12.2
		L-5	0.0110	11 300	4900	12.5
	Transverse	K-1	0.0105	12 300	-	21.5
		K-2	0.0108	12 100	5200	23.5
		K-3	0.0105	12 100	5300	21.5
		K-4	0.0108	11 900	-	22.0
		K-5	0.0105	11 800	5100	22.0
		K-6	0.0104	12 200	5600	22.0

Table A-9

TABLE A-10

EFFECT OF CHEMICAL MILLING ON THE MECHANICAL PROPERTIES OF 1100 ALUMINUM -
PARENT METAL - ANNEALED

Fabrication Process	Type Specimen	Specimen No.	Specimen Thickness inches	Tensile Strength psi	0.2% Yield Strength psi	Elongation % in 2 in.
Chemical Milled from 0.030 to 0.010	Longitudinal	C-1	0.0105	11 300	4900	15.0
		C-2	0.0105	12 200	5800	16.0
		C-3	0.0104	12 400	5300	16.5
		C-4	0.0103	11 800	4900	16.5
		C-5	0.0103	11 200	5500	11.0
		C-6	0.0105	11 300	5300	17.5
	Transverse	D-1	0.0104	12 400	5100	26.0
		D-2	0.0102	12 100	5400	15.5
		D-3	0.0108	12 400	5100	23.5
		D-4	0.0115	12 200	5700	16.5
		D-5	0.0090	12 500	6100	14.5
		D-6	0.0105	12 300	5200	24.0

Table A-10

TABLE A-11

MECHANICAL PROPERTIES OF 1100 ALUMINUM AT 75, -320, AND -423° F -
COMPLETELY ANNEALED PARENT METAL (CHEMICALLY MILLED FROM 0.030- TO 0.010-IN. THICKNESS)

Test Temperature °F	Type Specimen (Grain Direction)	Specimen No.	Specimen Thickness in.	Tensile Strength psi	0.2% Yield Strength psi	Elongation		
						% in 2 in.	% in 0.50 in.	% in 0.25 in.
75	Longitudinal	C-1	0.0105	11 300	4900	15.0	-	-
		C-2	0.0105	12 200	5800	16.0	-	-
		C-3	0.0104	12 400	5300	18.5	-	-
		C-4	0.0103	11 800	4900	16.5	-	-
		C-5	0.0103	11 200	5500	11.0	-	-
		C-6	0.0105	11 300	5300	17.5	-	-
		<u>AVERAGE</u>	<u>0.0104</u>	<u>11 700</u>	<u>5300</u>	<u>15.8</u>	<u>-</u>	<u>-</u>
	Transverse	D-1	0.0104	12 400	5100	26.0	-	-
		D-2	0.0102	12 100	5400	15.5	-	-
		D-3	0.0108	12 400	5100	23.5	-	-
		D-4	0.0115	12 200	5700	18.5	-	-
		D-5	0.0090	12 500	6100	14.5	-	-
		D-6	0.0105	12 300	5200	24.0	-	-
		<u>AVERAGE</u>	<u>0.0104</u>	<u>12 300</u>	<u>5400</u>	<u>20.3</u>	<u>-</u>	<u>-</u>
-320	Longitudinal	C-8	0.0105	23 800	6700	30.0	30.0	32.0
		C-10	0.0105	23 000	5200	26.5	22.0	22.0
		C-12	0.0110	24 700	6300	26.0	25.0	25.5
		<u>AVERAGE</u>	<u>0.0106</u>	<u>23 800</u>	<u>6000</u>	<u>27.5</u>	<u>25.7</u>	<u>26.5</u>
		D-17	0.0105	23 500	6200	38.0	44.0	36.0
	Transverse	D-8	0.0113	25 000	-	26.0	23.0	24.0
		D-9	0.0115	24 300	6900	42.5	36.0	36.0
		<u>AVERAGE</u>	<u>0.0111</u>	<u>24 300</u>	<u>6600</u>	<u>35.5</u>	<u>34.3</u>	<u>32.0</u>
		D-11	0.0110	38 300	-	31.5	32.0	32.0
-423	Longitudinal	C-15	0.0110	38 800	-	42.0	34.0	37.0
		C-16	0.0115	34 600	-	32.0	32.0	32.0
		C-18	0.0100	37 200	-	35.2	32.7	33.7
	Transverse	<u>AVERAGE</u>	<u>0.0108</u>	<u>37 900</u>	<u>-</u>	<u>44.0</u>	<u>42.7</u>	<u>43.3</u>
		D-12	0.0102	38 000	-	42.0	40.0	40.0
		D-14	0.0100	37 100	-	45.0	48.0	50.0
		<u>AVERAGE</u>	<u>0.0104</u>	<u>37 900</u>	<u>-</u>	<u>44.0</u>	<u>42.7</u>	<u>43.3</u>

Table A-11

TABLE A-12

MECHANICAL PROPERTIES OF 1100-O ALUMINUM WELDMENTS AT 75° F., COMPLETELY ANNEALED,
 TIG BUTT FUSION WELDED WITH 1100 ALUMINUM FILLER WIRE (MEMBRANE
 CHEMICALLY MILLED FROM 0.030- TO 0.010-IN. THICKNESS BEFORE WELDING)

Test Temperature °F	Type Specimen	Specimen No.	Specimen Thickness in.	Tensile Thickness in.	0.2% Yield Strength psi	Elongation			Failure Location
						% in 2 in.	% in 0.50 in.	% in 0.25 in.	
75	Longitudinal Grain/ Transverse Weld	M-1	0.0145	11 400	4500	10.2 ^a	13.0	-	H.A.Z.
		M-2	0.0135	10 200	3900	8.5 ^a	13.0	-	H.A.Z.
		M-3	0.0135	11 900	4200	19.5	12.0 ^a	-	Parent Metal
		M-4	0.0135	11 400	4300	11.0 ^a	12.0	-	H.A.Z.
		M-5	0.0135	11 800	3600	14.0	10.5 ^a	-	Parent Metal
		AVERAGE	0.0137	11 700	4100	16.7	12.7		
		N-1	0.0135	11 500	3900	10.2 ^a	10.0	-	H.A.Z.
		N-2	0.0140	18 000	3800	4.0 ^a	7.0	-	At Weld
		N-3	0.0140	12 000	3800	17.5	10.0 ^a	-	Parent Metal
		N-4	0.0135	12 300	4000	17.5	8.0 ^a	-	Parent Metal
		N-5	0.0140	11 800	4000	16.0 ^a	14.0	-	H.A.Z.
	Transverse Grain/ Transverse Weld	TW-1	0.0142	12 100	4200	21.5	-	-	Parent Metal
		TW-2	0.0142	12 600	4100	21.5 ^a	-	-	H.A.Z.
		TW-3	0.0140	12 500	3900	23.0	-	-	Parent Metal
		TW-4	0.0142	12 000	3800	17.0 ^a	-	-	H.A.Z.
		AVERAGE	0.0139	12 800	3900	19.9	10.3		

a

Not included in Average; These values for qualitative use only

TABLE A-13

MECHANICAL PROPERTIES OF 1100-0 ALUMINUM WELDMENTS AT 75° F., COMPLETELY ANNEALED, TIG BUTT FUSION WELDED WITH 1100 ALUMINUM FILLER WIRE, BENEFICIATED AFTER WELDING (MEMBRANE CHEMICALLY MILLED FROM 0.030- TO 0.010-IN. THICKNESS BEFORE WELDING)

Test Temperature °F	Type Specimen	Specimen No.	Specimen Thickness in.	Tensile Strength psi	0.2% Yield Strength psi	Elongation		Failure Location
						% in 2 in.	% in 0.50 in.	
75	Longitudinal Grain/ Transverse Weld	CW-1	0.0145	12 100	4300	18.7	9.0 ^a	-
		CW-2	0.0145	11 800	4000	17.0	10.5 ^a	Parent Metal
		CW-3	0.0145	10 300	4000	8.0 ^a	11.0	Parent Metal
		CW-4	0.0150	11 800	4200	18.0	13.0 ^a	H.A.Z.
		CW-5	0.0150	10 000	4000	6.5 ^a	10.0	Parent Metal
		AVERAGE	0.0147	11 200	4100	17.9	10.5	At Weld
Transverse Grain/ Transverse Weld	DW-1	0.0125	11 900	3900	19.0	9.0 ^a	-	Parent Metal
	DW-2	0.0125	11 700	4300	15.0	7.0 ^a	-	Parent Metal
	DW-3	0.0130	10 900	4100	15.0	7.0 ^a	-	Parent Metal
	DW-4	0.0135	11 800	4000	15.5	8.0 ^a	-	Parent Metal
	DW-5	0.0128	11 300	4300	13.5 ^a	12.0	-	H.A.Z.
	AVERAGE	0.0128	11 500	4100	16.1	N/A	-	
Longitudinal Grain/ Longitudinal Weld	O-1	0.0150	7000	3000	22.5	32.0 ^a	-	Center Center
	O-2	0.0155	6800	2800	18.0	29.0 ^a	-	
	P-1	0.0155	5800	2900	7.0	8.0 ^a	-	Center Specimen
	P-2	0.0155	7200	3200	18.5	20.0 ^a	-	Radius
-320	Longitudinal Grain/ Transverse Weld	AVERAGE	0.0153	6700	3000	16.5	N/A	
		CW-10	0.0125	22 200	6700	12.0 ^a	12.0 ^a	H.A.Z.
		CW-11	0.0135	24 700	6300	31.0	18.0 ^a	Parent Metal
		CW-12	0.0140	24 900	8100	29.0	18.0 ^a	Parent Metal
		CW-13	0.0145	24 700	7100	26.5 ^a	20.0 ^a	H.A.Z.
		AVERAGE	0.0136	24 100	7100	30.0	N/A	14.5

^a Not included in Average - these values for qualitative use only

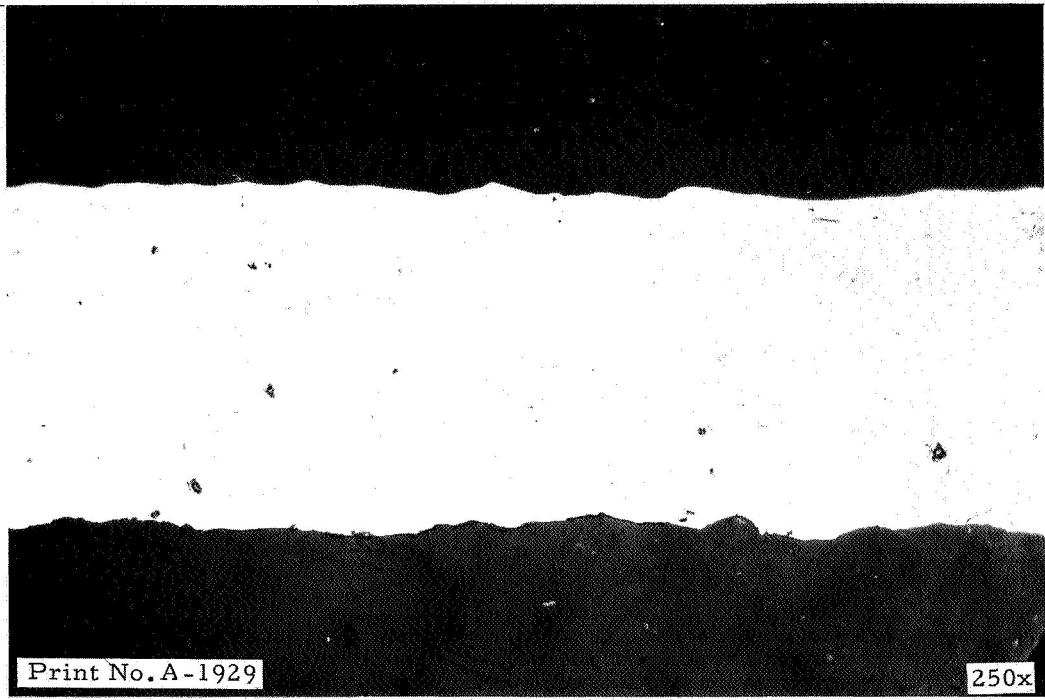
TABLE A-13 (con't.)

Test Temperature °F	Type Specimen	Specimen No.	Specimen Thickness in.	Tensile Strength psi	0.2% Yield Strength psi	Elongation % in. 0.50 in.	Elongation % in. 0.25 in.	Failure Location
-320	Transverse Grain/ Transverse Weld	DW-11	0.0130	18 700	-	10.0 ^a	10.0 ^a	Weld
		DW-12	0.0140	23 900	6700	28.0	16.0 ^a	Parent Metal
		DW-13	0.0138	24 500	5800	32.5	17.0 ^a	Parent Metal
		DW-14	0.0135	24 000	-	24.0	15.0 ^a	Parent Metal
		<u>AVERAGE</u>	<u>0.0136</u>	<u>22 800</u>	<u>6300</u>	<u>28.1</u>	<u>14.5</u>	<u>N/A</u>
-423	Longitudinal Grain/ Transverse Weld	CW-14	0.0145	38 200	-	35.0	30.0	21.0
		CW-15	0.0145	39 200	-	30.0	24.0	16.0
		CW-16	0.0142	40 100	-	35.0	24.0	16.0
		CW-17	0.0138	39 600	-	30.0	20.5	14.0
		<u>AVERAGE</u>	<u>0.0142</u>	<u>39 300</u>	<u>32.5</u>	<u>24.6</u>	<u>16.8</u>	
	Transverse Grain/ Transverse Weld	DW-15	0.0135	38 300	-	37.0	22.0	14.0
		DW-16	0.0128	38 600	-	32.0	24.0	16.0
		DW-17	0.0115	37 700	-	30.0	21.0	14.0
		DW-18	0.0130	40 100	-	36.5	24.0	14.0
		<u>AVERAGE</u>	<u>0.0127</u>	<u>38 700</u>	<u>33.9</u>	<u>22.8</u>	<u>14.5</u>	

a

Not included in Average - these values for qualitative use only

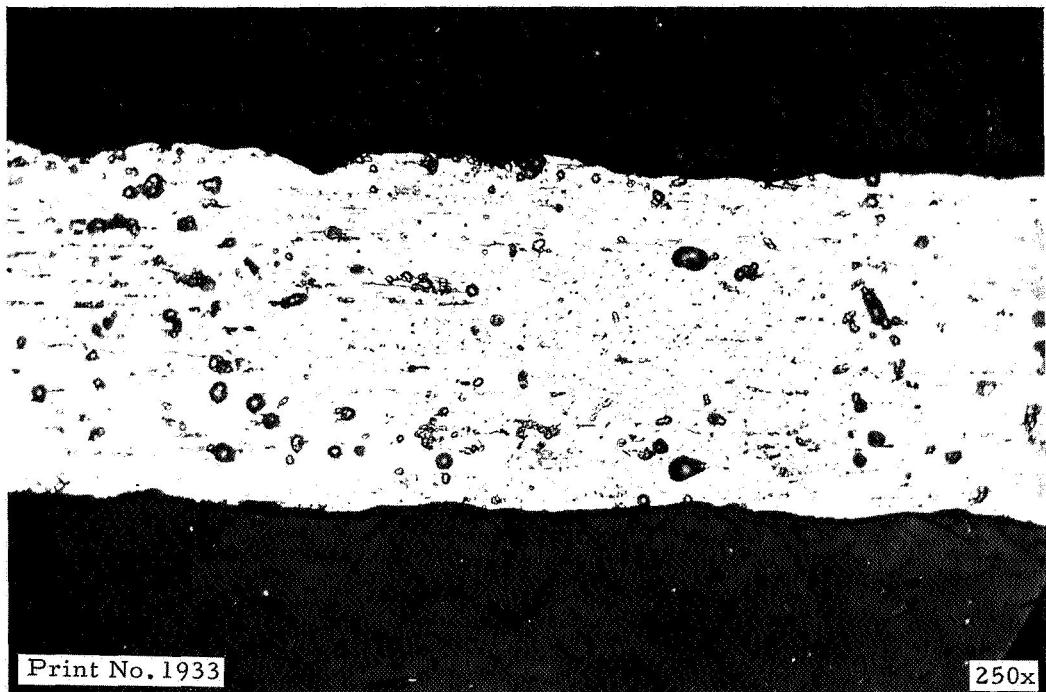
AEROJET
GENERAL^{PSI}
GENERAL



SECTION OF 6061 ALUMINUM ALLOY 0.010-IN. MEMBRANE
SHOWING EDGE ATTACK BY CHEMICAL MILLING SOLUTION - UNETCHED

10-067-118-

Figure A-1



SECTION OF 6061 ALUMINUM ALLOY 0.010-IN. MEMBRANE
SHOWING SOME SLIGHT INTERGRANULAR ATTACK BY CHEMICAL
MILLING SOLUTION - ETCHANT - 10% NaOH

EFFECT OF PROCESSING ON ELONGATION OF 6061 ALUMINUM ALLOY (PARENT METAL)

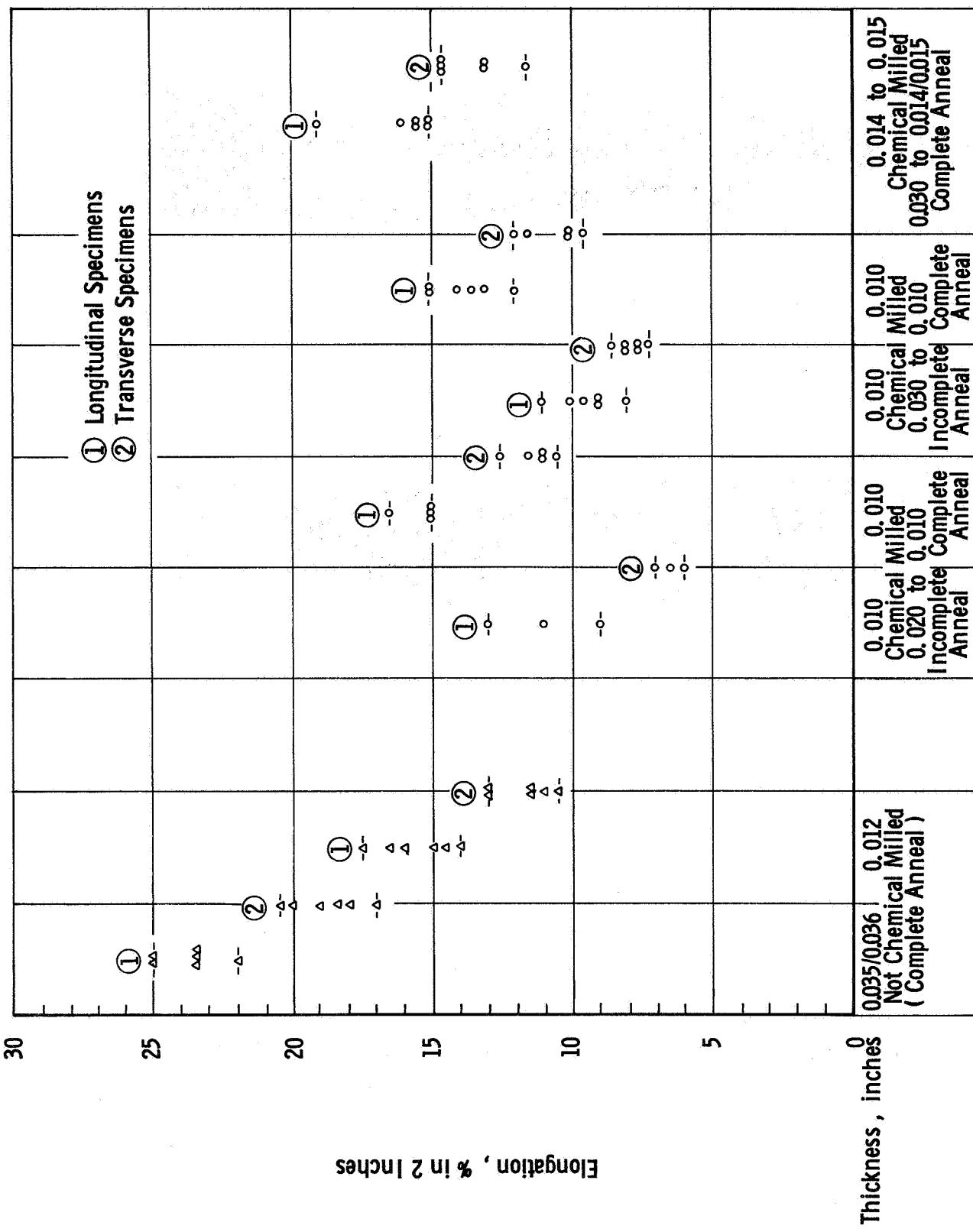
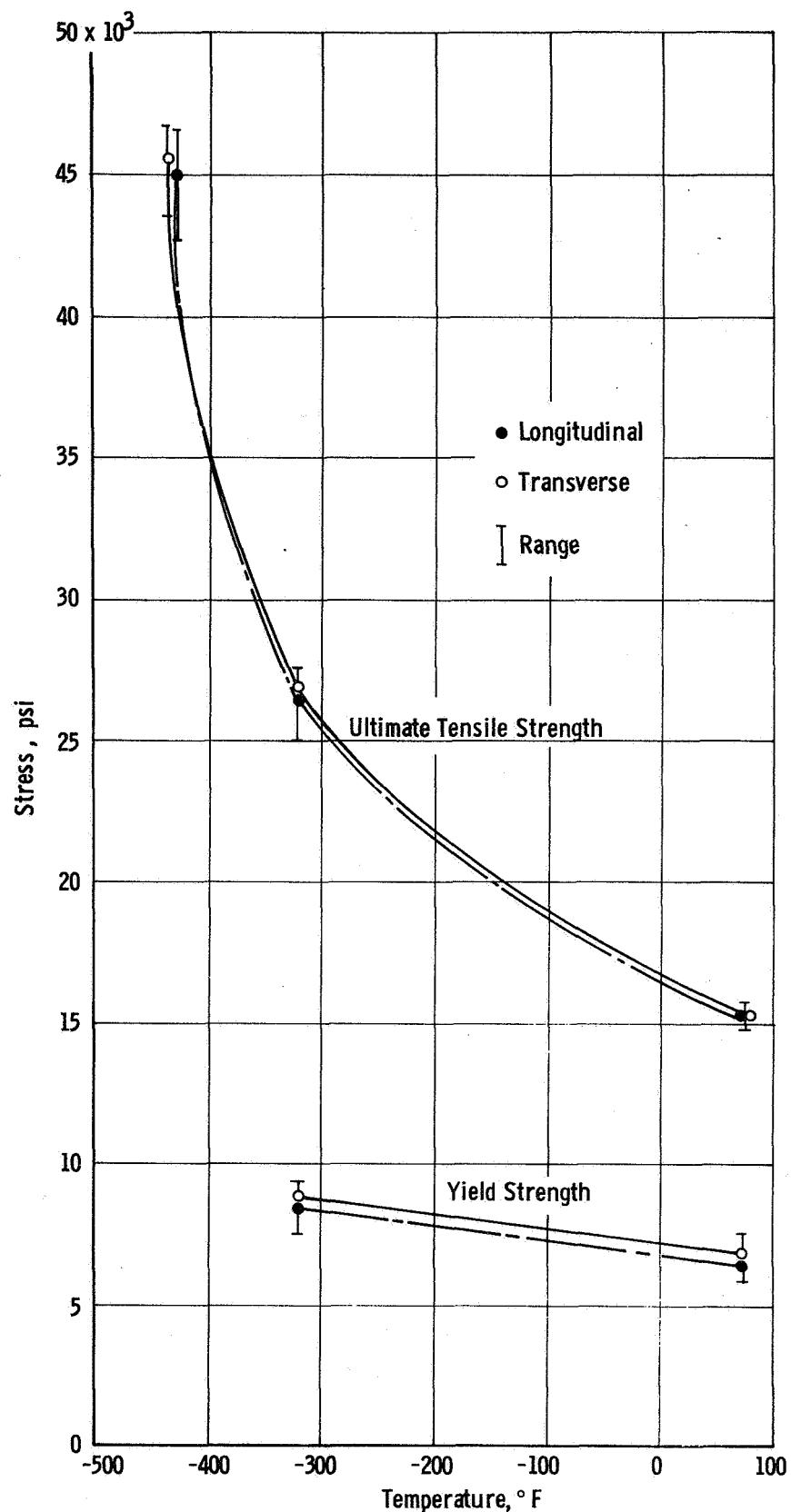
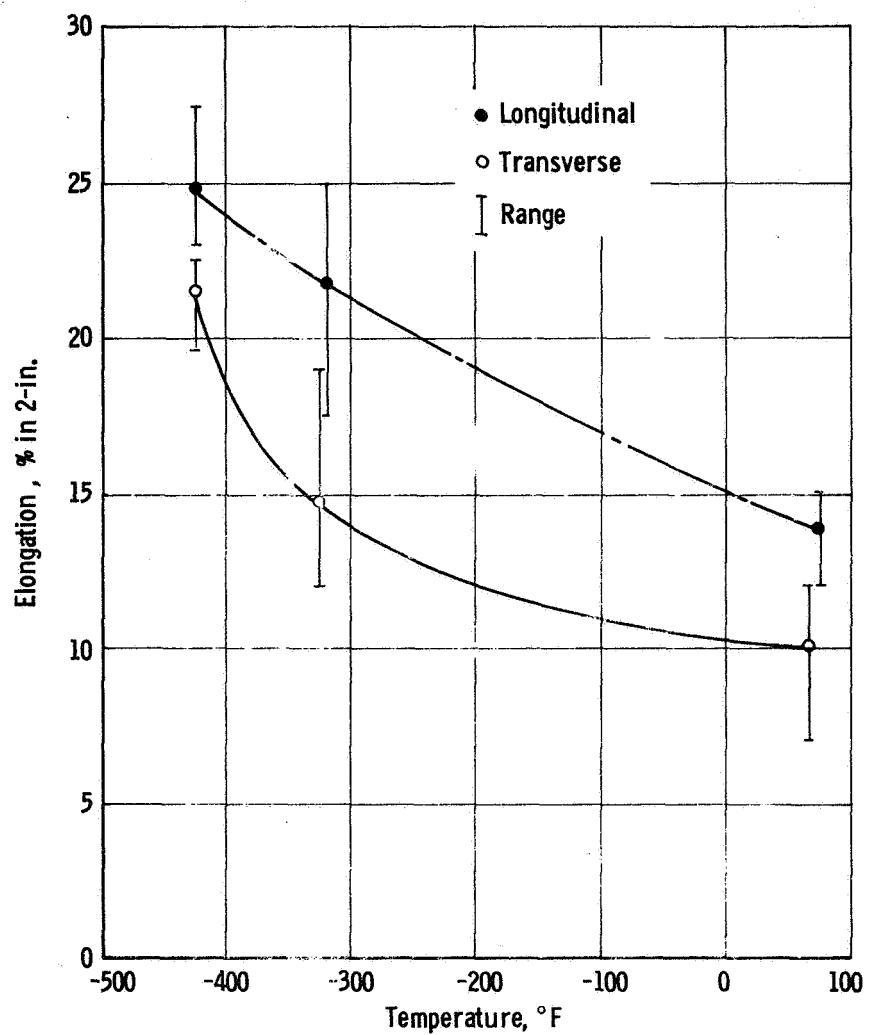


Figure A-3



TENSILE AND YIELD STRENGTHS OF 6061-O ALUMINUM ALLOY PARENT METAL
CHEMICALLY MILLED FROM 0.030 TO 0.010-IN. THICKNESS

Figure A-4



ELONGATION OF 6061-0 ALUMINUM ALLOY PARENT METAL,
CHEMICALLY MILLED FROM 0.030 TO 0.010-IN. THICKNESS

Figure A-5

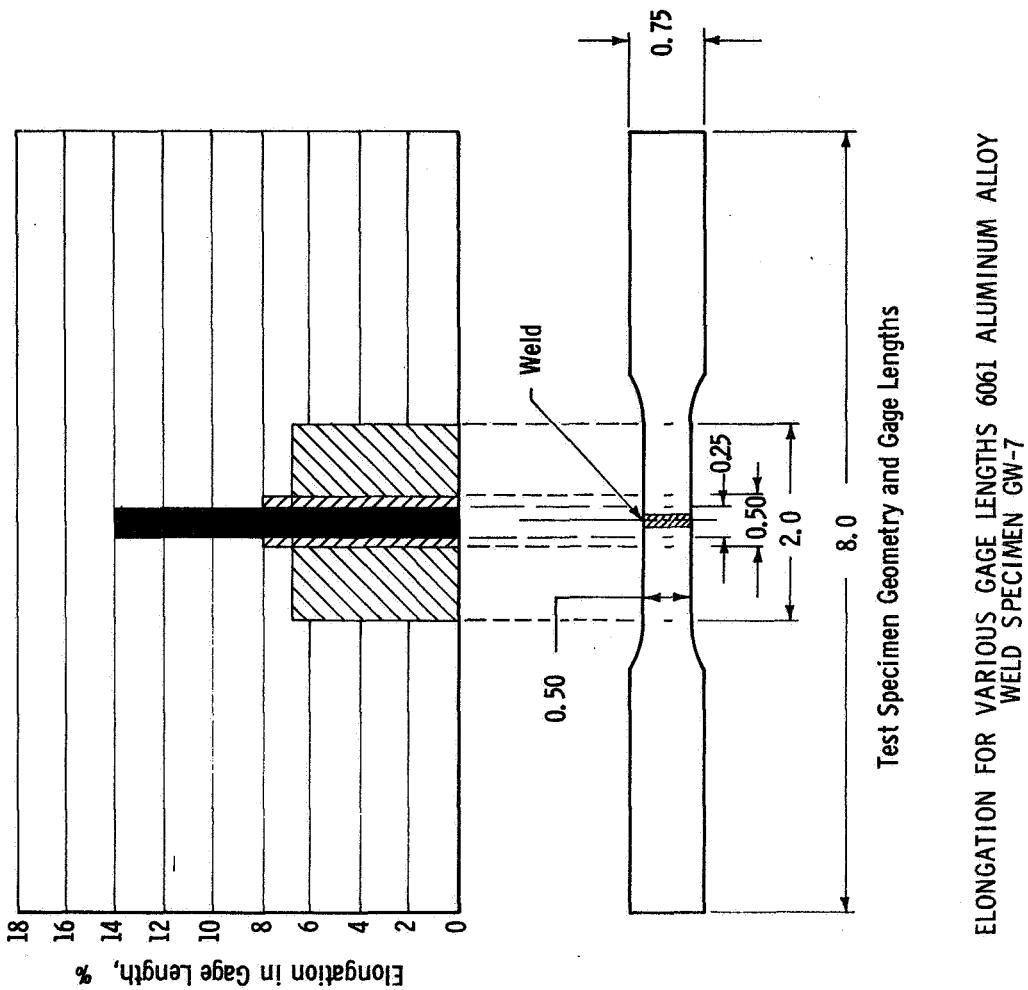
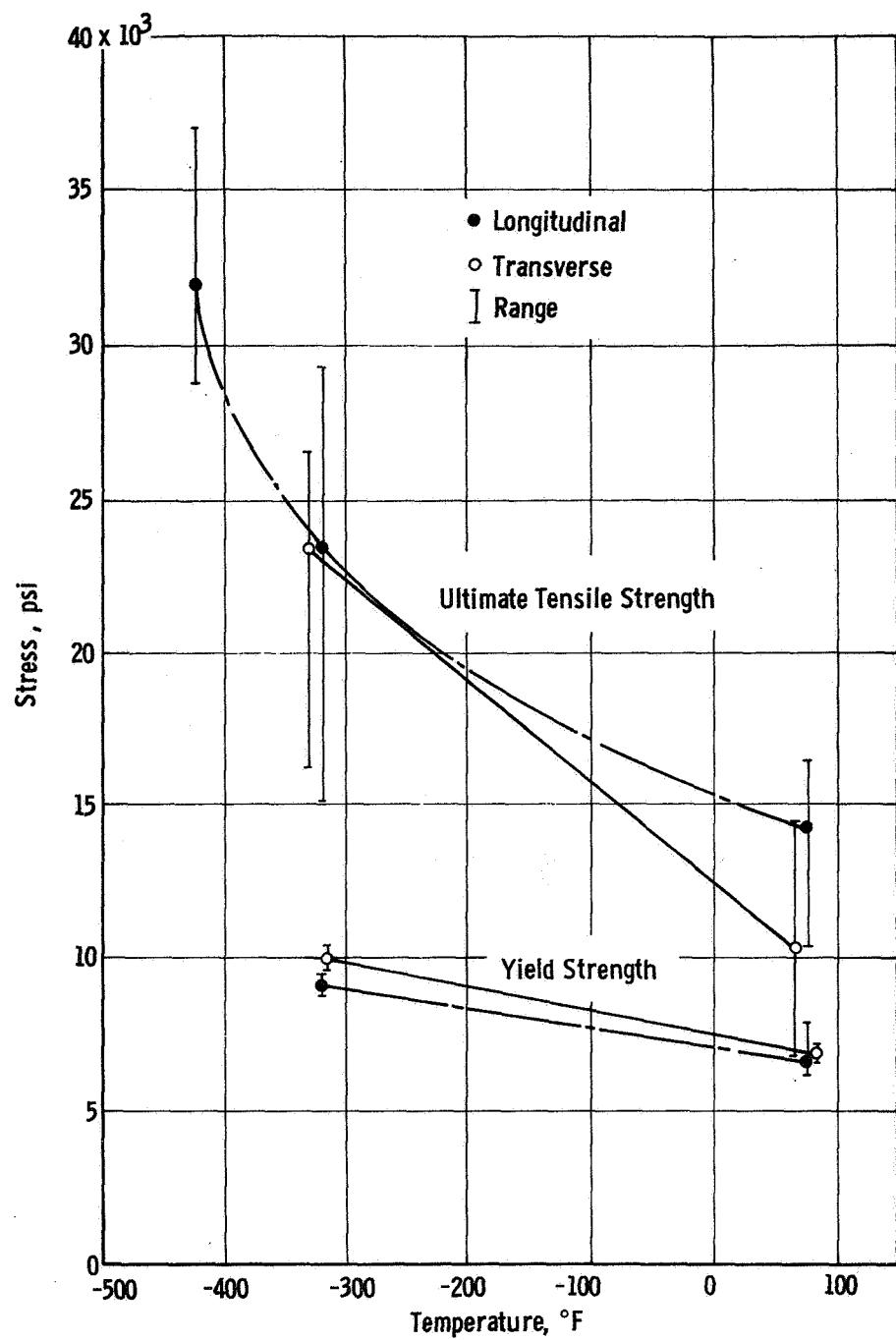
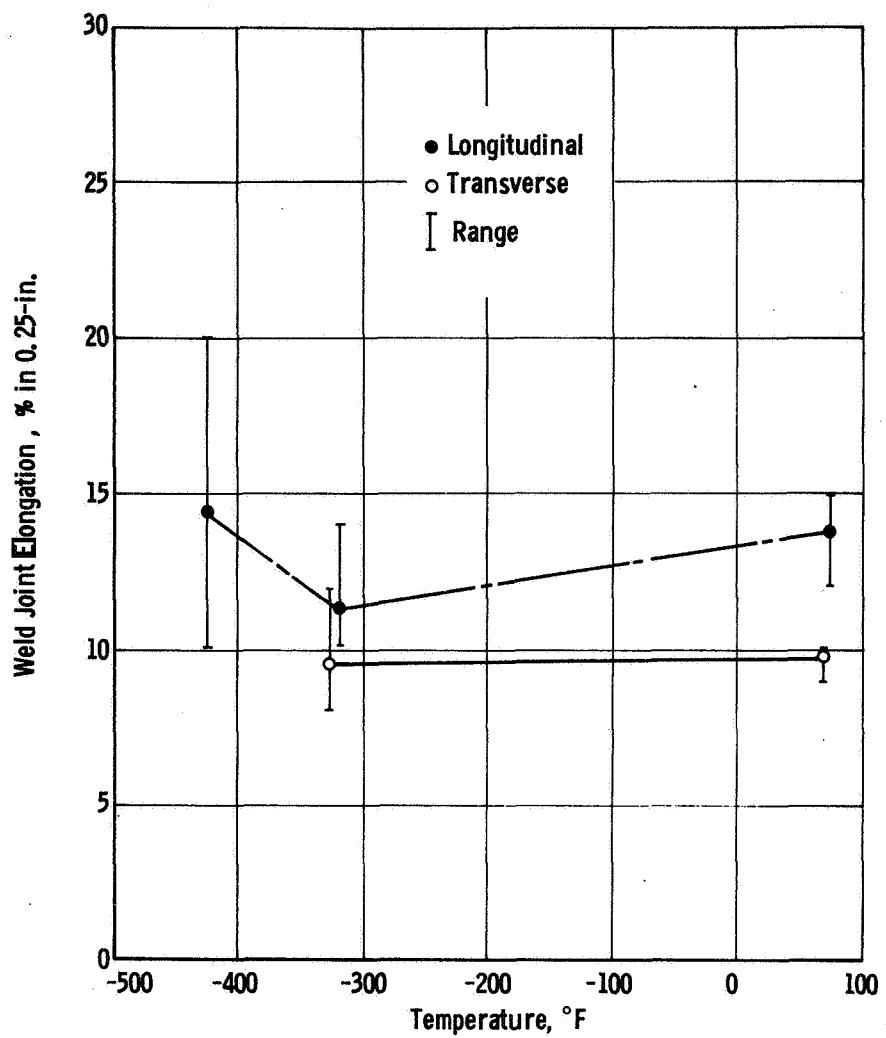


Figure A-6



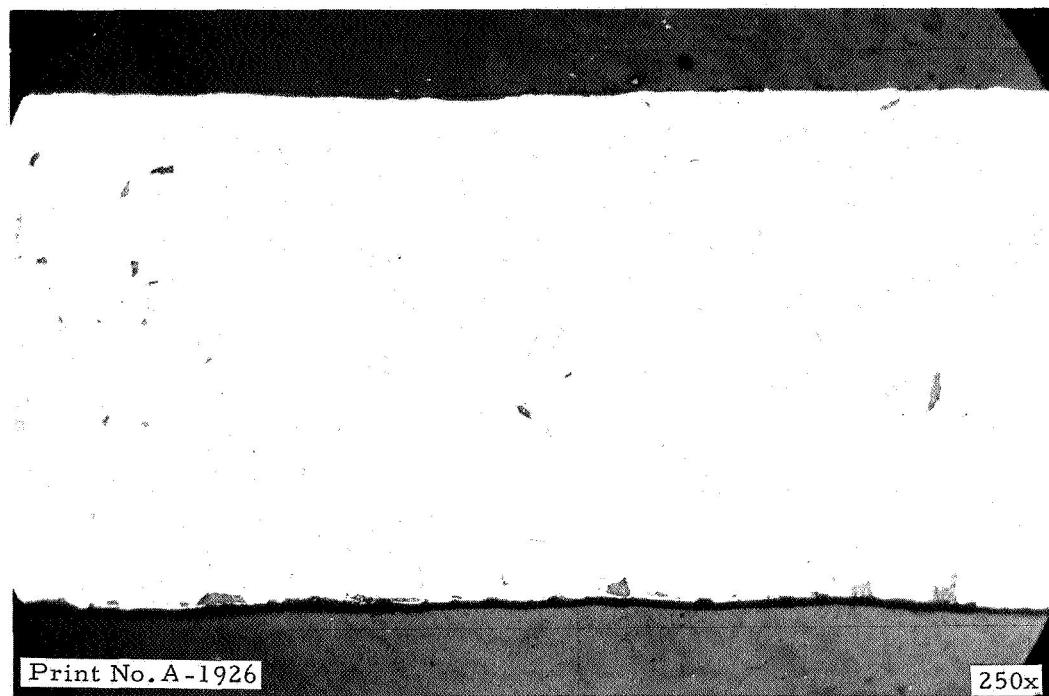
TENSILE AND YIELD STRENGTH OF 6061-0 ALUMINUM ALLOY, TIG BUTT FUSION WELDED
WITH 1100 ALUMINUM FILLER WIRE, BENEFICIATED AFTER WELDING, CHEMICALLY
MILLED FROM 0.030 TO 0.010-IN. THICKNESS

Figure A-7



ELONGATION OF 6061-0 ALUMINUM ALLOY, TIG BUTT FUSION WELDED
WITH 1100 ALUMINUM FILLER WIRE, BENEFICIATED AFTER WELDING,
CHEMICALLY MILLED FROM 0.030 TO 0.010-IN. THICKNESS

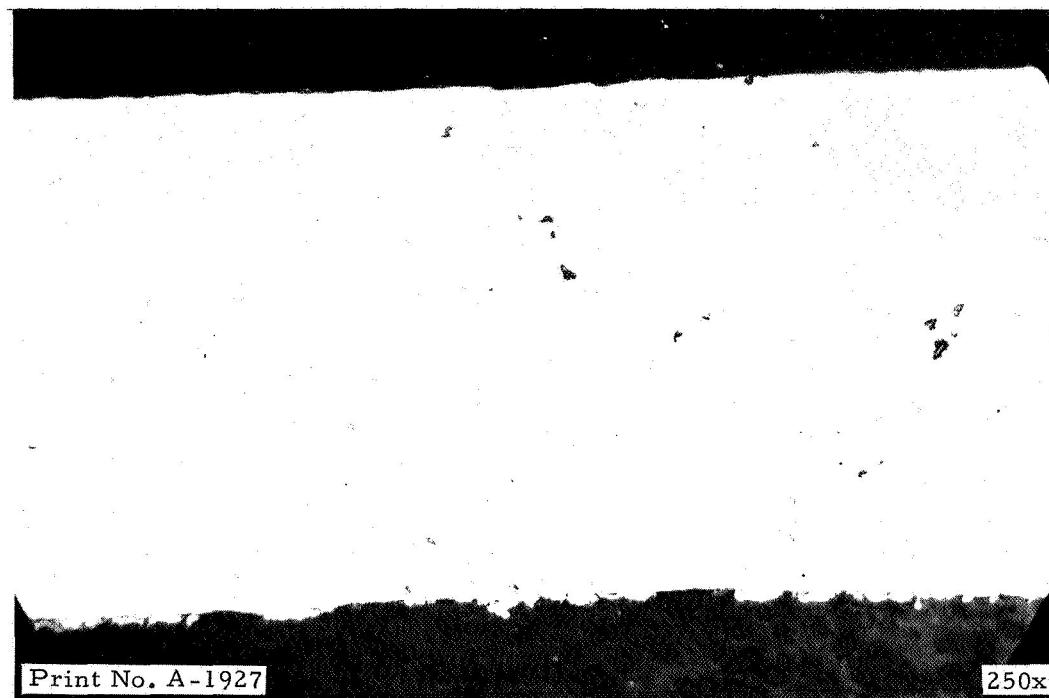
Figure A-8



SECTION OF 1100 ALUMINUM 0.010-IN. MEMBRANE
SHOWING UNIFORM EDGE ATTACK BY CHEMICAL
MILLING SOLUTION - UNETCHED

10-067-115-

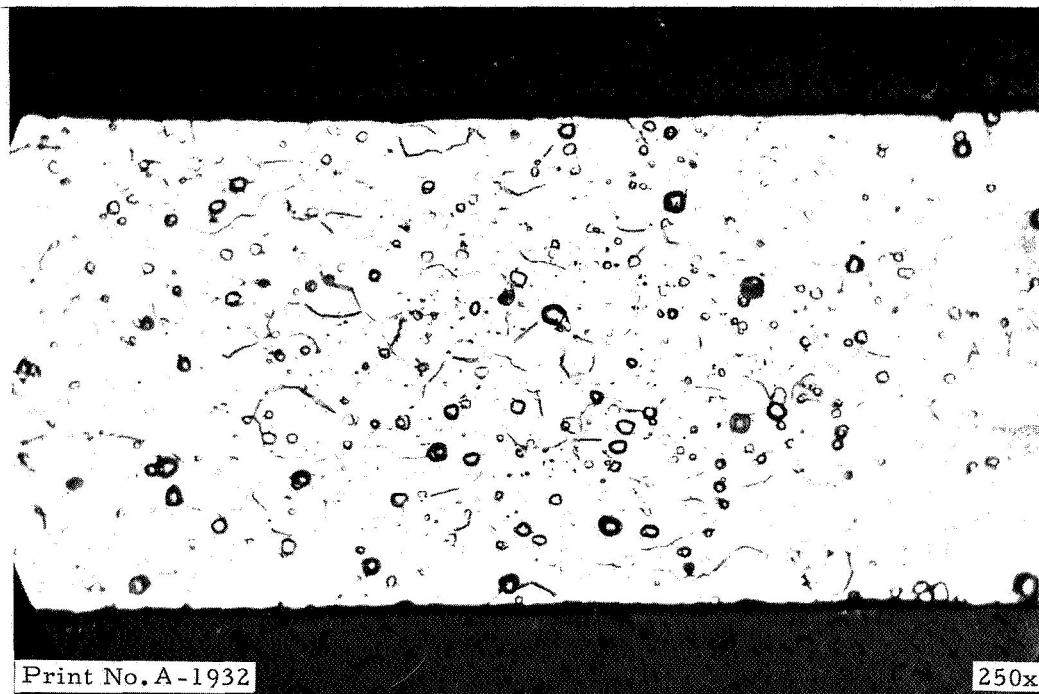
Figure A-9



**SECTION OF 1100 ALUMINUM 0.010-IN. MEMBRANE
SHOWING EVIDENCE OF SOME LOCALIZED INTERGRANULAR ATTACK
BY CHEMICAL MILLING SOLUTION - UNETCHED**

10-067-118-

Figure A-10



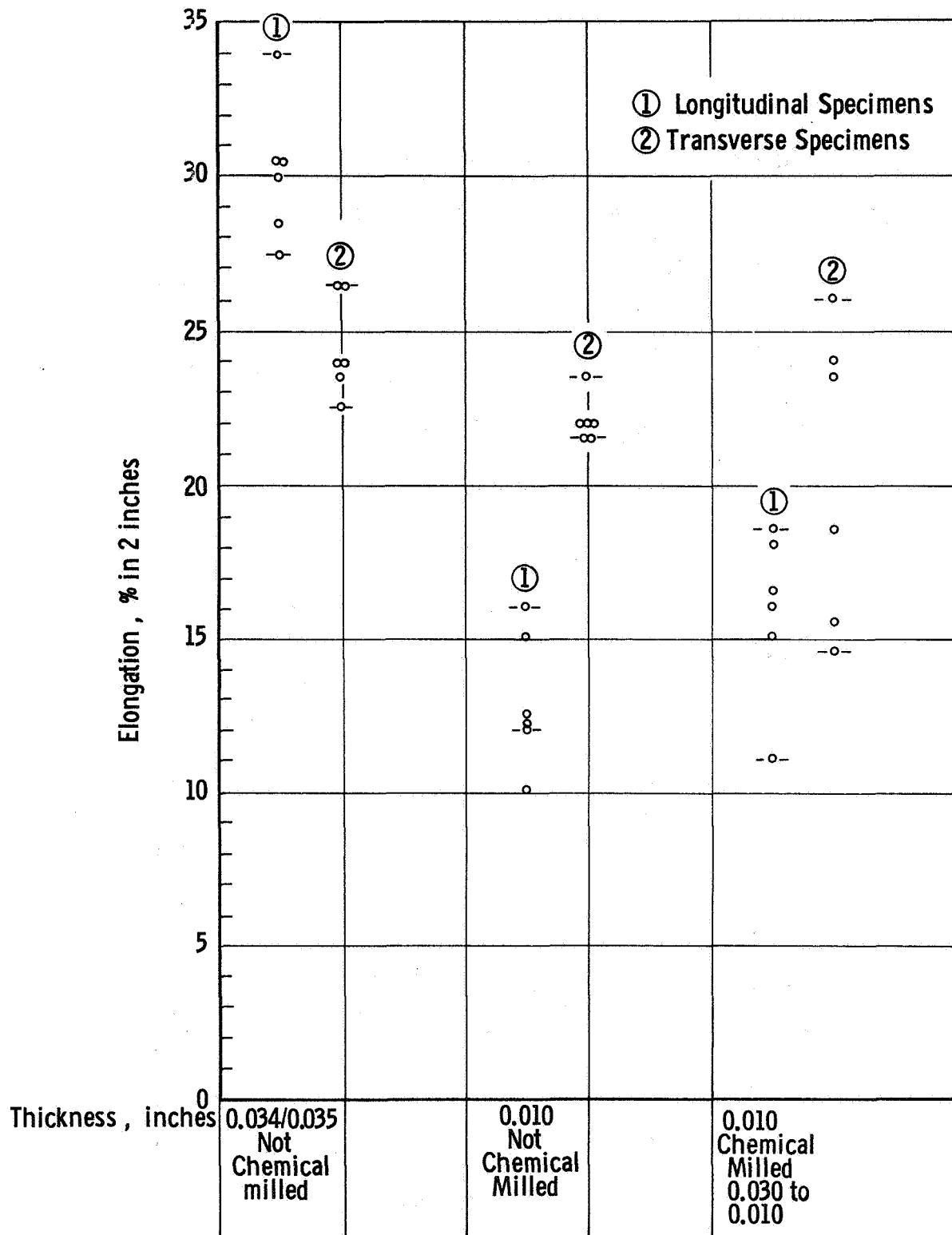
Print No. A-1932

250x

SECTION OF 1100 ALUMINUM 0.010-IN. MEMBRANE
SHOWING EVIDENCE OF SLIGHT INTERGRANULAR ATTACK
BY CHEMICAL MILLING SOLUTION - ETCHANT - 10% NaOH

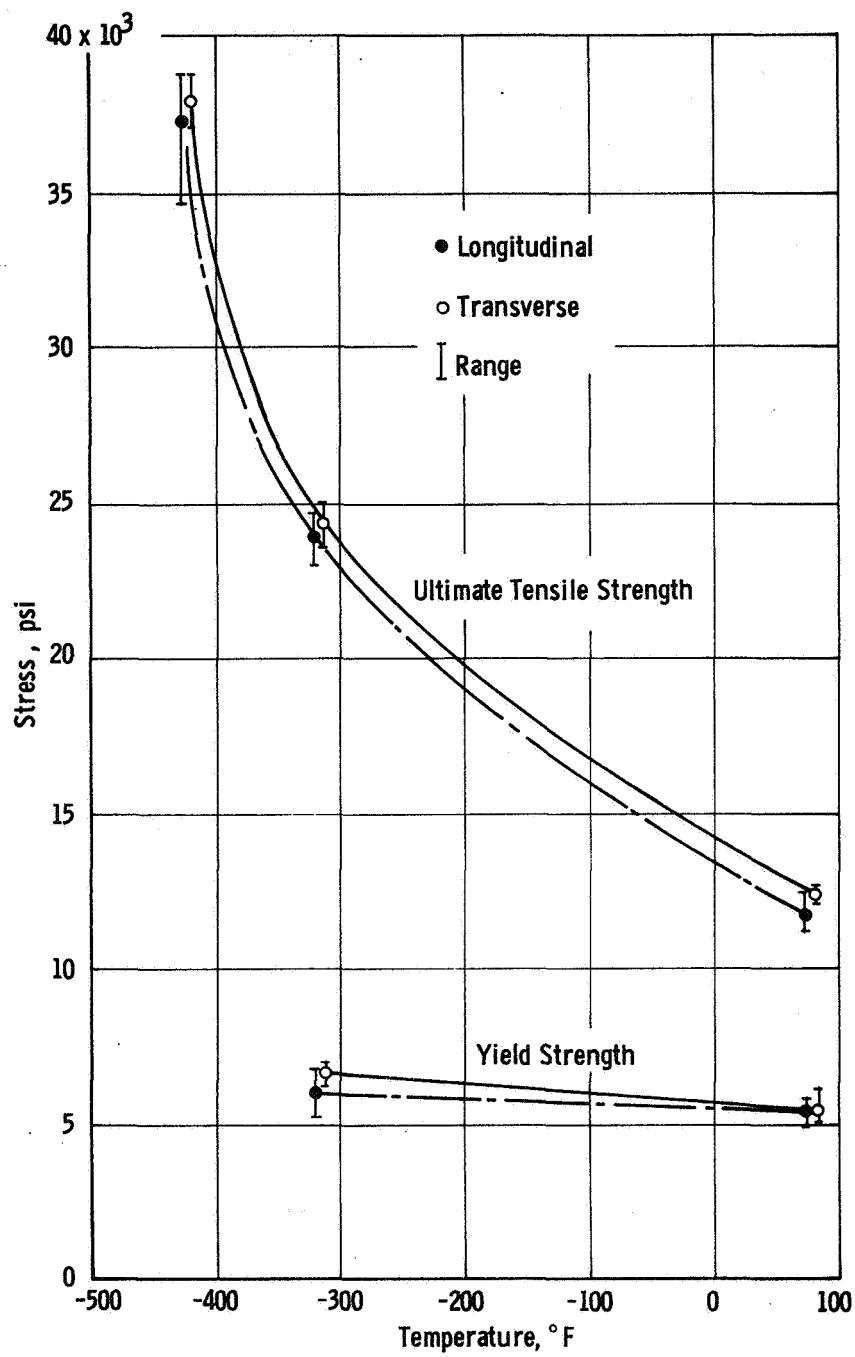
10-067-118-

Figure A-11

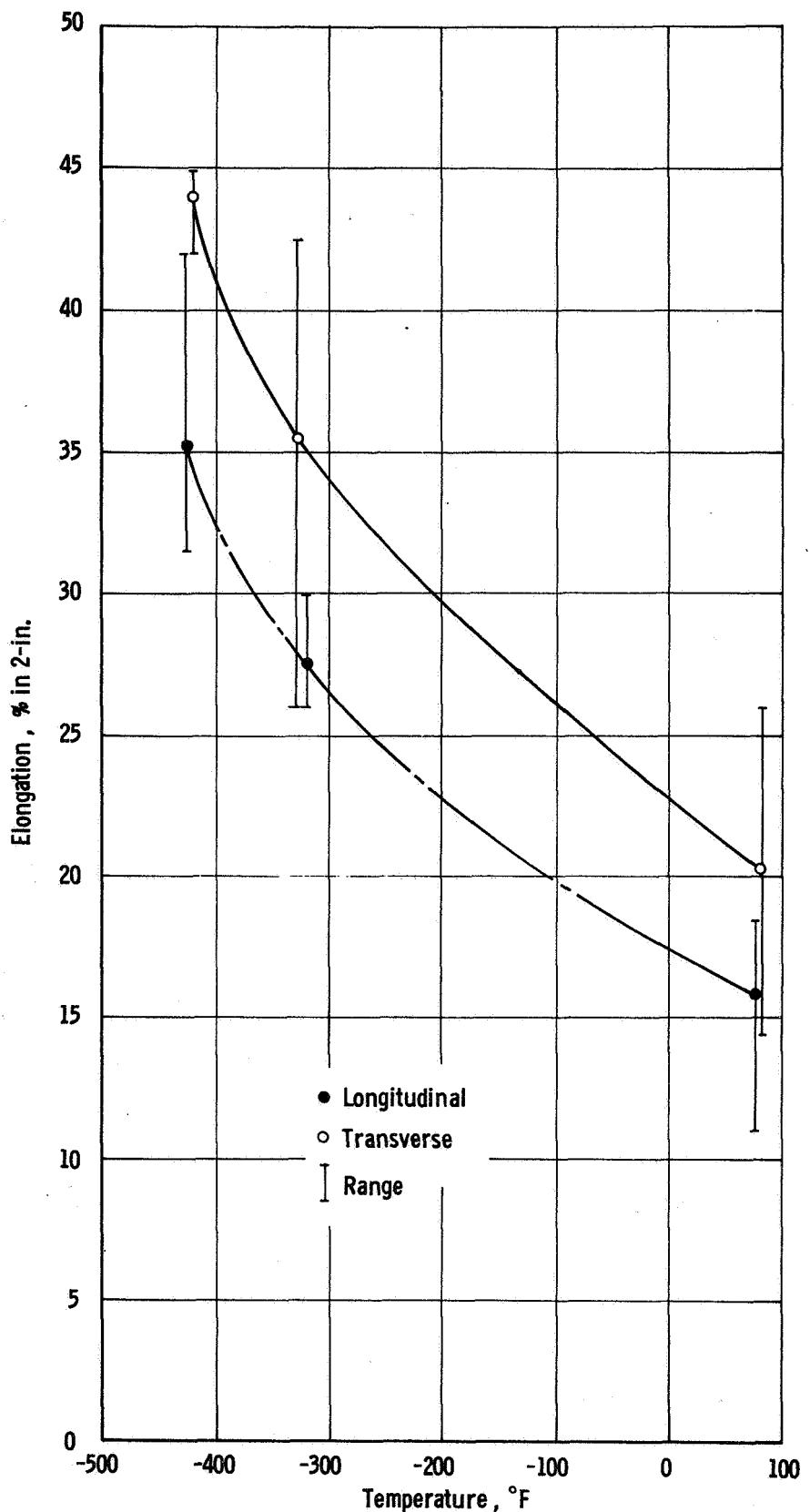


EFFECT OF PROCESSING ON ELONGATION OF 1100 ALUMINUM

Figure A-12

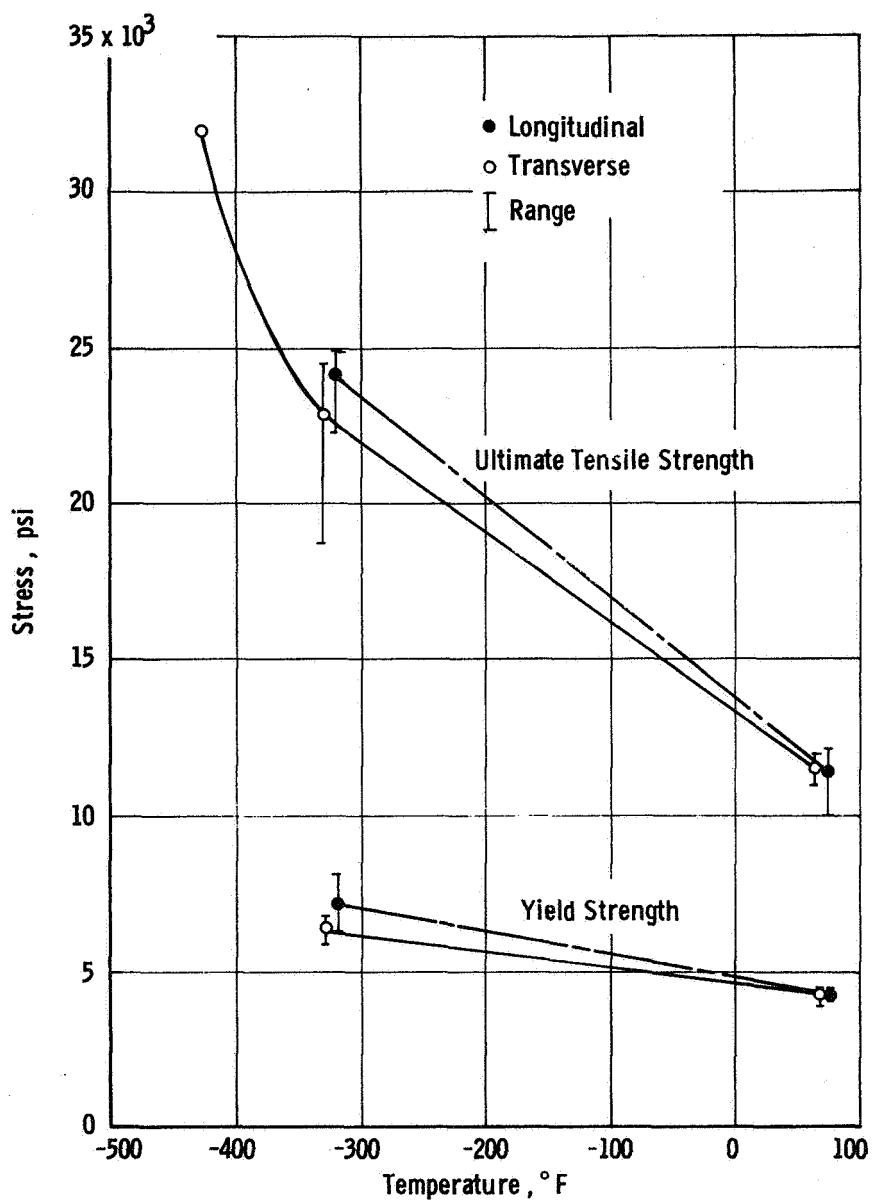


TENSILE AND YIELD STRENGTH OF 1100-O ALUMINUM PARENT METAL,
CHEMICALLY MILLED FROM 0.030 TO 0.010-IN. THICKNESS



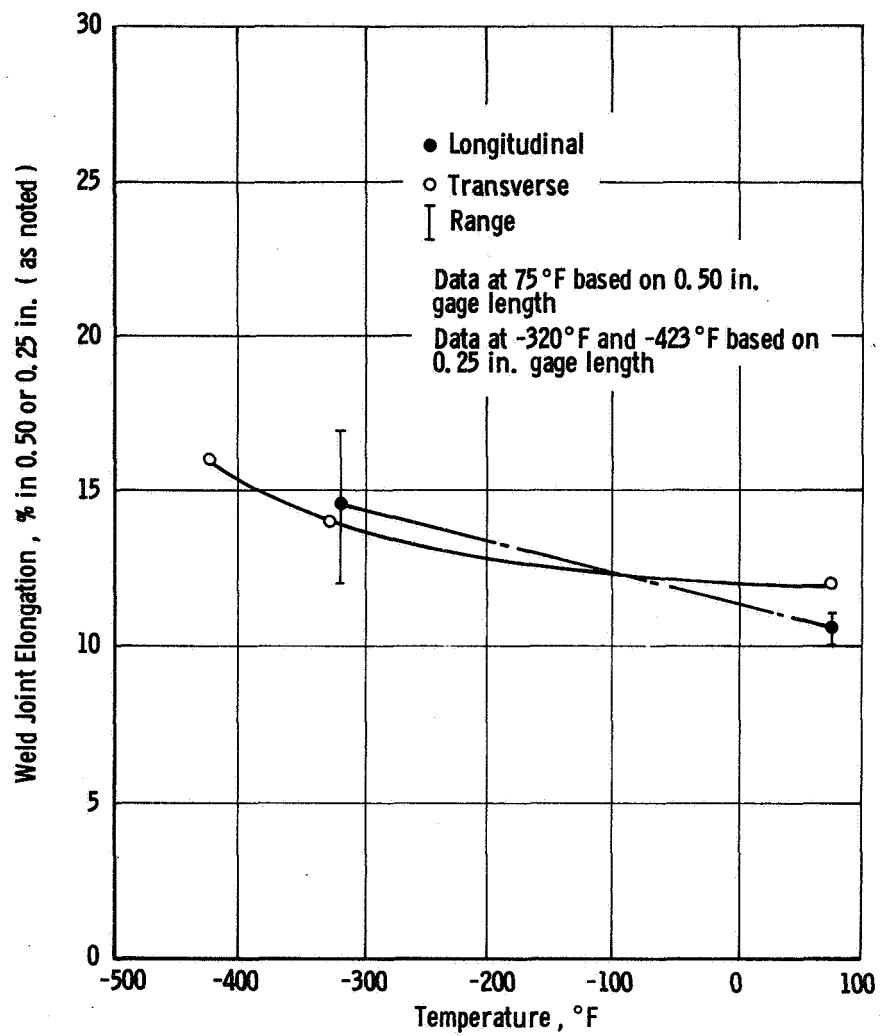
ELONGATION OF 1100-O ALUMINUM ALLOY PARENT METAL, CHEMICALLY MILLED
FROM 0.030 TO 0.010-IN. THICKNESS

Figure A-14



TENSILE AND YIELD STRENGTHS OF 1100-O ALUMINUM, TIG BUTT FUSION WELDED WITH 1100 ALUMINUM FILLER WIRE, BENEFICIATED AFTER WELDING, CHEMICALLY MILLED FROM 0.030 TO 0.010-IN. THICKNESS

Figure A-15



ELONGATION OF 1100-O ALUMINUM, TIG BUTT FUSION WELDED WITH
1100 ALUMINUM FILLER WIRE, BENEFICIATED AFTER WELDING,
CHEMICALLY MILLED FROM 0.030 TO 0.010-IN. THICKNESS

Figure A-16

APPENDIX B

DESIGN ANALYSIS OF PRESSURE-VESSEL MEMBRANE, HEAD-TO-CYLINDER JUNCTURE, WINDING PATTERN, AND METAL BOSSES*

I. CRITERIA

Two 12-in.-dia. by 18-in.-long aluminum-lined glass-filament-wound pressure vessel designs were prepared in accordance with the criteria listed in Section II-A of the main text.

II. DESIGN ALLOWABLE GLASS-FILAMENT STRENGTH

Aerojet/SCI has developed a systematic approach to the design of filament-wound vessels (Reference B-1, B-2, and B-3) and is using it in a number of applications. The method involves the use of pressure-vessel design factors, corresponding to a range of dimensional parameters, to determine the allowable strength for each configuration. The factors are based on data collected over the past 7 years from tests on several thousands of pressure vessels; these vessels ranged in diameter from 4 to 74 in. and had significant variations in their design parameters. Included as factors used for the selection of design-allowable values are the strength of the glass roving, resin content, envelope dimensions (length and diameter), internal pressure level, axial port diameters, temperature, sustained loading requirements, and cyclic loading requirements. The method was used in this analysis to establish realistic values for the allowable ultimate 75°F S-HTS glass-filament tensile strengths in the 12-in.-dia. by 18-in.-long aluminum-lined filament-wound test vessel.

A. LONGITUDINAL FILAMENTS

The allowable longitudinal-filament strength is given by

$$F_{f,1} = K_1 K_2 K_3 K_4 K_5 (\sec^2 \alpha) F_f$$

Symbols for this section are defined at the end of this appendix.

*

Presentation of these calculations in both S.I. and English systems would reduce the clarity of this Appendix. The English system only is used.

The following design factors (Reference B-3) are based on the specific vessel parameters:

<u>Parameter</u>	<u>Design Factor</u>
$D_c = 12.00 \text{ in.}$	0.815 (K_1)
$D_b/D_c = 0.11$	1.015 (K_2)
$L/D_c = 1.5$	1.000 (K_3)
$t_{f,1}/D_c \approx 0.00235$	0.920 (K_4)
$T = 75^\circ\text{F}$	1.000 (K_5)
$\alpha = 4^\circ$ (from geometry of vessel)	

For S-HTS glass filaments, the minimum ultimate tensile strength, F_f , is 415,000 psi.

The single-pressure-cycle allowable ultimate longitudinal filament strength is therefore

$$F_{f,1} = (0.815) (1.015) (1.000) (0.920) (1.000) (1.004) (415,000) \\ = 316,000 \text{ psi}$$

B. HOOP FILAMENTS

The allowable hoop-filament strength is given by

$$F_{f,h} = K_1 K_4 K_5 \left(1 - \frac{\tan^2 \alpha}{2}\right) F_f$$

The following design factors are based on the specific vessel parameters

<u>Parameter</u>	<u>Design Factor</u>
$D_c = 12.00 \text{ in.}$	0.890 (K_1)
$t_{f,h}/D_c \approx 0.00424$	0.960 (K_4)
$T = 75^\circ\text{F}$	1.000 (K_5)
$\alpha = 4^\circ$	

The single-pressure-cycle allowable ultimate hoop filament strength is therefore

$$F_{f,h} = (0.890) (0.960) (1.000) (1.000) \left[1 - \frac{0.00489}{2}\right] 415,000 \\ = 354,000 \text{ psi}$$

III. MEMBRANE ANALYSIS

A. METHOD

The vessel shape and component thicknesses were established with the previously developed computer program for analysis of metal-lined filament-wound pressure vessels (Reference B-4). The program was used to investigate the filament shell by means of a netting analysis, which assumes constant stresses along the filament path and that the resin matrix makes a negligible structural contribution. The filament and metal shells are combined by equating strains in the longitudinal and hoop directions and by adjusting the shell radii of curvature to match the combined material strengths at the design pressure.

The program established the optimum head contour and defined the component thicknesses and other dimensional coordinates, as well as the shell stresses and strains at zero pressure and the design pressure, the filament-path length, and the weight and volume of the components and complete vessel. It was also used to determine the stresses and strains in the two shells during vessel operation through the use of a series of pressures and temperatures.

B. COMPUTER INPUT AND OUTPUT

Input variables used for the computer pressure vessel design analysis are presented in Table B-1. The computer output described the pressure vessel membrane shape, component thickness and weights, and stress and strain conditions. The portions of the liner configuration and pressure vessel configuration dealing with the pressure vessel membrane are taken from the computer output, except as noted below.

The longitudinal filament-wound composite thickness requirements computed for the test vessels, based on a minimum allowable ultimate longitudinal filament stress of 316,000 psi and a design burst pressure of 3000 psig at 75° F, are the following:

Longitudinal Filament-Wound Composite Thickness in Cylinder (t_L)	0.042 in.
--	-----------

Equivalent Filament Thickness in Longitudinal Direction of Cylinder ($t_{f,1}$)	0.028 in.
--	-----------

The computerized analysis used the same allowable for the hoop filaments as for the longitudinal filaments (i.e., 316,000 psi), and the hoop filament-wound composite thickness requirements were computed to be the following:

Hoop Filament-Wound	0.084 in.
Composite Thickness in Cylinder (t_H)	

Equivalent Filament Thickness in Hoop Direction of Cylinder ($t_{f,h}$)	0.057 in.
--	-----------

Because the actual hoop filament minimum allowable ultimate stress, $F_{f,h}$, is 354,000 psi, the hoop wound composite thickness from the computer analysis, t_H , was reduced to bring the hoop filament stress up to 354,000 psi in order to obtain a balanced design with equal probability of failure in the hoop and longitudinal filaments. The load carried by the hoop filaments of the computer analysis is

$$F_{f,h} t_H = (316,000 \text{ psi}) (0.084 \text{ in.})$$

The new hoop-wound composite thickness, t'_H , required to develop a stress in the hoop filaments of 354,000 psi is given by

$$t'_H = \frac{316,000}{354,000} (0.084 \text{ in.}) = 0.075 \text{ in.}$$

This hoop-wound composite thickness is reflected in the vessel design shown in Figure 7 of the main text.

IV. HEAD-TO-CYLINDER JUNCTURE DISCONTINUITY ANALYSIS

A. OBJECTIVE

The purpose of this section of the report is to provide a discontinuity stress analysis of the head-to-cylinder juncture to establish the validity of the design shown in Figure 7 of the main text.

B. SUMMARY

Only the section at the juncture of the head-to-cylinder, shown schematically in Figure B-1, was considered in this analysis. Calculations indicate a maximum longitudinal composite stress of 213,300 psi (filament stress of 318,500 psi), which is 0.8% greater than the allowable design stress. This stress occurs in the cylindrical section approximately 0.1 inch from the tangent plane.

C. ANALYSIS

Since the meridional radius of curvature of the head changes very slowly in the area adjacent to the juncture of the head and cylinder, the head may be considered cylindrical at the discontinuity. Equations for the deflection and rotation at the head-cylinder juncture are taken from Reference B-5, cases 14 and 15, page 302. The deflection of the cylinder is

$$\delta_c = \delta_{cp} - \frac{V_o}{2D_c \lambda_c^3} - \frac{M_o}{2D_c \lambda_c^2}$$

and, the rotation of the cylinder is

$$\theta_c = \frac{V_o}{2D_c \lambda_c^2} + \frac{M_o}{D_c \lambda_c}$$

Deflection of the head is

$$\delta_h = \delta_{hp} + \frac{V_o}{2D_h \lambda_h^3} - \frac{M_o}{2D_h \lambda_h^2}$$

and, the rotation of the head is

$$\theta_h = \frac{V_o}{2D_h \lambda_h^2} - \frac{M_o}{D_h \lambda_h}$$

The following relationships are used to adapt the deflection and rotation equations to filament-wound cylinders:

1. Composite Beam Properties

a. Modulus

The composite modulus in the longitudinal direction is

$$E_L = \frac{E_{LL} t_L + E_{LM} t_M + E_{LH} t_H}{t_L + t_M + t_H}$$

where,

$$t_L = 0.042 \text{ in. (from Figure 7 of main text)}$$

$$t_M = 0.010 \text{ in.}$$

$$t_H = 0.075 \text{ in. (cylinder only, Figure 7 of main text)}$$

$$E_{LH} = 0.0 \text{ (resin crazes)}$$

The modulus of the longitudinal composite in the longitudinal direction (E_{LL}) is calculated from the following expression

$$E_{LL} = P_{vg} E_f \cos^2 \alpha_0$$

and with

$$E_f = 12.4 \times 10^6 \text{ psi (S-HTS glass filaments)}$$

$$P_{vg} = 0.673$$

$$\alpha_0 = 3.82^\circ \text{ (from computer analysis)}$$

$$E_{LL} = 0.673 (12.4 \times 10^6) (0.9956)$$

$$= 8.313 \times 10^6 \text{ psi}$$

Since the liner is strained beyond its yield stress, an effective modulus, based on total vessel strain, is used for the liner.

$$E_{LM} = \sigma_M (1 - \nu_M) \left(\frac{E_f}{\sigma_f, l} \right)$$

Where,

$$\nu_M = 0.325 \text{ for aluminum}$$

$$\sigma_f, l = 316,000 \text{ psi for S-HTS glass filaments at 3000 psi internal pressure}$$

$$\sigma_M = 13,400 \text{ psi (from computer analysis)}$$

$$E_{LM} = 13,400 (1-0.325) \left(\frac{12.4 \times 10^6}{316,000} \right)$$
$$= 0.355 \times 10^6 \text{ psi}$$

The composite modulus in the longitudinal direction for the cylinder is

$$E_{Lc} = \frac{8.313 \times 10^6 (0.42) + 0.355 \times 10^6 (0.010)}{0.042 + 0.010 + 0.075}$$
$$= 2.777 \times 10^6 \text{ psi}$$

and, for the head

$$E_{Lh} = \frac{8.313 \times 10^6 (0.042) + 0.355 \times 10^6 (0.010)}{0.042 + 0.010}$$
$$= 6.783 \times 10^6 \text{ psi}$$

The composite modulus in the hoop direction is

$$E_H = \frac{E_{HH} t_H + E_{HM} t_M + E_{HL} t_L}{t_L + t_M + t_H}$$

where,

$$\begin{aligned} E_{HH} &= P_{vg} E_f \\ &= 0.673 (12.4 \times 10^6) \\ &= 8.35 \times 10^6 \text{ psi} \end{aligned}$$

and

$$\begin{aligned} E_{HL} &= K E_f \sin^2 \alpha_0 \\ &= 0.673 (12.4 \times 10^6) (0.00443) \\ &= 0.037 \times 10^6 \text{ psi} \end{aligned}$$

The effective modulus of the liner in the hoop direction is

$$E_{HM} = \sigma_M (1 - \nu_M) \left(\frac{E_f}{\sigma_{f,h}} \right)$$

with,

$$\sigma_{f,h} = 354,000 \text{ psi for S-HTS hoop glass filaments at 3000 psi internal pressure}$$

$$\begin{aligned} E_{HM} &= 13,400 (1 - 0.325) \left(\frac{12.4 \times 10^6}{354,000} \right) \\ &= 0.317 \times 10^6 \text{ psi} \end{aligned}$$

The composite modulus in the hoop direction for the cylinder is

$$\begin{aligned} E_{Hc} &= \frac{8.35 \times 10^6 (0.075) + 0.317 \times 10^6 (0.010) + 0.037 \times 10^6 (0.042)}{0.042 + 0.010 + 0.075} \\ &= 4.968 \times 10^6 \text{ psi} \end{aligned}$$

and, for the head

$$\begin{aligned} E_{Hh} &= \frac{0.317 \times 10^6 (0.010) \times 0.037 \times 10^6 (0.042)}{0.042 + 0.010} \\ &= 0.091 \times 10^6 \text{ psi} \end{aligned}$$

b. Neutral Axis

The neutral axis of the cylinder is

$$\bar{Y}_c = \frac{E_{LL} t_L (t_M + t_L/2) + E_{LM} (t_M)^2/2}{(t_L + t_M + t_H) E_{Lc}}$$

$$\bar{Y}_c = \frac{8.313 \times 10^6 (0.042)(0.031) + 0.355 \times 10^6 (0.01)^2/2}{0.127 (2.777 \times 10^6)}$$

$$\bar{Y}_c = 0.031 \text{ in.}$$

and, for the head

$$\bar{Y}_h = \frac{E_{LL} t_L (t_M + t_L/2) + E_{LM} (t_M)^2/2}{(t_M + t_L) E_{Lh}}$$

$$\bar{Y}_h = \frac{8.313 \times 10^6 (0.042)(0.031) + 0.355 \times 10^6 (0.01)^2/2}{0.052 (6.783 \times 10^6)}$$

$$\bar{Y}_h = 0.031 \text{ in.}$$

c. Flexural Rigidity

The flexural rigidity is calculated from the equation

$$D = E_L I = \frac{1}{12} \left(t_M^3 E_{LM} + t_L^3 E_{LL} + t_H^3 E_{LH} \right)$$

$$+ t_M \left[\bar{Y} - t_M/2 \right]^2 E_{LM} + t_L \left[\bar{Y} - (t_M + t_L/2) \right]^2 E_{LL}$$

$$+ t_H \left[\bar{Y} - (t_M + t_L + t_H/2) \right]^2 E_{LH}$$

Since $\bar{Y}_c = \bar{Y}_h$, the head and cylinder flexural rigidities are

$$D_c = D_h = \frac{(0.01)^3 0.355 \times 10^6 + (0.042)^3 8.313 \times 10^6}{12}$$

$$+ 0.01 (0.031 - .005)^2 0.355 \times 10^6 = 53.753 \text{ lb-in.}$$

d. Stiffness

The modulus of the beam foundation (stiffness) is

$$k = \frac{E_H (t_L + t_M + t_H)}{R_2^2}$$

where,

$$R_2 = R = 6.00 \text{ in. (from computer analysis)}$$

For the cylinder

$$\begin{aligned} k_c &= \frac{4.968 \times 10^6 (0.127)}{(6)^2} \\ &= 17,530 \text{ lb/in.}^3 \end{aligned}$$

and for the head

$$\begin{aligned} k_h &= \frac{0.091 \times 10^6 (0.052)}{(6)^2} \\ &= 131.4 \text{ lb/in.}^3 \end{aligned}$$

e. Beam Characteristic

The beam characteristic (λ) is defined to be

$$\lambda^4 = \frac{k}{4D}$$

For the cylinder

$$\lambda_c^4 = \frac{17,530}{4(53.753)} = 81.53 \text{ in.}^{-1}$$

and for the head

$$\lambda_h^4 = \frac{131.4}{4(53.753)} = 0.6111 \text{ in.}^{-1}$$

2. Radial Membrane Deflections

a. Cylinder

$$\delta_{c_p} = \frac{pR^2}{E_H (t_M + t_L + t_H)}$$

With $p = 3000$ psi

$$\delta_{c_p} = \frac{3000 (6)^2}{4.968 \times 10^6 (0.127)} = 0.1712 \text{ in.}$$

b. Head

$$\delta_{H_p} = \frac{pR_2^2 (2 - R_2/R_1)}{2E_{H_h} (t_M + t_L)}$$

With $1/R_1 = 0.331 \text{ in.}^{-1}$

$$\begin{aligned} \delta_{H_p} &= \frac{3000 (6)^2 [2-6(0.331)]}{2(0.091 \times 10^6)(0.052)} \\ &= 0.1598 \text{ in.} \end{aligned}$$

3. Discontinuity Forces and Moments

a. Head-to-Cylinder Juncture

The discontinuity force and moment at the juncture of the head to cylinder may be found by matching head and cylinder rotation and deflection. The deflection of the cylinder is

$$\begin{aligned} \delta_c &= 0.1712 - \frac{V_o}{2(53.75)(27.13)} - \frac{M_o}{2(53.75)(9.029)} \\ \delta_c &= 0.1712 - 0.00034 V_o - 0.00103 M_o \end{aligned}$$

and the rotation of the cylinder is

$$\begin{aligned} \theta_c &= \frac{V_o}{2(53.75)(9.029)} + \frac{M_o}{53.75(3.005)} \\ \theta_c &= 0.00103 V_o + 0.00619 M_o \end{aligned}$$

The deflection of the head is

$$\delta_h = 0.1598 + \frac{V_o}{2(53.75)(0.6912)} - \frac{M_o}{2(53.75)(0.7817)}$$

$$\delta_h = 0.1598 + 0.01345 V_o - 0.1190 M_o$$

and the rotation of the head is

$$\theta_h = \frac{V_o}{2(53.75)(0.7817)} - \frac{M_o}{53.75(0.8841)}$$

$$\theta_h = 0.01190 V_o - 0.02104 M_o$$

Equating rotations and deflections yields

$$M_o = \left\{ \frac{0.01190 - 0.00103}{0.00619 + 0.02104} \right\} V_o$$

$$M_o = 0.39919 V_o$$

and

$$V_o = \frac{(0.1712 - 0.1598) + (0.01190 - 0.00103) M_o}{0.01345 + 0.00034}$$

$$V_o = 0.82668 + 0.78825 M_o$$

Simultaneous solution of the two equations yields

$$V_o = \frac{0.82668}{1 - 0.39919(0.78825)} = 1.206 \text{ lb/in.}$$

and

$$M_o = 0.39919 (1.206) = 0.481 \text{ in.-lb/in.}$$

b. Bending Moment Distribution

The bending moment distribution in the cylinder, including the moment due to shear, is calculated from the expression

$$M_c(Y) = e^{-\lambda_c Y} \left[M_o \cos \lambda_c Y + \left(M_o + \frac{V_o}{\lambda_c} \right) \sin \lambda_c Y \right]$$

and for the head

$$M_h(Y) = e^{-\lambda_h Y} \left[M_o \cos \lambda_h Y + \left(M_o - \frac{V_o}{\lambda_h} \right) \sin \lambda_h Y \right]$$

Results of calculations based on these equations are shown in Figure B-2. It can be seen that the maximum bending moment occurs in the cylinder approximately 0.10 in. from the tangency plane.

4. Maximum Stress

The maximum stress occurs in the longitudinal composite and is a combination of membrane and bending stresses. The longitudinal composite stress resulting from pressure is

$$\sigma_{LL_p} = P_{vg} \sigma_f, l \cos^2 \alpha_o$$

where,

$$\begin{aligned}\sigma_{LL_p} &= 0.673 (316,000)(0.9955) \\ &= 211,600 \text{ psi}\end{aligned}$$

The maximum tensile bending stress in the outside fibers of the longitudinal composite is

$$\begin{aligned}\sigma_{LL_B} &= \frac{M_y}{I_c} \left(\frac{E_{LL}}{E_L} \right)_c = \frac{M E_{LL}}{D_c} (\bar{Y} - t_M) \\ \sigma_{LL_B} &= \frac{0.535(8.313 \times 10^6)(0.031-0.010)}{53.75} \\ \sigma_{LL_B} &= 1740 \text{ psi}\end{aligned}$$

and the maximum combined (tensile) stress is

$$\begin{aligned}\sigma_{LL} &= \sigma_{LL_p} + \sigma_{LL_B} \\ \sigma_{LL} &= 211,600 + 1740 \\ \sigma_{LL} &= 213,340 \text{ psi}\end{aligned}$$

This longitudinal composite stress is equivalent to a longitudinal filament stress of 318,500 psi, which is 0.8% higher than the 316,000 psi allowable stress used for computer analysis of the membrane.

V. WINDING PATTERN ANALYSIS

The filament-wound vessel has two winding patterns: a longitudinal-in-plane pattern along the cylinder and over the end domes to provide the total

filament-wound composite strength in the heads and the longitudinal strength in the cylindrical section; and a circumferential pattern applied along the cylinder for hoop strength in this section.

The winding pattern for the pressure vessel requires the application of a specific quantity of glass roving in predetermined orientations in order to obtain the desired burst pressure. The pressure vessel membrane analysis of Section III-B showed that the required filament-wound composite and equivalent glass-filament thicknesses are the following:

	<u>Thickness, in.</u>
Longitudinal filament-wound composite thickness in cylinder	0.042
Equivalent filament thickness in longitudinal direction of cylinder	0.028
Hoop filament-wound composite thickness in cylinder	0.075
Equivalent filament thickness in hoop direction of cylinder	0.051

A. LONGITUDINAL PATTERN

The pattern is analyzed here on the basis of actual winding data and laboratory tests of glass roving and composite specimens, which have shown that a cured single layer of 20-end roving created by side-by-side orientation has a thickness ($t_{s,1}$) of 0.007 in.

The required number of layers of longitudinal winding (L_L) to make up the longitudinal composite thickness (T_L) is given by

$$L_L = \frac{T_L}{t_{s,1}} = \frac{0.042}{0.007} = 6 \text{ layers}$$

Two layers are formed for each revolution of the winding mandrel. The number of revolutions required (N_1) is therefore

$$N_1 = \frac{L_L}{2} = \frac{6}{2} = 3 \text{ revolutions}$$

The winding-tape width (W_L) is given by

$$W_L = \frac{N_2 A}{t_{s,1} P_{vg}}$$

where

N_2 = number of 20-end roving strands per tape, selected as 3

A = cross section of 20-end roving = 420×10^{-6} in.²

P_{vg} = glass-filament fraction in composite = 0.673

Thus,

$$w_L = \frac{(3)(420 \times 10^{-6})}{(0.007)(0.673)} = 0.268 \text{ in.}$$

The number of turns per revolution (N_3) must be an integer, and is given by

$$N_3 = \frac{\pi D_c \cos \alpha}{w_L + \epsilon_{t_p}} \quad \text{to the nearest integer}$$

where

D_c = vessel diameter = 12.00 in.

α = longitudinal in-plane winding angle = 3.82°

ϵ_{t_p} = space between tapes (which should equal zero)

Therefore,

$$N_3 = \frac{\pi (12.00)(0.998)}{0.268} = 140 \text{ turns per revolution}$$

B. Hoop Pattern

The required number of layers of hoop winding to make up the hoop composite thickness (t_H) is given by

$$L_H = \frac{t_H}{t_{s,h}}$$

where

$t_{s,h}$ = thickness of single cured layer of hoop winding

In this case $t_{s,h}$ may be set equal to 0.0075 in.

Then

$$L_H = \frac{0.075}{0.0075} = 10 \text{ layers}$$

The number of turns per inch of cylinder length (N_5) is given by

$$N_5 = \frac{L_c t_{s,h} P_{vg}}{N_4 A}$$

where

L_c = cylinder length, selected as 1 in.

N_4 = number of 20-end roving strands per tape, selected as 1

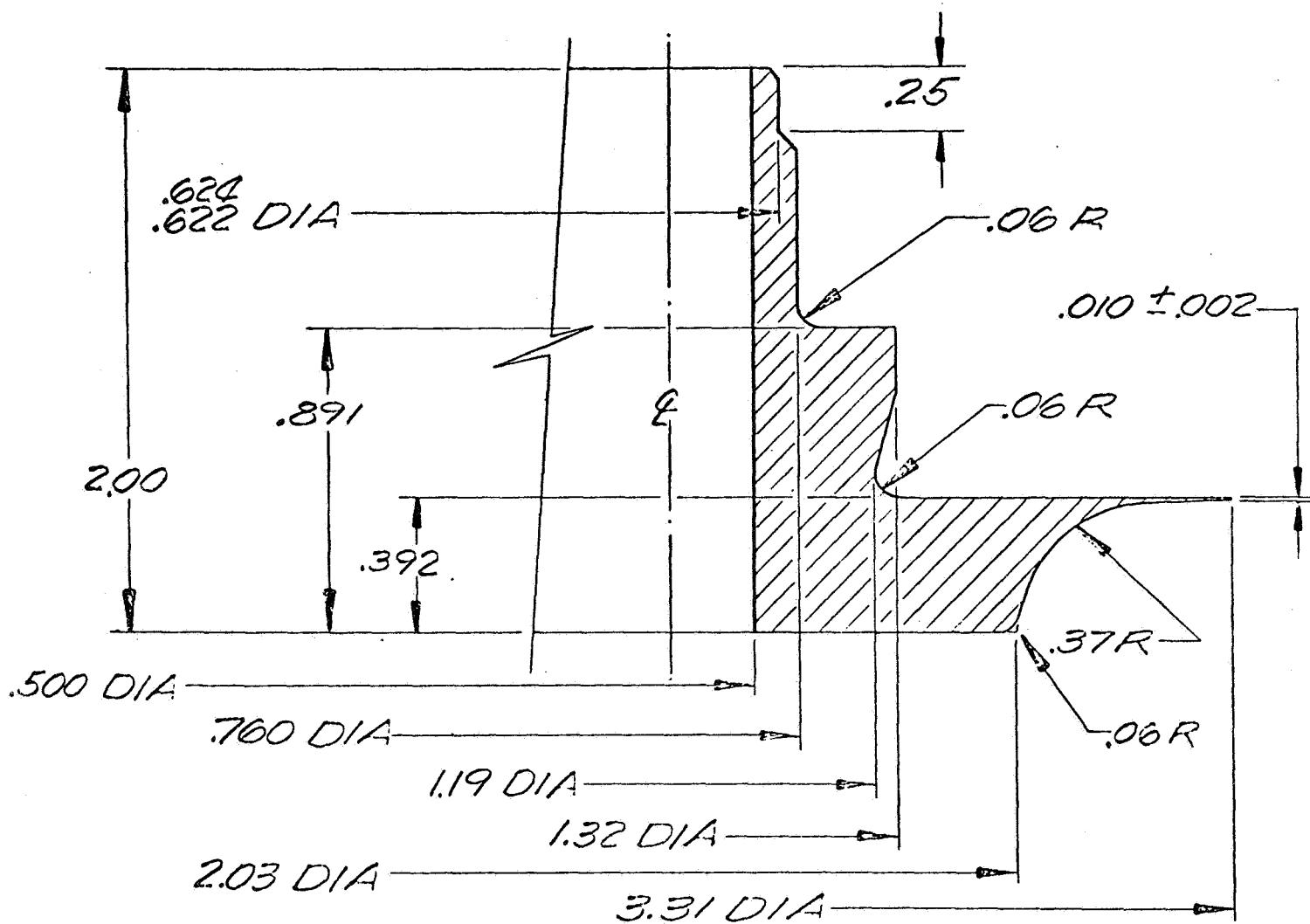
then

$$N_5 = \frac{(1.00)(0.0075)(0.673)}{(1) (420 \times 10^{-6})}$$
$$= 12.0 \text{ turns per inch layer.}$$

VI. DESIGN ANALYSIS OF BOSS

A. CONFIGURATION

The metal boss is fabricated from aluminum alloy 6061-T6. The significant dimensions of the boss for this analysis are given below (only one side of symmetrical boss shown).



B. MATERIAL PROPERTIES

Aluminum alloy 6061-T6 has the following design strength properties:

	Strength, psi		
	75°F	-320°F	-423°F
Ultimate, F_{tu}	42,000	54,000	64,000
Yield, F_{ty}	35,000	41,000	48,000
Shear, F_{su}	27,000	35,000	42,000

C. DESIGN CRITERIA

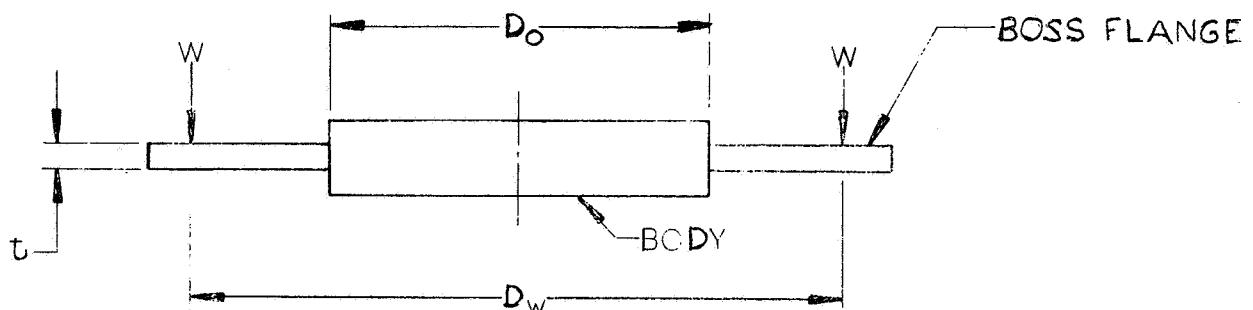
The metal boss is to be capable of sustaining the design burst pressure of the aluminum-lined filament-wound tank at 75°F , -320°F , and -423°F service temperatures. The design burst pressures (p_b) are 3000 psi at 75°F , 3750 psi at -320°F , and 3750 psi at -423°F .

D. ANALYSIS

Two separate analyses were performed on the boss to insure positive margins of safety at all sections of the boss.

1. Flange

The maximum stress in the flange is determined by using the conservative assumption that the flange is a flat plate with a concentrated annular load and a fixed inner edge (the body).



The end-for-end wrap pattern of the longitudinal filaments produces a rigid band around the boss that supports the flange. The load applied (W) is the reaction of the boss flange bearing against the composite structure.

The total load is therefore equivalent to the pressure acting over the area within the reaction circle. The diameter at which the load is assumed to act (D_w) is (from Reference 3).

$$D_w = (1 + \epsilon_{f,1}) D_o + 2.5 W_L$$

where

$$\epsilon_{f,1} = \frac{\sigma_{f,1}}{E_f} = \text{filament strain at ultimate stress, in./in.}$$

$$\sigma_{f,1} = \text{ultimate filament strength, psi} = 316,000 \text{ psi at } 75^{\circ}\text{F}, \\ \text{and } 395,000 \text{ psi at } -320 \text{ and } -423^{\circ}\text{F}$$

$$E_f = \text{filament modulus, psi} = 12.4 \times 10^6 \text{ psi at } 75^{\circ}\text{F, and} \\ 13.6 \times 10^6 \text{ psi at } -320 \text{ and } -423^{\circ}\text{F}$$

$$W_L = \text{filament-winding tape width (0.268-in.)}$$

The bending stress at the juncture of the flange and boss (σ_b) is calculated in accordance with formulas for loading on a flat plate (Reference B-5, Case 22, p. 201):

$$\sigma_b = \frac{\beta_{22} W}{t^2}$$

where

$$W = \frac{\pi p_b D_w^2}{4}$$

$$\beta_{22} \approx \frac{D_w}{D_o} - 1$$

$$t = \text{flange thickness, in.} = 0.392 \text{ in.}$$

a. Room Temperature Condition (75°F)

$$\epsilon_{f,1} = \frac{\sigma_{f,1}}{E_f} = \frac{316,000}{12.4 \times 10^6} = 2.55 \times 10^{-2} \text{ in./in.}$$

$$D_w = (1 + .0255) 1.190 + 2.5 (.268) = 1.890 \text{ in.}$$

$$W = \frac{\pi (3000)(1.890)^2}{4} = 8417 \text{ lbs}$$

$$\beta_{22} = \frac{1.890}{1.190} - 1 = 0.588$$

The bending stress is

$$\sigma_b = \frac{0.588 (8417)}{(0.392)^2} = 32,210 \text{ psi}$$

and, the margin of safety (M.S.) is given by

$$\text{M.S.} = \frac{F_{tu}}{\sigma_b} - 1$$

$$\text{M.S.} = \frac{42,000}{32,210} - 1 = + \underline{0.30}$$

b. Cryogenic Temperature Condition (-320°F critical)

$$\epsilon_{f,1} = \frac{395,000}{13.6 \times 10^6} = 2.90 \times 10^{-2} \text{ in./in.}$$

$$D_w = (1 + .0290) 1.190 + 2.5 (.268) = 1.895 \text{ in.}$$

$$W = \frac{\pi (3750)(1.895)^2}{4} = 10,576 \text{ lb.}$$

$$\beta_{22} = \frac{1.895}{1.190} - 1 = 0.592$$

The bending stress is

$$\sigma_b = \frac{0.592 (10,576)}{(0.392)^2} = 40,750 \text{ psi}$$

and, the margin of safety is

$$\text{M.S.} = \frac{54,000}{40,750} - 1 = + \underline{0.33}$$

2. Body

The body of the boss is analyzed by separation into three circular free bodies subjected to the loads and bending moments shown in Figure B-3. The equations for the rotation and deflection of each free body are written, and the discontinuity stresses at the free body junctures are established. It is assumed that the critical stresses will occur at the room temperature condition. This assumption is justified by the fact that the load increases less than the material strengths at cryogenic temperatures.

a. Plate Distortion

The plate is assumed to be simply supported along the outer edge and loaded by a uniform pressure (p), uniform load along the inner edge (F_y), and uniform edge moments (M).

The rotation (Reference B-5 Cases 13, 14 and 25, p. 242)

is

$$\theta_p = \frac{\lambda_{13} pa_p^3}{Et_p^3} + \frac{\lambda_{14} Pa_p}{Et_p^3} - \frac{\lambda_{25} M_1 a_p}{Et_p^3}$$

where, the coefficients (λ 's) are a function of the radius ratio

$$\frac{a_p}{b} = \frac{0.945}{0.25} = 3.78$$

and, from p. 241 of Reference B-5

$$\lambda_{13} = 1.250 - .78(1.250-1.007) = 1.092$$

$$\lambda_{14} = 1.238 - .78(1.238-1.082) = 1.116$$

$$\lambda_{25} = 5.52 - .78(5.52-4.08) = 4.40$$

With,

$$p = 3000 \text{ psi}$$

$$E = 10 \times 10^6 \text{ psi (for aluminum)}$$

$$t_p = 0.392 \text{ in.}$$

$$t_c = 0.125 \text{ in.}$$

$$r_o = b + t_c/2 = 0.25 + 0.0625 \\ = 0.3125 \text{ in.}$$

$$P = \frac{F_y}{y} (2\pi r_o) = \pi b^2 p = \pi (.25)^2 (3000) \\ = 589 \text{ lb.}$$

the rotation of the inner edge of the plate is

$$\theta_p = \frac{0.945}{10^7(0.392)^3} [1.092 (3000)(0.945)^2 + 1.116 (589) - 4.40 M_1]$$

$$\theta_p = [5621 - 6.904 M_1] \times 10^{-6}$$

The radial deflection of the plate is small and will be neglected.

$$\delta_p = 0$$

b. Ring Distortion

The ring is assumed to be subjected to a uniformly distributed twisting couple of M_t in.-lb. per linear in. which causes the ring to rotate about its centroid through an angle

$$\theta_r = \frac{M_t r_1^2}{EI_r} \quad \text{Reference B-5, p. 178}$$

The bending moment is

$$M_t r_1 = M_1 r_1 - (M_o - V_o y_o) r_o$$

and, assuming the ring to be of rectangular cross section with a width which is not small in comparison to the radius, the moment of inertia is

$$I_r = \frac{(2y_o)^3 \ln(r_2/b)}{12} \quad \text{Reference B-5, p. 179}$$

The rotation becomes

$$\theta_r = \frac{12 r_1}{8 E y_o^3 \ln(r_2/b)} [M_1 r_1 - (M_o - V_o y_o) r_o]$$

and for

$$r_1 = 0.4225 \text{ in.}$$

$$y_o = 0.25 \text{ in.}$$

$$r_2 = 0.595 \text{ in.}$$

$$\theta_r = \frac{12 (.4225)}{8 \times 10^7 (.25)^3 \ln(\frac{.595}{.25})} [.4225M_1 - .3125 (M_o - .25V_o)]$$

$$\theta_r = [1.977M_1 - 1.462M_o + 0.366V_o] \times 10^{-6}$$

The radial deflection of the plate is the sum of the deflections due to pressure and rotation. For the upper edge

$$\delta_r = \delta_p + y_o \theta_r$$

and for the lower edge

$$\delta = \delta_p - y_o \theta_r = 0$$

therefore, the deflection of the upper edge of the ring is

$$\delta_r = 2y_o \theta_r = 0.5\theta_r$$

c. Cylinder Distortion

The cylinder is thick-walled and subjected to pressure (p) and uniformly distributed continuity forces (V_o) and moments (M_o). The rotation (Reference B-5, Cases 14 and 15, p. 302) at the lower edge is

$$\theta_c = \frac{V_o}{2\lambda_c^2 D_c} + \frac{M_o}{\lambda_c D_c}$$

Where,

$$D_c = \frac{Et_c^3}{12(1-\nu^2)} = \frac{10^7 (.125)^3}{12 (.91)}$$

$$D_c = 1.789 \times 10^3$$

$$\lambda_c^4 = \frac{3(1-\nu^2)}{r_o^2 t_c^2} = \frac{3 (.91)}{[.3125 (.125)]^2}$$

$$\lambda_c^4 = 1.784 \times 10^3$$

$$\lambda_c^2 = 42.24, \lambda_c = 6.499$$

Therefore

$$\theta_c = \frac{V_o}{2(42.24)(1.789 \times 10^3)} + \frac{M_o}{6.499(1.789 \times 10^3)}$$

$$\theta_c = [6.617 V_o + 85.98 M_o] \times 10^{-6}$$

The radial deflection (Reference B-5 Cases 14, 15 and 35, p. 302 and 308) at the lower edge is

$$\delta_c = \Delta b - \frac{M_o}{2\lambda_c^2 D_c} - \frac{V_o}{2\lambda_c^3 D_c}$$

Where,

$$\Delta b = \frac{pb}{E} \left[\frac{a_c^2 + b^2}{a_c^2 - b^2} - \nu \left(\frac{b^2}{a_c^2 - b^2} - 1 \right) \right]$$

$$\Delta_b = \frac{3000 (.25)}{10^7} \left[\frac{(.375)^2 + (.25)^2}{(.375)^2 - (.25)^2} - .3 \left(\frac{(.25)^2}{(.375)^2 - (.25)^2} - 1 \right) \right]$$

$$\Delta_b = 0.199 \times 10^{-3} \text{ in.}$$

Therefore

$$\delta_c = 0.199 \times 10^{-3} - \frac{M_o}{2(42.24)(1.789 \times 10^3)} - \frac{V_o}{2(274.5)(1.789 \times 10^3)}$$

$$\delta_c = [199 - 6.617 M_o - 1.018 V_o] \times 10^{-6}$$

d. Discontinuity Forces and Moments

Equating the rotation and deflection of the upper edge of the ring to the lower edge of the cylinder, and the lower edge of the ring to the upper edge of the plate yields three equations for the calculation of discontinuity forces and moments.

$$M_1 = 44.2 M_o + 3.162 V_o$$

$$M_o = 33.8 - 0.204 V_o - 0.168 M_1$$

$$V_o = 15,360 - 24.27 M_1 + 3.995 M_o$$

The simultaneous solution of the three equations yields

$$M_1 = \frac{1708 - 855}{2.635 - 1.368} = 673 \text{ in-lb/in}$$

$$M_o = 1.368 (673) - 855 = 66 \text{ in-lb/in}$$

$$V_o = 15,360 - 24.27 (673) + 3.995 (66)$$
$$= -710 \text{ lb/in}$$

e. Maximum Stresses

The maximum stresses in the body of the boss are tensile stresses located at the outer edges of the free bodies which comprise the boss body.

(1) Meridional Stress in Cylinder

$$\sigma_{\varphi_c} = \frac{F_y}{t_c} + \frac{6 M_o}{t_c^2}$$

$$\sigma_{\varphi_c} = \frac{300}{.125} + \frac{6 (66)}{(.125)^2}$$

$$\sigma_{\varphi_c} = 2400 + 25,340 = 27,740 \text{ psi}$$

The margin of safety is

$$M.S. = \frac{42,000}{27,740} - 1 = + \underline{\underline{0.51}}$$

(2) Hoop Stress in Cylinder

$$\sigma_{\theta_c} = \frac{p (a_c^2 + b^2)}{a_c^2 - b^2} + \frac{2V_o \lambda_c r_o}{t_c} - \frac{2M_o \lambda_c^2 r_o}{t_c} + \frac{6M_o}{t_c^2}$$

$$\sigma_{\theta_c} = \frac{3000 [(.375)^2 + (.25)^2]}{(.375)^2 - (.25)^2} + \frac{2 (710)(6.499)(.3125)}{.125}$$
$$- \frac{2 (66)(42.24)(.3125)}{.125} + \frac{6 (.3)(66)}{(.125)^2}$$

$$\sigma_{\theta_c} = 7800 + 23,070 - 13,940 + 7600 = 24,530 \text{ psi}$$

The margin of safety is

$$M.S. = \frac{42,000}{24,530} - 1 = + \underline{\underline{0.71}}$$

(3) Shear Stress in Cylinder

$$\sigma_s = \frac{V_o}{t_c} = \frac{710}{.125} = 5680 \text{ psi}$$

The margin of safety is

$$M.S. = \frac{27,000}{5680} - 1 = + \underline{\underline{3.75}}$$

(4) Meridional Stress in Ring

The maximum stress in the meridan direction of the ring is a bending stress located at the juncture of the ring and the plate. With

$$t_r = r_2 - b = .595 - .250 = 0.345 \text{ in.}$$

the bending stress is

$$\sigma_{\phi_r} = \frac{6M_1}{t_r^2} = \frac{6(673)}{(.345)^2} = 33,920 \text{ psi}$$

and the margin of safety is

$$M.S. = \frac{42,000}{33,920} - 1 = + \underline{\underline{0.24}}$$

(5) Hoop Stress in Ring

The maximum hoop stress occurs at the upper outer edge of the ring and is given by

$$\sigma_{\theta_r} = \frac{p \left(\frac{r_2^2 + b^2}{r_2^2 - b^2} \right)}{I_r} + \frac{M_t r_1 y_o}{I_r}$$

With,

$$\begin{aligned} M_t r_1 &= M_1 r_1 - (M_o - V_o y_o) r_o \\ &= 673 (.4225) - [66 + 710 (.25)] .3125 \\ &= 193 \text{ in-lb} \end{aligned}$$

the maximum hoop stress is

$$\sigma_{\theta_r} = \frac{3000 \left\{ (.595)^2 + (.25)^2 \right\}}{(.595)^2 - (.25)^2} + \underline{193} (.25) \\ .00906$$

$$\sigma_{\theta_r} = 4290 + 5330 = 9620 \text{ psi}$$

and, the margin of safety is

$$M.S. = \frac{42,000}{9620} - 1 = \underline{\underline{3.37}}$$

NOMENCLATURE

<u>Symbol</u>	<u>Description</u>	<u>Units</u>
D	Flexural rigidity or diameter	lb-in or in
E	Modulus of elasticity	psi
F	Allowable ultimate strength	psi
I	Moment of inertia	in ³
k	Modulus of foundation	lb/in ³
K	Glass fraction by volume	--
M	Bending moment per unit width	in-lb/in
N	Force per unit width	lb/in
p	Internal pressure	psi
R	Radius	in.
R ₁	Radius of curvature in meridian direction	in.
R ₂	Radius of curvature in circumferential direction	in.
T	Temperature	
t	Thickness	in.
X	Axial coordinate	in.
y	Radial coordinate	in.
\bar{Y}	Distance from inside surface to neutral axis	in.
V	Shear force per unit width	lb/in
K ₁	Design factor based on chamber diameter	
K ₂	Design factor based on boss diameter	
K ₃	Design factor based on chamber length	
K ₄	Design factor based on chamber thickness	
K ₅	Design factor based on operating temperature	
K ₆	Design factor based on sustained pressure loading	
L	Chamber length	

Greek

α	Wrap angle	deg.
δ	Radial deflection	in.
θ	Rotation	radians
λ	Beam characteristic	in ⁻¹

NOMENCLATURE (Continued)

<u>Greek</u>	<u>Description</u>	<u>Units</u>
ν	Poisson's Ratio	--
σ	Stress	psi
η	Time	min.

Subscripts

B	due to bending
b	boss
c	cylinder
f	filament
f,h	hoop filaments
f,l	longitudinal filaments
h	head
H	hoop direction
Hf	hoop filaments
HH	hoop direction, hoop filament layer
HL	hoop direction, longitudinal filament layer
HM	hoop direction, metal liner
L	longitudinal direction
Lf	longitudinal filament
LH	longitudinal direction, hoop filament layer
LL	longitudinal direction, longitudinal filament layer
LM	longitudinal direction, metal liner
M	metal liner
o	at tangent plane
p	due to pressure

REFERENCES

B-1 F. J. Darms, R. Molho, and B. E. Chester, Improved Filament-Wound Construction for Cylindrical Pressure Vessels, ML-TDR-64-63, Volumes I and II, March 1964.

B-2 F. J. Darms and E. E. Morris, "Design Concepts and Procedures for Filament-Wound Composite Pressure Vessels," Paper presented at American Society for Mechanical Engineers Aviation and Space Conference, 16-18 March 1965, at Los Angeles, California.

B-3 Structural Materials Handbook, Aerojet-General Corporation, Structural Materials Division, February 1964.

B-4 F. J. Darms and R. E. Landes, Computer Program for the Analysis of Filament-Reinforced Metal Shell Pressure Vessels, NASA CR-72124 (Aerojet-General Report prepared under Contract NAS 3-6292), May 1966.

B-5 R. J. Roark, Formulas for Stress and Strain, 4th Edition, McGraw-Hill Book Company, 1965.

TABLE B-1
 DESIGN CRITERIA
 12-in-dia by 18-in-long Aluminum-Lined Glass Filament-
 Wound Pressure Vessels

Geometry and Pressure

Diameter, in.	12.000
Length, in.	18.000
Polar Boss Diameter, in.	1.200
Metal Liner Thickness, in.	0.010
Design Burst Pressure at 75°F, psig	3000
at -320°F, psig	3750
at -423°F, psig	3750

Material Properties

	Aluminum 6061-0	Glass-Filament- Wound Composite
Density, lb/in. ³	0.102	0.072
Coefficient of thermal expansion, in./in. - °F at +75 to -423°F	8.910 x 10 ⁻⁶	2.010 x 10 ⁻⁶
Tensile-yield strength, psi	8,000	-
Derivative of yield strength with respect to temperature, psi/°F	-7.9	..
Proportional limit, psi	8,000	..
Derivative of proportional limit with respect to temperature, psi/°F	-7.9	..
Elastic modulus, psi	10.25 x 10 ⁶	12.4 x 10 ⁶
Derivative of elastic modulus with respect to temperature, psi/°F	-1382	-2410
Plastic modulus, psi	116,500	..
Derivative of plastic modulus with respect to temperature, psi/°F	-516	..
Poisson's ratio	0.325	..
Derivative of Poisson's ratio with respect to temperature, 1/°F	0.201 x 10 ⁻⁴	..
Volume fraction of filament in composite	-	0.673
Longitudinal Filament, design- allowable stress, psi		
At +75°F	-	316,000
At -320°F	-	395,000
At -423°F	-	395,000

170-X-1123

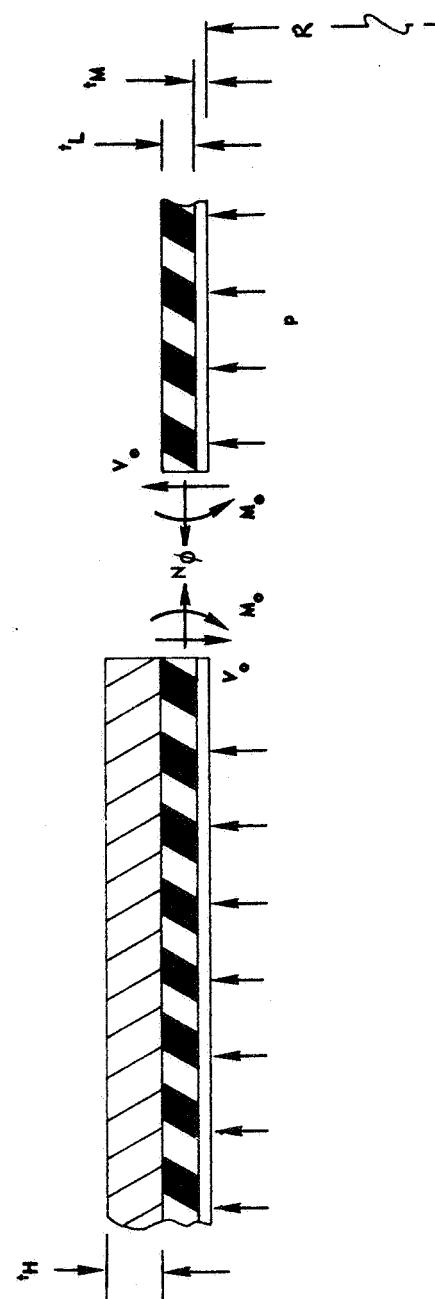
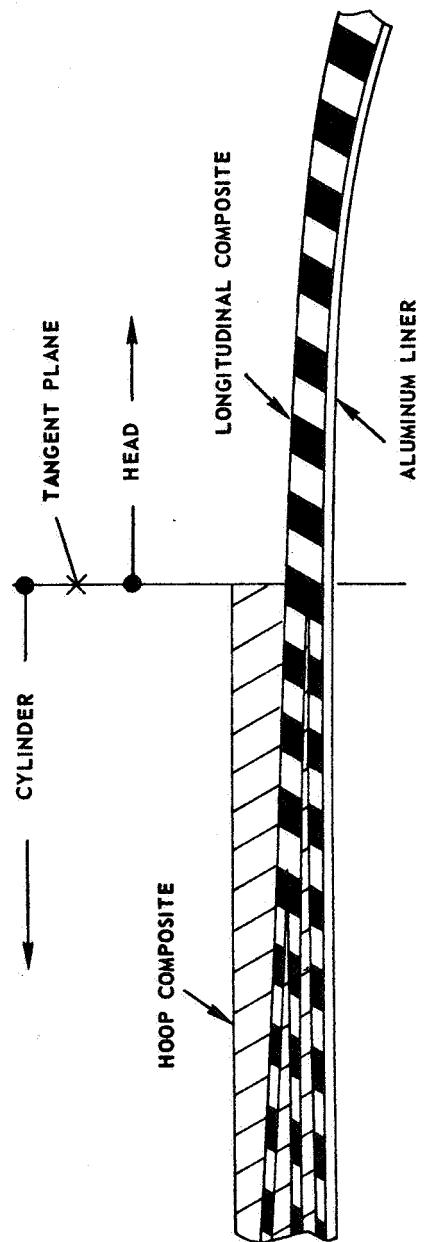


Figure B-1

Beam System for Analysis

170-X-1124

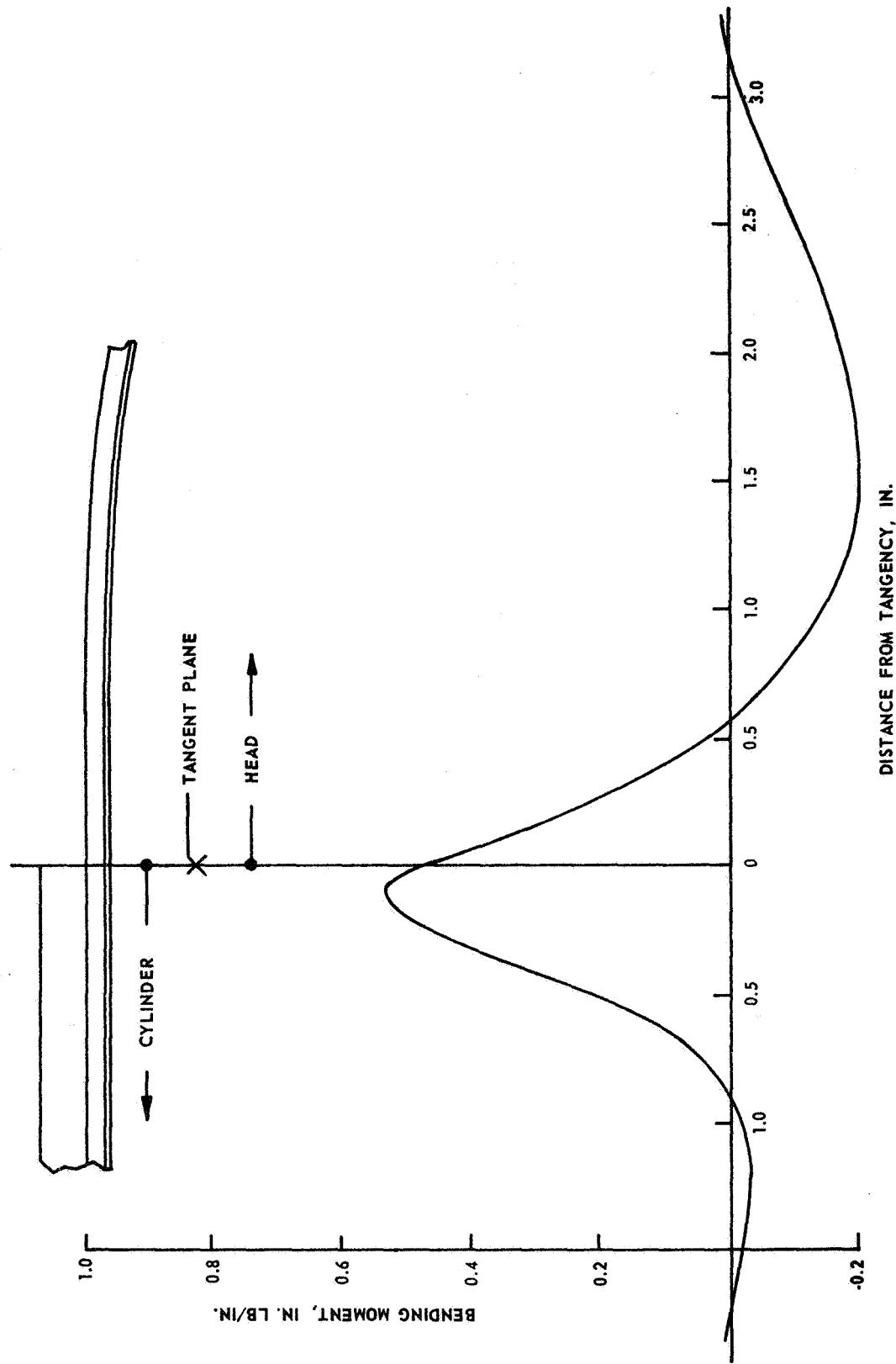
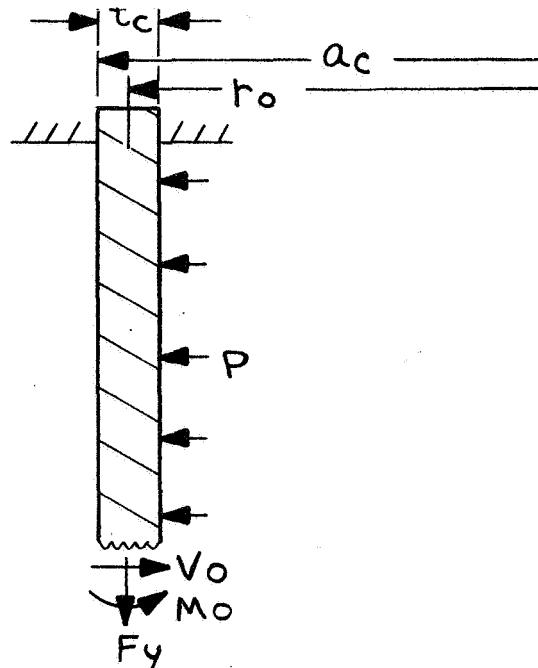


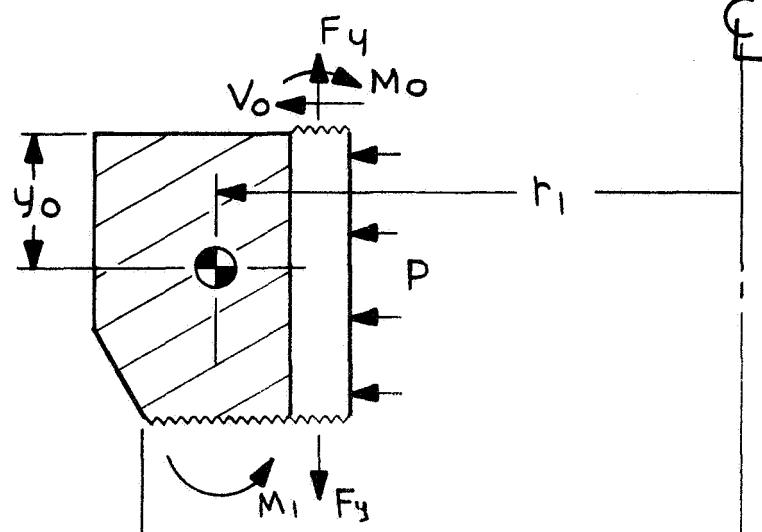
Figure B-2

Bending Moment Distribution at Head-to-Cylinder Juncture

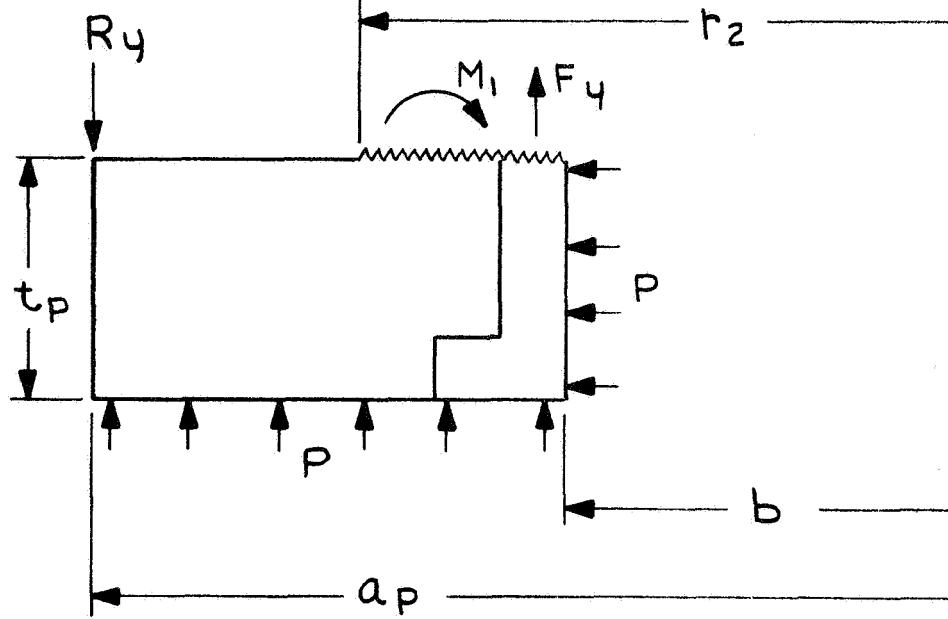
CYLINDER



RING



PLATE



BOSS BODY FREE BODIES

Figure B-3

APPENDIX C

SPECIMEN PREPARATION AND TEST PROCEDURE FOR EVALUATION OF ADHESIVE BOND STRENGTH BETWEEN ALUMINUM LINER AND GLASS FILAMENT COMPOSITE

I. METAL PREPARATION

A. The 2024 aluminum strips and the 6061 aluminum adherent were cleaned with carbon tetrachloride and with Hughson B-727 paste cleaner until a continuous film of water remained on the surface. The metal strips were air dried 60 minutes.

B. A coat of 3M XB3901 primer was brushed on the adhering surface of the metal strips, air dried 60 minutes and force dried 30 minutes at 190°F (360°K).

C. The 6061 aluminum adherent was coated on the adhering surface with the Adiprene L-100/Epirz 5101/MOCA adhesive.

D. A layer of nylon scrim was placed in the adhesive layer.

E. The prepared 6061 aluminum adherent was air cured 16 hours at room temperature, prior to assembly with the fabric when J P Stevens S-1852-2-400 scrim cloth was used. When J P Stevens 34168-2 scrim cloth was employed fabric was applied immediately followed by a 16 hour room temperature cure.

II. FABRIC PREPARATION

A. Type 181 glass fabric was impregnated with the Epon 828/Empol 1040/DSA/BDMA resin system and allowed to air dry 30 minutes.

B. 1-in.-(2.54-cm-) wide by 4-in.-(10.2-cm-) long strips were cut from the impregnated fabric.

III. SPECIMEN PREPARATION

A. Seven layers of the impregnated fabric were applied to the 1/8-in.-(0.3-cm-) thick 2024 aluminum strips.

B. The prepared 6061 aluminum adherent was placed on the resin coated side of the glass fabric layup and stitched down with a hand roller.

C. All specimens were cured 16 hours at room temperature plus 1 hour at 150°F (340°K) under 10 psi (6.9 N/cm²) pressure.

D. Six test specimens were subjected to each of the following cures under 10 psi (6.9 N/cm²) pressure:

<u>Specimen Type</u>	<u>Cure</u>
(1)	4 hours at 300°F (420°K)
(2)	6 hours at 300°F (420°K)
(3)	8 hours at 250°F (390°K)
(4)	16 hours at 250°F (390°K)
(5)	24 hours at 250°F (390°K)

IV. TESTING

A. The T-peel adhesion was determined per FTMS No. 601, Method 8031 on each specimen at

1. 75°F (297°K)
2. -320°F (-77°K)
3. -423°F (20°K)

B. A jaw separation speed of 0.5 in. per minute (1.3 cm/min) was used.

C. The specimens were immersed in liquid nitrogen or liquid hydrogen for the low temperature test.

D. The T-peel adhesion was calculated in lbf per inch of width.

APPENDIX D

FABRICATION SPECIFICATION FOR
1100 ALUMINUM LINER WITH BONDED BOSSES



AEROJET-GENERAL CORPORATION

CODE IDENT. NO. 70143

SPECIFICATION AGC-10587

LINER ASSEMBLY, 1100 ALUMINUM, 1269037-1,

FABRICATION OF

SUPERSEDING:

AGC- DATE	AGC- DATE	AGC- DATE
RELEASES (REPLACE PAGES IN SPECIFICATION WITH LATEST CHANGE BELOW.)		
REV LTR	RELEASE DATE	PAGE NUMBERS 1 2 3 4 5 6 7 8 9 10 11
	3 Jan 68	PAGE ADDITIONS

Authorized for Release by:

W.D. Knight

W. D. Knight
Chief Standards & Specifications Engineer
Engineering Documentation Dept.
Electronics Division

1. SCOPE

1.1 This specification establishes the requirements for the fabrication, inspection and acceptance testing of the 1100 aluminum metal liner assembly with bonded bosses, P/N 1269037-1, for use with glass filament-wound pressure vessels for cryogenic service.

2. APPLICABLE DOCUMENTS

2.1 Department of Defense documents.— Unless otherwise specified, the following documents, listed in the issue of the Department of Defense Index of Specifications and Standards in effect on the date of invitation for bids, shall form a part of this specification to the extent specified herein.

SPECIFICATIONS

Federal

QQ-A-225/8	Aluminum Alloy Bar, Rod, Wire, and Special Shapes, Rolled, Drawn, or Cold Finished, 6061
QQ-A-250/1	Aluminum 1100, Plate and Sheet
QQ-R-566	Rods, Welding, Aluminum and Aluminum Alloys
WW-T-700/6	Tube, Aluminum Alloy, Drawn, Seamless, 6061

Military

MIL-H-6088	Heat Treatment of Aluminum Alloys
------------	--------------------------------------

STANDARDS

Federal

FED-STD-151	Metals; Test Methods
-------------	----------------------

(Copies of documents required by contractors in connection with specific procurement functions should be obtained as indicated in the Department of Defense Index of Specifications and Standards.)

2.2 Aerojet-General Corporation documents.- Unless otherwise specified, the following documents of the latest issue in effect, shall form a part of this specification to the extent specified herein.

SPECIFICATIONS

AGC-13860

Radiographic Quality Levels,
Fusion Weldments

AGC-13972

Inspection, Dye Penetrant;
Metal Parts

STANDARDS

AGC-STD-1151

Inspection, Radiographic,
Materials, Procedures for

AGC-STD-1194

Welding, Fusion

AGC-STD-1194, Method 101 Aluminum Alloys, Fusion Welding

AGC-STD-4831

Aluminum and Aluminum Alloys,
Cleaning and Deoxidizing
Process Prior to Welding

ASD 5215

Marking, Methods of

DRAWINGS

1269037

1100 Aluminum Liner, with Bonded
Boss, 12-in.-dia. Filament-
Wound Pressure Vessel

3. REQUIREMENTS

3.1 Preproduction.- The metal liner furnished under this specification shall be subjected to preproduction testing as specified herein. A preproduction sample shall be submitted as specified herein.

3.2 Materials.-

3.2.1 Liner.- The metal liner half shell, P/N 1269037-2, shall be fabricated from 0.125-in. thick 1100-H14 aluminum sheet in accordance with Specification QQ-A-250/1 as the starting material.

3.2.2 Boss.- The boss, P/N 1269038-1, shall be fabricated from 6061-T6 aluminum alloy bar stock in accordance with Specification QQ-A-225/8.

3.2.3 Bleeder tube.- The bleeder tube, P/N 1269037-3, shall be fabricated from 6061-T6 aluminum alloy drawn seamless tubing in accordance with Specification WW-T-700/6.

3.2.4 Liner material identification.- Each blank cut from the 1100-H14 aluminum sheet for fabrication of P/N 1269037-2 shall be assigned a serial number (1, 2, 3, 4, etc.), the identification of which shall be maintained during all fabrication operations. This serial number along with the mill heat number for the plate from which the blank was cut shall be recorded for future reference.

3.3 Design.- The metal liner assembly furnished under this specification shall be fabricated in accordance with the requirements of AGC Drawing 1269037 and this specification.

3.4 Fabrication of aluminum liner half shell, P/N 1269037-2.- Unless otherwise specified, aluminum liner, P/N 1269037-2, shall be fabricated by utilizing the sequence of operations specified herein. The details of each operation shall be the responsibility of the fabricator.

Operation 1: Cut blank from the 1/8-in. thick 1100-H14 aluminum sheet and machine edge.

Operation 2: Form liner contour for half shell component, P/N 1269037-2. Anneal at 650°F in accordance with paragraph for "Annealing of Work Hardened Wrought Alloys" of Specification MIL-H-6088 between forming operations as required and after final forming operation.

Operation 3: Cut hole in dome area for installation of boss.

Operation 4: Machine to preweld configuration to provide a thickness of approximately 0.030-in. in the liner wall. The liner wall shall be located in an area approximately 0.030/0.035-in. below one surface of the original starting sheet.

Operation 5: Reduce thickness of liner wall to 0.010-in. by means of chemical milling, except in the weld joint area which shall be maintained at a thickness of approximately 0.020 to 0.030-in.

Operation 6: Perform preliminary machining of weld joint area as required.

Operation 7: Place in container and ship to Aerojet for installation of the boss.

3.5 Installation of boss in P/N 1269037-2.- A prefabricated boss, P/N 1269038-1, will be installed and bonded into the dome of each half liner, P/N 1269037-2, by Aerojet following procedure specified on Aerojet Drawing 1269037 and the component returned to the vendor.

3.6 Assembly of aluminum liner, P/N 1269037-1.- After installation of the boss, P/N 1269038-1 by Aerojet, two half shells shall be assembled to form the full liner, P/N 1269037-1, by utilizing the sequence of operations specified herein. The details of each operation shall be the responsibility of the fabricator.

- Operation 1: Perform the girth weld preparation machining of each liner half shell.
- Operation 2: Preform bleeder tube, P/N 1269037-3, and clean by following procedure in AGC-STD-4831.
- Operation 3: Install bleeder tube, P/N 1269037-3, inside the boss of one of the assembled liners as indicated on Drawing 1269037. Tack weld tube in place as required using gas tungsten-arc weld procedure in accordance with AGC-STD-1194, Method 101, and aluminum alloy weld rod of Specification QQ-R-566, Class 4043.
- Operation 4: Clean P/N 1269037-2 at weld joint area by following the procedure in AGC-STD-4831.
- Operation 5: Assemble two P/N's 1269037-2 together and gas tungsten-arc weld in accordance with AGC-STD-1194, Method 101, using weld rod of Specification QQ-R-566, Class 1100, to form assembly, P/N 1269037-1.
- Operation 6: Remove excess metal at girth weld joint by mechanical means to provide a weld seam height 0.004/0.006 in. above adjacent parent metal. Chemical milling of weld joint is not permitted.
- Operation 7: Beneficiate girth weld joint by planishing to attain 10 to 20% thickness reduction of as-welded and machined joint.
- Operation 8: Final machine weld seam to incorporate smooth surface free of irregularities for subsequent adhesive bonding.

Operation 9: Locally anneal girth weld joint by following the procedure of paragraph on "Annealing of Work Hardenable Wrought Alloys" of Specification MIL-H-6088 taking precautions that the bosses do not exceed 300°F as indicated by thermocouples, or Tempilstik or equivalent.

Operation 10: Clean the liner assembly by following the procedure of AGC-STD-4831.

3.7 Test coupons.- Four tensile test coupon blanks 3/4 in. wide x 8 in. long x 0.010 in. thick parallel to the direction of rolling shall be prepared from 1100-H14 aluminum sheet and accompany the one-half liner, P/N 1269037-2, through the final anneal (Operation 2 of 3.4). The aluminum sheet used for these coupons shall be from the same mill heat used to fabricate the two P/N 1269037-2 components. If sheet from different mill heats are used in one assembly, two coupons representing each mill heat shall accompany the components through the anneal operation.

3.7.1 Disposition of test coupons.- The test coupons shall accompany assembly, P/N 1269037-1, which they represent on its delivery to Aerojet. Tensile specimens machined from the coupons shall comply with the following tensile properties:

Ultimate tensile strength, psi	15,000 max.
Elongation in 2 in., percent	15.0 min.

3.8 Weld repairs.- Weld repairs shall be performed in accordance with the requirements of Standard AGC-STD-1194, "In-Process Rework."

3.9 Weld inspection.- The girth weld shall be dye penetrant inspected (see 4.5.3) and radiographic inspected (see 4.5.4).

3.9.1 Basis for rejection.-

3.9.1.1 Dye penetrant inspection.- The girth weld shall be free of external cracks or propagating defects. Surface porosity in excess of the limits specified in 3.9.1.2 is unacceptable.

3.9.1.2 Radiographic inspection.- The girth weld shall meet the requirements of Specification AGC-13860, Class 11 (eleven) with the following modifications:

- (a) Under scattered porosity - delete 0.010 in. max. diameter of cavity.
- (b) Excess penetration - delete T/4 and 0.032 in. max. and substitute 0.005 in. max.

(c) Delete excess crown limits - superseded by requirements of 3.6, Operations 6, 7 and 8.

3.10 Handling.- All handling operations of the liner assembly or the 1269037-2 half shells in the uncrated condition shall be performed using maximum care because of the susceptibility of the material to damage during the stages of fabrication. Components or assemblies damaged from handling shall be subject to rejection. The 1269037-2 components shall be kept in suitable containers or on pallets except when they are being worked.

3.11 Cleanliness.- After final machining, a cleaning method shall be employed to guarantee the liner assembly interior complete freedom from machining residue, shavings, and cuttings. After cleaning, the assembly openings shall remain sealed at all times, except when removal of seals is necessary for final fabrication or testing.

3.12 Identification of liner assembly.- The liner assembly shall be assigned serial numbers, A1, A2, A3, etc., which along with the assembly part number, shall be electrolytically etched as specified in Aerojet Standard ASD 5215, Method C, in the location indicated on Aerojet Drawing 1269037.

3.13 Preproduction sample tensile properties.- Parent metal and welded tensile specimens cut from the preproduction sample shall demonstrate capability to meet the following tensile properties when tested by Aerojet at the designated temperature. Six of each type specimen shall be tested at each temperature.

3.13.1 Tensile properties at 75° F.-

3.13.1.1 Parent metal.-

Ultimate tensile strength, psi	15,000 max.
Elongation in 2 in., percent	15.0 min.

3.13.1.2 Welded specimens.-

Ultimate tensile strength, psi	15,000 max.
Elongation in $\frac{1}{2}$ in., percent	11.0 min.

3.13.2 Tensile properties at -320° F.-

3.13.2.1 Parent metal.-

Elongation in 2 in., percent	28.0 min.
------------------------------	-----------

3.13.2.2 Welded specimens.-

Elongation in $\frac{1}{4}$ in., percent	14.0 min.
--	-----------

3.13.2.3 Ultimate tensile strength and yield strength at 0.2% offset shall be determined for each type specimen and reported for information only.

3.13.3 Tensile properties at -423°F.-3.13.3.1 Parent metal.-

Elongation in 2 in., percent	35.0 min.
------------------------------	-----------

3.13.3.2 Welded specimens.-

Elongation in $\frac{1}{2}$ in., percent	16.0 min.
--	-----------

3.13.3.3 Ultimate tensile strength and yield strength at 0.2% offset shall be determined for each type specimen and reported for information only.

3.14 Workmanship.- The liner assembly shall be fabricated, annealed, finished, and tested in a thoroughly workmanlike manner, particular attention shall be given to neatness and thoroughness with the processing and welding of the component parts. Non-conformance to the drawings and the requirements of this specification shall be cause for rejection.

4. QUALITY ASSURANCE PROVISIONS

4.1 Supplier responsibility.-

4.1.1 Inspection.- Unless otherwise specified, the supplier is responsible for the performance of all inspection requirements as specified herein and may use any facilities acceptable to the Aerojet-General Corporation (AGC).

4.1.2 Processing changes.- The supplier shall make no changes in processing techniques or other factors affecting the quality or performance of the product without prior written approval of AGC.

4.1.3 Preproduction sample.- The preproduction sample shall be fabricated using the same methods proposed for the fabrication of subsequent production lots of aluminum liner, P/N 1269037-1. It shall substantially represent the production liner to the extent that the evaluation described under 3.13 can be conducted. The preproduction sample shall be subjected to all preproduction tests

specified herein. Preproduction samples which do not meet the specified requirements shall be rejected. Fabrication of subsequent quantities for delivery and acceptance shall not be completed until written approval of the preproduction sample has been obtained from the AGC Project Engineer.

4.2 Sampling.-

4.2.1 Preproduction sample.- One aluminum liner, substantially representing P/N 1269037-1 in essential details as established by the AGC project engineer shall be submitted for preproduction testing.

4.2.2 Production sample.- All production units of aluminum alloy liner assembly, P/N 1269037-1 shall be submitted for quality conformance inspection.

4.3 Preproduction tests.- Testing of the preproduction sample shall be conducted by Aerojet-General Corporation and shall consist of the following inspections performed in the order listed:

- (a) Quality conformance inspections
- (b) Tensile strength tests (see Section 3.13)

4.4 Quality conformance inspections.- Inspection of all liner assemblies shall consist of tests to determine compliance with the following requirements of Section 3.

- (a) Examination of product
- (b) Tensile strength tests (see Section 3.7)
- (c) Dye penetrant inspection of girth weld
- (d) Radiographic inspection of girth weld

4.5 Test methods.-

4.5.1 Examination.- Each liner assembly shall be visually inspected for conformance to the requirements of Section 3 for which specific test methods are not specified and for conformance to the requirements of Section 5.

4.5.1.1 Certification of annealing procedure.- The supplier shall provide suitable evidence that the final annealing procedure specified in Operation 2 of paragraph 3.4 and in Operation 9 of paragraph 3.6 have been suitably controlled.

4.5.1.2 Certification of boss temper control.- The supplier shall provide suitable evidence that the bosses did not exceed 300°F during the annealing procedure specified in Operation 9 of paragraph 3.6.

4.5.2 Tensile strength test method.- The tensile strength properties shall be determined in accordance with FED-STD-151, Method 211.1 using the F2 test specimen.

4.5.3 Dye penetrant inspection.- Dye penetrant inspection in accordance with Specification AGC-13972 shall be performed on the girth weld of each liner assembly. After inspection, the weld shall be thoroughly cleaned.

4.5.4 Radiographic inspection.- Radiographic inspection in accordance with AGC-STD-1151 shall be performed on the girth weld of each liner assembly. Radiographs shall be subject to the interpretation and acceptance by designated Aerojet-General quality control and project representatives. Radiographic film shall be numbered to coincide with the identification markings of the liner assembly. China marking lead shall be used for marking weld identification so that exact location of weld areas with corresponding radiographs may be readily identified. All radiographic film shall become the property of Aerojet.

5. PREPARATION FOR DELIVERY

5.1 Packing.- The liner assembly shall be crated and firmly supported to prevent damage during shipment.

5.2 Marking.- The shipping container shall be marked with the following information:

- (a) Manufacturer's name
- (b) Liner Assembly, P/N 1269037-1
- (c) Liner serial number
- (d) Number and date of this specification
- (e) Purchase order number

6. NOTES

6.1 Intended use.- The aluminum alloy liner assembly is intended for use as a metal liner for glass filament-wound pressure vessels for storage of cryogenic fluids.

6.2 Ordering data.- Procurement documents should specify, but not be limited to, the following information:

- (a) Number and date of this specification
- (b) Place of inspection
- (c) Preproduction sample to be tested and approved prior to fabrication and acceptance of production quantities.
- (d) Place of delivery
- (e) Request for three copies of material certification and test results

PROCEDURE FOR BONDING OF BOSS TO LINER, P/N 1269037

1100 ALUMINUM LINER WITH BONDED BOSS,
12-IN.-DIA FILAMENT-WOUND PRESSURE VESSEL

Serial No: _____

Work Order: _____

Contract: _____

I. METAL PREPARATION

A. Clean the bonding surfaces of Part No. 1269037-2, 1100 Aluminum Liner Half Shell, and No. 1269038, Liner Boss, according to the following procedure:

1. Wipe the flange areas of the boss and within a 4.00-in.- (10.2-cm-) dia. area around the boss opening on the inside of the half section of the liner with MEK (methyl ethyl ketone) and air dry 30 minutes at 70-75°F (295-300°K).

2. Brush on a 5-8 mil (0.13-0.20 mm) thickness of Hughson EXB-727-6 paste cleaner to the top flange area of the boss and to the inside area in the liner previously wiped with MEK.

3. Allow to dry until the paste cleaner is powdery. This will require approximately 90 minutes.

4. Remove paste cleaner with tap water and continue washing until a film of water (water breakfree surface) remains on the bonding areas for 15 seconds.

5. Rinse surfaces with acetone to remove water and air dry for 30 minutes at 70-75°F (295-300°K).

B. Apply a primer as follows:

1. Brush a thin coat Minnesota Mining & Mfg. Company EC-3901 primer to the bonding areas of Part No. 1269037 and No. 1269038 and air dry 30 minutes at 70-75°F (295-300°K). Record acceptance tag numbers and serial numbers below:

	<u>Tag Number</u>	<u>Serial Number</u>
1269037-2 Liner	_____	_____
1269038-1 Boss	_____	_____
EC-3901 Primer	_____	N/A

2. Force dry the primer on both parts for 30 minutes at 190°F (360°K) in a circulating air oven.

C. Apply a 3 mil (0.08 mm) thickness of the following adhesive to the bonding areas:

<u>Composition</u>	<u>Ratio</u>	<u>Accept. Tag No.</u>
Adiprene L-100	80.00	_____
Epirez 5101	20.00	_____
MOCA	17.00	_____
	117.00	

Mixing Procedure: Mix Adiprene L-100 and Epirez 5101 resins together thoroughly. Heat MOCA to 200°F (367°K) until melted. Mix MOCA with mixed resins and degas in a vacuum dessicator for 15-20 minutes. Maintain the vacuum until the first foam created collapses.

II. PART FABRICATION

A. Allow the adhesive coated parts to air cure two to three hours at room temperature or until the adhesive has gelled slightly. The surfaces should still be slightly tacky.

B. Insert the boss, Part No. 1269038, in the opening of the liner section, Part No. 1269037-2, and press the liner halfshell firmly against the boss flange.

C. Apply 15 psi (10 N/cm^2) bonding pressure between the boss flange and the inside of the liner at the area in contact with the boss flange. The assembly must be supported in such a way that all of the pressure is applied to both sides of the bonding area.

D. Cure 24 hours at $70-75^{\circ}\text{F}$ ($295-300^{\circ}\text{K}$) under 15 psi (10 N/cm^2) pressure, followed by the following cure schedule

<u>Time</u>	<u>Temperature</u>	
	<u>$^{\circ}\text{F}$</u>	<u>$^{\circ}\text{K}$</u>
One hour	150	340
One hour	200	370
One hour	250	390
One hour	300	420

APPENDIX E

FABRICATION SPECIFICATION FOR
6061 ALUMINUM ALLOY LINER WITH INTEGRAL BOSS



AEROJET-GENERAL CORPORATION

CODE IDENT. NO. 70143

SPECIFICATION AGC-10586

LINER ASSEMBLY, 6061 ALUMINUM ALLOY, 1269036-1,

FABRICATION OF

SUPERSEDING:

AGC- DATE	AGC- DATE	AGC- DATE
RELEASES (REPLACE PAGES IN SPECIFICATION WITH LATEST CHANGE BELOW.)		
REV LTR	RELEASE DATE	PAGE NUMBERS
	3 Jan 68	1 2 3 4 5 6 7 8 9 10 11 12
		PAGE ADDITIONS

Authorized for Release by:

W. T. Knight
W. T. Knight
Chief Standards & Specifications Engineer
Engineering Documentation Dept.
Electronics Division

1. SCOPE

1.1 This specification establishes the requirements for the fabrication, inspection and acceptance testing of the 6061 aluminum alloy metal liner assembly with integral bosses, P/N 1269036-1 for use with glass filament-wound pressure vessels for cryogenic service.

2. APPLICABLE DOCUMENTS

2.1 Department of Defense documents.- Unless otherwise specified, the following documents, listed in the issue of the Department of Defense Index of Specifications and Standards in effect on the date of invitation for bids, shall form a part of this specification to the extent specified herein.

SPECIFICATIONS

Federal

QQ-A-225/8	Aluminum Alloy Bar, Rod, Wire, and Special Shapes; Rolled, Drawn, or Cold Finished, 6061
QQ-A-250/11	Aluminum Alloy 6061, Plate and Sheet
QQ-R-566	Rods, Welding, Aluminum and Aluminum Alloys
WW-T-700/6	Tube, Aluminum Alloy, Drawn, Seamless, 6061

Military

MIL-H-6088	Heat Treatment of Aluminum Alloys
------------	--------------------------------------

STANDARDS

Federal

FED-STD-151	Metals; Test Methods (Copies of documents required by contractor in connection with specific procurement functions should be obtained as indicated in the Department of Defense Index of Specific- ations and Standards.)
-------------	---

2.2 Aerojet-General Corporation documents.- Unless otherwise specified, the following documents of the latest issue in effect, shall form a part of this specification to the extent specified herein.

SPECIFICATIONS

AGC-13860

Radiographic Quality Levels,
Fusion Weldments

AGC-13972

Inspection, Dye Penetrant;
Metal Parts

STANDARDS

AGC-STD-1151

Inspection, Radiographic,
Materials, Procedures for

AGC-STD-1194

Welding, Fusion

AGC-STD-1194, Method 101 Aluminum Alloys, Fusion Welding

AGC-STD-4831

Aluminum and Aluminum Alloys,
Cleaning and Deoxidizing
Process Prior to Welding

ASD 5215

Marking, Methods of

DRAWINGS

1269036

6061 Aluminum Liner, 12-in.-dia.
Filament-Wound Pressure
Vessel

3. REQUIREMENTS

3.1 Preproduction.- The metal liner furnished under this specification shall be subjected to preproduction testing as specified herein. A preproduction sample shall be submitted as specified herein.

3.2 Materials.-

3.2.1 Liner.- The metal liner with integral bosses, P/N 1269036-2, shall be fabricated from 1-in.-thick 6061-T651 aluminum alloy plate in accordance with Specification QQ-A-250/11 as the starting material.

3.2.2 Extension.- The extension, P/N 1269036-3, shall be fabricated from 6061-T6 aluminum alloy bar stock in accordance with Specification QQ-A-225/8.

3.2.3 Bleeder tube.- The bleeder tube, P/N 1269036-4, shall be fabricated from 6061-T6 aluminum alloy drawn seamless tubing in accordance with Specification WW-T-700/6.

3.2.4 Liner material identification.- Each blank cut from the 6061-T651 aluminum alloy plate for fabrication of P/N 1269036-2 shall be assigned a serial number (1, 2, 3, 4, etc.), the identification of which shall be maintained during all fabrication operations. This serial number along with the mill heat number for the plate from which the blank was cut shall be recorded for future reference.

3.3 Design.- The metal liner assembly furnished under this specification shall be fabricated in accordance with the requirements of AGC Drawing 1269036 and this specification.

3.4 Fabrication and assembly of aluminum liner, P/N 1269036-1.- Unless otherwise specified, aluminum liner, P/N 1269036-1, shall be fabricated and assembled by utilizing the sequence of operations specified herein or as modified in 3.4.1. The details of each operation shall be the responsibility of the fabricator.

Operation 1: Upset the 6061-T651 aluminum alloy plate at a temperature of 650°F to make an internal projection for the boss area of the liner.

Operation 2: Machine the preformed plate to 0.125 in. nominal thickness except at the boss area which shall be machined to 1-in. thickness with appropriate transition from the boss area to the membrane section.

Operation 3: Anneal the machined preform by following the procedure of paragraph on "Annealing of Heat-Treated Wrought Alloys" of Specification MIL-H-6088.

Operation 4: Form liner contour for P/N 1269036-2. A stress-relief anneal at 650°F in accordance with paragraph on "Annealing of Work-Hardened Wrought Alloys" of Specification MIL-H-6088 shall be utilized between forming operations as required.

Operation 5: Solution heat treat and age the formed P/N 1269036-2 to T-6 condition in accordance with the procedure in Specification MIL-H-6088.

Operation 6: Machine contour to preweld configuration to provide a thickness of approximately 0.030-in. in the liner wall. The liner wall shall be located in an area not more than 0.125 in. below the surface of the original starting plate.

Operation 7: Reduce thickness of liner wall to 0.010-in. by means of chemical milling, except in the weld joint area which shall be maintained at a thickness of approximately 0.020 to 0.030 in.

Operation 8: Machine weld joint and boss area.

Operation 9: Clean internal surface of boss and the extension, P/N 1269036-3 by following the procedure in AGC-STD-4831.

Operation 10: Install extension *, P/N 1269036-3, in the boss and gas tungsten-arc weld as required in accordance with AGC-STD-1194, Method 101, using aluminum alloy weld rod of Specification QQ-R-566, Class 4043.

Operation 11: Preform bleeder tube, P/N 1269036-4, and clean by following procedure in AGC-STD-4831.

Operation 12: Install bleeder tube, P/N 1269036-4, inside the extension of the appropriate P/N 1269036-3 indicated on Drawing 1269036. Tack weld tube in place as required using gas tungsten-arc weld procedure in accordance with AGC-STD-1194, Method 101, and aluminum alloy weld rod of Specification QQ-R-566, Class 4043.

Operation 13: Clean P/N 1269036-2 at weld joint area by following the procedure in AGC-STD-4831.

Operation 14: Assemble two P/N's 1269036-2 together and gas tungsten-arc weld in accordance with AGC-STD-1194, Method 101, using weld rod of Specification QQ-R-566, Class 1100, to form assembly, P/N 1269036-1.

Operation 15: Remove excess metal at girth weld joint by mechanical means to provide a weld seam height 0.004/0.006 in. above adjacent parent metal. Chemical milling of weld joint is not permitted.

Operation 16: Beneficiate girth weld joint by planishing to attain 10 to 20% thickness reduction of the as-welded and machined joint.

Operation 17: Final machine weld seam to incorporate smooth surface free of irregularities for subsequent adhesive bonding.

Operation 18: Anneal liner membrane (including girth weld joint) by following the procedure of paragraph on "Annealing of Heat-Treated Wrought Alloys" of Specification MIL-H-6088. During this operation the boss areas of Drawing 1269036 shall be maintained at a temperature not exceeding 300°F as indicated by thermocouples, or Tempilstik or equivalent to retain T-6 properties in the boss.

Operation 19: Clean the liner assembly by following the procedure of AGC-STD-4831.

3.4.1 Alternate fabrication and assembly procedure.-

(a) Follow Operations 1 through 13 of paragraph 3.4, above.

(b) Anneal membrane portion of half liner, P/N 1269036-2 by following the procedure of paragraph on "Annealing of Heat-Treated Wrought Alloys" of Specification MIL-H-6088. During this operation the boss (J of Drawing 1269036) shall be maintained at a temperature not exceeding 300°F as indicated by thermocouples, or Tempilstik or equivalent to retain T-6 properties in the boss.

(c) Follow Operations 14, 15, 16 and 17 of paragraph 3.4, above.

(d) Locally anneal girth weld joint by following the procedure of paragraph on "Annealing of Heat-Treated Wrought Alloys" of Specification MIL-H-6088 taking precautions that the bosses do not exceed 300°F during the operation.

(e) Clean the liner assembly by following the procedure of AGC-STD-4831.

3.5 Test coupons.- Four tensile test coupon blanks 3/4 in. wide x 8 in. long x 0.010 in. thick transverse to the direction of rolling shall be prepared from 6061-T651 aluminum alloy plate and accompany the assembly, P/N 1269036-1 through the anneal (Operation 18 of 3.4 or Operation b of 3.4.1). The aluminum alloy plate used for these coupons shall be from the same mill heat used to fabricate the two P/N 1269036-2 components. If plate from different mill heats are used in one assembly, two coupons representing each mill heat shall accompany the assembly through the anneal operation.

3.5.1 Disposition of test coupons.- The test coupons shall accompany the assembly which they represent on its delivery to Aerojet. Tensile specimens machined from the coupons shall comply with the following tensile properties:

Ultimate tensile strength, psi	22,000 max.
Yield strength at 0.2% offset, psi	12,000 max.
Elongation in 2 in., percent	10.0 min.

3.6 Weld repairs.- Weld repairs shall be performed in accordance with the requirements of Standard AGC-STD-1194, "In-Process Rework."

3.7 Weld inspection.- The girth weld shall be dye penetrant inspected (see 4.5.3) and radiographic inspected (see 4.5.4).

3.7.1 Basis for rejection.-

3.7.1.1 Dye penetrant inspection.- The girth weld shall be free of external cracks or propagating defects. Surface porosity in excess of the limits specified in 3.7.1.2 is unacceptable.

3.7.1.2 Radiographic inspection.- The girth weld shall meet the requirements of Specification AGC-13860, Class 11 (eleven) with the following modifications:

(a) Under scattered porosity - delete 0.010 in. max. diameter of cavity.

(b) Excess penetration - delete T/4 and 0.032 in. max., and substitute 0.005 in. max.

(c) Delete excess crown limits - superseded by requirements of 3.4, Operation 15, 16 and 17.

3.8 Handling.- All handling operations of the liner assembly or the 1269036-2 components in the uncrated condition shall be performed using maximum care because of the susceptibility of the material to damage during the stages of fabrication. Components or assemblies damaged from handling shall be subject to rejection. The 1269036-2 components shall be kept in suitable container or on pallets except when they are being worked.

3.9 Cleanliness.- After final machining, a cleaning method shall be employed to guarantee the liner assembly interior complete freedom from machining residue, shavings, and cuttings. After cleaning, the assembly openings shall remain sealed at all times, except when removal of seals is necessary for final fabrication or testing.

3.10 Identification of liner assembly.- The liner assembly shall be assigned serial numbers A1, A2, A3, etc., which along with the assembly part number, shall be electrolytically etched as specified in Aerojet Standard ASD 5215, Method C, in the location indicated on Aerojet Drawing 1269036.

3.11 Preproduction sample tensile properties.- Parent metal and welded tensile specimens cut from the preproduction sample shall demonstrate capability to meet the following tensile properties when tested by Aerojet at the designated temperature. Six of each type specimen shall be tested at each temperature.

3.11.1 Tensile properties at 75° F.-

3.11.1.1 Parent metal.-

Ultimate tensile strength, psi	22,000 max.
Yield strength at 0.2% offset, psi	12,000 max.
Elongation in 2 in., percent	10.0 min.

3.11.1.2 Welded specimens.-

Ultimate tensile strength, psi	22,000 max.
Yield strength at 0.2% offset, psi	12,000 max.
Elongation in 1/4 in., percent	10.0 min.

3.11.2 Tensile properties at -320° F.-

3.11.2.1 Parent metal.-

Elongation in 2 in., percent 15.0 min.

3.11.2.2 Welded specimens.-

Elongation in $\frac{1}{4}$ in., percent 10.0 min.

3.11.2.3 Ultimate tensile strength and yield strength at 0.2% offset shall be determined for each type specimen and reported for information only.

3.11.3 Tensile properties at -423° F.-

3.11.3.1 Parent metal.-

Elongation in 2 in., percent 20.0 min.

3.11.3.2 Welded specimens.-

Elongation in $\frac{1}{4}$ in., percent 10.0 min.

3.11.3.3 Ultimate tensile strength and yield strength at 0.2% offset shall be determined for each type specimen and reported for information only.

3.12 Workmanship.-- The liner assembly shall be fabricated, heat treated, finished, and tested in a thoroughly workmanlike manner. Particular attention shall be given to neatness and thoroughness with the processing and welding of the component parts. Non-conformance to the drawing and the requirements of this specification can be cause for rejection.

4. QUALITY ASSURANCE PROVISIONS

4.1 Supplier responsibility.-

4.1.1 Inspection.-- Unless otherwise specified, the supplier is responsible for the performance of all inspection requirements as specified herein and may use any facilities acceptable to the Aerojet-General Corporation (AGC).

4.1.2 Processing changes.-- The supplier shall make no changes in processing techniques or other factors affecting the quality or performance of the product without prior written approval of AGC.

4.1.3 Preproduction sample.- The preproduction sample shall be fabricated using the same methods proposed for the fabrication of subsequent production lots of aluminum liner, P/N 1269036-1. It shall substantially represent the production liner to the extent that the evaluation described under 3.11 can be conducted. The preproduction sample shall be subjected to all preproduction tests specified herein. Preproduction samples which do not meet the specified requirements shall be rejected. Fabrication of subsequent quantities for delivery and acceptance shall not be completed until written approval of the preproduction sample has been obtained from the AGC Project Engineer.

4.2 Sampling.-

4.2.1 Preproduction sample.- One aluminum liner, substantially representing P/N 1269036-1 in essential details as established by the AGC project engineer, shall be submitted for preproduction testing.

4.2.2 Production sample.- All production units of aluminum alloy liner assembly, P/N 1269036-1 shall be submitted for quality conformance inspection.

4.3 Preproduction tests.- Testing of the preproduction sample shall be conducted by Aerojet-General Corporation and shall consist of the following inspections performed in the order listed:

- (a) Quality conformance inspections
- (b) Tensile strength tests (see Section 3.11).

4.4 Quality conformance inspections.- Inspection of all liner assemblies shall consist of tests to determine compliance with the following requirements of Section 3.

- (a) Examination of product
- (b) Tensile strength tests (see Section 3.5)
- (c) Dye penetrant inspection of girth weld
- (d) Radiographic inspection of girth weld

4.5 Test methods.-

4.5.1 Examination.- Each liner assembly shall be visually inspected for conformance to the requirements of Section 3 for which specific test methods are not specified and for conformance to the requirements of Section 5.

4.5.1.1 Certification of annealing procedure.- The supplier shall provide suitable evidence that the annealing procedure specified in Operation 18 of paragraph 3.4 or in (b) and (d) of paragraph 3.4.1, whichever is applicable, has been suitably controlled.

4.5.1.2 Certification of boss temper control.- The supplier shall provide suitable evidence that the boss areas (J of Drawing 1269036) did not exceed 300°F during the annealing procedure specified in Operation 18 of paragraph 3.4 or in (b) and (d) of paragraph 3.4.1, whichever is applicable.

4.5.2 Tensile strength test method.- The tensile strength properties shall be determined in accordance with FED-STD-151, Method 211.1, using the F2 test specimen.

4.5.3 Dye penetrant inspection.- Dye penetrant inspection in accordance with Specification AGC-13972 shall be performed on the girth weld of each liner assembly. After inspection, the weld shall be thoroughly cleaned.

4.5.4 Radiographic inspection.- Radiographic inspection in accordance with AGC-STD-1151 shall be performed on the girth weld of each liner assembly. Radiographs shall be subject to the interpretation and acceptance by designated Aerojet-General quality control and project representatives. Radiographic film shall be numbered to coincide with the identification markings of the liner assembly. China marking lead shall be used for marking weld identification so that exact location of weld areas with corresponding radiographs may be readily identified. All radiographic film shall become the property of Aerojet.

5. PREPARATION FOR DELIVERY

5.1 Packing.- The liner assembly shall be crated and firmly supported to prevent damage during shipment.

5.2 Marking.- The shipping container shall be marked with the following information:

- (a) Manufacturer's name
- (b) Liner Assembly, P/N 1269036-1
- (c) Liner serial number
- (d) Number and date of this specification
- (e) Purchase order number

6. NOTES

6.1 Intended use.- The aluminum alloy liner assembly is intended for use as a metal liner for glass filament-wound pressure vessels for storage of cryogenic fluids.

6.2 Ordering data.- Procurement documents should specify, but not be limited to, the following information:

- (a) Number and date of this specification
- (b) Place of inspection
- (c) Preproduction sample to be tested and approved prior to fabrication and acceptance of production quantities
- (d) Place of delivery
- (e) Request for three copies of material certification and test results.

Return this Form to Procuring Activity.

Document Preparing Activity:

AEROJET-GENERAL CORPORATION

Plant: Azusa

Address: 1100 W. Hollyvale Ave., Azusa

Organization: Engineering Documentation Dept.

DOCUMENT ANALYSIS SHEET

INSTRUCTIONS

This sheet may be completed by any activity involved in the use of this document. This sheet is for the express purpose of obtaining information relative to use of this document in order to insure that suitable products can be procured, manufactured, installed, or tested, with a minimum amount of delay and at the least cost. This Form and comments should be returned at any time its response is warranted. This Form may not be used to stipulate exceptions to this document taken in response to a request for quotation, nor may it be used to request waiver of requirements when performing under a contract invoking this document.

DOCUMENT TITLE: **Liner Assembly, 6061 Aluminum Alloy, 1269036-1, Fabrication of**

DOCUMENT NUMBER: **AGC-10586**

REVISION:

1. HAS ANY PART OF THE DOCUMENT CREATED PROBLEMS OR REQUIRED INTERPRETATIONS?

A. GIVE PARAGRAPH NUMBER AND WORDING.

B. RECOMMENDATIONS TO ALLEVIATE PROBLEM. (Include Attachments, If Applicable).

2. COMMENTS ON ANY REQUIREMENT, QUALITY ASSURANCE PROVISION, PACKAGING, CONTINUITY OF PROCEDURE, ETC., (Which appear to be too stringent or unnecessary, or incorrect).

3. IS THIS DOCUMENT EXCESSIVELY RESTRICTIVE?
IF ANSWER IS YES, IN WHAT WAY?

____ YES

____ NO

4. REMARKS: (Quality of Document, Clarity, Continuity, etc.)

SUBMITTED BY: (Name and Address to which further inquiry regarding comments should be directed).

DATE:

APPENDIX F

FILAMENT-WOUND VESSEL FABRICATION PROCEDURE ALUMINUM-LINED GLASS FILAMENT-WOUND PRESSURE VESSELS P/N 1268996 AND 1269232*

Reference Drawings:	<u>Number</u>	<u>Description</u>
	1269036	6061 Aluminum Liner with Integral Bosses
	1269037	1100 Aluminum Liner with Bonded Bosses
	1269231	1100 Aluminum Liner with Butt Welded Bosses
	1269227	1100 Aluminum Liner with Hinged Bosses

I. GENERAL INSTRUCTIONS

A. This data sheet is to be filled out in its entirety. Be sure that all weights, dimensions, winding pattern information, cure records, dates, and notes are entered as requested.

B. Any deviations from the specifications for fabrication are to be noted on this record so that all factors may be taken into account when analysis of the vessel is made after test.

C. This record will accompany the vessel through fabrication and be returned to the project engineer when complete.

D. All weights are to be recorded to nearest gram and all dimensions to 0.010 in. or better.

E. Verification of prior acceptance is to be made for all productive materials and acceptance tag numbers recorded.

F. Verification of calibration status for all data acquisition instruments is required. Serial numbers and calibration dates of instruments are to be recorded, as indicated.

II. INSPECTION OF ALUMINUM LINER

A. Wear clean white cotton gloves while handling aluminum liner.

B. Remove liner from container.

Record Acceptance Tag No. _____ of liner. Record serial number on Sheet 1.

* Presentation of fabrication procedures in both S.I. and English systems would reduce the clarity of this Appendix. The English system only is used.

C. Measure liner length, diameters, and weight and record them on Figure 1.

D. Replace liner in container.

III. PREPARATION OF SCRIM CLOTH TO COVER LINER HEADS

A. Obtain roll of J. P. Stevens Style 34168-2 nylon cloth, 36-in.-wide, scoured and heat set, natural color. Record Acceptance Tag No. _____.

B. Cut two flat patterns suitable for forming over each liner head past head-to-cylinder tangency point.

C. Cut circular hole in center of each pattern just large enough to permit positioning of them over metal boss of liner.

D. Protect cut patterns with plastic sheet and store.

IV. ASSEMBLY OF LINER TO WINDING SHAFT

A. Measure the boss-to-boss length and record actual _____. Subtract 22.480 in. from the actual length and record difference _____. Install the liner onto the winding shaft. Install retaining ring shim(s) equivalent in thickness to the length difference recorded above. Install and secure flange nut and swivel assembly.

B. Wear clean white cotton gloves while handling the aluminum liner.

C. Cover the liner/shaft assembly with a polyethylene bag if further processing is to be delayed in excess of 4-hours.

V. CLEANING AND PRIMING OF LINER

A. Apply .005 to .007-inch thick layer of Hughson EXB727-6 paste cleaner to outside surface of liner. Record Acceptance Tag No. _____.

B. Allow coating to air dry until it becomes powdery which will require approximately 90 minutes.

C. Remove paste cleaner coating by washing with tap water. Continue washing and rinsing until a continuous film of water (water break-free surface) is maintained for 15 seconds.

D. Wash with acetone to remove water and air dry for a minimum of 30 minutes.

E. Apply a thin coating of Minnesota Mining & Mfg. Co. EC-3901 primer to bonding surface and air dry 30 minutes. Record Acceptance Tag No. _____.

F. Force dry for approximately 30 minutes at 190°F with heat gun, infra red lamps, or quartz strip heaters.

NOTE: After application of the primer the liner may be stored at room temperature if necessary prior to subsequent operations. Protect primed liner with plastic sheet.

VI. APPLICATION OF ADHESIVE AND SCRIM CLOTH TO LINER

A. Cut a 10-1/2-inch by 39-inch panel of teflon coated glass fabric and wrap around the cylindrical section of the liner. Hold in place with adhesive tape over teflon fabric. DO NOT bond to primed surface.

B. Prepare small batches of adhesive (four batches required as described in Steps C, L, O, and V), according to following proportions and method of mixing:

<u>Composition</u>	<u>Parts by Weight</u>	<u>Acceptance Tag No.</u>
Adiprene L-100	80.0	_____
Epirez 5101	20.0	_____
MOCA	<u>17.0</u> <u>117.0</u>	_____

Mixing Method:

1. Blend Adiprene L-100 and Epirez 5101 resins thoroughly
2. Melt MOCA at 200°F and thoroughly mix into resin blend
3. Degas under vacuum until bubbling ceases

C. Brush coat adhesive on one head section of liner to a thickness of approximately .003-inch.

D. Unwrap plastic protective wrap from nylon scrim cloth head section.

E. Pull scrim cloth over shoulder of head section and stretch in place. Be sure opening in scrim cloth centered over boss.

F. Work scrim cloth into adhesive coated surface with clean brush until all air pockets and wrinkles in fabric disappear.

G. When scrim cloth head has been worked to edge of teflon coated fabric on liner cylindrical section, insert cutting ring under edge of cloth and locate scribe line on cutting ring normal to liner axis.

H. Remove all wrinkles in scrim cloth over cutting ring.

I. Cut scrim cloth at scribe line with razor blade cutting tool using a rocking motion to avoid displacement of fibers.

J. Remove cutting ring from under edge of scrim cloth and smooth fabric with brush. Carefully inspect cut edge of scrim cloth for uniformity and remove any frayed threads. Repeat Steps G to J until scrim cloth has been cut around the liner circumference.

K. Apply more adhesive over scrim cloth and brush carefully.

L. Repeat Steps C through K for other head section.

M. Remove teflon coated fabric from cylindrical section of liner.

N. Cut an 11-inch by 39-inch panel of No. 34168-2 nylon scrim cloth and roll it on a 2-inch diameter by 12-inch long paper tube. Carefully inspect left edge for uniformity and remove any frayed edges.

O. Apply approximately .003-inch thickness of adhesive over cylindrical section of liner. Avoid any movement of edges of scrim cloth head sections already in place.

P. Apply scrim cloth to cylindrical section by unrolling from tube. Make butt joint at left edge between cylindrical section scrim cloth and scrim cloth head section already in place.

Q. Work left edge of cylindrical section scrim cloth with brush to insure a butt joint with no gaps between head section and cylindrical section.

R. Insert cutting jig under scrim cloth at right edge of cylindrical section. Adjust accurately so that scribe line coincides exactly with edge of the head section scrim cloth already in place.

S. Cut right edge of cylindrical section scrim cloth on scribe line of jig in the same manner as the head sections were cut.

T. Cut the longitudinal joint of the cylindrical section scrim cloth by use of a razor blade knife on a flat metal strip attached to the liner

bosses.

U. After both ends of scrim cloth longitudinal joint are cut, work the edges together with a brush until no gaps remain at the butt joint.

V. Apply additional adhesive over scrim cloth of hoop area until a uniform coat is obtained. Avoid any movement of the fabric.

VII. POSITIONING OF LINER IN WINDING MACHINE

Prior to this operation, liner cleaning and adhesive application and shaft assembly will have been completed as described in Section III, IV, V, and VI.

A. Wear clean white cotton gloves while handling the liner.

B. Remove the liner/winding shaft assembly from the handling stand. Carry and secure the assembly in the winding machine.

C. Protect the liner with plastic sheet if it is not to be overwrapped immediately.

VIII. WINDING MACHINE SETUP AND CALIBRATION

Refer to Drawing 1268966 or 1269232, "12-in.-dia Aluminum-Lined Glass-Filament-Wound Pressure Vessel" during operations described below:

A. Setup resin impregnation systems on winding machines.

B. Dry run the machines (without paying off roving) and check machine settings to obtain the required uniform distribution of the design number of winding arm turns per mandrel revolution for longitudinal winding and turns per inch for hoop winding.

C. Install (3) rolls of 20-end glass roving into the tension devices for longitudinal winding and one roll for hoop winding. Thread the roving through the guide rollers and impregnation system. Secure the roving ends and set the tension at approximately 7 pounds per 20 ends roving.

D. For longitudinal winding, adjust the rollers as required to assure a uniform thickness, tape of the design width formed from three 20-end rovings at final payoff to liner.

E. Ensure that the tape passes tangent to each boss for longitudinal winding, with a maximum permissible distance between the boss and tape edge of 0.020-inch, by making a few winding arm transverses on the mandrel. Make adjustments as required to provide the specified longitudinal winding pattern.

F. Calibrate the tension devices to provide a dynamic tension of 7 pounds per 20-end roving for longitudinal rolls and 10 pounds for the hoop roll at the roving payoff. Calibrate the tension devices statically then dynamically. Record on Table F1 the static tension needed to provide the required dynamic tension. Also record there the tension device settings.

IX. GENERAL INSTRUCTIONS FOR HANDLING OF GLASS ROVING

A. Keep each roll of 20-end glass-filament roving in its protective plastic bag with end plates in place of its individual box in cold storage at 32°F or lower, except when it is being used to overwind one or more liners on a given day.

B. Weigh each spool of roving before initiating winding. For subsequent weighing, plastic-bag any scrap obtained during winding.

C. At the completion of winding each day, immediately remove each roll of roving from the tension devices, repackage it with end plates in its plastic bag and box, and return it to cold storage (32°F or lower).

X. RESIN PREPARATION

A. Obtain the Epon 828, DSA, Empol 1040, and BDMA resin constituents.

B. Measure out the following quantities of each constituent for each of three batches:

	<u>Quantity, g.</u>	<u>Acceptance Tag No.</u>
Epon 828	200 ± 0.5	_____
DSA	231 ± 0.5	_____
Empol 1040	40 ± 0.5	_____
BDMA	2 ± 0.0	_____

C. Mix and warm the Epon 828 and Empol 1040 to 212°F. Cool the mixture to room temperature and add the DSA and BDMA. Thoroughly mix the constituents. Heat the mixed resin to 85 to 100°F.

XI. OVERWRAPPING OF ALUMINUM LINER

A. General Notes - (1) Stop overwrapping, remove the winding, and restart the process, if any of the following should occur: (a) filament breakage, (b) loss of end or ends on guide roller, (c) loss of roving tension,

(d) lack of resin impregnation in roving, (e) winding-pattern gapping, or (f) excessive variation of filament-tape width; and (2) retain in a plastic bag all excessive roving not used in winding but included in the initially recorded roving-spool weights; weigh it and record the weight on Table F-1.

B. Obtain three rolls of 20-end glass roving (S/HTS per WS-1126, B/1, Notice 2) and weigh each roll. Record the roll number and weight on Table F-1, and place the rolls on tension-device spindles. Record on Table the number of the spindle on which each roll is mounted. Record Acceptance Tag Numbers _____ and _____.

C. Move the winding machine payoff head into position for longitudinal winding. Thread the three 20-end rovings through the guide rollers and payoff head tangent to the metal liner boss and secure them in place.

D. Pour one batch of the mixed resin in the impregnation pot. Brush-impregnate the roving between the impregnation pot and the liner. Maintain the mixed resin bath at a temperature of 85 to 100°F. Add additional batches of mixed resin as required.

E. Set the machine-turn counter and record the reading in Table F-1.

F. Identify the starting position of the winding-shaft mount in relation to the stationary point on the machine immediately adjacent to the mount.

G. Overwind the aluminum liner as specified on Drawing 1268966 or 1269232 and described in Steps H to I following.

H. Start the longitudinal filament winding making sure that the design tape width is maintained. If required, brush on extra resin or remove excess resin on filaments.

I. Stop winding at the completion of the first liner revolution of 360° (which will close the pattern). Maintain the tension on the roving. Enter the counter reading at completion of one revolution on Table F-1.

J. Tie off the three 20-end rovings. Secure each roving to the payoff head.

K. Move liner to hoop winding machine.

L. Move the winding machine payoff head into position for hoop winding the cylindrical section, starting at the left end. Thread one 20-end roving through the payoff roller and onto the liner cylindrical section along a tangency plane. Secure in place. Use 10-pounds tension per roll for all hoop winding.

M. Enter the counter reading in Table F-1. Start the hoop winding with the design number of turns per inch along the 10.74-inch cylindrical section from left to right. Stop winding at the completion of the first hoop layer and enter counter reading in Table F-1. Enter the counter reading at completion of the second hoop layer in Table F-1.

O. Wind back to the right along the cylinder to 0.50-inch from the tangent plane and tie off the roving. Secure the roving to the payoff head. Enter the counter reading at completion of the third hoop layer in Table F-1.

P. Move the liner back to the longitudinal winding machine. Thread the three 20-end rovings through the guide rollers and payoff head tangent to the metal liner boss and secure them in place.

Q. Repeat Steps H to J to complete second revolution of longitudinal winding.

R. Apply three more layers of hoop winding in accordance with the general procedure of Steps K to O and specific dimensional and pressure requirements of Drawing 1268966 or 1269232 and Table F-1.

S. Apply a third revolution of longitudinal winding following the general procedure of Steps P and Q.

T. Complete hoop winding by applying four more layers plus fill-in in accordance with the general procedure of Steps K to O and specific dimensional and pressure requirements of Drawing 1268966 or 1269232 and Table F-1. As last hoop layer is being applied, locate four instrument terminals on cylinder under windings; locate two of them 180° apart and 0.50-inch up on one end of the cylinder and the remaining two at the other end of the cylinder along a longitudinal line from each of the first two terminals and 0.50-inch up on the cylinder. At the same time, locate temperature sensors under hoop winding 90° away from instrument terminals.

U. Remove the three spools of roving from the tension devices, weigh them, and record their weights on Table F-1.

V. Weigh the scrap roving, and enter this weight on Table F-1. Compute the total weight of roving used.

XII. PREPARATION FOR CURING OF COMPOSITE STRUCTURE

A. In vacuum-bagging the wound tank shell for the cure, use one layer of 2353 dacron cloth for release/bleeder cloth.

B. Bag the shell with 6-mil polyvinyl alcohol (PVA) sheet tailored to avoid excess wrinkles.

- C. Seal the bag with zinc chromate putty.
- D. Install a vacuum valve over the dacron pad in the cylindrical section.
- E. Evacuate the bag to 20-inch Hydrogen or better, and check for leaks.

NOTE: An alternative to vacuum bagging is to periodically (every 20 or 30 minutes) wipe the excess resin off the composite. This should be continued until the resin stops flowing, approximately 2-1/2 hours. Enter the type of resin control used in the note section below.

XIII. CURING OF COMPOSITE STRUCTURE

- A. Transfer the unit to the curing oven.
- B. Mount the winding shaft on the support fixtures in the oven.
- C. Cure at 150^oF for 2 hours and at 300^oF for 4 hours. Keep a record of the cure on the continuous recording chart. Record calibration date _____ and Serial Number _____ on recorder.
- D. Reduce the oven temperature to 100^oF at a rate not to exceed 100^oF/hour.
- E. Attach copy of cure chart to this page.
- F. Remove the cured tank from the oven.

XIV. CLEANING, DIMENSION CHECKING, AND WEIGHING

- A. Disassemble tank from shaft.
- B. Clean tank interior by flushing with solvent, then detergent and water, then water rinse. Tank should not be exposed to water for more than 30 minutes. The tank may then be dried by flushing with acetone or by baking 200^oF for one hour.
- C. Identify tank with part number and serial number per drawing.
- D. Measure the wound-tank length, diameters and weight and record them on Figure F-1.
- E. Place the wound tank in the storage box. Deliver this "Fabrication Instructions" with tank, along with all other fabrication and inspection documents in the folder.

TABLE F-1
WINDING DATA

Machine Settings

Longitudinal Winding

Hoop Winding

Tension Settings

Static tension at payoff required for dynamic tension of 10 ± 1 lb/20-end roving at payoff

<u>Tension-Device Spindle No.</u>	<u>Static Tension Pound</u>	<u>Tension-Device Setting</u>
A	_____	_____
B	_____	_____
C	_____	_____

Glass Roving Data

<u>Roll No.</u>	<u>Tension-Device Spindle No.</u>	<u>Starting</u>	<u>Final</u>	<u>Roving</u>	<u>Weight, g.</u>
—	_____	_____	_____	_____	_____
—	_____	_____	_____	_____	_____
—	_____	_____	_____	_____	_____
—	_____	_____	_____	_____	_____
Total					_____
Less scrap weight (subtract)					_____
Total roving on tank					_____ g.
Tensiometer Serial No. _____; calibration date _____					

TABLE F-1 (Cont.)

WINDING DATA

Longitu- dinal Revolu- tion No.	Layer No.	Layer No.	Hoop		Actual			Design		
			End of Layer Distance, in.		From Left	Total Tangent Plane	Counter Reading At Start	Total Length, in.	At End	Total Turns per Revolution or per Hoop Layer
-	1	-	-	-	-	-	-	-	-	140 ± 4
1	2	-	0.00	0.00	0.00	10.74	-	-	-	126
-	-	1	0.00	0.00	0.00	19.24	-	-	-	120
-	-	2	0.50	0.50	0.50	9.74	-	-	-	114
-	-	3	0.50	0.50	-	-	-	-	-	140 ± 4
-	-	3	-	-	-	-	-	-	-	108
-	-	4	-	-	-	-	-	-	-	102
-	-	2	1.00	0.50	0.50	9.24	-	-	-	96
-	-	4	1.00	1.00	1.00	8.74	-	-	-	140 ± 4
-	-	5	1.00	1.00	1.00	8.24	-	-	-	126
-	-	6	1.50	1.50	1.50	-	-	-	-	126
-	-	5	-	-	-	-	-	-	-	126
-	-	6	-	-	-	-	-	-	-	126
3	-	-	-	-	-	-	-	-	-	126
-	-	-	Fill in left end of cylinder as required in accordance with Drawing							
-	-	-	7	0.00	0.00	10.74	-	-	-	126
-	-	-	Fill in right end of cylinder as required in accordance with Drawing							
-	-	-	8	0.00	0.00	10.74	-	-	-	126
-	-	-	9	0.00	0.00	10.74	-	-	-	126
-	-	-	10	0.00	0.00	10.74	-	-	-	126

NOTES _____

DATE/TIME _____

SIGNATURE _____

FIGURE I

INSPECTION OF ALUMINUM LINER AND FILAMENT-WOUND VESSEL ASSEMBLY (FORM)

Serial No. _____

Record serial number and calibration date of instruments used.

Before-winding data: Date _____ Siganture _____

After-winding data: Date _____ Siganture _____

Tangent Plane Weld Joint +

Tangent Plane

		Instruments	
	Serial No.	Calib. No.	
Outside Diameter Before Winding and Cure	_____	_____	_____
Outside Diameter After Winding and Cure	_____	_____	_____
Cylinder Length			
2.85		2.85	
Before Winding			
After Winding and Cure			
Overall Length			
Before Winding		After Winding and Cure	
Weight of liner before winding _____ g			
Weight of vessel after winding and cure _____ g			

APPENDIX G

FABRICATION SPECIFICATION FOR
1100 ALUMINUM LINERS WITH BUTT-WELDED AND HINGED BOSSES



AEROJET-GENERAL CORPORATION

CODE IDENT. NO. 70143

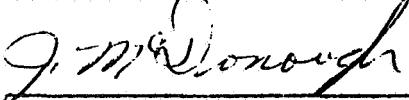
SPECIFICATION AGC-10598 A

LINER ASSEMBLY, PRESSURE VESSEL, 1100 ALUMINUM, FABRICATION OF

SUPERSEDED:

AGC - 10598 DATE 21 March 1969		AGC - DATE	AGC - DATE
RELEASES (REPLACE PAGES IN SPECIFICATION WITH LATEST CHANGE BELOW)			
REV LTR	RELEASE DATE	PAGE NUMBERS	PAGE ADDITIONS
	21 Mar 69	1 1 2 3 4 5 6 7 8 A-1 A-2	
A	17 Apr 70	A A A A A A A A A A	Appendix A

Authorized for Release:


J. Coff
for J. Coff, Supervisor
Specifications and Standards
Mechanical Systems Operations
Electronics Division
Azusa Facility

1. SCOPE

1.1 Scope.- This specification establishes the requirements for the fabrication and quality conformance inspection of two types of 1100 aluminum metal liner assemblies for use with glass filament-wound pressure vessels for cryogenic service.

1.2 Classification.- The aluminum liner assemblies shall be classified as follows:

<u>Suffix Number</u>	<u>Description</u>	<u>Part No.</u>
-1	Hinged Boss Concept	1269227-1
-2	Butt Welded Boss Concept	1269231-1

Each classification shall be specified by referencing the specification number and suffix number for the liner desired.

Example: Fabricate and inspect liner in accordance with AGC-10598-1

2. APPLICABLE DOCUMENTS

2.1 Department of Defense documents.- Unless otherwise specified, the following documents, listed in the issue of the Department of Defense Index of Specifications and Standards in effect on the date of invitation for bids, shall form a part of this specification to the extent specified herein.

SPECIFICATIONS

Federal

(A)	QQ-A-225/1	Aluminum 1100, Bar, Rod and Wire, Rolled, Drawn, or Cold Finished
(A)	QQ-A-250/1	Aluminum Alloy 1100, Plate and Sheet

Military

MIL-H-6088	Heat Treatment of Aluminum Alloys
MIL-I-6866	Inspection, Penetrant Method of

STANDARDS

Military

MIL-STD-453	Inspection, Radiographic
-------------	--------------------------

Industry

ASTM-E-8	Tension Testing of Metallic Materials
----------	---------------------------------------

(Copies of documents required by contractors in connection with specific procurement functions should be obtained as indicated in the Department of Defense Index of Specifications and Standards.)

2.2 Aerojet-General Corporation documents.- Unless otherwise specified, the following documents of the latest issue in effect, shall form a part of this specification to the extent specified herein.

SPECIFICATION

AGC-13860

Radiographic Quality Levels, Fusion Weldments

STANDARDS

AGC-STD-1317

Electron Beam Welding

AGC-STD-4831

Aluminum and Aluminum Alloys, Cleaning and Deoxidizing Process Prior to Welding

ASD 5215

Marking, Methods of

DRAWINGS

1269226

Liner Components, Hinged Boss Concept
12-in-dia, Filament-Wound Vessel

1269227

Liner Assembly, Welded-Hinged Boss Concept,
12-in-dia, Filament-Wound Vessel

1269229

Liner, Butt-Welded Boss Concept, 12-in-dia
Filament-Wound Vessel

(A)

1269230

Boss, Butt-Welded Concept, 12-in-dia
Filament-Wound Vessel

1269231

Liner Assembly, Welded-Butt Welded Boss
Concept, 12-in-dia Filament-Wound Vessel

(A)

1269236

Back-up Ring, Expendable, Filament
Wound Vessel 12-in-dia

3. REQUIREMENTS

3.1 Materials.-

3.1.1 Liner.- The metal-liner half-shell, P/N 1269226-2 and P/N 1269229-1 shall be fabricated from Type 1100 aluminum sheet in accordance with Specification QQ-A-250/1 as the starting material.

3.1.2 Boss.- The bosses P/N 1269226-3 and P/N 1269230-1, shall be fabricated from 2219-T87 aluminum alloy fully-wrought, forged bar stock, commercial grade, with a minimum ultimate tensile strength of 60,000 psi, minimum yield strength of 48,000 psi and minimum elongation of 6 percent in a 2-inch gage length.

3.1.3 Collar.- The collar, P/N 1269226-4 shall be fabricated from 2219-T87 aluminum alloy fully-wrought, forged bar stock, commercial grade with a minimum ultimate tensile strength of 60,000 psi, a minimum yield strength of 48,000 psi, and a minimum elongation of 6 percent in 2-inch gage length.

3.1.4 Flange.- The hot section flange, P/N 1269226-5 shall be fabricated from Type 1100 aluminum bar stock in accordance with QQ-A-225/1 or Type 1100 aluminum plate or sheet stock per QQ-A-250/1 as the starting material.

(A) 3.1.5 Liner material identification.- Each blank cut from the Type 1100 aluminum sheet for fabrication of P/N 1269226-2 or P/N 1269229-1 shall be identified with the serial number assigned by AGC, the identification of which shall be maintained during all fabrication operations. This serial number along with the mill heat number for the sheet from which the blank was cut shall be recorded for future reference.

3.2 Design.- The metal-liner assembly furnished under this specification shall be fabricated in accordance with the requirements of AGC Drawing 1269227 or 1269231, as applicable, and this specification.

(A) 3.3 Fabrication of aluminum liner half shell.- Unless otherwise specified, aluminum liner half-shells, P/N 1269226-2 and P/N 1269229-1 shall be fabricated by utilizing the following sequence of operations. The details of each operation shall be the responsibility of the fabricator. Throughout the processing operations, care shall be taken to prevent physical damage or chemical contamination to the liner components.

(A) Operation 1: Cut at least 4 tensile specimens for each mill heat involved and verify satisfactory elongation and tensile strength in accordance with 4.4.2 and 3.6 before forming half-shells.

(A) Operation 2: Prepare 5 tensile test blanks and process with half shells in accordance with 3.6. Form liner contour for half-shell component P/N 1269226-2 or P/N 1269229-1. Anneal at 650°F in accordance with paragraph for "Annealing of Work Hardened Wrought Alloys" of Specification MIL-H-6088 between forming operations, as required, and after the final forming operation.

Operation 3: Reduce thickness of liner wall to 0.010 inch by means of chemical milling, except in the weld joint area and boss area which shall be maintained at the thicknesses shown on the drawing.

(A) Operation 4: Cut hole in dome area for installation of boss or flange, as applicable.

(A) Operation 5: Apply Teflon coating to liner half-shell, P/N 1269226-2 in accordance with the drawing.

(A) Operation 6: Place in container, prepare for shipment in accordance with Section 5, and ship to Aerojet for welding of boss in each half shell in accordance with 3.4.

(A) Operation 7: After welding of bosses, machine girth weld area to pre-weld configuration in accordance with drawings 1269226 or 1269229, as applicable.

(A) Operation 8: Weigh each half shell to nearest 0.1 ounce. Record and forward weight to Aerojet with the liner. Weight of the half shell shall be 1¹/₄ ounces or less.

(A) Operation 9: Package and mark item in accordance with Section 5 and ship to Aerojet.

(A) 3.4 Welding of boss in liner half-shell.- A prefabricated flange P/N 1269226-5; boss P/N 1269226-3; and collar P/N 1269226-4 shall be welded into P/N 1269226-2 half-shell; and a prefabricated boss P/N 1269230-1 shall be welded into P/N 1269229-1 half-shell. The welding shall be performed at Aerojet-General Corporation (AGC) in accordance with the following operations:

- (A) Operation 1: Match machine boss P/N 1269230-1 or boss P/N 1269226-3, collar P/N 1269226-4, and flange P/N 1269226-5 to opening in head of liner shell as specified on applicable drawing.
- Operation 2: All tooling shall be vapor-degreased prior to installation in the electron-beam weld cabinet.
- (A) Operation 3: Clean boss, collar, flange, and half liner at the weld joint with spectrometric grade acetone.
- Operation 4: If an aluminum liner weldment has not been made within the previous two working-days, a flat-plate test weldment shall be run on aluminum sheet in accordance with the approved weld schedule to verify the performance of the welding machine prior to proceeding with liner weldments.
- (A) Operation 5: Assemble boss or boss, collar, and flange in half-liner. Electron-beam weld in accordance with the approved weld schedule, Drawing 1269227 or 1269231, and AGC-STD-1317. Weld repairs are not permitted, except as specified in 3.7.
- (A) Operation 6: Inspect welds in accordance with 4.4.3 and 4.4.4.

(A) 3.5 Assembly of aluminum liner.- After installation of the boss in each liner half-shell, the two half-shells shall be assembled to form the full liner, P/N 1269227-1 or P/N 1269231-1 by utilizing the following sequence of operations:

- (A) Operation 1: Clean half-shells at girth weld-joint area in accordance with the procedures specified in AGC-STD-4831 followed by cleaning with spectrometric grade acetone. Verify that weight of half shells is available; if not, weigh to nearest 0.1 ounce and record.
- (A) Operation 2: Assemble two matching half-shells together utilizing copper backup ring P/N 1269226-1. Maximum gapping at butt weld joint and the maximum mismatch at the joint shall not exceed the requirements on drawing 1269227 or 1269229, as applicable.
- (A) Operation 3: Electron-beam weld joint in accordance with approved weld schedule, Drawing 1269227 or 1269231, and AGC-STD-1317. The quality level and any required repairs shall be in accordance with 3.8 and 3.7.

- (A) Operation 4: Remove copper backup ring by means of chemical etching in accordance with Appendix A. Care shall be taken to mask liner bosses and collars to prevent contact with nitric acid.
- (A) Operation 5: Inspect weld in accordance with 4.4.3 and 4.4.4. In addition to weld quality, check X-ray film for no evidence of residual copper from backup ring.
- (A) Operation 6: Helium leak test liner assembly in accordance with special test procedure prepared for the assembly. Leakage shall not exceed 1×10^{-5} scc/sec at 5 ± 2 psid.
- Operation 7: Anneal liner assembly at 600°F for one hour.

(A) 3.6 Test coupons.- Prior to starting processing of liner half-shells, P/N 1269226-2 or 1269229-1, the ultimate tensile strength and elongation in a 2-inch gage length shall be verified with at least 4 tensile specimens from each mill heat involved. Subsequently five tensile test blanks 3/4 inch wide by 8 inches long shall be cut from the Type 1100 aluminum sheet parallel to the direction of rolling, and accompany each lot of liner half-shells, P/N 1269226-2 or 1269229-1, through the final anneal and delivery to AGC. The aluminum sheet used for these coupons shall be from the same mill heats used to fabricate the half-shells. Tensile specimens shall be tested in accordance with 4.4.2 and shall comply with the following tensile properties:

(a)	Ultimate tensile strength, psi	15,000 maximum
(b)	Elongation in 2 inches, percent	15.0 minimum

(A) 3.7 Weld repairs.- Weld repairs shall be limited to those directed by the project engineer.

(A) 3.8 Weld acceptance criteria.- Welds shall meet the following quality requirements:

(A) 3.8.1 Dye penetrant inspection.- The welds shall be free of external cracks or propagating defects. Surface porosity in excess of the limits specified in 3.8.2 is unacceptable.

(A) 3.8.2 Radiographic inspection.- The welds shall meet the quality level requirements of Specification AGC-13860, Class 11 (eleven) with the following modifications:

- (a) Under scattered porosity - delete 0.010 inch maximum diameter of cavity.
- (A) (b) Under excess crown limits substitute "weld crown shall be removed only as specified by the project engineer."

3.9 Handling.- All handling operations of the liner assembly or the half-shells in the uncrated condition shall be performed using maximum care because of the susceptibility of the material to damage during the stages of fabrication. Components or assemblies damaged from handling shall be subject to rejection. The components shall be kept in suitable containers except when they are being worked.

(A) 3.10 Cleanliness.- After final machining, a cleaning method shall be employed to guarantee the liner assembly interior is completely free from machining residue, shavings, and cuttings. After cleaning, the assembly openings shall remain sealed at all times, except when removal of seals is necessary for final fabrication or testing. The cleaning method shall not damage the aluminum materials.

(A) 3.11 Identification of liner assembly.- Each liner assembly shall be marked with the part number and assigned serial number, by electrolytic etch, as specified by Aerojet Standard ASD 5215, Method C, in the location indicated on Aerojet Drawing 1269227 or 1269231.

3.12 Workmanship.- The liner assembly shall be fabricated, annealed, finished, and tested in a thoroughly workmanlike manner. Particular attention shall be given to neatness and thoroughness of the processing and welding of the component parts. Nonconformance to the drawings and the requirements of this specification shall be cause for rejection.

4. QUALITY ASSURANCE PROVISIONS

4.1 Supplier responsibility.-

(A) 4.1.1 Inspection.- Unless otherwise specified, the supplier shall be responsible for the performance of all inspection requirements specified herein and may use any facilities acceptable to the Aerojet-General Corporation (AGC).

4.1.2 Processing changes.- The supplier shall make no changes in processing techniques or other factors affecting the quality or performance of the product without prior written approval of AGC.

4.2 Sampling.-

4.2.1 Production sample.- All production units of aluminum alloy liner assembly, P/N 1269227-1 or 1269231-1 shall be subjected to quality conformance inspection.

4.3 Quality conformance inspections.- Inspection of all liner assemblies shall consist of the following quality conformance inspection to determine compliance with the requirements herein:

- (A) (a) Dimensional and visual inspection (see 4.4.1).
- (b) Tensile strength tests (see 4.4.2)
- (A) (c) Dye penetrant inspection of girth and boss welds (see 4.4.3)
- (A) (d) Radiographic inspection of girth and boss welds (see 4.4.4)

4.4 Test methods.-

(A) 4.4.1 Examination.- Each liner assembly shall be measured and visually inspected for conformance to the requirements of Section 3, Section 5 and the drawings.

(A) 4.4.2 Tensile strength test method.- The tensile strength properties shall be determined in accordance with ASTM-E-8, using the standard sheet-type test specimen with a 2 in. gage length to verify compliance with 3.6.

(A) 4.4.3 Dye penetrant inspection.- Dye penetrant inspection in accordance with Specification MIL-I-6866, Type I, Method A shall be performed on all welds of each liner assembly to verify compliance with 3.8.1. After inspection, the weld shall be thoroughly cleaned.

(A) 4.4.4 Radiographic inspection.- Radiographic inspection in accordance with MIL-STD-453 shall be performed on all girth welds, on the flange to half-shell weld (see 1269227), and on the boss to half-shell weld (see 1269231). Radiographs shall be subject to the interpretation and acceptance in accordance with 3.8.2 by designated Aerojet-General quality control and project representatives. Radiographic film shall be numbered to coincide with the identification markings of the liner assembly. China marking lead shall be used for marking weld identification so that exact location of weld areas with corresponding radiographs may be readily identified. All radiographic film shall become the property of the Aerojet-General Corporation.

5. PREPARATION FOR DELIVERY

(A) 5.1 Packing.- Liner components, and the liner assembly shall be crated and firmly supported to prevent damage during storage, handling or shipment.

5.2 Marking.- The shipping container shall be marked with the following information:

- (a) Manufacturer's name
- (b) Part number
- (c) Serial number
- (d) Number, revision letter, and date of this specification
- (e) Purchase order number

6. NOTES

6.1 Intended use.- The aluminum alloy liner assembly is intended for use as a metal liner for glass filament-wound pressure vessels for storage of cryogenic fluids.

6.2 Ordering data.- Procurement documents should specify, but not be limited to, the following information:

- (a) Number, revision letter, and date of this specification
- (b) Request for three copies of material certification and test results
- (c) Responsibility for testing tensile test coupons before forming half-shells (see 3.6)
- (A) (d) Operations to be performed by the supplier
- (e) Place of delivery for tensile test coupons, half-shell liners, and finished units.
- (A) (f) Serial numbers to be assigned.

APPENDIX A

Copper Weld Backup Ring Etch Removal Procedure

10. SCOPE

10.1 This appendix covers the procedure to be used for preparation of a chemical etchant and removal of the copper backup ring from 1100 Aluminum Liners, AGC Part Nos. 1269227-1 and 1269231-1.

20. APPLICABLE DOCUMENTS

20.1 Aerojet-General Corporation documents.- Unless otherwise specified, the following documents of the latest issue in effect, shall form a part of this appendix to the extent specified herein.

DRAWINGS

1269227	Liner assembly, Welded-Hinged Boss Concept, 12-in-dia, Fialment-Wound Vessel
1269231	Liner Assembly, Welded-Butt Welded Boss Concept, 12-in-dia Fialment-Wound Vessel
1269236	Backup Ring, Expendable, Filament Wound Vessel 12-in-dia

30. OPERATING PROCEDURE

30.1 Copper backup ring removal by chemical etching.- After assembly of the two matching half-shells has been accomplished and inspected, utilizing the copper backup ring P/N 1269236-1 and electron-beam welding of the joint, prepare a chemical etchant and remove the copper ring as follows:

- (a) Prepare etchant by adding 6 gallons of Nitric Acid, 42° Baumé to 8 gallons of water and stir. Let solution cool to 100°F and add 13 1/2 ounces of Chromic Acid Flake. Stir until fully dissolved and cool again to 100°F.
- (b) Check etch rate to confirm 0.0005 inch per minute copper removal.
- (c) Mask bosses and collars; then fully immerse liner assembly in etchant.
- (d) Check etchant solution temperature every 15 minutes to insure that temperature is below 105°F and absence of a brown nitrous oxide fume.
- (e) Drain liner completely every hour to minimize internal concentration of copper precipitate in the liner and re-submerge liner in the same etchant bath.

APPENDIX A

- (f) When etching is complete, rinse liner assembly by submerging in four (4) successive fresh water rinses. This operation must be completed in 30 minutes or less. Make final rinse of liner by submerging in de-ionized water.
- (g) Remove liner from water bath, drain completely, and dry in an oven at 225°F for 30 minutes. Remove liner and allow to cool to room temperature.
- (h) Weigh liner and compare to measurement specified in 3.5, operation 1 to confirm complete removal of copper ring.

APPENDIX H
FILAMENT STRESS ANALYSIS

Filament stresses in a metal-lined filament-wound pressure vessel are a function of the amount of fiber, fiber orientation, applied load, and the load taken by the metal liner. The relations defining these factors in the cylindrical section of a vessel are summarized in the following paragraphs followed by sample calculations for a specific vessel (A-3), to demonstrate the methods used.

I. EQUIVALENT FILAMENT THICKNESS

The equivalent filament thickness per layer of S-glass/epoxy tape used in vessel winding may be determined from the expression

$$t_f = N_2 A_f / W_l \quad (H1)$$

where

$$A_f = \text{cross section of 20-end roving} = \\ 4.20 \times 10^{-4} \text{ in}^2 (0.0027 \text{ cm}^2)$$

$$W_l = \text{winding tape width, selected as} \\ 0.255 \text{ in (0.648 cm)}$$

$$N_2 = \text{number of 20-end roving strands} \\ \text{per tape, selected as } 3$$

Therefore, for all vessels in this program the equivalent filament thickness per layer, based on equation (H1), is

$$t_f = 3(4.20 \times 10^{-4})/0.255$$

$$t_f = 0.00494 \text{ in. (0.125 mm)}$$

II. LOAD TAKEN BY METAL LINER

The load taken by the thin 1100-0 aluminum liner at the pressures of interest can be calculated from measured strain data. Assuming the liner is subjected to a 1:1 biaxial stress field, the strain equation in the inelastic region of the material is

$$\epsilon = \frac{F_{ty}(1-\mu_e)}{E} + \frac{(\sigma - F_{ty})(1-\mu_p)}{E_p} \quad (H2)$$

Where, an effective plastic modulus (E_p) can be derived from the expression

$$E_p = \frac{F_{tu} - F_{ty}}{\epsilon_{tu} - F_{ty}/E} \quad (H3)$$

with the following material properties (room temperature values shown)

$$\text{Ultimate tensile strength, } F_{tu} = 12300 \text{ psi (8480 N/cm}^2\text{)}$$

$$\text{Tensile yield strength, } F_{ty} = 5400 \text{ psi (3720 N/cm}^2\text{)}$$

$$\text{Ultimate tensile strain, } \epsilon_{tu} = 0.203$$

$$\text{Elastic Poisson's ratio, } \mu_e = 0.325$$

$$\text{Plastic Poisson's ratio, } \mu_p = 0.5$$

$$\text{Elastic modulus, } E = 10.25 \times 10^6 \text{ psi (70.7 GN/m}^2\text{)}$$

Thus, the plastic modulus, at room temperature, is

$$E_p = \frac{12300 - 5400}{0.203 - 5400/10.25 \times 10^6}$$

$$E_p = 34000 \text{ psi (0.23 GN/m}^2\text{)}$$

and the strain equation, rearranged for stress calculations, is

$$\sigma = \frac{\epsilon + 0.0791}{1.471 \times 10^{-5}} \quad (H2a)$$

III. GEOMETRIC RELATIONS

A. VOLUME FRACTION OF GLASS

The following procedure was used to arrive at the volume fraction of glass (P_{vg}) in the composite. The weight fraction of glass was calculated from measured values for composite weight (W_g) by the equation

$$P_{wg} = \frac{W_g}{W_c} \quad (H4)$$

Assuming a void free composite, the volume fraction of glass was then determined from the figure included in this Appendix.

B. COMPOSITE THICKNESSES

The thickness of the longitudinal composite is

$$t_L = N_L t_f / P_{vg} \quad (H5)$$

The hoop composite thickness is

$$t_H = N_H t_f / P_{vg} \quad (H6)$$

and the total composite wall thickness in the cylinder is

$$t_C = t_L + t_H \quad (H7)$$

where

N_L = number of longitudinally oriented layers, selected as 6

N_H = number of hoop oriented layers, selected as 10

C. VESSEL INSIDE RADIUS

The inside radius (R) of the pressurized vessel is

$$R = D_i(1 + \epsilon_\theta)/2 \quad (H8)$$

where,

ϵ_θ = hoop strain

D_i = average (unloaded) inside diameter = $D_o - 2t_c$, in (cm)

D_o = outside diameter of vessel, in (cm)

IV. FILAMENT STRESSES

In order to calculate vessel filament stresses at the pressures of interest, load balance relations are required which take into account loads carried by the metal liner and oriented filaments in both directions.

A. LONGITUDINAL DIRECTION

Assuming the loads carried by the matrix material are insignificant, the load balance in the longitudinal direction of the cylinder is

$$\sigma_{f,l} (N t_f) \cos^2 \alpha_o + \sigma_{\text{om}} t_m = pR/2 \quad (H9)$$

where

$\sigma_{f,l}$ = longitudinal filament stress, psi (N/cm^2)

α_o = orientation of longitudinal filaments with respect to axis of rotation,
3.82 degrees (0.067 rad)

σ_{om} = longitudinal stress in liner, psi (N/cm^2)

t_m = thickness of liner, 0.010 in (0.254 mm)

p = internal pressure, psi (N/cm^2)

Rearrangement of the load balance relation results in the following equation for calculation of longitudinal filament stress

$$\sigma_{f,l} = \frac{pR/2 - \sigma_{\theta m} t_m}{N_L t_f \cos^2 \alpha_o} \quad (\text{H9a})$$

B. HOOP DIRECTION

The load balance in the hoop direction of the cylinder is

$$\sigma_{f,h}(N_H t_f) + \sigma_{f,l}(N_L t_f) \sin^2 \alpha_o + \sigma_{\theta m} t_m = pR \quad (\text{H10})$$

where

$\sigma_{f,h}$ = hoop filament stress, psi (N/cm^2)

$\sigma_{\theta m}$ = hoop stress in liner, psi (N/cm^2)

Rearrangement of the load balance relation results in the following equation for calculation of hoop filament stress

$$\sigma_{f,h} = \frac{pR(1-.5 \tan^2 \alpha_o) - \sigma_{\theta m} t_m (1-\tan^2 \alpha_o)}{N_H t_f} \quad (\text{H10a})$$

V. SAMPLE CALCULATION

Fabrication data and room temperature single cycle burst data from Vessel A-3 were used to provide sample calculations. The required data are

$$D_o = 12.339 \text{ in } (31.341 \text{ cm})$$

$$W_g = 1990 \text{ grams}$$

$$W_c = 2344 \text{ grams}$$

$$\epsilon_{\theta} = 0.0212$$

$$\epsilon_{\phi} = (0.0175 + 0.0146)/2 = 0.0161$$

$$p = 2250 \text{ psi } (1550 \text{ N/cm}^2)$$

A. METAL LINER STRESSES

Based on equation (H2a), the hoop stress in the metal liner at pressure is

$$\sigma_{\theta m} = \frac{0.0212 + 0.0791}{1.471 \times 10^{-5}} = 6820 \text{ psi } (4700 \text{ N/cm}^2)$$

and the longitudinal stress in the liner is

$$\sigma_{\phi m} = \frac{0.0161 + 0.0791}{1.471 \times 10^{-5}} = 6470 \text{ psi } (4460 \text{ N/cm}^2)$$

B. VOLUME FRACTION OF GLASS

The weight fraction of glass from equation (H4), is

$$P_{wg} = \frac{1990}{2344} = 0.849$$

and the corresponding volume fraction from the included figure is

$$P_{vg} = 0.715$$

C. COMPOSITE THICKNESSES

The thickness of the longitudinal composite is computed from equation (H5) as

$$t_L = 6(0.00494)/0.715 = 0.0415 \text{ in } (0.105 \text{ cm})$$

The hoop composite thickness, from equation (H6), is

$$t_H = 10(0.00494)/0.715 = 0.0691 \text{ in } (0.176 \text{ cm})$$

and the total composite wall thickness in the cylinder, based on equation (H7), is

$$t_c = 0.0415 + 0.0691 = 0.1106 \text{ in } (0.281 \text{ cm})$$

D. VESSEL INSIDE RADIUS

The inside diameter of the cylindrical section of the vessel is

$$D_i = 12.339 - 2(0.1106) = 12.118 \text{ in } (30.779 \text{ cm})$$

and from equation (H8), the corresponding radius, at pressure, is

$$R = 12.118 (1 + 0.0212)/2 = 6.187 \text{ in } (15.716 \text{ cm})$$

E. FILAMENT STRESSES

The stress in the longitudinal filaments is calculated from equation (H9a) as

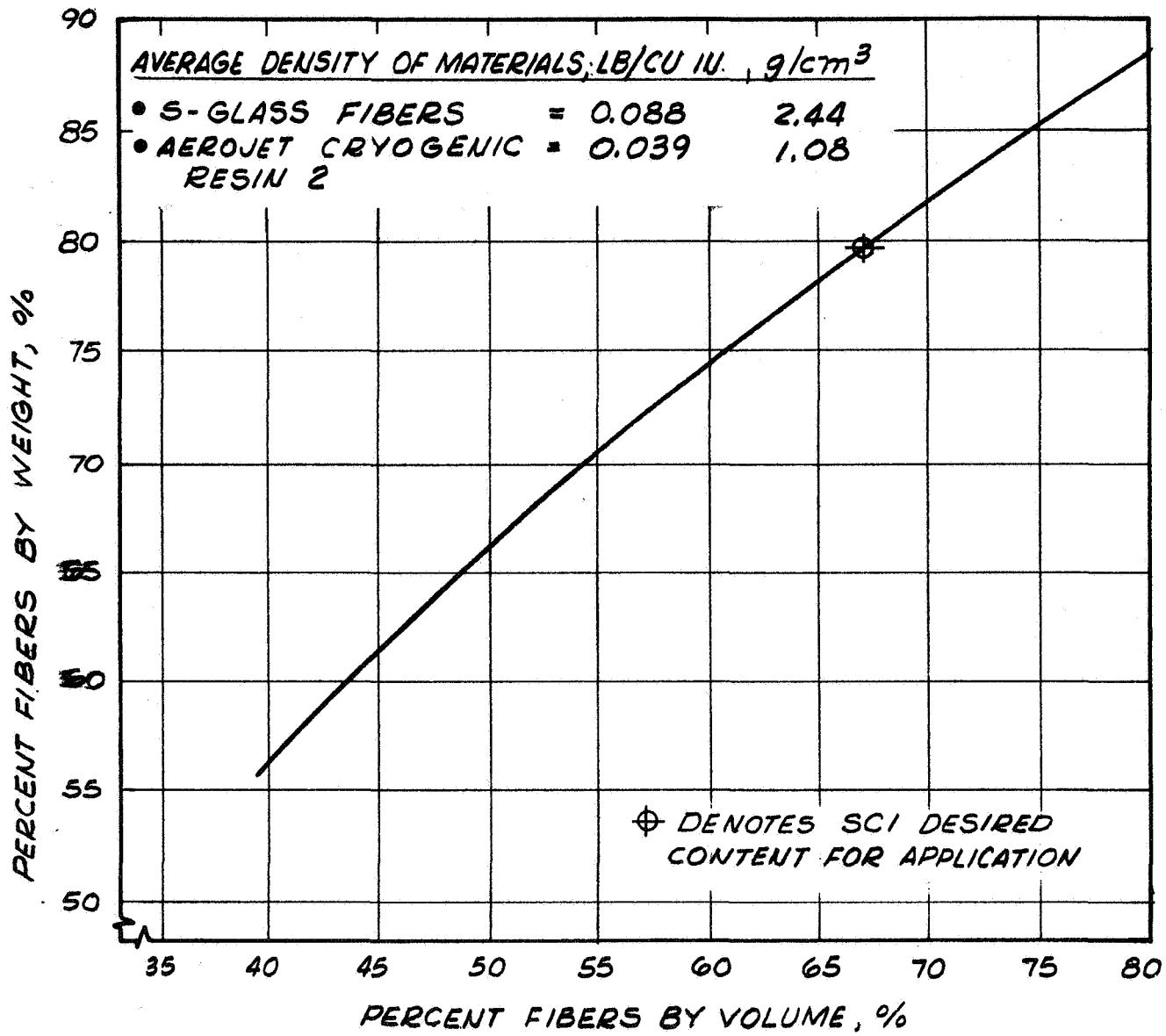
$$\sigma_{f,l} = \frac{2250(6.187)/2 - 6470(0.010)}{6(0.00494)(.998)^2}$$

$$\sigma_{f,l} = 234\ 000 \text{ psi } (161\ 000 \text{ N/cm}^2)$$

and the stress in the hoop filaments, from equation (H10a), is

$$\sigma_{f,h} = \frac{2250(6.187)\{1 - .5(0.0667)^2\} - 6820(0.01)\{1 - (0.0667)^2\}}{10 (0.00494)}$$

$$\sigma_{f,h} = 280\ 000 \text{ psi } (193\ 000 \text{ N/cm}^2)$$



Filter Content Relation
for S-Glass Roving/Resin #2 Composites

Figure H-1

DISTRIBUTION

REPORT
COPIES
R D

RECIPIENT

DESIGNEE

National Aeronautics & Space Administration
Lewis Research Center
21000 Brookpark Road
Cleveland, Ohio 44135

1 Attn: Contracting Officer, MS 500-313
5 Liquid Rocket Technology Branch, MS 500-209
1 Technical Report Control Office, MS 5-5
1 Technology Utilization Office, MS 3-16
2 AFSC Liaison Office, MS 4-1
2 Library
1 Office of Reliability & Quality Assurance,
MS 500-111
1 D. L. Nored, Chief, LRTB, MS 500-209
3 J. R. Barber Project Manager, MS 500-209
1 E. W. Conrad, MS 500-204
1 R. H. Kemp, MS 49-1

2 Chief, Liquid Experimental Engineering, RPX
Office of Advanced Research & Technology
NASA Headquarters
Washington, D.C. 20546

2 Chief, Liquid Propulsion Technology, RPL
Office of Advanced Research & Technology
NASA Headquarters
Washington, D.C. 20546

1 Director, Launch Vehicles & Propulsion, SV
Office of Space Science & Applications
NASA Headquarters
Washington, D.C. 20546

1 Chief, Environmental Factors & Aerodynamics
Code RV-1
Office of Advanced Research & Technology
Washington, D.C. 20546

1 Chief, Space Vehicles Structures
Office of Advanced Research & Technology
NASA Headquarters
Washington, D.C. 20546

REPORT
COPIES
R D

	<u>RECIPIENT</u>	<u>DESIGNEE</u>
1	Director, Advanced Manned Missions, MT Office of Manned Space Flight NASA Headquarters Washington, D.C. 20546	
6	NASA Scientific & Technical Information Facility P.O. Box 33 College Park, Maryland 20740	
1	Director, Technology Utilization Division Office of Technology Utilization NASA Headquarters Washington, D.C. 20546	
1 1	National Aeronautics & Space Administration Ames Research Center Moffett Field, California 94035 Attn: Library	C. A. Syvertson
1	National Aeronautics & Space Administration Flight Research Center P.O. Box 273 Edwards, California 93523 Attn: Library	
1	National Aeronautics & Space Administration Goddard Space Flight Center Greenbelt, Maryland 20771 Attn: Library	
1	National Aeronautics & Space Administration John F. Kennedy Space Center Cocoa Beach, Florida 32931 Attn: Library	
1	National Aeronautics & Space Administration Langley Research Center Langley Station Hampton, Virginia 23365 Attn: Library	
1	National Aeronautics & Space Administration Manned Spacecraft Center Houston, Texas 77001 Attn: Library	J. G. Thiobaudaux, Jr. Chief, Propulsion & Power Division

REPORT
COPIES
R D

RECIPIENT

DESIGNEE

1 1	National Aeronautics & Space Administration George C. Marshall Space Flight Center Huntsville, Alabama 35812 Attn: Library	J. Blumrich
1 1	Jet Propulsion Laboratory 4800 Oak Grove Drive Pasadena, California 91103 Attn: Library	W. Jensen
1	Defense Documentation Center Cameron Station Building 5 5010 Duke Street Alexandria, Virginia 22314 Attn: TISIA	
1	Office of the Director of Defense Research & Engineering Washington, D.C. 20301 Attn: Office of Asst. Dir. (Chem. Technology)	
1	RTD (RTNP) Bolling Air Force Base Washington, D.C. 20332	
1	Arnold Engineering Development Center Air Force Systems Command Tullahoma, Tennessee 37389 Attn: Library	Dr. H. K. Doetsch
1	Advanced Research Projects Agency Washington, D.C. 20525 Attn: Library	D. E. Mock
1	Aeronautical Systems Division Air Force Systems Command Wright-Patterson Air Force Base, Dayton, Ohio Attn: Library	D. L. Schmidt Code ARSCNC-2

REPORT
COPIES
R D

	<u>RECIPIENT</u>	<u>DESIGNEE</u>
1	Air Force Missile Test Center Patrick Air Force Base, Florida Attn: Library	L. J. Ullian
1	Air Force Systems Command Andrews Air Force Base Washington, D.C. 20332 Attn: Library	Capt. S. W. Bowen SCLT
1	Air Force Rocket Propulsion Laboratory (RPR) Edwards, California 93523 Attn: Library	
1	Air Force Rocket Propulsion Laboratory (RPM) Edwards, California 93523 Attn: Library	
1	Air Force FTC (FTAT-2) Edwards Air Force Base, California 93523 Attn: Library	Donald Ross
1	Air Force Office of Scientific Research Washington, D.C. 20333 Attn: Library	SREP, Dr. J. F. Masi
1	Space & Missile Systems Organization Air Force Unit Post Office Los Angeles, California 90045 Attn: Technical Data Center	
1 1	Office of Research Analyses (OAR) Holloman Air Force Base, New Mexico 88330 Attn: Library RRRD	
1	U. S. Air Force Washington, D.C. Attn: Library	Col. C. K. Stambaugh, Code AFRST
1	Commanding Officer U. S. Army Research Office (Durham) Box CM, Duke Station Durham, North Carolina 27706 Attn: Library	

REPORT
COPIES
R D

	<u>RECIPIENT</u>	<u>DESIGNEE</u>
1	U. S. Army Missile Command Redstone Scientific Information Center Redstone Arsenal, Alabama 35808 Attn: Document Section	Dr. W. Wharton
1	Bureau of Naval Weapons Department of the Navy Washington, D.C. Attn: Library	J. Kay, Code RTMS-41
1	Commander U. S. Naval Missile Center Point Mugu, California 93041 Attn: Technical Library	
1	Commander U. S. Naval Weapons Center China Lake, California 93557 Attn: Library	W. F. Thorm Code 4562
1	Commanding Officer Naval Research Branch Office 1030 E. Green Street Pasadena, California 91101 Attn: Library	
1	Director (Code 6T80) U. S. Naval Research Laboratory Washington, D.C. 20390 Attn: Library	H. W. Carhart J. M. Kralli
1	Picatinny Arsenal Dover, New Jersey 07801 Attn: Library	I. Forsten
1	Air Force Aero Propulsion Laboratory Research & Technology Division Air Force Systems Command United States Air Force Wright-Patterson AFB, Ohio 45433 Attn: APRP (Library)	R. Quigley C. M. Donaldson

REPORT
COPIES

R D

RECIPIENT

DESIGNEE

1	Space Division Aerojet-General Corporation 9200 East Flair Drive El Monte, California 91734 Attn: Library	S. Machlawski
1 1	Ordnance Division Aerojet-General Corporation 11711 South Woodruff Avenue Downey, California 90241 Attn: Library	W. L. Arter
1	Propulsion Division Aerojet-General Corporation P.O. Box 15847 Sacramento, California 95803 Attn: Technical Library 2484-2015A	R. Stiff
1	Aerospace Corporation P.O. Box 95085 Los Angeles, California 90045 Attn: Library-Documents	
1	Air Products and Chemicals Company Allentown, Pennsylvania, 18105 Attn: P. J. DeRea	
1	ARDE, Incorporated 193 Route 17 Paramus, New Jersey 07652	
1	ARO, Incorporated Arnold Engineering Development Center Arnold Air Force Station, Tennessee 37389 Attn: Dr. S. H. Goethert Chief Scientist	
1	Atlantic Research Corporation Shirley Highway & Edsall Road Alexandria, Virginia 22314 Attn: Security Office for Library	
1	Battelle Memorial Institute 505 King Avenue Columbus, Ohio 43201 Attn: Defense Metals Information Center	

REPORT
COPIES

R D

RECIPIENT

DESIGNEE

1	Bell Aerosystems Box 1, Buffalo, New York 14205 Attn: T. Rainhardt	
1	The Boeing Company Aero Space Division P.O. Box 3707 Seattle, Washington 98124 Attn: Ruth E. Peerenboom (1190)	
1 1	Aerojet Nuclear Systems Company P.O. Box 13070 Sacramento, California 95813	G. L. Ryland
1	Western Division McDonnell Douglas Aircraft Company, Inc. 3000 Ocean Park Blvd. Santa Monica, California 90406 Attn: J. M. Toth	J. L. Waisman
1	Hercules Powder Company Chemical Propulsion Division 910 Market Street Wilmington, Delaware 19804	
1	Narmco Research & Development Co. Whittaker Corporation 131 N. Ludlow Street Dayton, Ohio 45402	
1	Plastics Technical Evaluation Center Picatinny Arsenal Dover, New Jersey 07801	
1	Rocketdyne 6633 Canoga Avenue Canoga Park, California 91304 Attn: Library, Department 596-306	
1	Rohr Corporation Department 145 Chula Vista, California 91312	

REPORT
COPIES
R D

RECIPIENT

DESIGNEE

1 TRW Systems
1 Space Park
Redondo Beach, California 90200
Attn: Tech. Lib. Doc. Acquisitions

1 Sandia Corporation
Sandia Base
Albuquerque, New Mexico 87115
Attn: H. E. Montgomery

1 Swedlow, Incorporated
6986 Bandini Blvd.,
Los Angeles, California 90022

1 Thiokol Chemical Corporation D. Hess
Wasatch Division
P.O. Box 524, Brigham City, Utah 84302
Attn: Library Section

1 United Aircraft Corporation
United Technology Center
P.O. Box 358
Sunnyvale, California 94088
Attn: Librarian

1 Chemical Propulsion Information Agency
Applied Physics Laboratory
8621 Georgia Avenue
Silver Spring, Maryland 20910

1 The Garrett Corporation
20545 Center Ridge Road
Cleveland, Ohio 44116

1 Grumman Aircraft Engineering Corp.
Bethpage
Long Island, New York

1 General Dynamics/Convair
P.O. Box 1128
San Diego, California 92712
Attn: Library and Information Services (128-00)

1 B. F. Goodrich Company
Aerospace & Defense Products
500 South Main Street
Akron, Ohio 44311

<u>REPORT COPIES</u>	<u>RECIPIENT</u>	<u>DESIGNEE</u>
<u>R D</u>		
1	Goodyear Aerospace Corporation 1210 Massillon Rd Akron, Ohio 44306	
1	Hamilton Standard Corporation Windsor Locks, Connecticut 06096 Attn: Library	
1	ABL, Division of Hercules Powder Company Cumberland, Maryland 21502 Attn: Thomas Bates	
1	IIT Research Institute Technology Center Chicago, Illinois 60616 Attn: C. K. Hersh, Chemistry Division	
1	Martin-Marietta Company Denver, Colorado 80201 Attn: A. Feldman	
1	North American Aviation, Inc. Space & Information Systems Division 12214 Lakewood Blvd. Downey, California 90242 Attn: Technical Information Center D/096-722 (A107)	
1	U. S. Rubber Company Mishawaka, Indiana 46544	
1	General Electric Company Apollo Support Dept., P.O. Box 2500 Daytona Beach, Florida 32015 Attn: C. Day	
1	Aerojet-General Corporation Park West Building - Suite 227 20545 Center Ridge Road Cleveland, Ohio 44116 Attn: W. Snapp	
1	Marine Engineering Laboratory NSRDC ANNADIV Annapolis, Md. 21402 Attn: Karl H. Keller, Code 560	

REPORT
COPIES
R D

RECIPIENT

DESIGNEE

1 Brunswick Corporation
Defense Products Division
P.O. Box 4594
43000 Industrial Ave.,
Lincoln, Nebraska 68504
Attn: J. Carter

1 Celanese Corp.
Box 1000
Summit, New Jersey 07901
Attn: J. D. Lassiter

1 Aeronutronic Division of Philco Ford Corp. Dr. L. H. Linder
Ford Road
Newport Beach, California 92663
Attn: Technical Information Department